MAR 18 1997

SANDIA REPORT

SAND96–2765 • UC-~~721~~ 2000
Unlimited Release
Printed February 1997

Laboratory Creep and Mechanical Tests on Salt Data Report (1975–1996)

Waste Isolation Pilot Plant (WIPP) Thermal/Structural Interactions Program

Kirby D. Mellegard, Darrell E. Munson

Prepared by
Sandia National Laboratories
Albuquerque, New Mexico 87185 and Livermore, California 94550
for the United States Department of Energy
under Contract DE-AC04-94AL85000

SF2900Q(8-81)

Issued by Sandia National Laboratories, operated for the United States Department of Energy by Sandia Corporation.

Printed in the United States of America. This report has been reproduced directly from the best available copy.

Available to DOE and DOE contractors from
Office of Scientific and Technical Information
P.O. Box 62
Oak Ridge, TN 37831

Prices available from (615) 576-8401, FTS 626-8401

Available to the public from
National Technical Information Service
U.S. Department of Commerce
5285 Port Royal Rd
Springfield, VA 22161

NTIS price codes
Printed copy: A23
Microfiche copy: A01

SAND96-2765
Unlimited Release
Printed February 1997

Distribution
Category UC-~~721~~ 2000

Laboratory Creep and Mechanical Tests on Salt Data Report (1975 – 1996)

Waste Isolation Pilot Plant (WIPP) Thermal/Structural Interactions Program

K.D. Mellegard
RE/SPEC Inc., Rapid City, SD 57709-0725

D.E. Munson
Sandia National Laboratories, Albuquerque, NM 87185-5800

ABSTRACT

The Waste Isolation Pilot Plant (WIPP), a facility located in a bedded salt formation in Carlsbad, New Mexico, is being used by the U.S. Department of Energy to demonstrate the technology for safe handling and disposal of transuranic wastes produced by defense activities in the United States. In support of that demonstration, mechanical tests on salt were conducted in the laboratory to characterize material behavior at the stresses and temperatures expected for a nuclear waste repository. Many of those laboratory test programs have been carried out in the RE/SPEC Inc. rock mechanics laboratory in Rapid City, South Dakota; the first program being authorized in 1975 followed by additional testing programs that continue to the present. All of the WIPP laboratory data generated on salt at RE/SPEC Inc. over the last 20 years is presented in this data report. A variety of test procedures were used in performance of the work including quasi-static triaxial compression tests, constant stress (creep) tests, damage recovery tests, and multiaxial creep tests. The detailed data is presented in individual plots for each specimen tested. Typically, the controlled test conditions applied to each specimen are presented in a plot followed by additional plots of the measured specimen response. Extensive tables are included to summarize the tests that were performed. Both the tables and the plots contain cross-references to the technical reports where the data were originally reported. Also included are general descriptions of laboratory facilities, equipment, and procedures used to perform the work.

CONTENTS

CONTENTS (Continued)

TABLES

TABLES (Continued)

FIGURES

1.0 INTRODUCTION

1.1 BACKGROUND

The Waste Isolation Pilot Plant (WIPP) is a facility sited in a bedded salt formation in southeastern New Mexico. The purpose of the WIPP is to demonstrate the technology for safe handling and disposal of transuranic (TRU) radioactive wastes produced by defense activities of the United States. This technology is being developed in support of performance assessment calculations and activities necessary to demonstrate compliance to the regulatory requirements promulgated by the Environmental Protection Agency (EPA).

One of the necessary inputs the WIPP Project has used to fulfill its mission is rock mechanics testing performed in a materials testing laboratory. Much of that laboratory work was performed by RE/SPEC Inc. in their rock mechanics laboratory located in Rapid City, South Dakota. The first laboratory testing contract between Sandia National Laboratories (SNL) and RE/SPEC Inc. was issued in 1975 when the pre-WIPP conceptual repository designs were being considered by SNL. After that first contract, additional laboratory investigations were conducted over the years and continue today. The results of those laboratory testing programs were published in technical reports and a summary listing is presented in Table 1-1.

Throughout many of the reports in Table 1-1 there are references to a set of constitutive equations known as the Multimechanism Deformation (M-D) model which is based on the micromechanisms thought to control the deformation of salt at the stresses and temperatures expected for a nuclear waste repository (Munson and Dawson, 1979; Munson and Dawson, 1982a; Munson and Dawson, 1982b; Munson and Dawson, 1984; Munson, 1979; Munson et al., 1989b). Typical test programs were directed at quantifying either elastic or inelastic parameters appearing in this constitutive model (Fossum et al., 1994), while some other programs were designed to evaluate or guide the development and refinement of the forms of the constitutive model. This especially pertains to the testing performed in support of the Multimechanism Deformation Coupled Fracture (MDCF) model (Chan et al., 1992; Chan et al., 1996) and the experiments define the form of the flow potential (Munson et al., 1989a; Munson et al., 1989b). Another specialized testing program was directed at determining the thermomechanical damage recovery parameters that impacted WIPP sealing systems (Brodsky and Munson, 1994).

The salt creep and mechanical response data which are given in this data report are fundamentally independent of any constitutive model, as is appropriate. The data were, however, ultimately analyzed by well established methods to give the parameters specifically required for the M-D and MDCF models. These methods and the results of the analysis used for this parameter determination have been presented elsewhere for the determination of discrete parameter values (Munson et al., 1989a; Munson et al., 1989b) and for the determination of parameter distribution functions (Pfeifle et al., 1992; Fossum et al., 1994).

1.2 APPROACH AND SCOPE

This report is a summary presentation of laboratory results that have been generated at RE/SPEC Inc. and documented in the reports listed in Table 1-1. In keeping within the intent of a data report, there have been no data analyses performed on the data; however, simple changes in data format have been performed to make the original data sets compatible with modern personal computer systems. For the oldest data sets, old technology "punch card" listings of data were transcribed for modern magnetic disk storage. Where plots were generated for this report, they simply represent data extracted from the reports in Table 1-1 and only the graphical format may have changed. Some of the older data were originally reported using English units and those results have been converted to SI units for this report.

Table 1-1. Summary List of WIPP-Related Laboratory Investigations at RE/SPEC Inc.

Report No.	Author(s)	Title
SAND93-7111	Brodsky, N. S.	*Thermomechanical Damage Recovery Parameters for Rocksalt From the Waste Isolation Pilot Plant*
SAND92-7291	Mellegard, K. D. Pfeifle, T. W.	*Creep Tests on Clean and Argillaceous Salt From the Waste Isolation Pilot Plant*
SAND91-7083	Mellegard, K. D. Callahan, G. D. Senseny, P. E.	*Multiaxial Creep of Natural Rock Salt*
SAND90-7076	Brodsky, N. S.	*Crack Closure and Healing Studies in WIPP Salt Using Compressional Wave Velocity and Attenuation Measurements: Test Methods and Results*
SAND89-7098	Senseny, P. E.	*Creep of Salt From the ERDA–9 Borehole and the WIPP Workings*
SAND85-7261	Senseny, P. E.	*Triaxial Compression Creep Tests on Salt From the Waste Isolation Pilot Plant*
SAND80-7114	Hansen, F. D. Mellegard, K. D.	*Further Creep Behavior of Bedded Salt From Southeastern New Mexico at Elevated Temperature*
SAND79-7030	Hansen, F. D. Mellegard, K. D.	*Creep Behavior of Bedded Salt From Southeastern New Mexico at Elevated Temperature*
SAND79-7045	Hansen, F. D.	*Triaxial Quasi-Static Compression and Creep Behavior of Bedded Salt From Southeastern New Mexico*

The approach used in this report is to present sufficient background information, in a general way, to place the material studies into the proper context, followed by the detailed test results. As part of the background information, the work gives some general history of salt core acquisition along with information on specimen preparation and handling. General information is also provided on typical laboratory procedures and equipment. The various types of tests that were performed are described along with general notes on how the acquired data were reduced to obtain meaningful test results.

The bulk of the report presents the detailed results from individual tests. These results are presented only in graphical form because many of the data sets contain hundreds (and in some cases thousands) of lines of acquired data. Also included are summary tables that are cross-referenced to the individual plots of data by a test number and/or a specimen identification number. Each result (either tabular or graphical) is also cross-referenced to the report where that result originally appeared.

1.3 PERMANENT RECORDS RETENTION

The supporting information for each of the reports in Table 1-1 was collected and organized in an orderly fashion by following the guidelines presented in the SNL Quality Assurance Procedure QAP 20-3, entitled *Qualification of Existing Data*, Rev. 2, 6-28-95 (Scully, 1995). Specifically, the guidelines for developing a Laboratory Data Notebook presented in Appendix B of QAP 20-3 were used to assemble a data records package for each report. These individual data packages followed the format detailed in Appendix B of QAP 20-3 and those files are in the Sandia WIPP Central Files (SWCF) for records retention and future reference. These records packages contain the original complete test objectives, statements of work, calibrations, data, and all other relevant documents of the tests, including core identification and specimen identification. These records also include documentation of procedures, including coring, core identification, calibration, testing, and data reduction.

1.4 TRANSMISSION TO PERFORMANCE ASSESSMENT

As is consistent within the intent of a data report, the data presented reflect only simple data reduction (e.g., conversion of measured forces and displacements to stresses and strains). The data presented in this report have not been the subject of any analysis. The complete analysis of the data has been performed in other work which determines material parameters for specific constitutive models (Munson et al., 1989a; Munson et al., 1989b) and the statistical distributions of those parameters (Pfeifle et al., 1992; Fossum et al., 1994). The parameters resulting from those analyses, performed subsequent to the laboratory testing, are the quantities transmitted to Performance Assessment for support of numerical studies.

1.5 REPORT ORGANIZATION

The remainder of this report is organized into eight chapters. The next chapter, Chapter 2.0, covers topics related to core acquisition and specimen preparation. Chapters 3.0, 4.0, and 5.0 present general information on typical laboratory facilities, test equipment, and test procedures, respectively. Chapter 6.0 describes the processes by which test systems were calibrated and verified. Chapter 7.0 presents all the tabulated test results. Chapter 8.0 is a brief summary. Chapter 9.0 is a list of cited references followed by appendices that contain the detailed test results in graphical form. Appendix A holds the plots of the quasi-static triaxial compression tests. Appendix B contains detailed results from creep testing of specimens from boreholes drilled in the vicinity of the WIPP facility. Appendix C is also dedicated to creep testing, but for specimens taken from the WIPP mine workings. The detailed results of the specialized multiaxial testing are given in Appendix D. Lastly, Appendix E presents the detailed results obtained from the damage recovery testing program.

2.0 TEST SPECIMENS

2.1 CORE ACQUISITION

The specific sources of core are generally given in the individual reports listed in Table 1-1. The bulk of the WIPP-related core came from two sources. The first source was the AEC7 and ERDA9 deep boreholes drilled from the ground surface and located in the vicinity of the WIPP. The borehole core was greater than 100 mm (4 inches) in diameter and could be subcored in the laboratory to provide testable specimens of 50 mm diameter. The second source of core was the WIPP mine workings. The core obtained directly from the WIPP mine workings was generally large diameter which required subcoring to 100 mm in diameter. The salt core obtained from the WIPP mine workings was classified as clean salt or argillaceous salt. The clean salt was relatively free of impurities while the argillaceous salt had a significant clay content. The salt core obtained from the AEC7 and ERDA9 boreholes was not classified and has an unknown clay content. A non-WIPP source of salt core was the International Salt Mine in Avery Island, Louisiana. The Avery Island core was used in a testing program that was designed solely to determine the creep flow potential criterion that should be used for salt.

The acquisition of core samples was typically performed by SNL field and contract personnel. The core was marked to designate its source and depth of recovery. The recovered core varied in length and each individual piece was given a unique marking. The individual pieces were packaged in core boxes and shipped in temperature controlled trucks (to prevent freezing of the specimen) to RE/SPEC Inc. in Rapid City, South Dakota. Upon arrival in Rapid City, the core was inspected for damage and logged into an inventory for control purposes. The core was stored in a controlled environment where the core was protected from extremes in temperature. The core remained in storage protected from extremes in temperature until it was retrieved for specimen preparation purposes.

A chain of custody was implemented by logging the initial core information into a core inventory system. As the core moved through the processes of specimen preparation and laboratory testing, additional core inventory records were generated to document specimen usage and storage locations.

2.2 SPECIMEN PREPARATION

The preparation and control of testable specimens from the core samples was done by RE/SPEC using standard RE/SPEC laboratory procedures that have evolved as an integral part of a corporate quality assurance program (RE/SPEC, 1995). The prepared specimens were labeled such that they could be traced back to the original core sample which in turn should be traceable to a recovery site in the field. This specimen labeling scheme often followed the outline of an SNL procedure designated WIPP-092 that was devised for maintaining traceability of specimens. The specimen label became a unique identifier for each individual specimen and was used in the published reports to link the reported test results to specific specimens. In later sections of this report, those same identifiers will be seen on the plots and in the summary tables.

The typical specimen preparation procedure comprised a sequence of machining operations which were conducted at the RE/SPEC laboratory. First, the core sample was sawn to appropriate lengths in a bandsaw. The sawn pieces were then subcored in a vertical milling machine to obtain specimens of the appropriate diameter. Typical length-to-diameter (L:D) ratios were constrained to about L:D = 2. The ends of the cored specimens were then finished flat and parallel in a milling machine or lathe. The finished specimen represented a right-circular-cylinder which had dimensions that could be determined using standard dimensional measurement tools; e.g., micrometers, calipers, V-blocks, height gage, and a granite surface plate. These specimen dimensions were recorded for each specimen for later use in data reduction.

A special specimen preparation procedure was devised for creating large thin-walled hollow cylinders of salt needed for multiaxial testing. Starting with a large diameter core, the core was sawn to an appropriate length and then the outside surface was finished in a lathe. A thin-walled cylinder was then created with a boring tool on a lathe to cut the appropriate inside diameter. The inner surface and the ends of the hollow cylinder were then finished to produce the final specimen.

3.0 LABORATORY FACILITIES

When the first laboratory testing contract between RE/SPEC and SNL was placed in 1975, the RE/SPEC laboratory was housed in facilities located near the present site of the laboratory. In 1980, the laboratory was moved to a new facility which had a design based on the need for a laboratory setting that was dedicated to rock mechanics testing. The new facility covered a total of 30,000 square feet with about 10,000 square feet dedicated to laboratory operations. The new facility incorporated an earth-sheltered concept that enhanced constant temperature control within the laboratory portion. The entire facility was equipped with a backup power system that could support electrical power needs during periods of commercial utility power outages.

A floor plan of the laboratory portion of the current facility is shown in Figure 3-1. The General Lab Area at the east end is a high bay area used for shipping/receiving and storage of core. Adjacent to that area is a Specimen Preparation room that is equipped with saws, lathes, milling machines, and grinders that are available for use in preparing testable specimens. Machined specimens are taken into the Metrology room where dimensional and mass measurements can be made. The Metrology room also houses the calibration standards that are kept on site, such as load cells, dead weight pressure systems, temperature baths, gage blocks, and electrical standards. The largest area on the floor plan is dedicated to the Rock Lab where the test systems are located. Those test systems are discussed in Chapter 4.0 of this report. The remainder of the laboratory space is dedicated to petrographic and thermal studies along with facility support services; e.g., office space, drafting, mechanical/utility rooms, storage areas, and a Quality Assurance fireproof storage vault.

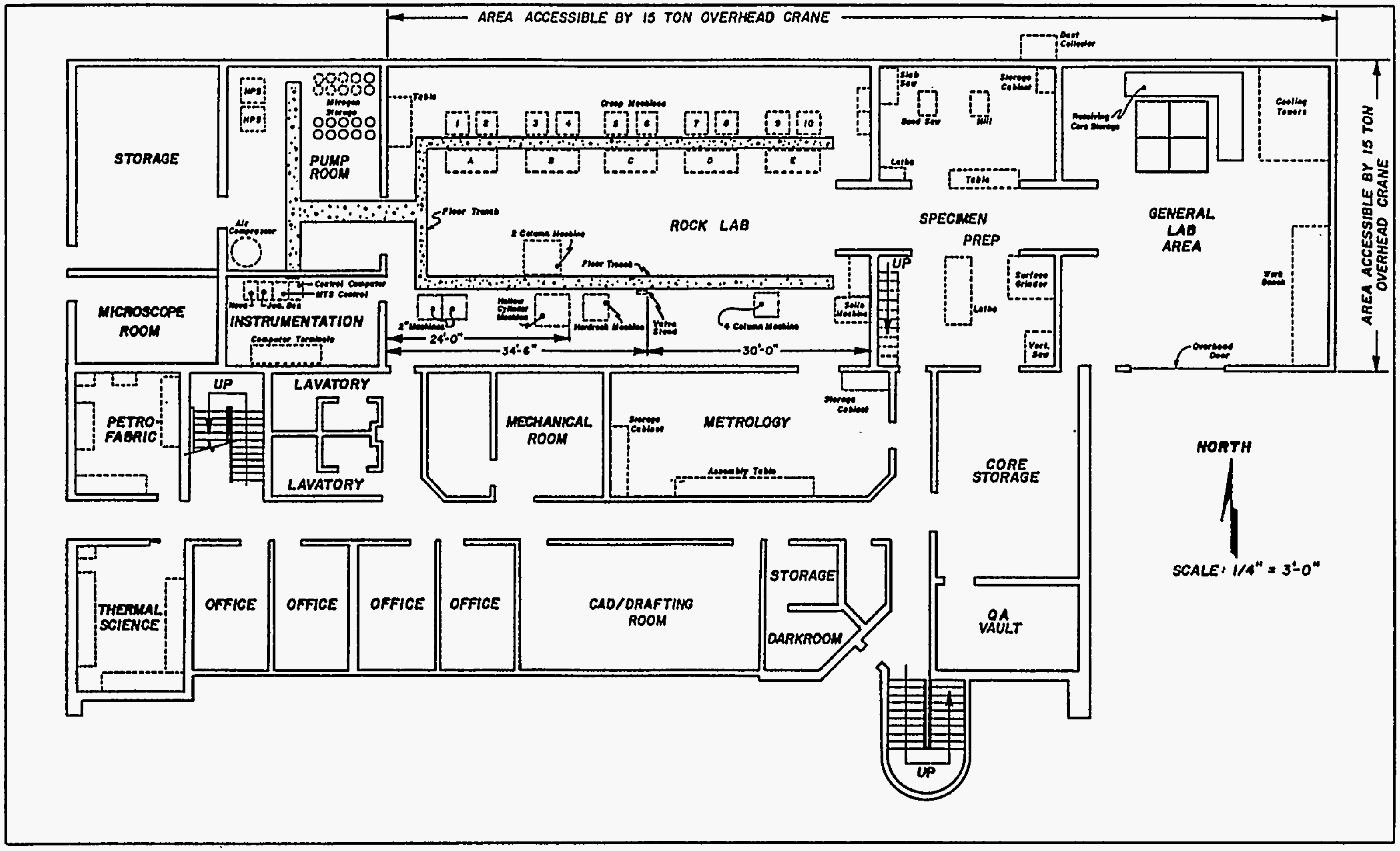

Figure 3-1. Floor Plan of Laboratory Facility in Rapid City, South Dakota.

4.0 TEST EQUIPMENT

4.1 TEST FRAMES

The mechanical test results contained in this report were generated using a variety of test frames available in the RE/SPEC laboratory. The laboratory supports 16 different test frames including 4 computer-controlled servohydraulic frames built by MTS Systems Inc. of Eden Prairie, Minnesota, 10 fully automated and computer-controlled static triaxial compression systems, and 2 manually operated static triaxial compression systems. The 2 manually operated machines and the 10 automated machines are custom systems. The configuration and use of any of the available test frames is well documented within the original reports listed in Table 1-1. The general details of those test frames used for the work in Table 1-1 are presented here for easy reference.

4.1.1 Static Triaxial Compression Machines

Twelve test frames are equipped with a system of accumulators and dilatometers for maintaining loads and pressures on the test specimens. These test frames are termed static systems and are usually used for constant stress (creep) tests on cylindrical specimens, but can be operated manually to effect a quasi-static, stress-rate controlled, triaxial compression test.

Two of the systems were originally designed and built by Dr. Wolfgang R. Wawersik at the University of Utah. The operation and capabilities of those two test frames were well documented (Wawersik, 1975; Dropek, 1976). Additional documentation is contained in the early reports listed in Table 1-1. These two frames are limited to testing 50-mm-diameter specimens.

The design for the two small systems served as a basis for Wawersik's subsequent design of a larger test frame (Wawersik, 1979). The new design allowed for specimens as large as 100 mm diameter and that design was adopted by RE/SPEC for construction of four similar machines. Shortly thereafter, six additional frames of the same design were procured as a custom order from the Instron Corporation of Canton, Massachusetts. Instron also equipped all ten of the larger systems with computerized data acquisition and process control for maintaining constant stress as inelastic deformations cause an increase in specimen area. A schematic drawing of the larger test system is given in Figure 4-1. Specific information on the ten larger test frames and the two smaller test frames is given in Table 4-1.

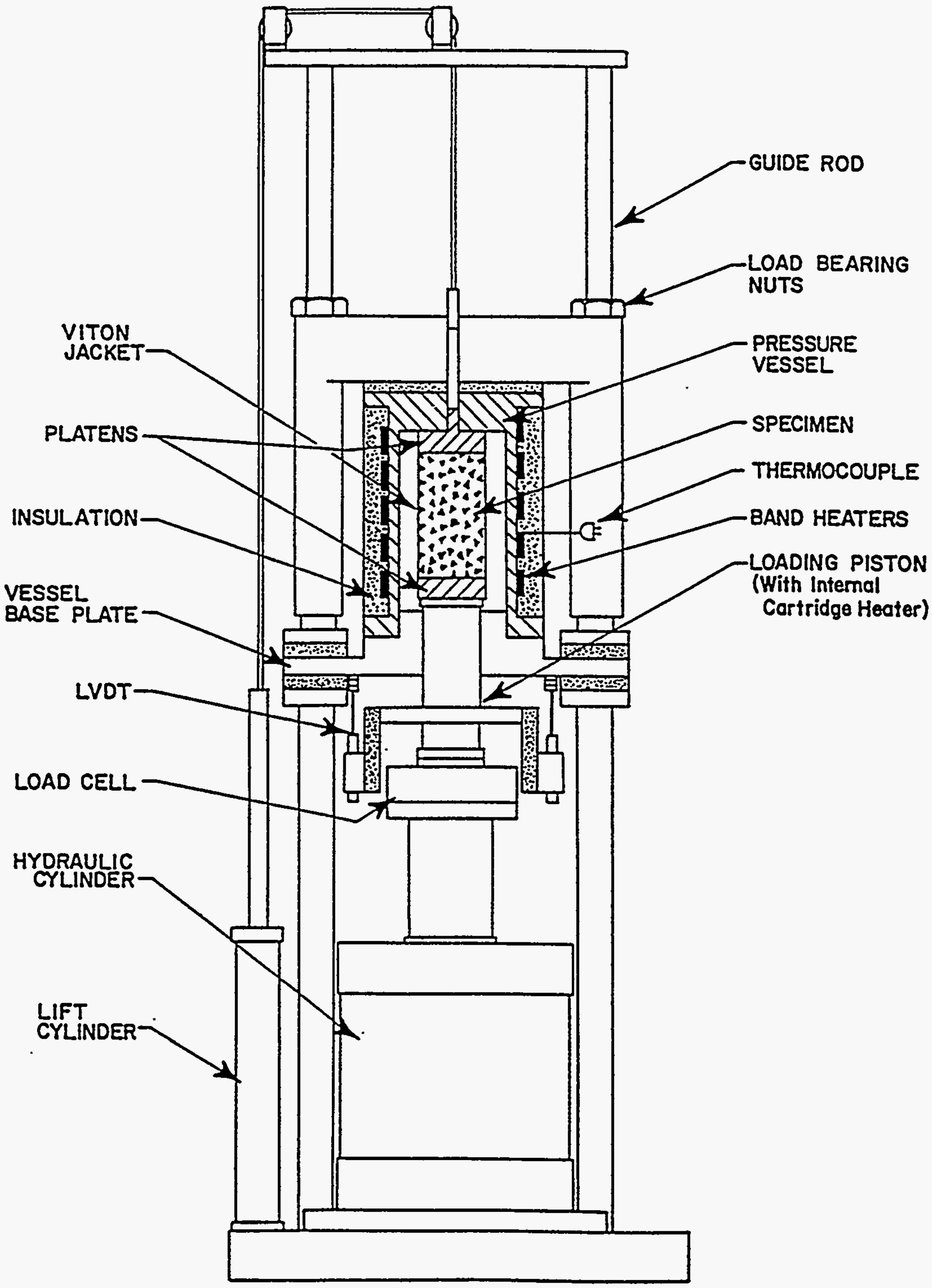

Figure 4-1. Schematic Diagram of a Static Triaxial Compression Test System.

4.1.2 Servohydraulic Test Frames

There are four servohydraulic test frames built by MTS Systems, Inc. All four systems are similar in that they include (1) a frame and load actuator that provides the reaction and axial force, respectively, (2) a control console that houses servoloop controllers and transducer signal conditioning, and (3) a computer that provides software control and data acquisition. Only two of the four servohydraulic test systems were used and specific information on those two test frames is given in Table 4-2.

Table 4-1. Static Triaxial Compression Test Frames

Test System Name	Capabilities			
	Axial Force (MN)	Specimen Temperature (°C)	Confining Pressure (MPa)	Specimen Diameter (mm)
Instron 1	1.5	200	70	100
Instron 2	1.5	200	70	100
Instron 3	1.5	200	70	100
Instron 4	1.5	200	70	100
Instron 5	1.5	200	70	100
Instron 6	1.5	200	70	100
Instron 7	1.5	200	70	100
Instron 8	1.5	200	70	100
Instron 9	1.5	200	70	100
Instron 10	1.5	200	70	100
WRW 1	0.27	200	70	50
WRW 2	0.54	200	70	50

Table 4-2. Servohydraulic Test Frames

Test System Name[a]	MTS Model Number	Capabilities			
		Axial Force (MN)	Specimen Temperature (°C)	Confining Pressure (MPa)	Pore Pressure (MPa)
UTS2	312.41	0.5	300	70	70
HCS	315.03	3.4	200	35	–

[a] UTS2 = Two-column universal frame with movable crosshead.
HCS = High stiffness frame with fixed crosshead (hollow cylinder configuration).

The UTS2 machine is used routinely for uniaxial and triaxial compression tests at both room and elevated temperature. A schematic drawing of this style of machine is given in Figure 4-2. This machine can be equipped with either a pressure vessel for triaxial compression testing or an environmental chamber for testing at elevated temperatures.

The HCS machine is a custom designed system equipped with an annular pressure vessel designed for testing thin-walled cylindrical specimens. The HCS machine has three independent axes of servocontrol; one for axial load, one for internal pressure, and one for external pressure. This configuration allows each of the three principal stresses to be uniquely specified.

4.2 INSTRUMENTATION/DATA ACQUISITION

The test systems used to conduct the experiments described in the reports listed in Table 1-1 were instrumented to measure specimen response under controlled test conditions. Typical physical quantities that were measured during testing were time, force, pressure, displacement, and temperature. The instrumentation and data acquisition methods that were used varied depending upon which test system was used and also the state of the art in electronics at the time the test was run.

4.2.1 Static Triaxial Compression Machines

The first test systems in use at RE/SPEC were the static loading frames. These frames were designed primarily to perform creep tests, but they could also be used to perform slow loading (quasi-static) stress-rate-controlled triaxial compression tests. Their primary instrumentation systems are comprised of two Linear Variable Differential Transformers (LVDTs) for measuring axial displacement, a dilatometer capable of measuring volume changes at constant confining pressure, a load cell for measuring total axial force, in-line pressure transducers for measurements of confining pressure (and sometimes pore pressure), a thermocouple for temperature measurement, and some type of clocking device to record elapsed time.

The two diametrically opposed LVDTs were mounted so their average signal output represented the displacement of the axial force generation ram relative to the fixed pressure vessel containing the specimen. When this relative displacement measurement was corrected for nonspecimen deformations (e.g., compression of the steel ram and platens), the net change in displacement represented the axial deformation of the specimen. The dilatometer was a screw-driven intensifier in which the screw rotation could be measured to determine the volume of oil that had to be extracted from the test vessel to maintain a constant pressure. This volumetric measurement was corrected for temperature changes in the oil and intrusion of the axial force ram to obtain the net volume change of the specimen.

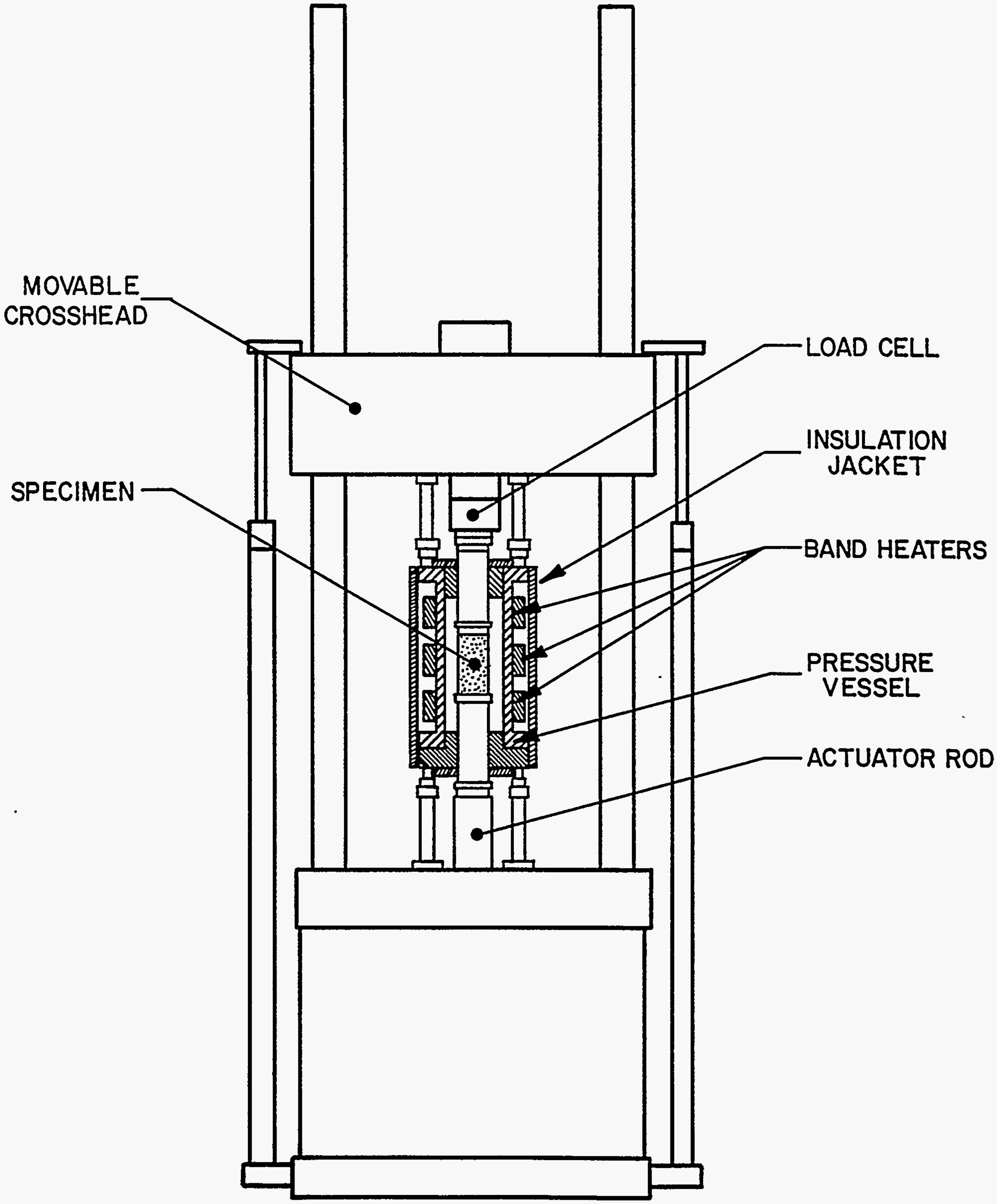

Figure 4-2. Schematic Diagram of a Universal Test System.

A strain-gage-based load cell was placed between the axial loading ram and test vessel loading column to measure the total axial force applied to the system. When the forces required to react against the confining pressure were subtracted from the total force measurement, the net axial force on the specimen could be determined. Pressure transducers were used in the lines leading to the test vessel to monitor confining pressure. Embedded in the wall of the test vessel was a thermocouple used to record system temperature.

During the early years of the laboratory, the transducer signal conditioning was provided by individual electronic units whose high-level signal outputs were fed to a single master display. The display module could feed data at predetermined intervals to a paper tape printer where data values were recorded for later processing. The resolution of the system was limited to that provided by the 4½ digit display meter. With the procurement of new test machines from the Instron Corporation, new data acquisition electronics became available. The new system used board-level signal conditioning and the high-level signal outputs were fed to individual channels on an analog-to-digital (A/D) conversion board. The A/D board was embedded in a Digital Equipment Corporation (DEC) computer system with an LSI 11/23 microprocessor platform. Custom software purchased with the system allowed 14-bit resolution of the data signals through the A/D boards and automated scanning of all data channels.

4.2.2 Servohydraulic Test Frames

The two servohydraulic test machines were used for programmable load path testing which primarily consisted of quasi-static triaxial compression, hydrostatic compression, and multiaxial creep tests. They both use a DEC microprocessor that allows computer control of both test conditions and data acquisition. The data acquisition is performed by a 14-bit A/D board that is fed signal voltages from electronic signal conditioner modules that service individual transducers.

The specimen deformation measurement techniques are similar on both machines in that while indirect measurements (like those made on the static machines) are possible, the primary method of measuring specimen deformations uses direct-contact extensometers. This type of instrumentation can be placed directly on the specimen, even when the specimen is contained within a pressurized and heated test vessel. A typical direct-contact extensometer mounting configuration used on the UTS2 machine is shown in Figure 4-3. The axial extensometer measures axial specimen deformation over the prescribed gage length; the circumferential extensometer effectively measures the change in specimen diameter. The circumferential extensometer is mounted at the ends of a roller-link chain wrapped around the mid-height of the specimen. In some configurations, the circumferential extensometer is replaced by a diametral gage. A diametral gage comprises a strain-gaged ring attached to two vertical posts that hold mounting pins which contact opposite ends of a diameter through the mid-height of the specimen. The diametral gage thus measures the change in specimen diameter along a horizontal axis whereas the circumferential gage measures the average change in specimen diameter.

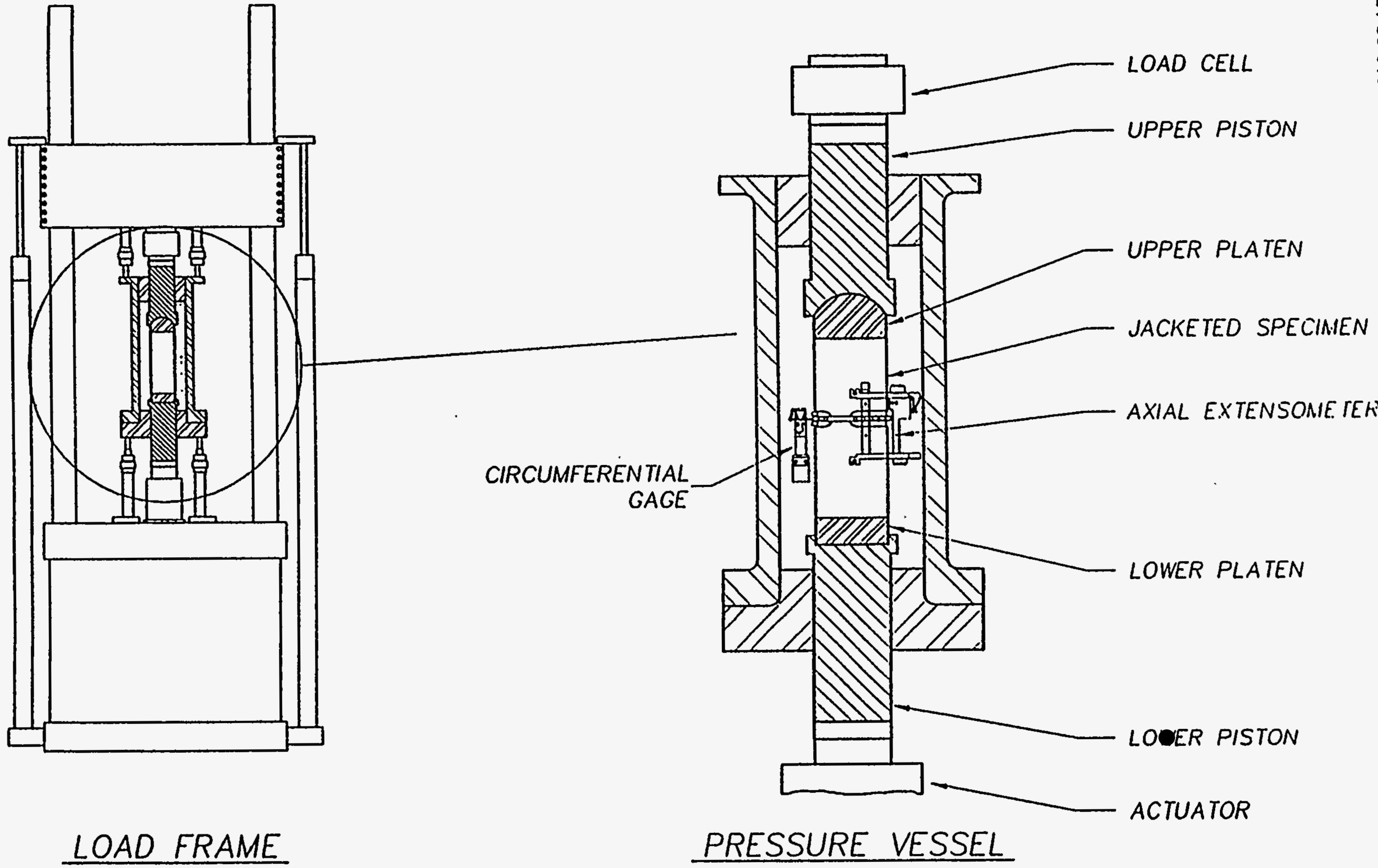

Figure 4-3. Direct-Contact Extensometers.

The specialized test system used for testing hollow cylinders was equipped with a unique configuration of extensometers that were capable of measuring the changes in inner and outer diameters of the specimen. This was accomplished by mounting four extensometers at 90° intervals on a ring that was spring loaded to hold it in place against the specimen. The four extensometers then provide four measurements of the distance from the specimen wall to the fixed diameter ring and those four measurements could be averaged. Two such rings were used; one for the inside of the specimen and one for the outside.

The UTS2 universal test system has a movable crosshead with an attached strain-gaged load cell that measures the total axial force applied to the test column. This approach is similar to the static load frames in that the force required to react against the confining pressure within the test vessel must be subtracted from the load cell measurement to obtain the net axial force applied to the specimen. The HCS system (used for testing of hollow cylinders) does not have a load cell at all. Rather, it uses a differential pressure transducer to measure the pressure difference between the chambers above and below the axial force actuator. This difference is linearly related to the level of total axial force and can be calibrated to read in units of force. Again, the reactive force necessary to support the pressures within the annular pressure vessel must be subtracted from the total to obtain the net axial force on the specimen.

In both systems, standard pressure transducers are connected in the lines leading from the servohydraulic pressure control intensifiers to the pressure vessel to monitor the confining pressures applied to the specimen. Again, thermocouples are used to track the system temperatures and the computer system provides a clocking device to record the elapsed time during the test.

The acoustic data generated in two of the reports required specialized equipment in addition to the standard capabilities available with a servohydraulic test frame. The additional equipment was an ultrasonic velocity measurement system that included two pairs of compressional wave velocity transducers, a switching box, a pulser/receiver, a preamplifier with power supply, and a digital oscilloscope. One set of velocity transducers was mounted in the platens above and below the specimen for measurements parallel to the specimen axis, and a second set of transducers was held by springs against the sides of the specimen for measurements perpendicular to the axis. During measurement, a main pulse was sent to one of the pulsing transducers at the same time a trigger pulse was sent to the oscilloscope. The main pulse traveled through the specimen to the receiving transducer and the oscilloscope recorded both the pulsing signal waveform and the receiving signal waveform. The two recorded waveforms were then analyzed to determine arrival times and amplitudes.

5.0 TEST PROCEDURES

5.1 QUASI-STATIC

One of the common types of mechanical test is the quasi-static triaxial compression test. Initially, this type of test was run using the static frames to impose a constant stress rate by manually incrementing the axial load at prescribed intervals of time. Later, with the advent of servohydraulic test systems, this type of test was usually run as a constant strain rate test using the axial strain measurement as feedback to the control loop.

The generalized procedure used for running the quasi-static tests required placing a cylindrical specimen between two metal platens and then encasing the assembly in an elastomer protective sleeve (or jacket). This test assembly was placed in a pressure vessel and subjected to a constant confining pressure. If the test was to be performed at elevated temperatures, the whole assembly was heated to the desired temperature and allowed to stabilize for several hours. The heating was applied at a low rate and while the specimen was under pressure to avoid thermal cracking of the specimen. The axial force was then increased in either of two modes, constant stress rate or constant strain rate, until the specimen failed or some other limiting condition was reached. An excursion in the loading was allowed whereby the axial loading could be reversed and then reapplied to create an unload/reload sequence.

The measured mechanical data generally were recorded as values of force, pressure, and displacement. Data reduction involved using the recorded data with knowledge of initial specimen geometry to convert the measurements into values of principal stresses and strains. The calculation of axial strain was straightforward. The measurement of the net change in specimen length was used to calculate a true (or logarithmic) axial strain. The measurement of net change in specimen diameter was used to calculate a true lateral strain under the assumption that the deformed shape of the specimen remained as a right circular cylinder. The axial stress was calculated using the measurement of net axial force on the specimen and the current area of the deformed specimen. This calculation gave a Cauchy stress measure for axial stress. The radial stress component was simply the value of the measured confining pressure.

5.2 CREEP

The scope of many of the test programs involved performance of the triaxial compression creep test. This type of test required application of constant stress states over long periods of time and the static load frames were designed specifically for this purpose.

The generalized procedure used for performing the creep tests required placing a cylindrical specimen between two metal platens and then encasing the assembly in an elastomer protective sleeve (or jacket). This test assembly was placed in a pressure vessel and subjected to a constant confining pressure. If the test was to be performed at elevated temperatures, the whole assembly was heated to the desired temperature and allowed to stabilize for several hours. The heating was applied at a low rate and while the specimen was under pressure to avoid thermal cracking of the specimen. The axial force was then increased while holding the confining pressure constant until the desired axial stress difference was imposed. This static stress state was then maintained over long periods of time while recording the inelastic deformation of the specimen. The maintenance of a constant axial stress required that the axial force on the system be periodically adjusted to compensate for measured changes in specimen diameter. On the ten Instron frames, this adjustment was performed automatically under computer control.

Most of the creep tests were performed as single-stage tests; that is, the specimen strains were allowed to accumulate at a fixed stress state for some time and then the stress was removed and the test was complete. In contrast, some of the creep tests were run using a multistage load path whereby the stress state or temperature was changed at specified times. Thus, the stages subsequent to the initial loading stage could be viewed as individual creep tests; but they each might have a unique strain history depending upon the deformations that occurred in prior stages.

The measured mechanical data generally were recorded as values of force, pressure, and displacement. Data reduction involved using the recorded data with knowledge of initial specimen geometry to convert the measurements into values of principal stresses and strains. The calculation of axial strain was straightforward. The measurement of the net change in specimen length was used to calculate a true (or logarithmic) axial strain. The measurement of net change in specimen diameter was used to calculate a true lateral strain under the assumption that the deformed shape of the specimen remained as a right circular cylinder. The net change in specimen diameter was deduced from an algorithm that used the volumetric measurement provided by the dilatometer and the axial displacement measurement (Dropek, 1976). The axial stress was calculated using the measurement of net axial force on the specimen and the current area of the deformed specimen. This calculation gave a Cauchy stress measure for axial stress. The radial stress component was simply the value of the measured confining pressure.

5.3 MULTIAXIAL (HOLLOW CYLINDER)

The multiaxial tests used thin-walled hollow cylinders of salt that were jacketed with elastomer tubes both inside and outside. After assembly into an annular pressure vessel, three independent servocontrol systems were activated to control the pressure applied to the outside surface of the specimen, the pressure applied to the inside surface of the specimen, and the axial force imposed on the specimen. The three controlled loads (outer pressure, inner pressure, and axial force) were ramped up under computer control to a desired hydrostatic stress state. At the operator's command, a computer program would then quickly ramp all three controlled variables along a proportional stress path to apply the desired shear stresses while maintaining a constant mean stress and Lode angle. Once the desired level of shear stress was applied, that level was then maintained constant for long periods of time as prescribed for a creep test.

The measured mechanical data generally were recorded as values of force, pressure, and displacement. Data reduction involved using the recorded data with knowledge of initial specimen geometry to convert the measurements into values of principal stresses and strains. The calculation of axial strain was straightforward. The measurement of the net change in specimen length was used to calculate a true (or logarithmic) axial strain. The measurements of net change in the inner and outer specimen diameters were used to calculate the true circumferential and radial strains. The circumferential strain was calculated using the change in average specimen diameter. The radial strain was calculated using the change in the thickness of the thin specimen wall. The axial stress was calculated using the measurement of net axial force on the specimen and the current annular area of the specimen. The radial and circumferential principal stresses were calculated from the measurements of internal and external pressure. The radial stress was assumed to resist changes in wall thickness and was calculated as the sum of the radial stresses at the middle of the wall required to equilibrate the inner pressure acting on the inner wall and the outer pressure acting on the outer wall. The circumferential stress was assumed to resist changes in average specimen diameter and was calculated as the stress acting over the wall thickness to balance the difference between the forces of the outer pressure acting on the outer wall and the inner pressure acting on the inner wall.

5.4 DAMAGE RECOVERY

The intent of the damage recovery tests was to investigate the introduction of damage and damage recovery in intact WIPP specimens. Damage was introduced during a standard constant strain rate test performed at low confining pressure. Subsequently, the damaged specimen was subjected to hydrostatic pressurization at either room or elevated temperatures. During both the damage and damage recovery phases, the ultrasonic compressional waves were monitored along with the corresponding axial and lateral specimen strains. During data analysis, the ultrasonic data was correlated to the levels of specimen strain (damage).

6.0 CALIBRATION/VERIFICATION PROCESSES

6.1 CALIBRATION

The general approach to calibration followed the guidelines set forth in a national Performance Test Code on Measurement Uncertainty (ANSI/ASME, 1985). That test code suggests that insofar as possible, "the calibration process should include a reasonable simulation of instrument test-like conditions." Following this guideline, the transducers on the test systems were calibrated by bringing reference calibration standards to the test system rather than taking the transducers to a calibration facility.

During a typical calibration, transducers were connected in their normal orientations on the test system and their outputs were recorded through an analog-to-digital converter at the data collection computer. A typical calibration consisted of applying 20 known standard inputs to the transducer and reading the corresponding transducer outputs at the data collection point. The correlation between the transducer outputs and known standard inputs provided the sensitivity and offset for that transducer. Standard inputs were provided by standards that were traceable to the U.S. National Institute for Standards and Technology (formerly National Bureau of Standards).

The calibration constants determined for each transducer were periodically checked by verifying them against the standards. This was usually done during the interval available between the termination of one test and the initiation of the next test. This transducer verification provided a check on anomalies that could arise in the data acquisition process (e.g., transducer drift, power supply fluctuations, wire breaks, etc.).

In addition to the transducer calibrations, system calibrations were also performed. System calibrations are those correction factors used to account for changes in the transducer output that are unrelated to specimen behavior. For example, when axial specimen deformation is measured with extensometers that are connected between a loading ram and a fixed point on a test vessel, a portion of the displacement reading represents deformation of the test system and not deformation of the specimen. This is often referred to as the "machine softness" component of the reading. Calibration factors that account for machine softness were determined and used when reducing axial deformation data. Other typical system calibration factors that were determined to account for such biases included (1) the temperature gradient between the thermocouple location and the midpoint of the specimen, (2) temperature corrections on dilatometer volume measurements, (3) pressure and temperature effects on transducers subjected to hostile environments, (4) delay times for acoustic transducers, and (5) the influence of the protective jackets used when performing triaxial compression tests. The specific details of these types of system calibrations are too extensive to be presented here, but they are contained in the individual reports listed in Table 1-1.

6.2 VERIFICATION

After all calibration constants have been determined, there is still a need to verify (or validate) that the test system is responding as expected. A typical verification technique involved testing a specimen fabricated from material with known properties, like steel and aluminum, and checking the test result to verify that the expected response was observed. This common technique of verification was often carried out just prior to starting production testing on the rock samples and was reported in the final results, if appropriate.

Another method of verifying proper system operation was to test a specimen of rock that had been previously characterized, either by RE/SPEC or perhaps some other agency. The test results could be compared to the previously published results to gain confidence that the test system was operating properly. Again, such comparative verification exercises were reported in the final results, if appropriate.

7.0 DATA

This chapter comprises the bulk of this report and holds the compilation of data from the various sources listed in the introduction. This chapter is organized into four sections, each of which presents data for a particular type of test. The four test types are (1) quasi-static triaxial compression, (2) constant stress (creep), (3) multiaxial, and (4) damage recovery. Moreover, the section on creep data is further organized as to source of specimens. The creep data results are presented separately for specimens that came from boreholes in the vicinity of the WIPP and specimens that came directly from the WIPP mine workings.

7.1 QUASI-STATIC TRIAXIAL COMPRESSION

Within this subsection, two tables have been included that summarize the complete work performed and documented in the reports for borehole specimens. The first table represents the matrix of tests that were performed and the second table presents a summary of the test results. All of the specimens used for quasi-static triaxial compression tests came from the boreholes AEC7 and ERDA9 drilled in the vicinity of the WIPP.

A text matrix is given in Table 7-1. The source where the data were originally reported is indicated in the table. The first column in the table is the specimen identification label that was assigned in the original report. The next two columns are the original nominal diameter of the specimen and the specimen's length-to-diameter ratio. The nominal test conditions are given in columns four through six as specimen temperature, confining pressure, and axial stress difference loading rate, respectively.

Each test listed in a test matrix produced a result generated from an analysis of the data. The various test results are summarized for borehole specimens in Table 7-2 along with comments on the tests.

Plots have been created to present the salient features of each test listed in Table 7-1 to demonstrate control of desired test conditions and observations of the resulting specimen behavior. Thus, data plots consist of curves tracing the control variables as a function of time and also plots of stress versus strain. These plots can be found in Appendix A.

7.2 CONSTANT STRESS (CREEP)

Within each of the following two subsections (one for borehole specimens and one for specimens from the mine workings), two tables have been included that summarize the complete work performed and documented in the reports. The first table represents the matrix of tests that were performed, and the second table presents a summary of the test results. In all the tables, the source references are given in subheadings to indicate where the data were originally reported. The sign convention in the tables is that compression is positive.

Table 7-1. Quasi-Static Test Matrix for Borehole Specimens

Specimen I.D.	Nominal Dimensions[a]		Specimen Temperature (°C)	σ_3 (MPa)	Load Rate
	D (mm)	L:D			$\Delta\dot{\sigma}$ (MPa/min)
Following Data From SAND79-7045					
AEC7-1953 (Test RQ-1)	50	2	28	3.45	0.21
AEC7-1954 (B) (Test RQ-2)	50	2	100	13.8	0.14
AEC7-2721.5 (A) (Test RQ-3)	50	2	28	3.45	0.14
AEC7-2721.5 (B) (Test RQ-4)	50	2	28	13.8	0.12

(a) D = diameter
L:D = length-to-diameter ratio.

Table 7-2. Quasi-Static Test Results for Borehole Specimens

Specimen I.D.	$\Delta\sigma_{max}$ (MPa)	ε_1^{max}	E (GPa)	ν	Comments
Following Data From SAND79-7045					
AEC7-1953 (Test RQ-1)	39	0.0644	3.0	0.46	The maximum stress and strain values are not ultimate values. Loading was terminated at machine limits. The elastic parameters were not determined from an unload/reload cycle. They are an integrated modulus calculated over the initial 1 percent of axial strain.
AEC7-1954 (B) (Test RQ-2)	26	0.0769	2.0	0.37	
AEC7-2721.5 (A) (Test RQ-3)	36	0.0619	1.4	0.26	
AEC7-2721.5 (B) (Test RQ-4)	40	0.0765	2.5	0.29	

7.2.1 Boreholes

A composite text matrix for the tests on specimens from boreholes is given in Table 7-3. The first column in the table identifies the specimen as it was identified in the original report. The second column is the stage of loading for that specimen. The next column designates the load path for that portion of the test where the designation "A" means application of the load and "C" means the constant stress portion of the test. The nominal test conditions are given in columns four through six and column seven is the test duration. The durations are given in units of seconds (s), minutes (m), or days (d).

The test results for the specimens listed in the test matrix are summarized in Table 7-4. Included as a test result in Table 7-4 are the increments of strain induced in the specimen during the application of an axial stress difference to initiate the creep test and during the creep portion of the test. The sign convention on the strain values is that compression is positive. Also included in Table 7-4 are test comments that may reflect unusual specimen behavior, aberrations in test control, or some other special characteristic of that test that deserves consideration.

Plots have been created to present the salient features of each test to demonstrate control of desired test conditions and observations of the resulting specimen behavior. Thus, typical plots consist of curves tracing the control variables as a function of time and also plots of strain versus time. Most of the tests were initiated by applying the axial stress difference at a relatively slow rate. For these tests, plots are included that present the test conditions as a function of time during the load application. Also included are plots of the stress versus strain response for the load application. All plots can be found in Appendix B where the sign convention is that compression is positive.

7.2.2 WIPP Mine Workings

A composite text matrix for the tests on specimens from the WIPP mine workings is given in Table 7-5. The first column in the table identifies the specimen as it was identified in the original report. The second column is the stage of loading for that specimen. The next column designates the load path for that portion of the test where the designation "A" means application of the load and "C" means the constant stress portion of the test. The nominal test conditions are given in columns four through six and column seven is the test duration. The durations are given in units of seconds (s), minutes (m), or days (d).

The test results for the specimens listed in the test matrix are summarized in Table 7-6. Included as a test result in Table 7-6 are the increments of strain induced in the specimen during the initial application of an axial stress difference to initiate the creep test and during the creep portion of the test. The sign convention on the strain values is that compression is positive. Also included in Table 7-6 are test comments that may reflect unusual specimen behavior, aberrations in test control, or some other special characteristic of that test that deserves consideration.

Table 7-3. Constant Stress (Creep) Test Matrix for Borehole Specimens (Page 1 of 6)

Specimen I.D.	Stage	Load Path[a]	Temperature (°C)	$\sigma_1 - \sigma_3$ (MPa)	σ_3 (MPa)	Test Duration[b]
Following Data From SAND89-7098 (Nominal Specimen Diameter = 100 mm and L:D = 2)						
ERDA9/88/2127-0/1 (Test I.D. 2127)	1	A	25	0–10	15	<30 s
		C	25	10	15	337 d
ERDA9/88/2124-0/1 (Test I.D. 2124)	1	A	22	0–11.7	20.7	<30 s
		C	22	11.7	20.7	216 d
ERDA9/88/2126-0/1 (Test I.D. 2126)	1	A	25	0–15	15	<30 s
		C	25	15	15	244 d
Following Data From SAND80-7114 (Nominal Specimen Diameter = 50 mm and L:D = 2)						
SLA/79/1/2 (Test I.D. 1)	1	A	24	0–10.3	0	15 m
		C	24	10.3	0	8.9 d
SLA/79/4A/2 (Test I.D. 1R)	1	A	24	0–10.3	0	15 m
		C	24	10.3	0	26.9 d
	2	A	24-70	10.3	0	44 m
		C	70	10.3	0	14.9 d
SLA/79/18C/1 (Test I.D. 2)	1	A	24	0–20.7	17.2	30 m
		C	24	20.7	17.2	61.8 d

Table 7-3. Constant Stress (Creep) Test Matrix for Borehole Specimens (Page 2 of 6)

Specimen I.D.	Stage	Load Path[a]	Temperature (°C)	$\sigma_1 - \sigma_3$ (MPa)	σ_3 (MPa)	Test Duration[b]
SLA/79/19A/2 (Test I.D. 3)	1	A	24	0–20.7	3.5	30 m
		C	24	20.7	3.5	41.8 d
SLA/79/11/2 (Test I.D. 4)	1	A	24	0–10.3	20.7	15 m
		C	24	10.3	20.7	8.8 d
SLA/79/1/1 (Test I.D. 4R)	1	A	24	0–10.3	20.7	15 m
		C	24	10.3	20.7	60.9 d
	2	A	24–100	10.3	20.7	56 m
		C	100	10.3	20.7	20.2 d
SLA/79/15A/2 (Test I.D. 5)	1	A	70	0–10.3	20.7	15 m
		C	70	10.3	20.7	44.9 d
SLA/79/19A/1 (Test I.D. 6)	1	A	100	0–10.3	20.7	15 m
		C	100	10.3	20.7	48.9 d
SLA/79/15A/1 (Test I.D. 7)	1	A	200	0–10.3	20.7	15 m
		C	200	10.3	20.7	1.0 d
SLA/79/18B/2 (Test I.D. 8)	1	A	200	0–5.5	0	8 m
		C	200	5.5	0	10.9 d
SLA/79/18C/2 (Test I.D. 9)	1	A	200	0–5.5	3.4	8 m
		C	200	5.5	3.4	19.0 d

Table 7-3. Constant Stress (Creep) Test Matrix for Borehole Specimens (Page 3 of 6)

Specimen I.D.	Stage	Load Path[a]	Temperature (°C)	$\sigma_1 - \sigma_3$ (MPa)	σ_3 (MPa)	Test Duration[b]
SLA/79/20/2 (Test I.D. 10)	1	A	200	0–5.5	20.7	8 m
		C	200	5.5	20.7	20.1 d
SLA/79/20/1 (Test I.D. 11)	1	A	70	0–20.7	17.2	30 m
		C	70	20.7	17.2	29.8 d
SLA/79/18B/1 (Test I.D. 12)	1	A	70	0–5.5	20.7	8 m
		C	70	5.5	20.7	14.0 d
SLA/79/14B/1 (Test I.D. 12R)	1	A	70	0–5.5	20.7	8 m
		C	70	5.5	20.7	37.8 d
Following Data From SAND79-7030 (Nominal Specimen Diameter = 50 mm and L:D = 2)						
ERDA9-2668.5 (A) (Test I.D. 1)	1	A	24	0–10.3	0	12 m
		C	24	10.3	0	5.1 d
ERDA9-2668.5 (A) (Test I.D. 1A)	1	A	24	0–10.3	0	13 m
		C	24	10.3	0	15 d
ERDA9-2668.5 (B) (Test I.D. 2)	1	A	70	0–10.3	0	15 m
		C	70	10.3	0	21 d
ERDA9-2662.0 (Test I.D. 3)	1	A	100	0–10.3	0	15 m
		C	100	10.3	0	21 d
ERDA9-2678.0 (A) (Test I.D. 4)	1	A	24	0–20.7	0	11 m
		C	24	20.7	0	0.2 d

Table 7-3. Constant Stress (Creep) Test Matrix for Borehole Specimens (Page 4 of 6)

Specimen I.D.	Stage	Load Path[a]	Temperature (°C)	$\sigma_1 - \sigma_3$ (MPa)	σ_3 (MPa)	Test Duration[b]
ERDA9-2674.5 (A) (Test I.D. 5)	1	A	24	0–20.7	17.2	40 m
		C	24	20.7	17.2	15 d
ERDA9-2674.5 (B) (Test I.D. 6)	1	A	70	0–20.7	17.2	19 m
		C	70	20.7	17.2	6.7 d
ERDA9-2679.0 (B) (Test I.D. 7)	1	A	100	0–20.7	17.2	31 m
		C	100	20.7	17.2	1.8 d
ERDA9-2605.0 (B) (Test I.D. 8)	1	A	100	0–10.3	20.7	15 m
		C	100	10.3	20.7	15.1 d
ERDA9-2678.0 (B) (Test I.D. 9)	1	A	24	0–10.3	0	7 m
		C	24	10.3	0	6.8 d
	2	A	24	10.3–20.7	0	15 m
		C	24	20.7	0	15 m
ERDA9-2606.0 (B) (Test I.D. 10)	1	A	24	0–10.3	17.2	15 m
		C	24	10.3	17.2	7.1 d
	2	A	24	10.3–20.7	17.2	15 m
		C	24	20.7	17.2	7.9 d
ERDA9-2679.0 (A) (Test I.D. 11)	1	A	100	0–10.3	0	15 m
		C	100	10.3	0	5.2 d
	2	A	100	10.3–20.7	0	21 m
		C	100	20.7	0	0 d

Table 7-3. Constant Stress (Creep) Test Matrix for Borehole Specimens (Page 5 of 6)

Specimen I.D.	Stage	Load Path[a]	Temperature (°C)	$\sigma_1 - \sigma_3$ (MPa)	σ_3 (MPa)	Test Duration[b]
ERDA9-2678.3 (B) (Test I.D. 12)	1	A	100	0–10.3	17.2	15 m
		C	100	10.3	17.2	5.7 d
	1	A	100	10.3–20.7	17.2	15 m
		C	100	20.7	17.2	0.5 d
ERDA9-2605.5 (B) (Test I.D. 13)	1	A	24	0–31	13.8	45 m
		C	24	31	13.8	10.9 d
ERDA9-2678.7 (B) (Test I.D. 14)	1	A	24	0–41.4	10.3	60 m
		C	24	41.4	10.3	3.7 d
Following Data From SAND79-7045 (Nominal Specimen Diameter = 50 mm and L:D = 2)						
AEC7-2729 (Test I.D. RC-1)	1	A	28	0–10.3	3.45	28 m
		C	28	10.3	3.45	9.7 d
	2	A	28	10.3–20.7	3.45	9 m
		C	28	20.7	3.45	5.2 d
	3	A	28	20.7–31.0	3.45	7 m
		C	28	31.0	3.45	4.7 d
AEC7-2715 (B) (Test I.D. RC-2)	1	A	100	0–10.3	3.45	18 m
		C	100	10.3	3.45	9.9 d
	2	A	100	10.3–20.7	3.45	18 m
		C	100	20.7	3.45	5.1 d

Table 7-3. Constant Stress (Creep) Test Matrix for Borehole Specimens (Page 6 of 6)

Specimen I.D.	Stage	Load Path[a]	Temperature (°C)	$\sigma_1 - \sigma_3$ (MPa)	σ_3 (MPa)	Test Duration[b]
AEC7-2715 (A) (Test I.D. RC-3)	1	A	28	0–10.3	13.8	9 m
		C	28	10.3	13.8	8.9 d
	2	A	28	10.3–20.7	13.8	5 m
		C	28	20.7	13.8	4.9 d
	3	A	28	0–31	13.8	7 m
		C	28	31	13.8	4.9 d
AEC7-2711 (A) (Test I.D. RC-4)	1	A	29	0–20.7	13.8	29 m
		C	29	20.7	13.8	12.2 d
	2	A	29	20.7–31.0	13.8	5 m
		C	29	31.0	13.8	5.8 d
AEC7-2711 (B) (Test I.D. RC-5)	1	A	100	0–10.3	13.8	11 m
		C	100	10.3	13.8	10.9 d
	2	A	100	10.3–20.7	13.8	16 m
		C	100	20.7	13.8	4.7 d
AEC7-2715.5 (Test I.D. RC-6)	1	A	100	0–20.7	13.8	16 m
		C	100	20.7	13.8	4.7 d

(a) A = application load-up to initiate creep test
C = constant stress (creep) portion of test.

(b) s = seconds
m = minutes
d = days.

Table 7-4. Constant Stress (Creep) Test Results for Borehole Specimens (Page 1 of 6)

Specimen I.D.	Stage	Load Path[a]	Strain Increments, % ε_1	Strain Increments, % ε_3	Comments
Following Data From SAND89-7098 (Nominal Specimen Diameter = 100 mm and L:D = 2)					
ERDA9/88/2127-0/1 (Test I.D. 2127)	1	A	0.166	−0.083	
		C	0.317	−0.219	
ERDA9/88/2124-0/1 (Test I.D. 2124)	1	A	0.228	−0.102	
		C	0.698	−0.141	
ERDA9/88/2126-0/1 (Test I.D. 2126)	1	A	0.438	−0.118	
		C	2.399	−1.118	
Following Data From SAND80-7114 (Nominal Specimen Diameter = 50 mm and L:D = 2)					
SLA/79/1/2 (Test I.D. 1)	1	A	0.253	—	
		C	0.540	—	Data acquisition failure at ~9 days. Data prior to 9 days is valid.
SLA/79/4A/2 (Test I.D. 1R)	1	A	0.224	—	
		C	0.131	—	
	2	A	—	—	
		C	0.595	—	
SLA/79/18C/1 (Test I.D. 2)	1	A	0.752	−0.301	
		C	3.27	−1.58	

Table 7-4. Constant Stress (Creep) Test Results for Borehole Specimens (Page 2 of 6)

Specimen I.D.	Stage	Load Path[(a)]	Strain Increments, %		Comments
			ε_1	ε_3	
SLA/79/19A/2 (Test I.D. 3)	1	A	1.01	−0.431	
		C	5.22	−2.84	
SLA/79/11/2 (Test I.D. 4)	1	A	0.098	−0.028	Data acquisition failure at ~9 days. Poor lateral strain data. Possible leak in dilatometer system.
		C	0.325	–	
SLA/79/1/1 (Test I.D. 4R)	1	A	0.074	−0.025	
		C	0.298	−0.139	
	2	A	–	–	
		C	4.54	−2.28	
SLA/79/15A/2 (Test I.D. 5)	1	A	0.129	−0.052	
		C	1.28	−0.582	
SLA/79/19A/1 (Test I.D. 6)	1	A	0.150	−0.058	
		C	5.02	−2.57	
SLA/79/15A/1 (Test I.D. 7)	1	A	0.912	−0.436	
		C	24.6	−15.8	
SLA/79/18B/2 (Test I.D. 8)	1	A	0.181	–	
		C	10.8	–	
SLA/18C/2 (Test I.D. 9)	1	A	0.086	−0.022	
		C	18.7	−10.9	

Table 7-4. Constant Stress (Creep) Test Results for Borehole Specimens (Page 3 of 6)

Specimen I.D.	Stage	Load Path[(a)]	Strain Increments, % ε_1	Strain Increments, % ε_3	Comments
SLA/79/20/2 (Test I.D. 10)	1	A	0.066	−0.023	
		C	14.3	−8.50	
SLA/79/20/1 (Test I.D. 11)	1	A	1.04	−0.473	
		C	27.0	−16.6	
SLA/79/18B/1 (Test I.D. 12)	1	A	0.026	−0.021	
		C	0.081	0.557	
SLA/79/14B/1 (Test I.D. 12R)	1	A	0.016	−0.010	
		C	0.276	−0.032	
Following Data From SAND79-7030 (Nominal Specimen Diameter = 50 mm and L:D = 2)					
ERDA9-2668.5 (A) (Test I.D. 1)	1	A	0.34	–	
		C	0.47	–	Leak required unload at 5.1 days. Data is valid.
ERDA9-2668.5 (A) (Test I.D. 1A)	1	A	0.17	–	
		C	0.07	–	Test restarted and data appended to Test 1. Data was reported as Test 1.
ERDA9-2668.5 (B) (Test I.D. 2)	1	A	0.42	–	
		C	3.27	–	
ERDA9-2662.0 (Test I.D. 3)	1	A	0.81	–	
		C	10.9	–	
ERDA9-2678.0 (A) (Test I.D. 4)	1	A	1.45	–	
		C	2.75	–	Specimen ruptured.

Table 7-4. Constant Stress (Creep) Test Results for Borehole Specimens (Page 4 of 6)

Specimen I.D.	Stage	Load Path[a]	Strain Increments, %		Comments
			ε_1	ε_3	
ERDA9-2674.5 (A) (Test I.D. 5)	1	A	0.79	–0.29	
		C	4.11	–1.80	
ERDA9-2674.5 (B) (Test I.D. 6)	1	A	1.54	–0.70	
		C	43.0	–20.5	Specimen contacted vessel wall at 150 hours.
ERDA9-2679.0 (B) (Test I.D. 7)	1	A	1.18	–0.48	
		C	39.8	–28.4	Specimen contacted vessel wall at end of test.
ERDA9-2605.0 (B) (Test I.D. 8)	1	A	0.20	–0.09	
		C	6.55	–3.14	
ERDA9-2678.0 (B) (Test I.D. 9)	1	A	0.24	–	
		C	0.36	–	
	2	A	0.87	–	
		C	0.89	–	Specimen ruptured.
ERDA9-2606.0 (B) (Test I.D. 10)	1	A	0.12	–0.05	
		C	0.35	–0.22	
	2	A	0.51	–0.22	
		C	2.91	–1.43	
ERDA9-2679.0 (A) (Test I.D. 11)	1	A	0.61	–	
		C	7.82	–	
	2	A	6.97	–	Specimen contacted vessel wall.
		C	–	–	Never started.

Table 7-4. Constant Stress (Creep) Test Results for Borehole Specimens (Page 5 of 6)

Specimen I.D.	Stage	Load Path[a]	Strain Increments, %		Comments
			ε_1	ε_3	
ERDA9-2678.3 (B) (Test I.D. 12)	1	A	0.28	–0.11	
		C	5.27	–2.67	
	2	A	1.66	–0.82	
		C	20.5	–11.2	
ERDA9-2605.5 (B) (Test I.D. 13)	1	A	0.78	–0.26	
		C	12.2	–6.55	
ERDA9-2678.7 (B) (Test I.D. 14)	1	A	4.37	–2.11	
		C	22.8	–13.5	
Following Data From SAND79-7045 (Nominal Specimen Diameter = 50 mm and L:D = 2)					
AEC7-2729 (Test I.D. RC-1)	1	A	0.392	–0.104	
		C	0.509	–0.236	
	2	A	0.608	–0.311	
		C	2.73	–1.45	
	3	A	0.603	–0.302	
		C	7.14	–3.80	
AEC7-2715 (B) (Test I.D. RC-2)	1	A	0.585	–0.171	
		C	4.36	–1.19	
	2	A	1.32	–0.657	
		C	20.1	–10.5	

Table 7-4. Constant Stress (Creep) Test Results for Borehole Specimens (Page 6 of 6)

Specimen I.D.	Stage	Load Path[a]	Strain Increments, % ε_1	Strain Increments, % ε_3	Comments
AEC7-2715 (A) (Test I.D. RC-3)	1	A	0.148	–0.053	
		C	0.438	–0.156	
	2	A	0.396	–0.191	
		C	2.12	–0.854	
	3	A	0.492	–0.246	
		C	6.22	–3.05	
AEC7-2711 (A) (Test I.D. RC-4)	1	A	0.751	–0.314	
		C	3.16	–1.40	
	2	A	0.551	–0.276	
		C	6.81	–3.44	
AEC7-2711 (B) (Test I.D. RC-5)	1	A	0.178	–0.083	
		C	5.34	–2.37	
	2	A	1.40	–0.608	
		C	24.4	–13.8	
AEC7-2715.5 (Test I.D. RC-6)	1	A	2.25	–0.924	
		C	23.9	–12.9	

(a) A = application load-up to initiate creep test.
C = constant stress (creep) portion of test.

Table 7-5. Constant Stress (Creep) Test Matrix for Mine Workings Specimens (Page 1 of 6)

Specimen I.D.	Stage	Load Path[a]	Temperature (°C)	$\sigma_1 - \sigma_3$ (MPa)	σ_3 (MPa)	Test Duration[b]
Following Data From SAND92-7291 (Nominal Specimen Diameter = 100 mm and L:D = 2)						
C1X01-1/3-3/7-1	1	A	25	0–11.5	15	<30 s
		C	25	11.5	15	184 d
C1X01-1/3-3/1-1	1	A	25	0–15	15	<30 s
		C	25	15	15	461 d
C1X01-1/3-3/4-1	1	A	25	0–17	15	<30 s
		C	25	17	15	248 d
C1X01-1/3-3/2-1	1	A	25	0–21	15	< 30 s
		C	25	21	15	159 d
C1X01-1/3-3/6-1	1	A	100	0–3.5	15	< 30 s
		C	100	3.5	15	433 d
C1X01-1/3-2/7-1	1	A	100	0–5	15	< 30 s
		C	100	5	15	211 d
MCE36-1/1-1/2-2/2	1	A	100	0–7	15	< 30 s
		C	100	7	15	326 d
L4X01-6/1-2/1-2/1	1	A	25	0–10	15	< 30 s
		C	25	10	15	615 d

Table 7-5. Constant Stress (Creep) Test Matrix for Mine Workings Specimens (Page 2 of 6)

Specimen I.D.	Stage	Load Path[a]	Temperature (°C)	$\sigma_1 - \sigma_3$ (MPa)	σ_3 (MPa)	Test Duration[b]
L4X01-6/1-2/1-4/1	1	A	25	0–11.5	15	< 30 s
		C	25	11.5	15	449 d
L4X01-6/1-1/1-1/1	1	A	25	0–13	15	< 30 s
		C	25	13	15	468 d
L4X01-6/1-1/1-2/1	1	A	25	0–15	15	<30 s
		C	25	15	15	22.6 d
L4X01-5/1-1/1-7/1	1	A	25	0–15	15	<30 s
		C	25	15	15	101 d
L4X01-6/1-1/1-3/1	1	A	100	0–3.5	15	<30 s
		C	100	3.5	15	340 d
L4X01-6/1-2/1-7/1	1	A	100	0–5	15	< 30 s
		C	100	5	15	70.8 d
L4X01-7/1-2/1-4/1	1	A	100	0–5	15	< 30 s
		C	100	5	15	410 d
Following Data From SAND89-7098 (Nominal Specimen Diameter = 100 mm and L:D = 2)						
C1X01-04/1-3/1-2 (Test I.D. C1X041)	1	A	25	0–10	15	< 30 s
		C	25	10	15	219 d

Table 7-5. Constant Stress (Creep) Test Matrix for Mine Workings Specimens (Page 3 of 6)

Specimen I.D.	Stage	Load Path[a]	Temperature (°C)	$\sigma_1 - \sigma_3$ (MPa)	σ_3 (MPa)	Test Duration[b]
C1X01-04/1-3/2-2 (Test I.D. C1X042)	1	A	25	0–15	15	< 30 s
		C	25	15	15	166 d
C1X01-02/1-3/1-2 (Test I.D. C1X021)	1	A	25	0–15	15	< 30 s
		C	25	15	15	281 d
Following Data From SAND85-7261 (Nominal Specimen Diameter = 100 mm and L:D = 2)						
P4X18-4/4-1-2	1	A	25	0–10	15	<30 s
		C	25	10	15	217 d
P4X18-1/5-1-2	1	A	25	0–10	15	< 30 s
		C	25	10	15	172 d
P4X18-1/3-1-2	1	A	25	0–15	15	< 30 s
		C	25	15	15	48 d
P4X18-4/2-1-2	1	A	25	0–15	15	<30 s
		C	25	15	15	114 d
P4X18-1/6-1-2	1	A	25	0–21	15	<30 s
		C	25	21	15	96 d
P4X18-4/1-1-2	1	A	100	0–3.5	15	<30 s
		C	100	3.5	15	82 d

Table 7-5. Constant Stress (Creep) Test Matrix for Mine Workings Specimens (Page 4 of 6)

Specimen I.D.	Stage	Load Path[a]	Temperature (°C)	$\sigma_1 - \sigma_3$ (MPa)	σ_3 (MPa)	Test Duration[b]
P4X18-2/3-1-2	1	A	100	0–7	15	< 30 s
		C	100	7	15	115 d
P4X18-4/5-1-2	1	A	200	0–2	15	< 30 s
		C	200	2	15	85 d
P4X18-2/4-1-2	1	A	200	0–3.5	15	<30 s
		C	200	3.5	15	38 d
DX16-2/7-1-2	1	A	25	0–10	15	< 30 s
		C	25	10	15	285 d
DX19-5/7-1-2	1	A	25	0–10	15	< 30 s
		C	25	10	15	183 d
DX19-5/5-1-2	1	A	25	0–13	15	<30 s
		C	25	13	15	250 d
DX16-2/1-1-2	1	A	25	0–15	15	<30 s
		C	25	15	15	75 d
DX16-2/4-1-2	1	A	25	0–17	15	<30 s
		C	25	17	15	272 d
DX16-2/8-1-2	1	A	25	0–19	15	<30 s
		C	25	19	15	270 d

Table 7-5. Constant Stress (Creep) Test Matrix for Mine Workings Specimens (Page 5 of 6)

Specimen I.D.	Stage	Load Path[a]	Temperature (°C)	$\sigma_1 - \sigma_3$ (MPa)	σ_3 (MPa)	Test Duration[b]
DX19-5/6-1-2	1	A	25	0–19	15	< 30 s
		C	25	19	15	208 d
DX16-2/6-1-2	1	A	25	0–21	15	< 30 s
		C	25	21	15	174 d
DX19-5/1-1-2	1	A	25	0–25	15	<30 s
		C	25	25	15	44 d
DX19-5/2-1-2	1	A	25	0–30	15	< 30 s
		C	25	30	15	10.3 d
DX19-5/3-1-2	1	A	25	0–30	15	< 30 s
		C	25	30	15	11.7 d
DX16-2/3-1-2	1	A	100	0–3.5	15	<30 s
		C	100	3.5	15	68 d
DX19-4/4-1-2	1	A	100	0–7	15	<30 s
		C	100	7	15	180 d
DX19-5/4-1-2	1	A	100	0–17	15	<30 s
		C	100	17	15	2.8 d
DX16-2/2-1-2	1	A	200	0–2	15	<30 s
		C	200	2	15	47 d

Table 7-5. Constant Stress (Creep) Test Matrix for Mine Workings Specimens (Page 6 of 6)

Specimen I.D.	Stage	Load Path[a]	Temperature (°C)	$\sigma_1 - \sigma_3$ (MPa)	σ_3 (MPa)	Test Duration[b]
DX16-2/5-1-2	1	A	200	0–2	15	< 30 s
		C	200	2	15	231 d
DX19-4/3-1-2	1	A	200	0–3.5	15	< 30 s
		C	200	3.5	15	37 d

(a) A = application load-up to initiate creep test
C = constant stress (creep) portion of test.

(b) s = seconds
m = minutes
d = days.

Table 7-6. Constant Stress (Creep) Test Results for Mine Workings Specimens (Page 1 of 6)

Specimen I.D.	Stage	Load Path[a]	Strain Increments, % ε_1	Strain Increments, % ε_3	Comments
Following Data From SAND92-7291 (Nominal Specimen Diameter = 100 mm and L:D = 2)					
C1X01-1/3-3/7-1	1	A	0.096	−0.027	
		C	0.560	−0.332	
C1X01-1/3-3/1-1	1	A	0.164	−0.061	
		C	4.103	−1.713	
C1X01-1/3-3/4-1	1	A	0.316	−0.125	
		C	6.420	−3.193	
C1X01-1/3-3/2-1	1	A	0.471	−0.213	
		C	12.24	−5.677	
C1X01-1/3-3/6-1	1	A	0.028	−0.010	
		C	0.385	0.071	
C1X01-1/3-2/7-1	1	A	0.075	−0.036	
		C	0.714	−0.251	
MCE36-1/1-1/2-2/2	1	A	0.083	−0.034	
		C	7.436	−3.677	
L4X01-6/1-2/1-2/1	1	A	0.100	−0.043	
		C	4.921	0.828	

Table 7-6. Constant Stress (Creep) Test Results for Mine Workings Specimens (Page 2 of 6)

Specimen I.D.	Stage	Load Path[a]	Strain Increments, %		Comments
			ε_1	ε_3	
L4X01-6/1-2/1-4/1	1	A	0.219	−0.103	
		C	10.26	−3.780	
L4X01-6/1-1/1-1/1	1	A	0.190	−0.083	
		C	5.236	−2.418	
L4X01-6/1-1/1-2/1	1	A	0.269	−0.124	
		C	1.839	−0.771	
L4X01-5/1-1/1-7/1	1	A	0.759	−0.367	
		C	12.62	−5.67	
L4X01-6/1-1/1-3/1	1	A	0.061	−0.023	
		C	2.120	−1.096	
L4X01-6/1-2/1-7/1	1	A	0.072	−0.035	
		C	2.807	−1.327	
L4X01-7/1-2/1-4/1	1	A	0.043	−0.016	
		C	8.563	−4.230	
Following Data From SAND89-7098 (Nominal Specimen Diameter = 100 mm and L:D = 2)					
C1X01-04/1-3/1-2 (Test I.D. C1X041)	1	A	0.151	−0.073	
		C	0.453	−0.134	

Table 7-6. Constant Stress (Creep) Test Results for Mine Workings Specimens (Page 3 of 6)

Specimen I.D.	Stage	Load Path[(a)]	Strain Increments, %		Comments
			ε_1	ε_3	
C1X01-04/1-3/2-2 (Test I.D. C1X042)	1	A	0.399	–0.181	
		C	1.901	–0.780	
C1X01-02/1-3/1-2 (Test I.D. C1X021)	1	A	0.216	–0.085	
		C	1.979	–1.059	
Following Data From SAND85-7261 (Nominal Specimen Diameter = 100 mm and L:D = 2)					
P4X18-4/4-1-2	1	A	0.097	–0.029	
		C	0.525	–0.204	
P4X18-1/5-1-2	1	A	0.212	–0.075	
		C	1.133	–0.045	
P4X18-1/3-1-2	1	A	0.316	–0.124	
		C	12.97	–6.445	Anomalous test result. Localized deformation along clay seams.
P4X18-4/2-1-2	1	A	0.165	–0.059	
		C	2.272	–0.943	
P4X18-1/6-1-2	1	A	0.372	–0.051	
		C	12.91	–2.059	
P4X18-4/1-1-2	1	A	0.044	–0.022	
		C	0.437	–0.233	

Table 7-6. Constant Stress (Creep) Test Results for Mine Workings Specimens (Page 4 of 6)

Specimen I.D.	Stage	Load Path[a]	Strain Increments, %		Comments
			ε_1	ε_3	
P4X18-2/3-1-2	1	A	0.059	–0.017	
		C	12.07	–7.039	Possible moisture effects.
P4X18-4/5-1-2	1	A	0.074	–0.033	
		C	1.559	–0.339	
P4X18-2/4-1-2	1	A	0.098	–0.037	
		C	12.15	–7.325	Possible moisture effects.
DX16-2/7-1-2	1	A	0.074	–0.032	
		C	0.346	–0.198	
DX19-5/7-1-2	1	A	0.093	–0.039	
		C	0.313	N/A	
DX19-5/5-1-2	1	A	0.229	–0.104	
		C	1.152	–0.402	
DX16-2/1-1-2	1	A	0.156	–0.060	
		C	1.529	–0.683	
DX16-2/4-1-2	1	A	0.344	–0.157	
		C	8.637	–1.514	Possible machine malfunction.
DX16-2/8-1-2	1	A	0.408	–0.158	
		C	12.60	–5.426	

Table 7-6. Constant Stress (Creep) Test Results for Mine Workings Specimens (Page 5 of 6)

Specimen I.D.	Stage	Load Path[(a)]	Strain Increments, %		Comments
			ε_1	ε_3	
DX19-5/6-1-2	1	A	0.366	–0.164	
		C	9.874	–4.525	
DX16-2/6-1-2	1	A	0.615	–0.261	
		C	12.98	–6.362	Possible jacket leak near end of test.
DX19-5/1-1-2	1	A	0.890	–0.426	
		C	12.28	–5.752	
DX19-5/2-1-2	1	A	1.387	–0.672	
		C	11.89	–5.901	
DX19-5/3-1-2	1	A	1.366	–0.664	
		C	11.53	–5.833	
DX16-2/3-1-2	1	A	0.025	–0.009	
		C	0.137	–0.100	
DX19-4/4-1-2	1	A	0.059	–0.021	
		C	7.403	–1.985	Anomalous test result.
DX19-5/4-1-2	1	A	1.004	–0.497	
		C	12.41	–6.217	
DX16-2/2-1-2	1	A	0.005	–0.003	
		C	0.228	–0.678	Anomalous test result.

Table 7-6. Constant Stress (Creep) Test Results for Mine Workings Specimens (Page 6 of 6)

Specimen I.D.	Stage	Load Path[a]	Strain Increments, %		Comments
			ε_1	ε_3	
DX16-2/5-1-2	1	A	0.034	−0.014	
		C	3.683	−2.279	Anomalous test result.
DX19-4/3-1-2	1	A	0.107	−0.047	
		C	13.26	7.193	

(a) A = application load-up to initiate creep test.
C = constant stress (creep) portion of test.

Plots have been created to present the salient features of each test to demonstrate control of desired test conditions and observations of the resulting specimen behavior. Thus, data plots consist of curves tracing the control variables as a function of time and also plots of strain versus time. These creep tests were initiated by applying the desired axial stress difference very quickly (<30s) and no data were collected during that time. Thus, there are no stress application plots as were produced for the borehole specimens. All creep data plots can be found in Appendix C where the sign convention is that compression is positive. For those specimens classified as argillaceous salt, a notation is included in the figure caption.

7.3 MULTIAXIAL STRESS

This section presents the data obtained from a highly specialized type of test that required the use of large, thin walled, hollow cylinders of salt. For this work, the relatively uniform and pure dome salt from Avery Island, Louisiana, was used. The use of a non-WIPP salt type was acceptable because these tests were designed to investigate the role of the intermediate principal stress on the creep potential of salt and no site specific material properties were sought. Two tables have been included to summarize the work performed. The first table represents the matrix of tests that were performed and the second table presents a summary of the test results.

The text matrix that was followed is given in Table 7-7. The first column in the table is the test identification label that was given in the original report. The remaining columns give the test conditions in three equivalent forms; first as stress invariants, then as principal stresses, and finally as the values of the controlled variables. All of the tests were performed on specimens with the same nominal dimensions; a length of 610 mm, an outer diameter of 305 mm, and a wall thickness of 25 mm. All tests were conducted at laboratory room temperature (20°C) and were performed on a single special purpose test system.

The numerical test results are summarized in Table 7-8. For this analysis, the test results were represented by the Lode angle for stress calculated from the measured stresses and the principal strain rates observed at the end of the test. The principal strain rate values were used to calculate Lode angles for strain rates which were then plotted against Lode angles for stresses. Each test provided a single data point on the Lode angle plot and they appear as shown in Figure 7-1. There are two theoretical curves in Figure 7-1; one represents the theoretical response if the creep potential of salt is governed by a Mises criterion and the other represents the theoretical response if the creep potential of salt is governed by a Tresca criterion. A comparison of the two theoretical curves with the experimental data led to the conclusion that the creep potential of salt was best represented by a Tresca criterion.

Plots have been created to present the salient features of each test to demonstrate control of desired test conditions and observations of the resulting specimen behavior and those plots can be found in Appendix D. The figures in Appendix D are plots of curves that trace the control variables as a function of time and also plots of all three principal strains versus time.

Table 7-7. Multiaxial Test Matrix for Avery Island Salt[a]

Specimen I.D.	I_1 (MPa)	J_2 (MPa)^2	ψ^σ	σ_{rr} (MPa)	$\sigma_{\theta\theta}$ (MPa)	σ_{zz} (MPa)	F (MN)	P_o (MPa)	P_i (MPa)
AI/82/C′1	–55	33.33	0°	–18.33	–12.56	–24.11	–0.538	–17.85	–18.91
AI/86/C′3/1 AI/86/A′1/11	–55	33.33	10°	–17.18	–13.23	–24.60	–0.549	–16.85	–17.57
AI/86/C′4/1 AI/86/A′12/1	–55	33.33	20°	–16.05	–14.05	–24.90	–0.555	–15.89	–16.25
AI/82/C′7	–55	33.33	30°	–15.00	–15.00	–25.00	–0.557	–15.00	–15.00
AI/86/A′10/1	–55	52.08	20°	–15.48	–12.98	–26.54	–0.592	–15.27	–15.73

(a) Symbol Definitions:
I_1 = First invariant of stress
J_2 = Second invariant of stress deviator
ψ^σ = Lode angle for stress
σ_{rr} = Radial principal stress
$\sigma_{\theta\theta}$ = Circumferential principal stress
σ_{zz} = Axial principal stress
F = Net axial force on specimen
P_o = Pressure acting on outer wall of specimen
P_i = Pressure acting on inner wall of specimen.

The control variables are presented in terms of two stress invariants and the Lode angle for stresses because they are common measures used when dealing with multiaxial states of stress. In the strain versus time plots, the strain values include the elastic and inelastic strains induced during the loading to initiate the creep tests. The multiaxial tests were originally reported using a positive sign for tension and that convention has been retained in this section and in Appendix D.

Table 7-8. Multiaxial Test Results for Avery Island Salt

Specimen I.D.	Stress Lode Angle, ψ^σ	Principal Strain Rates at End of Test (s^{-1})		
		$\dot{\varepsilon}_{rr}$	$\dot{\varepsilon}_{\theta\theta}$	$\dot{\varepsilon}_{zz}$
AI/82/C'1	0.78°	0	6.83×10^{-10}	-5.64×10^{-10}
AI/86/C'3/1	10.23°	0	6.73×10^{-10}	-6.63×10^{-10}
AI/86/A'1/1	10.21°	0	0.59×10^{-10}	-0.59×10^{-10}
AI/86/C'4/1	19.85°	0	3.36×10^{-10}	-4.35×10^{-10}
AI/86/A'12/1	20.65°	0	0.89×10^{-10}	-3.17×10^{-10}
AI/82/C'7	29.59°	1.88×10^{-10}	1.88×10^{-10}	-3.17×10^{-10}
AI/86/A'10/1	20.52°	0	1.94×10^{-10}	-2.07×10^{-10}

7.4 DAMAGE RECOVERY

This section presents the data obtained from a specialized testing program devised to assess the effects of time, temperature, hydrostatic stress, and damage level on crack closure and healing of salt specimens retrieved from the WIPP mine workings. Table 7-9 has been included to summarize the work performed and it represents the matrix of tests that were performed.

The tests listed in Table 7-9 were used to generate data that could be used to address questions in two separate experiments. In the first experiment, three specimens that had been subjected to a controlled level of damage (1 percent axial strain) in a strain rate controlled triaxial compression test, were healed at one of three different pressures (5, 10, and 15 MPa). Crack closure and healing, as indicated by changes in ultrasonic compressional wave amplitudes and velocities, were observed as a function of time by recording the recoveries of the amplitudes and velocities. In the second experiment, the effect of different damage levels was investigated. Specimens that had been subjected to one of three controlled levels of damage (0.5, 1.0, or 1.5 percent axial strain) were all healed at a pressure of 15 MPa. Again, the recoveries of the wave amplitudes and velocities were measured as a function of time to assess the effect of initial damage level on the healing process.

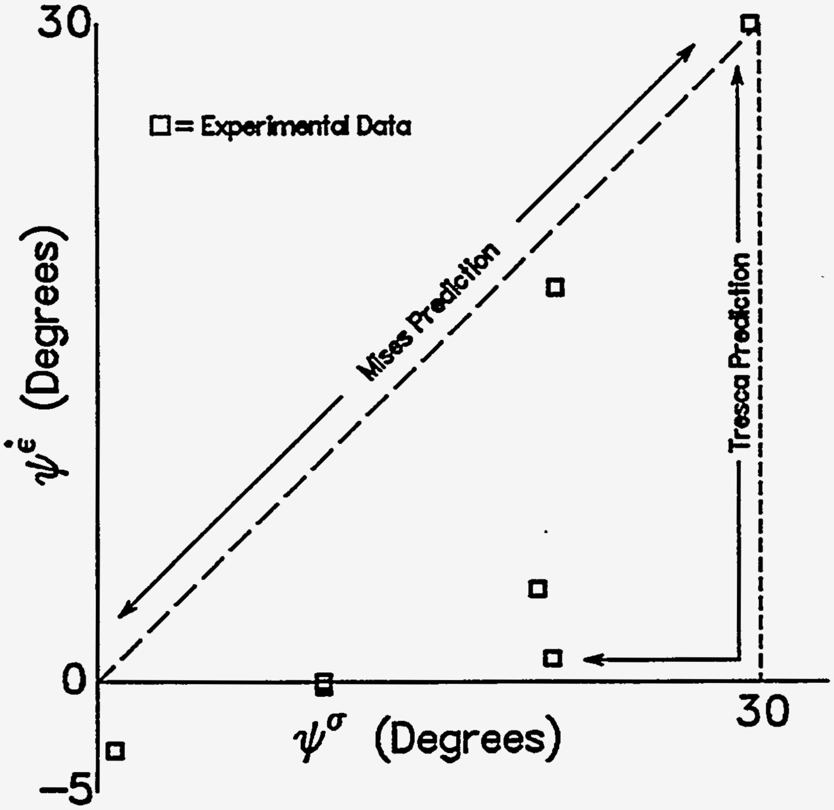

Figure 7-1. Strain Rate Lode Angle Versus Stress Lode Angle.

The results of the testing are graphical in nature, so there is no tabulation of test results contained within this section. Plots have been created to present the data measured during each test. Included are plots of strain versus time and plots of wave amplitude and velocity versus time. These plots can be found in Appendix E. The sign convention for the damage recovery work was that compression is positive.

Table 7-9. Damage Recovery Test Matrix for WIPP Mine Workings Salt

Test	Specimen I.D.	Temperature (°C)	Pressure (MPa)	Damage Level (Axial Strain, %)
The Following Data From SAND93-7111				
LCH015	C1X01-02/1-4/2-2[(a)]	21	15	1.5
LDR001	MCE36-1/2-1/2-7/2	70	15	1.5
LDR002	MCE36-1/2-1/2-6/2	70	15	1.5
LDR005	MCE36-1/2-1/2-1/2	46	15	1.5
LDR006	MCE36-1/1-1/2-7/2	46	15	1.5
The Following Data From SAND90-7076				
1	C1X01-04/1-4/2-2	21	10	1.0
2	C1X01-03/1-4/4-2	21	5	1.0
3	C1X01-04/1-2/4-2	21	15	1.0
4	C1X01-04/1-2/3-2	21	15	0.5
5	C1X01-02/1-4/4-2	21	15	1.0
6	C1X01-02/1-4/2-2[(a)]	21	15	1.5
7	C1X01-04/1-4/4-2	21	15	0.5

(a) This test was originally reported in SAND90-7076 (Brodsky, 1990) and then referenced again in SAND93-7111 (Brodsky, 1993).

8.0 SUMMARY

Twenty-one years of laboratory testing performed by RE/SPEC Inc. in support of the WIPP has been summarized and compiled into this single document. The types of tests performed over that period and included here represent quasi-static triaxial compression, constant stress (creep), multiaxial creep, and damage recovery. All tests performed over that period and included here have been previously reported.

The data contained herein are essentially only a reproduction of previously published results. There has been no new data reduction performed in preparation of this report. A substantial part of the current effort involved retrieval of archived information for the given reports from the RE/SPEC file system. This information was reformatted for incorporation into the standard Laboratory Notebook System format now in use at the WIPP and described in Appendix B of SNL Quality Assurance Procedure QAP 20-03 entitled *Qualification of Existing Data* (Scully, 1995). Those Laboratory Notebooks provide all the supporting information for the data presented in this summary report and they will be transferred to Sandia WIPP Central Filing for future reference and records retention.

9.0 REFERENCES

ANSI/ASME. 1985. *Part 1: Measurement Uncertainty Instruments and Apparatus.* PTC19.1-1985. New York, NY: American Society of Mechanical Engineers.

Brodsky, N. S. 1990. *Crack Closure and Healing Studies in WIPP Salt Using Compressional Wave Velocity and Attenuation Measurements: Test Methods and Results.* SAND90-7076. Prepared by RE/SPEC Inc., Rapid City, SD. Albuquerque, NM: Sandia National Laboratories.

Brodsky, N. S. 1993. *Thermomechanical Damage Recovery Parameters for Rocksalt From the Waste Isolation Pilot Plant.* SAND93-7111. Prepared by RE/SPEC Inc., Rapid City, SD. Albuquerque, NM: Sandia National Laboratories.

Brodsky, N. S., and D. E. Munson. 1994. "Thermomechanical Damage Recovery Parameters for Rocksalt From the Waste Isolation Pilot Plant," *Rock Mechanics: Models and Measurements, Challenges From Industry, Proceedings of the 1st North American Rock Mechanics Symposium, University of Texas at Austin, June 1–3, 1994.* Eds. P. P. Nelson and S. E. Laubach. Brookfield, VT: A. A. Balkema. 731–738.

Chan, K. S., S. R. Bodner, A. F. Fossum, and D. E. Munson. 1992. "A Constitutive Model for Inelastic Flow and Damage Evolution in Solids Under Triaxial Compression," *Mechanics of Materials.* Vol. 14, No. 1, 1–14.

Chan, K. S., D. E. Munson, A. F. Fossum, and S. R. Bodner, 1996. "A Constitutive Model for Representing Coupled Creep, Fracture, and Healing in Rock Salt," *4th Conference on the Mechanical Behavior of Salt, University of Montreal, École Polytechnique de Montréal, June 17–18, 1996.* SAND96-0376C. Albuquerque, NM: Sandia National Laboratories. (Copy on file in the Sandia WIPP Central Files, Sandia National Laboratories, Albuquerque, NM as WPO33791.)

Dropek, R. K., 1976. "Pressure-Temperature Creep Testing as Applied to a Commercial Rock Salt." Master's Thesis. Salt Lake City, UT: University of Utah, Department of Civil Engineering. (Copy on file in the Sandia WIPP Central Files, Sandia National Laboratories, Albuquerque, NM as WPO38426.)

Fossum, A. F., T. W. Pfeifle, K. D. Mellegard, and D. E. Munson, 1994. "Probability Distributions for Parameters of the Munson-Dawson Salt Creep Model," *Rock Mechanics: Models and Measurements, Challenges From Industry, Proceedings of the 1st North American Rock Mechanics Symposium, University of Texas at Austin, June 1–3, 1994.* Eds. P. P. Nelson and S. E. Laubach. Brookfield, VT: A. A. Balkema. 715–722.

Hansen, F. D., 1979. *Triaxial Quasi-Static Compression and Creep Behavior of Bedded Salt From Southeastern New Mexico.* SAND79-7045. Prepared by RE/SPEC Inc., Rapid City, SD. Albuquerque, NM: Sandia National Laboratories.

Hansen, F. D. and K. D. Mellegard, 1979. *Creep Behavior of Bedded Salt From Southeastern New Mexico at Elevated Temperature.* SAND79-7030. Prepared by RE/SPEC Inc., Rapid City, SD. Albuquerque, NM: Sandia National Laboratories.

Hansen, F. D. and K. D. Mellegard, 1980. *Further Creep Behavior of Bedded Salt From Southeastern New Mexico at Elevated Temperature.* SAND80-7114. Prepared by RE/SPEC Inc., Rapid City, SD. Albuquerque, NM: Sandia National Laboratories.

Mellegard, K. D. and T. W. Pfeifle, 1993. *Creep Tests on Clean and Argillaceous Salt From the Waste Isolation Pilot Plant.* SAND92-7291. Prepared by RE/SPEC Inc., Rapid City, SD. Albuquerque, NM: Sandia National Laboratories.

Mellegard, K. D., G. D. Callahan, and P. E. Senseny, 1992. *Multiaxial Creep of Natural Rock Salt.* SAND91-7083. Prepared by RE/SPEC Inc., Rapid City, SD. Albuquerque, NM: Sandia National Laboratories.

Munson, D. E., 1979. *Preliminary Deformation-Mechanism Map for Salt (With Application to WIPP).* SAND79-0076. Albuquerque, NM: Sandia National Laboratories.

Munson, D. E. and P. R. Dawson, 1979. *Constitutive Model for the Low Temperature Creep of Salt (With Application to WIPP).* SAND79-1853. Albuquerque, NM: Sandia National Laboratories.

Munson, D. E. and P. R. Dawson, 1982a. *A Transient Creep Model for Salt During Stress Loading and Unloading.* SAND82-0962. Albuquerque, NM: Sandia National Laboratories.

Munson, D. E. and P. R. Dawson, 1982b. "A Workhardening/Recovery Model of Transient Creep of Salt During Stress Loading and Unloading," *Issues in Rock Mechanics, Proceedings of the 23rd U.S. Symposium on Rock Mechanics, University of California, Berkeley, CA, August 25–27, 1982.* Eds. R. E. Goodman and F. E. Heuze. New York, NY: Society of Mining Engineers of the American Institute of Mining, Metallurgical and Petroleum Engineers. 299–306.

Munson, D. E. and P. R. Dawson, 1984. "Salt Constitutive Modeling Using Mechanism Maps," *The Mechanical Behavior of Salt, Proceedings of the First Conference, Pennsylvania State University, University Park, PA, November 9–11, 1981.* Eds. H. R. Hardy and M. Langer. Rockport, MA: Karl Distributors. 718–737.

Munson, D. E., A. F. Fossum, and P. E. Senseny, 1989a. *Advances in Resolution of Discrepancies Between Predicted and Measured In Situ WIPP Room Closures*. SAND88-2948. Albuquerque, NM: Sandia National Laboratories.

Munson, D. E., A. F. Fossum, and P. E. Senseny, 1989b. "Approach to First Principles Model Prediction of Measured WIPP In Situ Room Closure in Salt," *Rock Mechanics as a Guide for Efficient Utilization of Natural Resources: Proceedings, 30th U.S. Symposium, West Virginia University, Morgantown, WV, June 19–22, 1989.* Ed. A. W. Khair. Brookfield, VT: A. A. Balkema. 673–680.

Pfeifle, T. W., K. D. Mellegard, and D. E. Munson, 1992. "Determination of Probability Density Functions for Parameters in the Munson-Dawson Model for Creep Behavior of Salt." *Probabilistic Method in Geomechanics, AMD-Vol. 134,* (A. F. Fossum, ed.). ASME, New York, NY: 41–56.

RE/SPEC Inc. 1995. "Quality Assurance Manual." Rev. 4. RSI/SIR-95-01. Rapid City, SD: RE/SPEC Inc. (Copy on file in Sandia WIPP Central Files, Sandia National Laboratories, Albuquerque, NM as WPO37027.)

Scully, L. W. 1995. "Qualification of Existing Data." Quality Assurance Procedure QAP 20-3, Revision 2. Albuquerque, NM: Sandia National Laboratories, Waste Isolation Pilot Plant. (Copy of superseded procedure on file in Sandia WIPP Central Files, Sandia National Laboratories, Albuquerque, NM as WPO10893.)

Senseny, P. E., 1986. *Triaxial Compression Creep Tests on Salt From the Waste Isolation Pilot Plant*. SAND85-7261. Prepared by RE/SPEC Inc., Rapid City, SD. Albuquerque, NM: Sandia National Laboratories.

Senseny, P. E., 1990. *Creep of Salt From the ERDA-9 Borehole and the WIPP Workings*. SAND89-7098. Prepared by RE/SPEC Inc., Rapid City, SD. Albuquerque, NM: Sandia National Laboratories.

Wawersik, W. R., 1975. "Technique and Apparatus for Strain Measurements on Rock in Constant Confining Pressure Experiments," *Rock Mechanics,* Vol. 7, no. 4, 231–241.

Wawersik, W. R., 1979. *Indirect Deformation (Strain) Measurements and Calibrations in Sandia Triaxial Apparatus for Rock Testing to 250°C*. SAND79-0114. Albuquerque, NM: Sandia National Laboratories.

[illegible]

APPENDIX A

QUASI-STATIC TRIAXIAL COMPRESSION TESTS

FIGURES

FIGURE **PAGE**

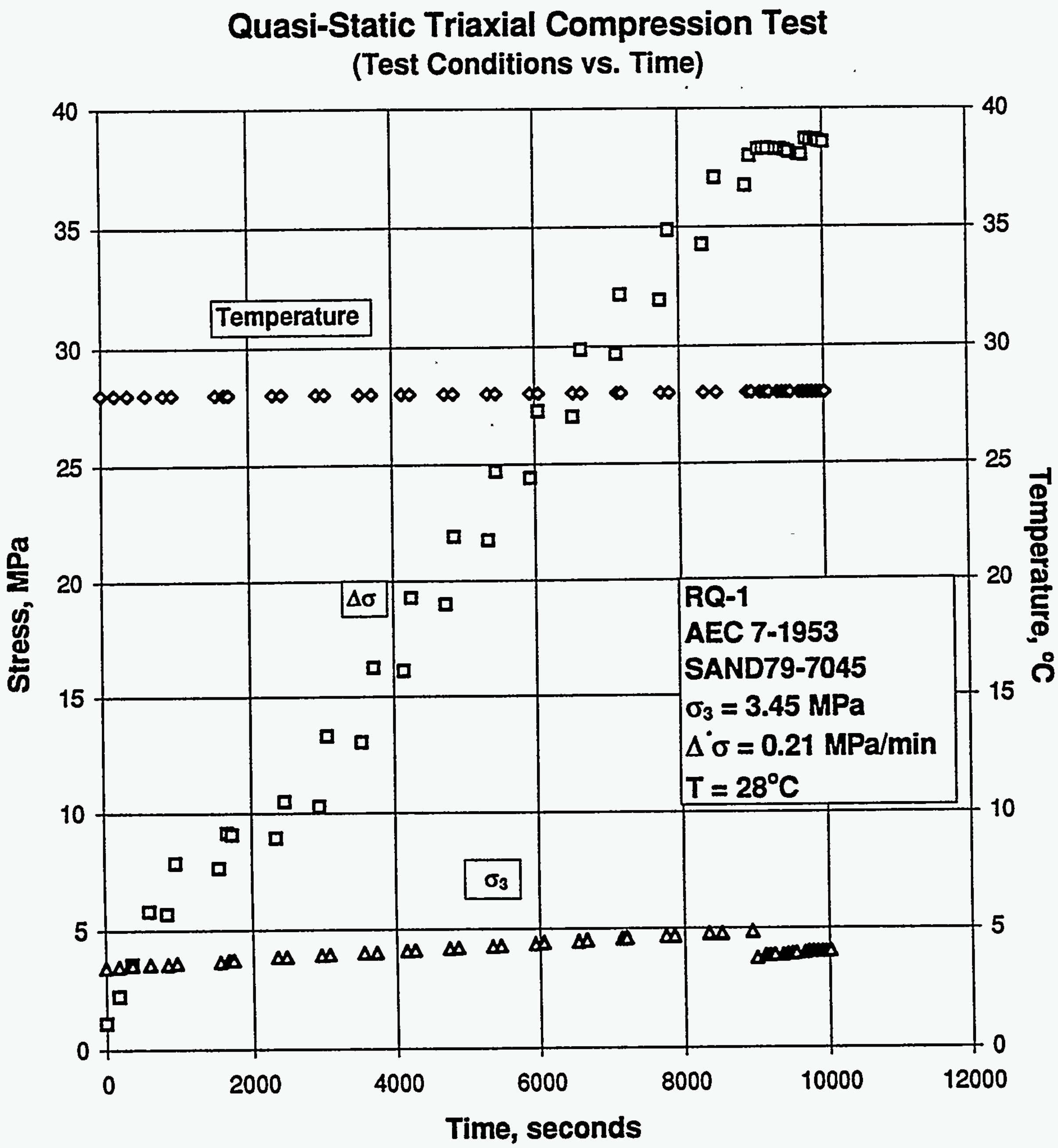

Figure A-1. Test Conditions Versus Time for a Quasi-Static Triaxial Compression Test: Specimen AEC7-1953.

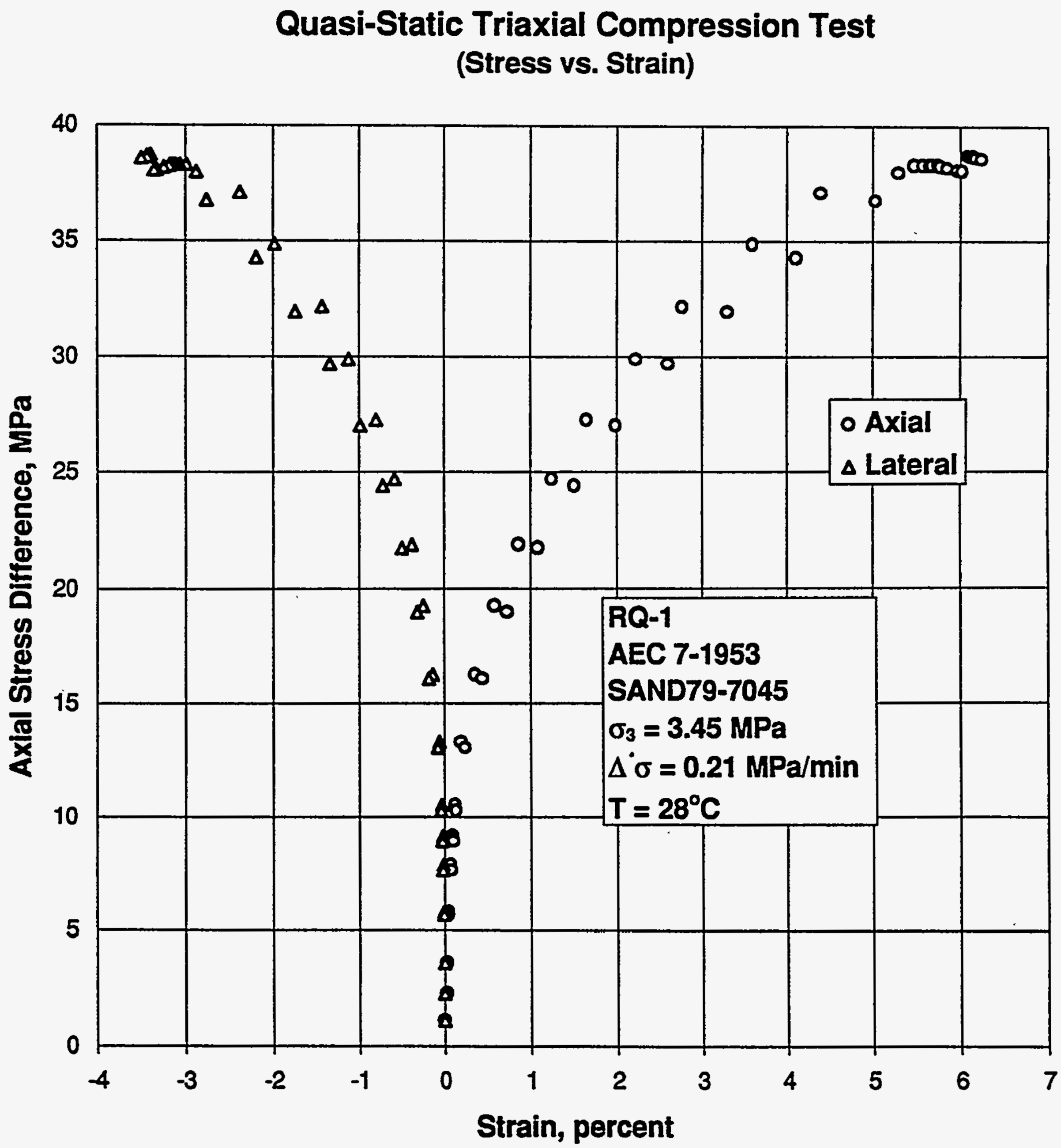

Figure A-2. Axial Stress Difference Versus Axial and Lateral Strain for a Quasi-Static Triaxial Compression Test: Specimen AEC7-1953.

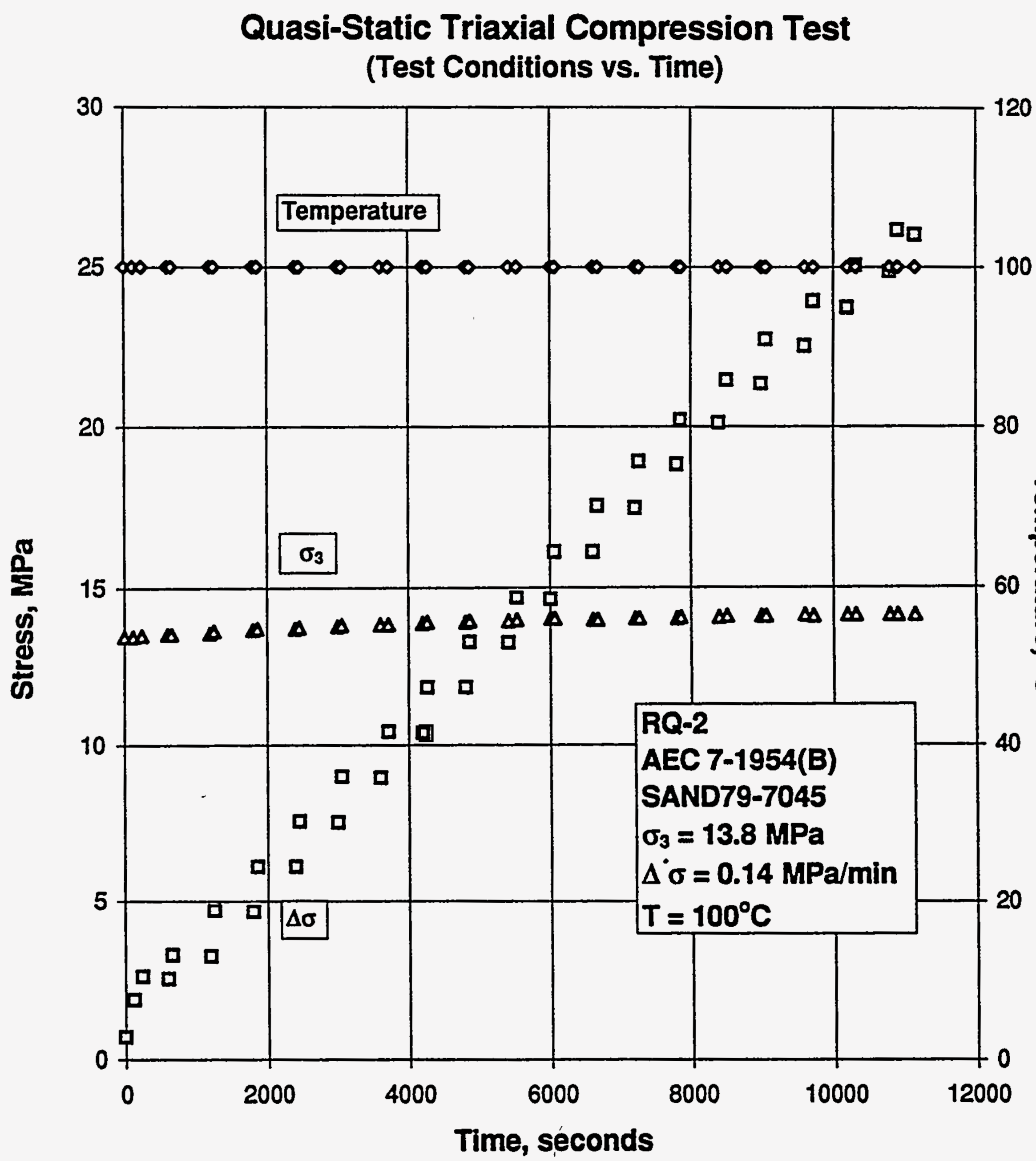

Figure A-3. Test Conditions Versus Time for a Quasi-Static Triaxial Compression Test: Specimen AEC7-1954 (B).

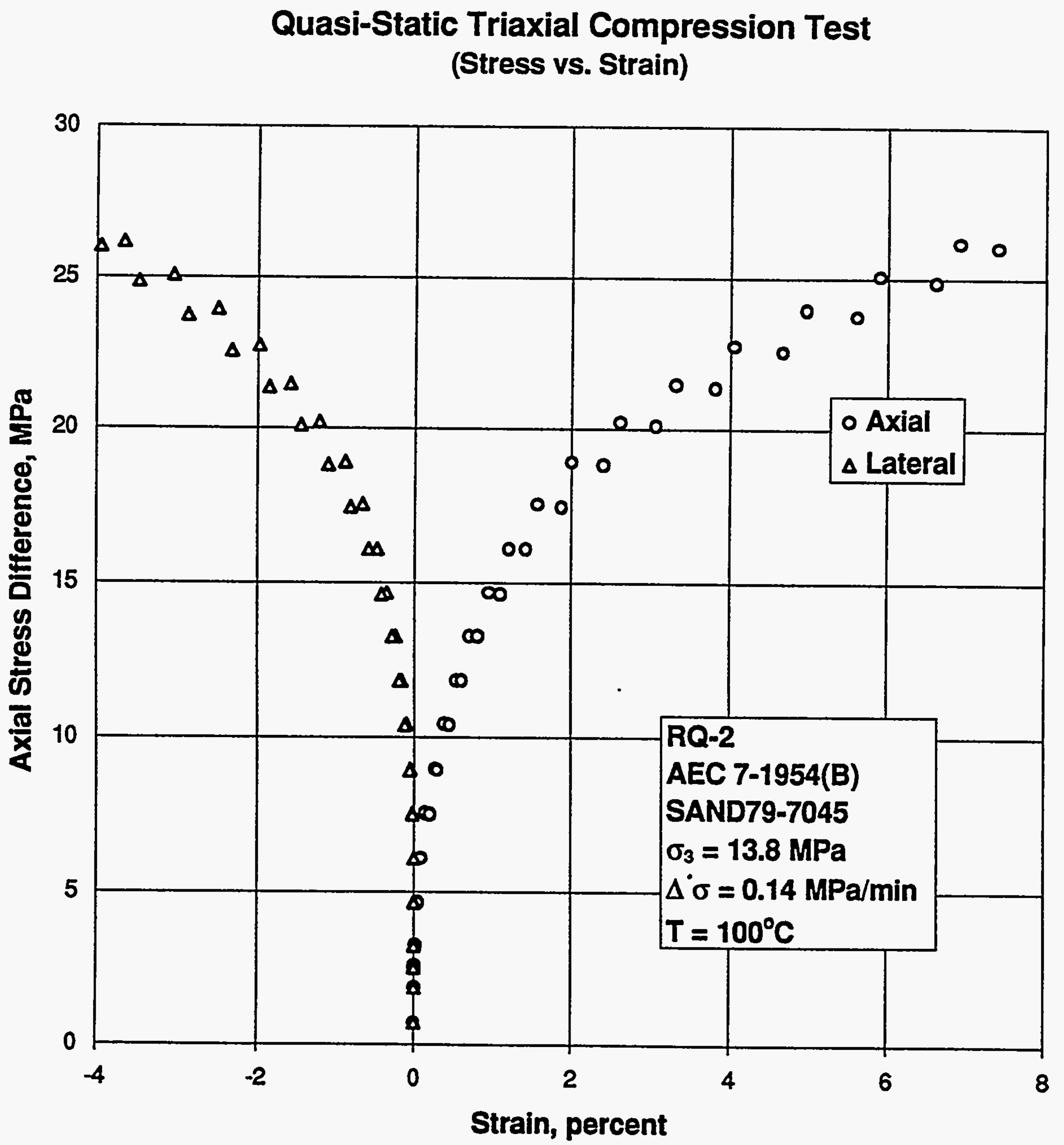

Figure A-4. Axial Stress Difference Versus Axial and Lateral Strain for a Quasi-Static Triaxial Compression Test: Specimen AEC7-1954 (B).

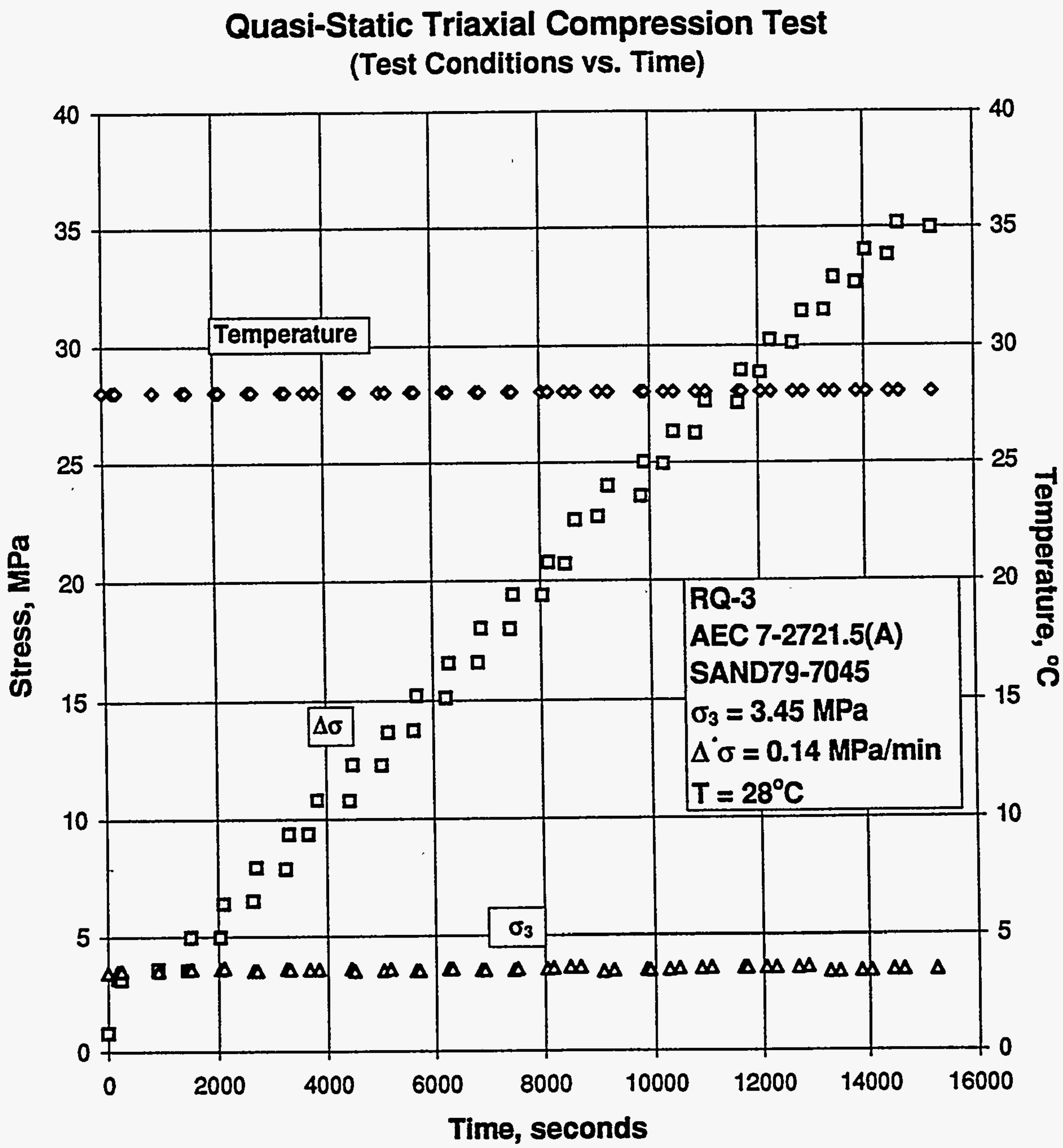

Figure A-5. Test Conditions Versus Time for a Quasi-Static Triaxial Compression Test: Specimen AEC7-2721.5 (A).

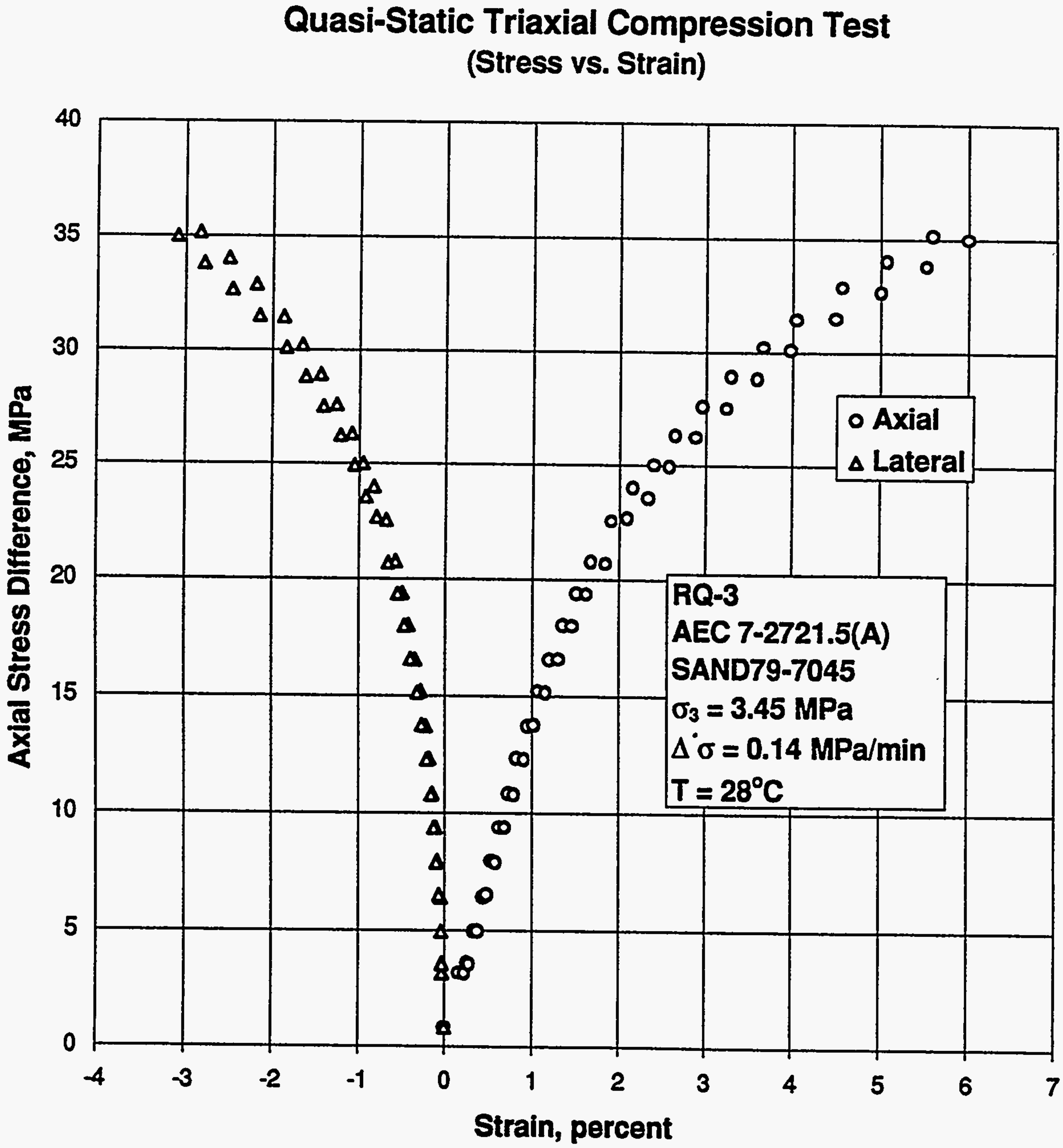

Figure A-6. Axial Stress Difference Versus Axial and Lateral Strain for a Quasi-Static Triaxial Compression Test: Specimen AEC7-2721.5 (A).

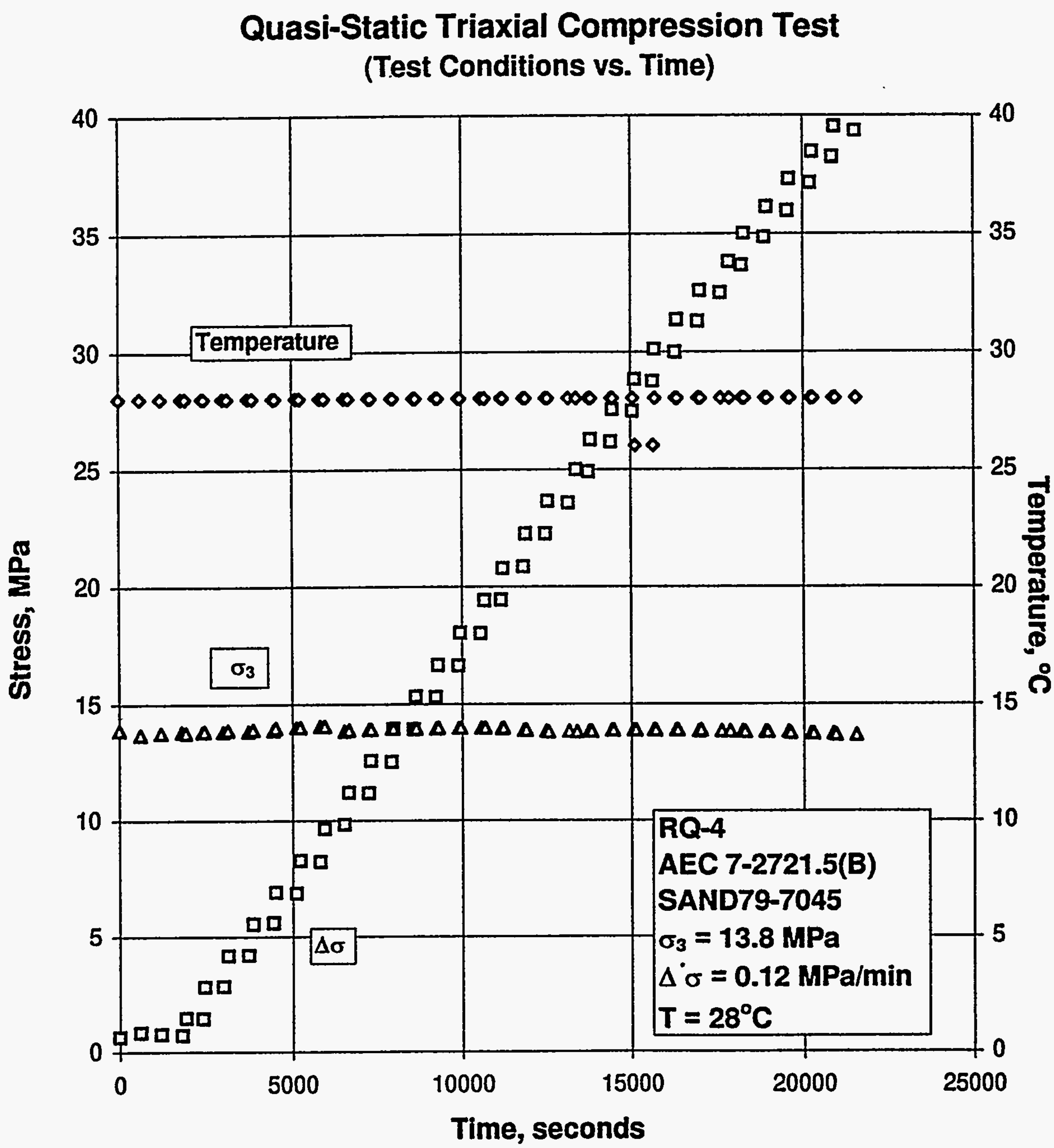

Figure A-7. Test Conditions Versus Time for a Quasi-Static Triaxial Compression Test: Specimen AEC7-2721.5 (B).

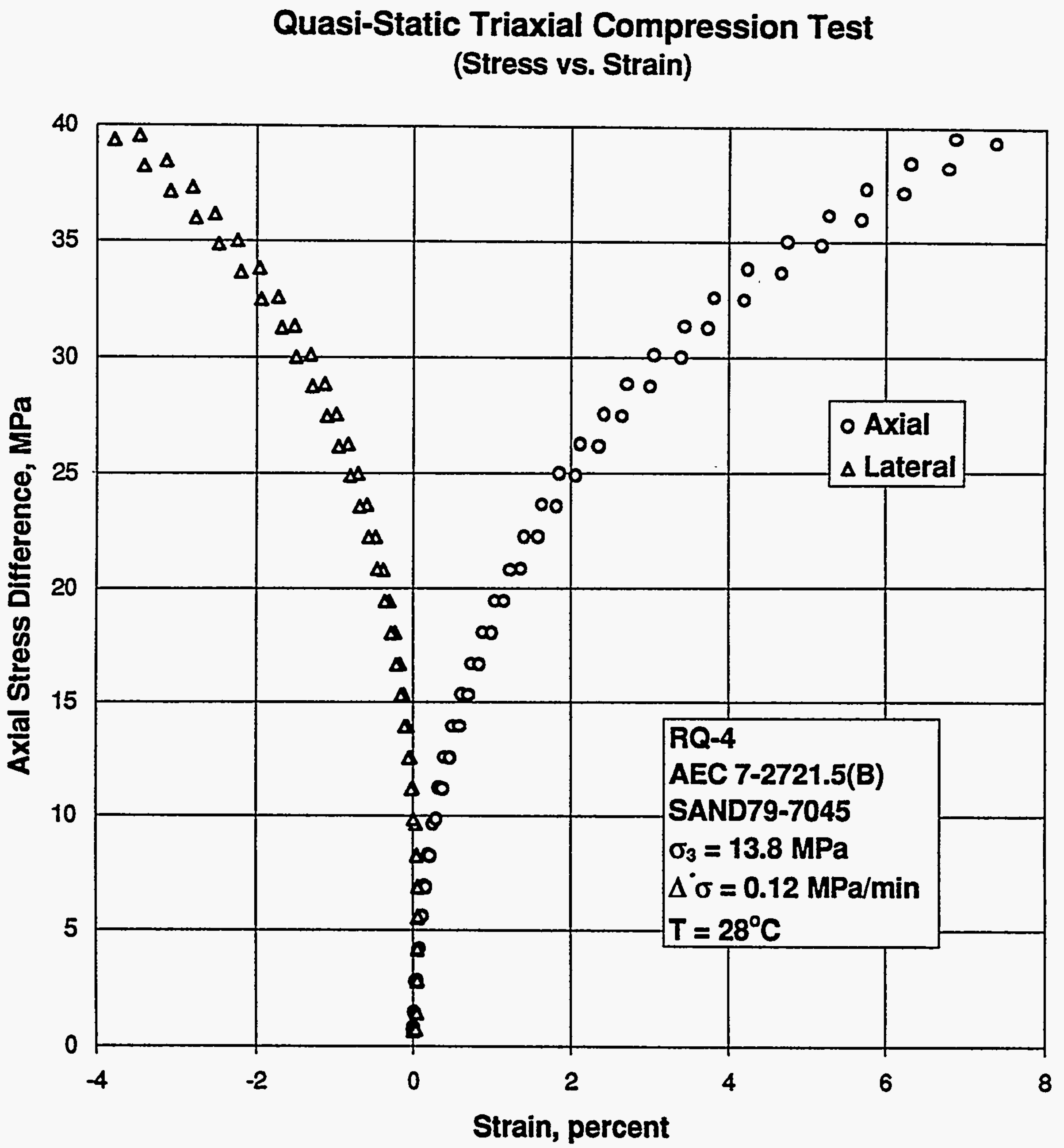

Figure A-8. Axial Stress Difference Versus Axial and Lateral Strain for a Quasi-Static Triaxial Compression Test: Specimen AEC7-2721.5 (B).

APPENDIX B

CREEP TESTS ON BOREHOLE SPECIMENS

FIGURES

FIGURES (Continued)

FIGURES (Continued)

FIGURE PAGE

FIGURES (Continued)

FIGURES (Continued)

FIGURES (Continued)

FIGURE PAGE

FIGURES (Continued)

FIGURE PAGE

FIGURES (Continued)

FIGURE PAGE

FIGURES (Continued)

FIGURE PAGE

FIGURES (Continued)

FIGURES (Continued)

FIGURE PAGE

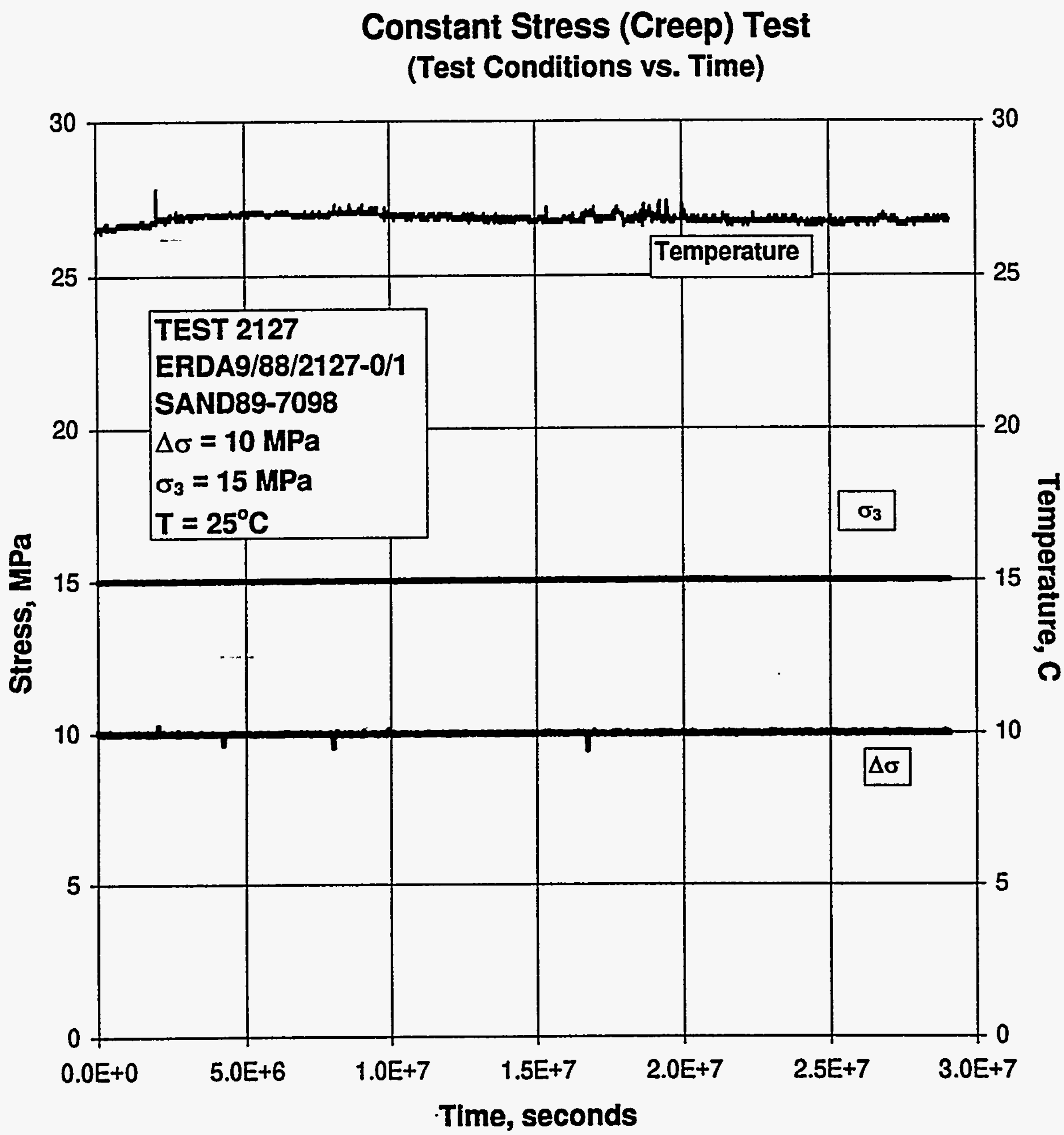

Figure B-1. Test Conditions Versus Time for a Creep Test: Specimen ERDA9/88/2127-0/1; Stage 1 of 1.

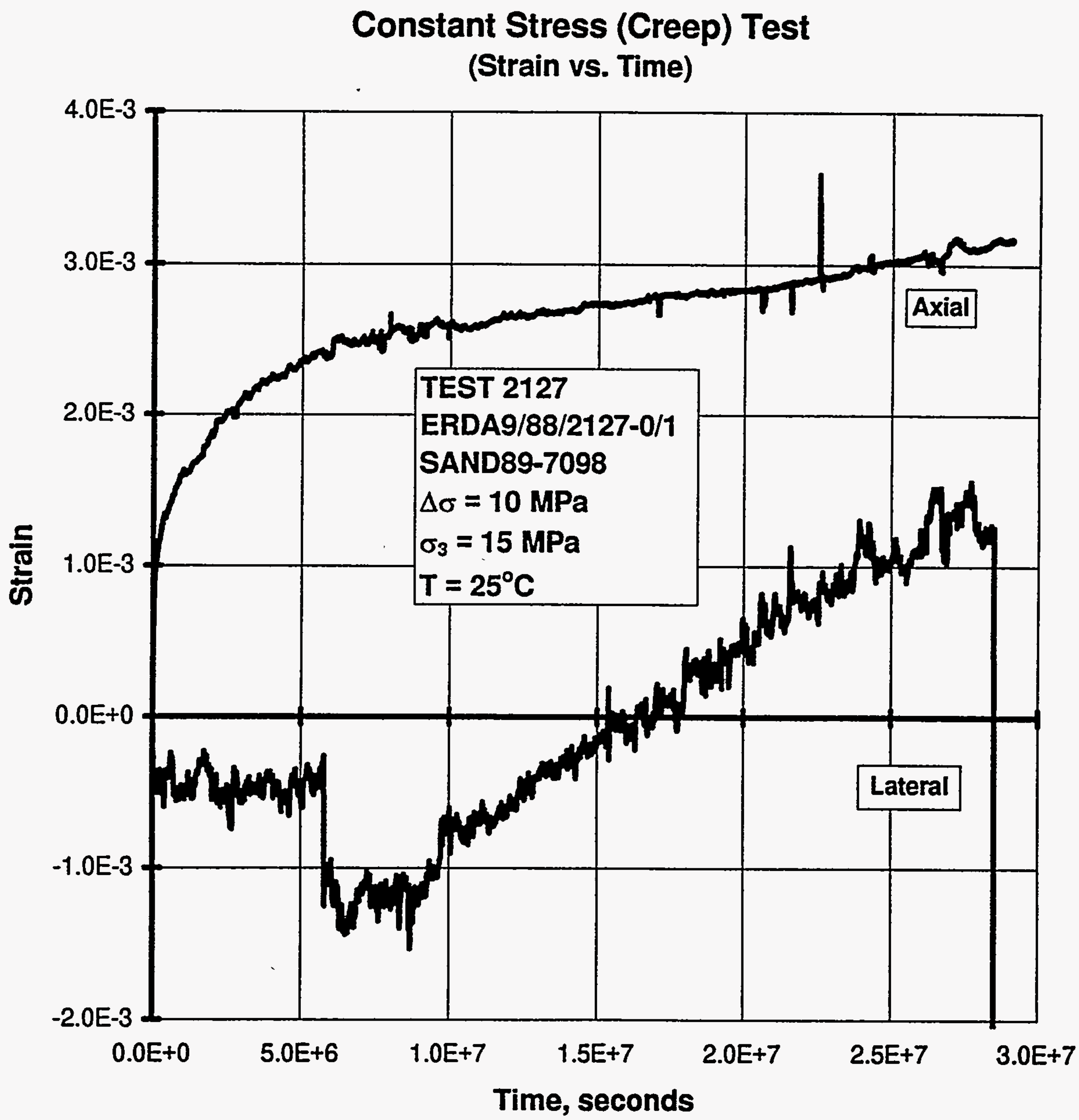

Figure B-2. Axial Strain and Lateral Strain Versus Time for a Creep Test: Specimen ERDA9/88/2127-0/1; Stage 1 of 1.

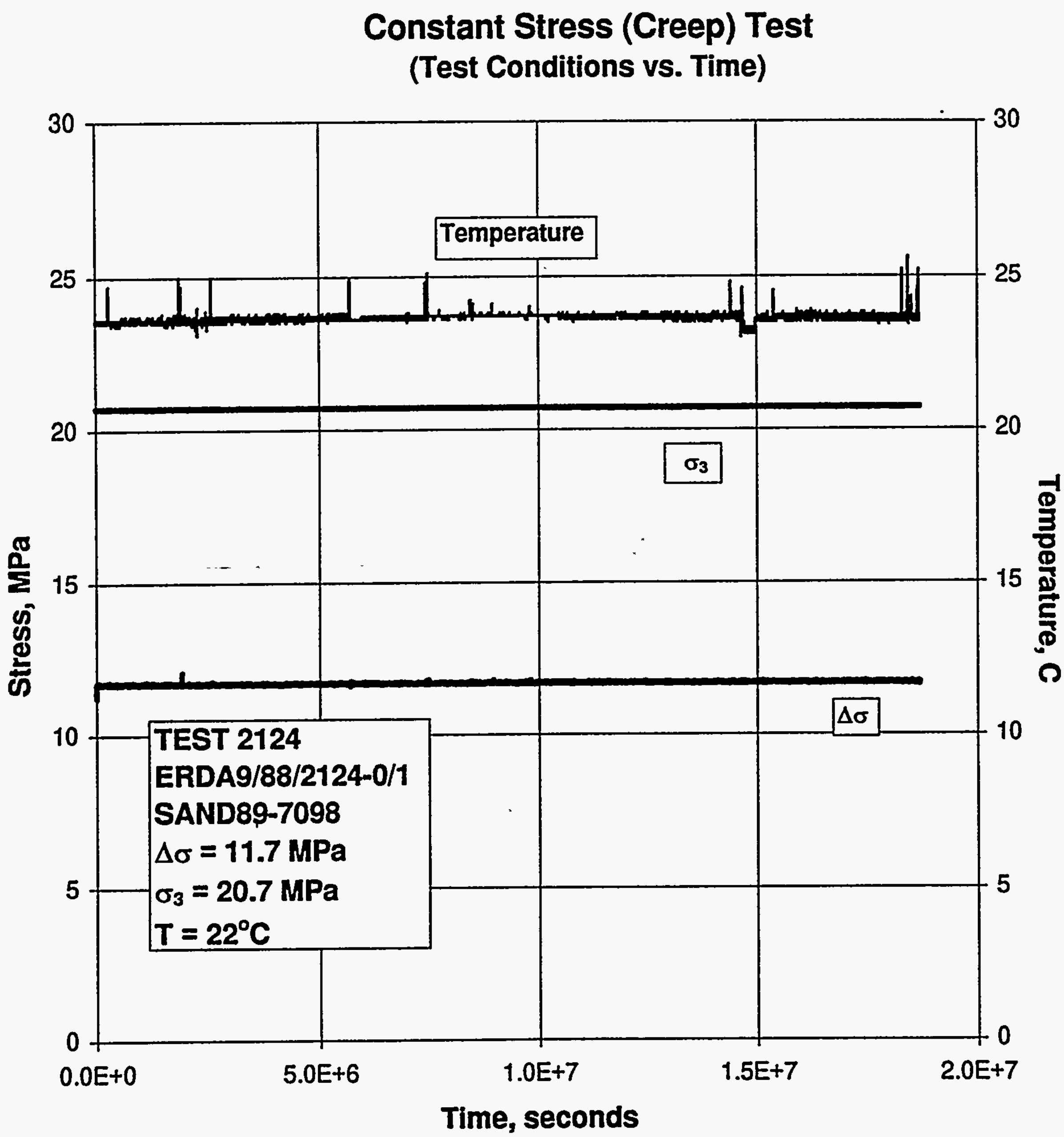

Figure B-3. Test Conditions Versus Time for a Creep Test: Specimen ERDA9/88/2124-0/1; Stage 1 of 1.

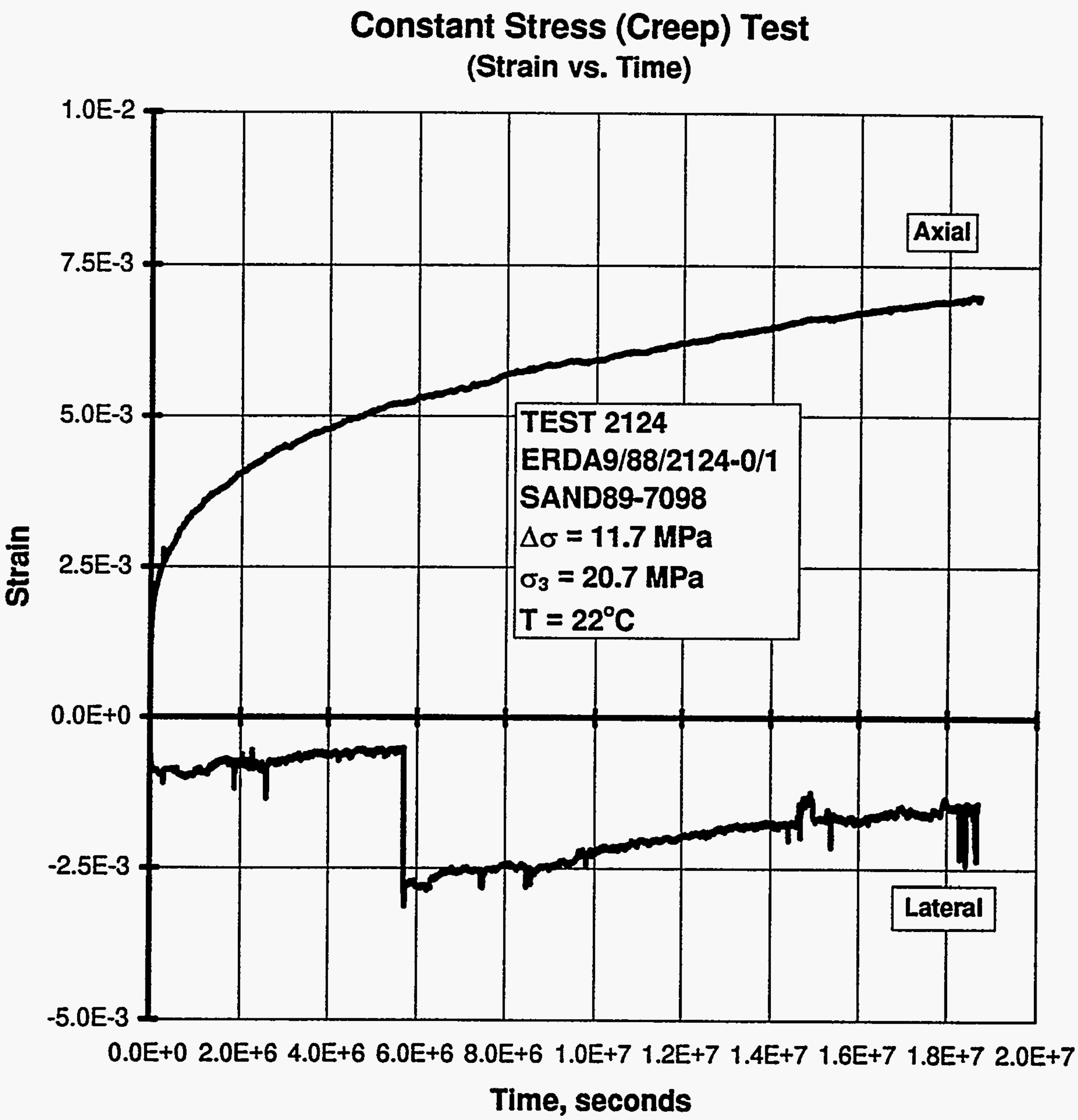

Figure B-4. Axial Strain and Lateral Strain Versus Time for a Creep Test: Specimen ERDA9/88/2124-0/1; Stage 1 of 1.

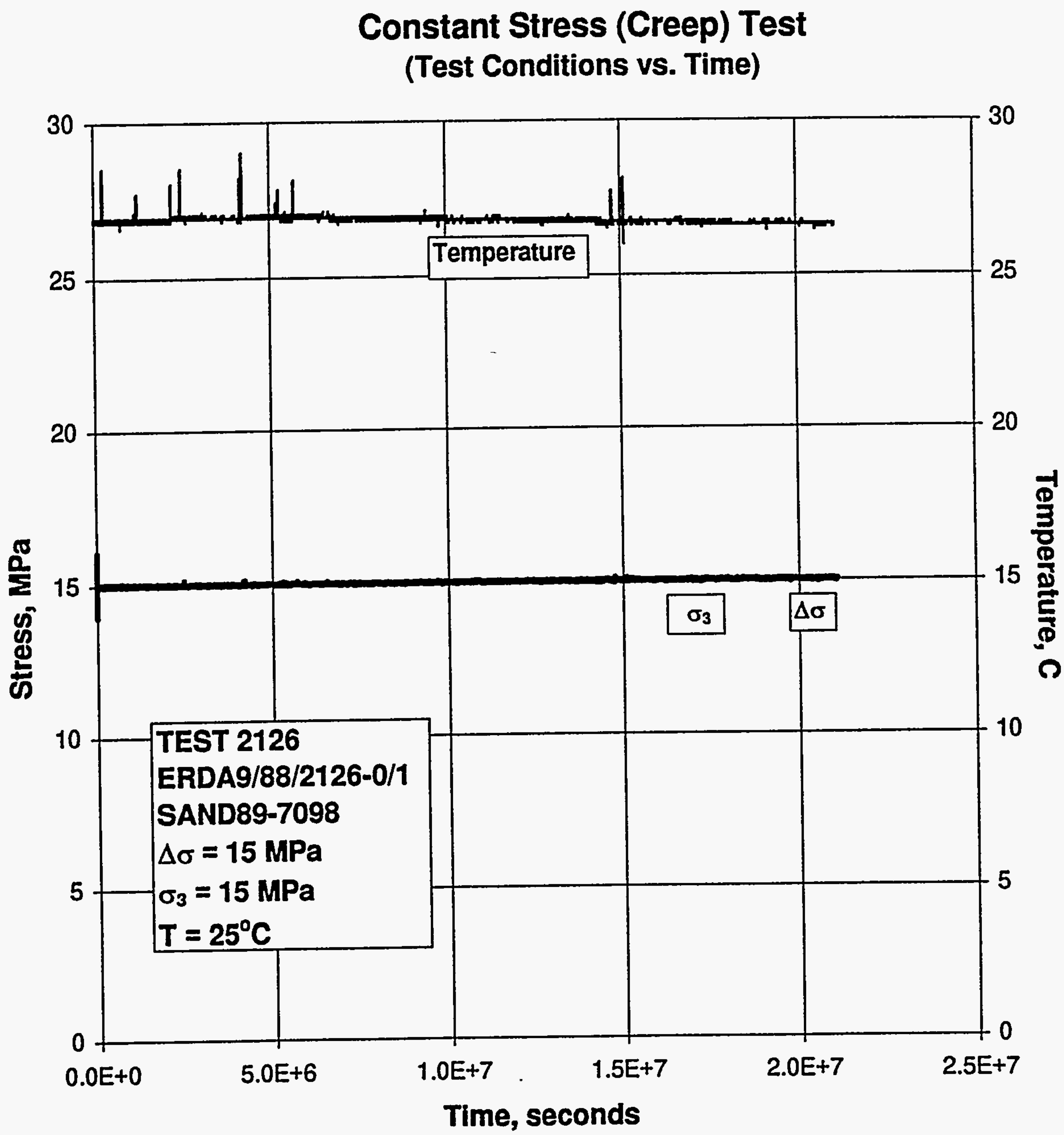

Figure B-5. Test Conditions Versus Time for a Creep Test: Specimen ERDA9/88/2126-0/1; Stage 1 of 1.

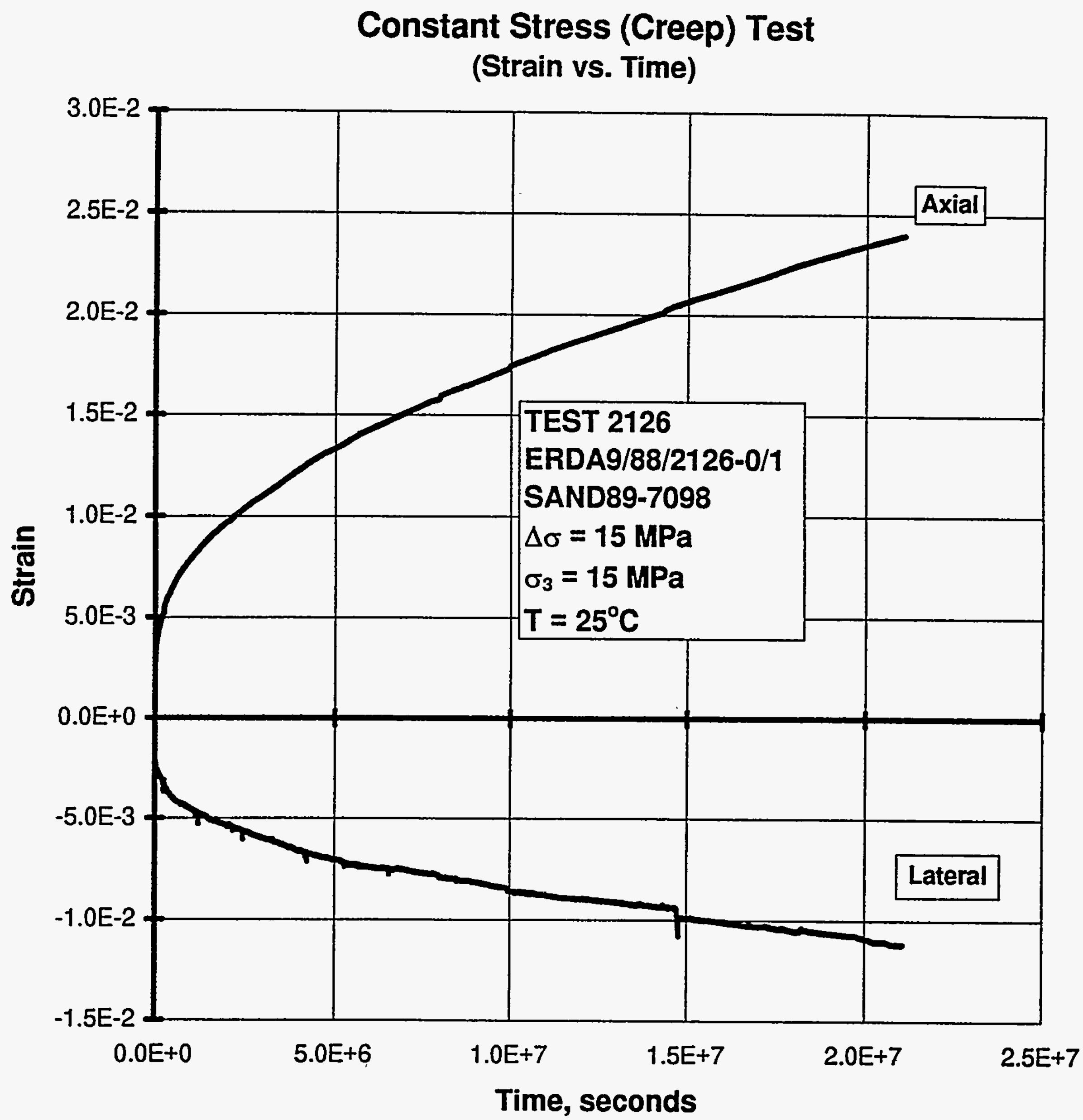

Figure B-6. Axial Strain and Lateral Strain Versus Time for a Creep Test: Specimen ERDA9/88/2126-0/1; Stage 1 of 1.

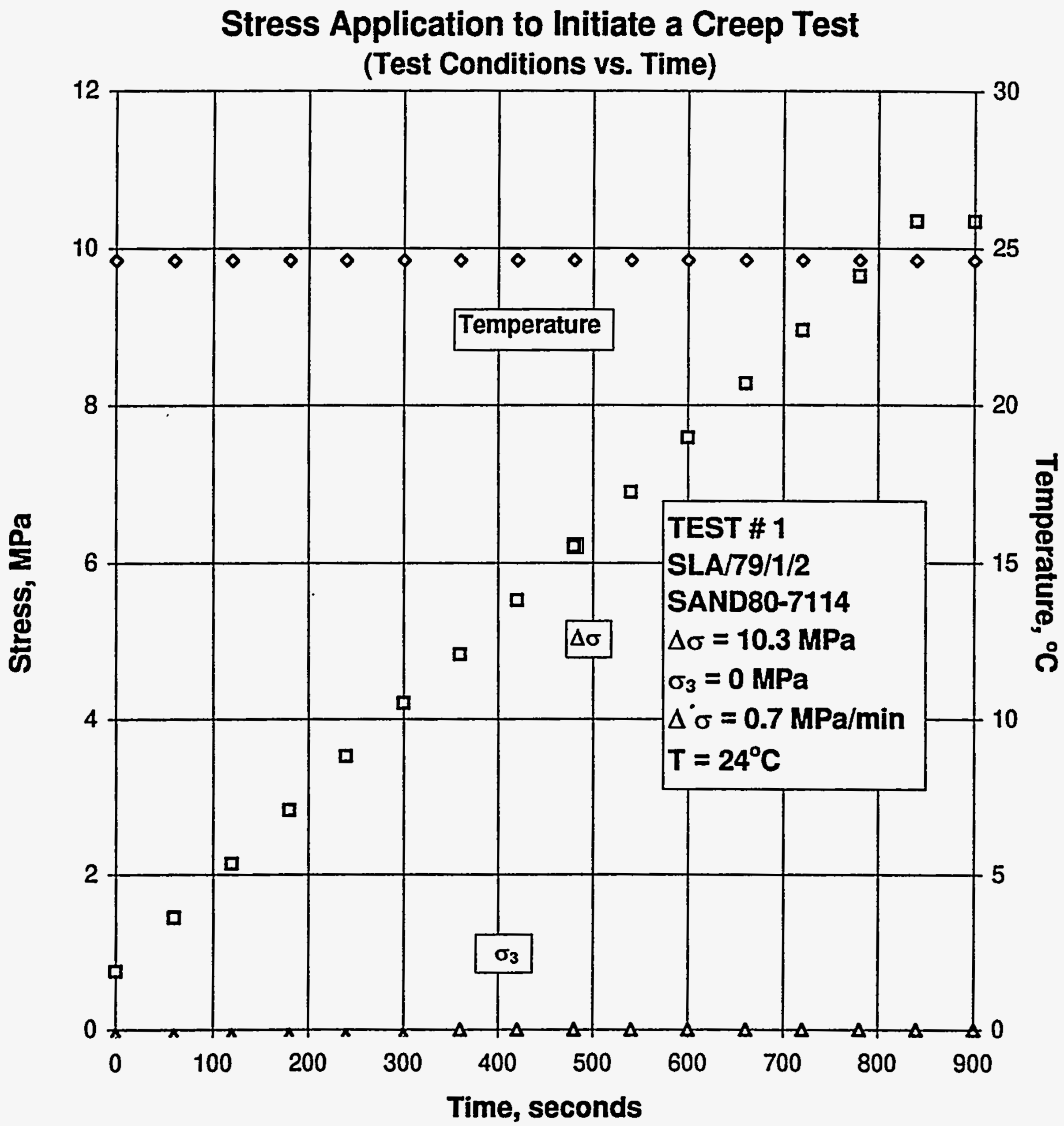

Figure B-7. Test Conditions Versus Time for Stress Application to Initiate a Creep Test: Specimen SLA/79/1/2; Stage 1 of 1.

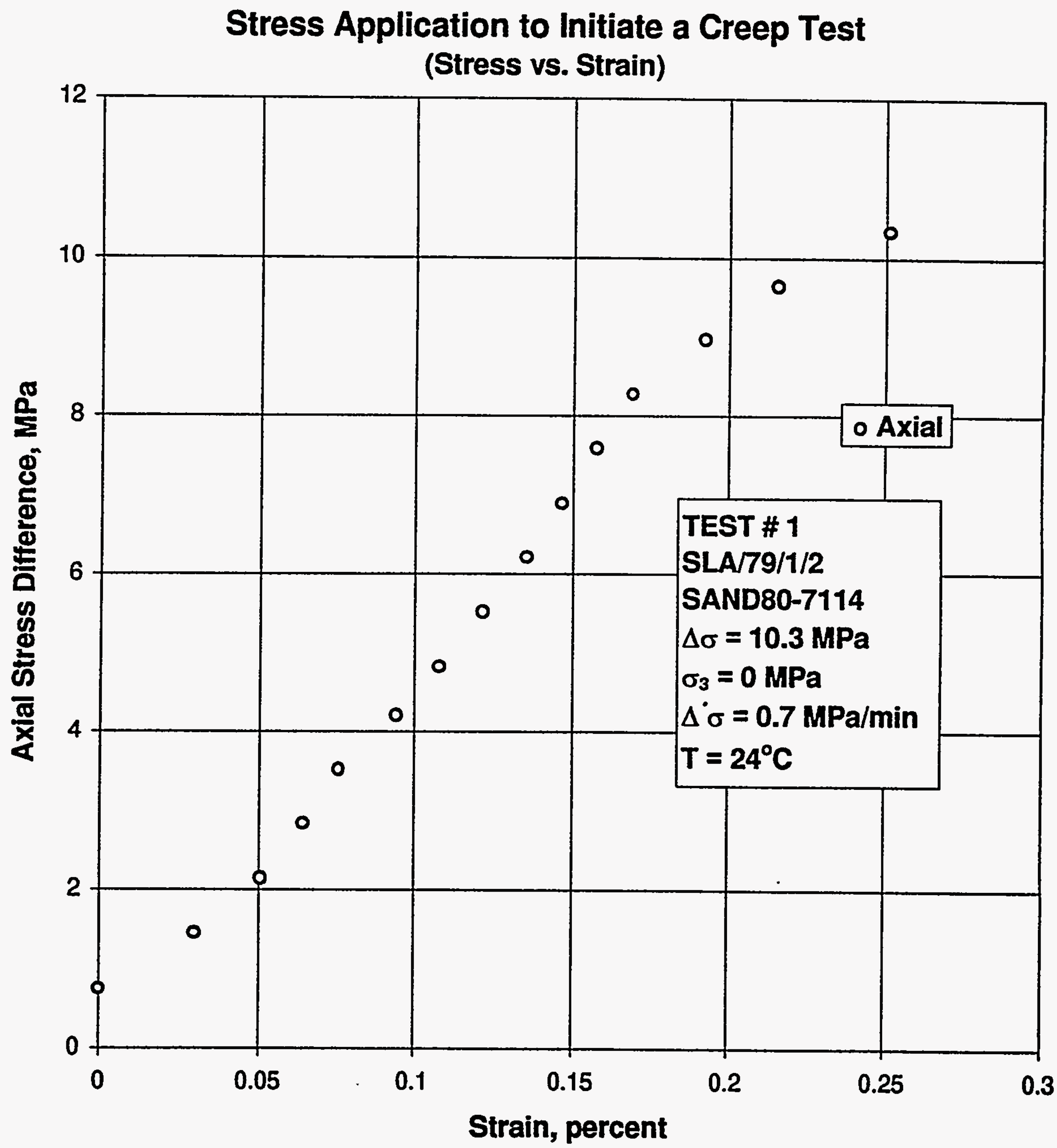

Figure B-8. Axial Stress Difference Versus Axial and Lateral Strain for Stress Application to Initiate a Creep Test: Specimen SLA/79/1/2; Stage 1 of 1.

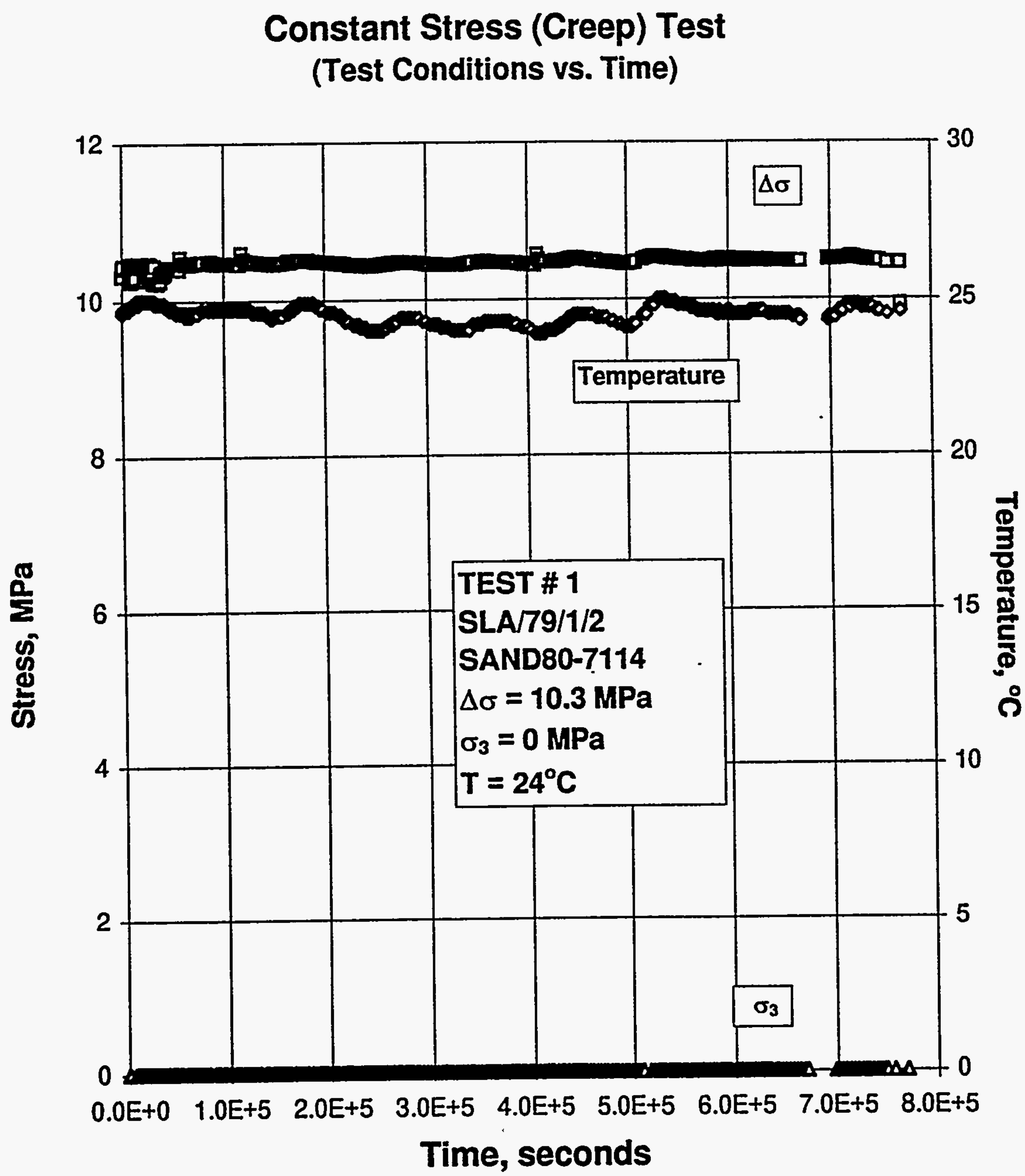

Figure B-9. Test Conditions Versus Time for a Creep Test: Specimen SLA/79/1/2; Stage 1 of 1.

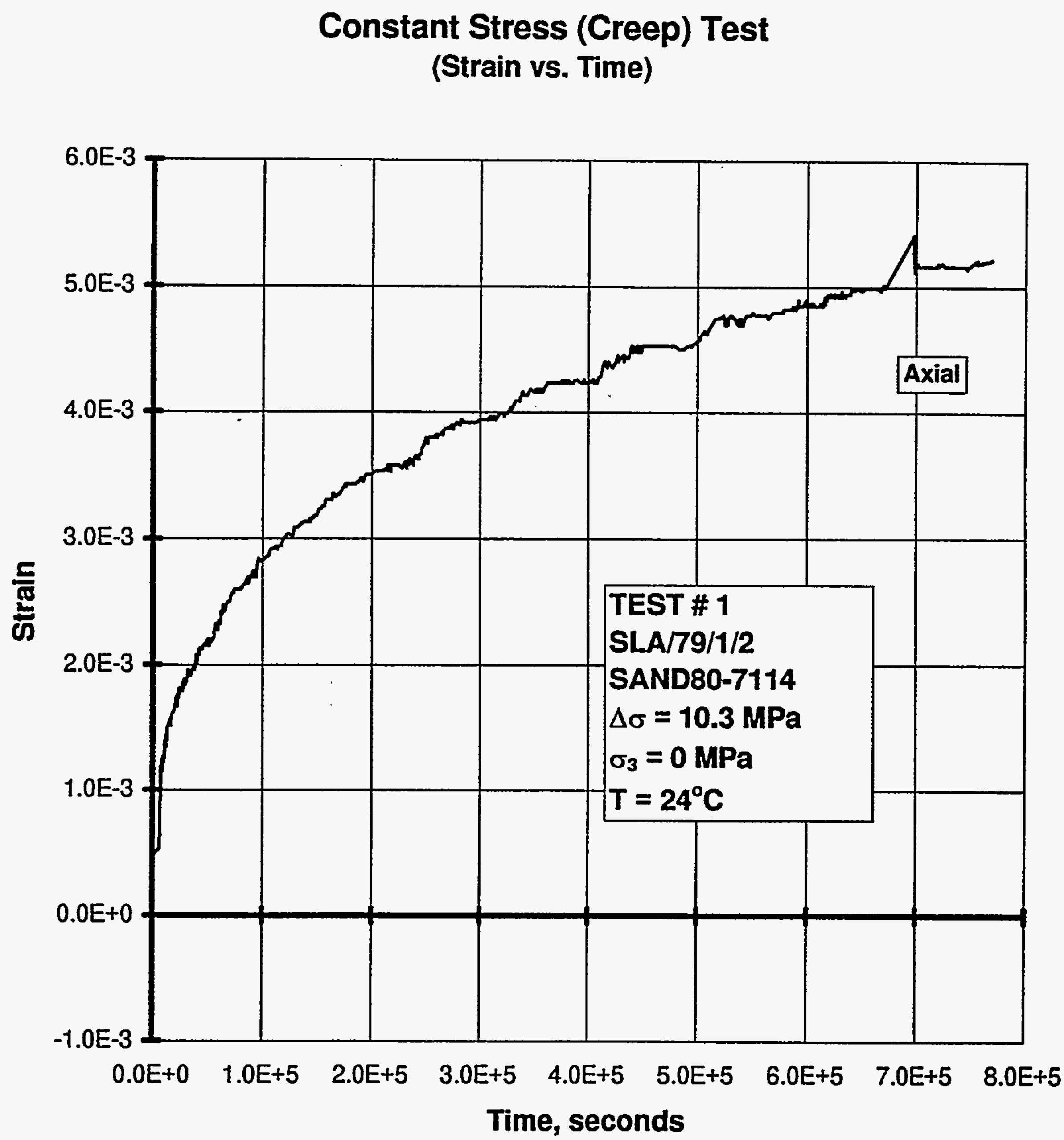

Figure B-10. Axial Strain and Lateral Strain Versus Time for a Creep Test: Specimen SLA/79/1/2; Stage 1 of 1 (Data Acquisition Failure at 9 Days. Data Before 9 Days is Valid).

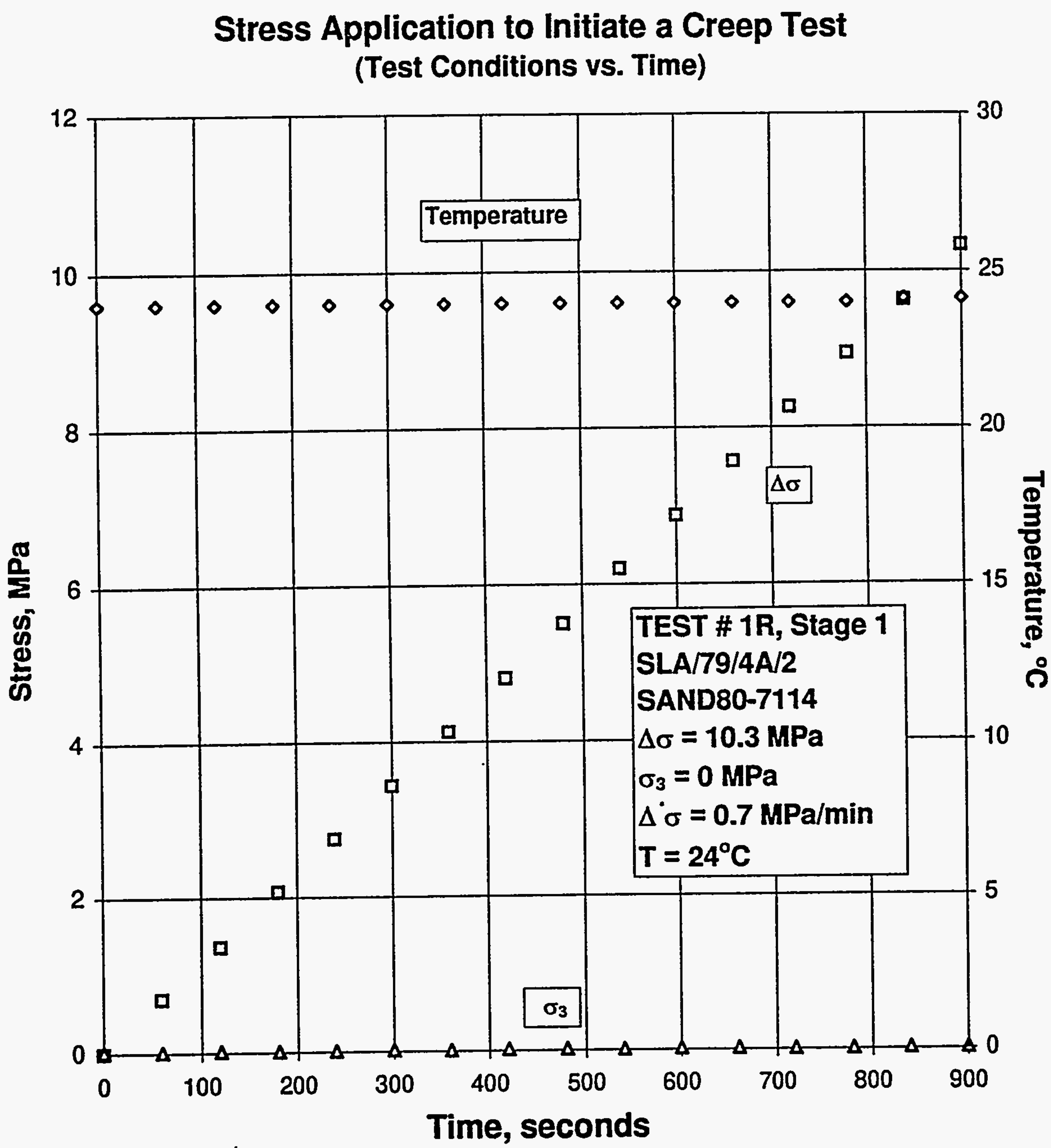

Figure B-11. Test Conditions Versus Time for Stress Application to Initiate a Creep Test: Specimen SLA/79/4A/2; Stage 1 of 2.

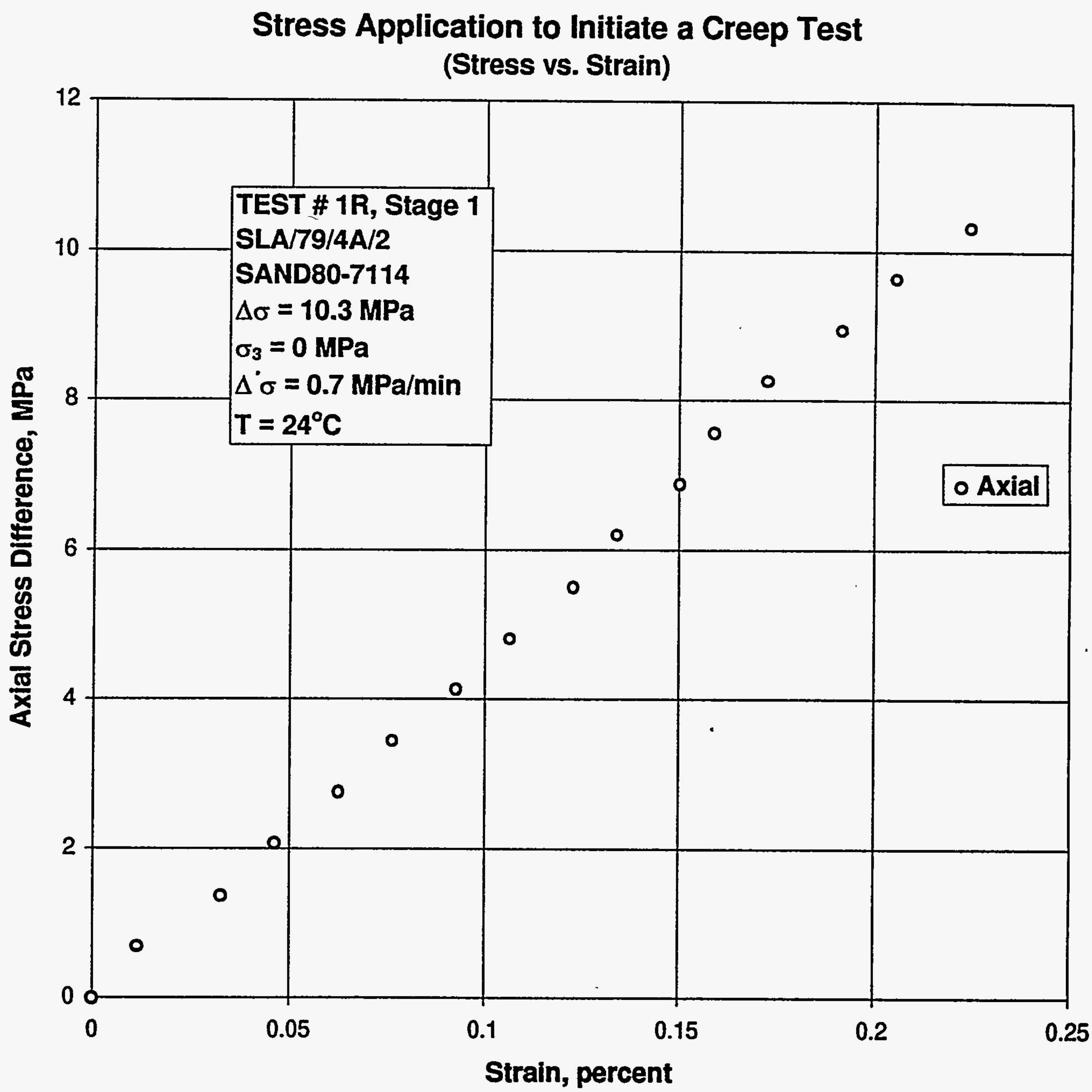

Figure B-12. Axial Stress Difference Versus Axial and Lateral Strain for Stress Application to Initiate a Creep Test: Specimen SLA/79/4A/2; Stage 1 on 2.

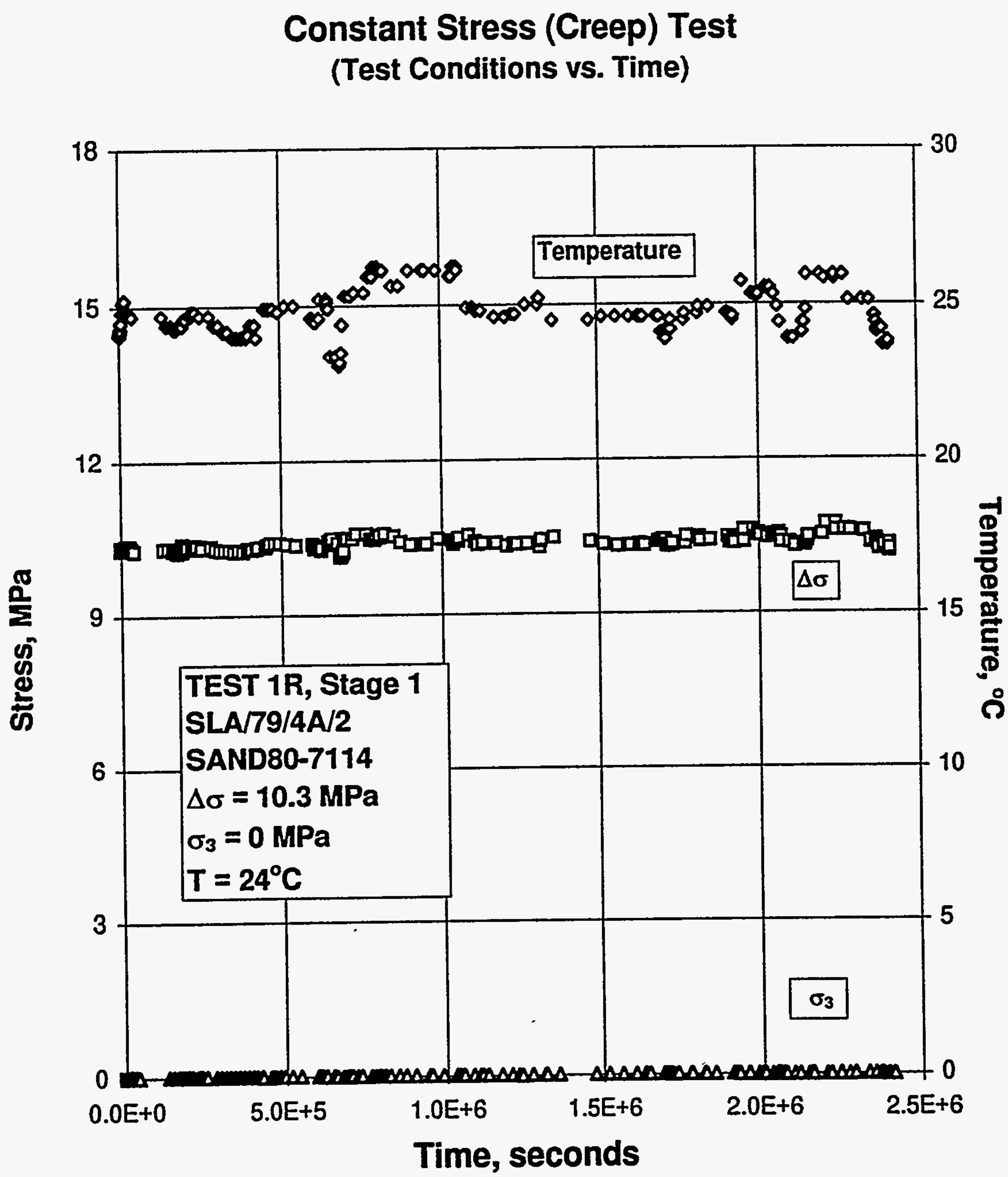

Figure B-13. Test Conditions Versus Time for a Creep Test: Specimen SLA/79/4A/2; Stage 1 of 2.

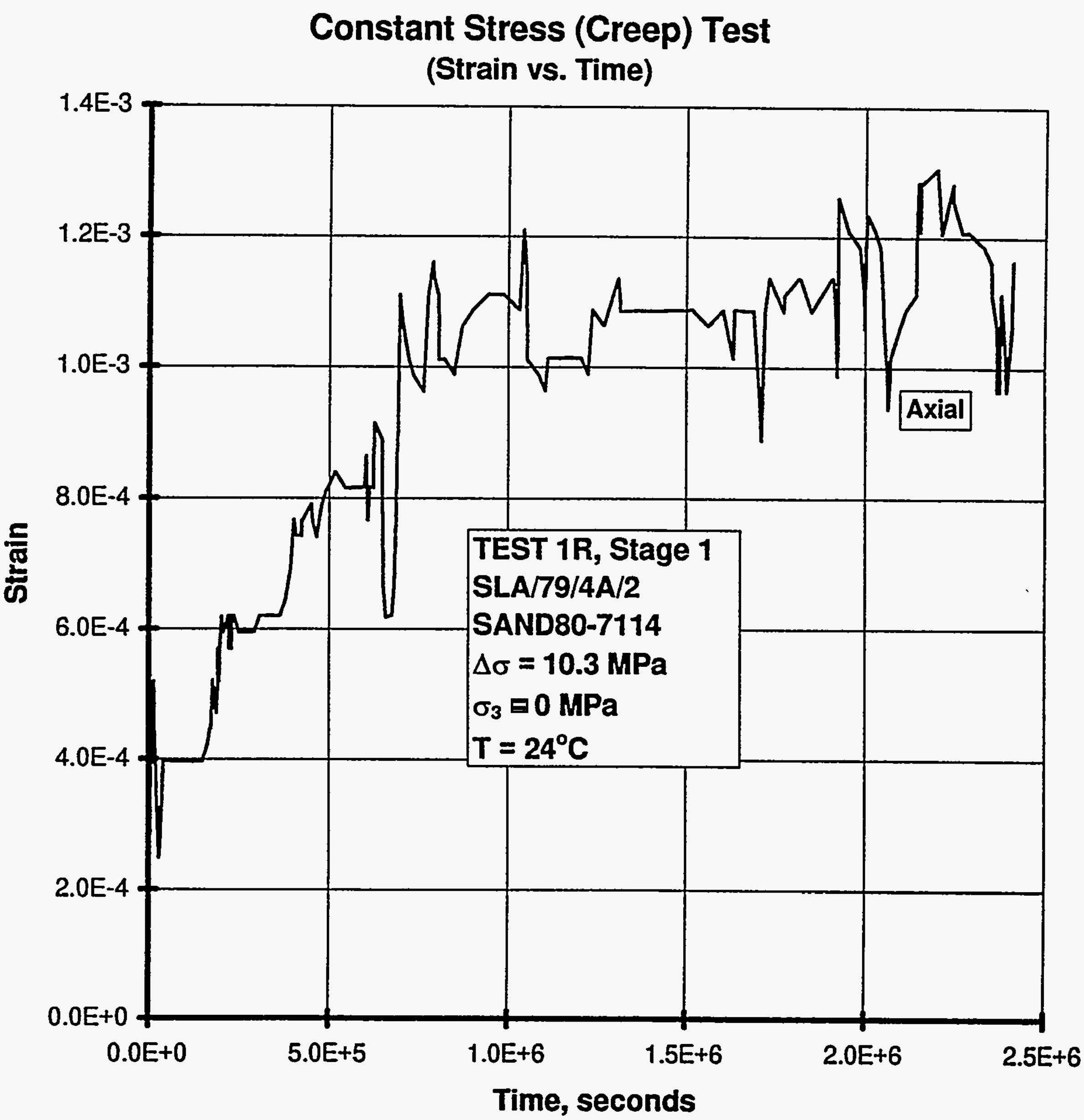

Figure B-14. Axial Strain and Lateral Strain Versus Time for a Creep Test: Specimen SLA/79/4A/2; Stage 1 of 2.

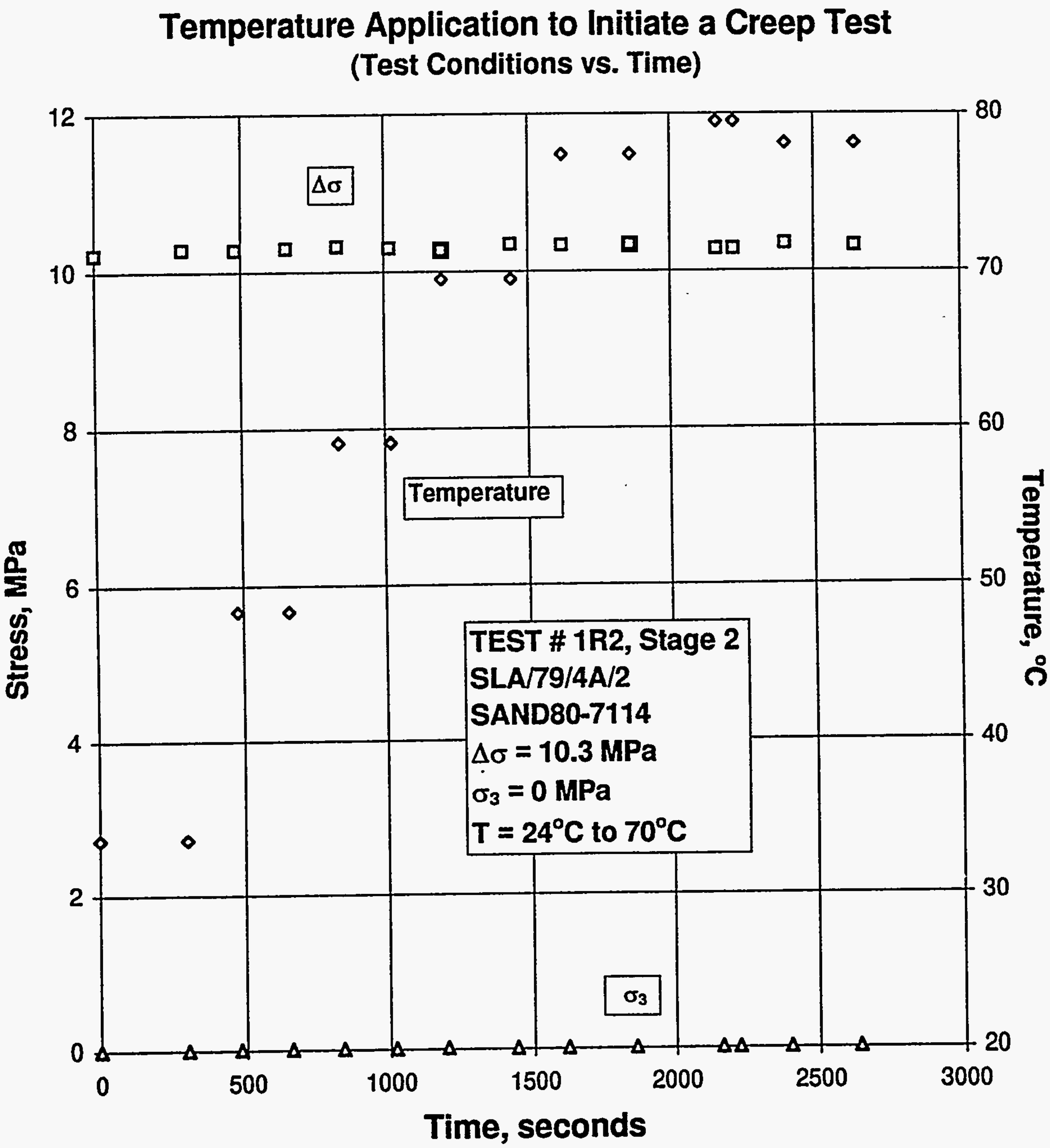

Figure B-15. Test Conditions Versus Time for Temperature Application to Initiate a Creep Test: Specimen SLA/79/4A/2; Stage 2 of 2.

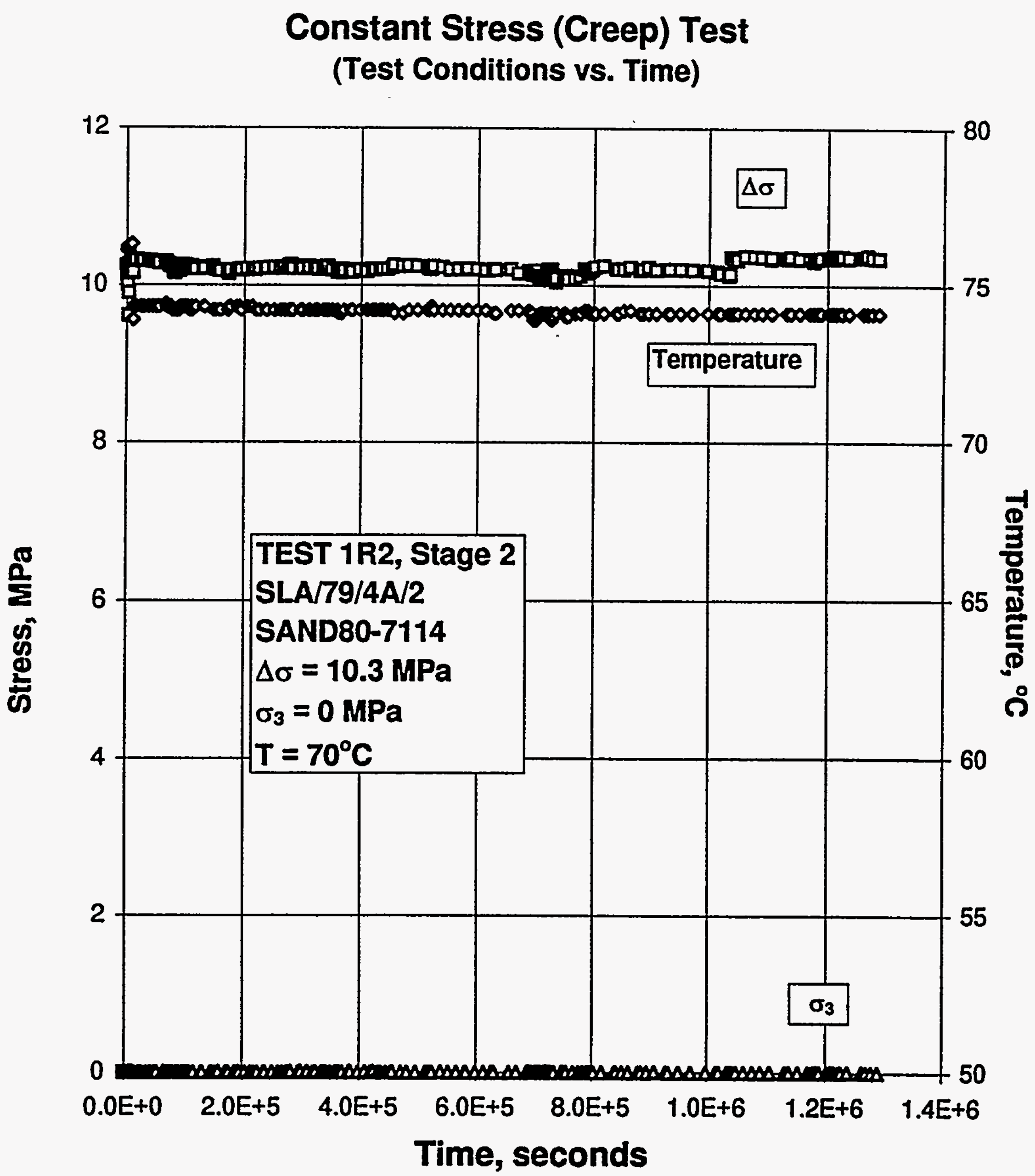

Figure B-16. Test Conditions Versus Time for a Creep Test: Specimen SLA/79/4A/2; Stage 2 of 2.

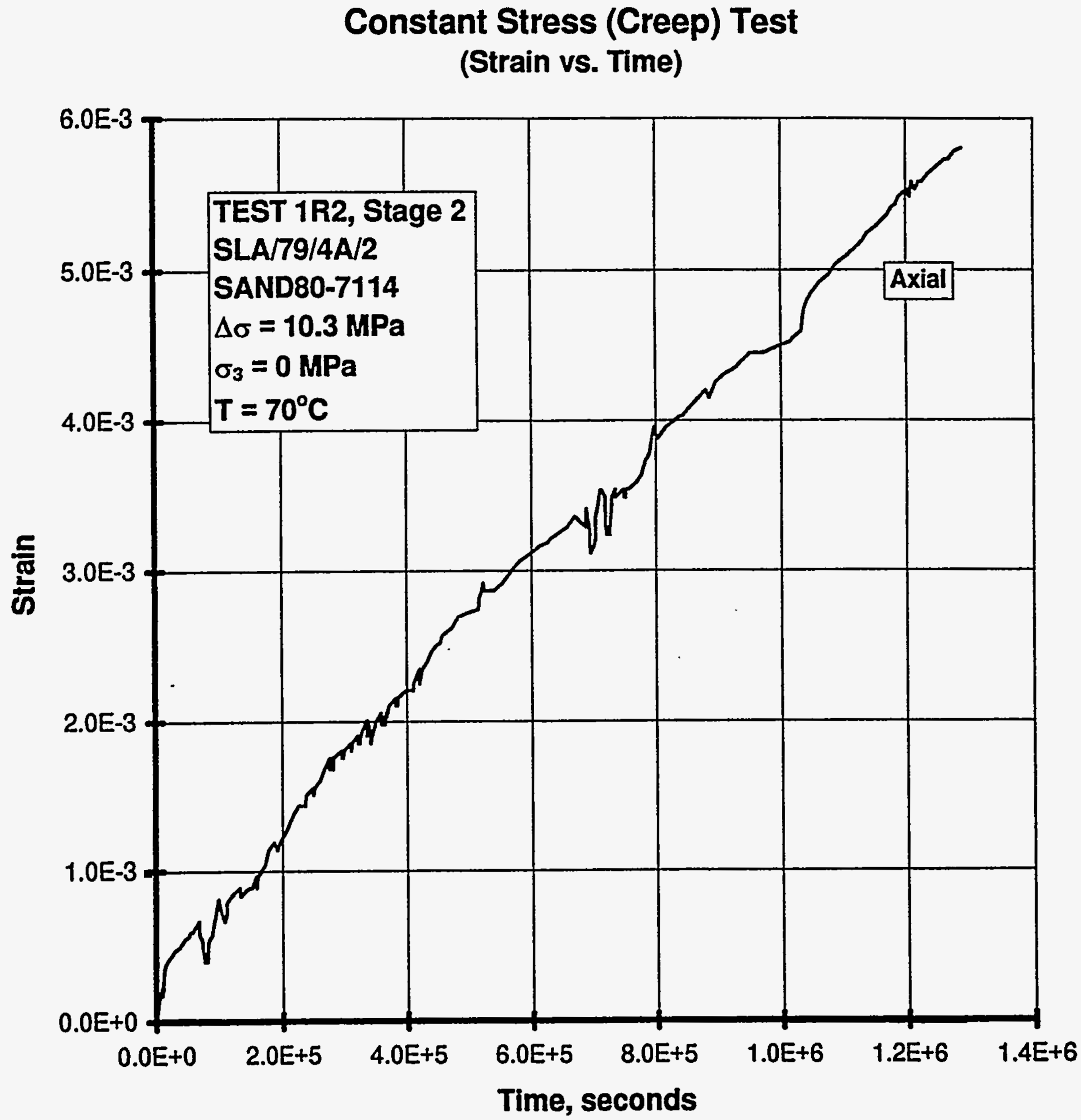

Figure B-17. Axial Strain and Lateral Strain Versus Time for a Creep Test: Specimen SLA/79/4A/2; Stage 2 of 2.

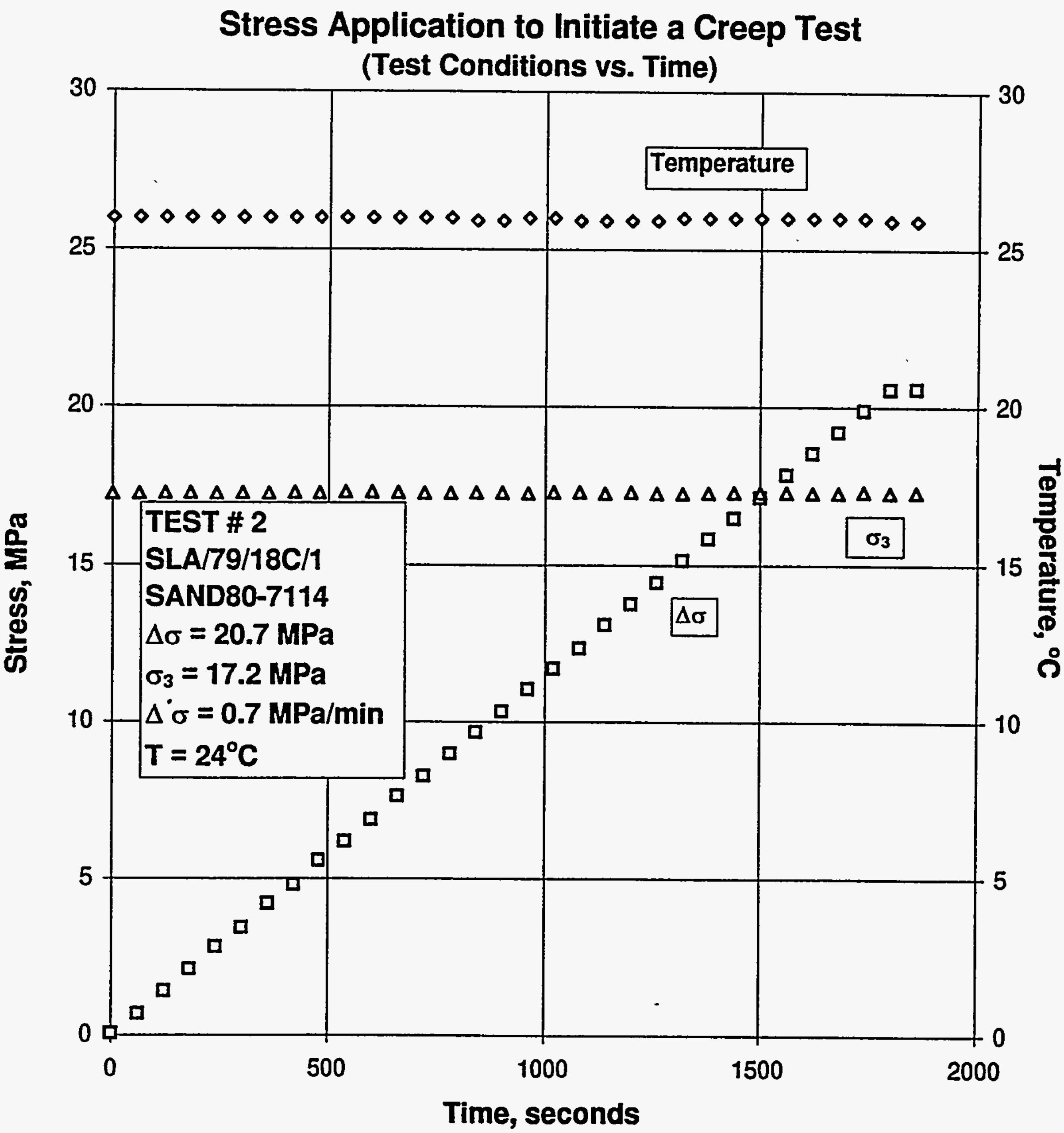

Figure B-18. Test Conditions Versus Time for Stress Application to Initiate a Creep Test: Specimen SLA/79/18C/1; Stage 1 of 1.

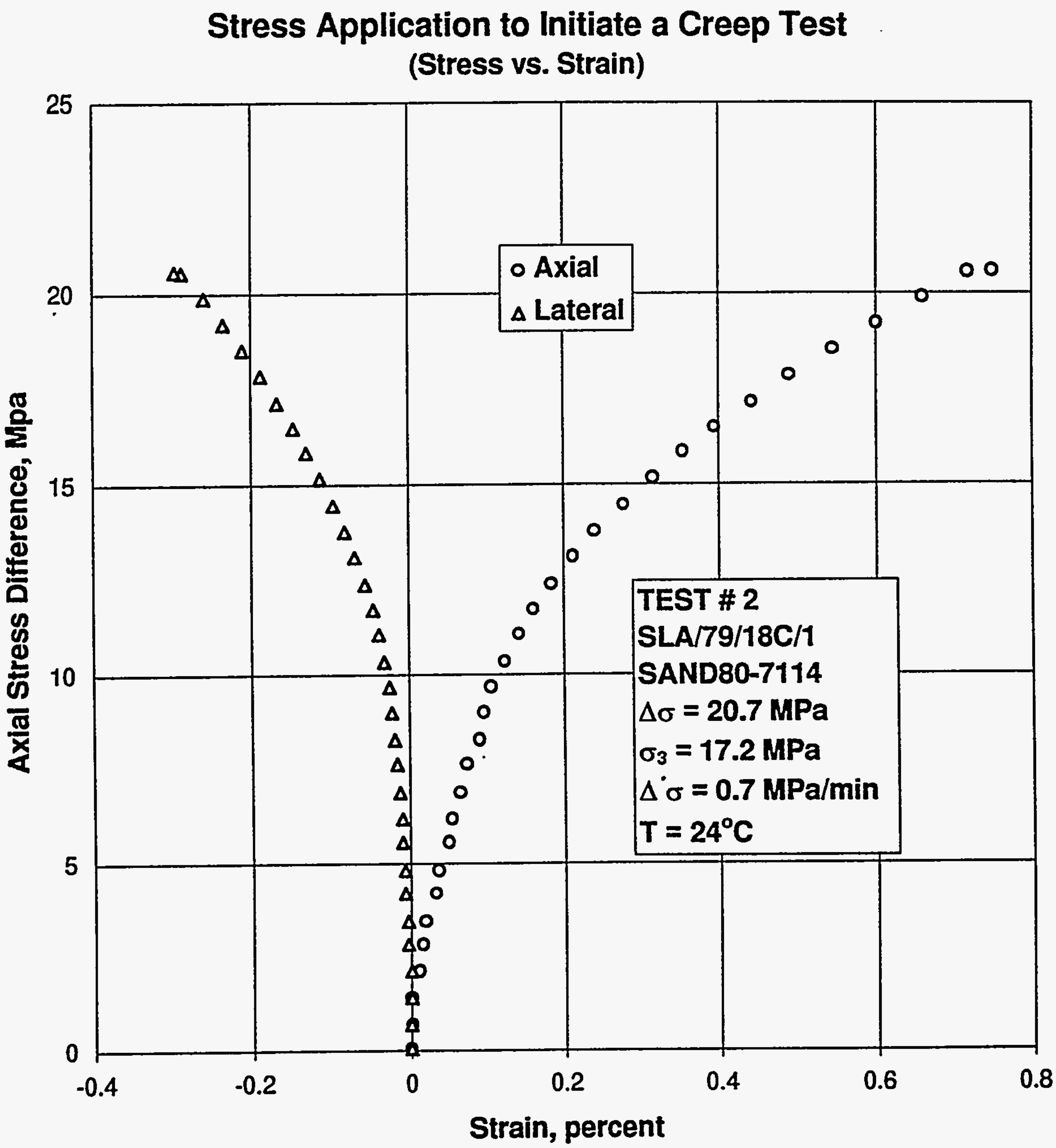

Figure B-19. Axial Stress Difference Versus Axial and Lateral Strain for Stress Application to Initiate a Creep Test: Specimen SLA/79/18C/1; Stage 1 of 1.

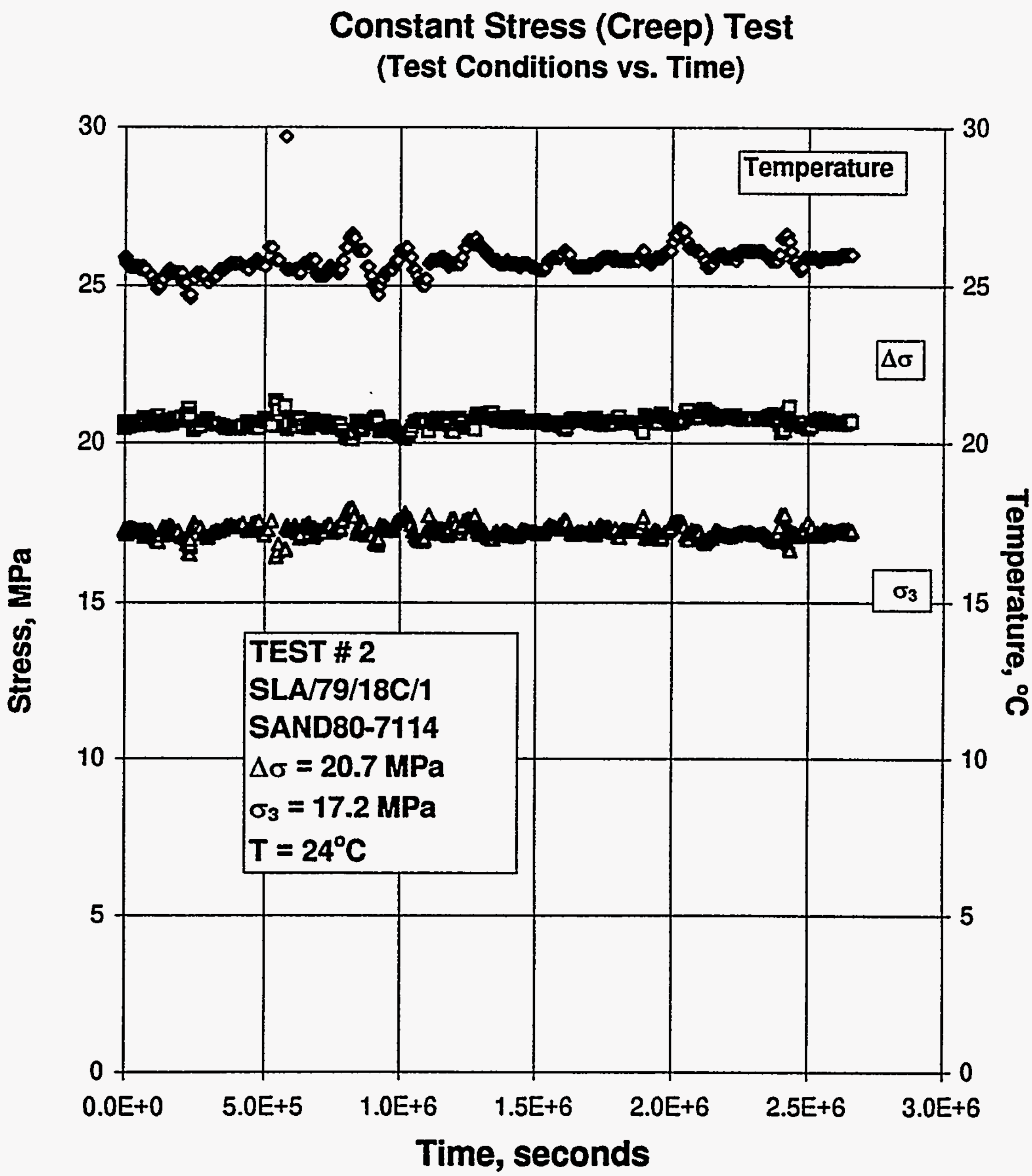

Figure B-20. Test Conditions Versus Time for a Creep Test: Specimen SLA/79/18C/1; Stage 1 of 1.

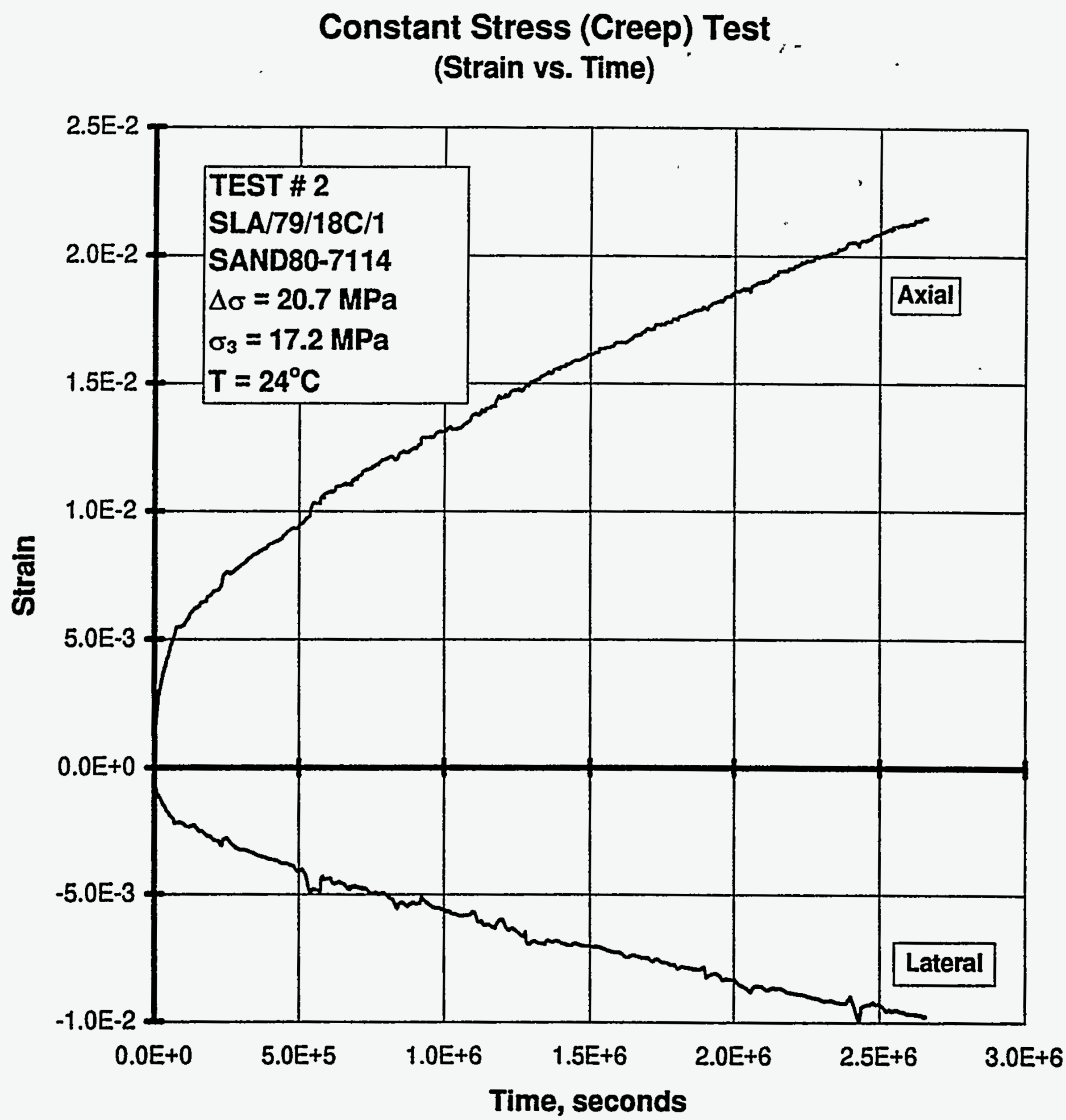

Figure B-21. Axial Strain and Lateral Strain Versus Time for a Creep Test: Specimen SLA/79/18C/1; Stage 1 of 1.

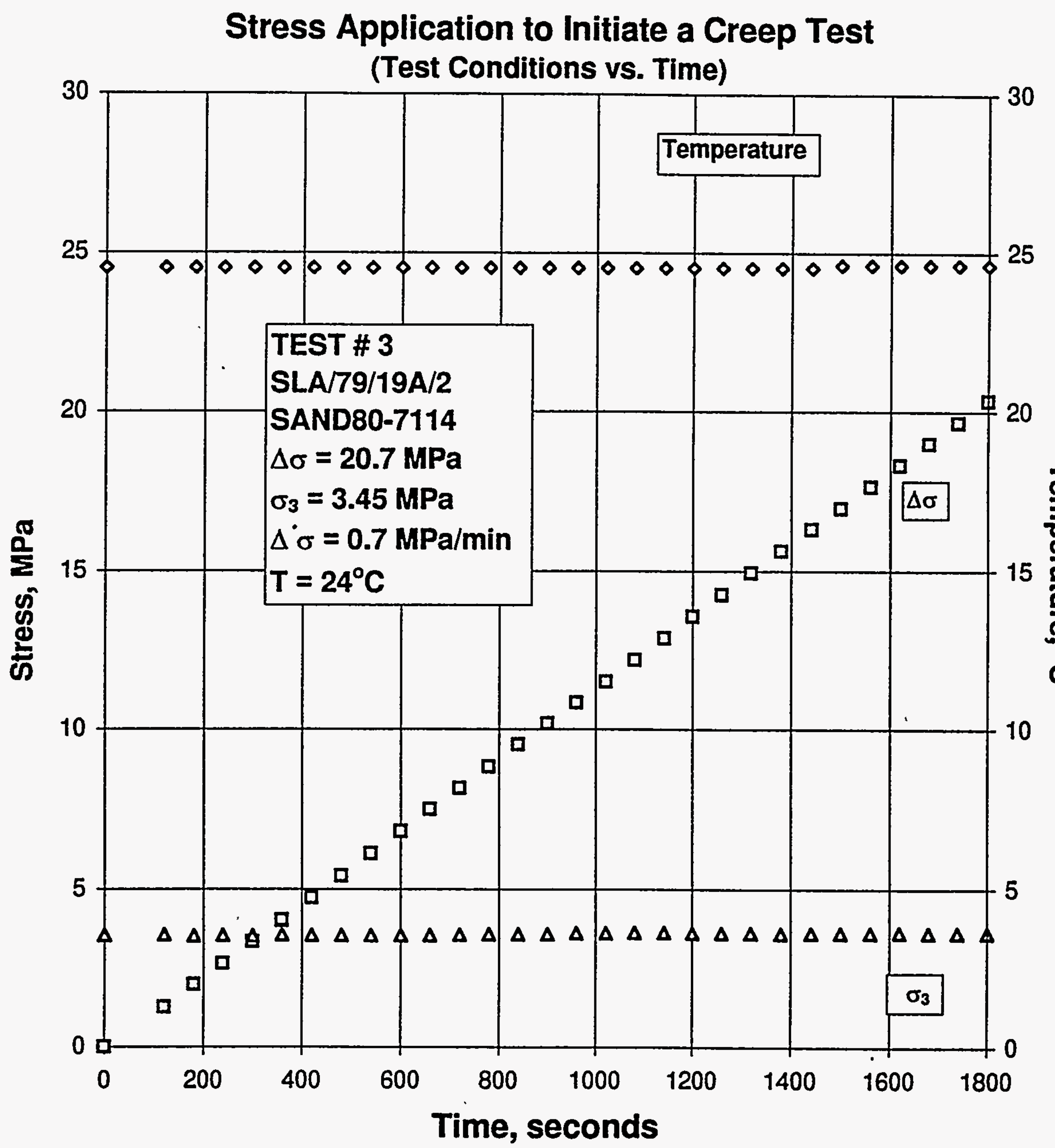

Figure B-22. Test Conditions Versus Time for Stress Application to Initiate a Creep Test: Specimen SLA/79/19A/2; Stage 1 of 1.

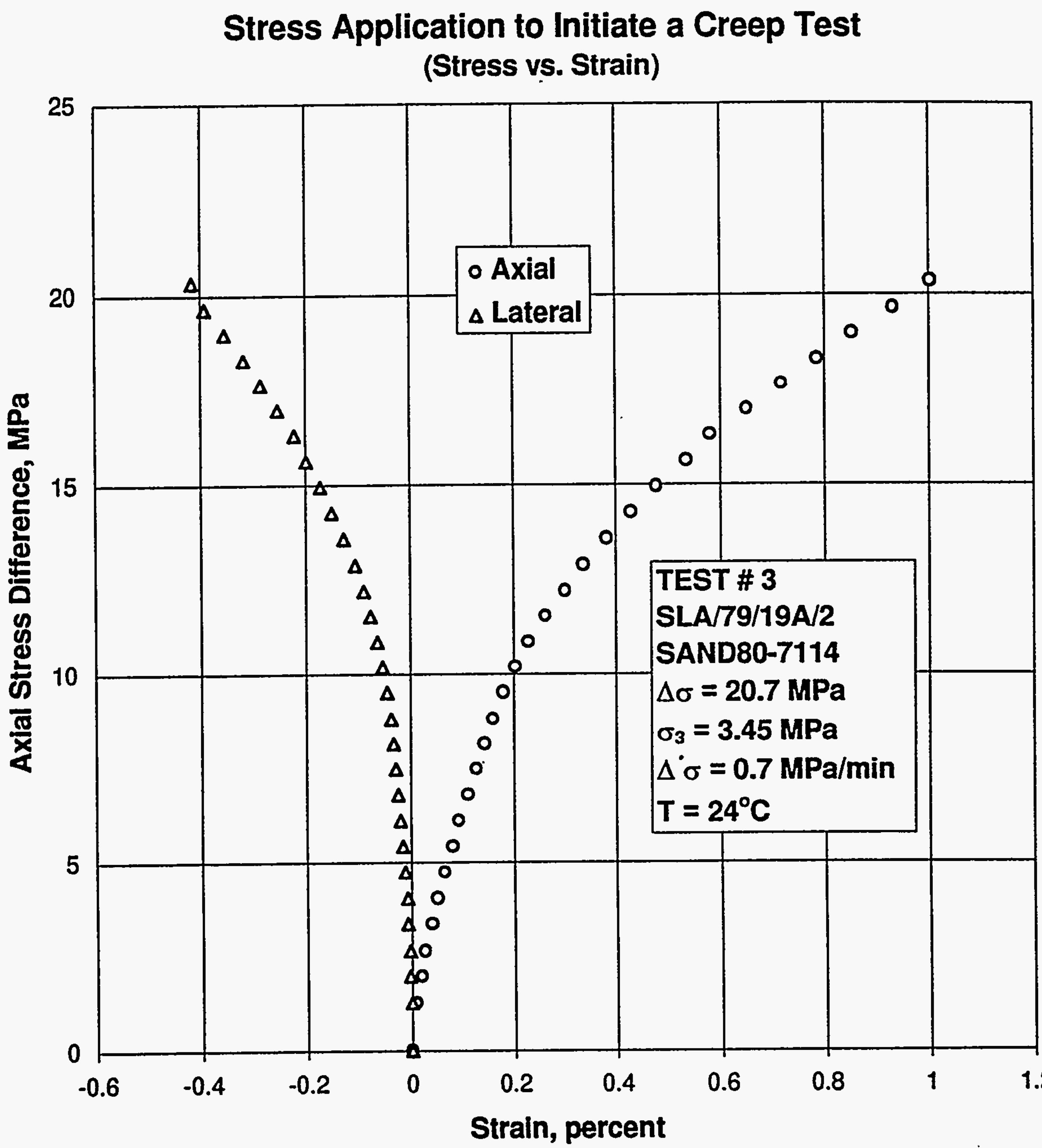

Figure B-23. Axial Stress Difference Versus Axial and Lateral Strain for Stress Application to Initiate a Creep Test: Specimen SLA/79/19A/2; Stage 1 of 1.

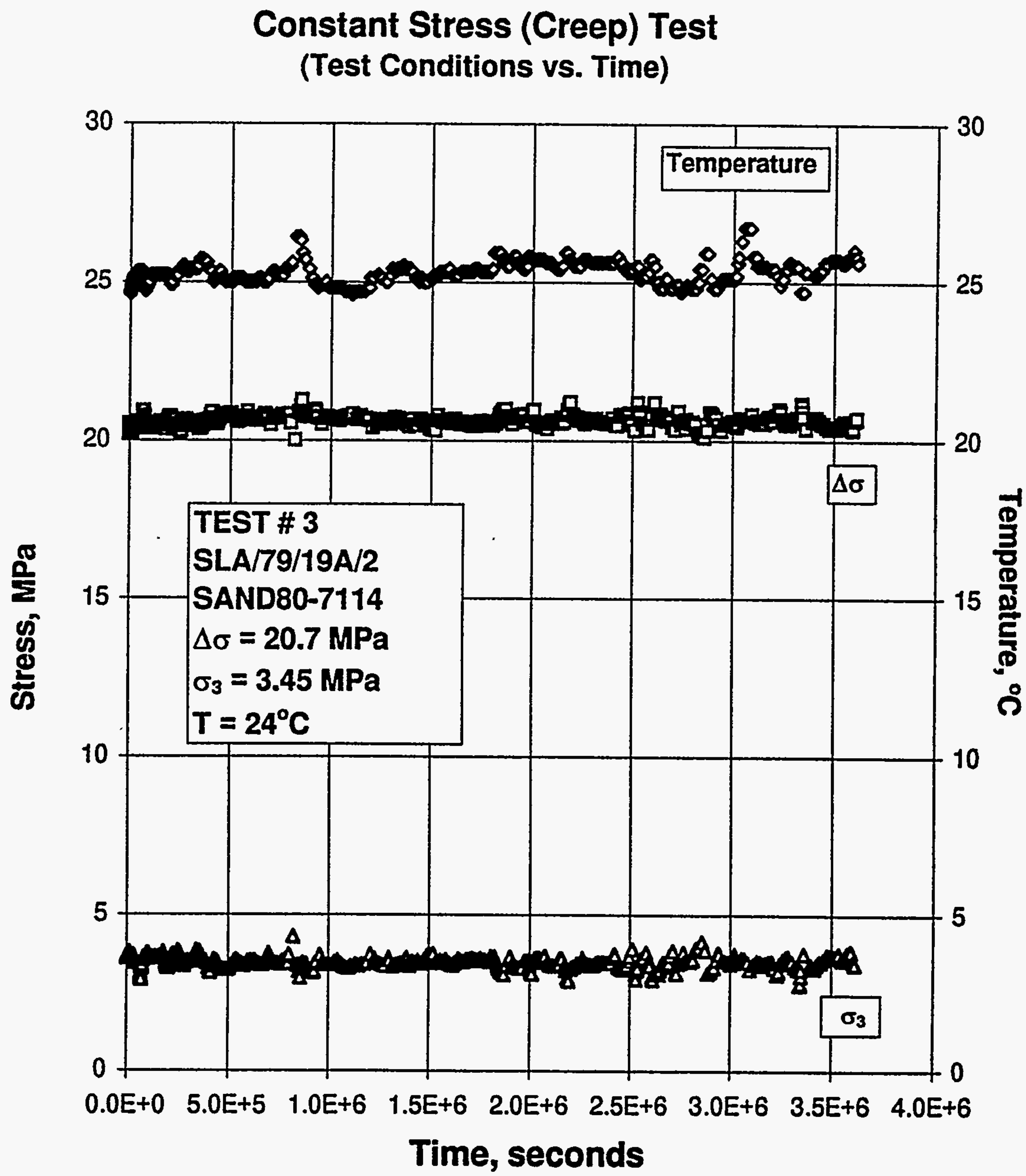

Figure B-24. Test Conditions Versus Time for a Creep Test: Specimen SLA/79/19A/2; Stage 1 of 1.

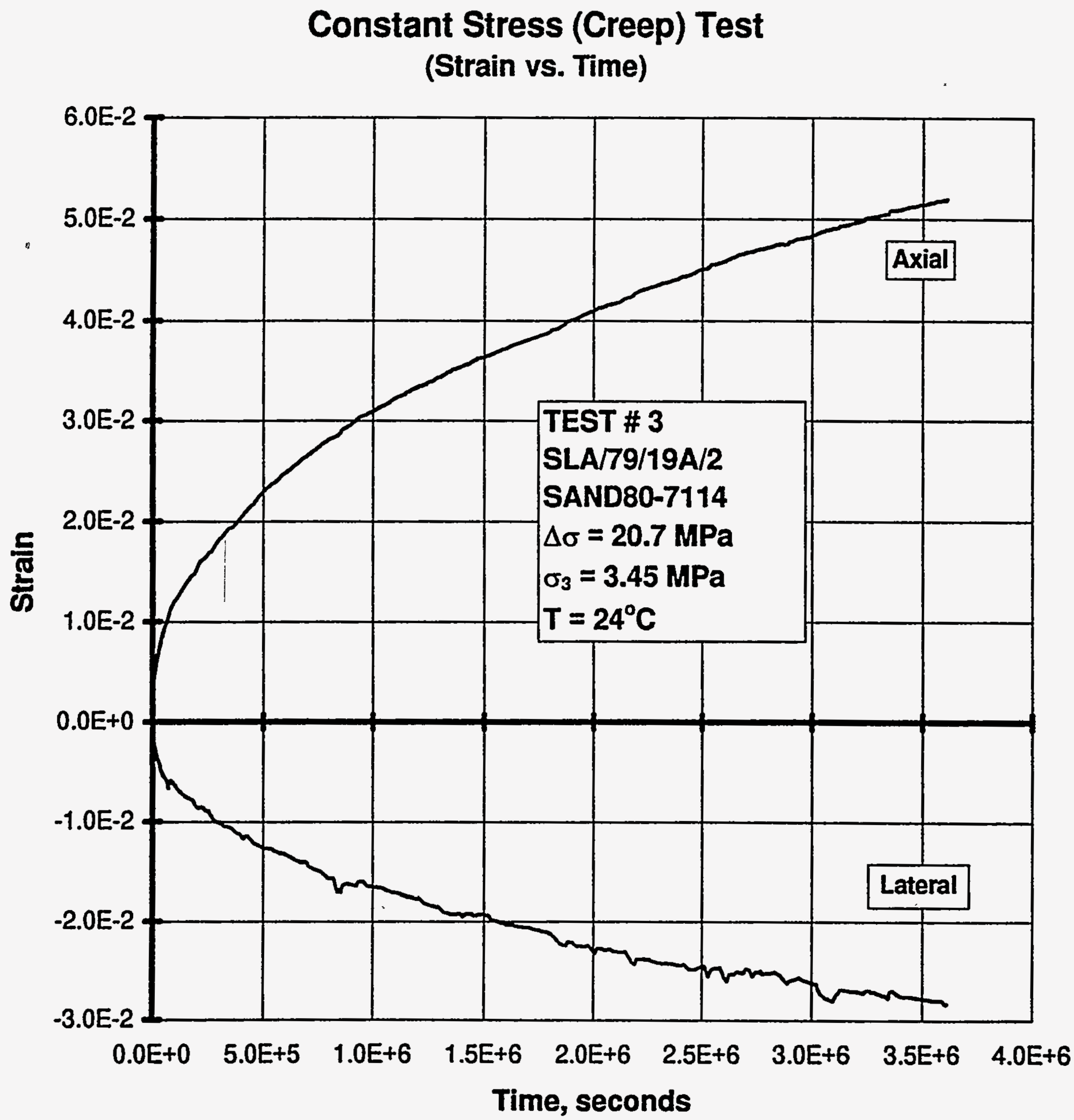

Figure B-25. Axial Strain and Lateral Strain Versus Time for a Creep Test: Specimen SLA/79/19A/2; Stage 1 of 1.

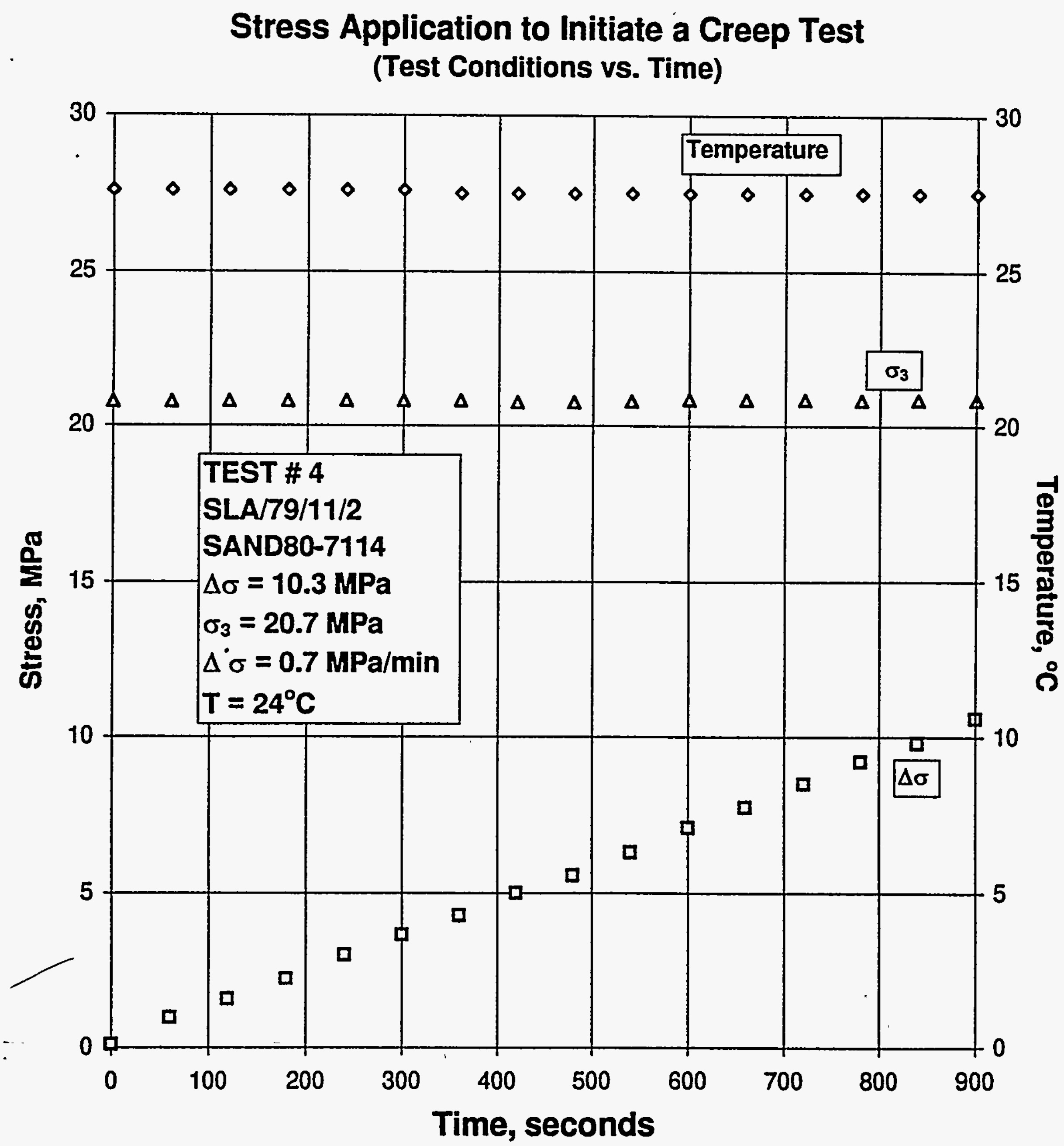

Figure B-26. Test Conditions Versus Time for Stress Application to Initiate a Creep Test: Specimen SLA/79/11/2; Stage 1 of 1.

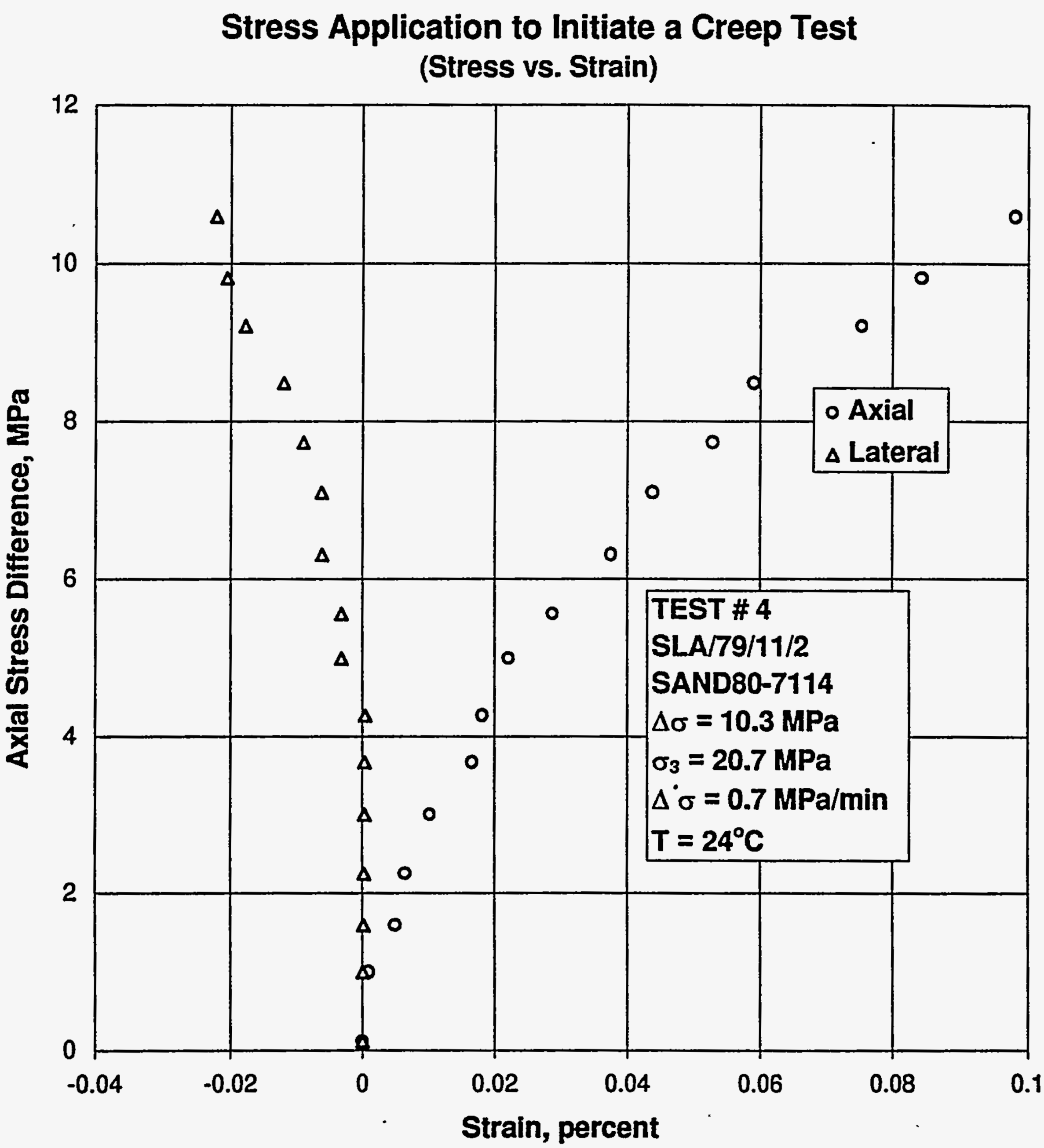

Figure B-27. Axial Stress Difference Versus Axial and Lateral Strain for Stress Application to Initiate a Creep Test: Specimen SLA/79/11/2; Stage 1 of 1.

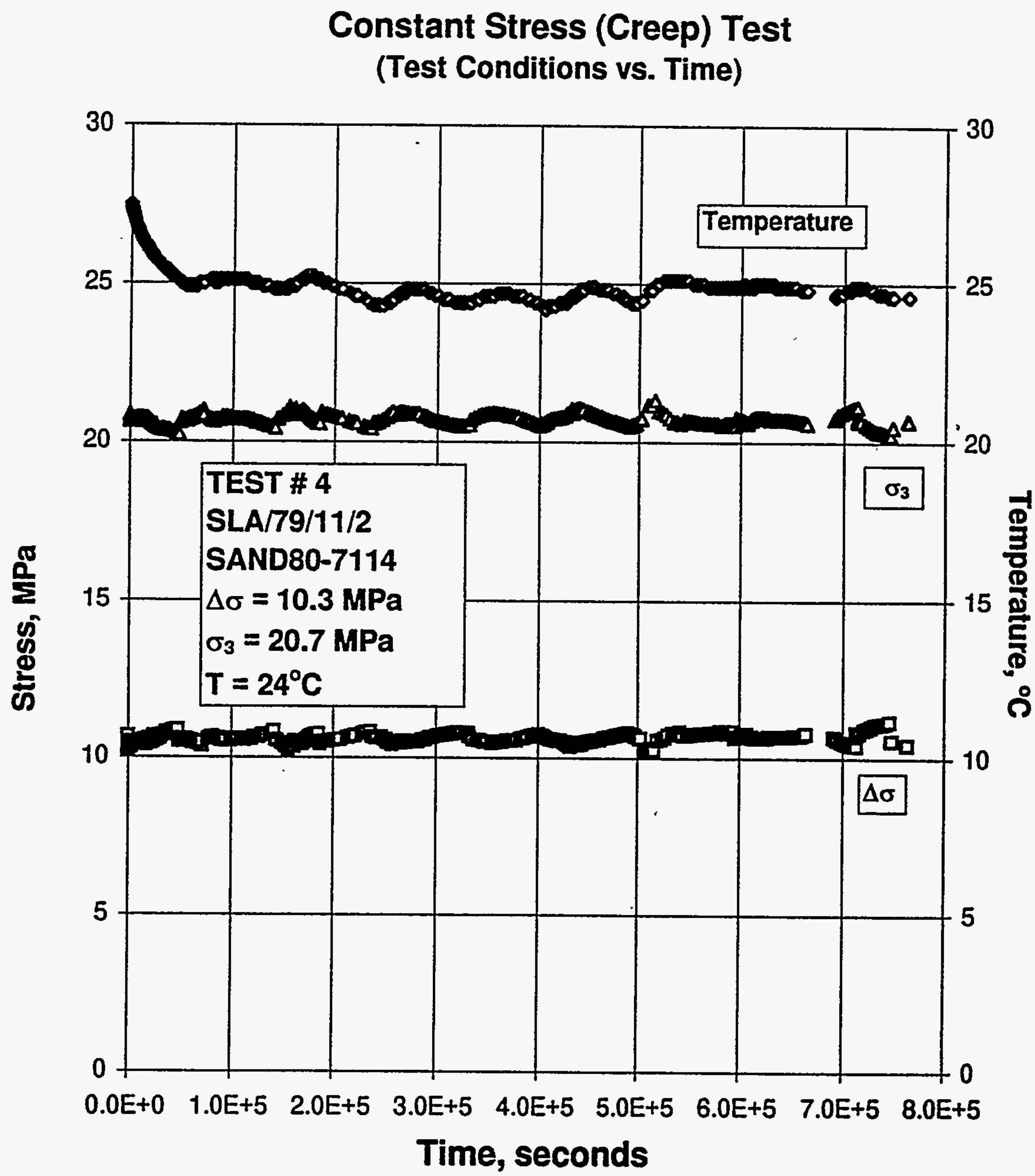

Figure B-28. Test Conditions Versus Time for a Creep Test: Specimen SLA/79/11/2; Stage 1 of 1.

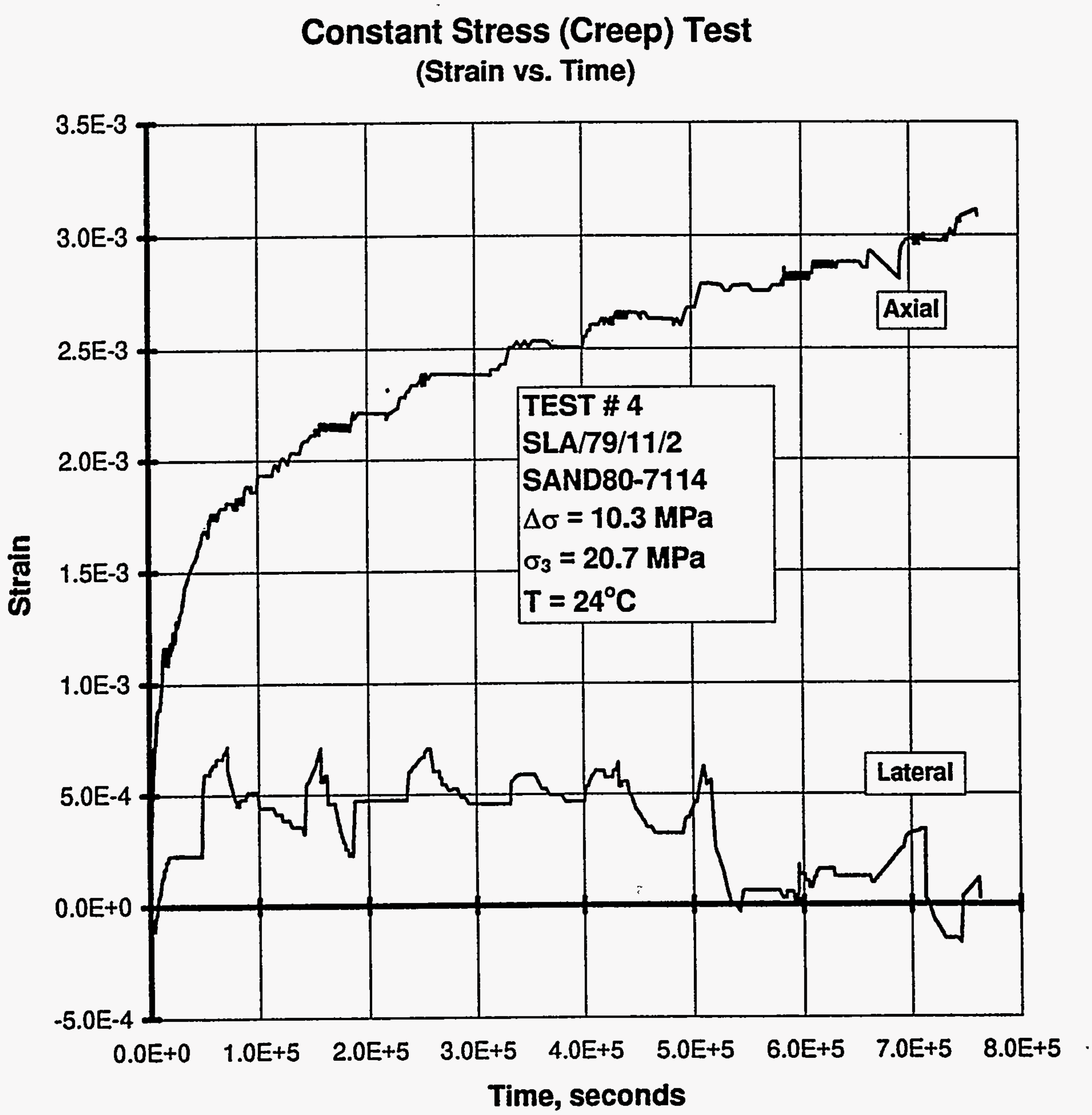

Figure B-29. Axial Strain and Lateral Strain Versus Time for a Creep Test: Specimen SLA/79/11/2; Stage 1 of 1 (Data Acquisition Failure at 9 Days. Data Before 9 Days is Valid. Poor Lateral Data Caused by Dilatometer Leak).

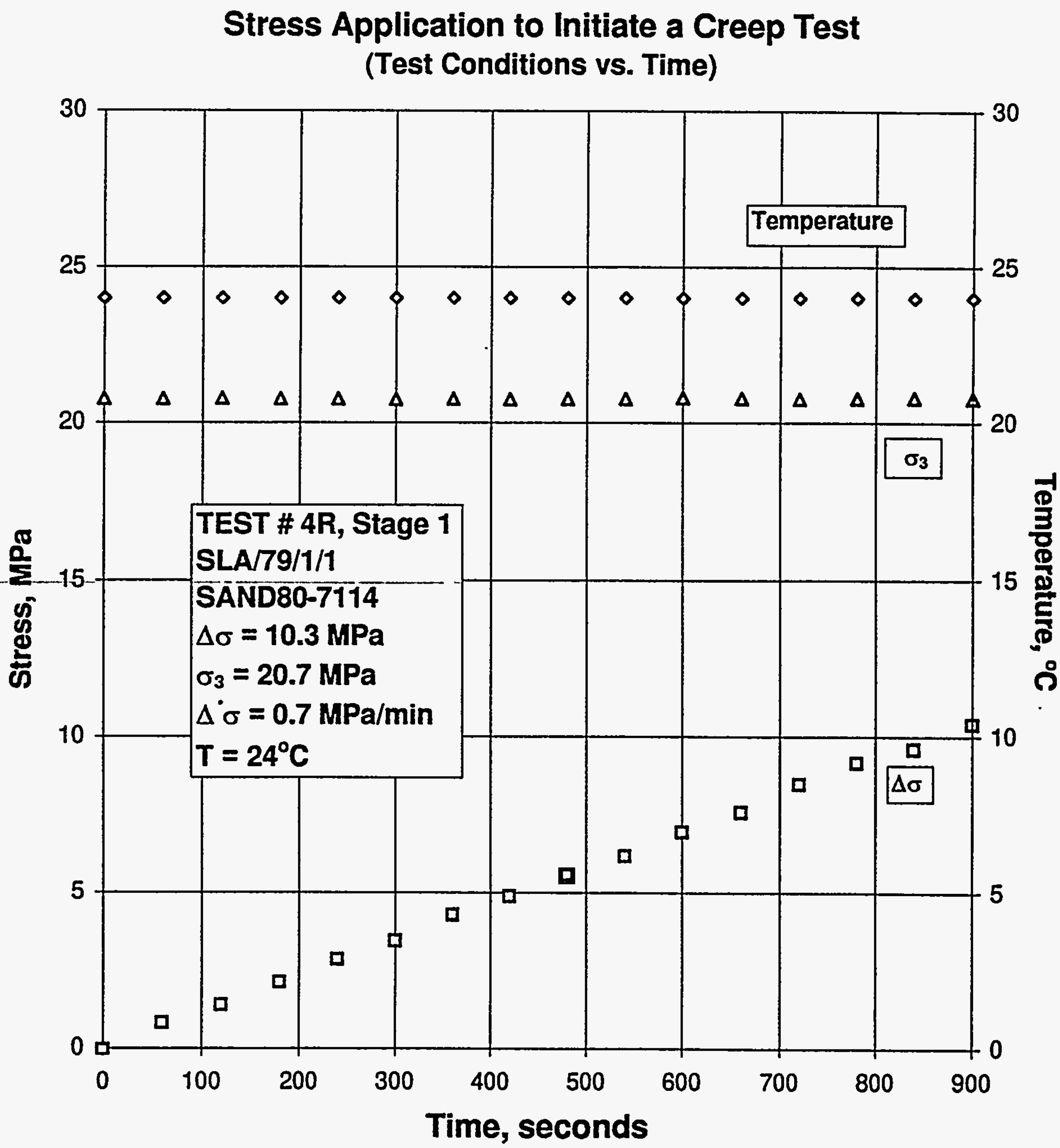

Figure B-30. Test Conditions Versus Time for Stress Application to Initiate a Creep Test: Specimen SLA/79/1/1; Stage 1 of 2.

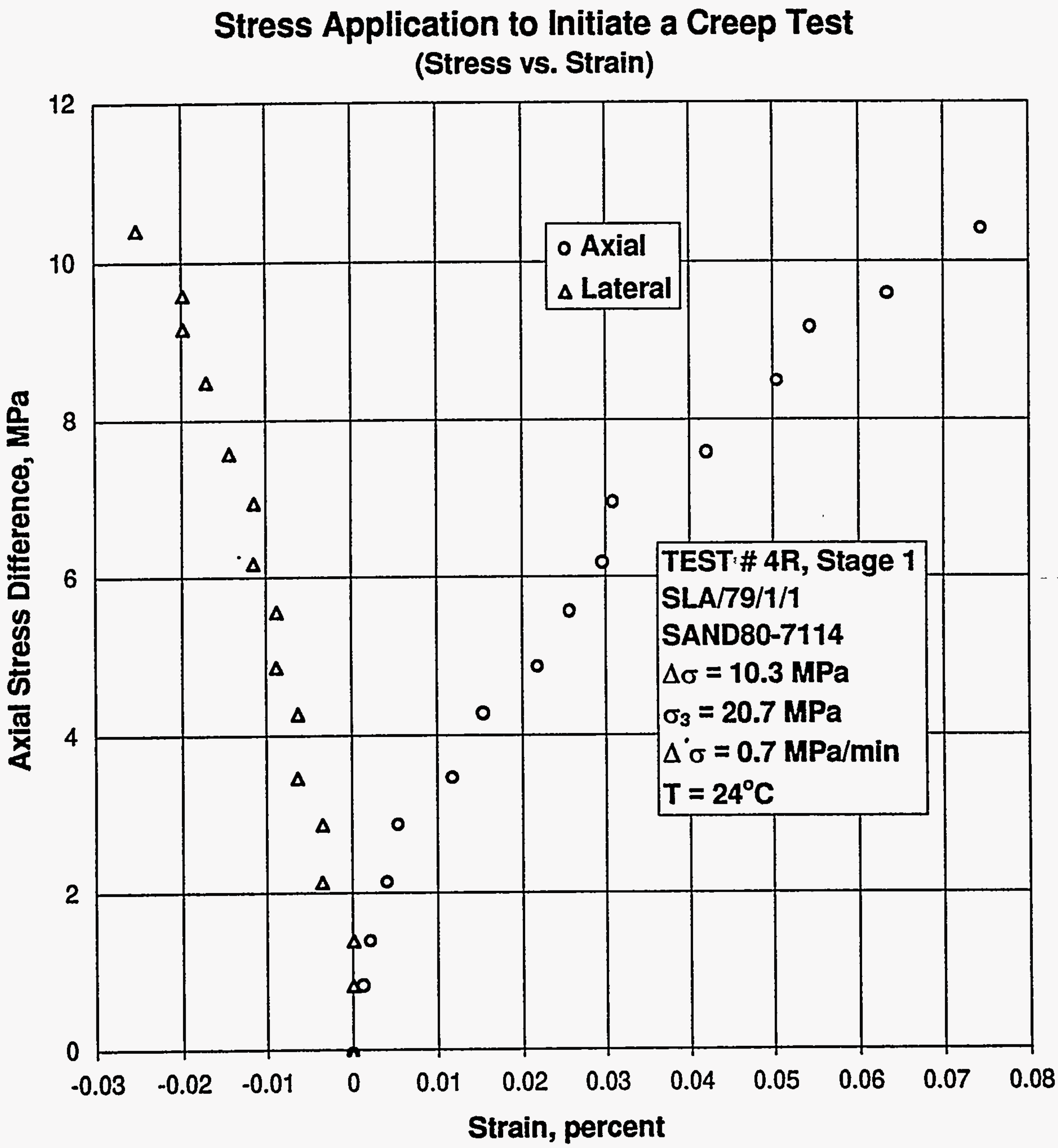

Figure B-31. Axial Stress Difference Versus Axial and Lateral Strain for Stress Application to Initiate a Creep Test: Specimen SLA/79/1/1; Stage 1 of 2.

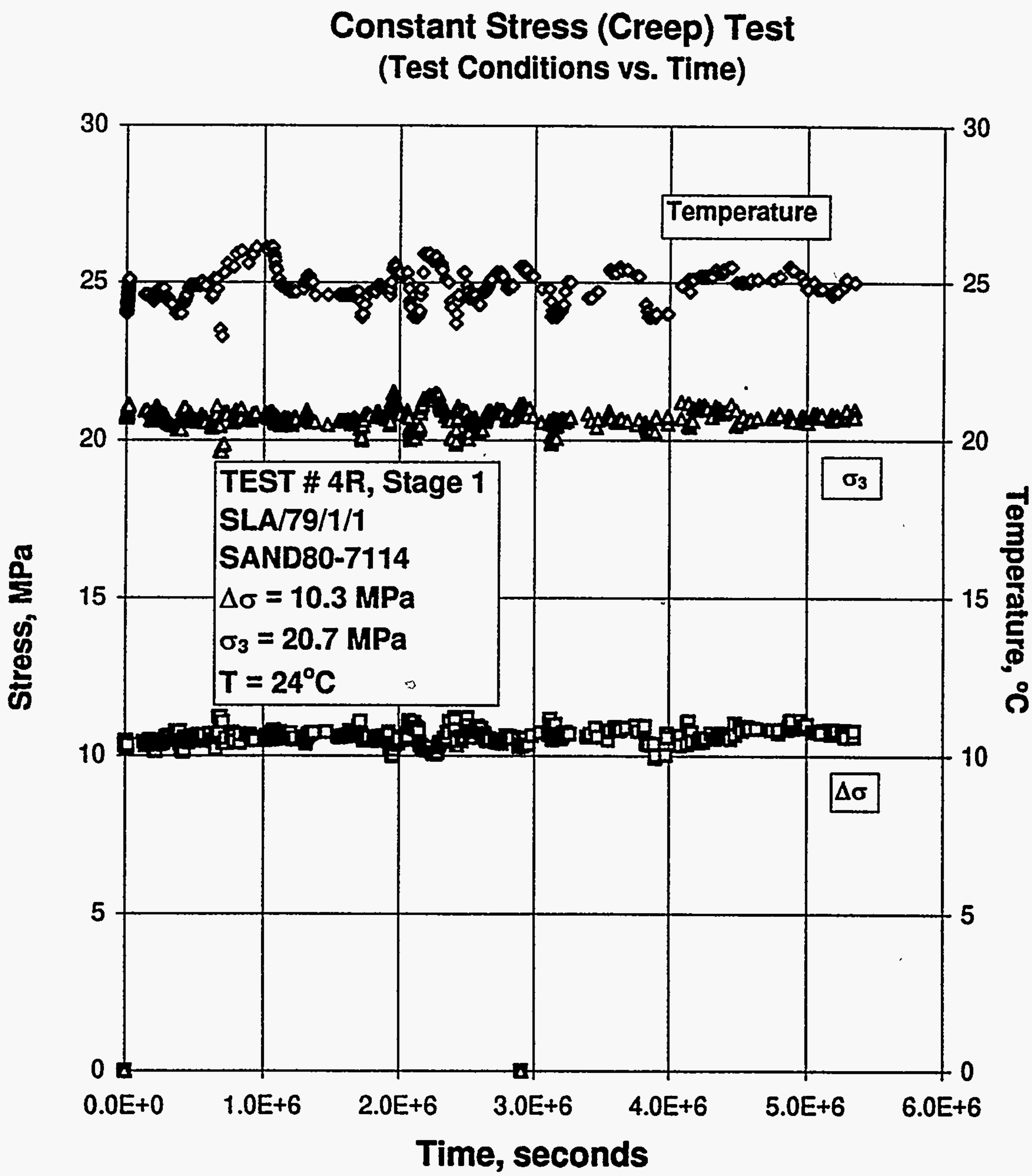

Figure B-32. Test Conditions Versus Time for a Creep Test: Specimen SLA/79/1/1; Stage 1 of 2.

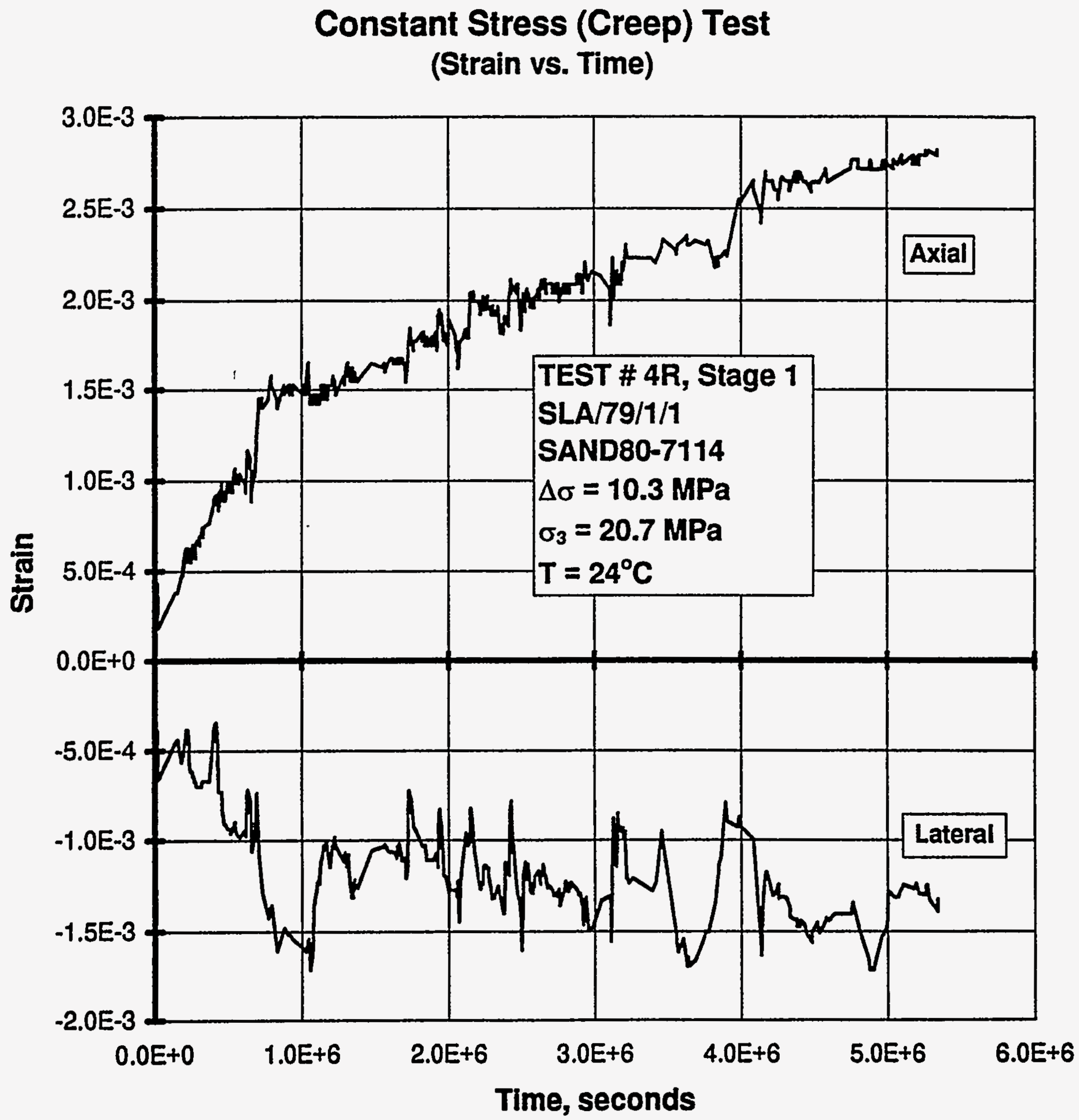

Figure B-33. Axial Strain and Lateral Strain Versus Time for a Creep Test: Specimen SLA/79/1/1; Stage 1 of 2.

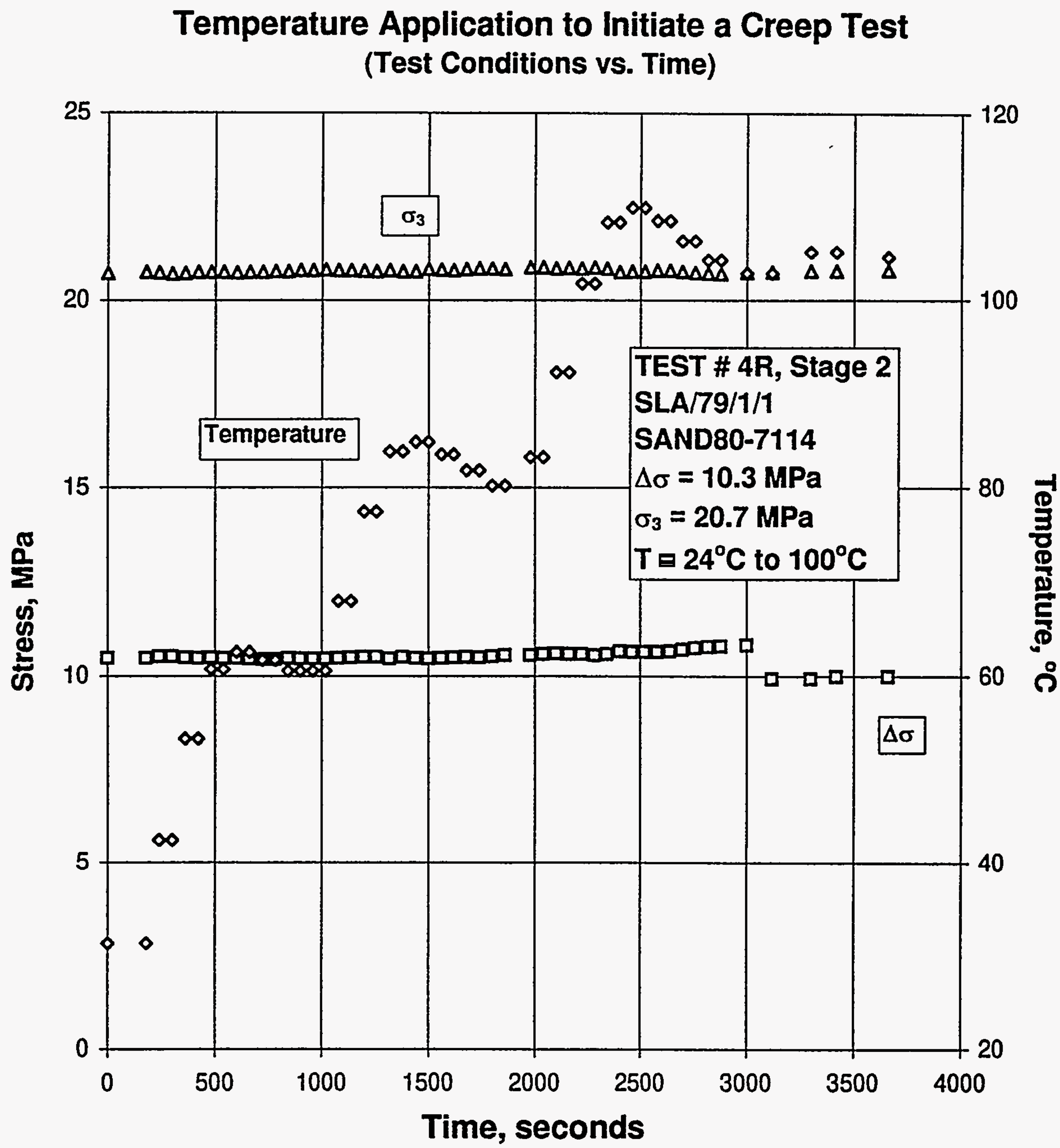

Figure B-34. Test Conditions Versus Time for Temperature Application to Initiate a Creep Test: Specimen SLA/79/1/1; Stage 2 of 2.

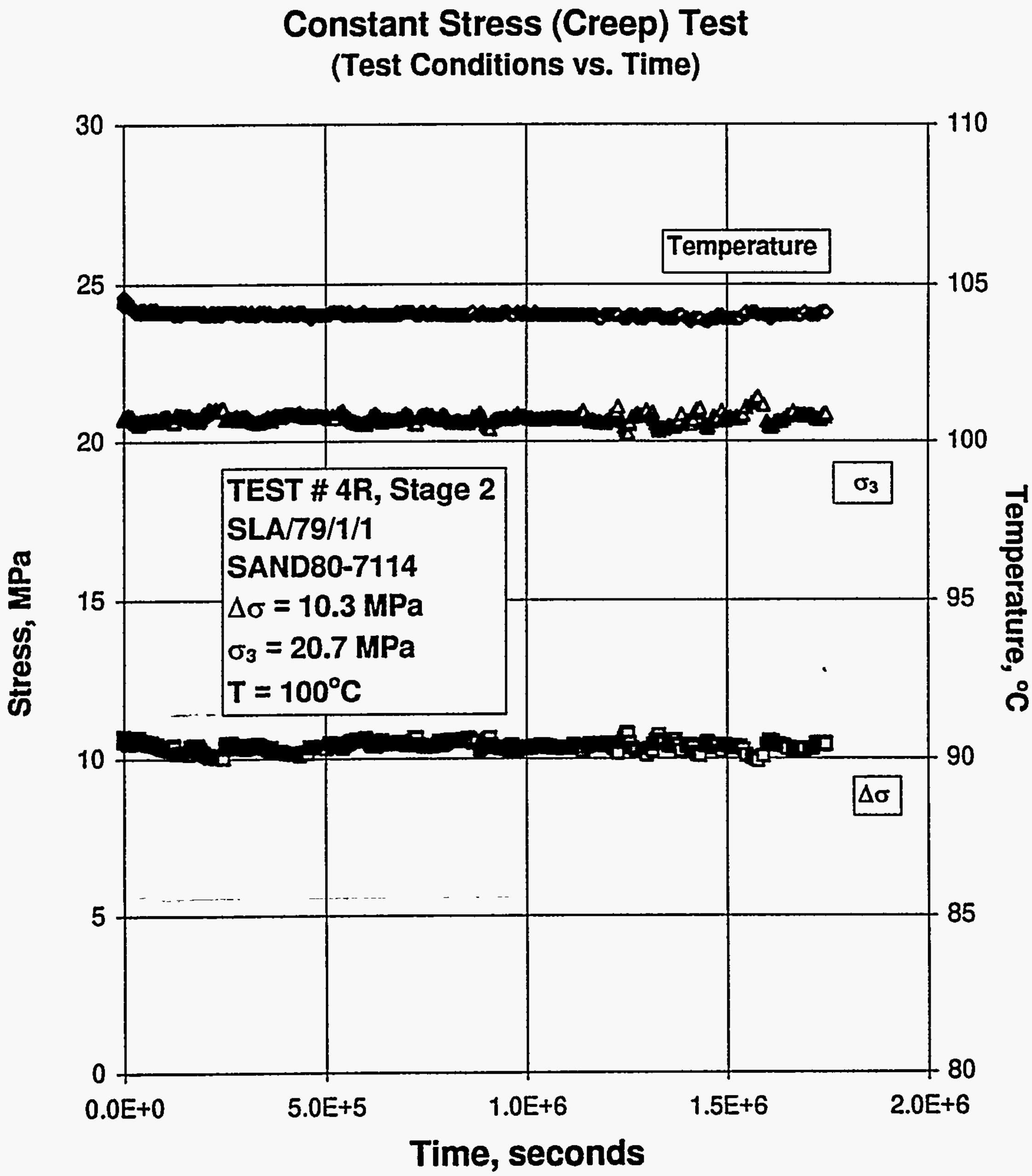

Figure B-35. Test Conditions Versus Time for a Creep Test: Specimen SLA/79/1/1; Stage 2 of 2.

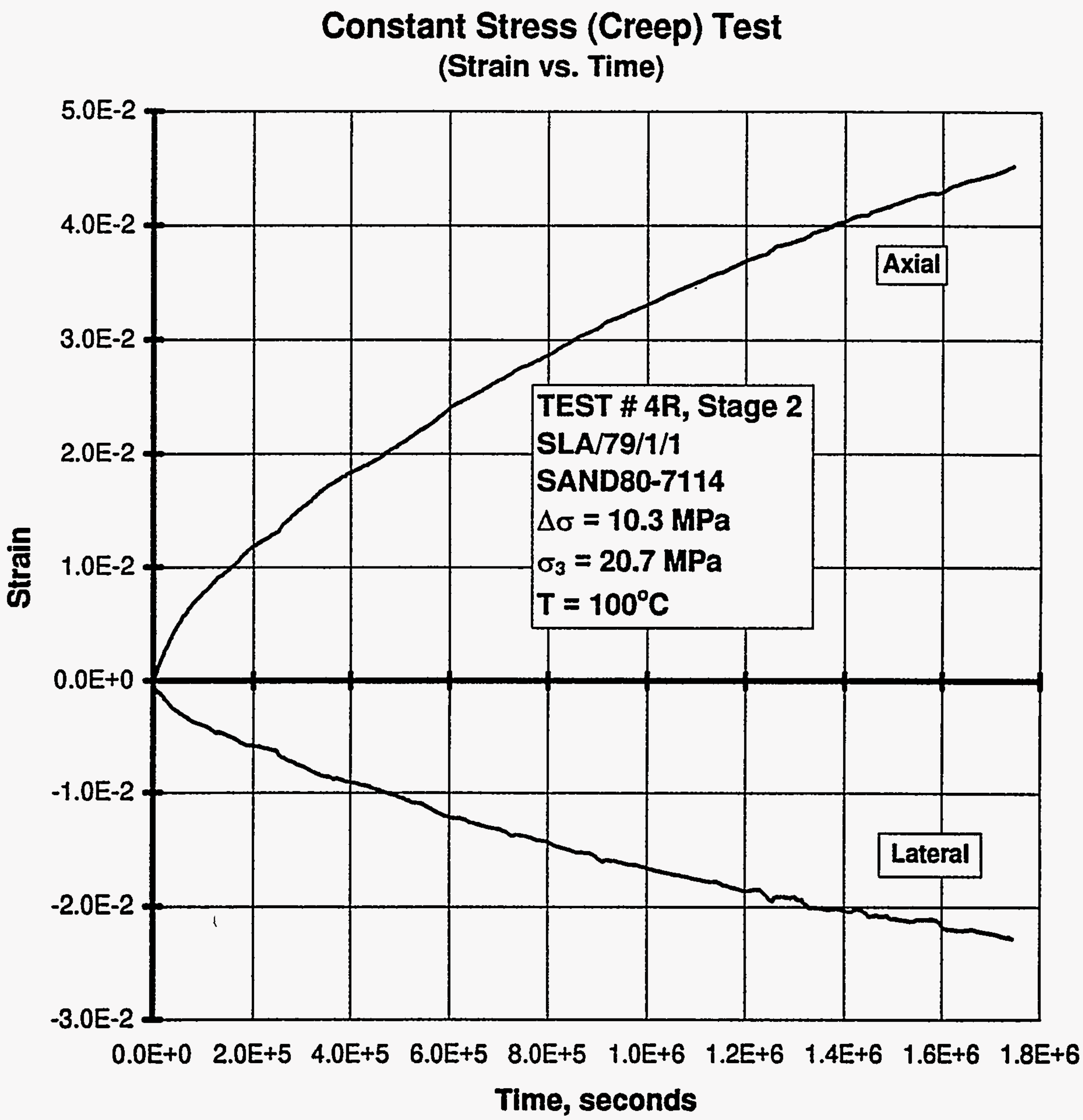

Figure B-36. Axial Strain and Lateral Strain Versus Time for a Creep Test: Specimen SLA/79/1/1; Stage 2 of 2.

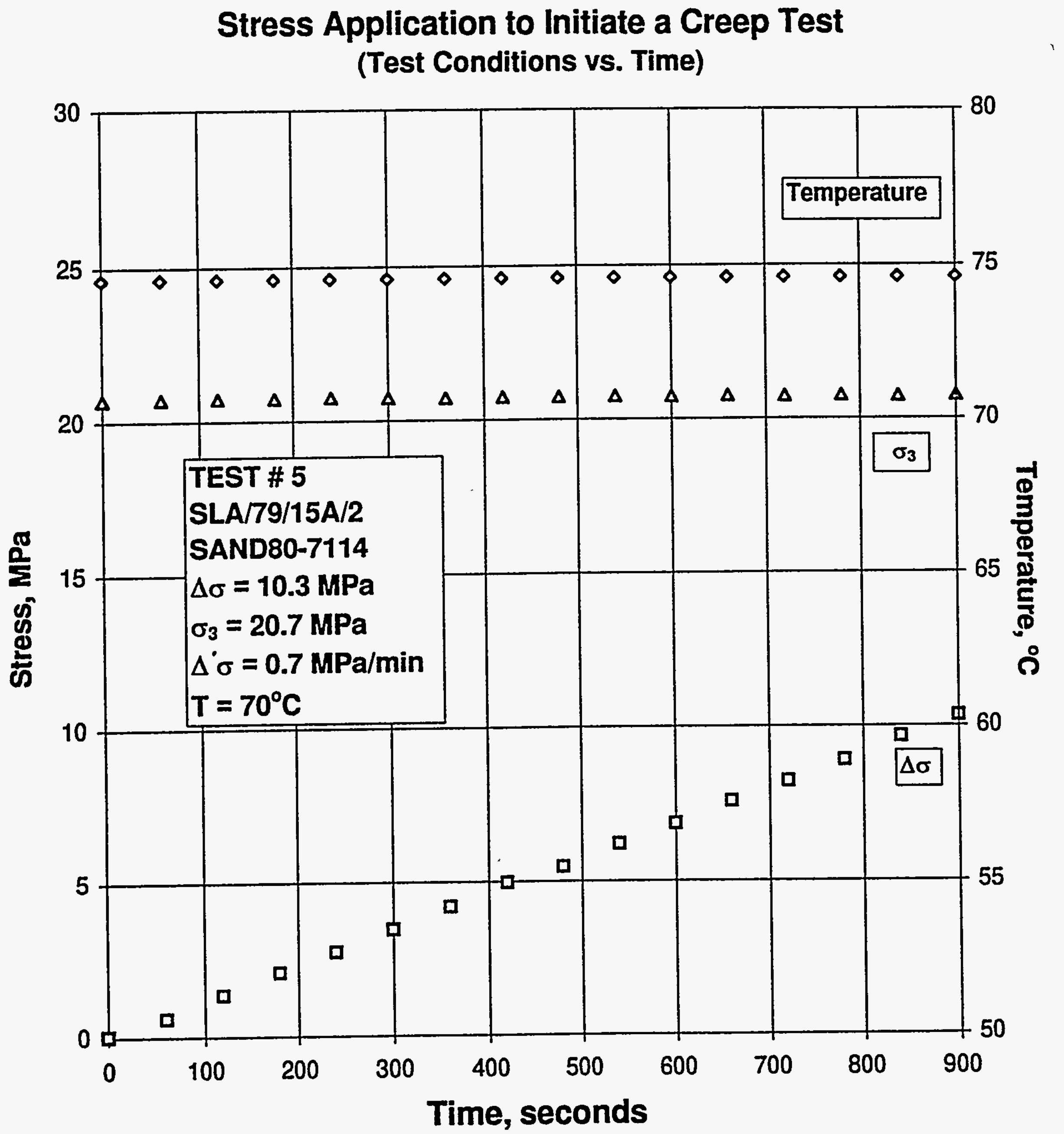

Figure B-37. Test Conditions Versus Time for Stress Application to Initiate a Creep Test: Specimen SLA/79/15A/2; Stage 1 of 1.

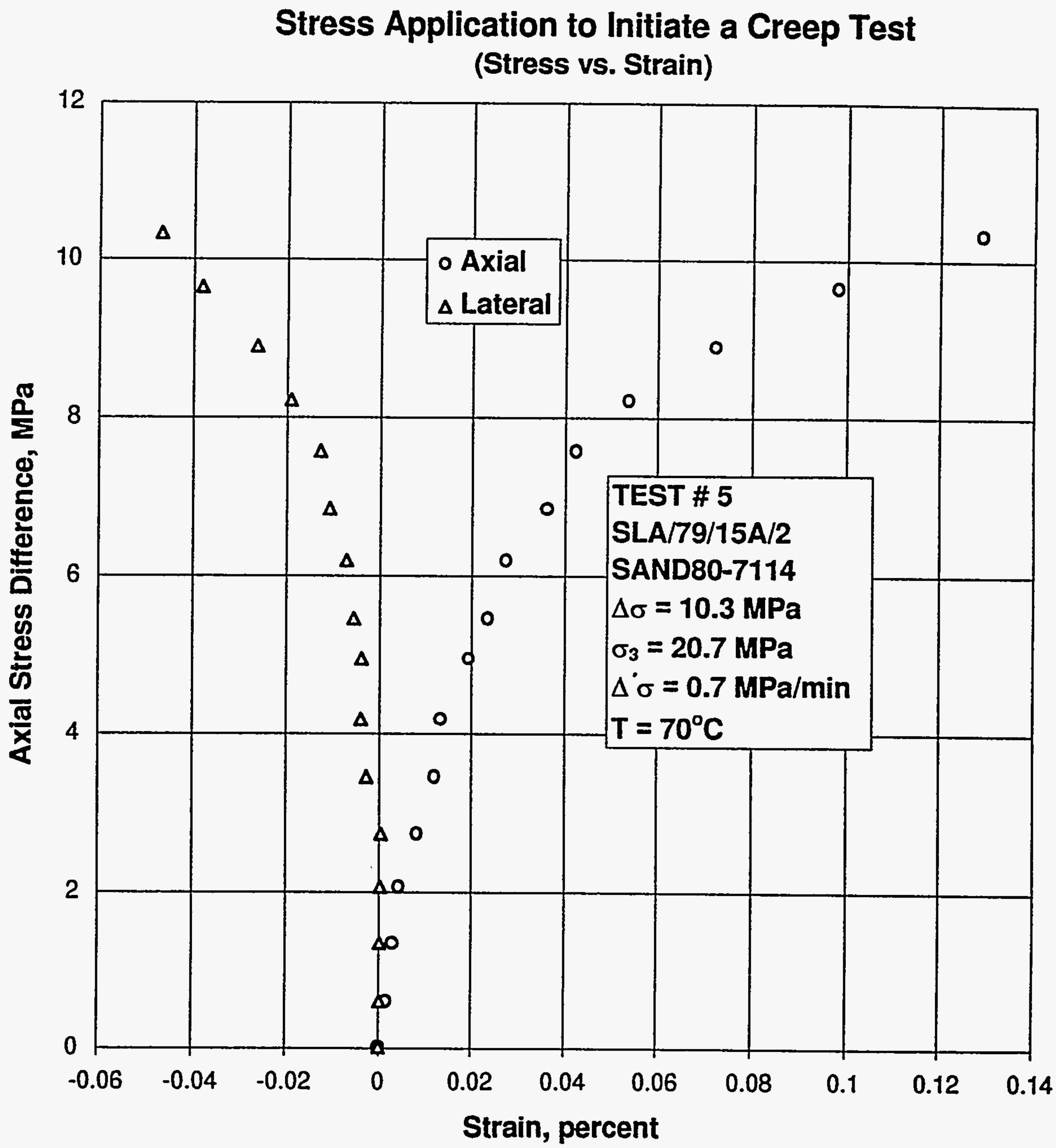

Figure B-38. Axial Stress Difference Versus Axial and Lateral Strain for Stress Application to Initiate a Creep Test: Specimen SLA/79/15A/2; Stage 1 of 1.

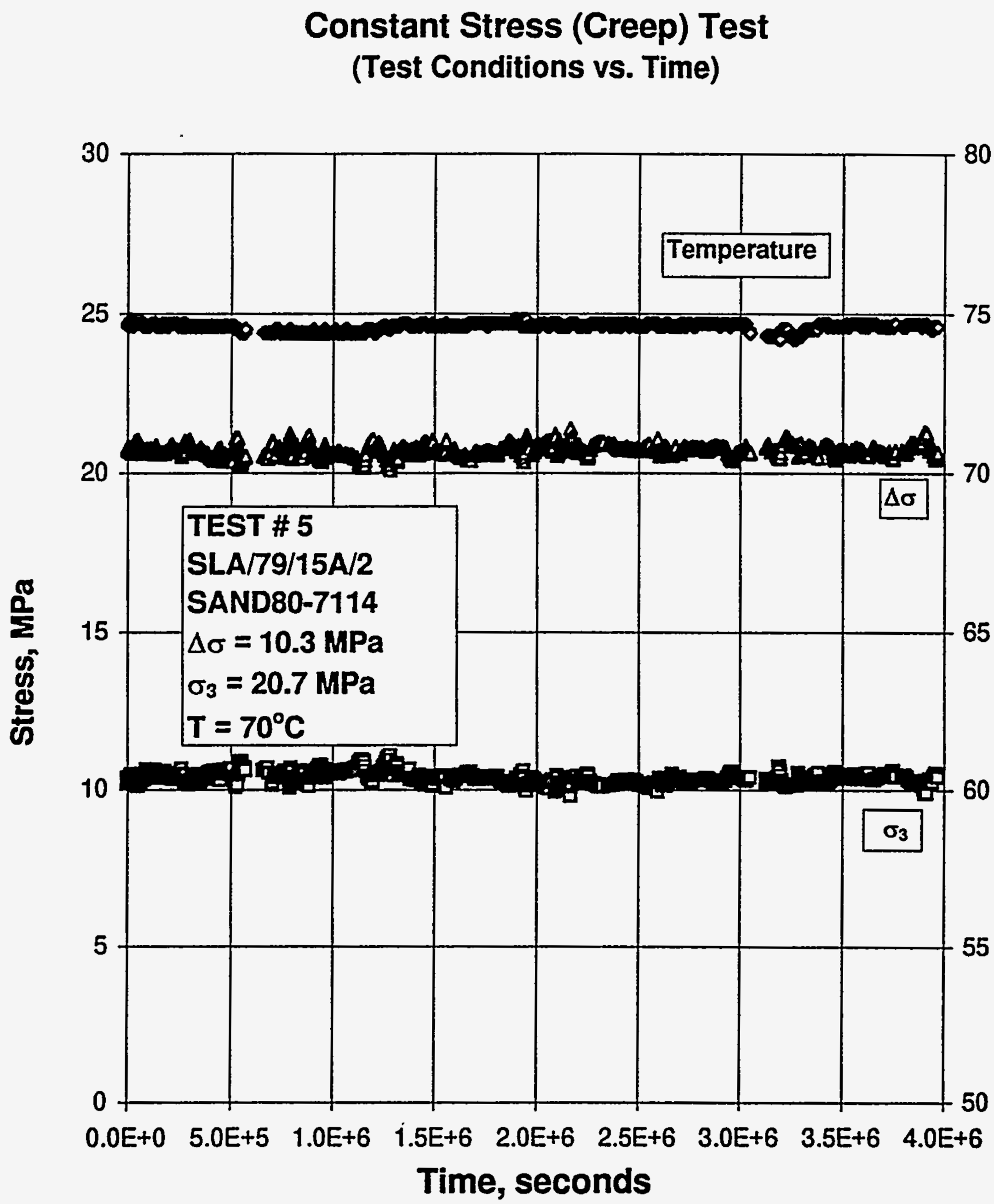

Figure B-39. Test Conditions Versus Time for a Creep Test: Specimen SLA/79/15A/2; Stage 1 of 1.

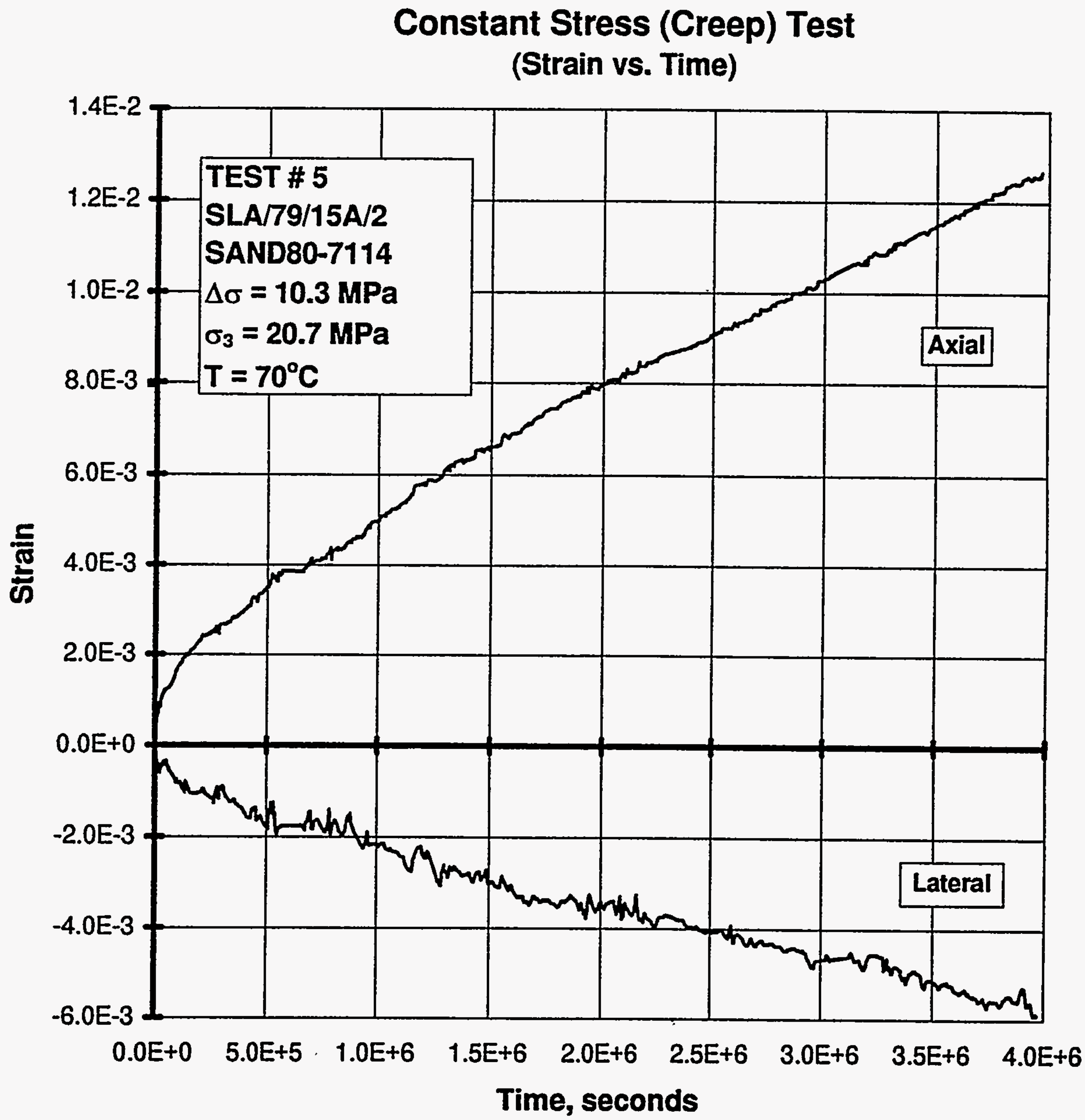

Figure B-40. Axial Strain and Lateral Strain Versus Time for a Creep Test: Specimen SLA/79/15A/2; Stage 1 of 1.

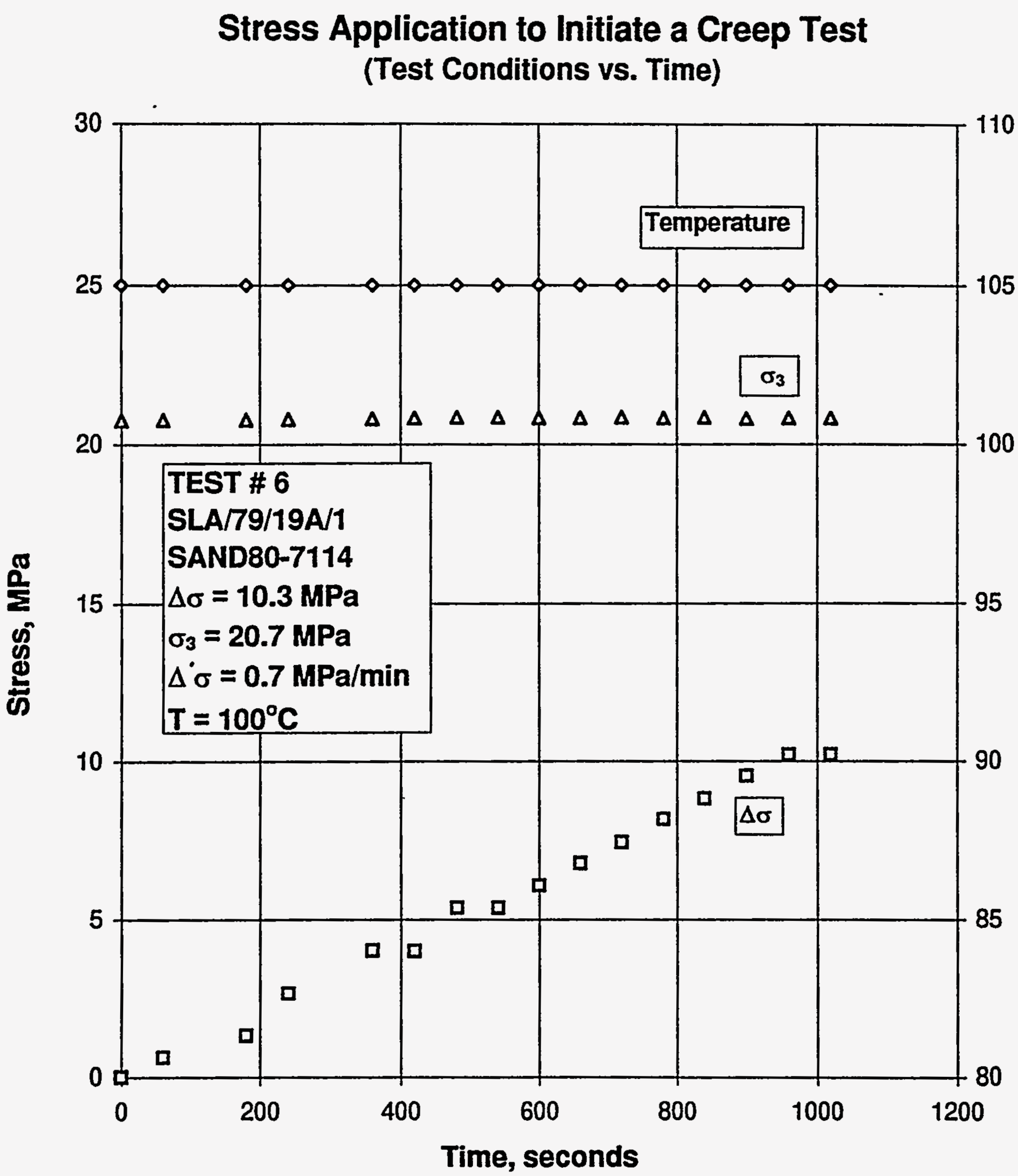

Figure B-41. Test Conditions Versus Time for Stress Application to Initiate a Creep Test: Specimen SLA/79/19A/1; Stage 1 of 1.

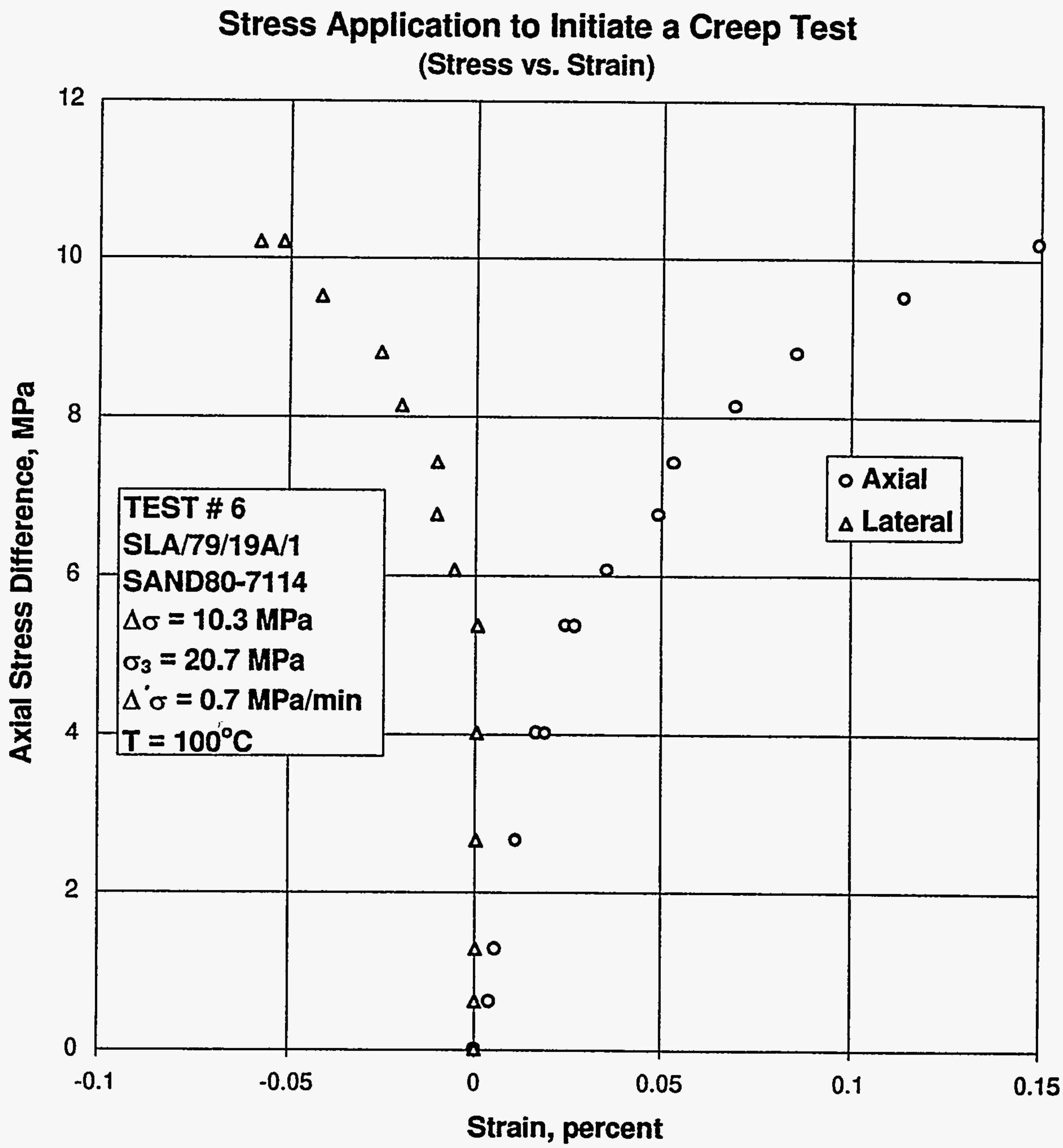

Figure B-42. Axial Stress Difference Versus Axial and Lateral Strain for Stress Application to Initiate a Creep Test: Specimen SLA/79/19A/1; Stage 1 of 1.

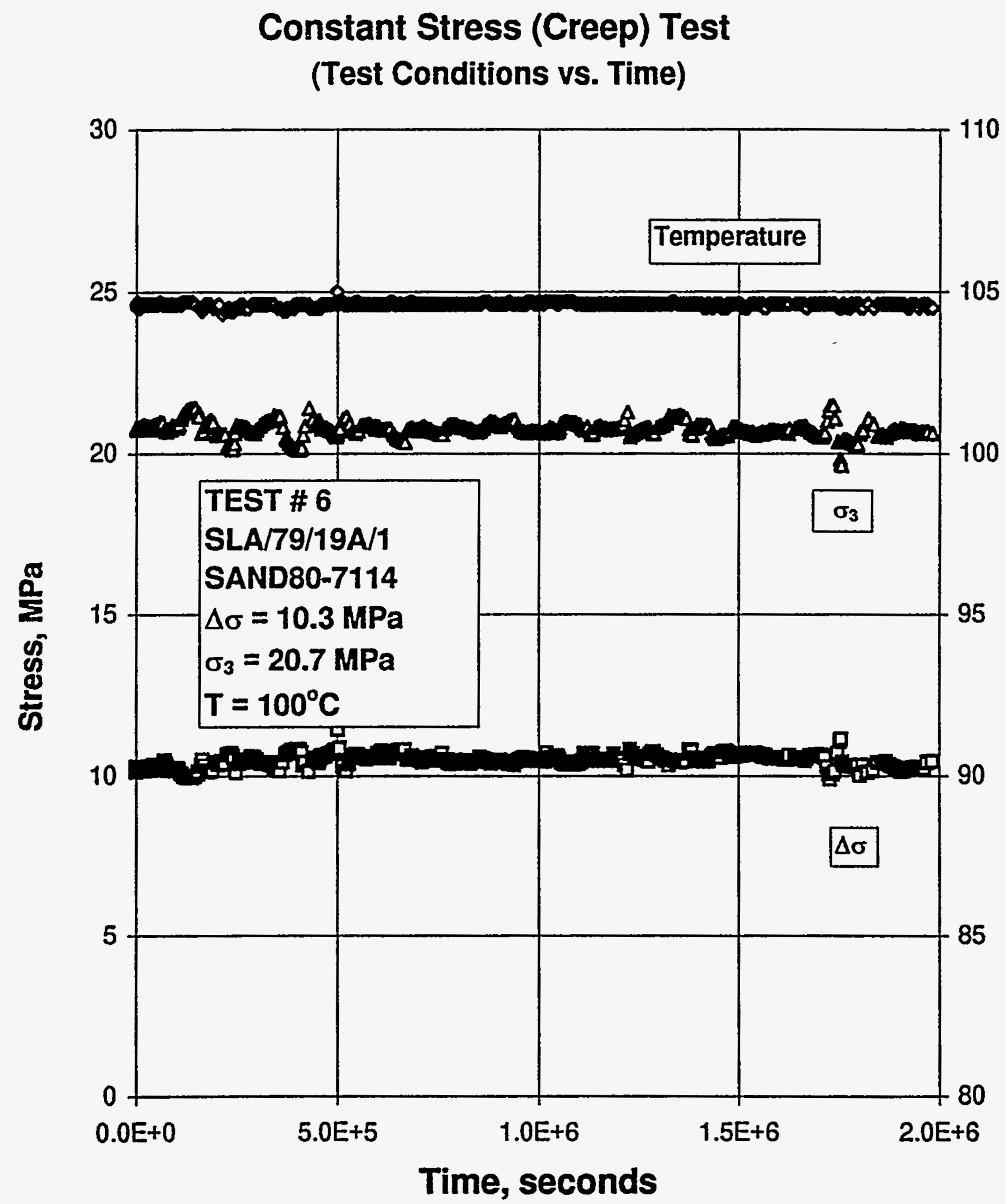

Figure B-43. Test Conditions Versus Time for a Creep Test: Specimen SLA/79/19A/1; Stage 1 of 1.

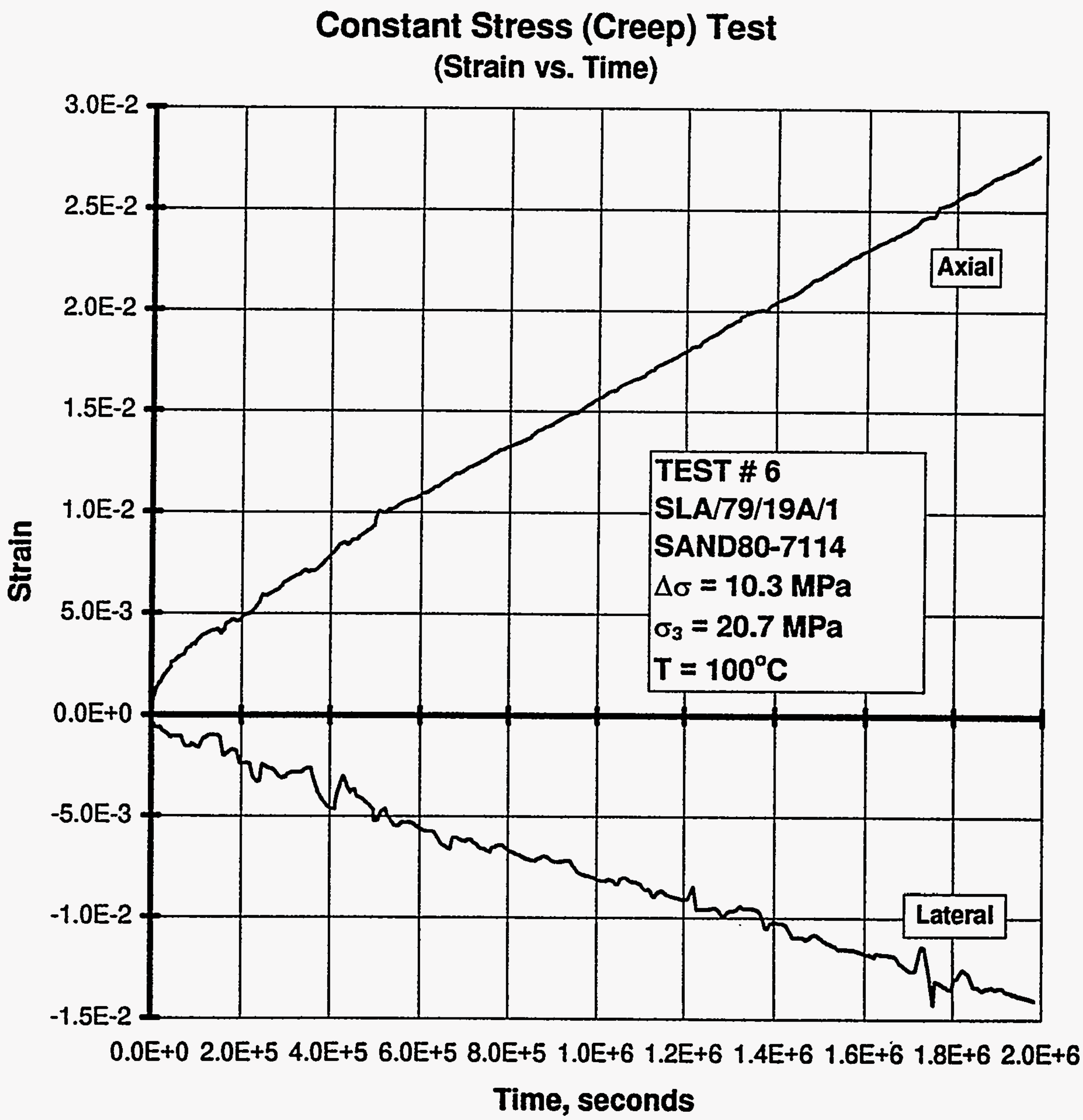

Figure B-44. Axial Strain and Lateral Strain Versus Time for a Creep Test: Specimen SLA/79/19A/1; Stage 1 of 1.

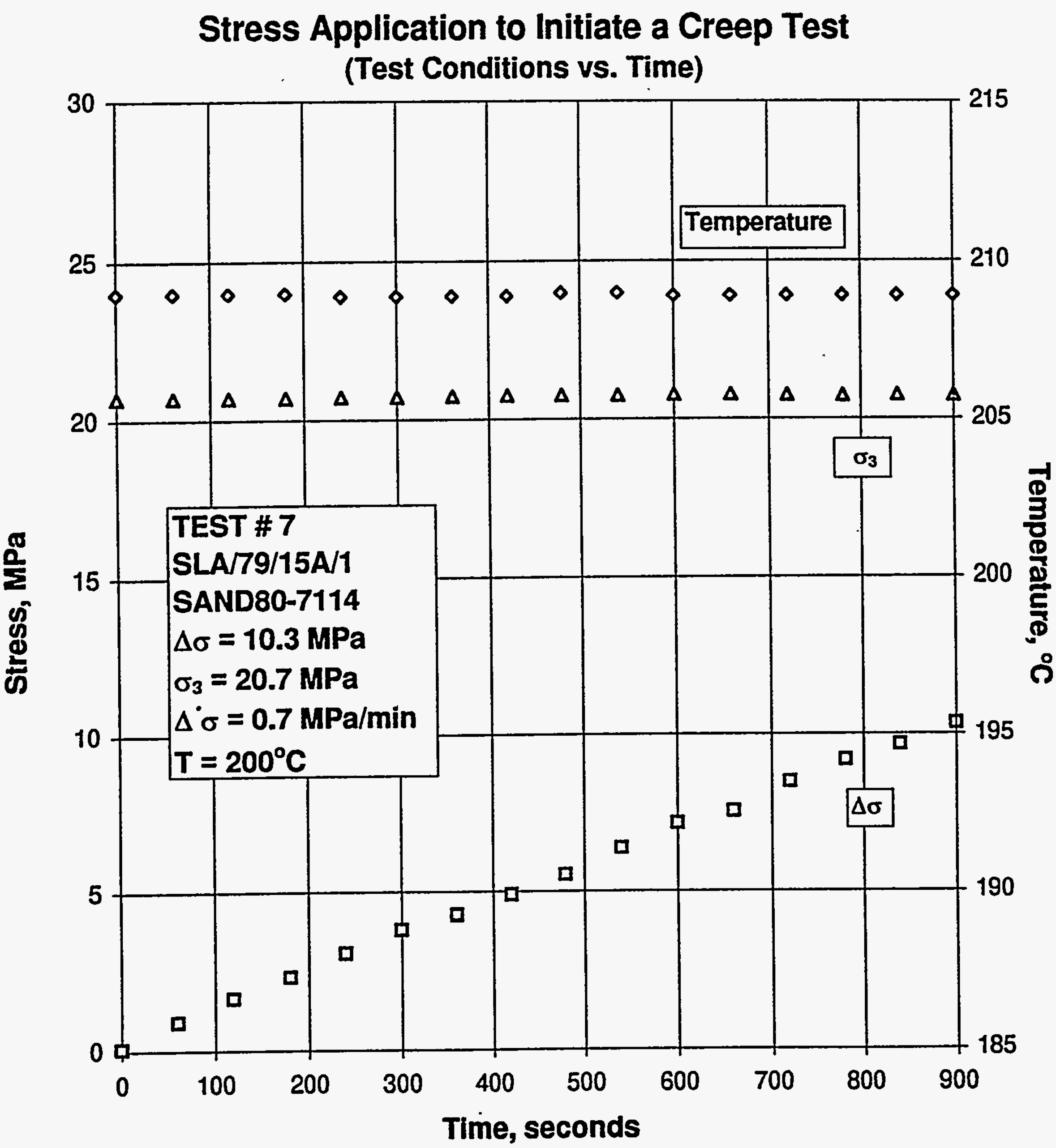

Figure B-45. Test Conditions Versus Time for Stress Application to Initiate a Creep Test: Specimen SLA/79/15A/1; Stage 1 of 1.

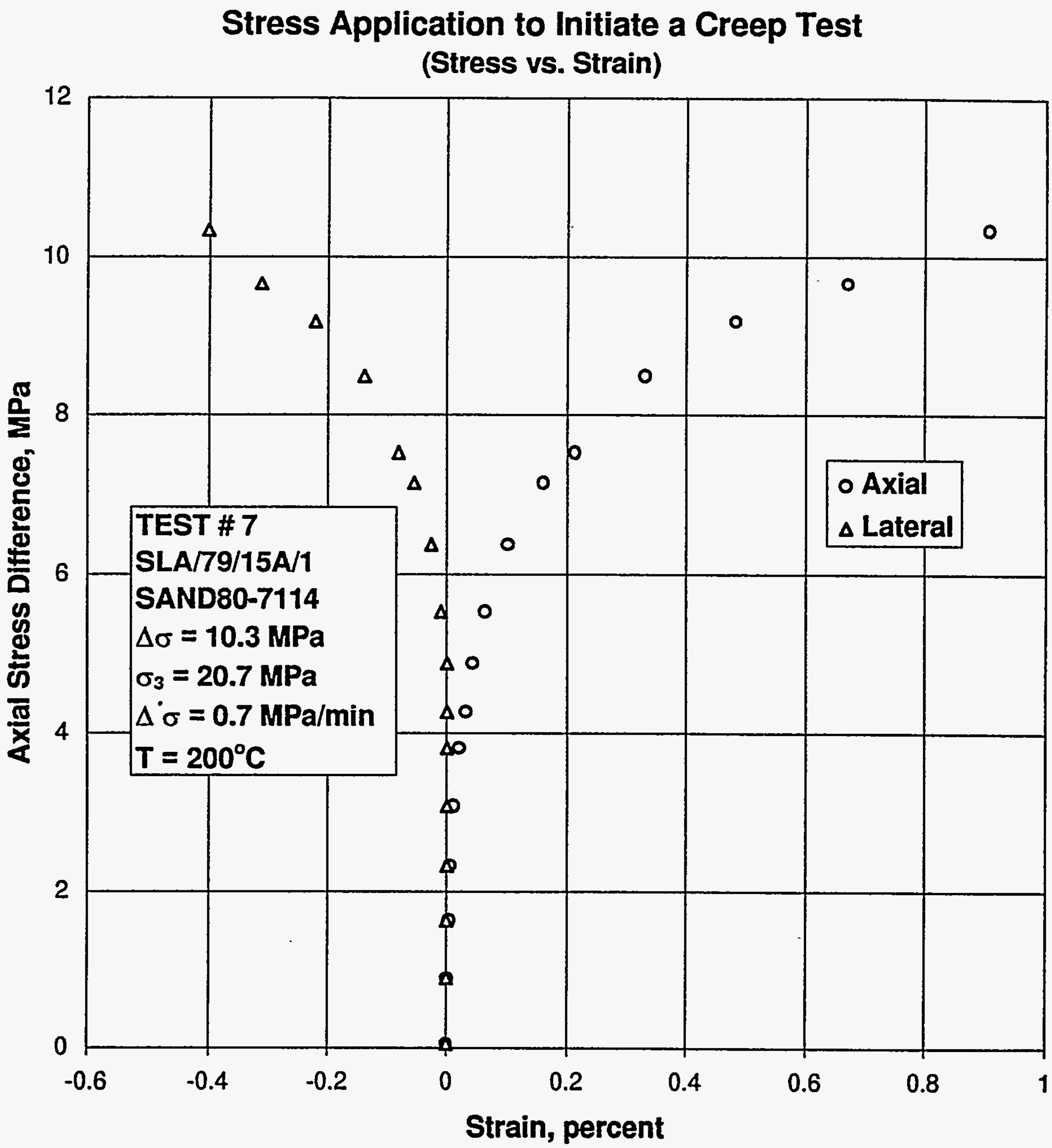

Figure B-46. Axial Stress Difference Versus Axial and Lateral Strain for Stress Application to Initiate a Creep Test: Specimen SLA/79/15A/1; Stage 1 of 1.

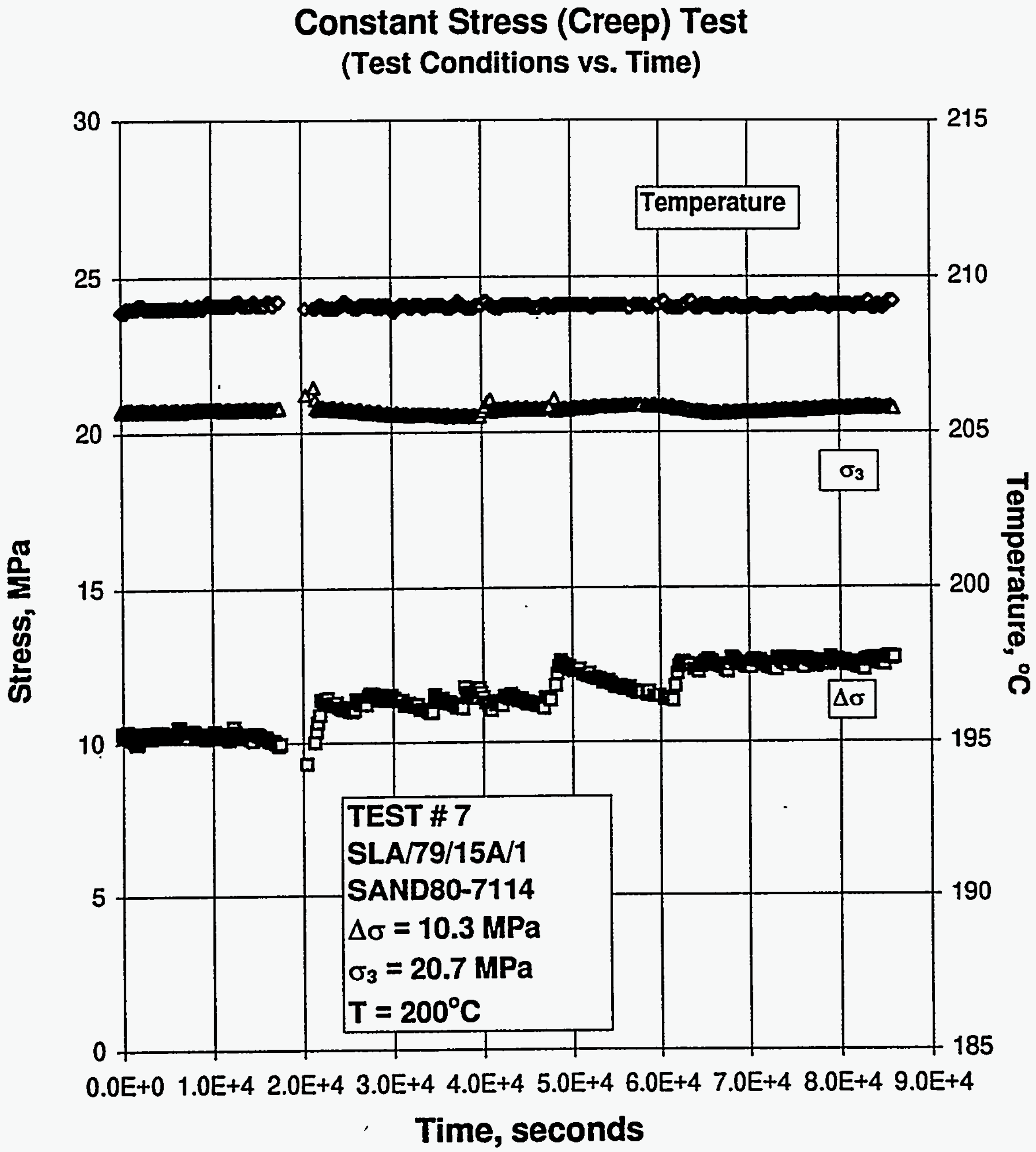

Figure B-47. Test Conditions Versus Time for a Creep Test: Specimen SLA/79/15A/1; Stage 1 of 1.

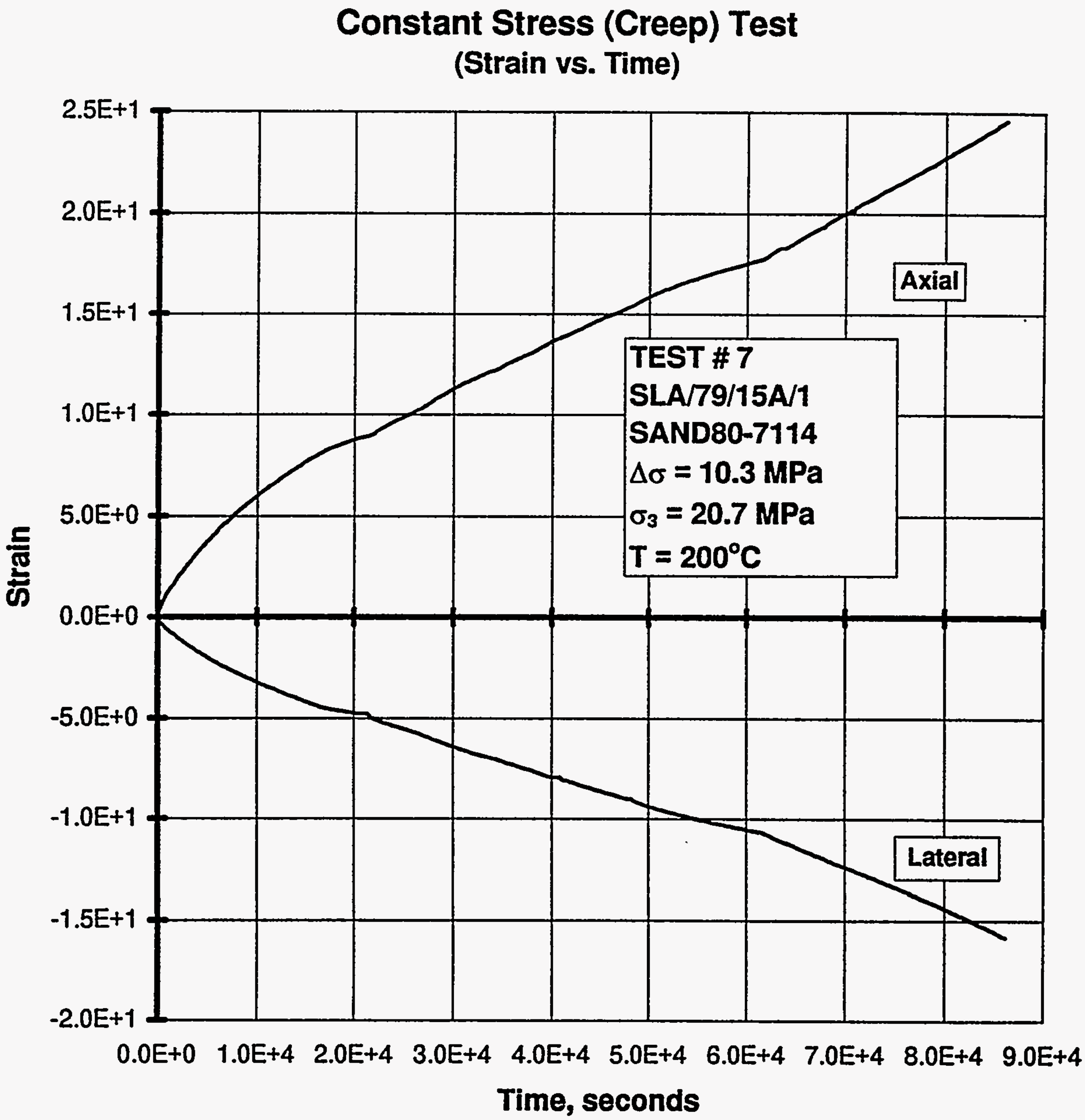

Figure B-48. Axial Strain and Lateral Strain Versus Time for a Creep Test: Specimen SLA/79/15A/1; Stage 1 of 1.

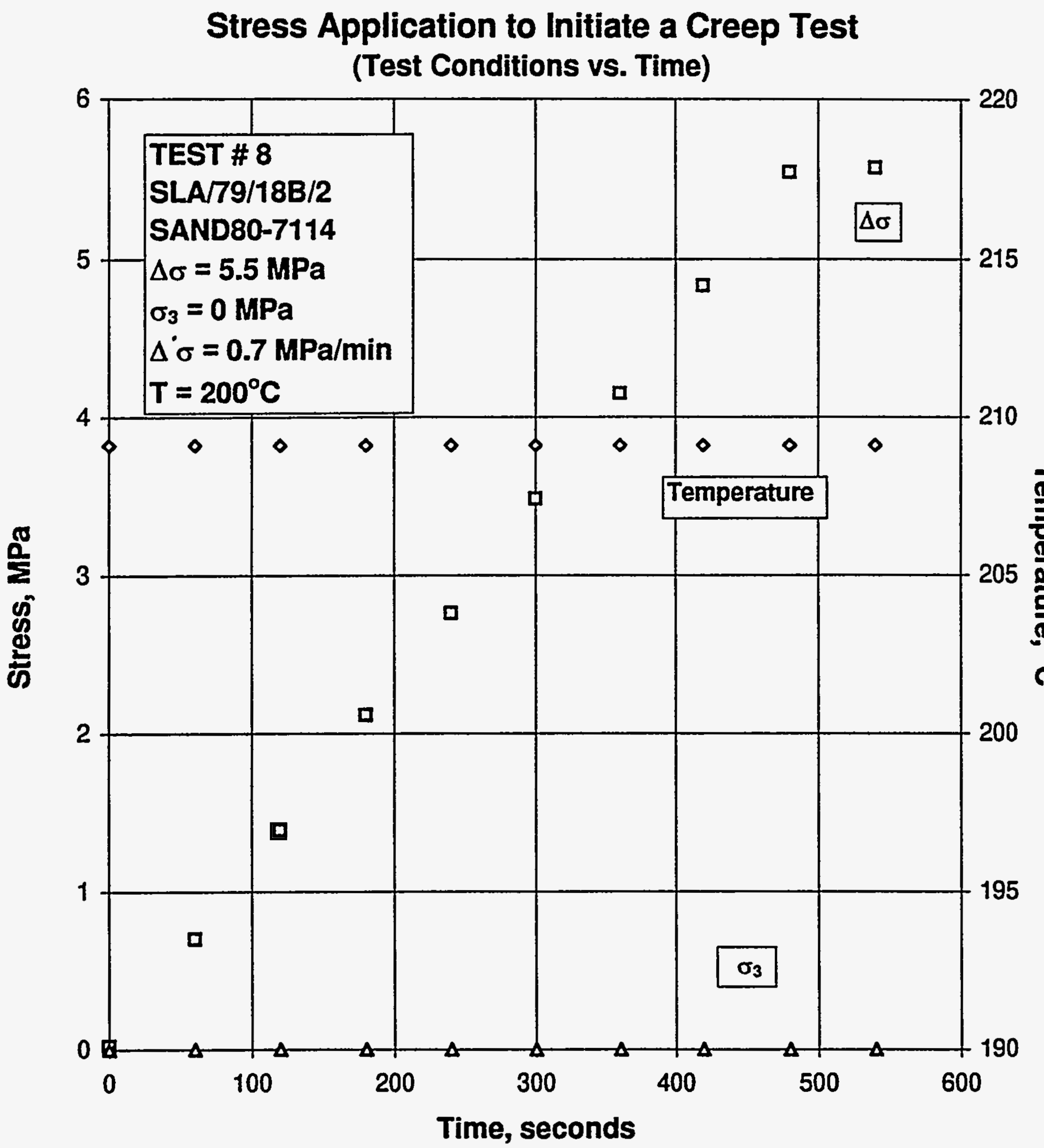

Figure B-49. Test Conditions Versus Time for Stress Application to Initiate a Creep Test: Specimen SLA/79/18B/2; Stage 1 of 1.

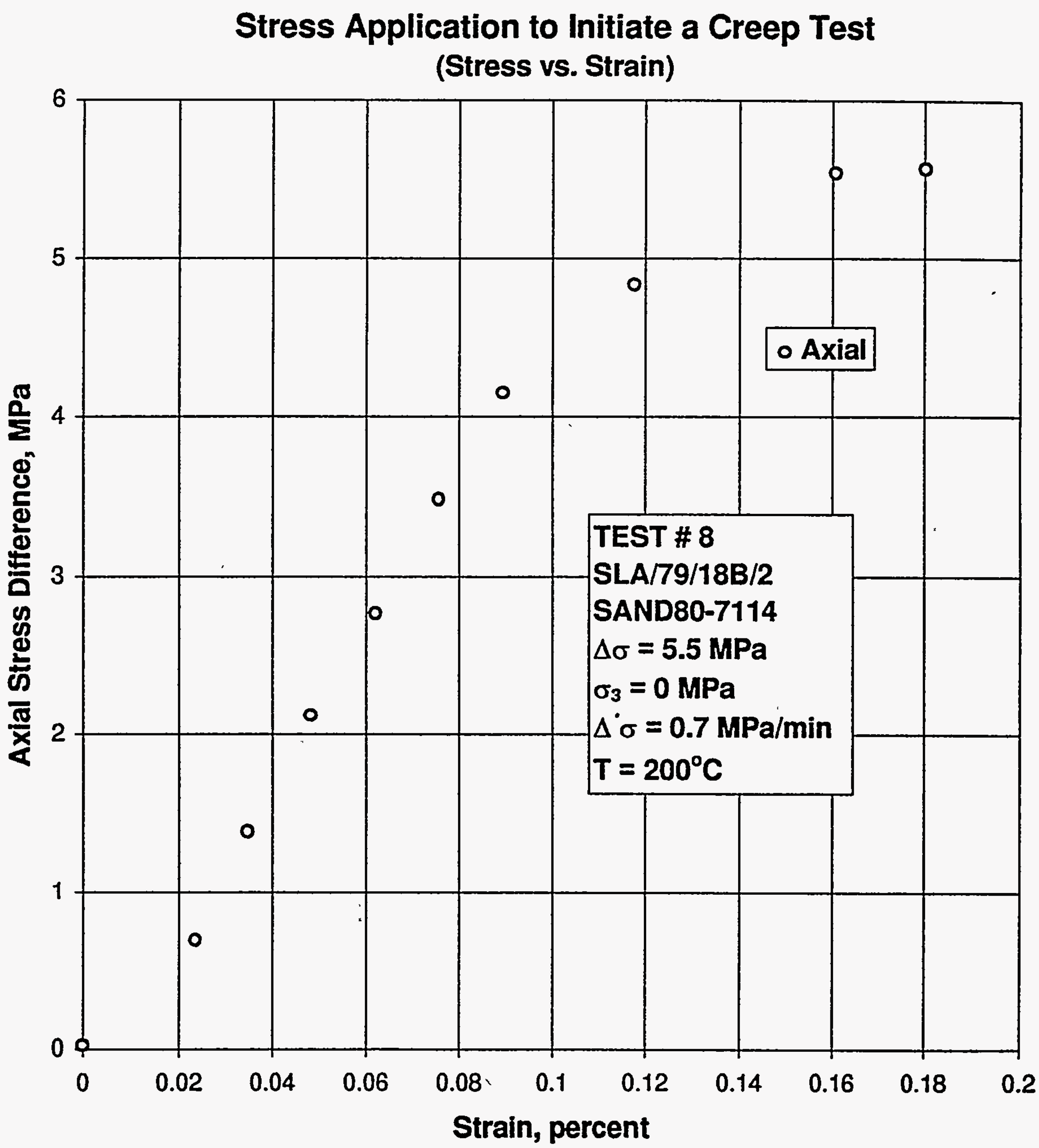

Figure B-50. Axial Stress Difference Versus Axial and Lateral Strain for Stress Application to Initiate a Creep Test: Specimen SLA/79/18B/2; Stage 1 of 1.

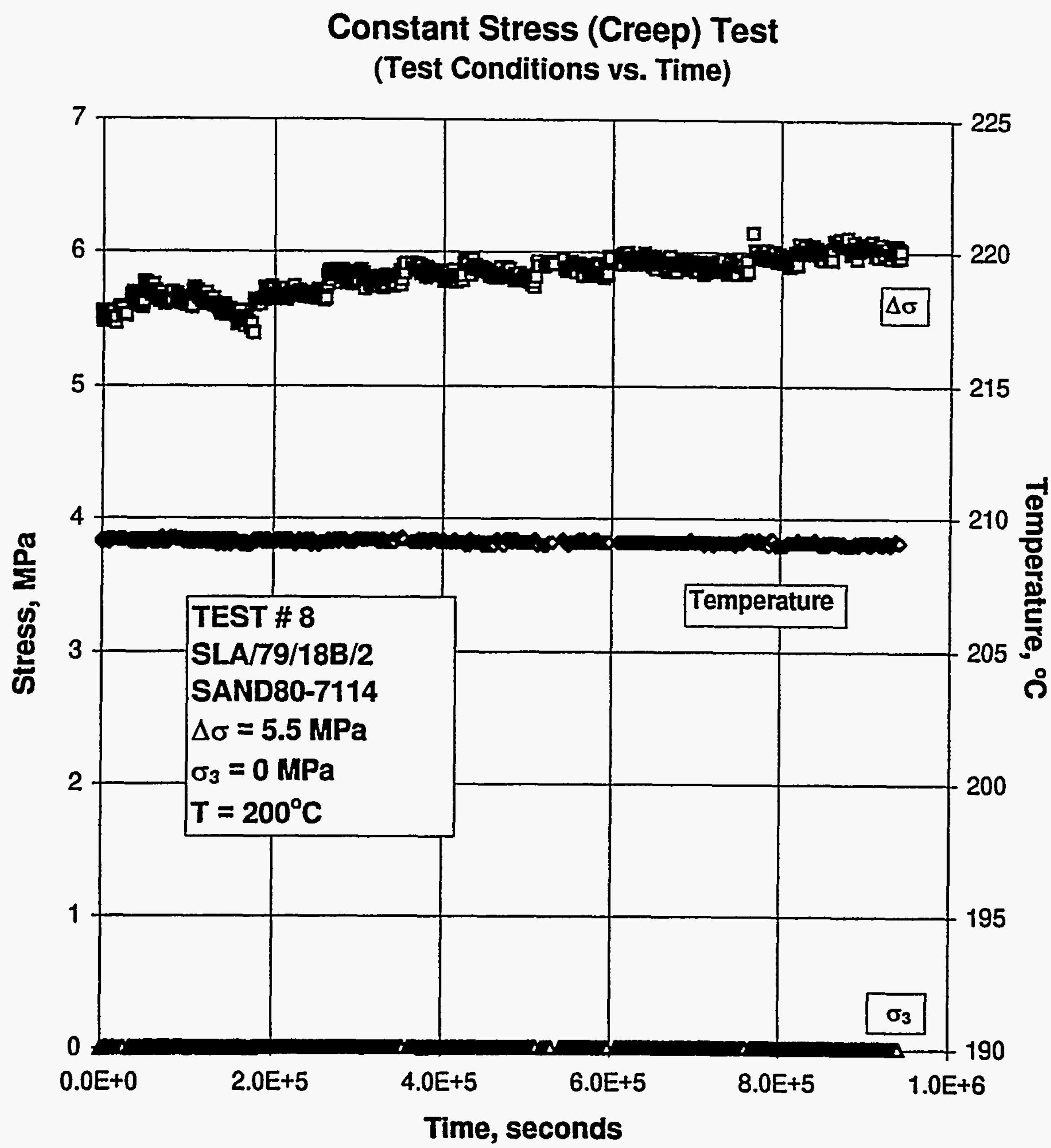

Figure B-51. Test Conditions Versus Time for a Creep Test: Specimen SLA/79/18B/2; Stage 1 of 1.

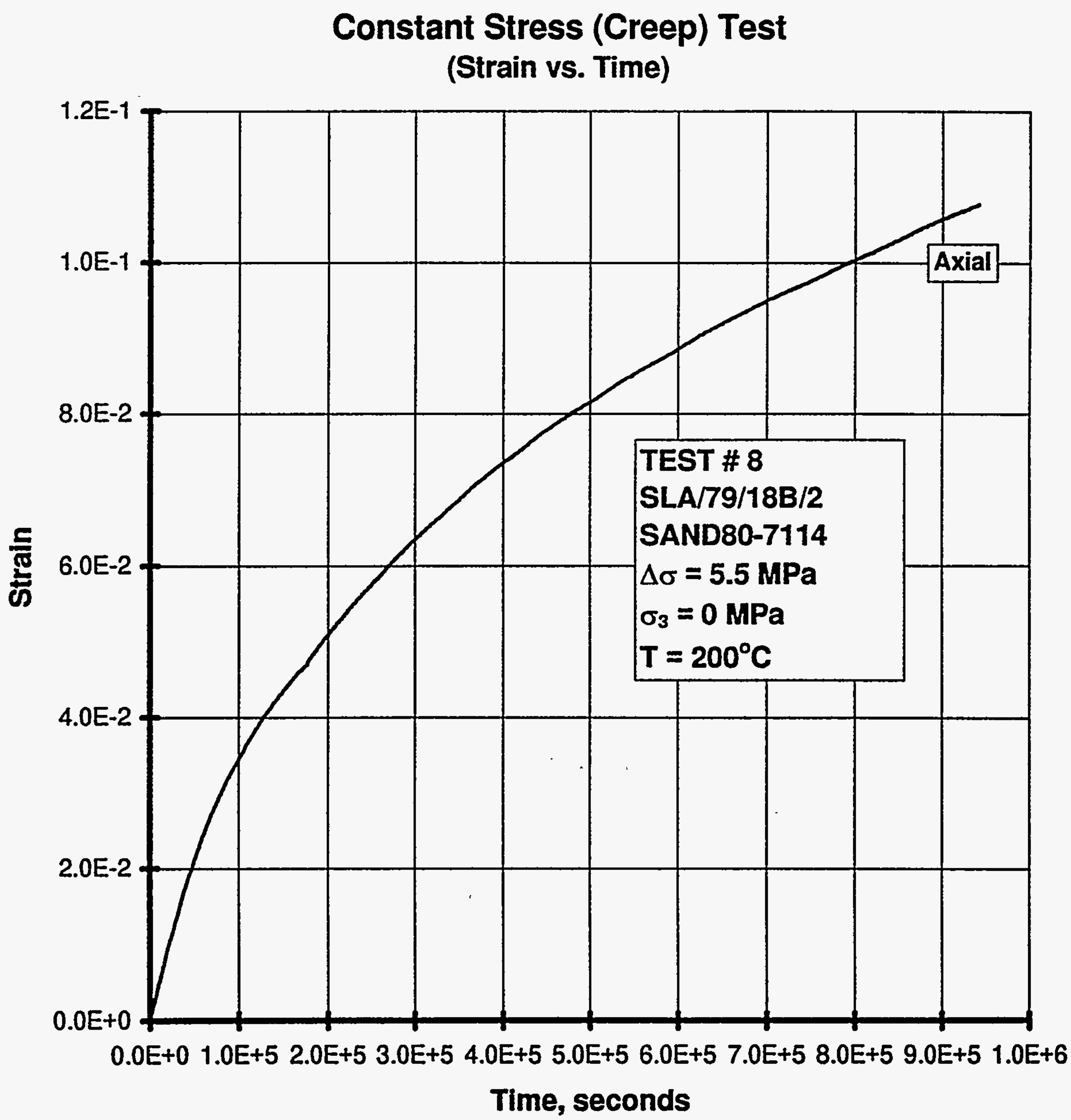

Figure B-52. Axial Strain and Lateral Strain Versus Time for a Creep Test: Specimen SLA/79/18B/2; Stage 1 of 1.

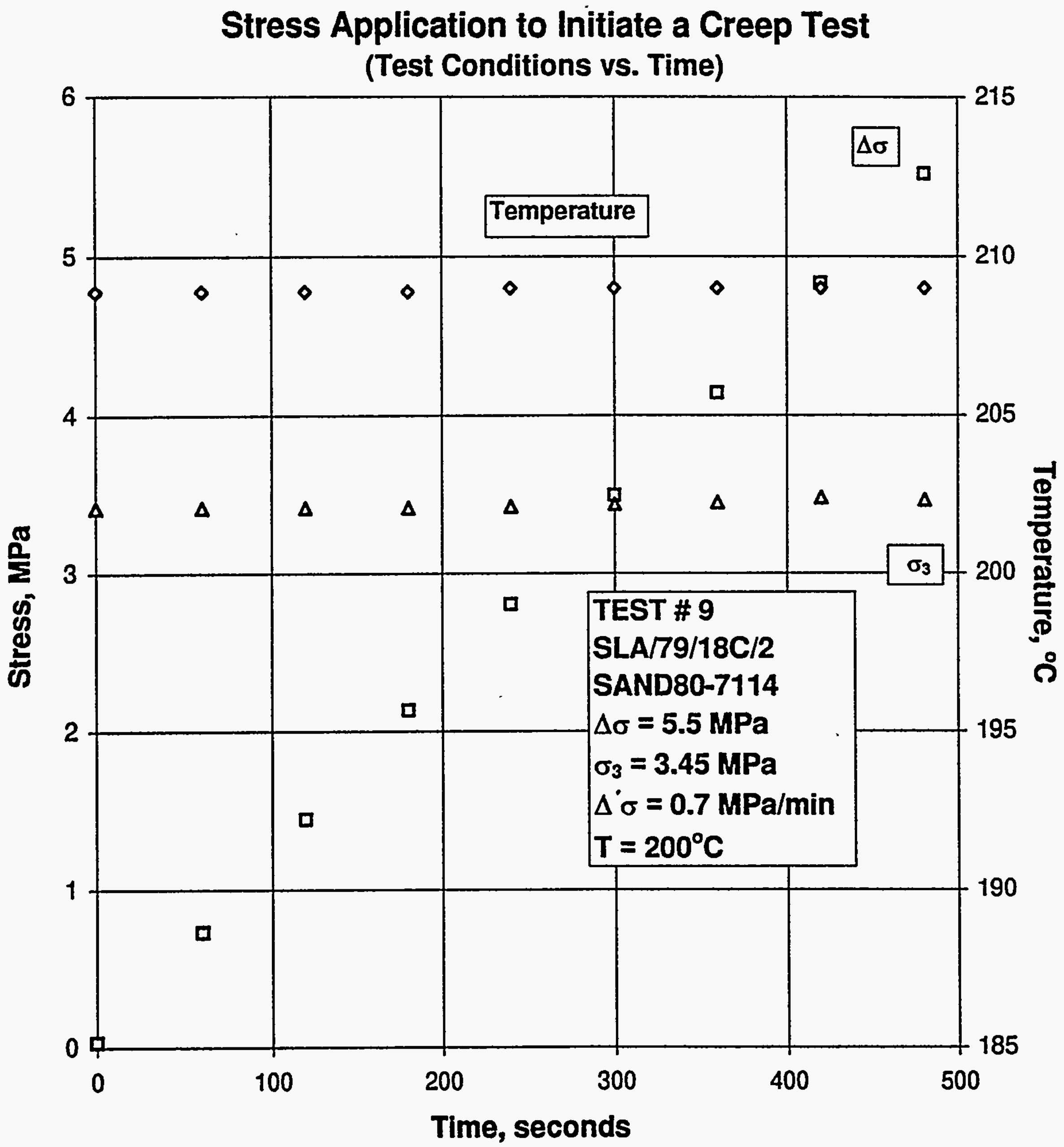

Figure B-53. Test Conditions Versus Time for Stress Application to Initiate a Creep Test: Specimen SLA/79/18C/2; Stage 1 of 1.

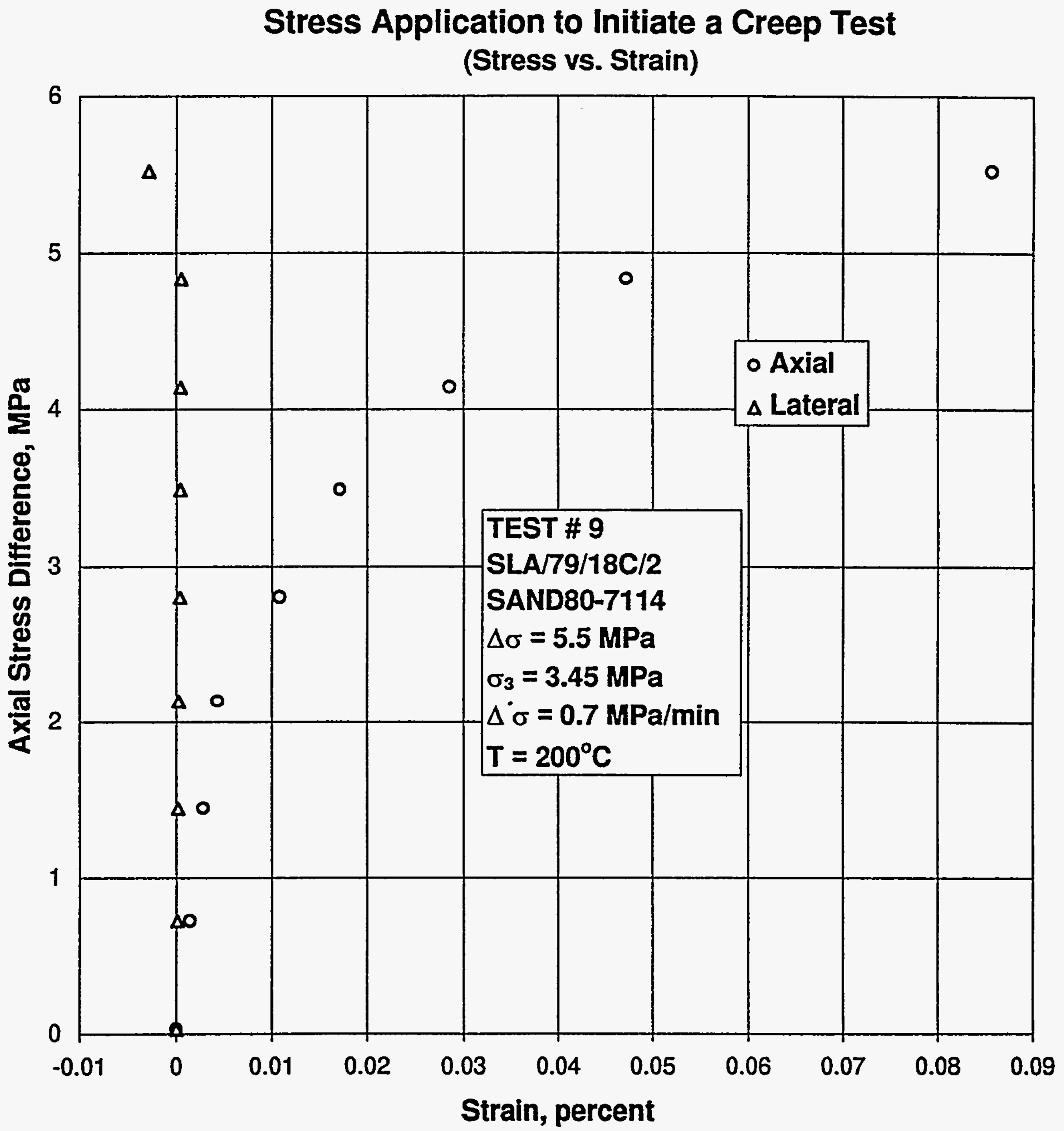

Figure B-54. Axial Stress Difference Versus Axial and Lateral Strain for Stress Application to Initiate a Creep Test: Specimen SLA/79/18C/2; Stage 1 of 1.

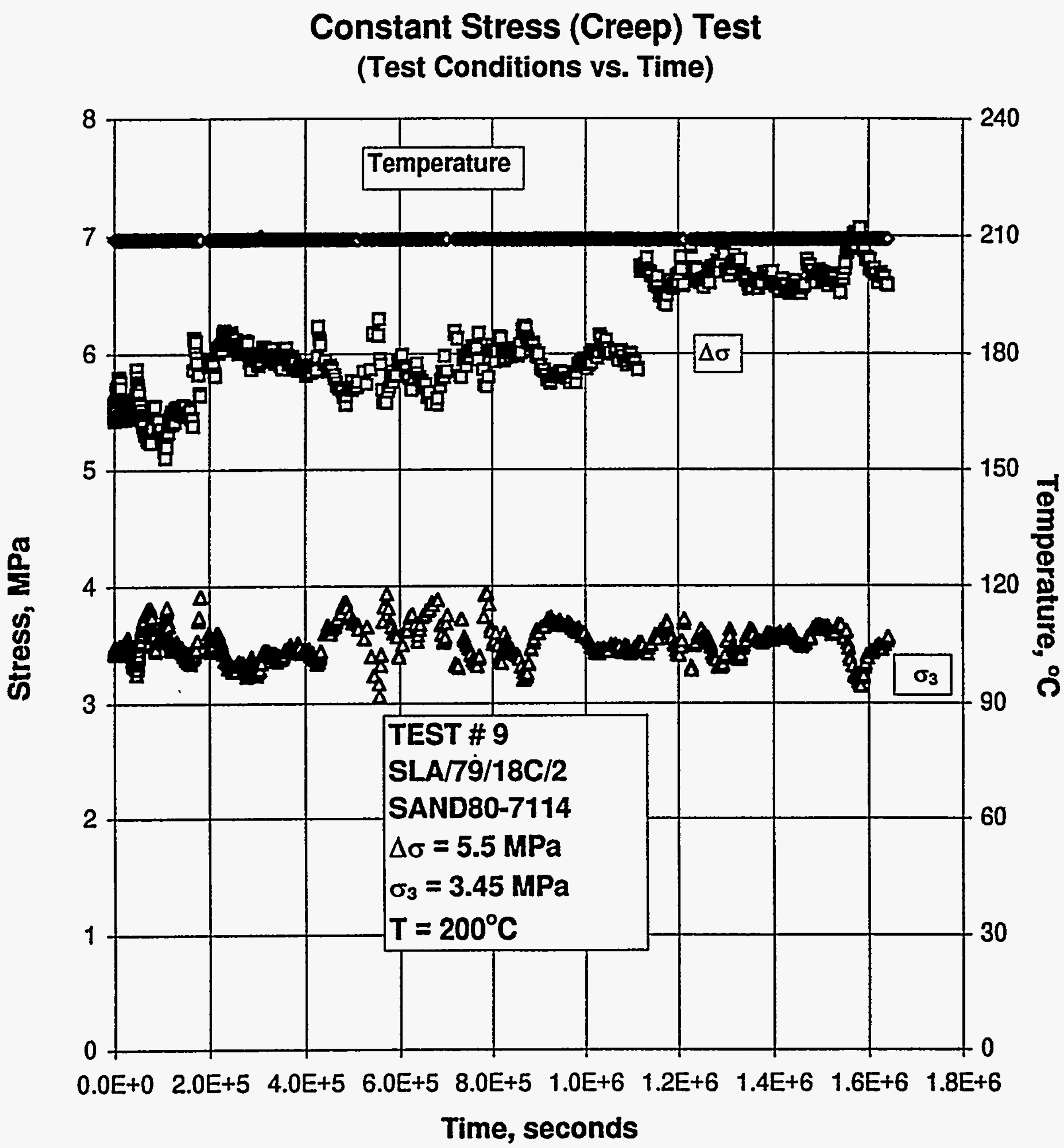

Figure B-55. Test Conditions Versus Time for a Creep Test: Specimen SLA/79/18C/2; Stage 1 of 1.

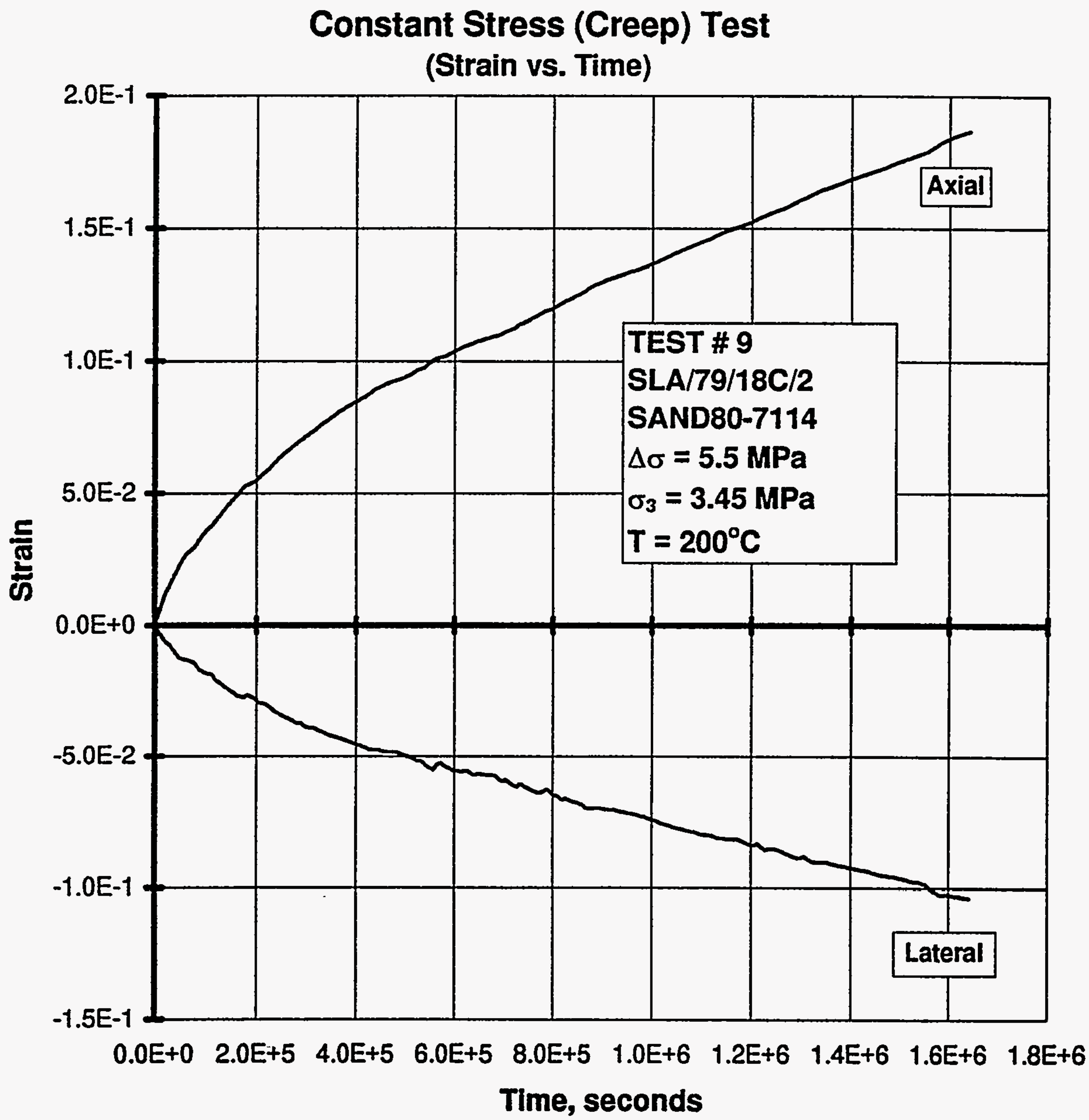

Figure B-56. Axial Strain and Lateral Strain Versus Time for a Creep Test: Specimen SLA/79/18C/2; Stage 1 of 1.

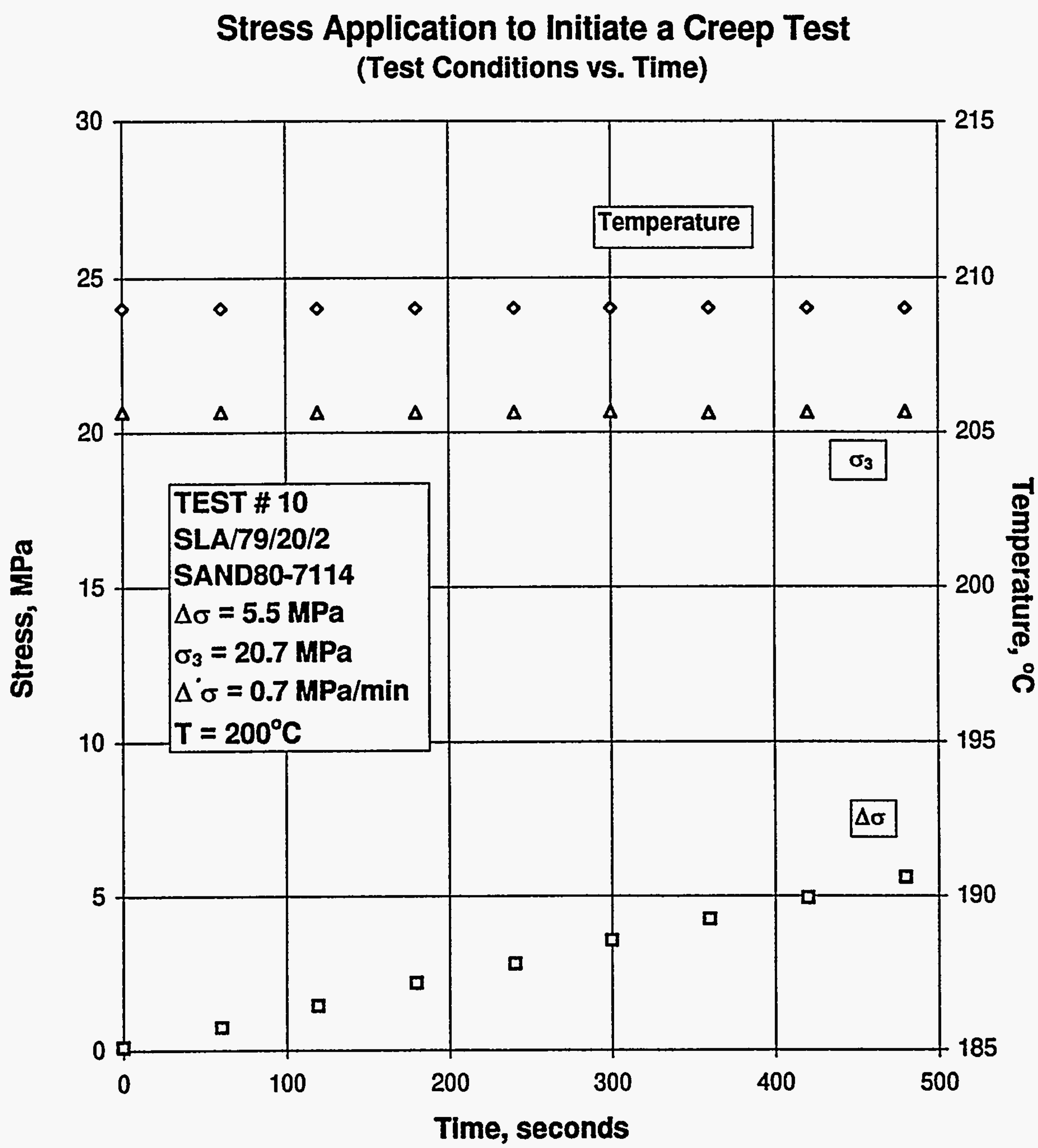

Figure B-57. Test Conditions Versus Time for Stress Application to Initiate a Creep Test: Specimen SLA/79/20/2; Stage 1 of 1.

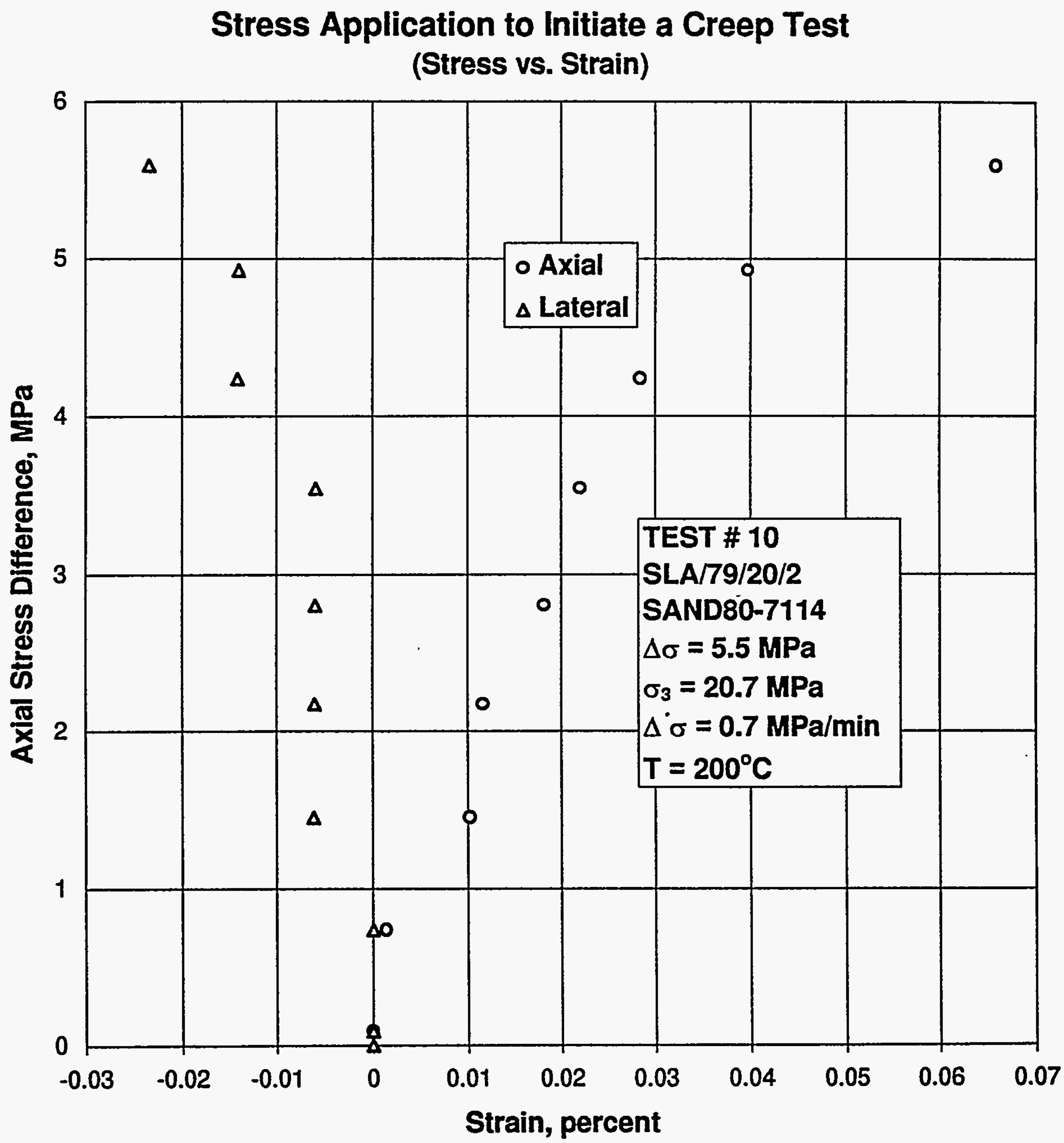

Figure B-58. Axial Stress Difference Versus Axial and Lateral Strain for Stress Application to Initiate a Creep Test: Specimen SLA/79/20/2; Stage 1 of 1.

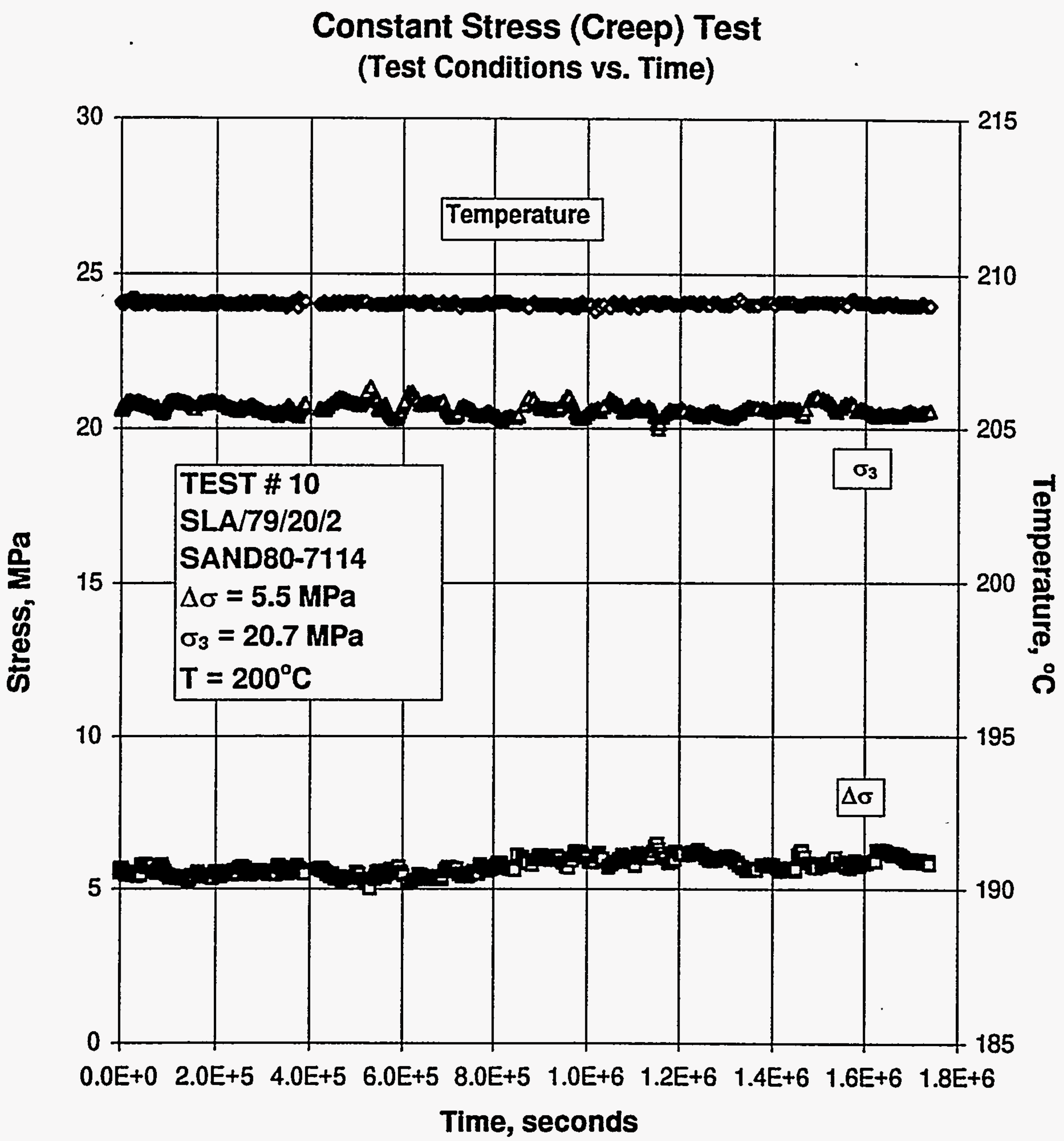

Figure B-59. Test Conditions Versus Time for a Creep Test: Specimen SLA/79/20/2; Stage 1 of 1.

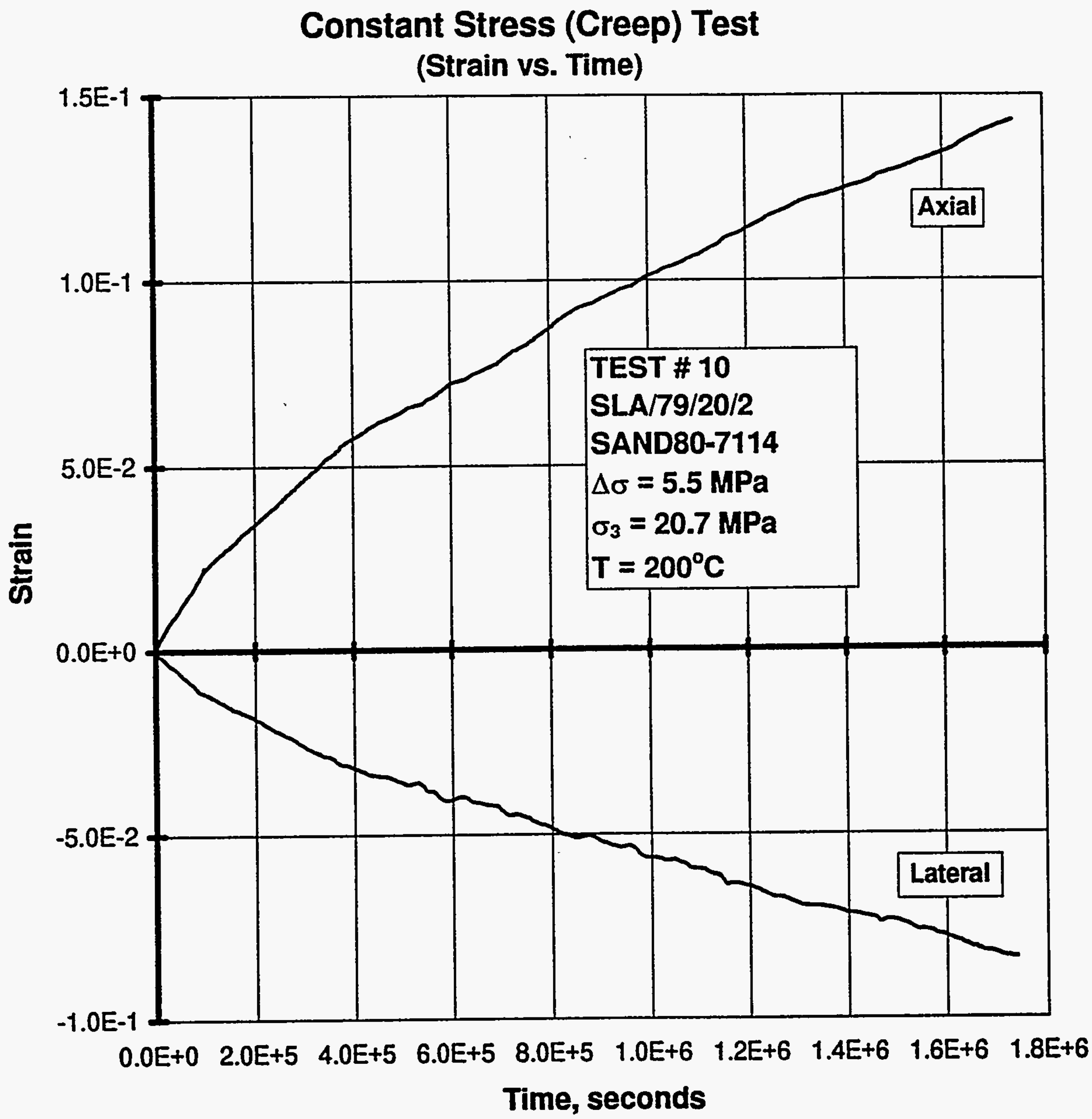

Figure B-60. Axial Strain and Lateral Strain Versus Time for a Creep Test: Specimen SLA/79/20/2; Stage 1 of 1.

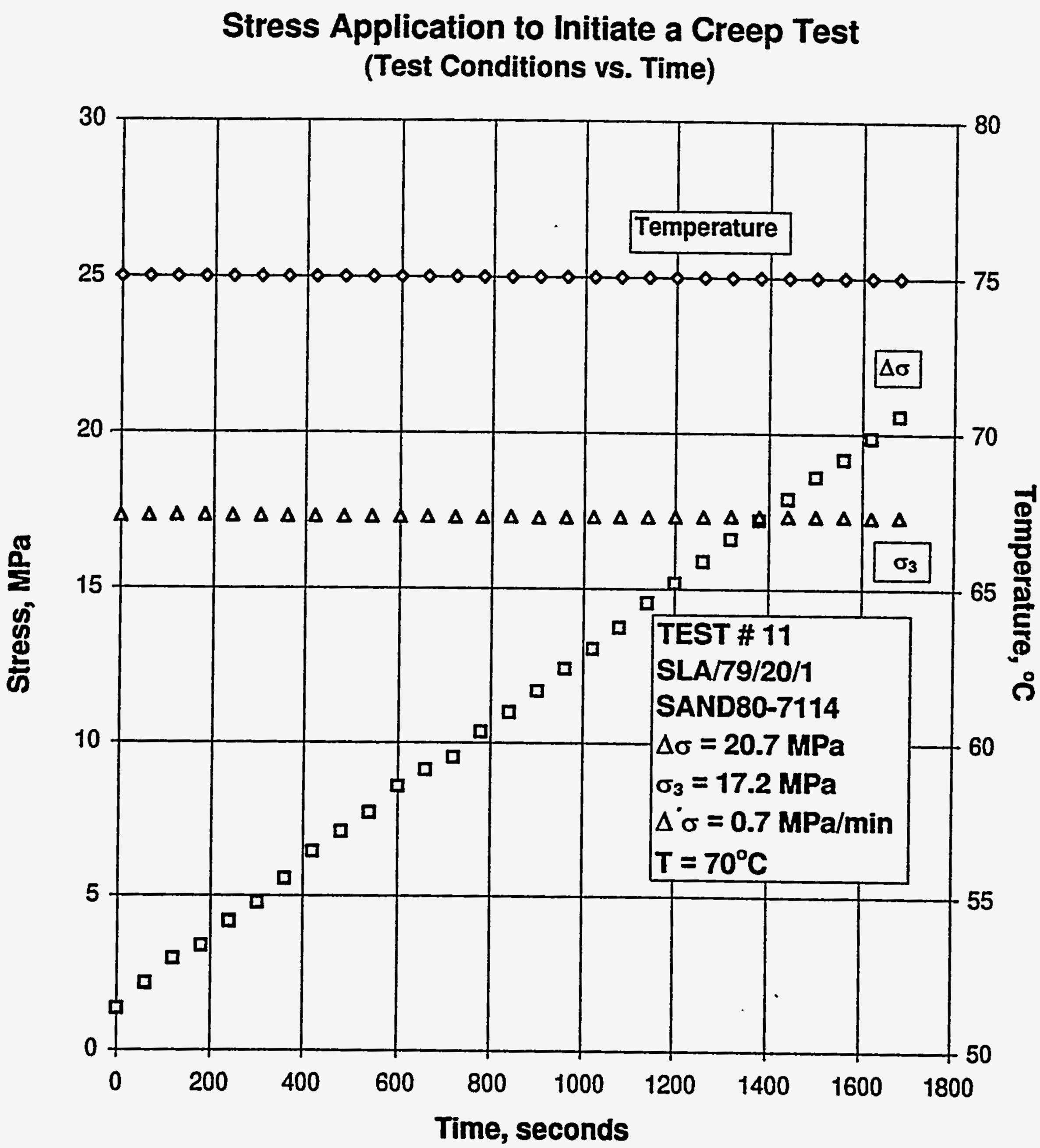

Figure B-61. Test Conditions Versus Time for Stress Application to Initiate a Creep Test: Specimen SLA/79/20/1; Stage 1 of 1.

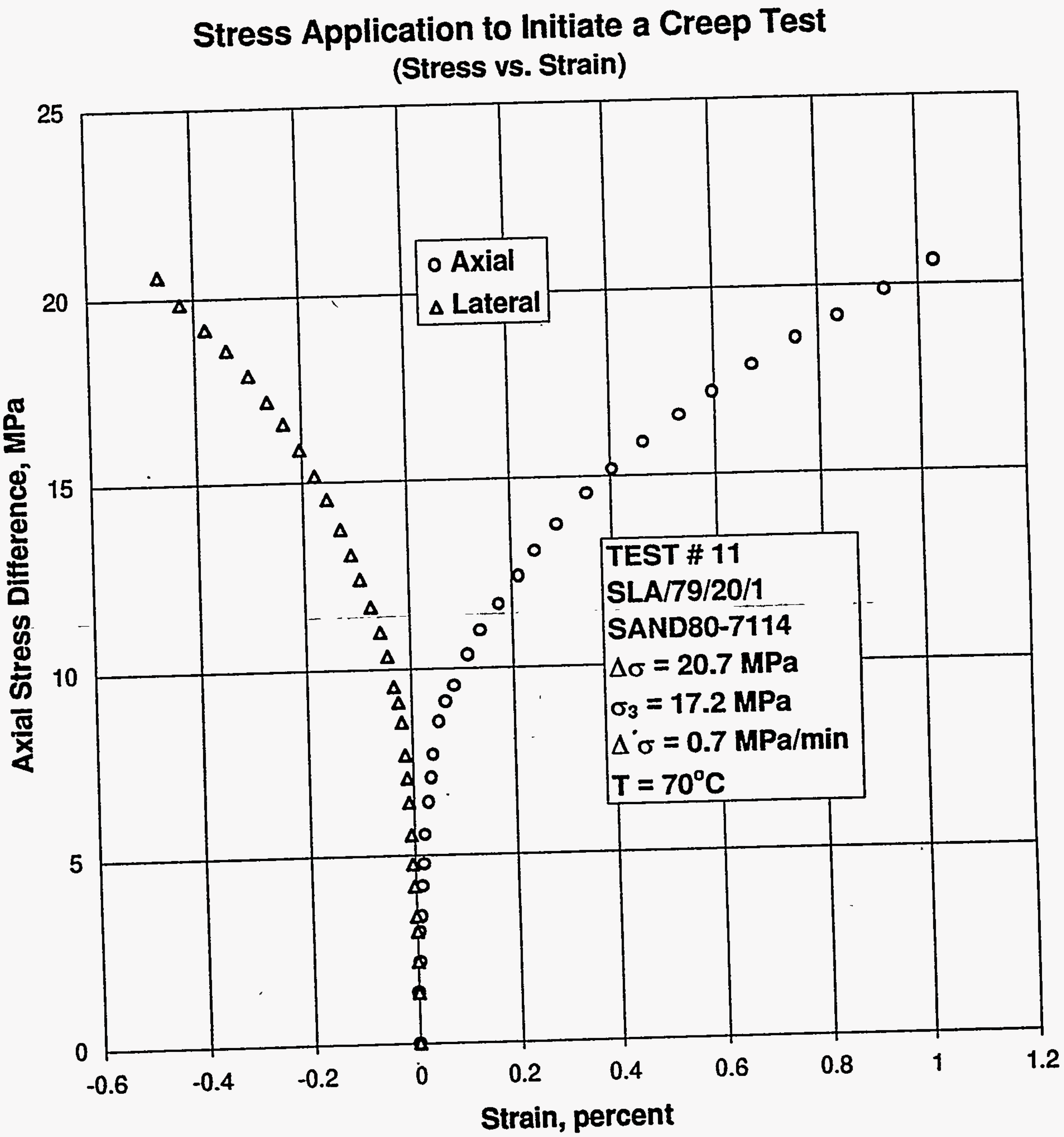

Figure B-62. Axial Stress Difference Versus Axial and Lateral Strain for Stress Application to Initiate a Creep Test: Specimen SLA/79/20/1; Stage 1 of 1.

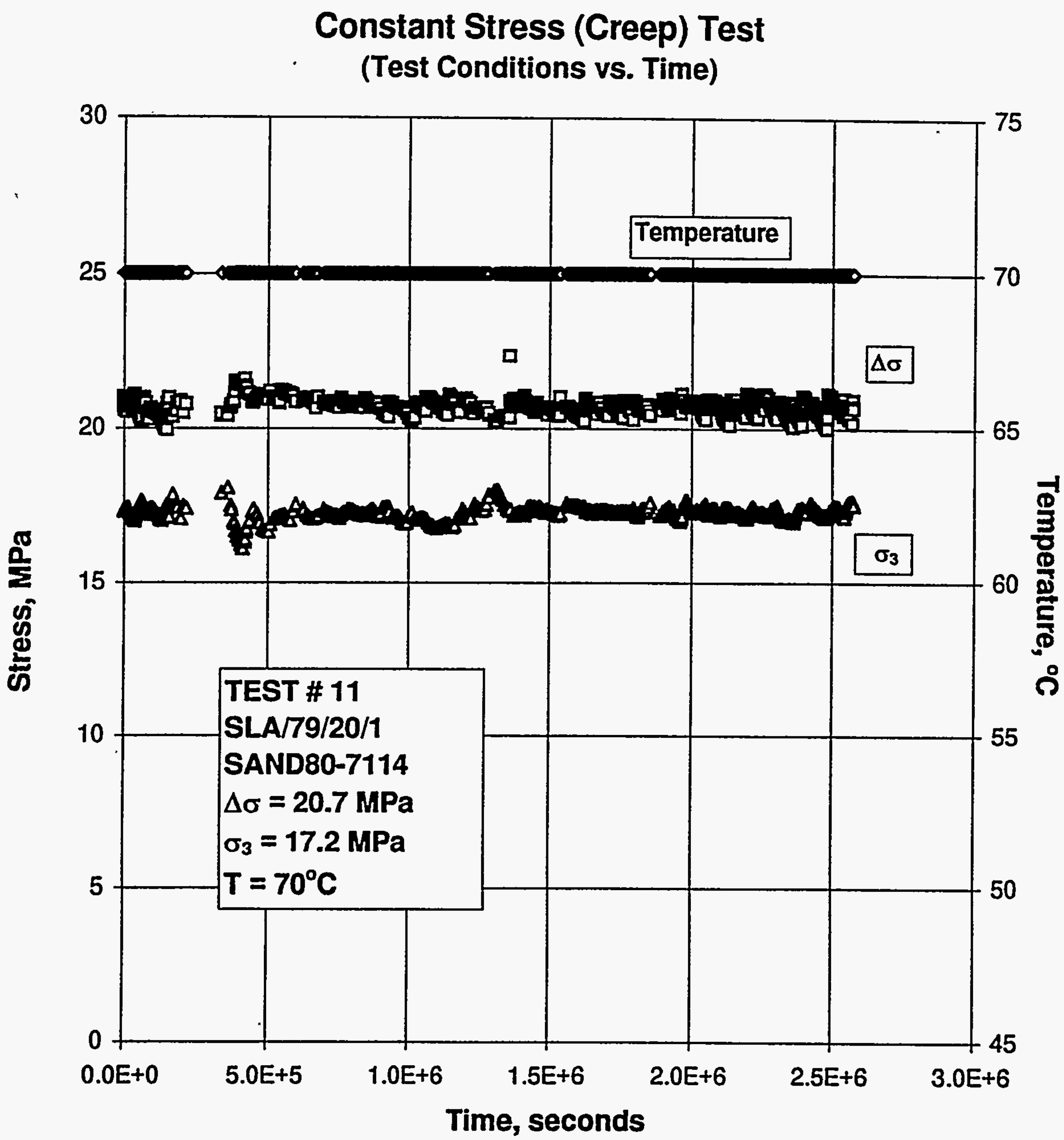

Figure B-63. Test Conditions Versus Time for a Creep Test: Specimen SLA/79/20/1; Stage 1 of 1.

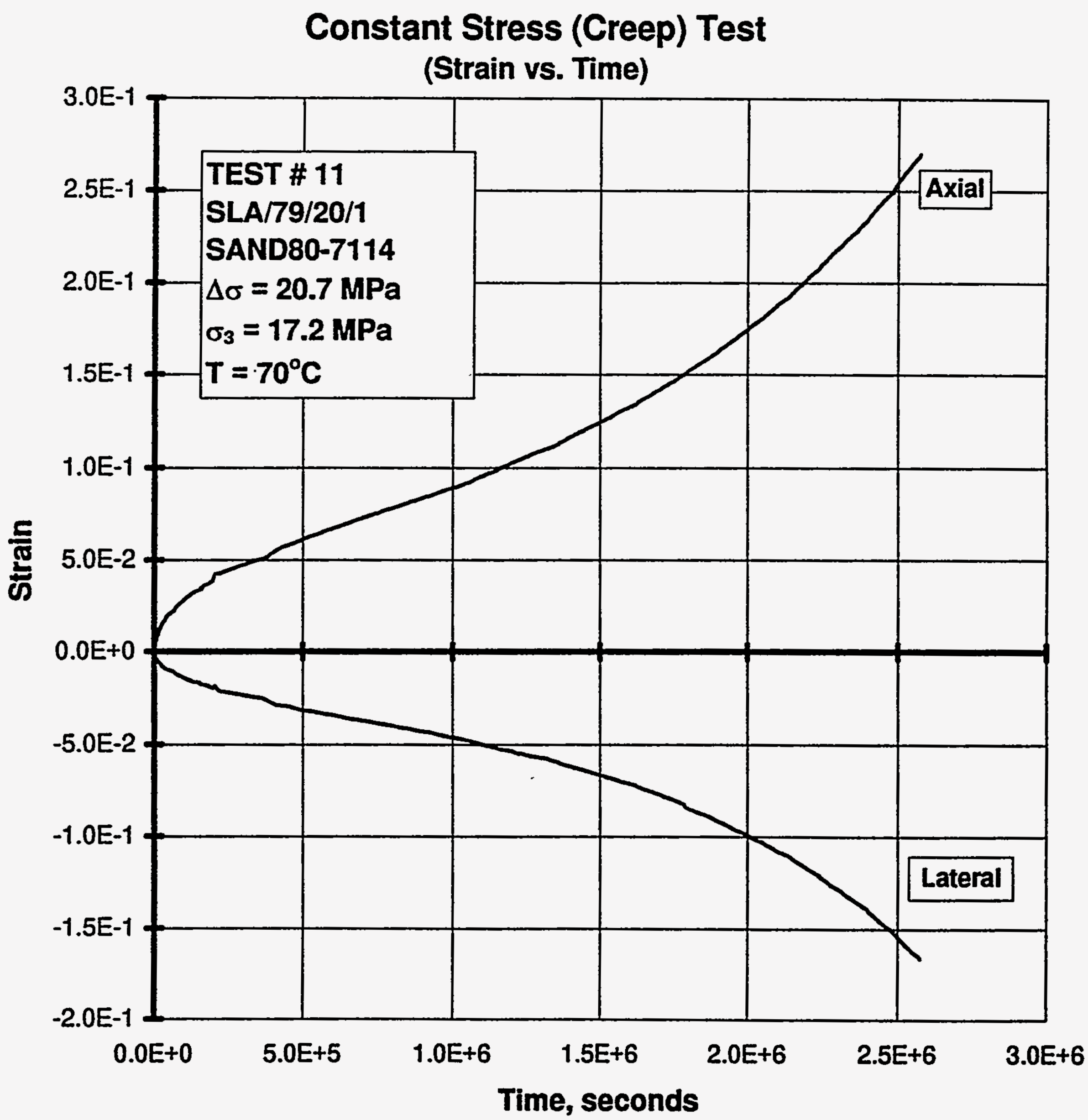

Figure B-64. Axial Strain and Lateral Strain Versus Time for a Creep Test: Specimen SLA/79/20/1; Stage 1 of 1.

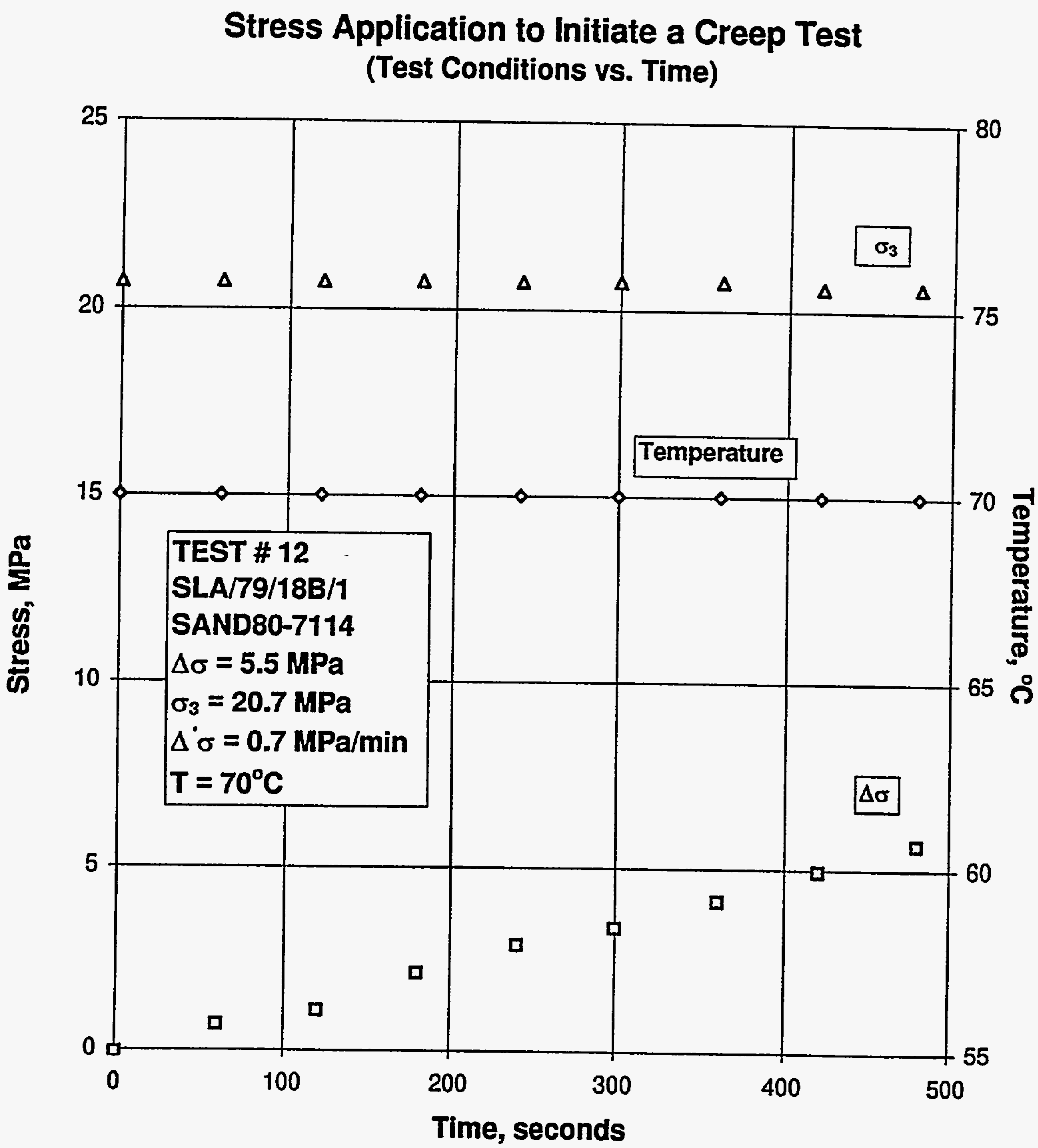

Figure B-65. Test Conditions Versus Time for Stress Application to Initiate a Creep Test: Specimen SLA/79/18B/1; Stage 1 of 1.

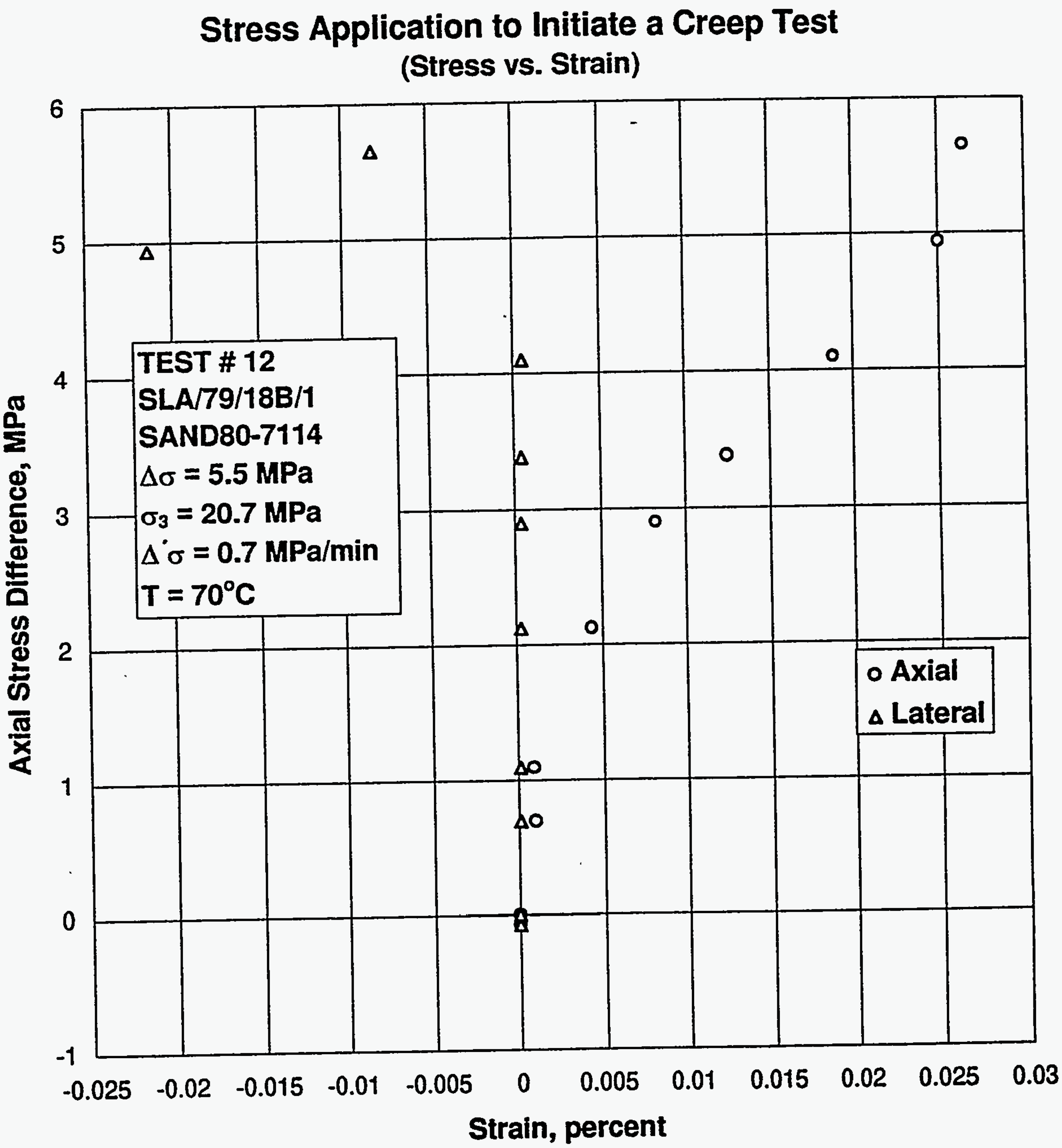

Figure B-66. Axial Stress Difference Versus Axial and Lateral Strain for Stress Application to Initiate a Creep Test: Specimen SLA/79/18B/1; Stage 1 of 1.

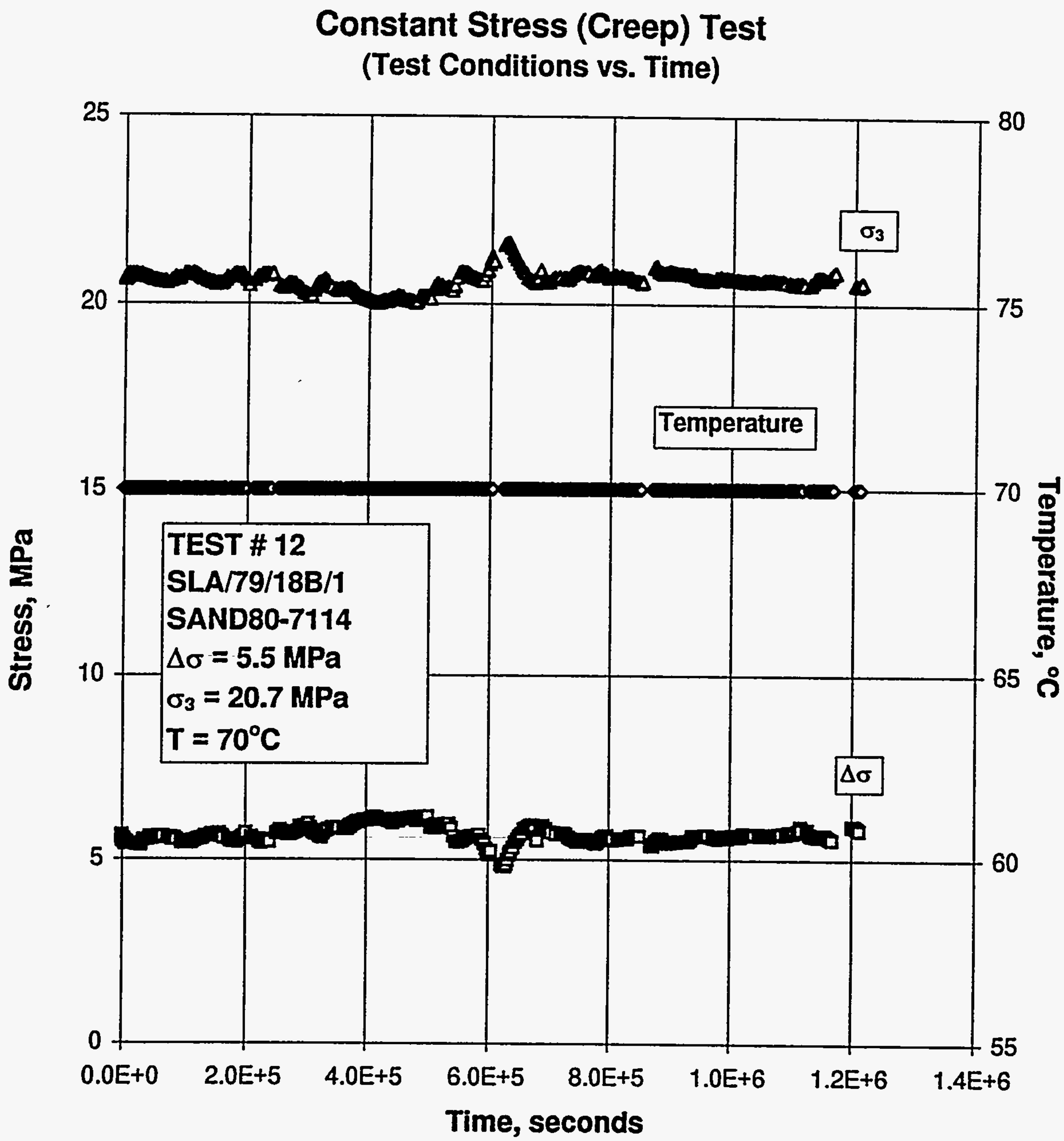

Figure B-67. Test Conditions Versus Time for a Creep Test: Specimen SLA/79/18B/1; Stage 1 of 1.

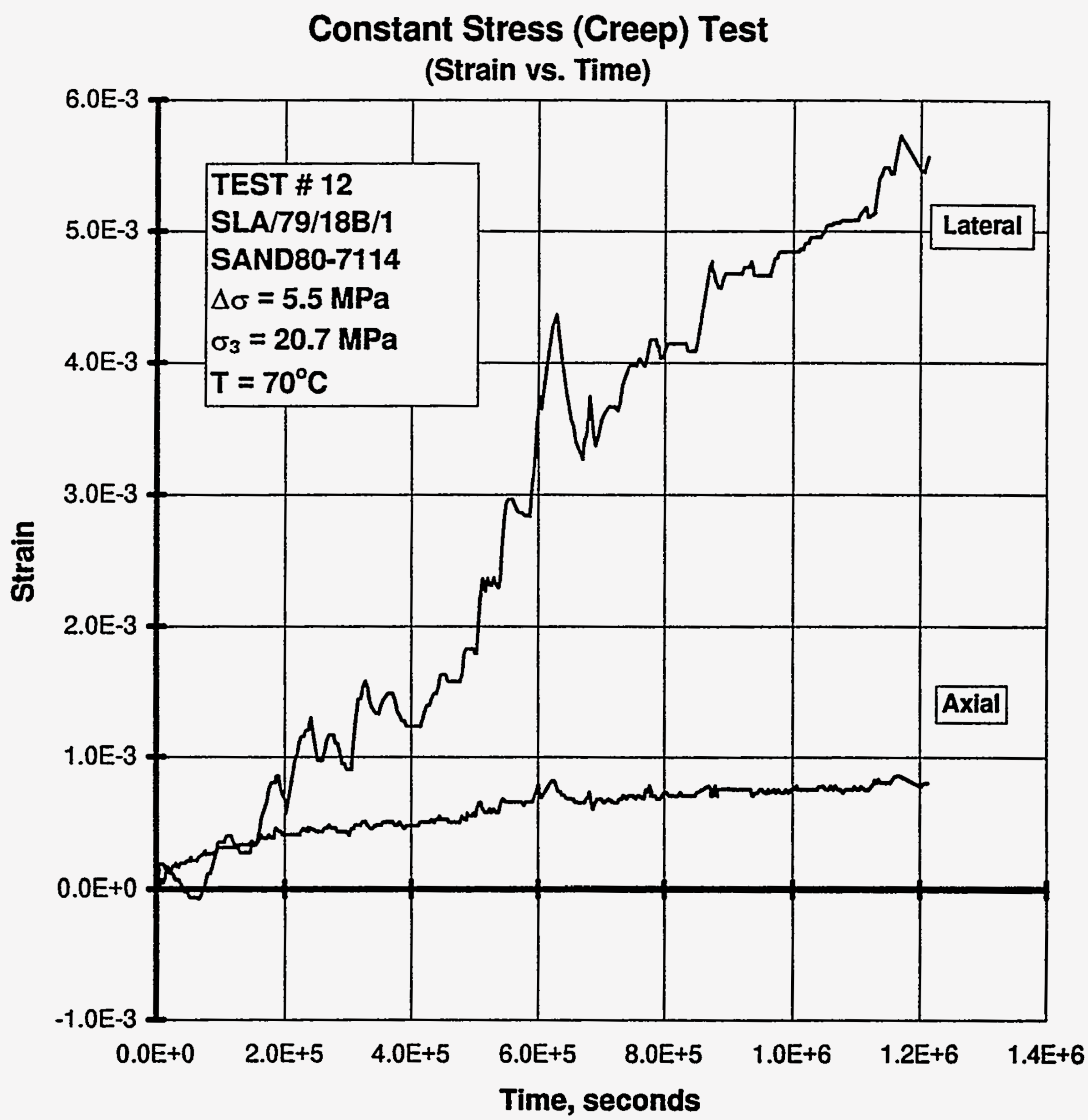

Figure B-68. Axial Strain and Lateral Strain Versus Time for a Creep Test: Specimen SLA/79/18B/1; Stage 1 of 1.

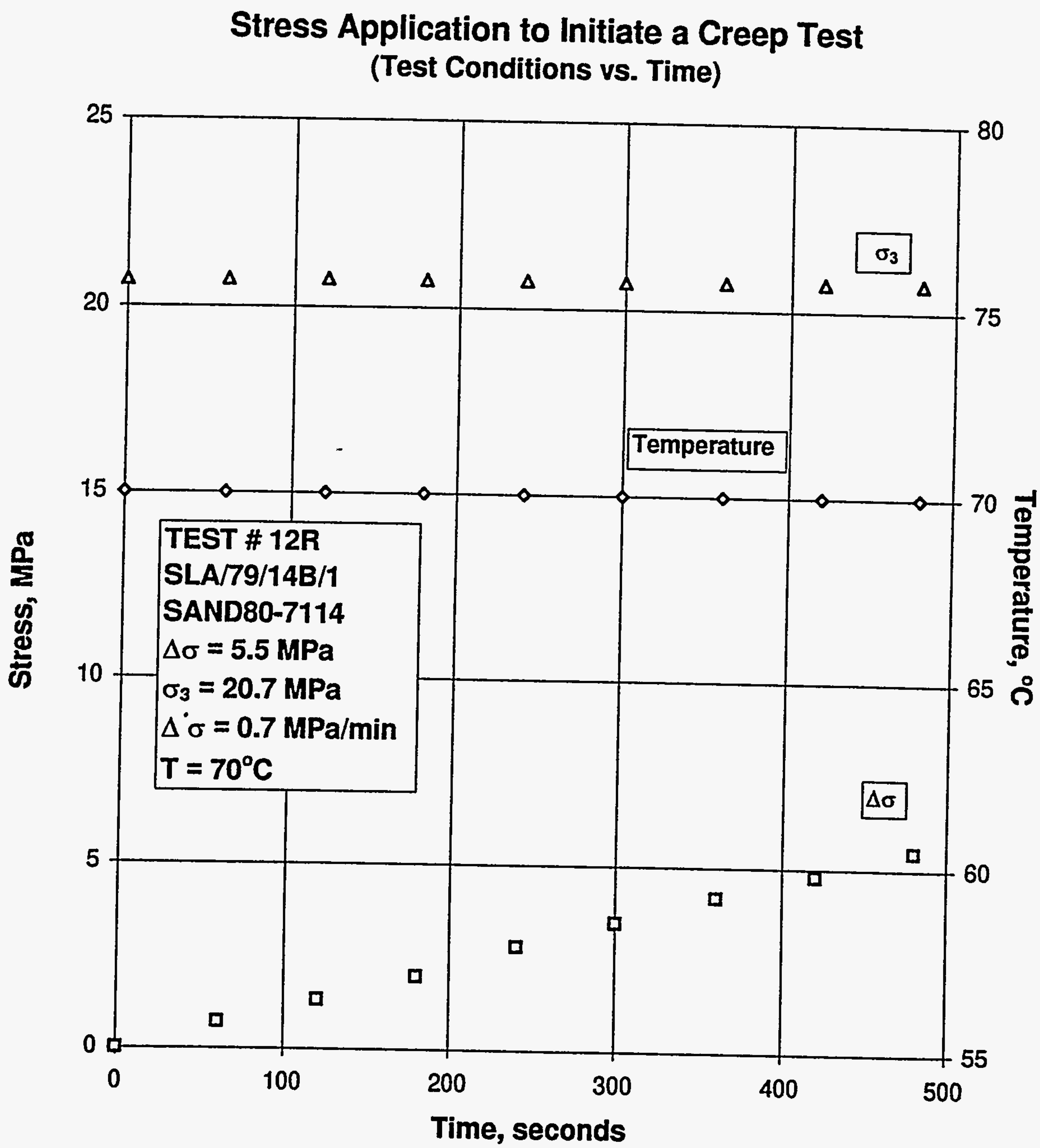

Figure B-69. Test Conditions Versus Time for Stress Application to Initiate a Creep Test: Specimen SLA/79/14B/1; Stage 1 of 1.

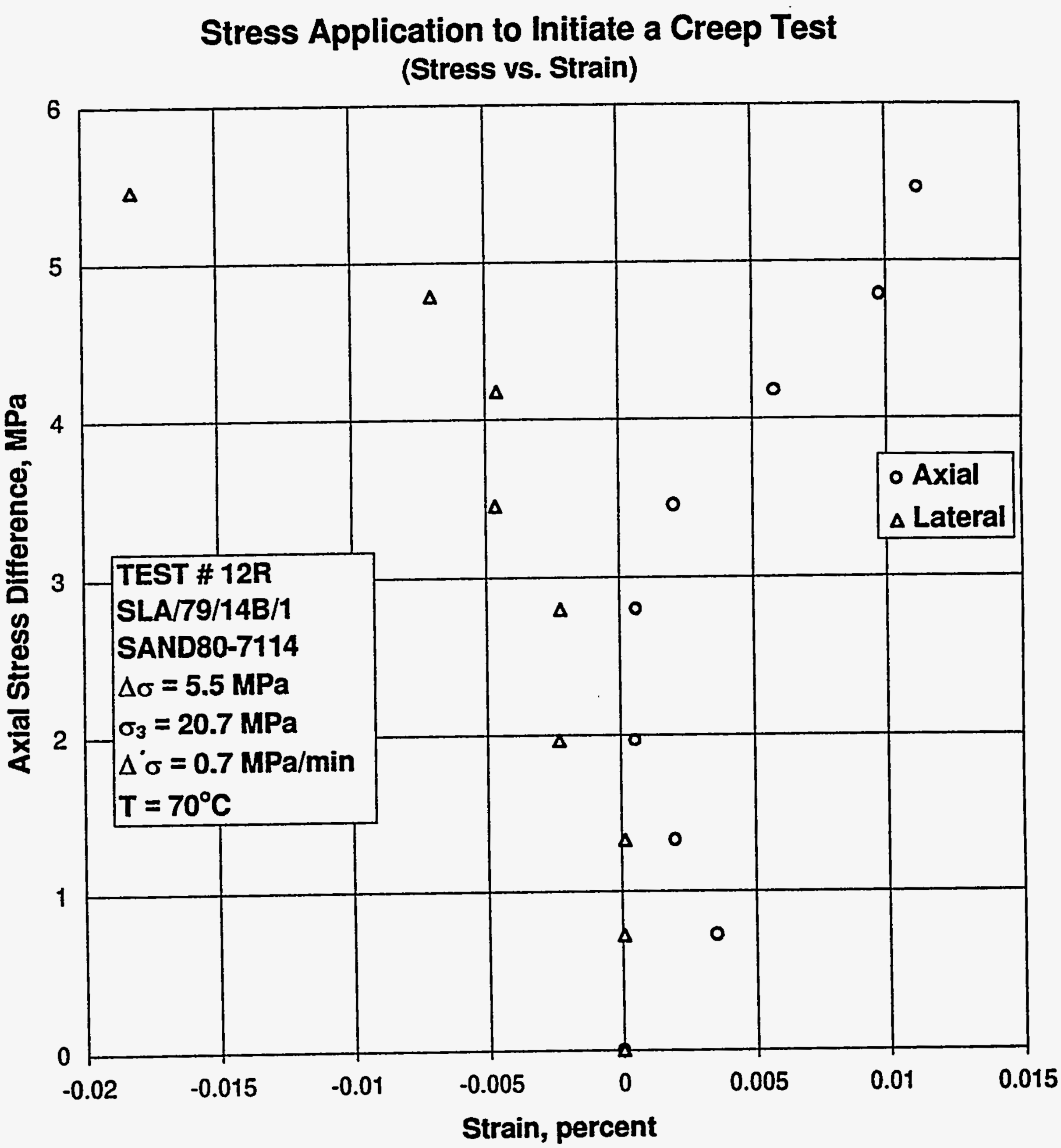

Figure B-70. Axial Stress Difference Versus Axial and Lateral Strain for Stress Application to Initiate a Creep Test: Specimen SLA/79/14B/1; Stage 1 of 1.

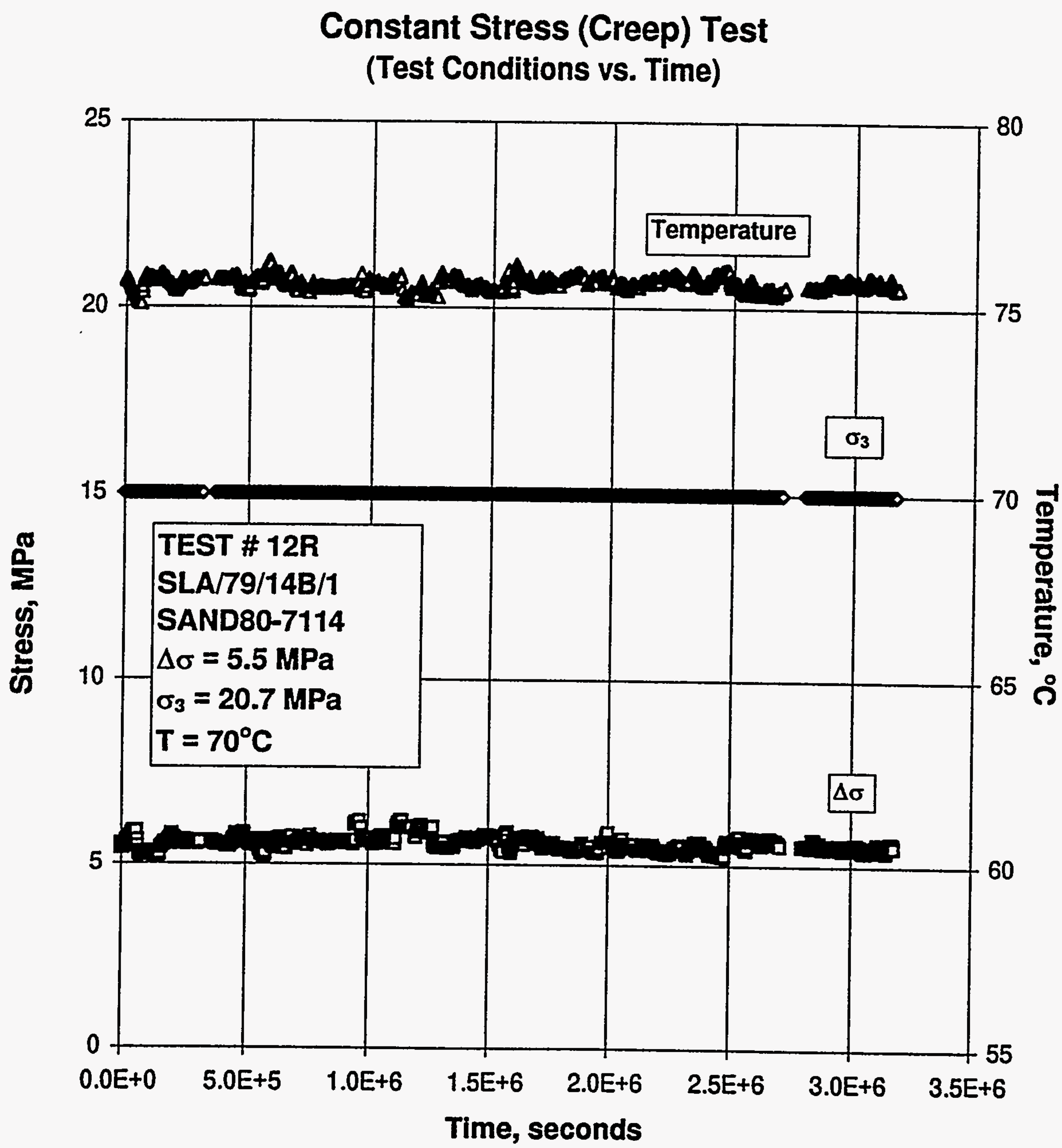

Figure B-71. Test Conditions Versus Time for a Creep Test: Specimen SLA/79/14B/1; Stage 1 of 1.

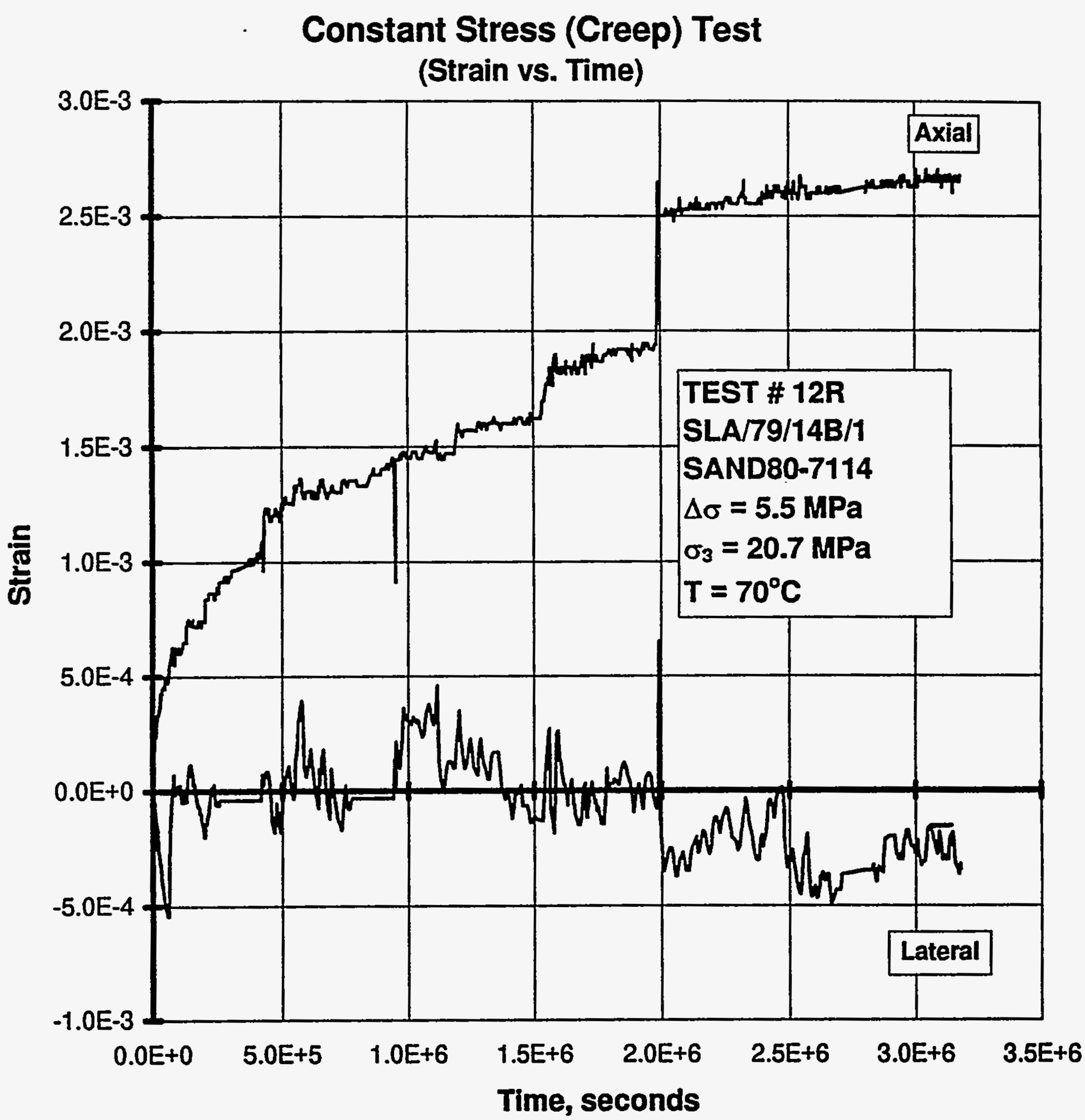

Figure B-72. Axial Strain and Lateral Strain Versus Time for a Creep Test: Specimen SLA/79/14B/1; Stage 1 of 1.

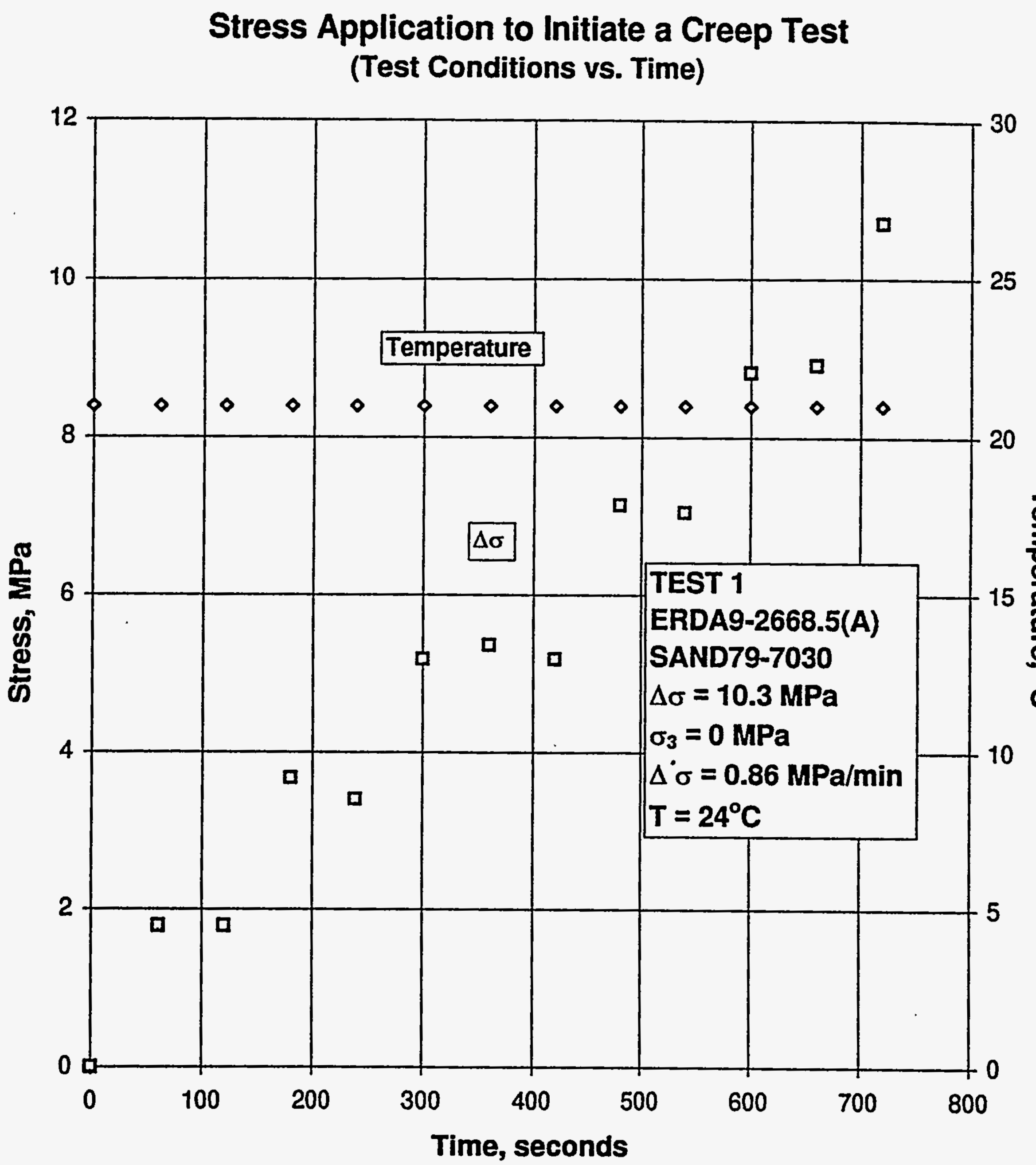

Figure B-73. Test Conditions Versus Time for Stress Application to Initiate a Creep Test: Specimen ERDA9-2668.5 (A); Stage 1 of 1.

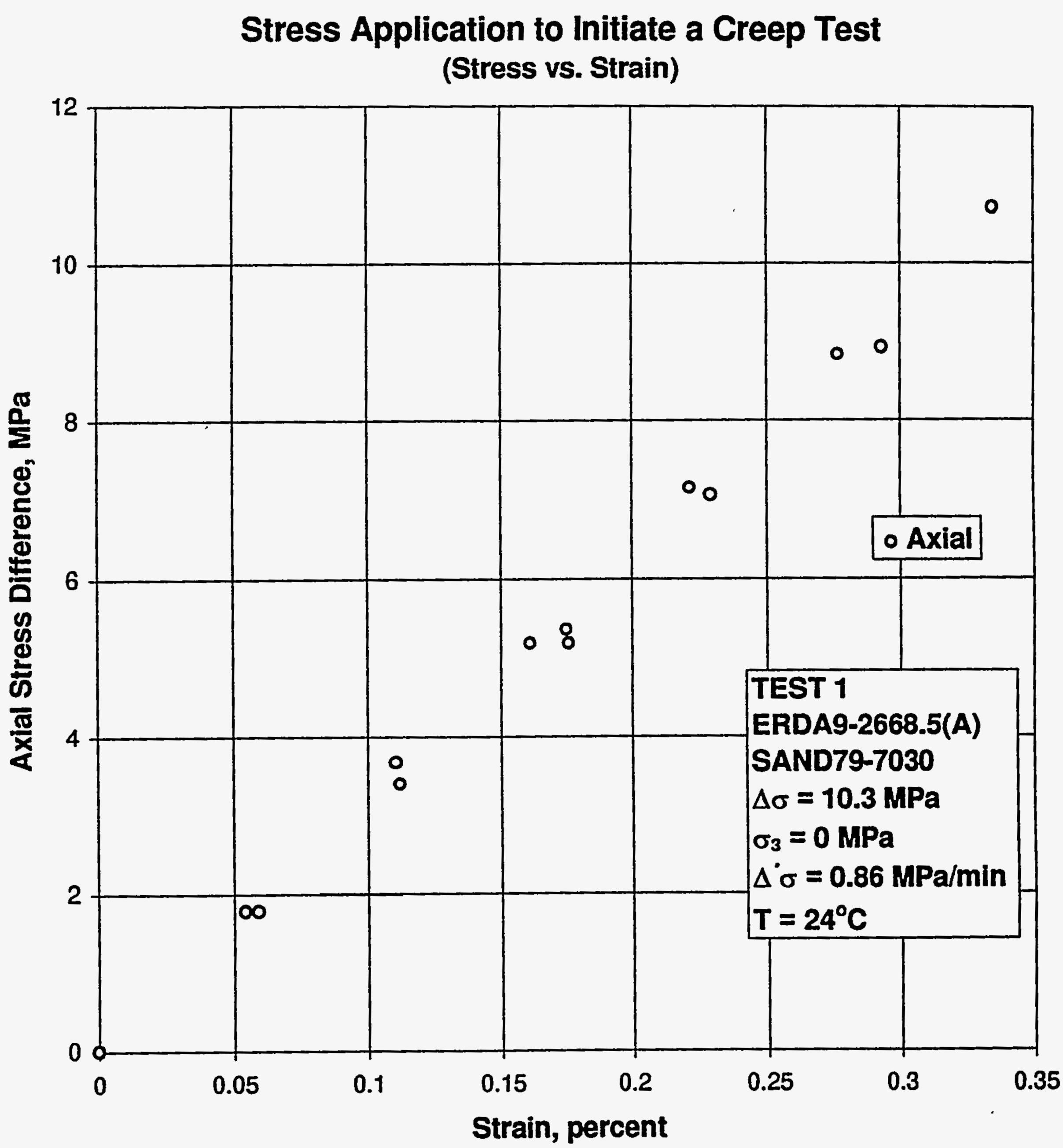

Figure B-74. Axial Stress Difference Versus Axial and Lateral Strain for Stress Application to Initiate a Creep Test: Specimen ERDA9-2668.5 (A); Stage 1 of 1.

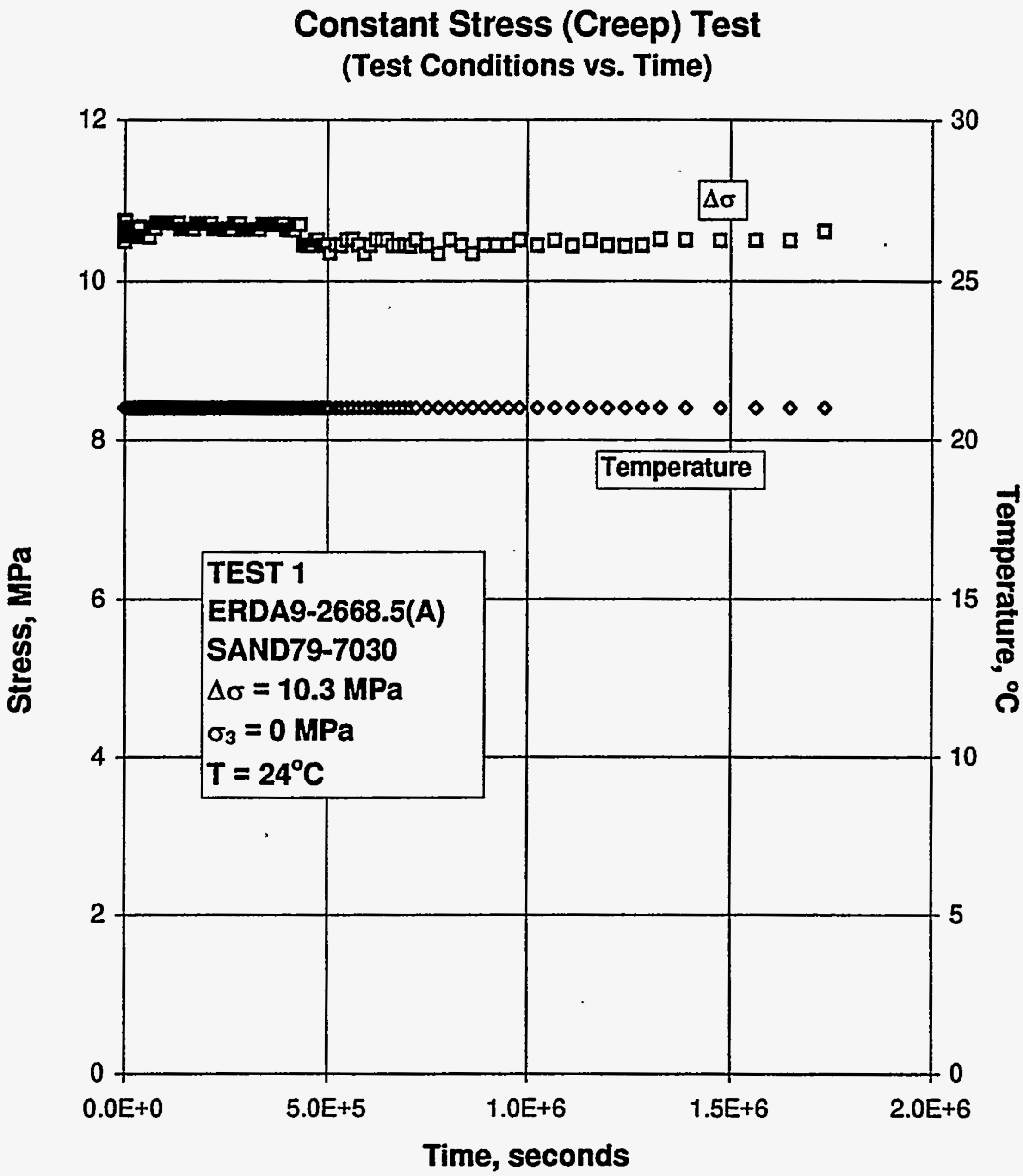

Figure B-75. Test Conditions Versus Time for a Creep Test: Specimen ERDA9-2668.5 (A); Stage 1 of 1 (System Malfunction at 5.1 Days. Test was Restarted After Repair).

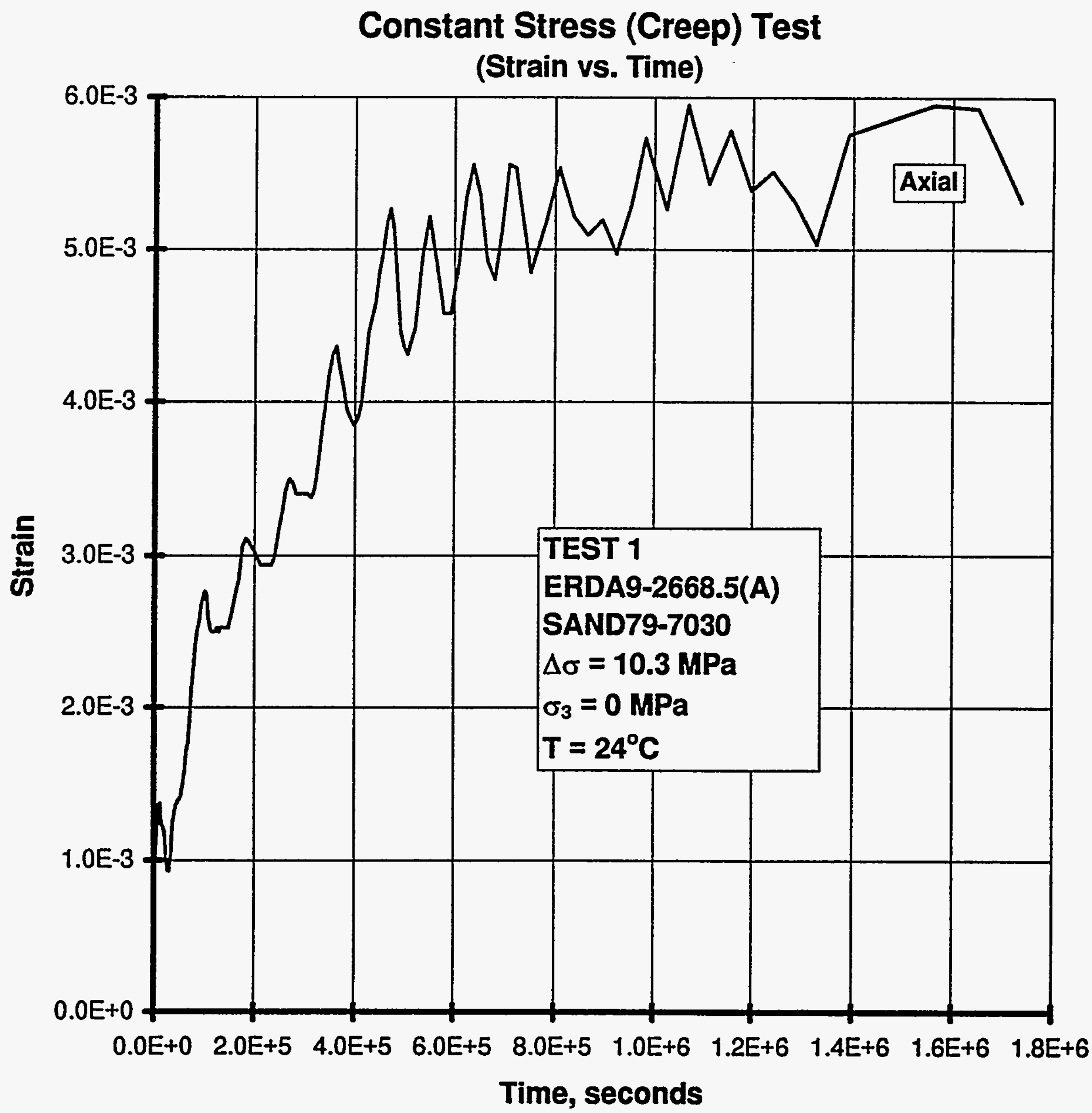

Figure B-76. Axial Strain and Lateral Strain Versus Time for a Creep Test: Specimen ERDA9-2668.5 (A); Stage 1 of 1 (System Malfunction at 5.1 Days. Test was Restarted After Repair).

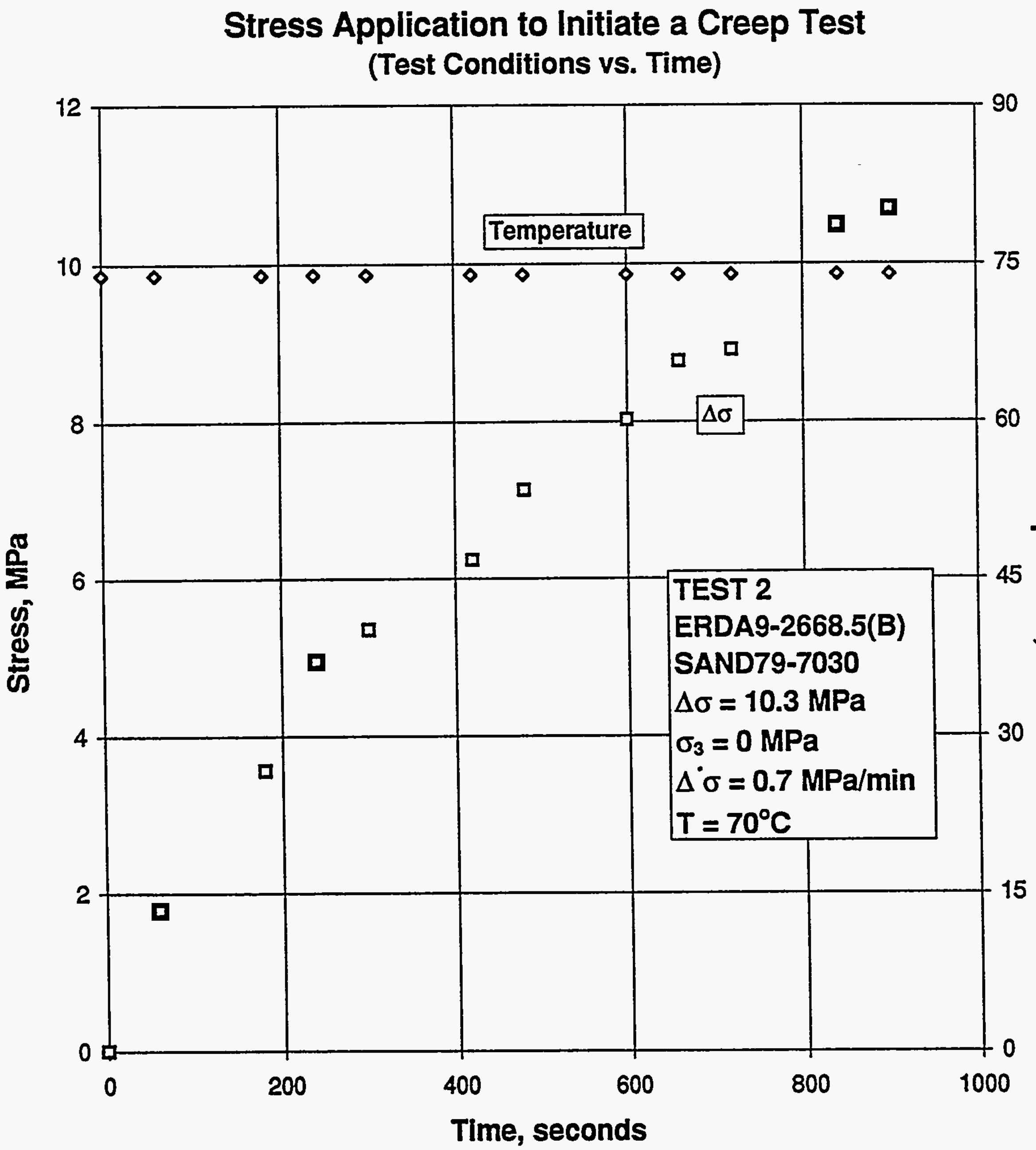

Figure B-77. Test Conditions Versus Time for Stress Application to Initiate a Creep Test: Specimen ERDA9-2668.5 (B); Stage 1 of 1.

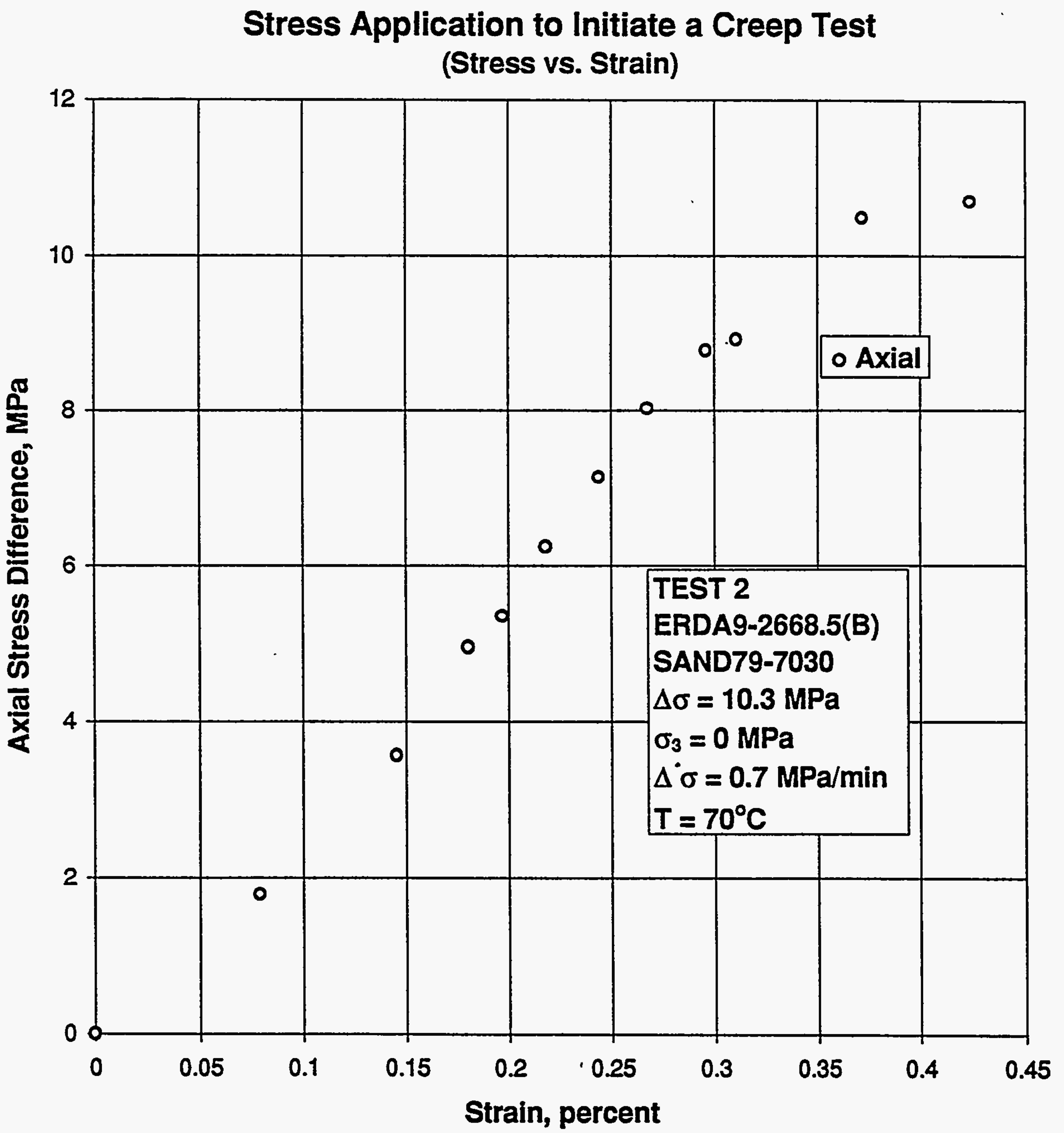

Figure B-78. Axial Stress Difference Versus Axial and Lateral Strain for Stress Application to Initiate a Creep Test: Specimen ERDA9-2668.5 (B); Stage 1 of 1.

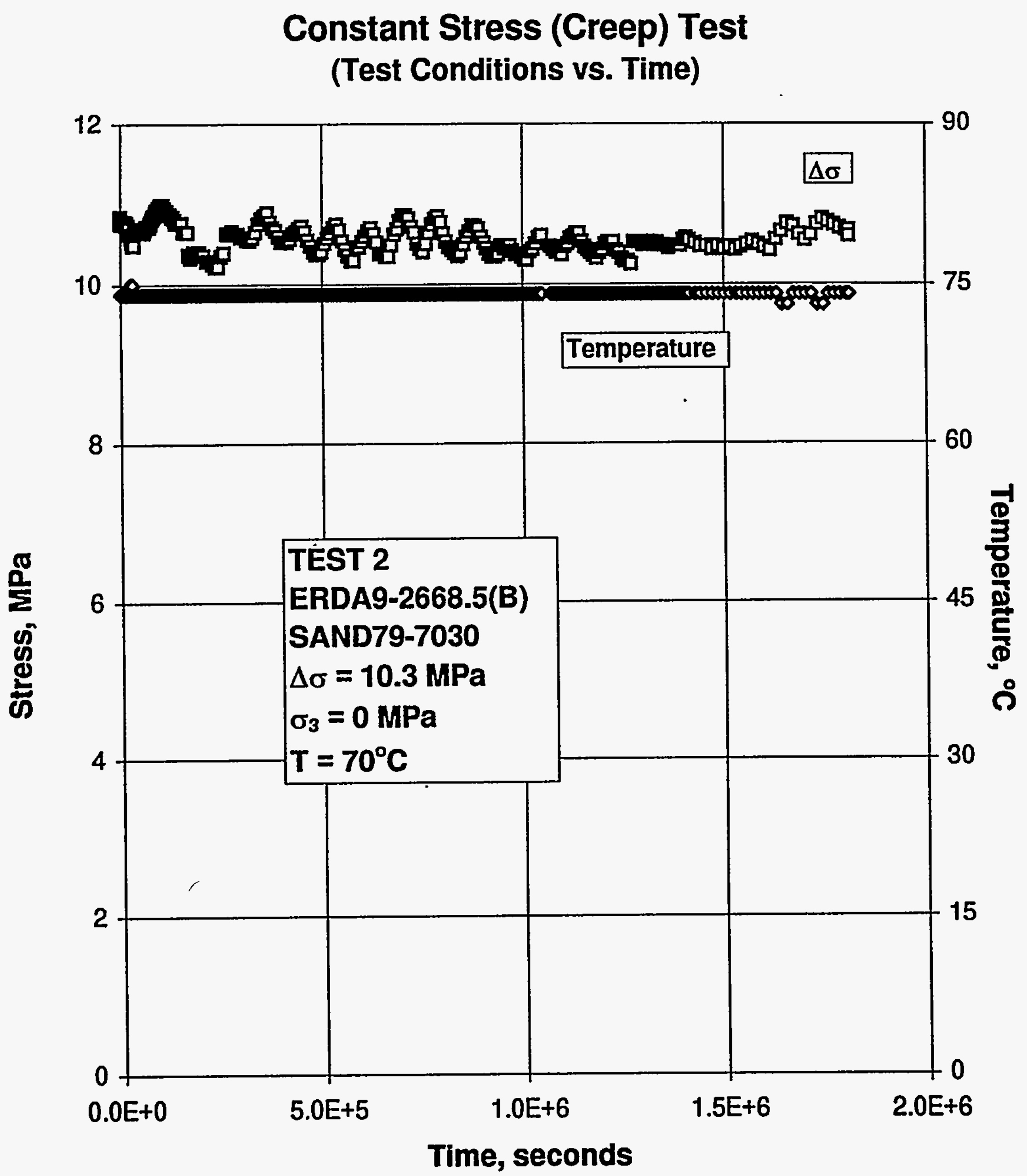

Figure B-79. Test Conditions Versus Time for a Creep Test: Specimen ERDA9-2668.5 (B); Stage 1 of 1.

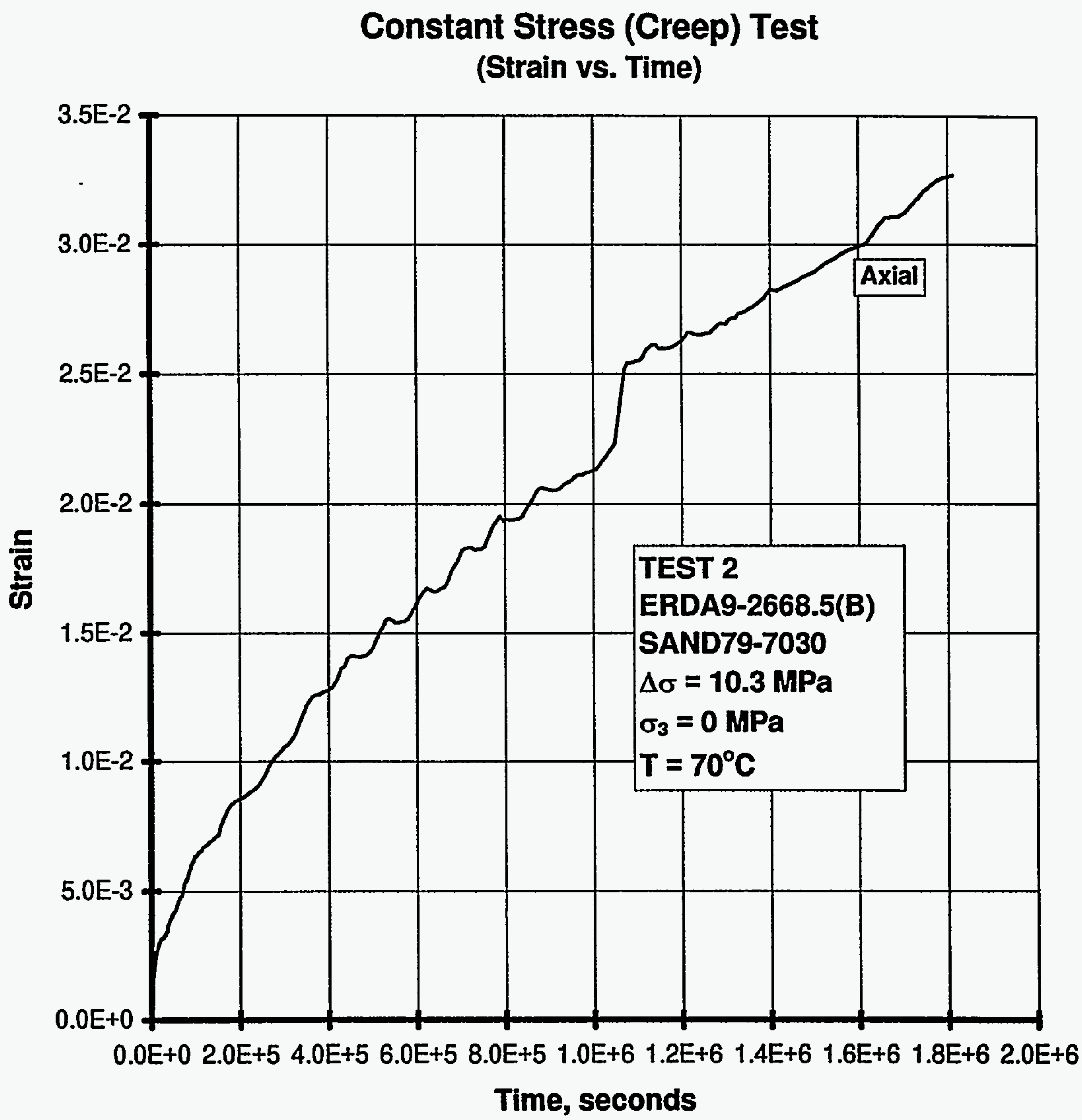

Figure B-80. Axial Strain and Lateral Strain Versus Time for a Creep Test: Specimen ERDA9-2668.5 (B); Stage 1 of 1.

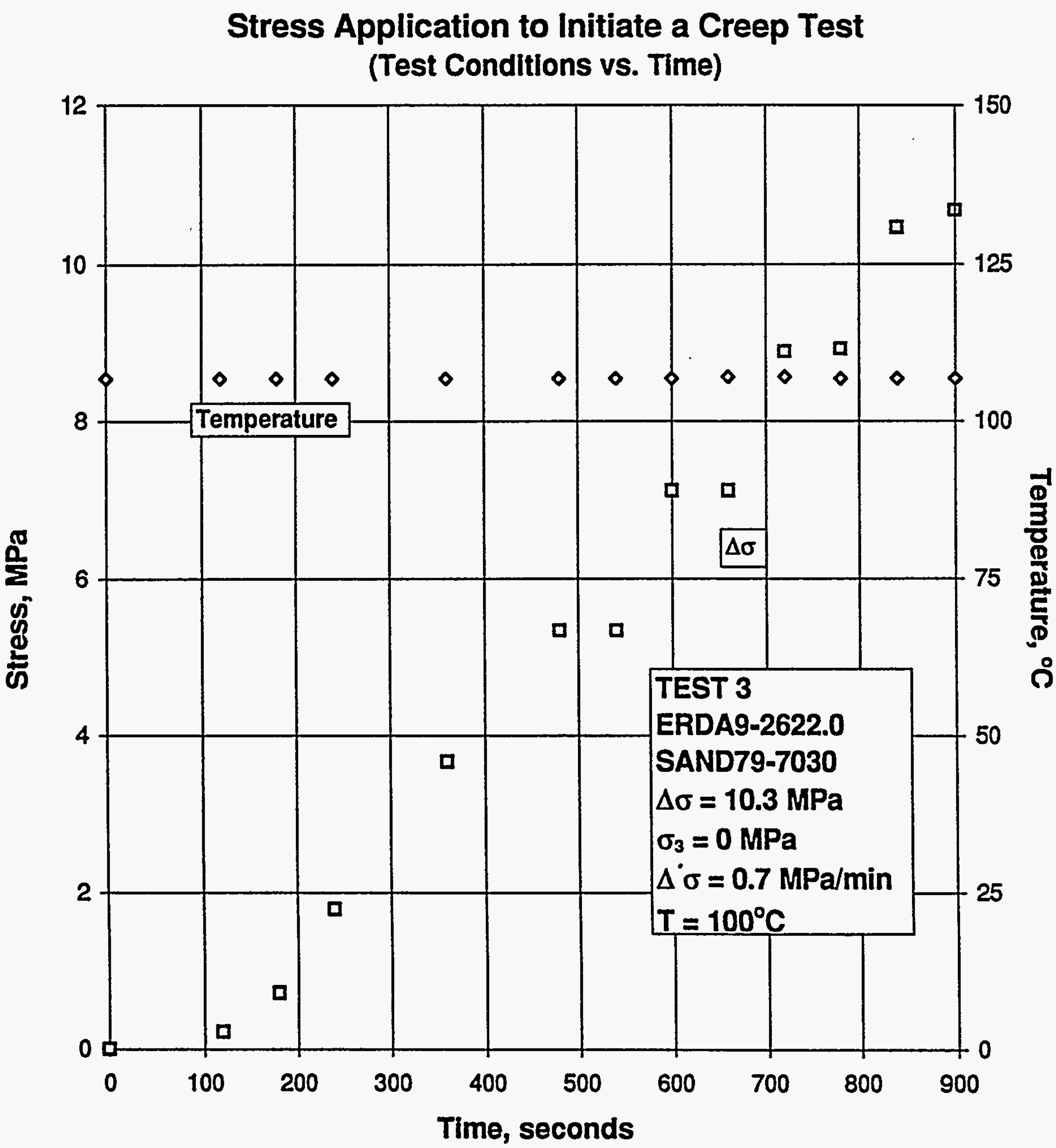

Figure B-81. Test Conditions Versus Time for Stress Application to Initiate a Creep Test: Specimen ERDA9-2622.0; Stage 1 of 1.

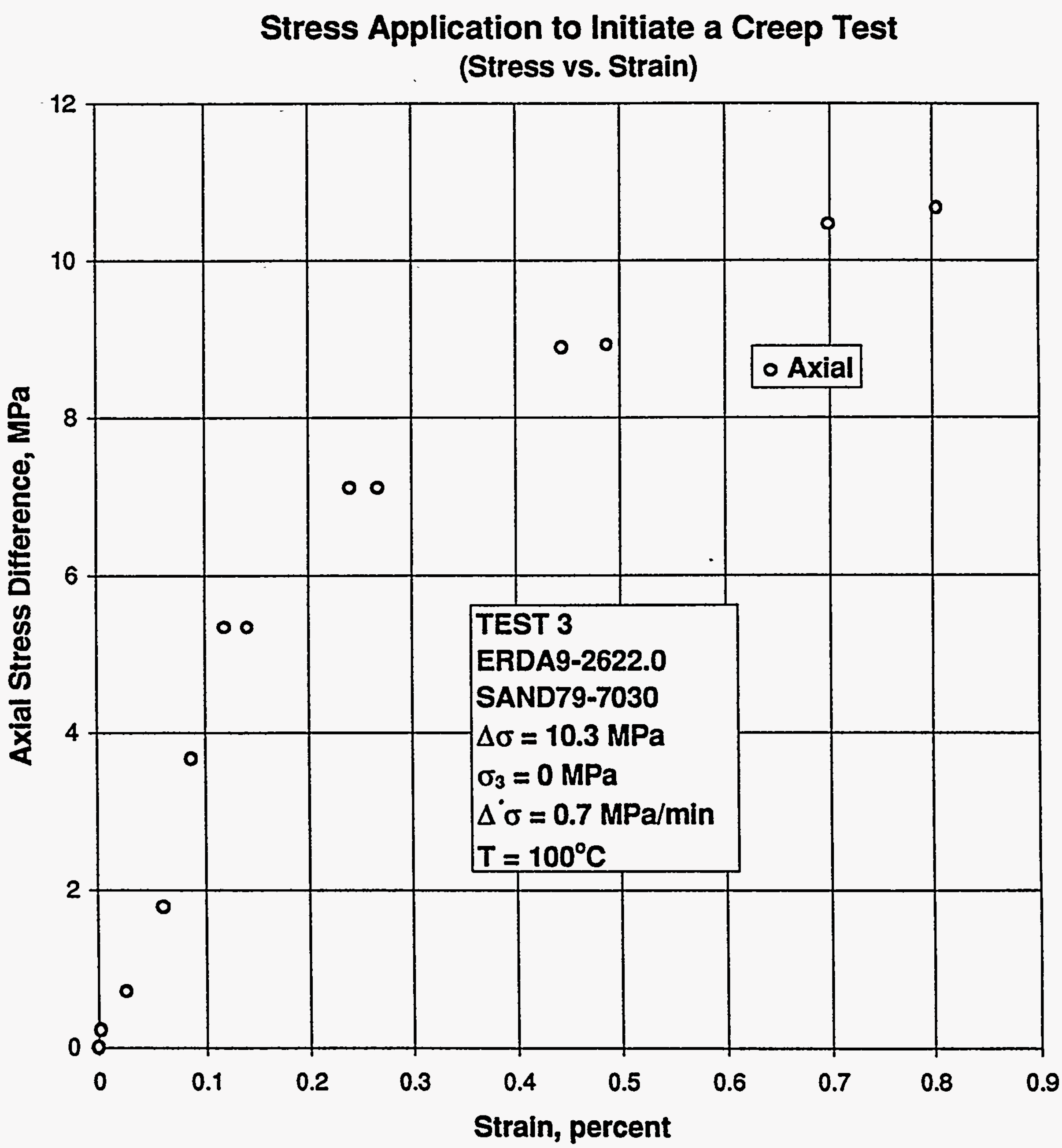

Figure B-82. Axial Stress Difference Versus Axial and Lateral Strain for Stress Application to Initiate a Creep Test: Specimen ERDA9-2622.0; Stage 1 of 1.

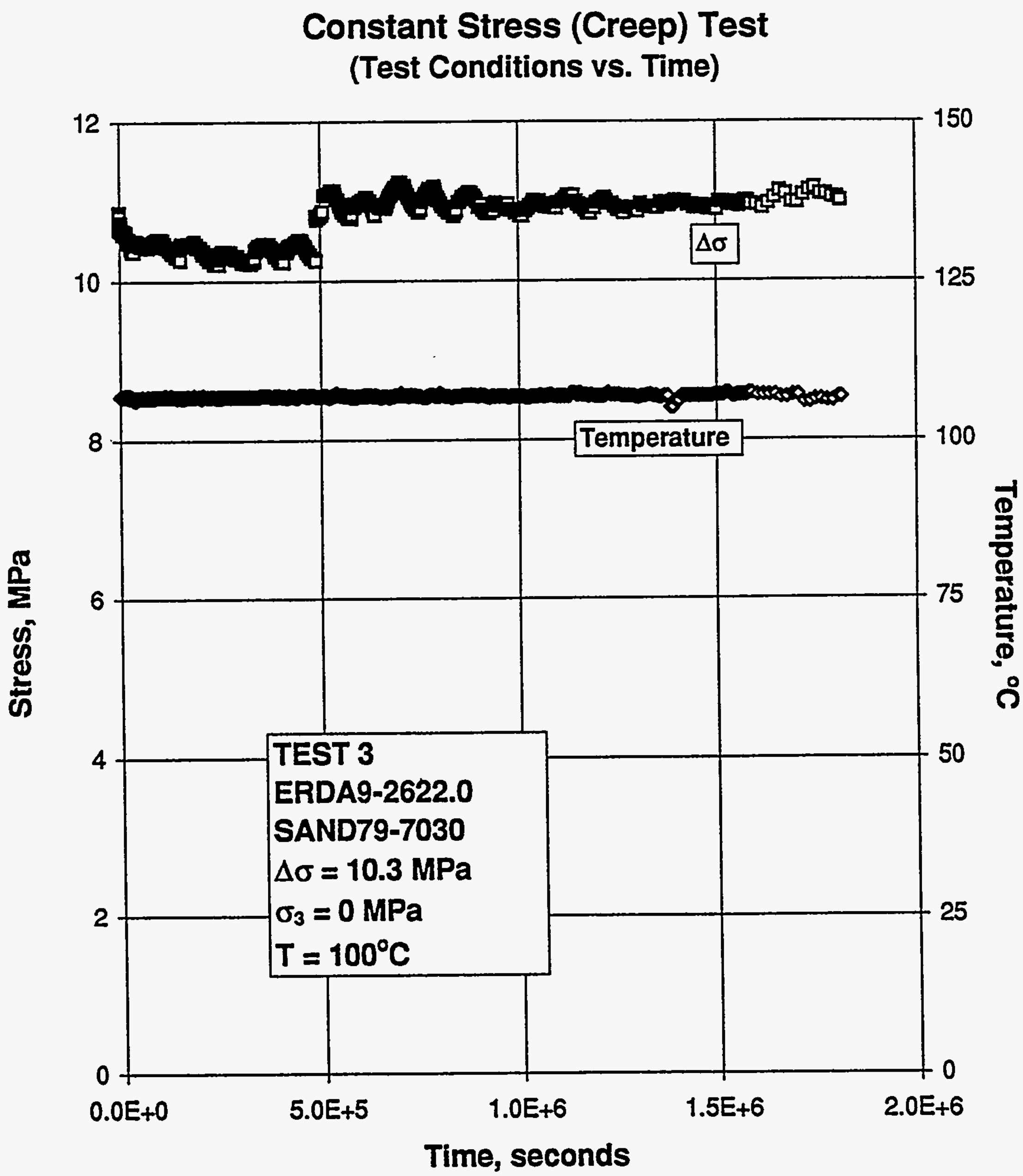

Figure B-83. Test Conditions Versus Time for a Creep Test: Specimen ERDA9-2622.0; Stage 1 of 1.

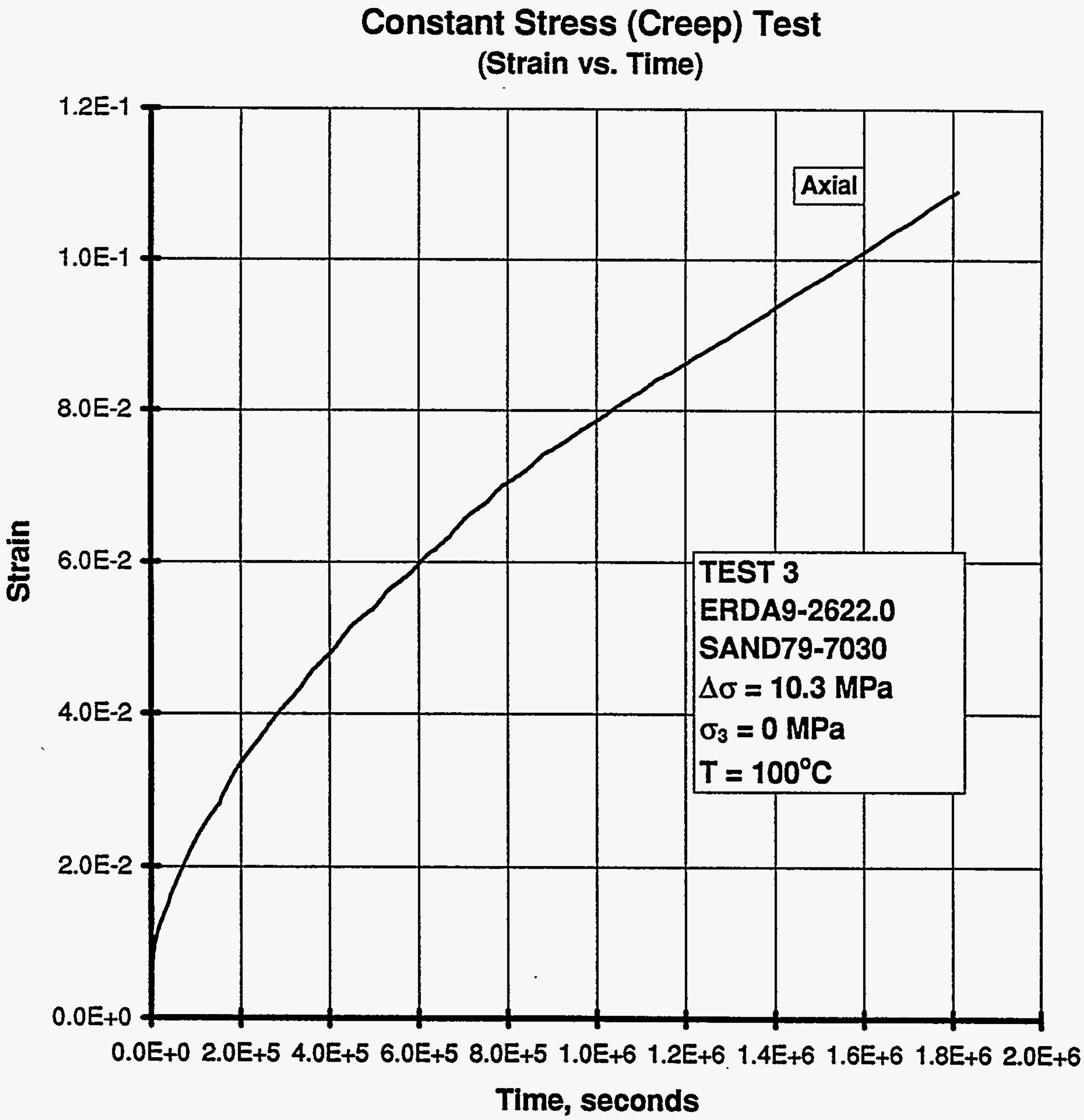

Figure B-84. Axial Strain and Lateral Strain Versus Time for a Creep Test: Specimen ERDA9-2622.0; Stage 1 of 1.

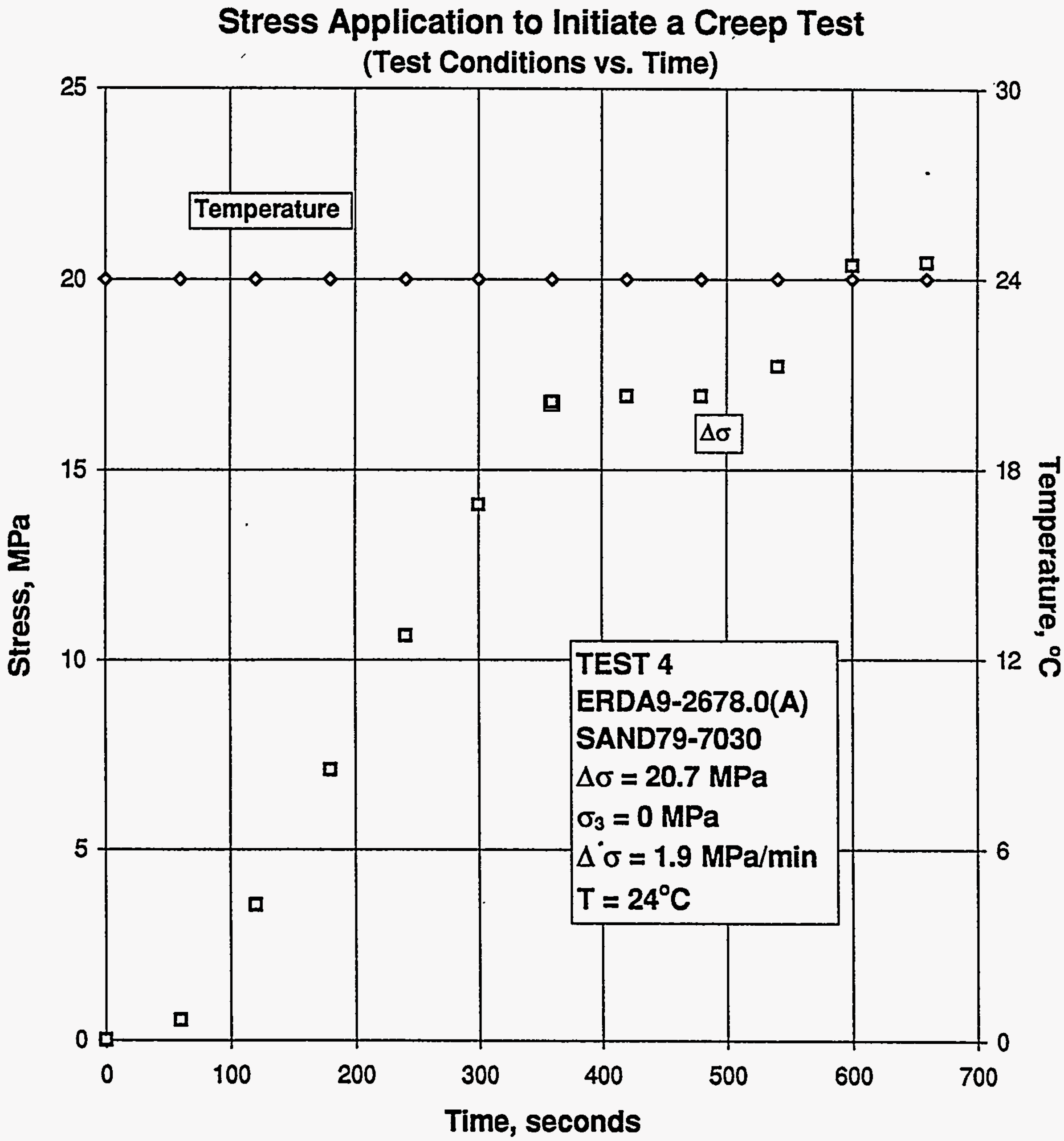

Figure B-85. Test Conditions Versus Time for Stress Application to Initiate a Creep Test: Specimen ERDA9-2678.0 (A); Stage 1 of 1.

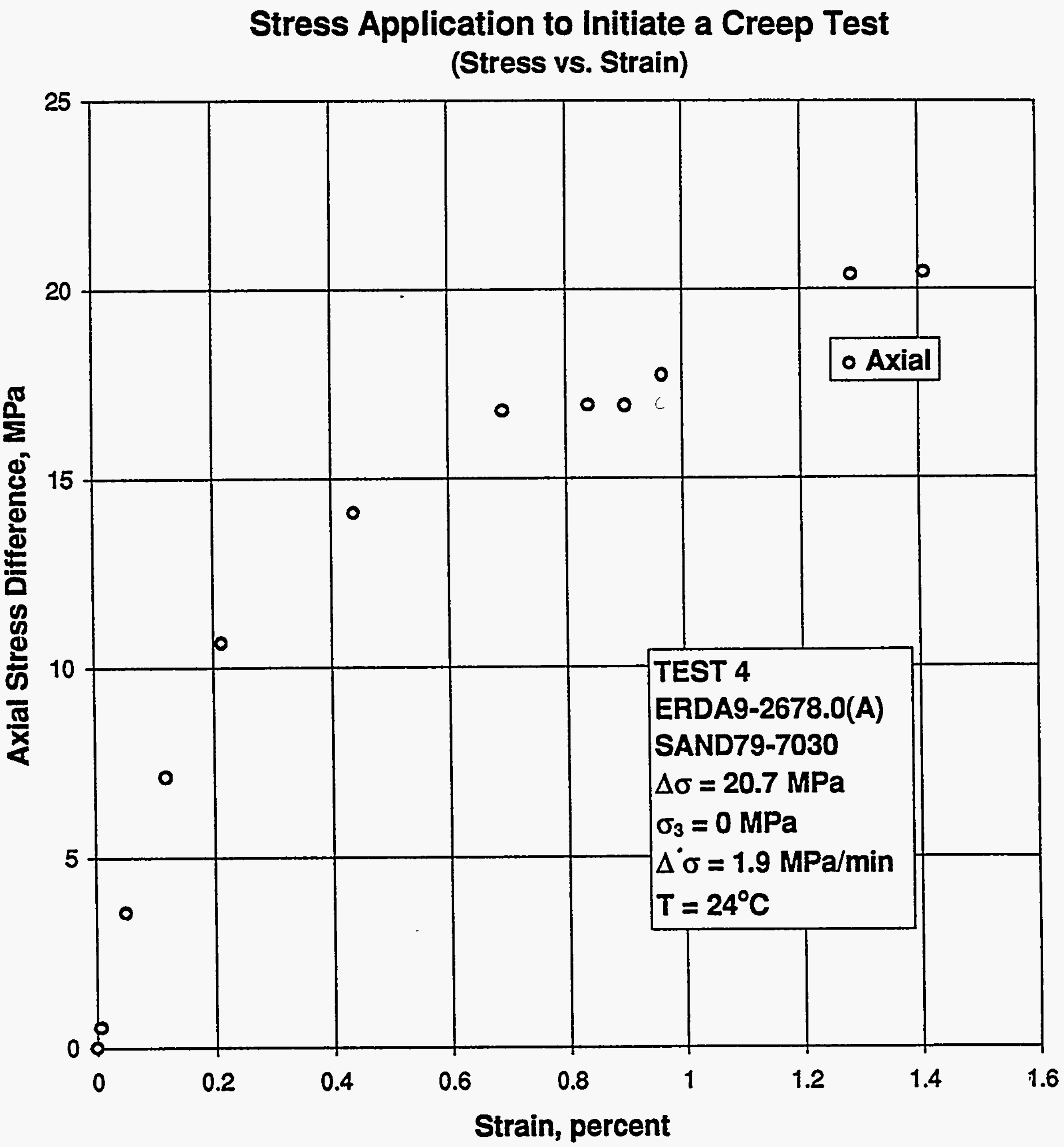

Figure B-86. Axial Stress Difference Versus Axial and Lateral Strain for Stress Application to Initiate a Creep Test: Specimen ERDA9-2678.0 (A); Stage 1 of 1.

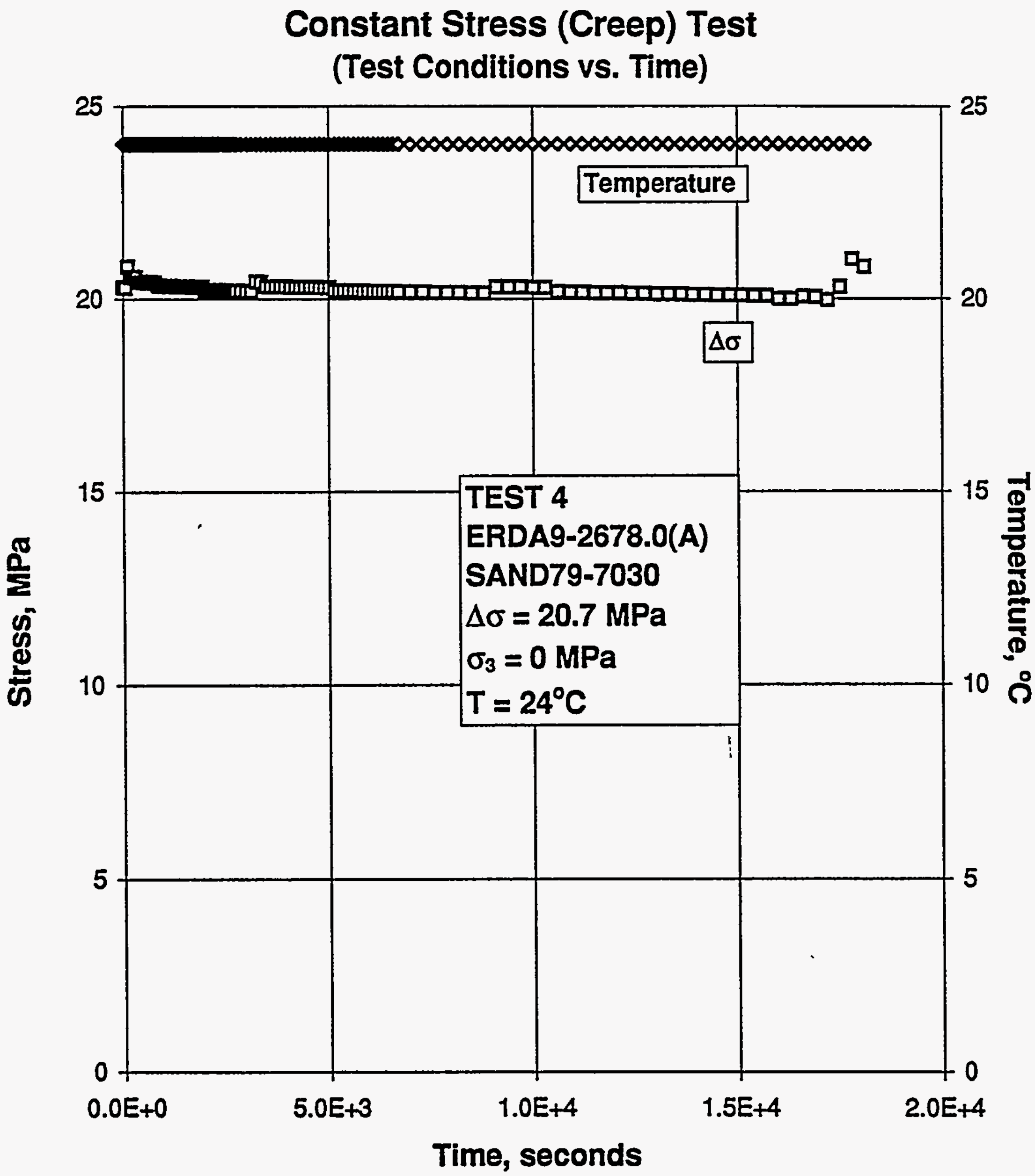

Figure B-87. Test Conditions Versus Time for a Creep Test: Specimen ERDA9-2678.0 (A); Stage 1 of 1 (Specimen Rupture Terminated Test).

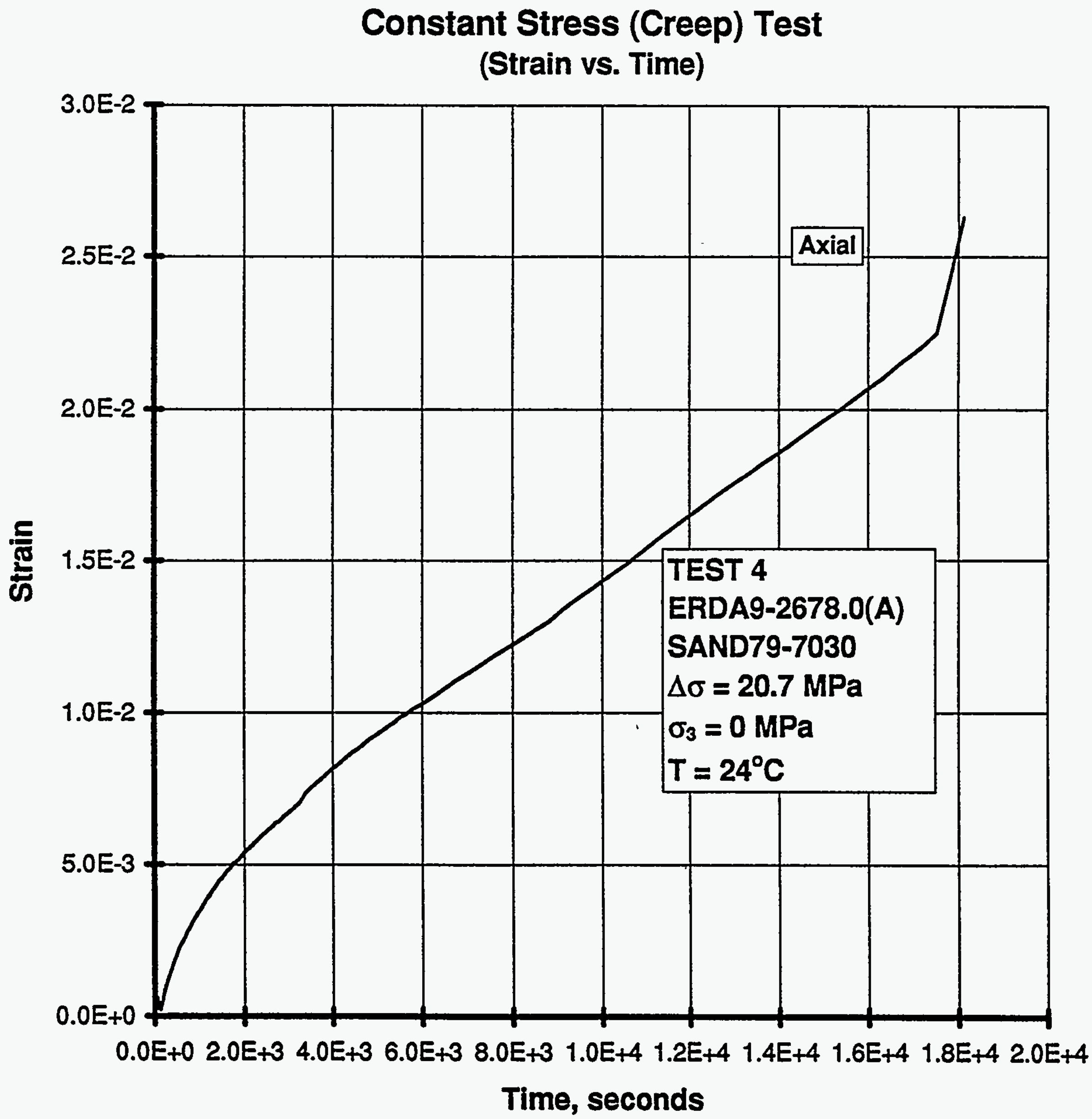

Figure B-88. Axial Strain and Lateral Strain Versus Time for a Creep Test: Specimen ERDA9-2678.0 (A); Stage 1 of 1 (Specimen Rupture Terminated Test).

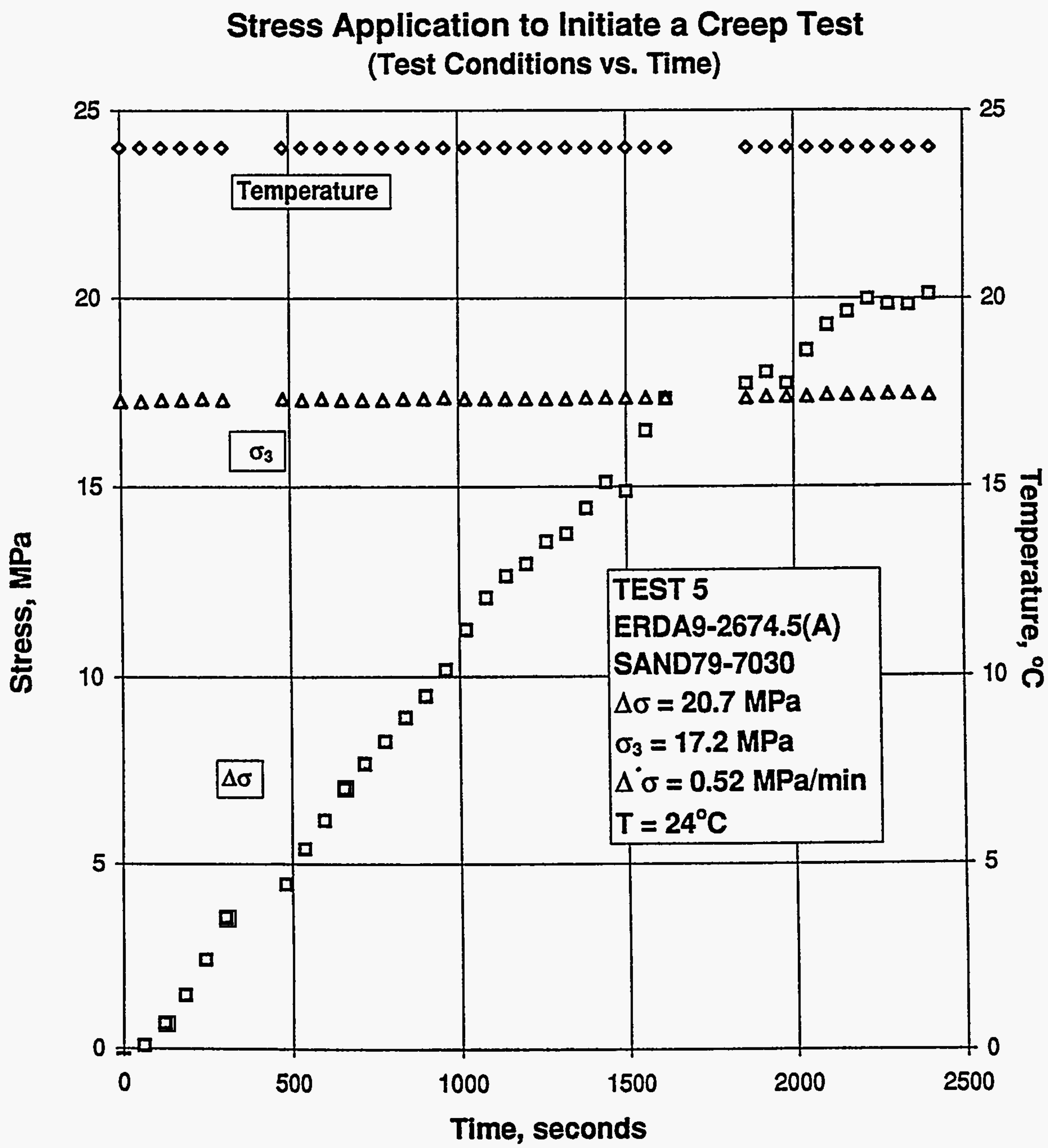

Figure B-89. Test Conditions Versus Time for Stress Application to Initiate a Creep Test: Specimen ERDA9-2674.5 (A); Stage 1 of 1.

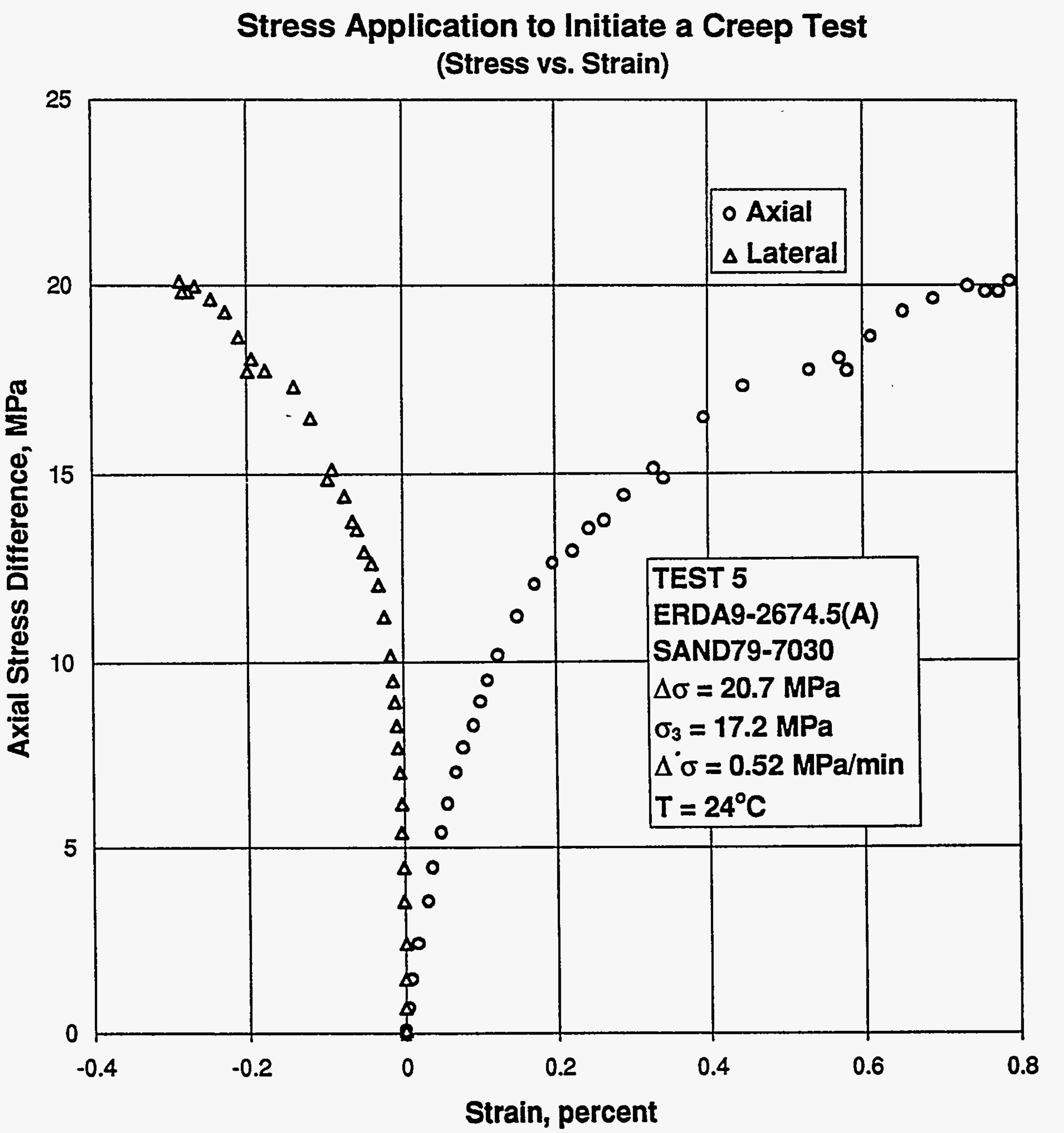

Figure B-90. Axial Stress Difference Versus Axial and Lateral Strain for Stress Application to Initiate a Creep Test: Specimen ERDA9-2674.5 (A); Stage 1 of 1.

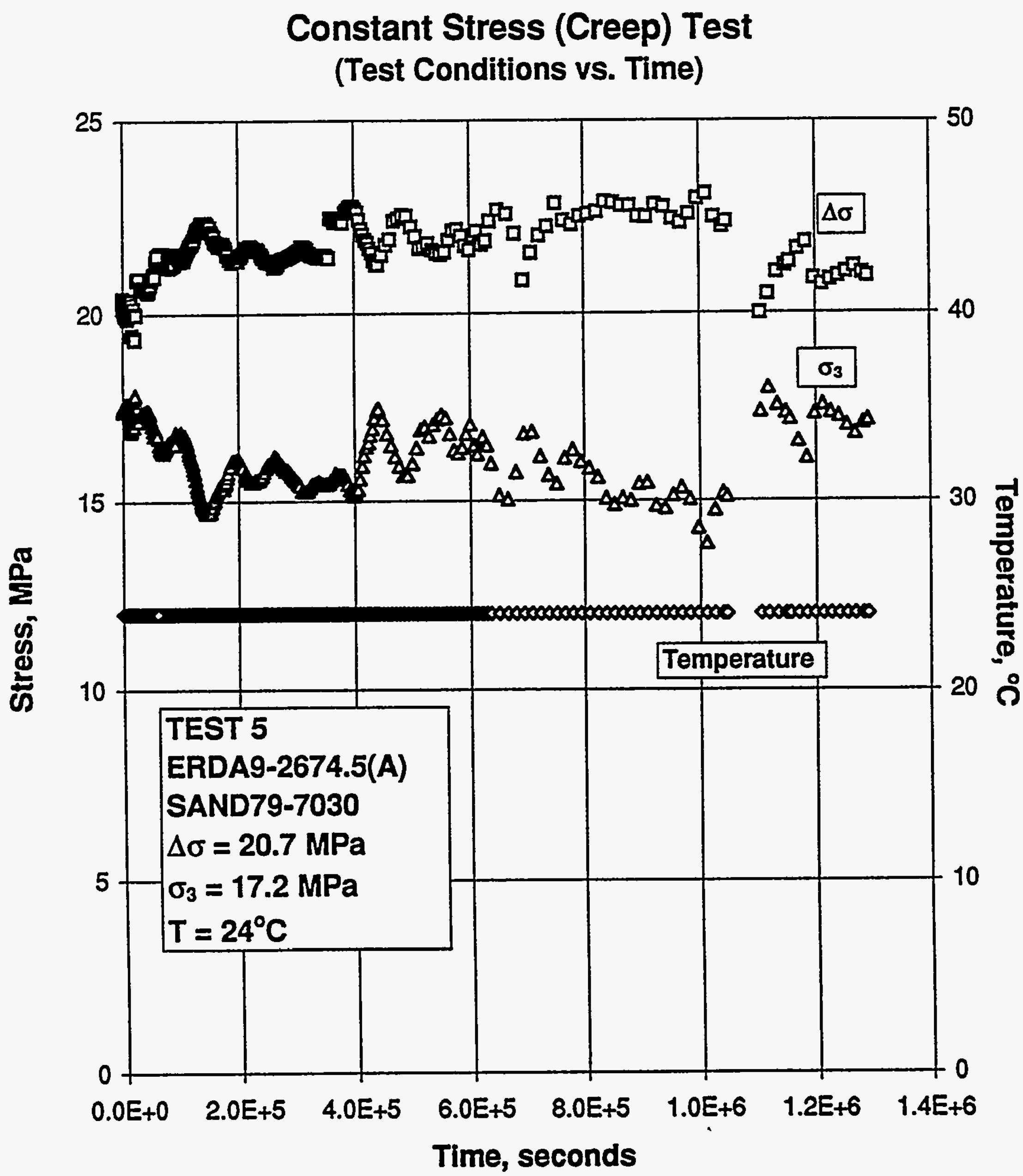

Figure B-91. Test Conditions Versus Time for a Creep Test: Specimen ERDA9-2674.5 (A); Stage 1 of 1.

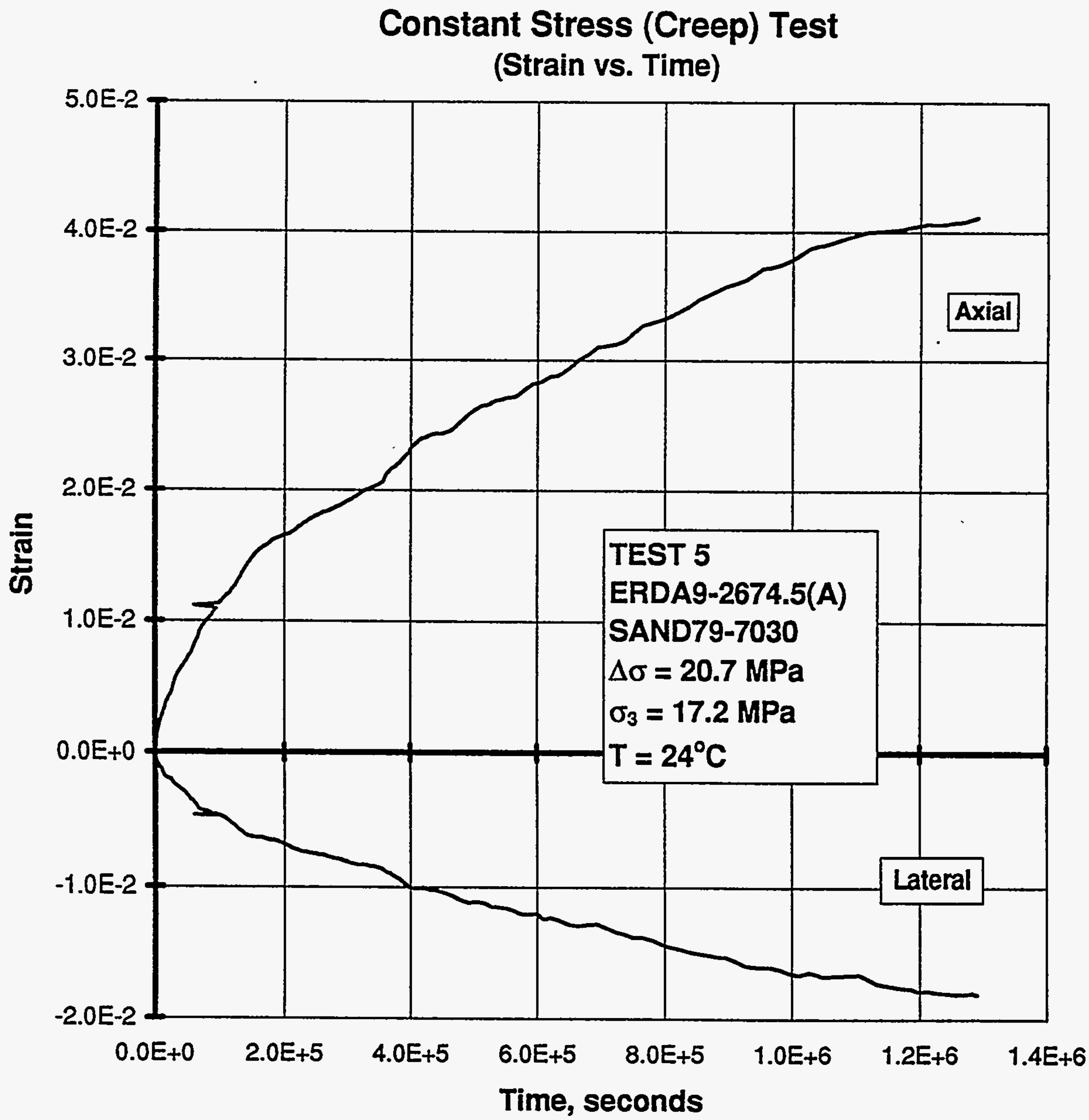

Figure B-92. Axial Strain and Lateral Strain Versus Time for a Creep Test: Specimen ERDA9-2674.5 (A); Stage 1 of 1.

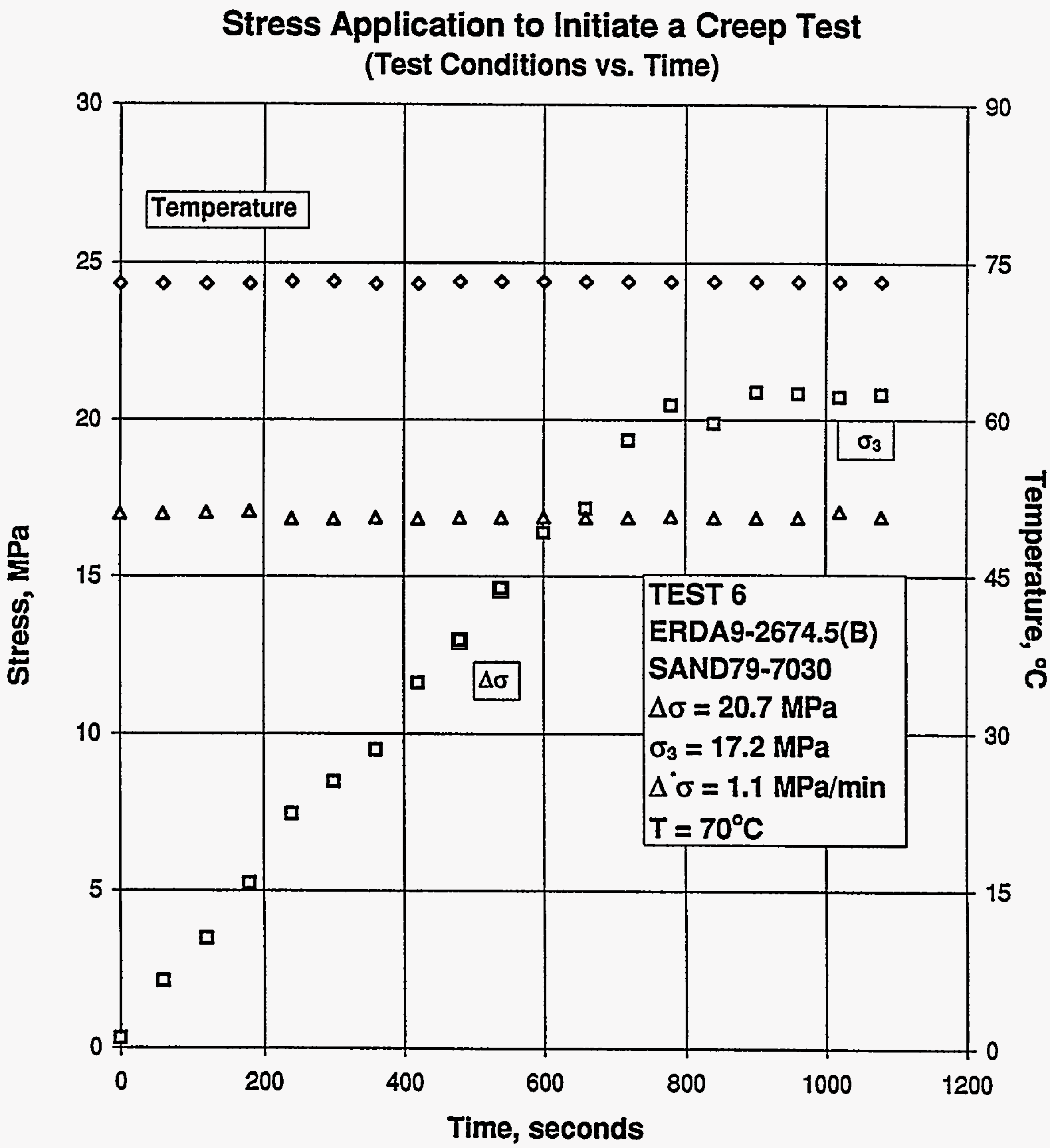

Figure B-93. Test Conditions Versus Time for Stress Application to Initiate a Creep Test: Specimen ERDA9-2674.5 (B); Stage 1 of 1.

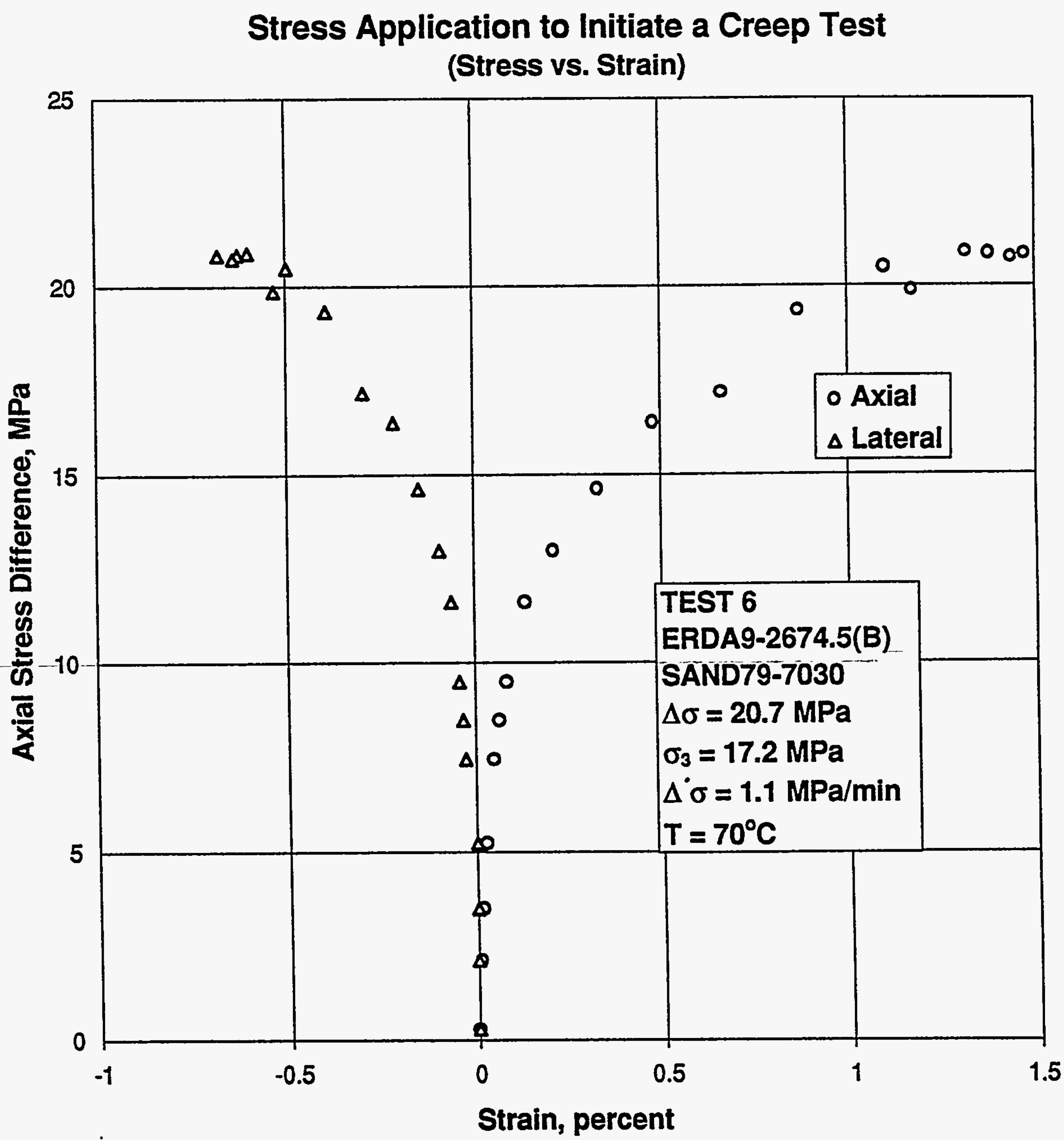

Figure B-94. Axial Stress Difference Versus Axial and Lateral Strain for Stress Application to Initiate a Creep Test: Specimen ERDA9-2674.5 (B); Stage 1 of 1.

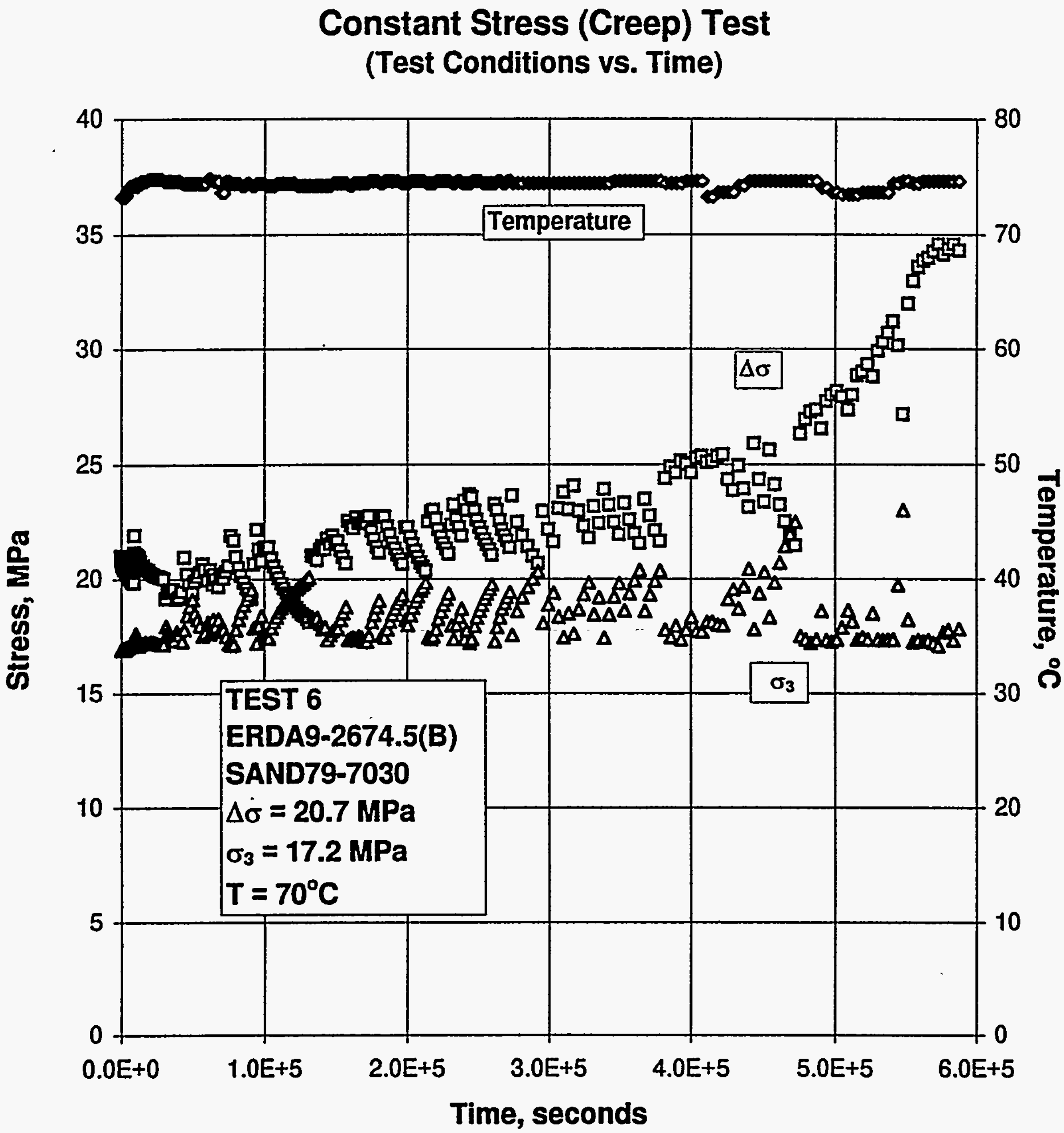

Figure B-95. Test Conditions Versus Time for a Creep Test: Specimen ERDA9-2674.5 (B); Stage 1 of 1 (Specimen Contacted Vessel Wall at 150 Hours).

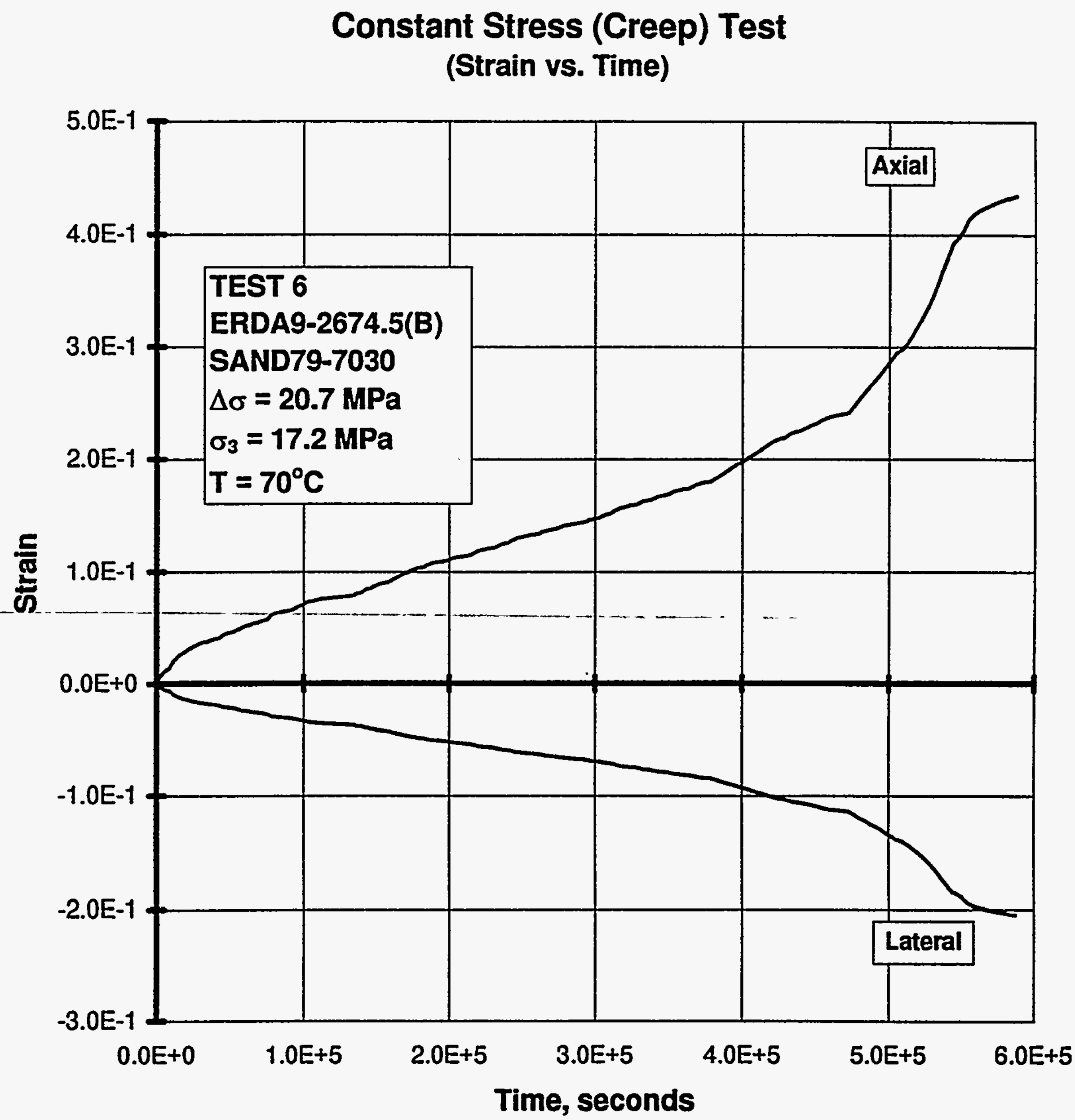

Figure B-96. Axial Strain and Lateral Strain Versus Time for a Creep Test: Specimen ERDA9-2674.5 (B); Stage 1 of 1 (Specimen Contacted Vessel Wall at 150 Hours).

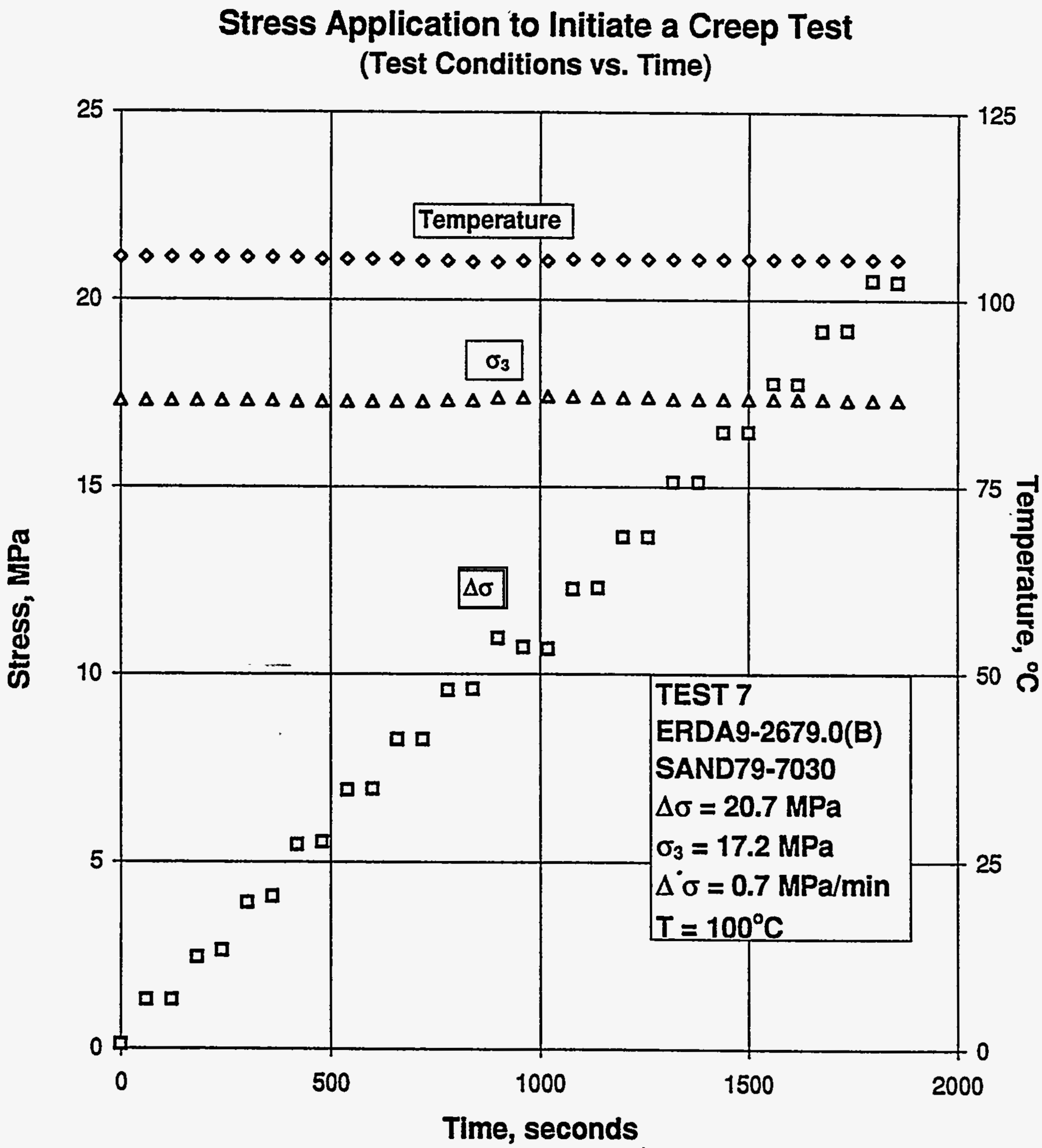

Figure B-97. Test Conditions Versus Time for Stress Application to Initiate a Creep Test: Specimen ERDA9-2679.0 (B); Stage 1 of 1.

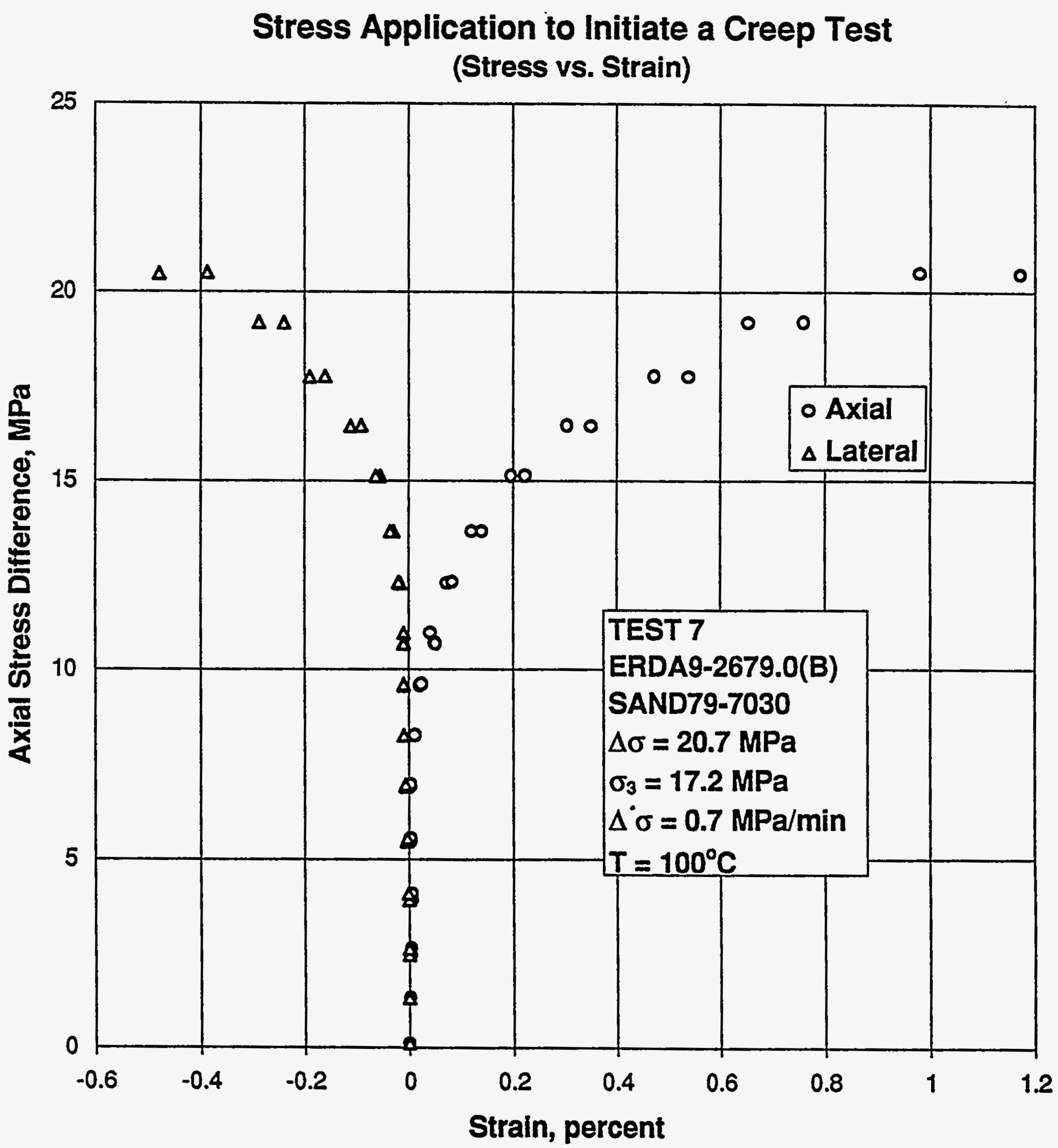

Figure B-98. Axial Stress Difference Versus Axial and Lateral Strain for Stress Application to Initiate a Creep Test: Specimen ERDA9-2679.0 (B); Stage 1 of 1.

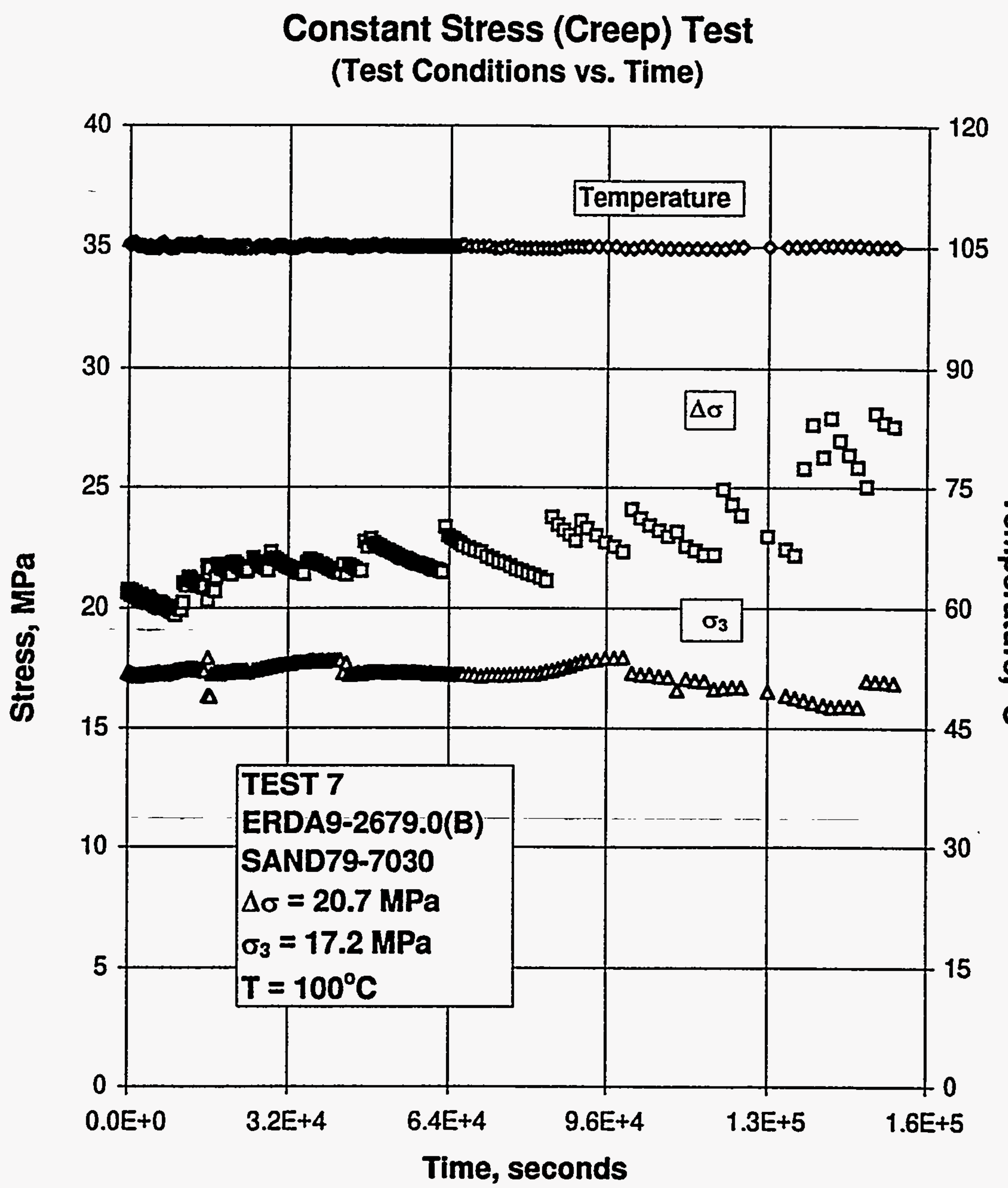

Figure B-99. Test Conditions Versus Time for a Creep Test: Specimen ERDA9-2679.0 (B); Stage 1 of 1 (Specimen Contacted Vessel Wall at End of Test).

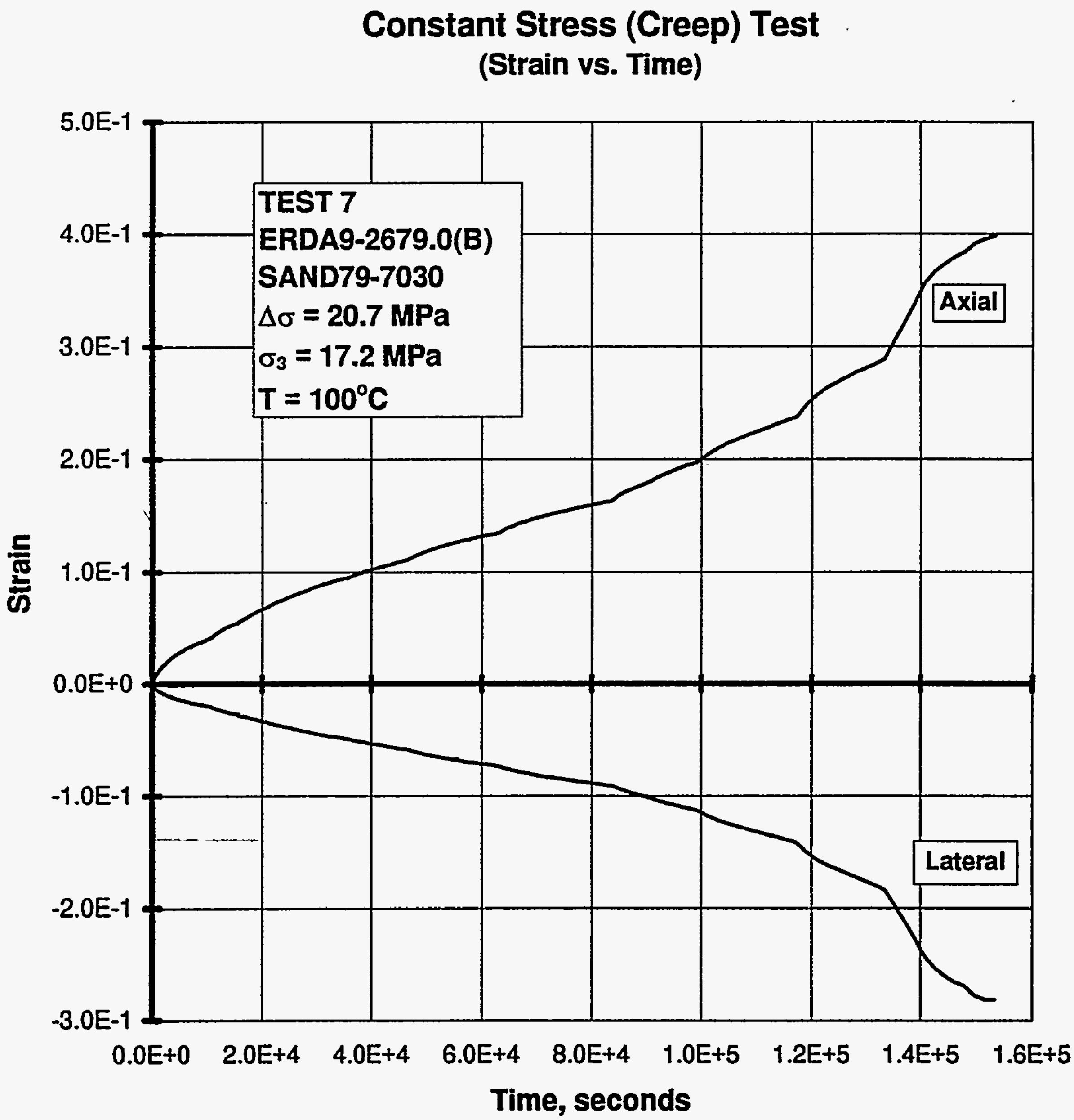

Figure B-100. Axial Strain and Lateral Strain Versus Time for a Creep Test: Specimen ERDA9-2679.0 (B); Stage 1 of 1 (Specimen Contacted Vessel Wall at End of Test).

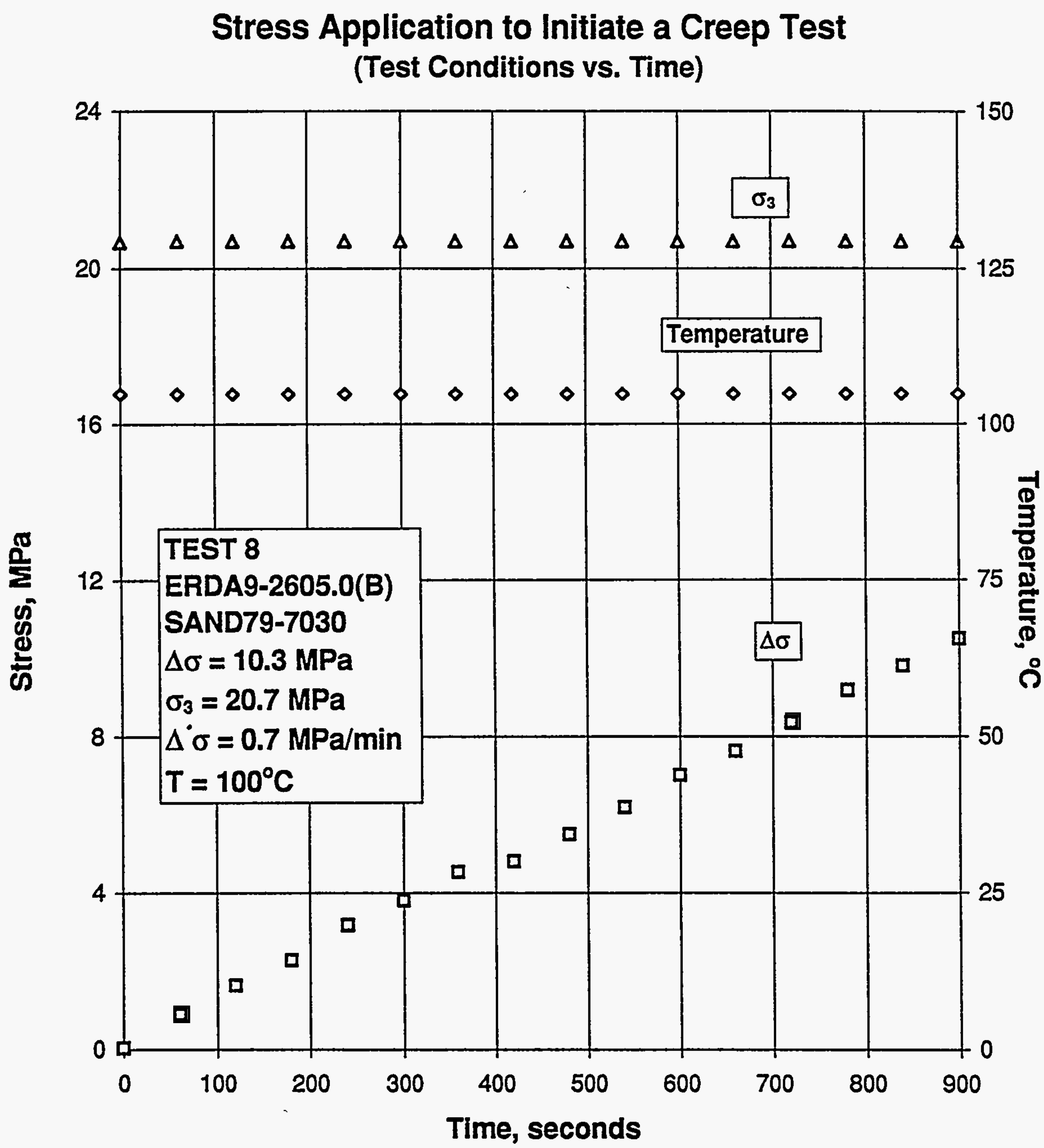

Figure B-101. Test Conditions Versus Time for Stress Application to Initiate a Creep Test: Specimen ERDA9-2605.0 (B); Stage 1 of 1.

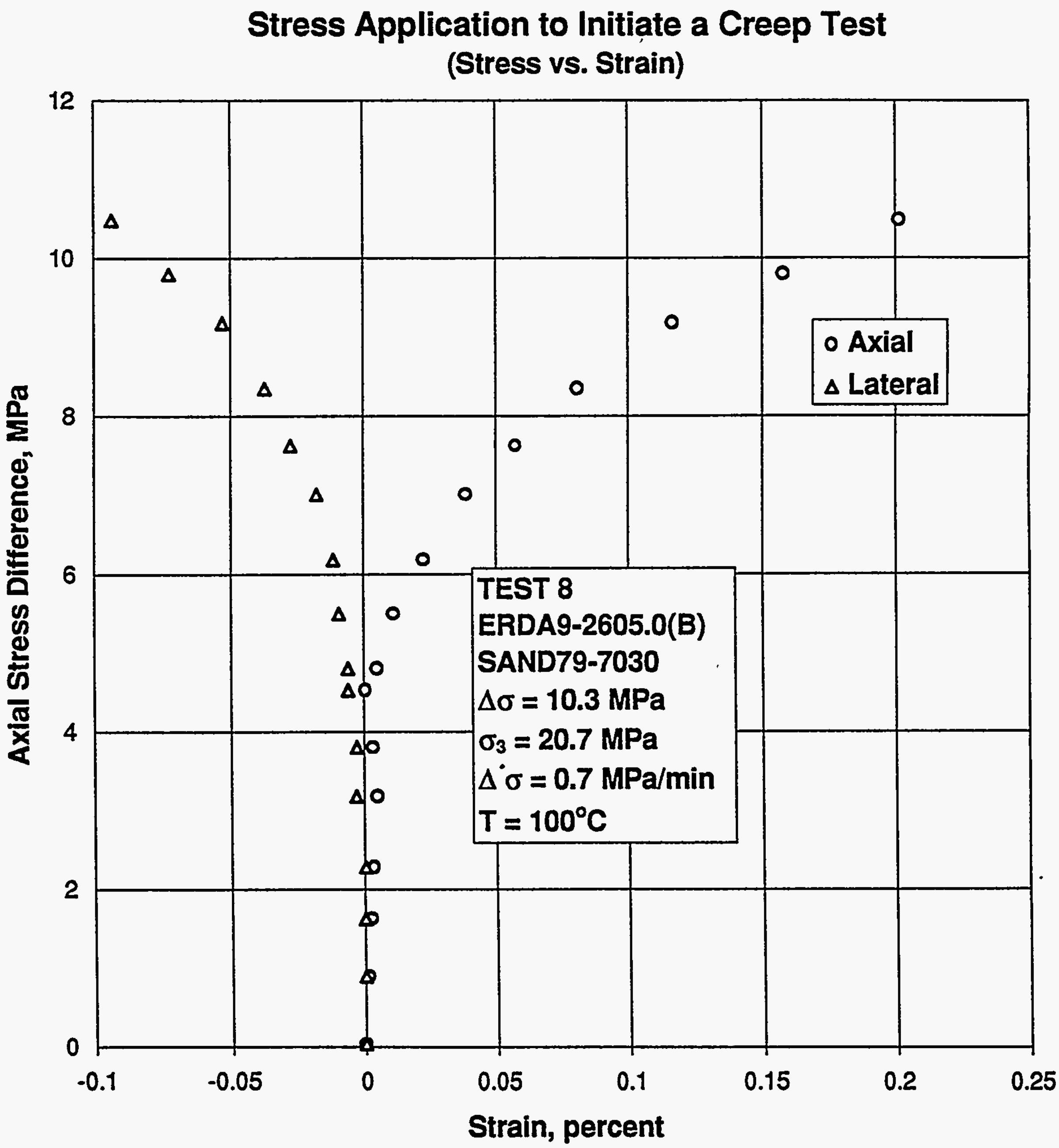

Figure B-102. Axial Stress Difference Versus Axial and Lateral Strain for Stress Application to Initiate a Creep Test: Specimen ERDA9-2605.0 (B); Stage 1 of 1.

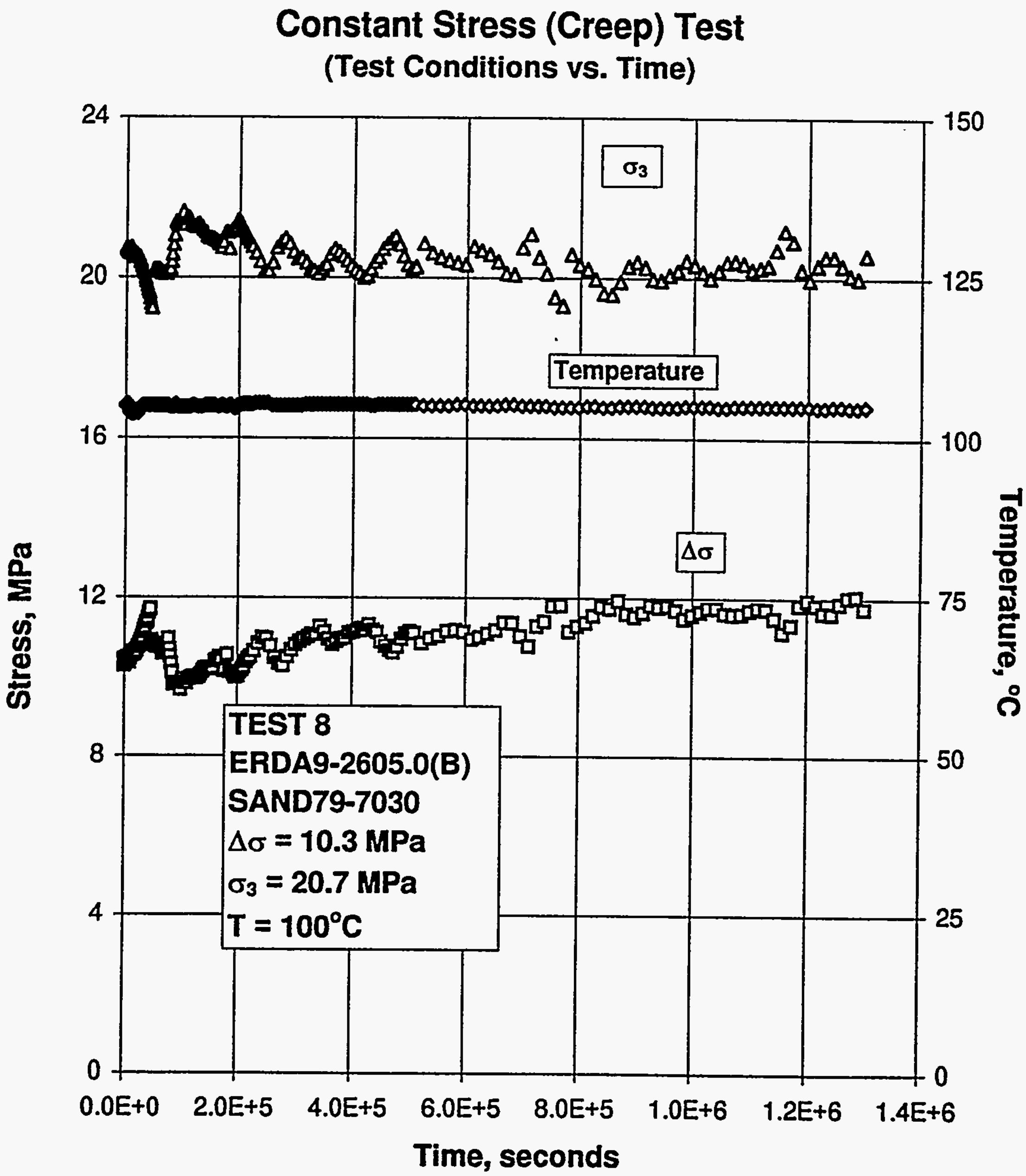

Figure B-103. Test Conditions Versus Time for a Creep Test: Specimen ERDA9-2605.0 (B); Stage 1 of 1.

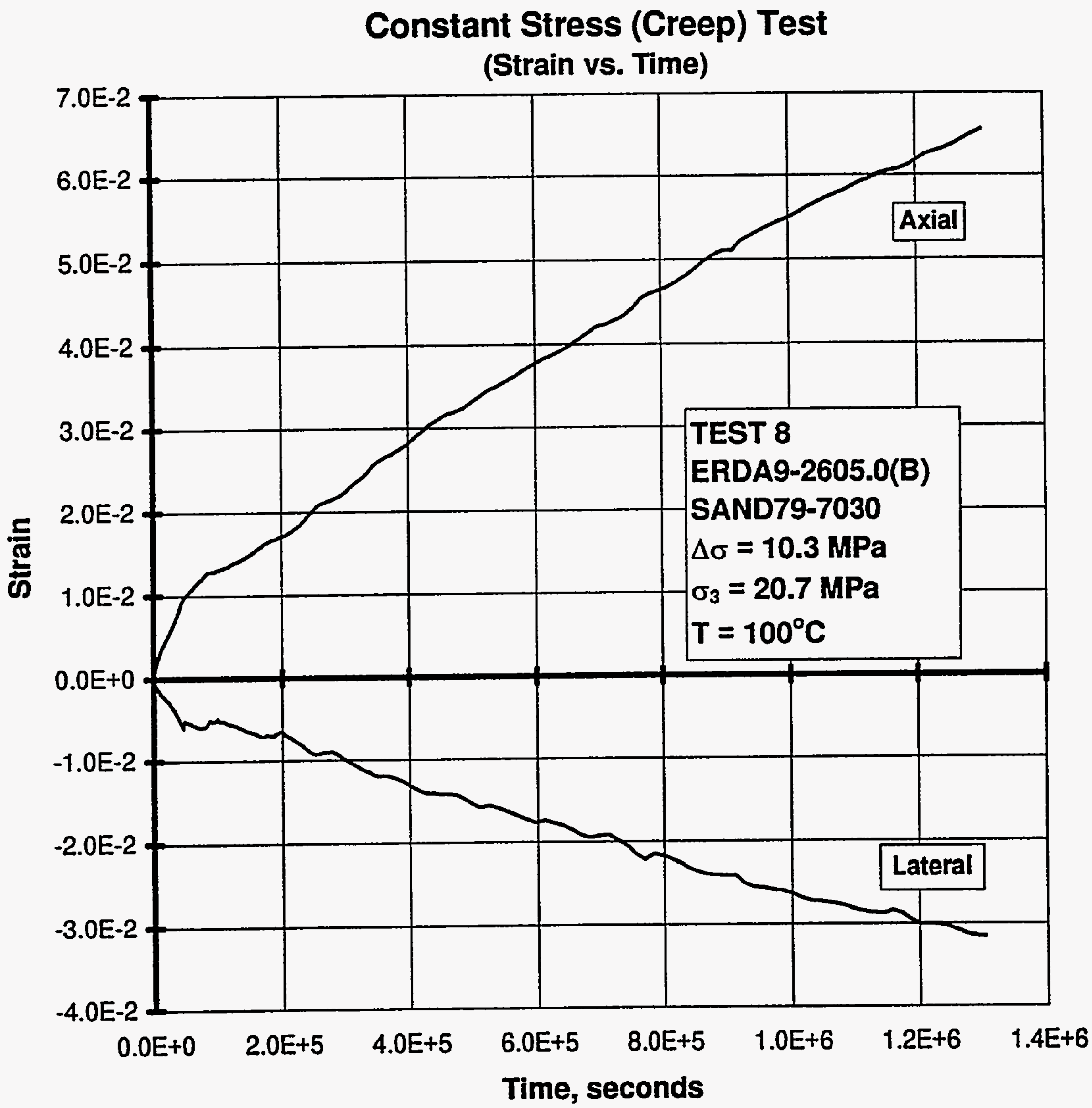

Figure B-104. Axial Strain and Lateral Strain Versus Time for a Creep Test: Specimen ERDA9-2605.0 (B); Stage 1 of 1.

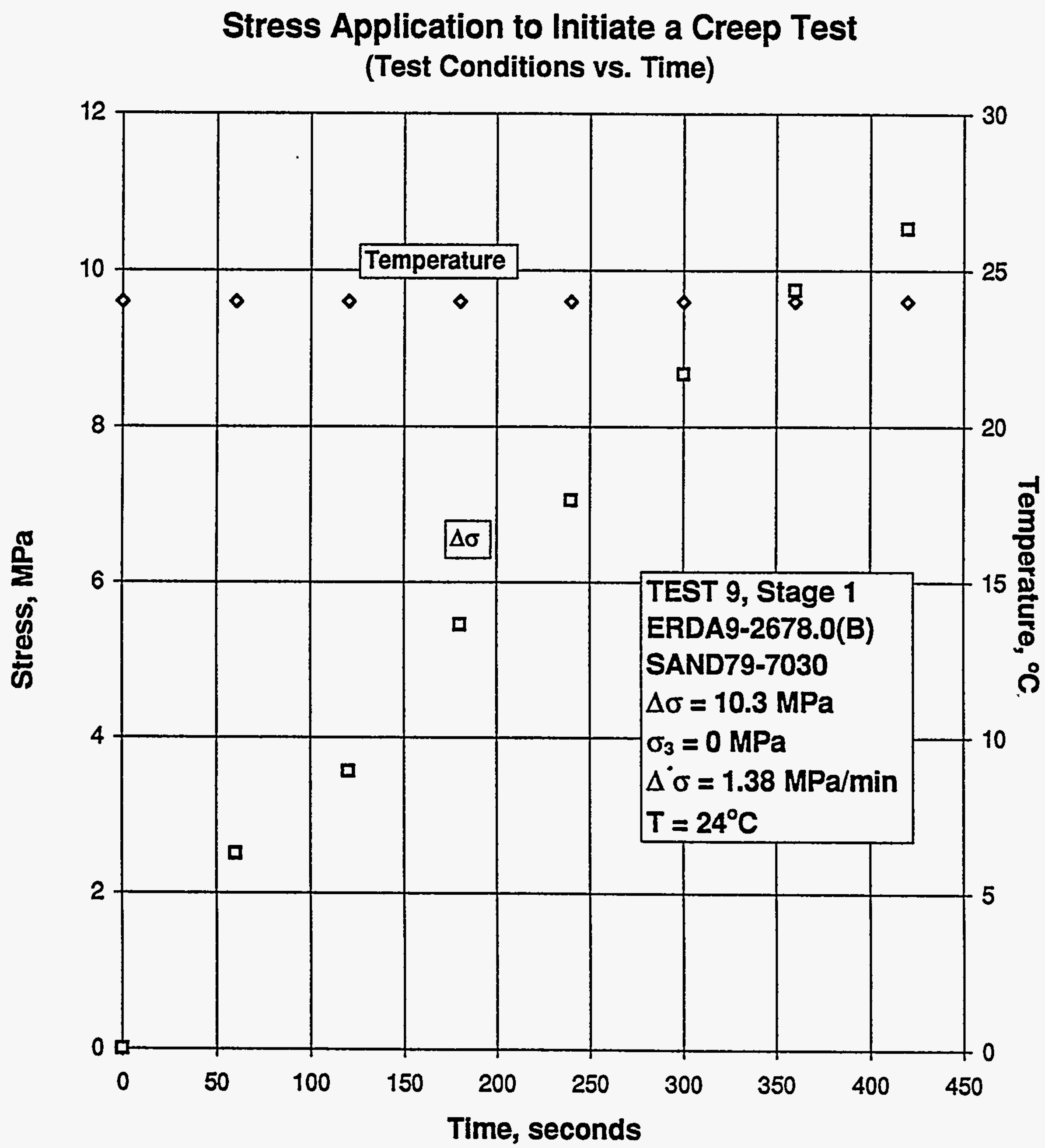

Figure B-105. Test Conditions Versus Time for Stress Application to Initiate a Creep Test: Specimen ERDA9-2678.0 (B); Stage 1 of 2.

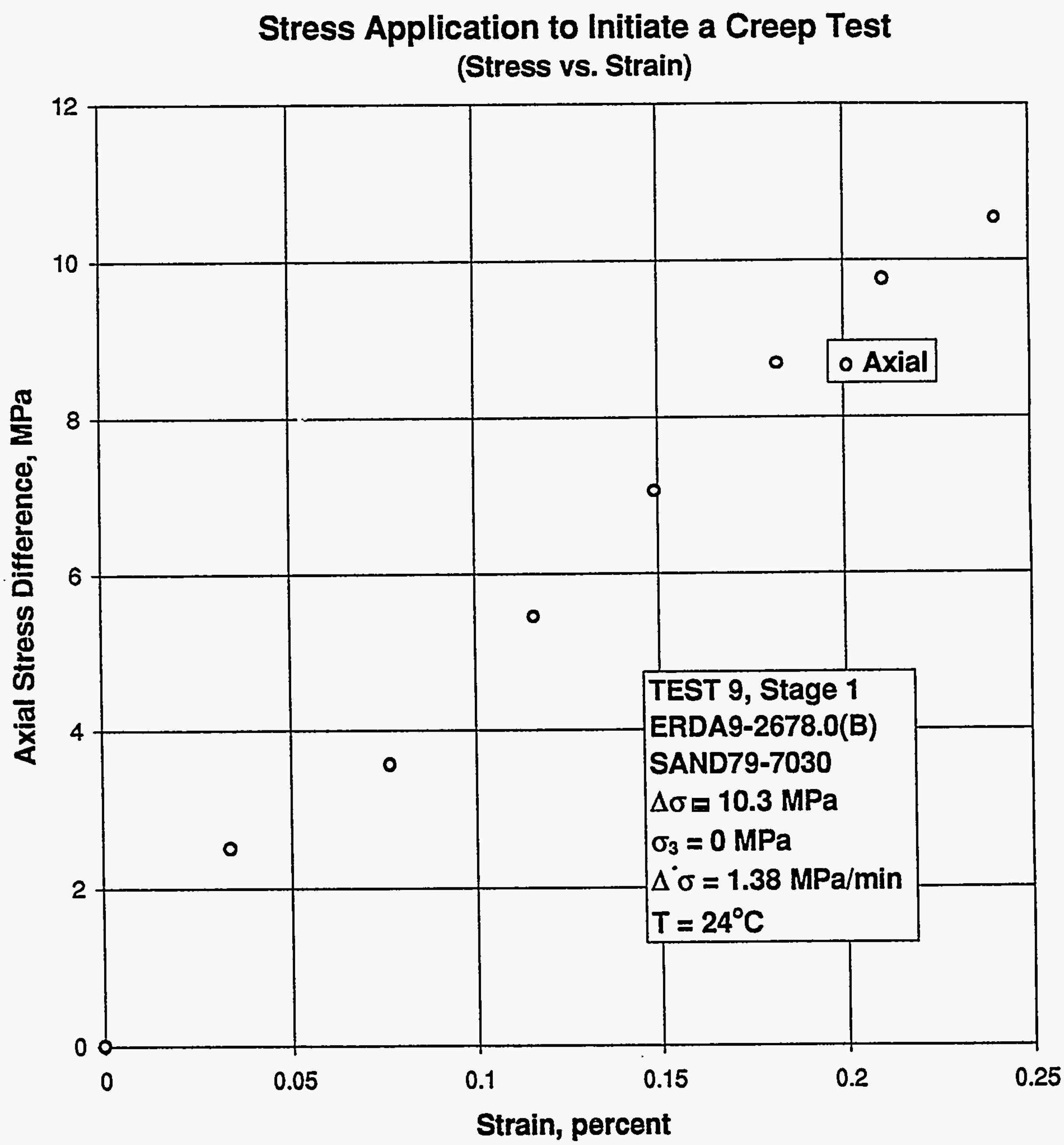

Figure B-106. Axial Stress Difference Versus Axial and Lateral Strain for Stress Application to Initiate a Creep Test: Specimen ERDA9-2678.0 (B); Stage 1 of 2.

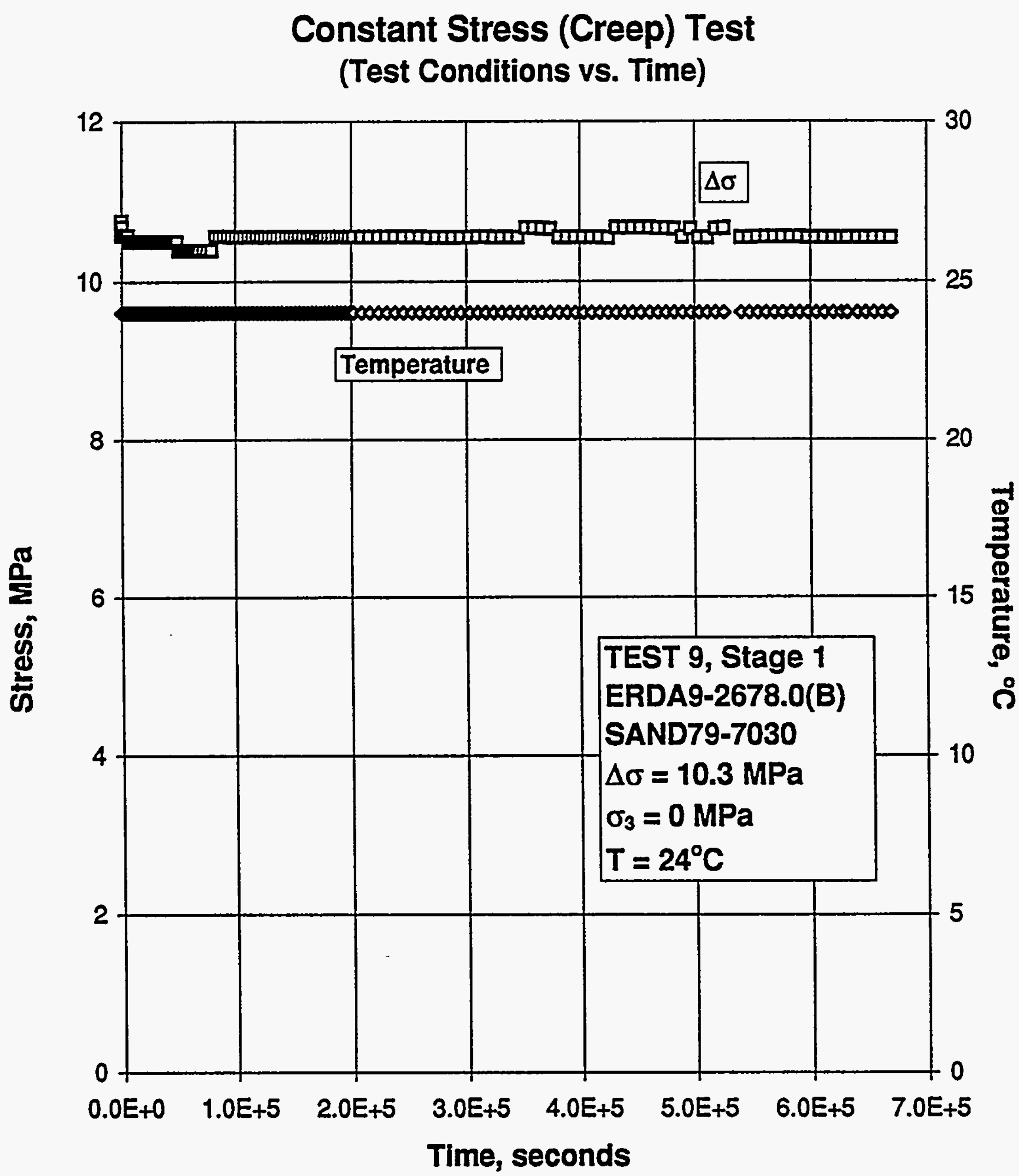

Figure B-107. Test Conditions Versus Time for a Creep Test: Specimen ERDA9-2678.0 (B); Stage 1 of 2.

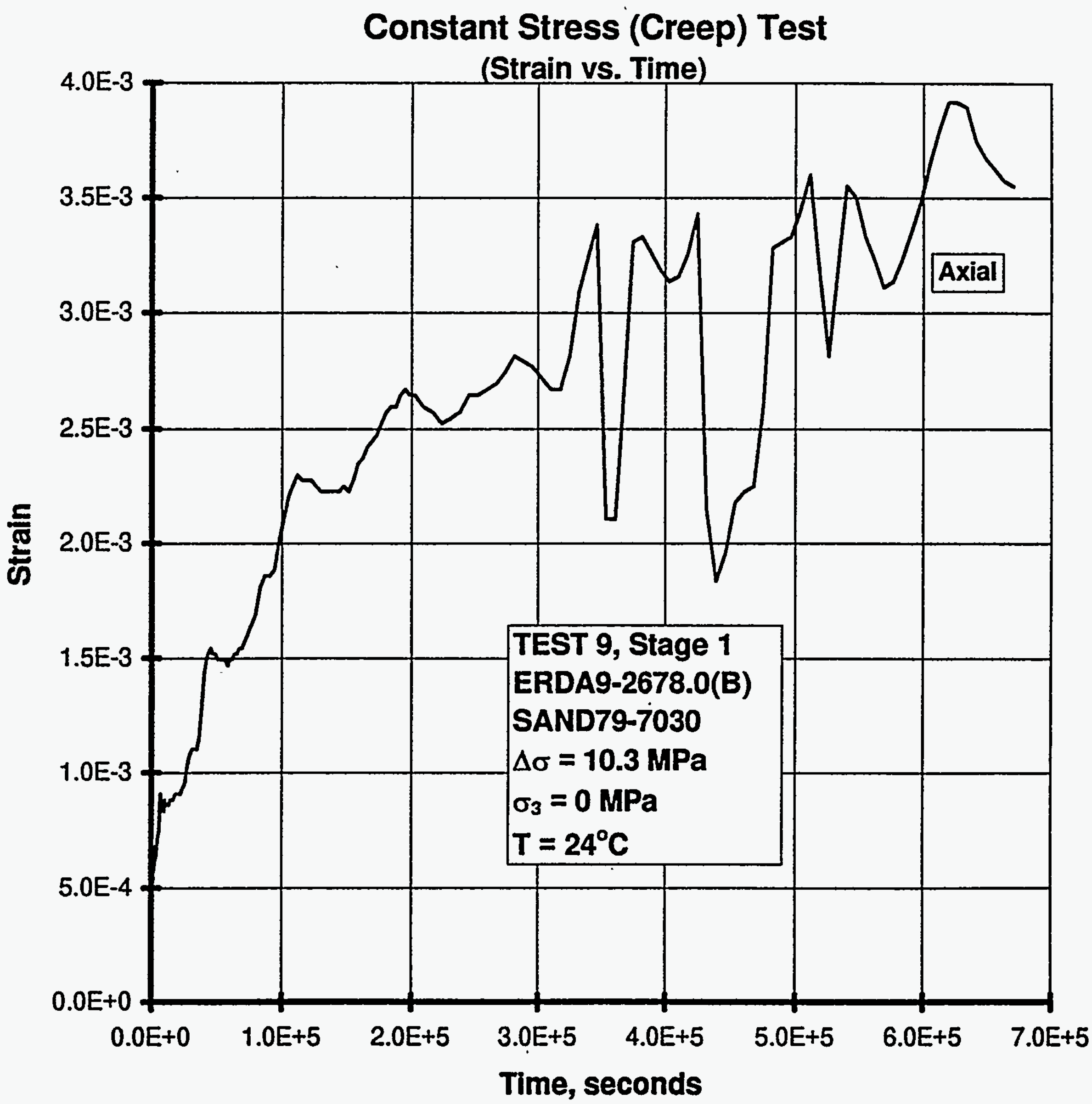

Figure B-108. Axial Strain and Lateral Strain Versus Time for a Creep Test: Specimen ERDA9-2678.0 (B); Stage 1 of 2.

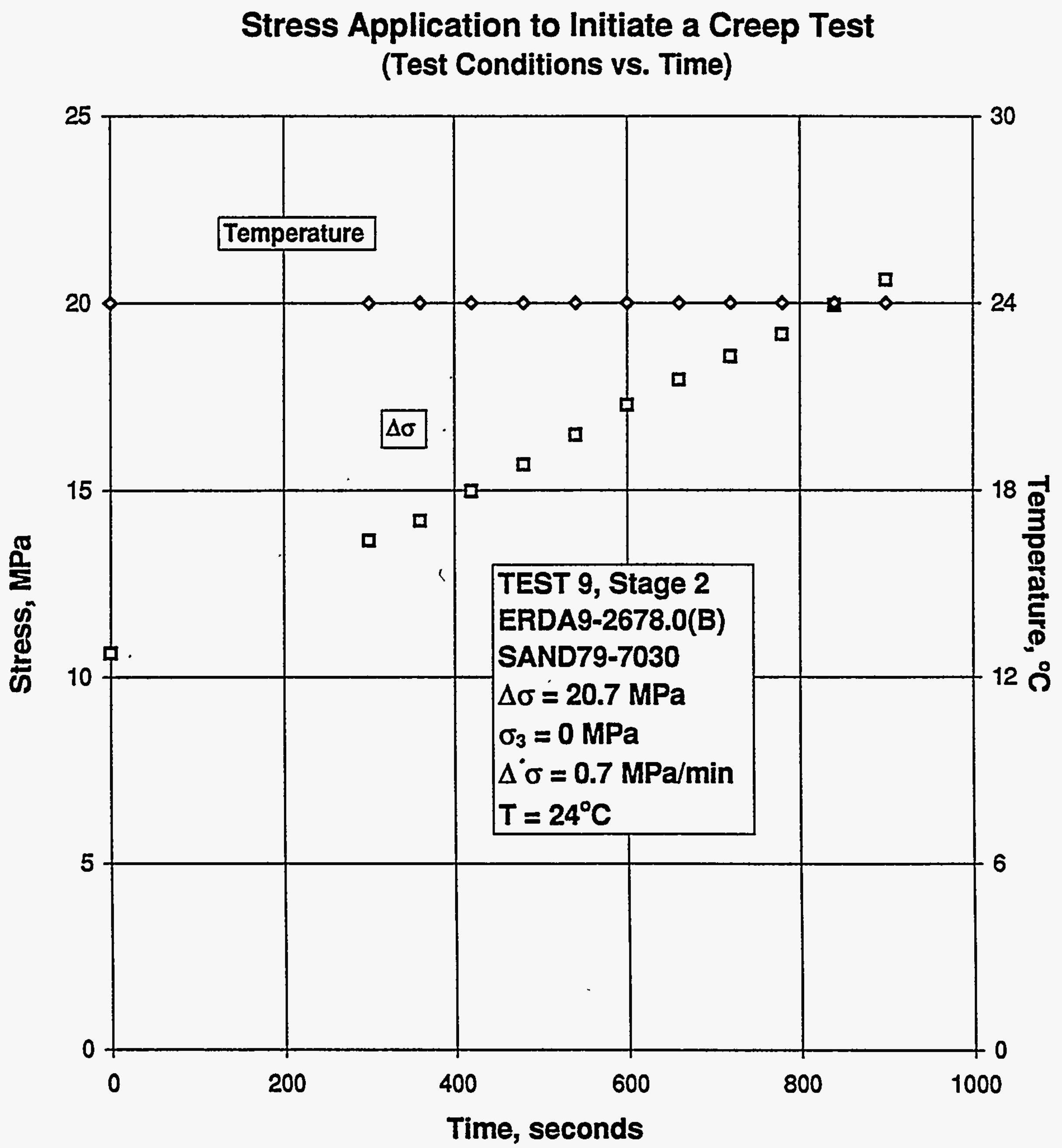

Figure B-109. Test Conditions Versus Time for Stress Application to Initiate a Creep Test: Specimen ERDA9-2678.0 (B); Stage 2 of 2.

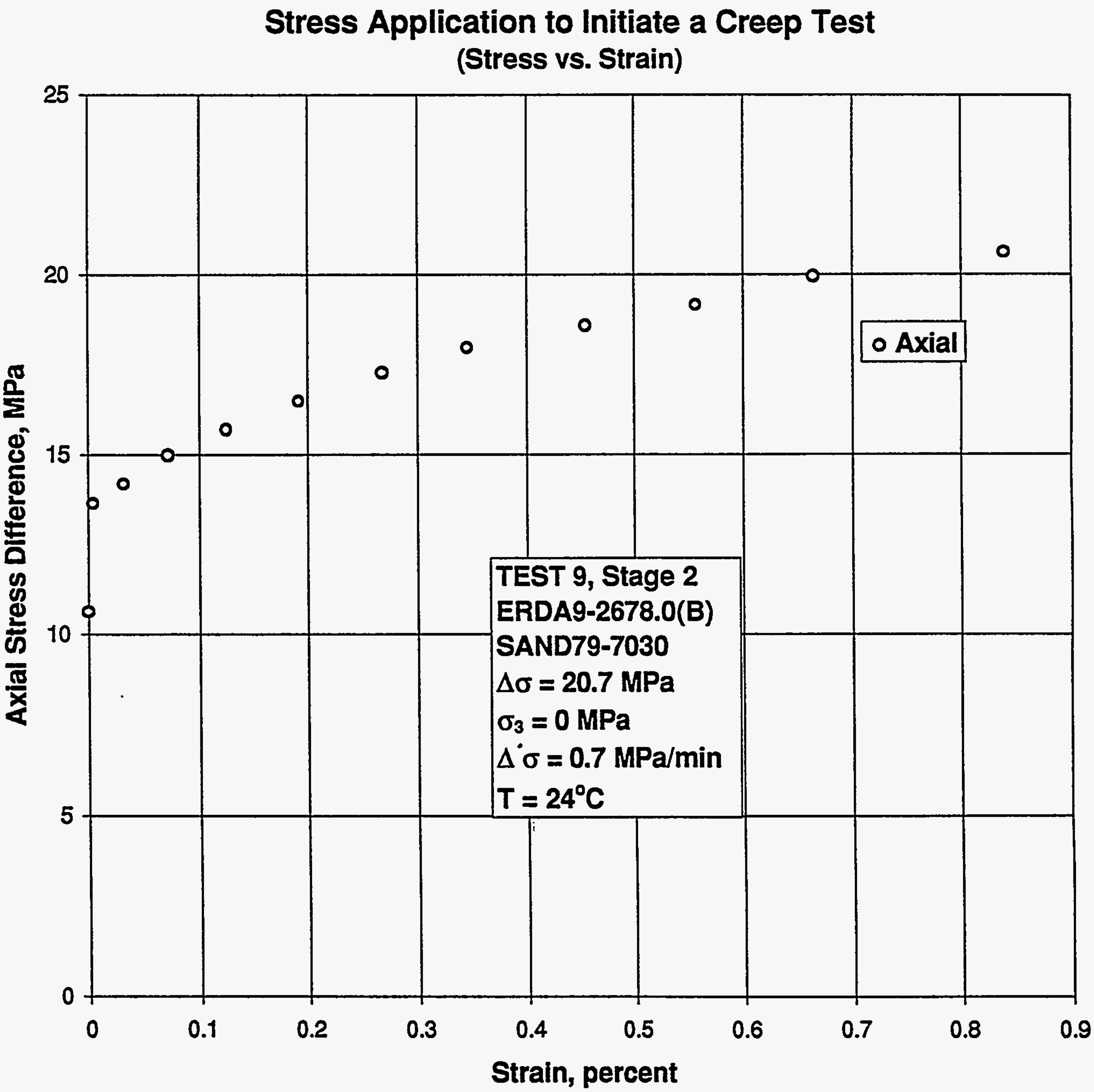

Figure B-110. Axial Stress Difference Versus Axial and Lateral Strain for Stress Application to Initiate a Creep Test: Specimen ERDA9-2678.0 (B); Stage 2 of 2.

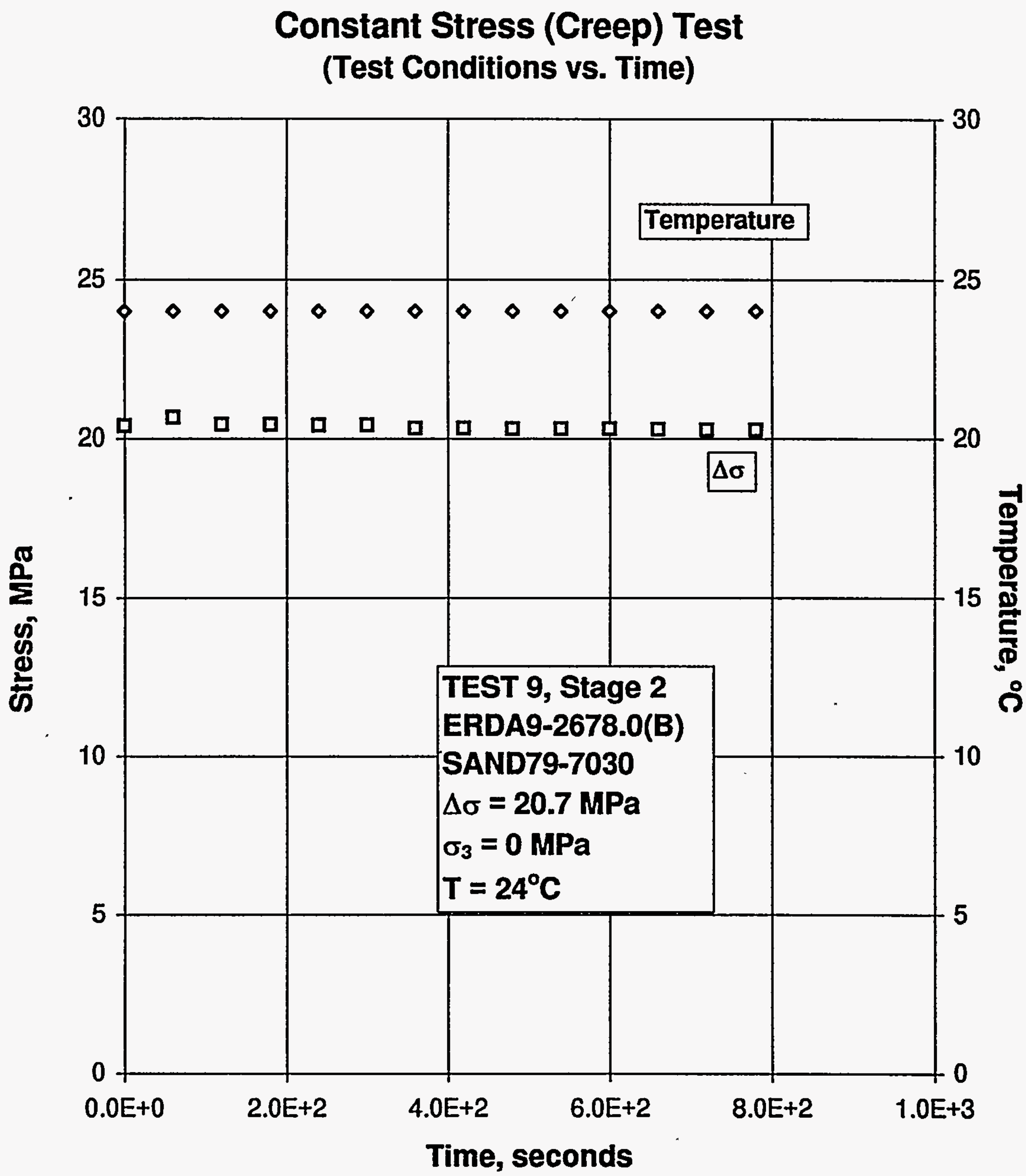

Figure B-111. Test Conditions Versus Time for a Creep Test: Specimen ERDA9-2678.0 (B); Stage 2 of 2 (Specimen Rupture Terminated Test).

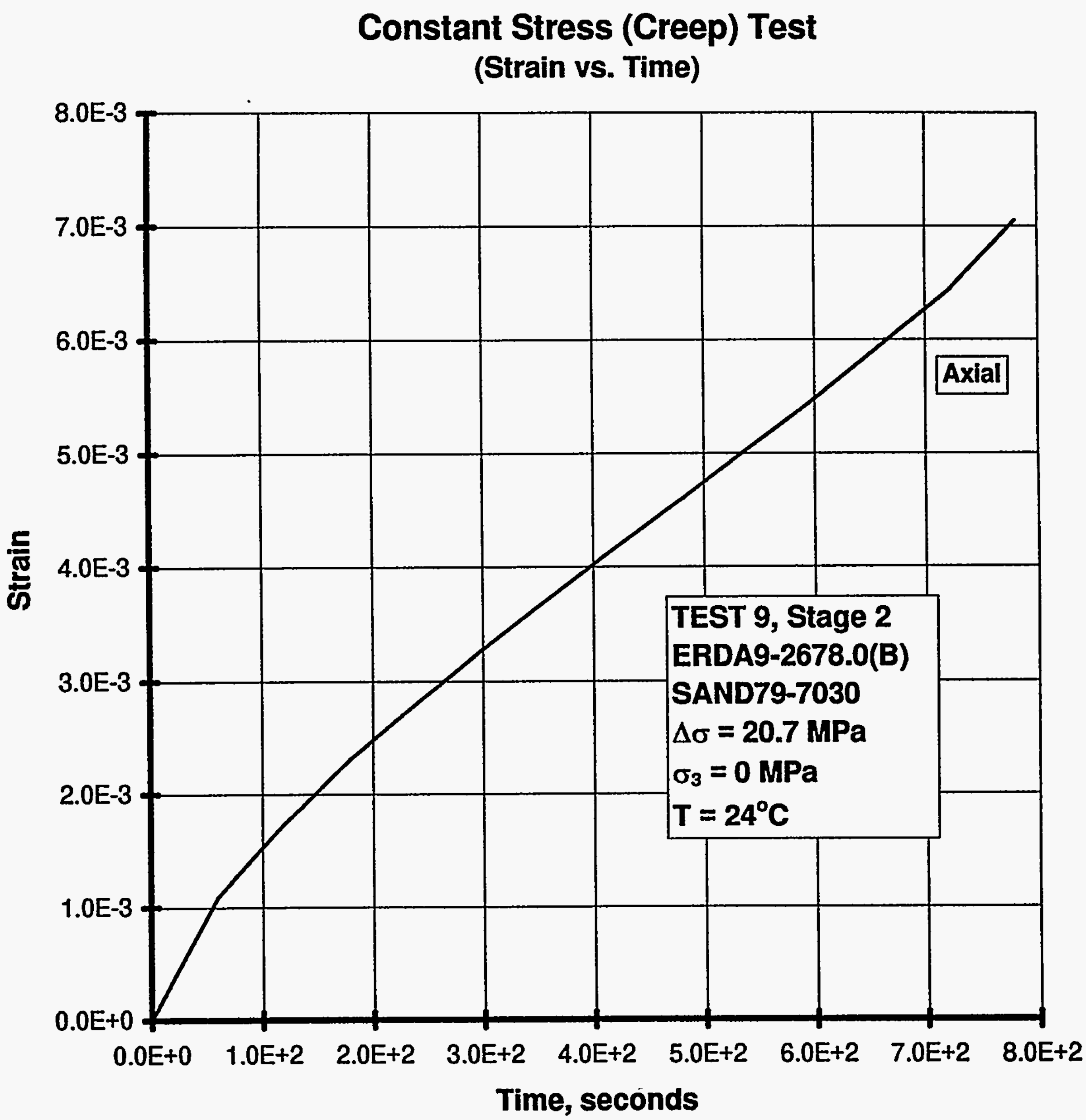

Figure B-112. Axial Strain and Lateral Strain Versus Time for a Creep Test: Specimen ERDA9-2678.0 (B); Stage 2 of 2 (Specimen Rupture Terminated Test).

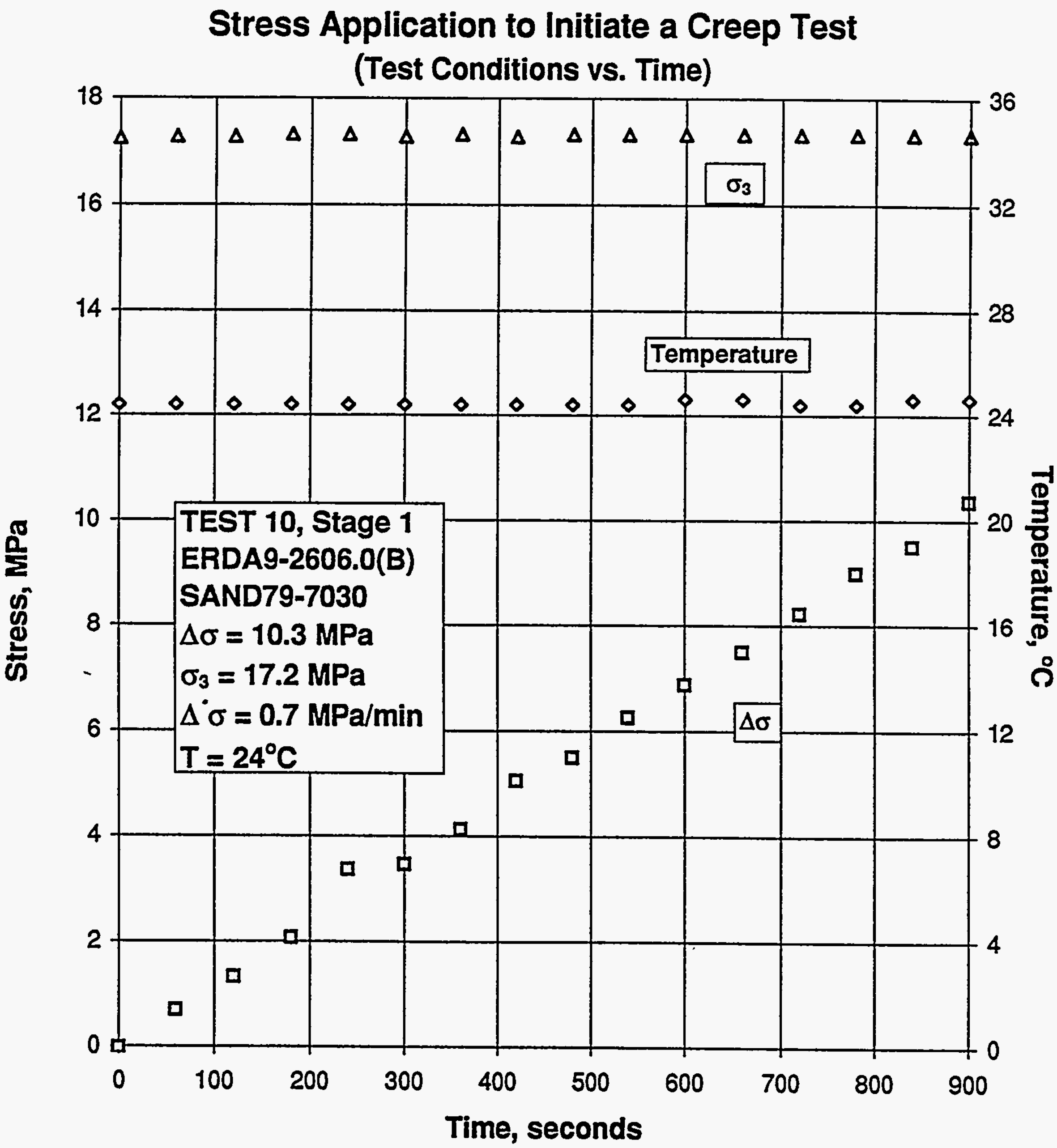

Figure B-113. Test Conditions Versus Time for Stress Application to Initiate a Creep Test: Specimen ERDA9-2606.0 (B); Stage 1 of 2.

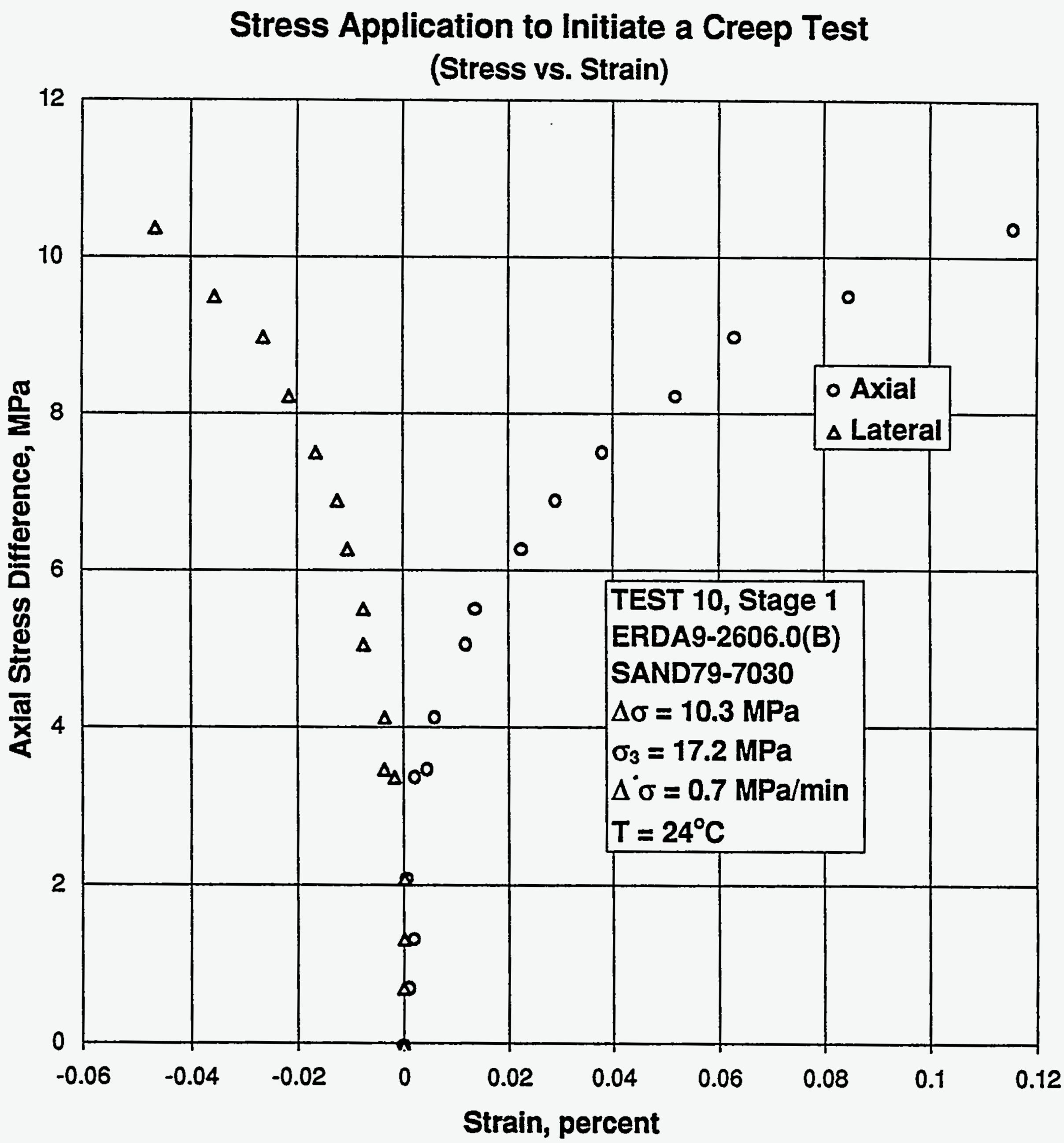

Figure B-114. Axial Stress Difference Versus Axial and Lateral Strain for Stress Application to Initiate a Creep Test: Specimen ERDA9-2606.0 (B); Stage 1 of 2.

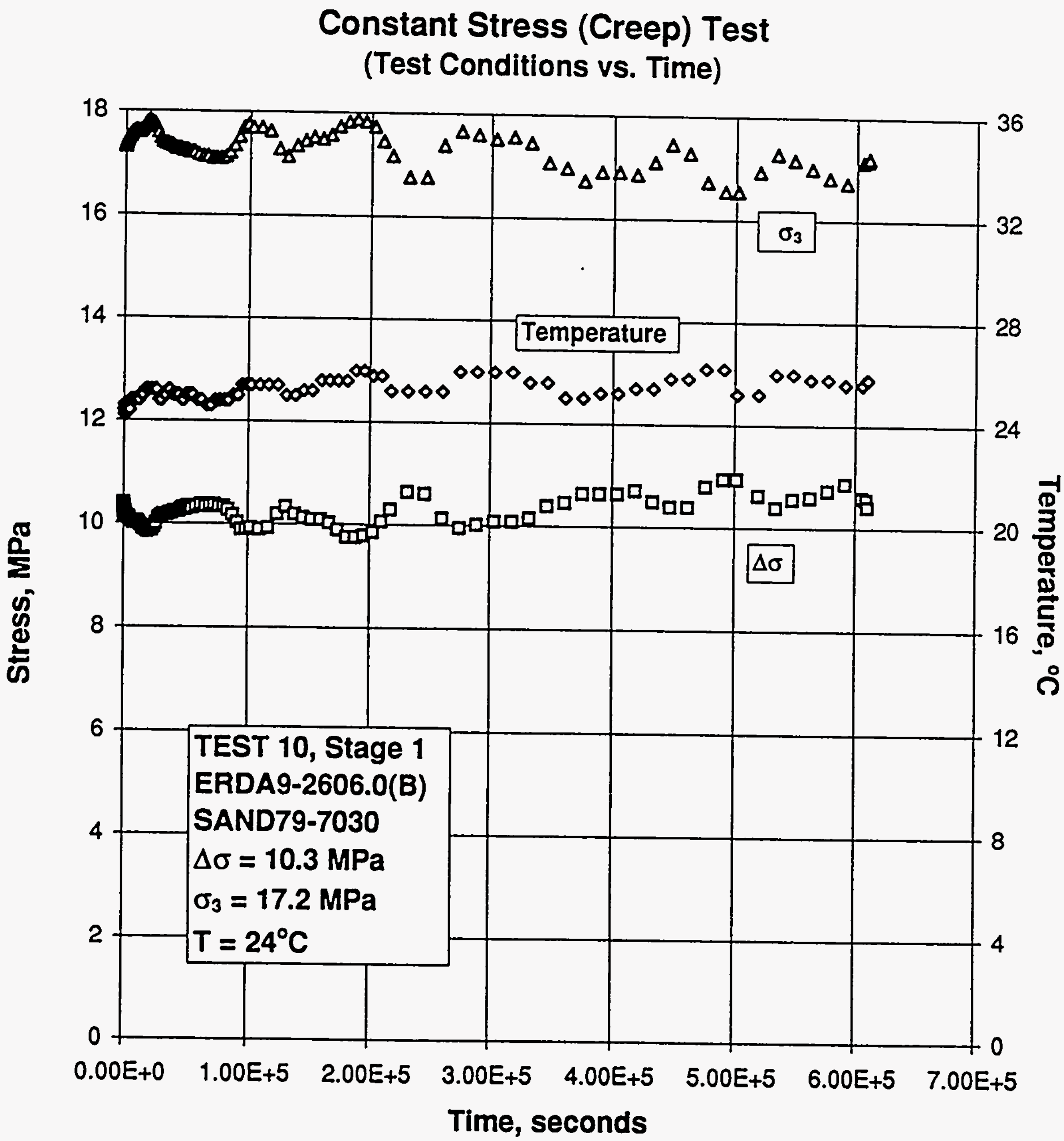

Figure B-115. Test Conditions Versus Time for a Creep Test: Specimen ERDA9-2606.0 (B); Stage 1 of 2.

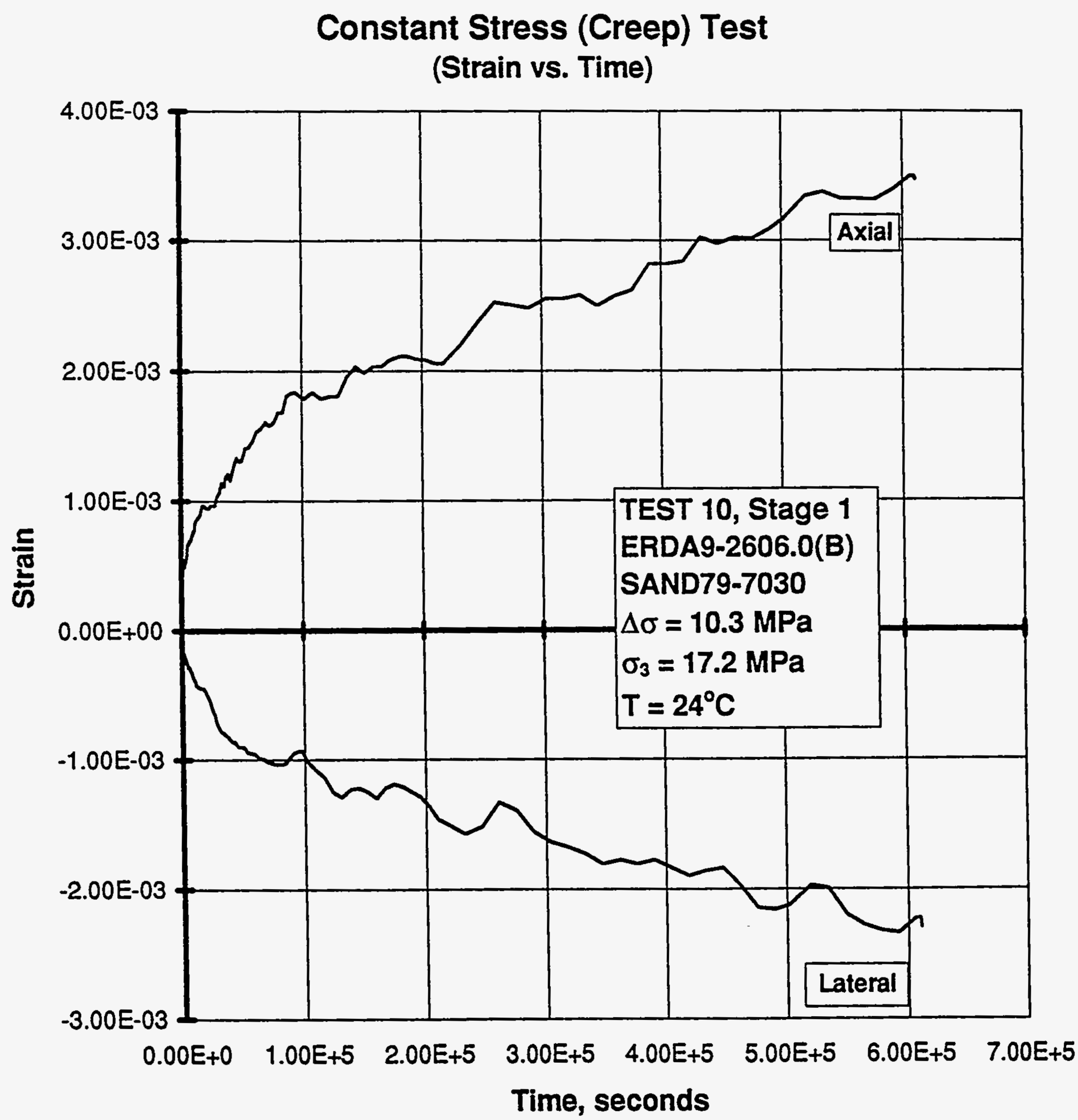

Figure B-116. Axial Strain and Lateral Strain Versus Time for a Creep Test: Specimen ERDA9-2606.0 (B); Stage 1 of 2.

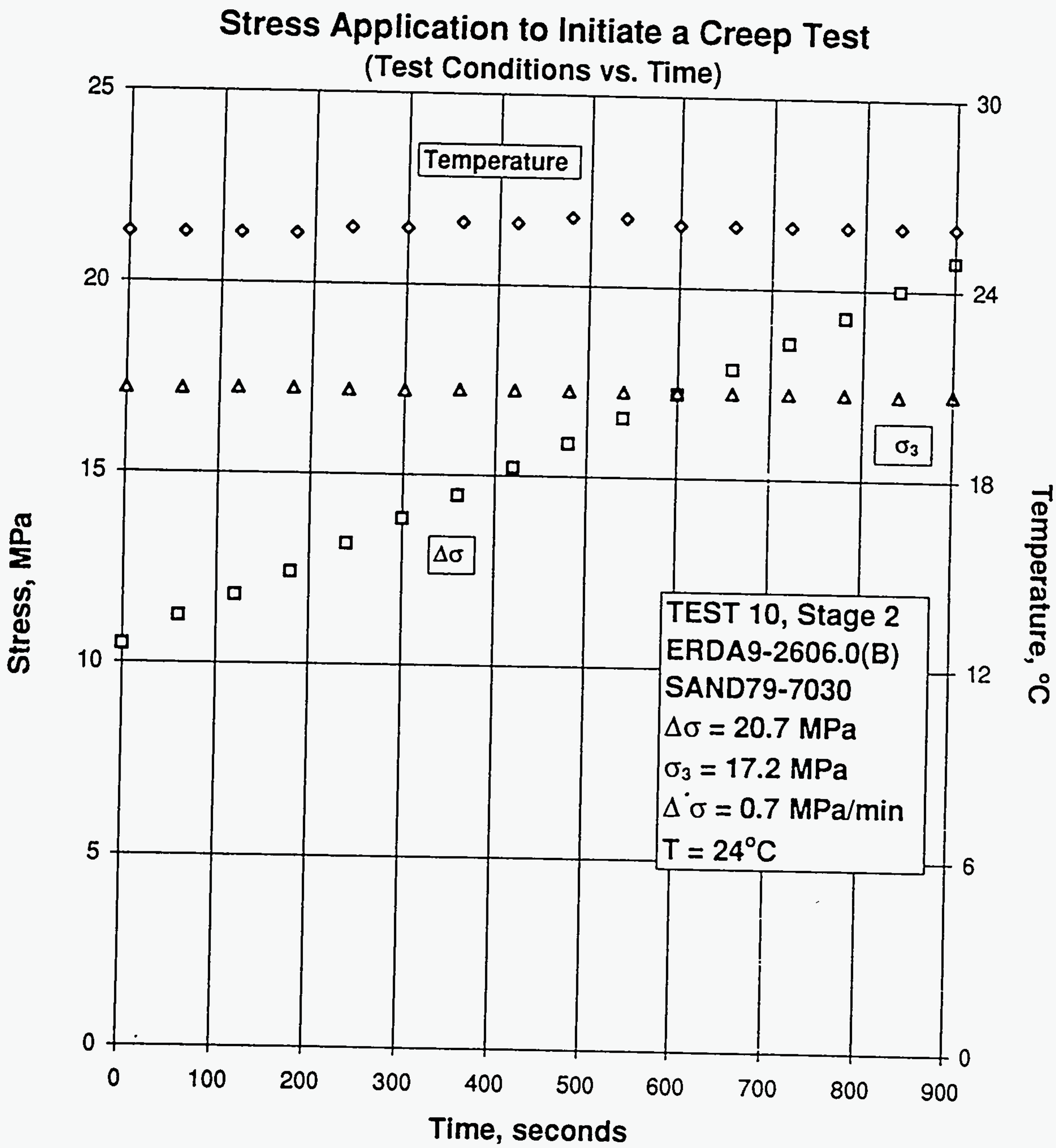

Figure B-117. Test Conditions Versus Time for Stress Application to Initiate a Creep Test: Specimen ERDA9-2606.0 (B); Stage 2 of 2.

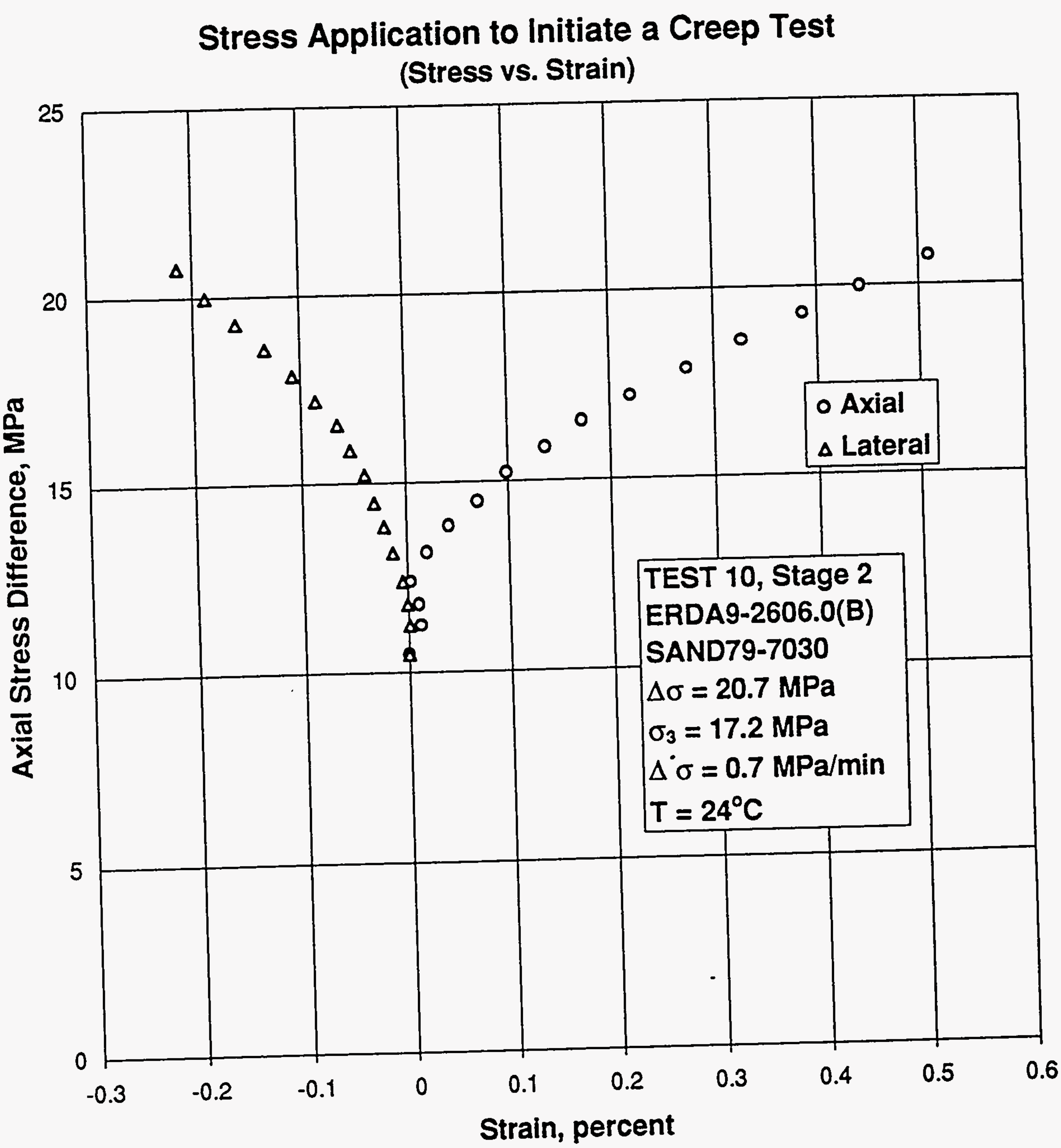

Figure B-118. Axial Stress Difference Versus Axial and Lateral Strain for Stress Application to Initiate a Creep Test: Specimen ERDA9-2606.0 (B); Stage 2 of 2.

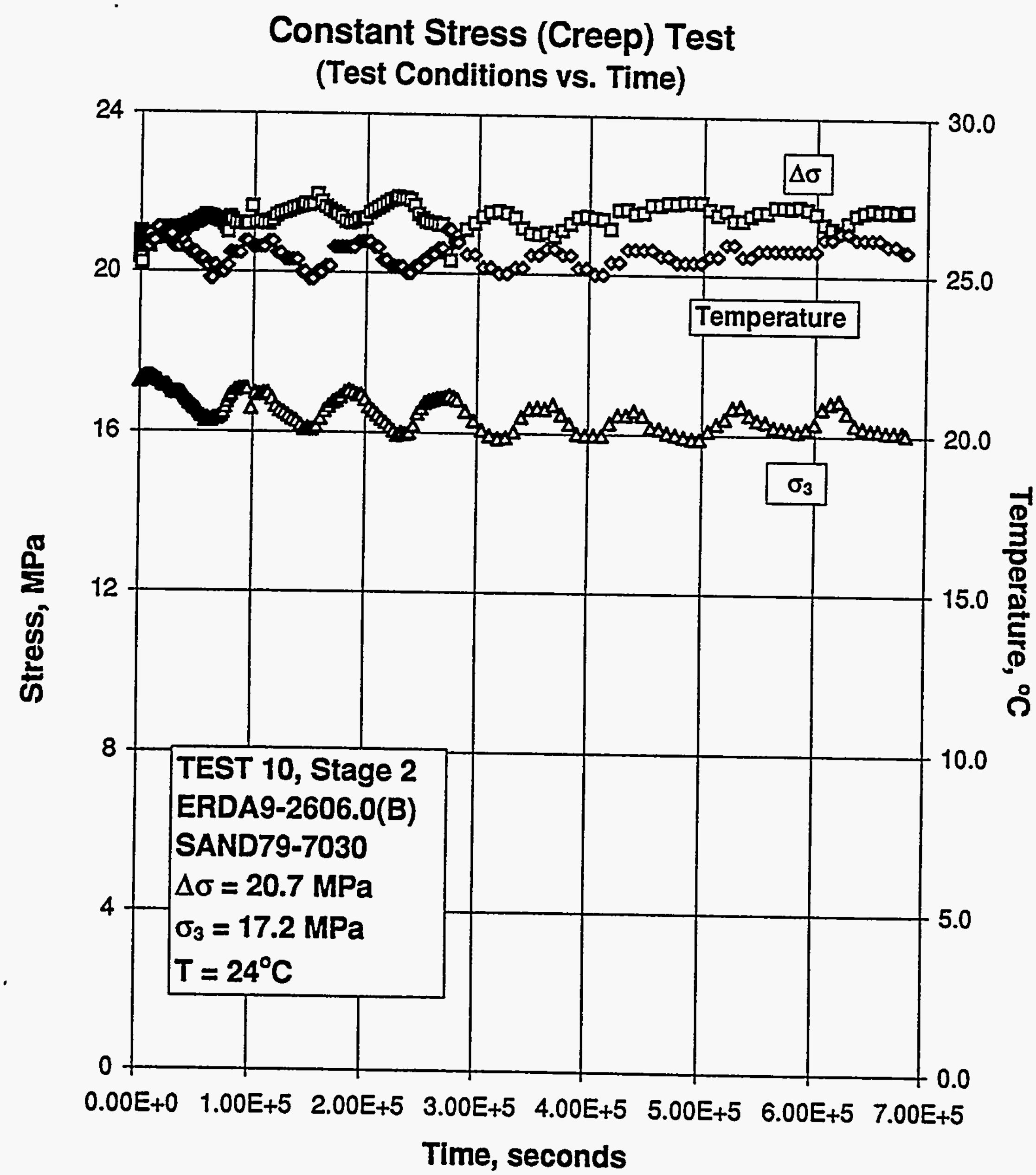

Figure B-119. Test Conditions Versus Time for a Creep Test: Specimen ERDA9-2606.0 (B); Stage 2 of 2.

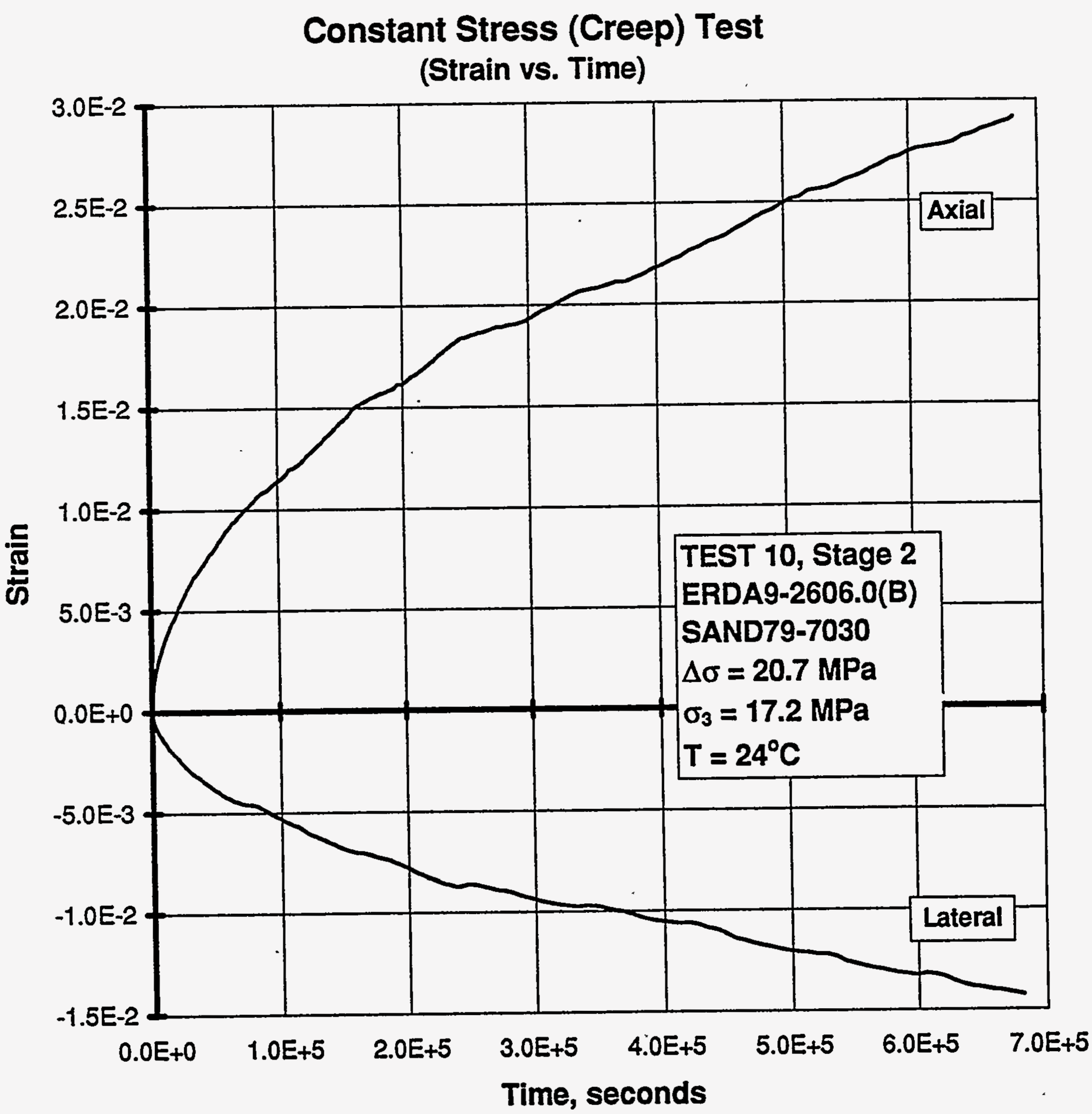

Figure B-120. Axial Strain and Lateral Strain Versus Time for a Creep Test: Specimen ERDA9-2606.0 (B); Stage 2 of 2.

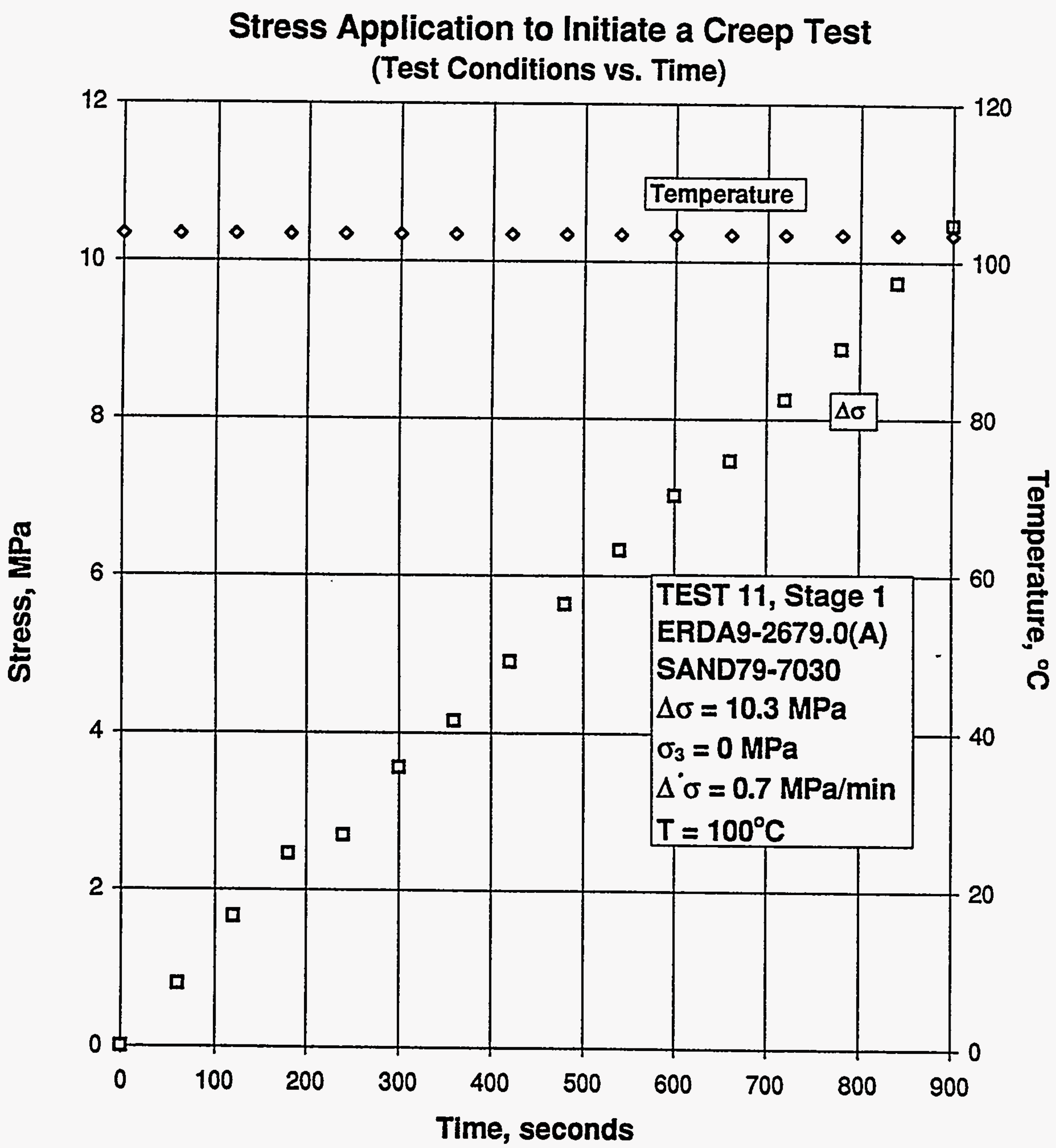

Figure B-121. Test Conditions Versus Time for Stress Application to Initiate a Creep Test: Specimen ERDA9-2679.0 (A); Stage 1 of 2.

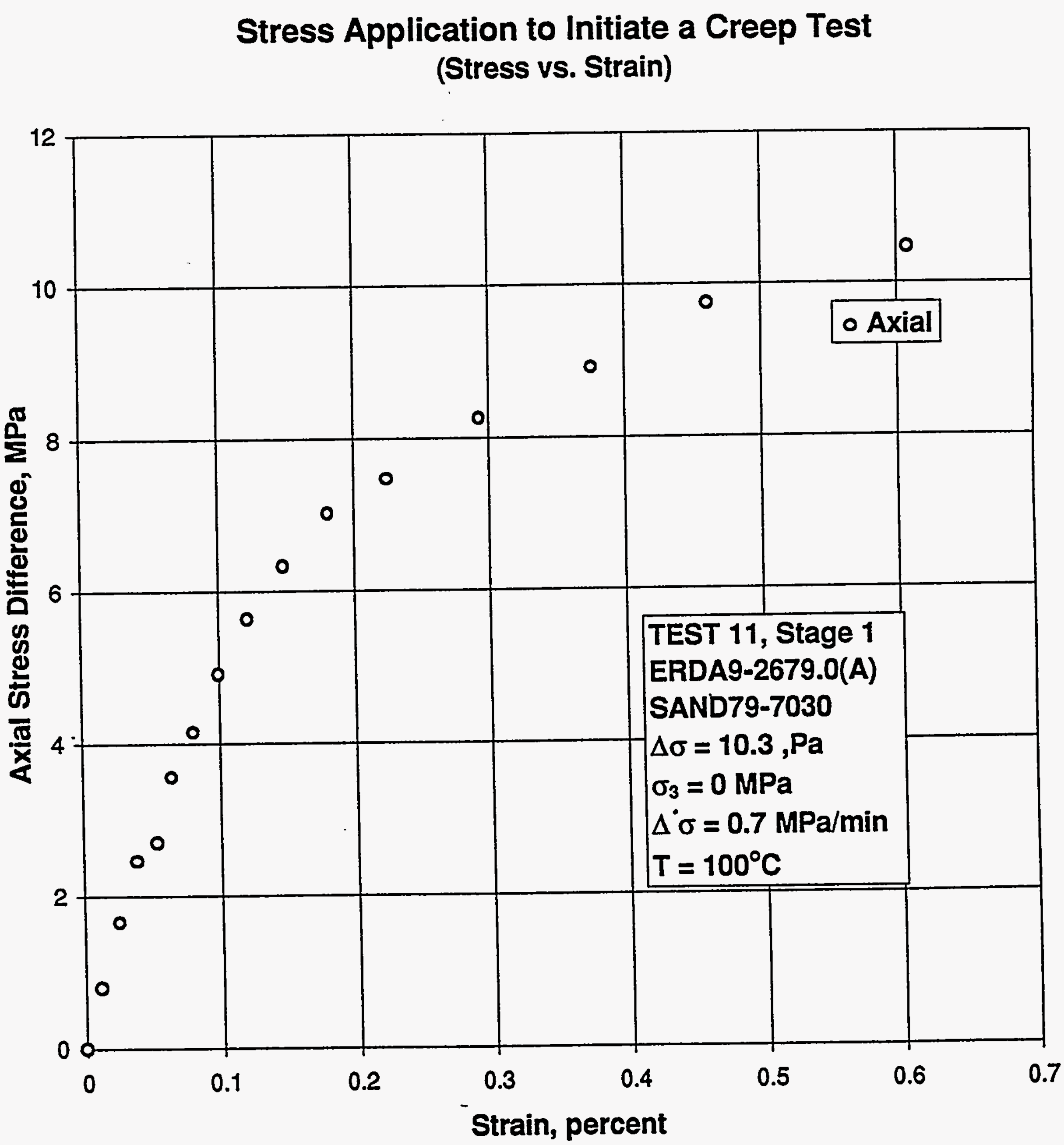

Figure B-122. Axial Stress Difference Versus Axial and Lateral Strain for Stress Application to Initiate a Creep Test: Specimen ERDA9-2679.0 (A); Stage 1 of 2.

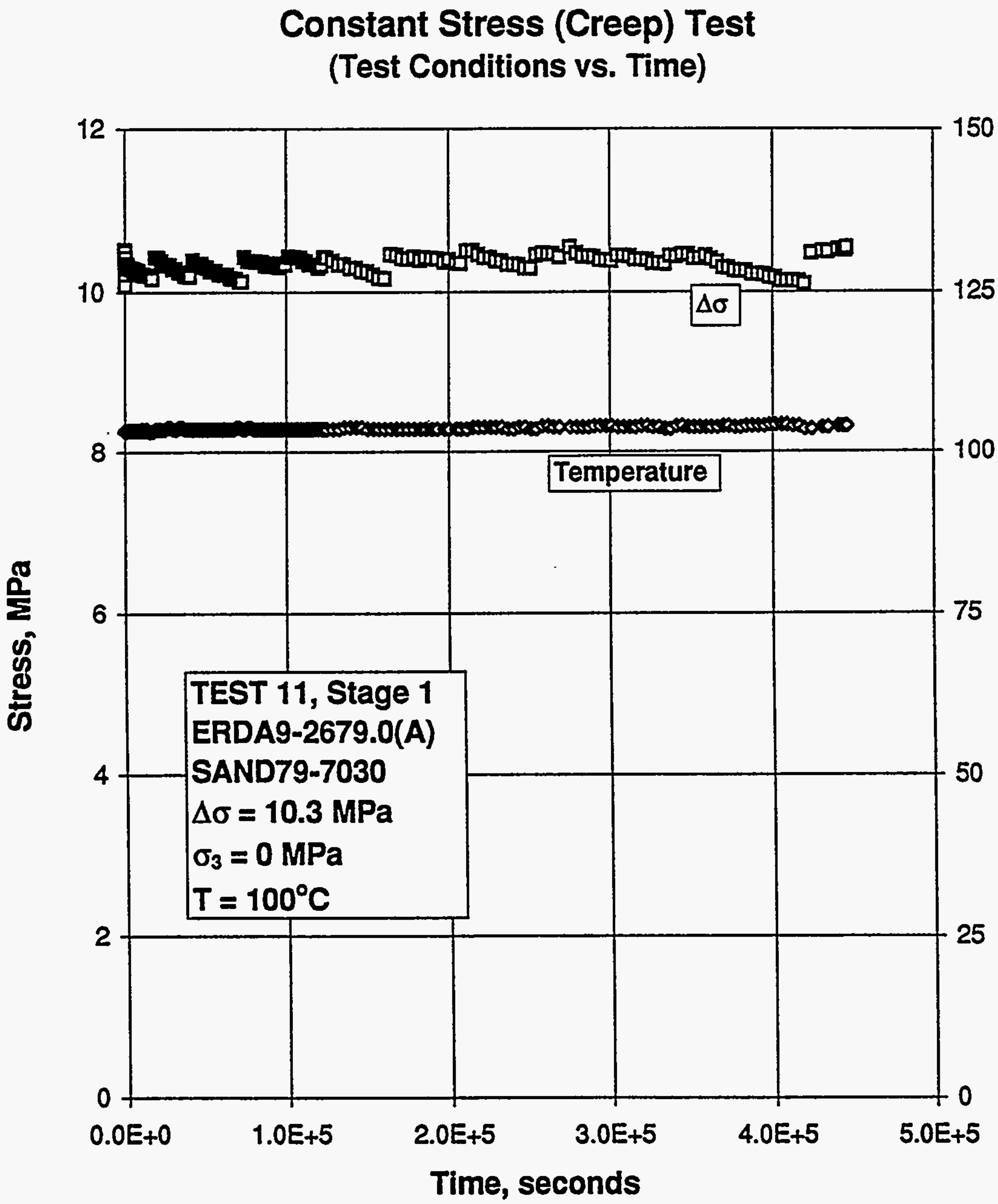

Figure B-123. Test Conditions Versus Time for a Creep Test: Specimen ERDA9-2679.0 (A); Stage 1 of 2.

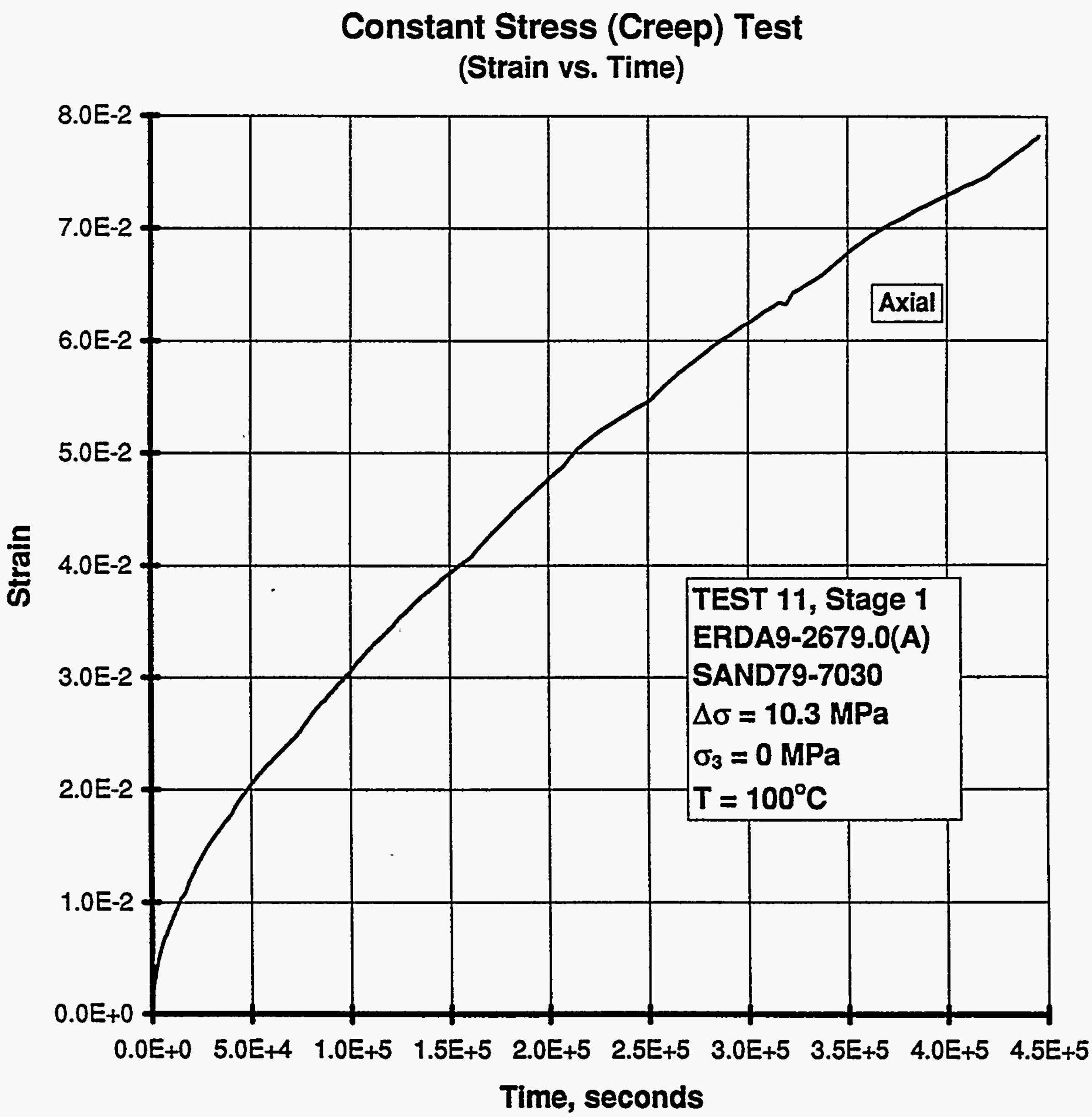

Figure B-124. Axial Strain and Lateral Strain Versus Time for a Creep Test: Specimen ERDA9-2679.0 (A); Stage 1 of 2.

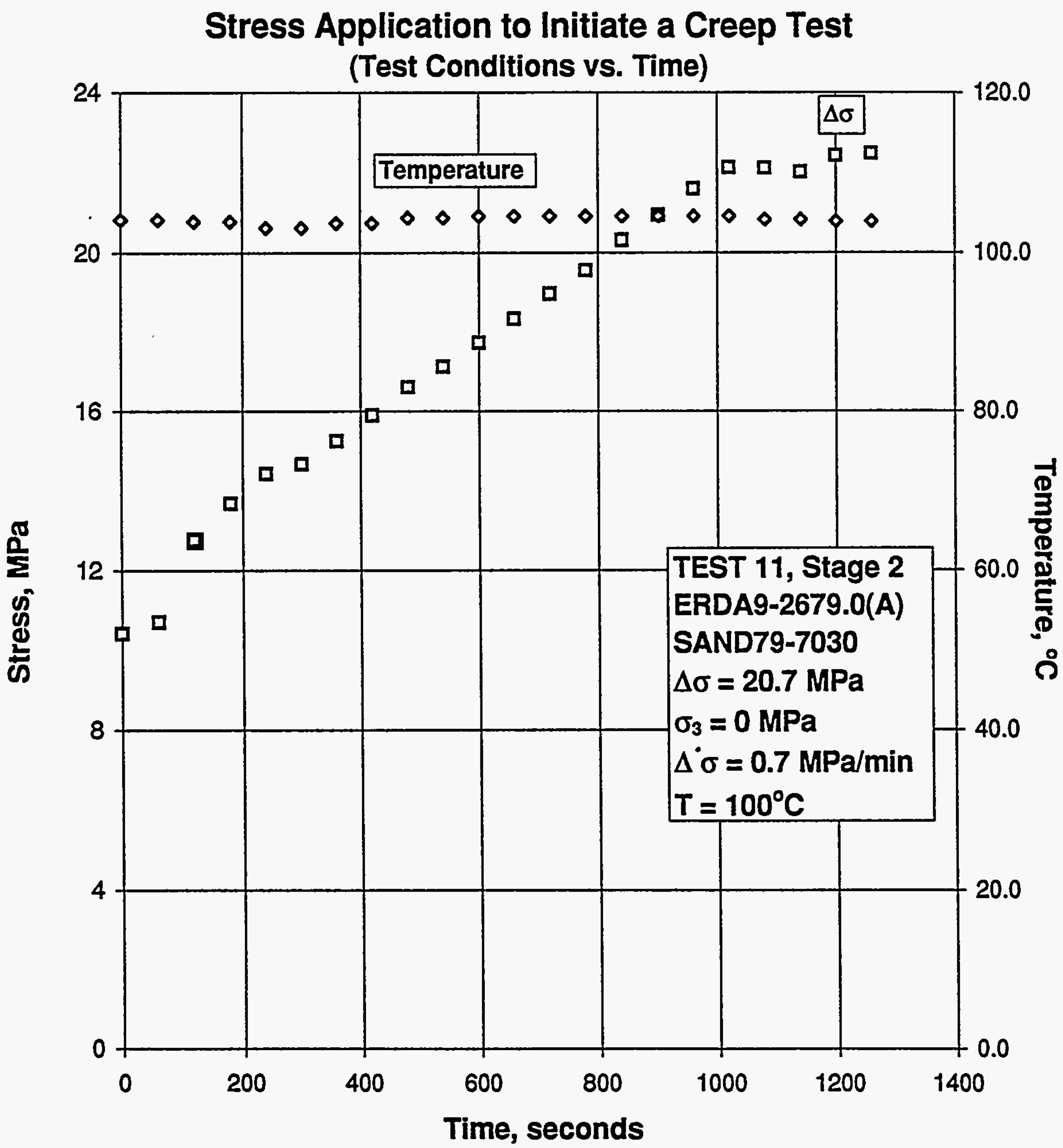

Figure B-125. Test Conditions Versus Time for Stress Application to Initiate a Creep Test: Specimen ERDA9-2679.0 (A); Stage 2 of 2 (Specimen Contacted Vessel Wall. No Creep Stage).

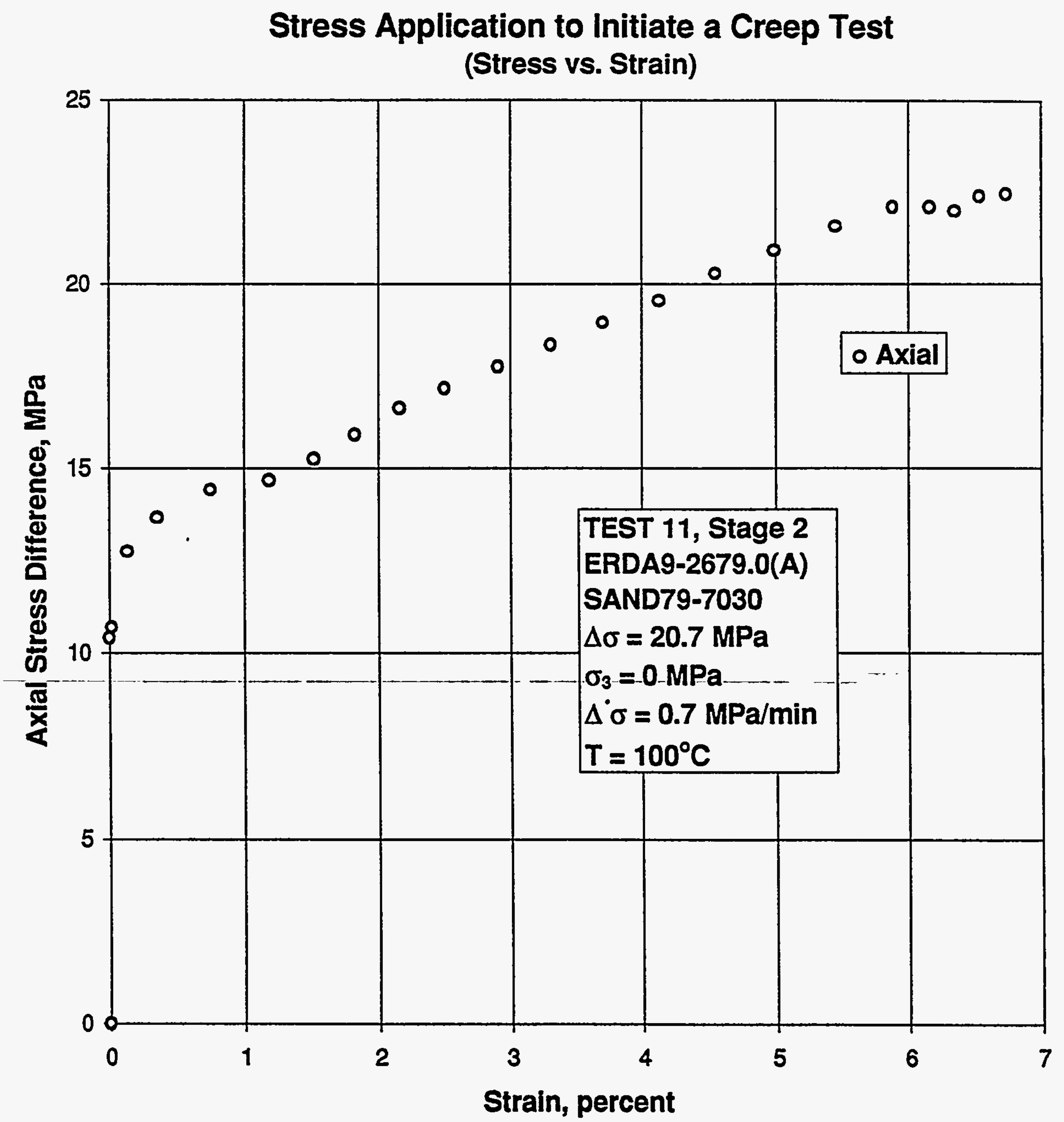

Figure B-126. Axial Stress Difference Versus Axial and Lateral Strain for Stress Application to Initiate a Creep Test: Specimen ERDA9-2679.0 (A); Stage 2 of 2 (Specimen Contacted Vessel Wall. No Creep Stage).

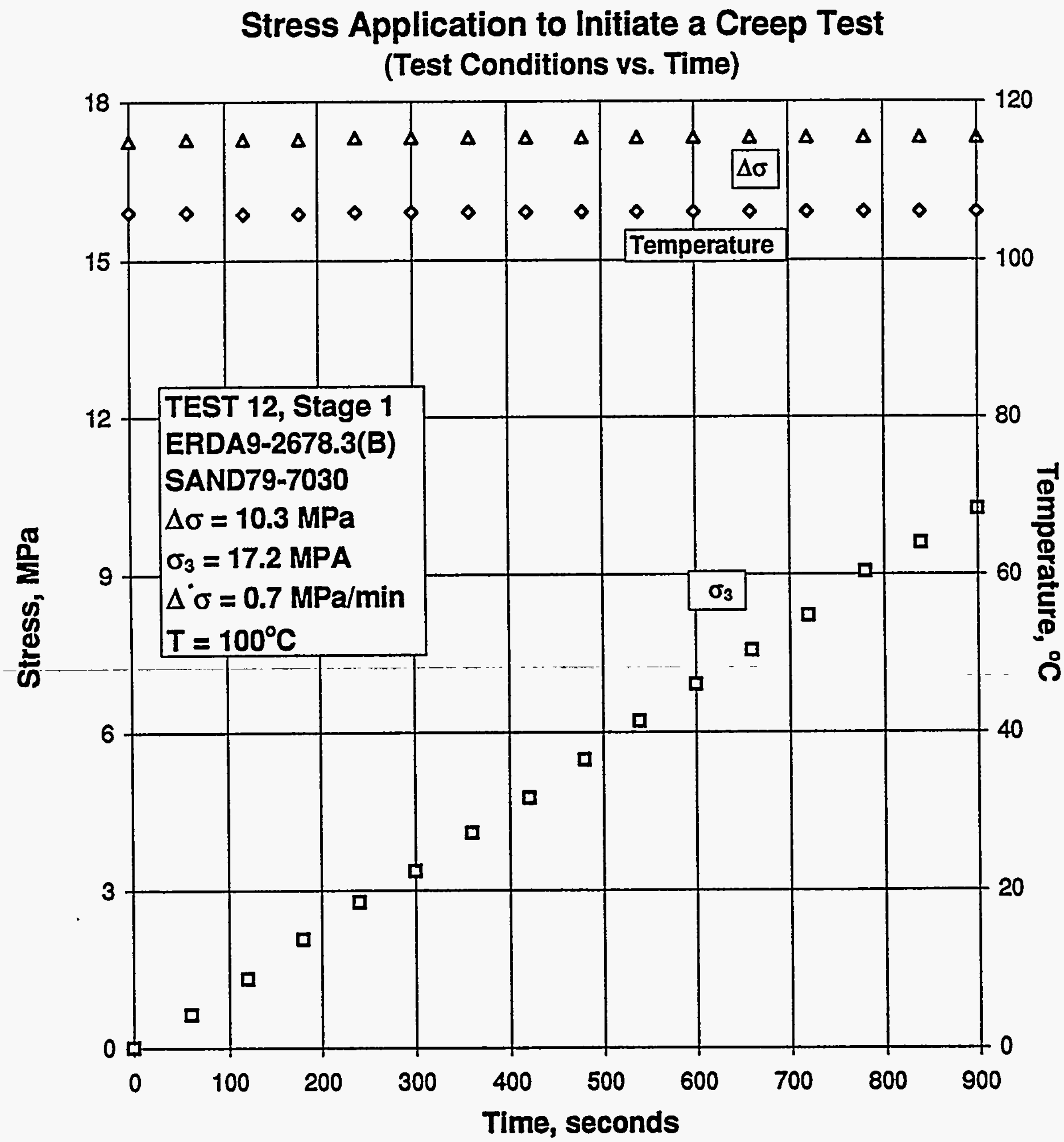

Figure B-127. Test Conditions Versus Time for Stress Application to Initiate a Creep Test: Specimen ERDA9-2678.3 (B); Stage 1 of 2.

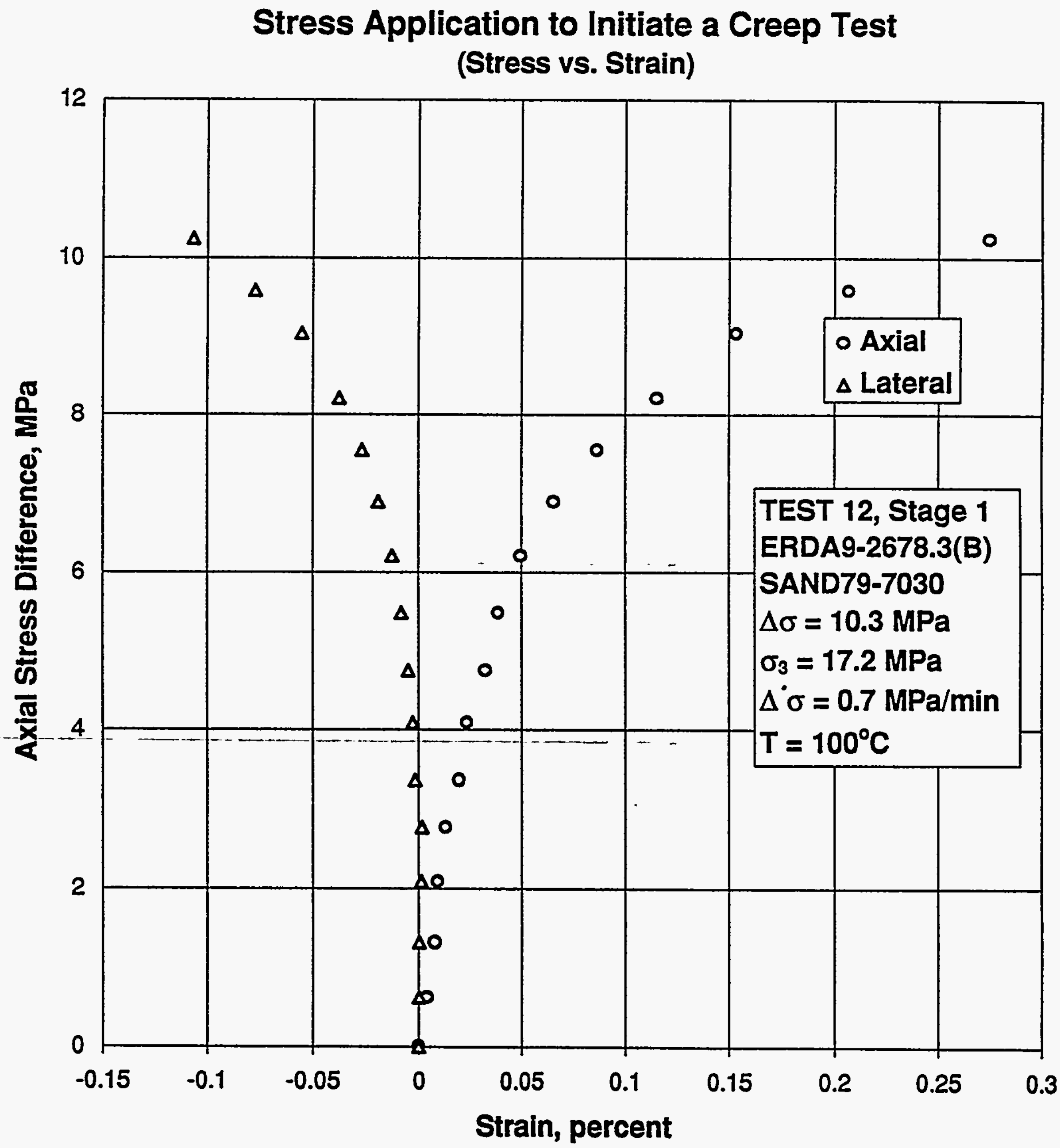

Figure B-128. Axial Stress Difference Versus Axial and Lateral Strain for Stress Application to Initiate a Creep Test: Specimen ERDA9-2678.3 (B); Stage 1 of 2.

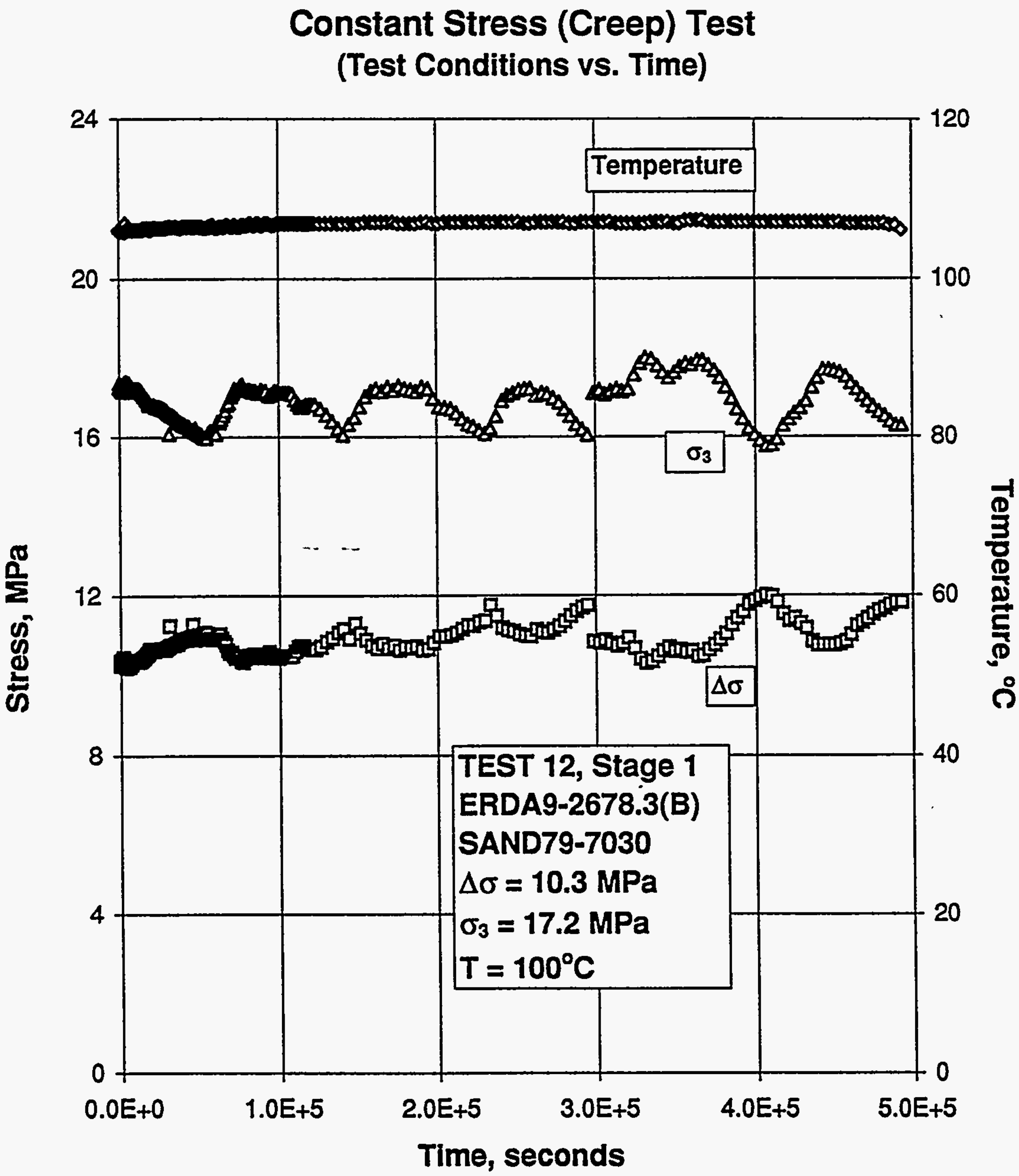

Figure B-129. Test Conditions Versus Time for a Creep Test: Specimen ERDA9-2678.3 (B); Stage 1 of 2.

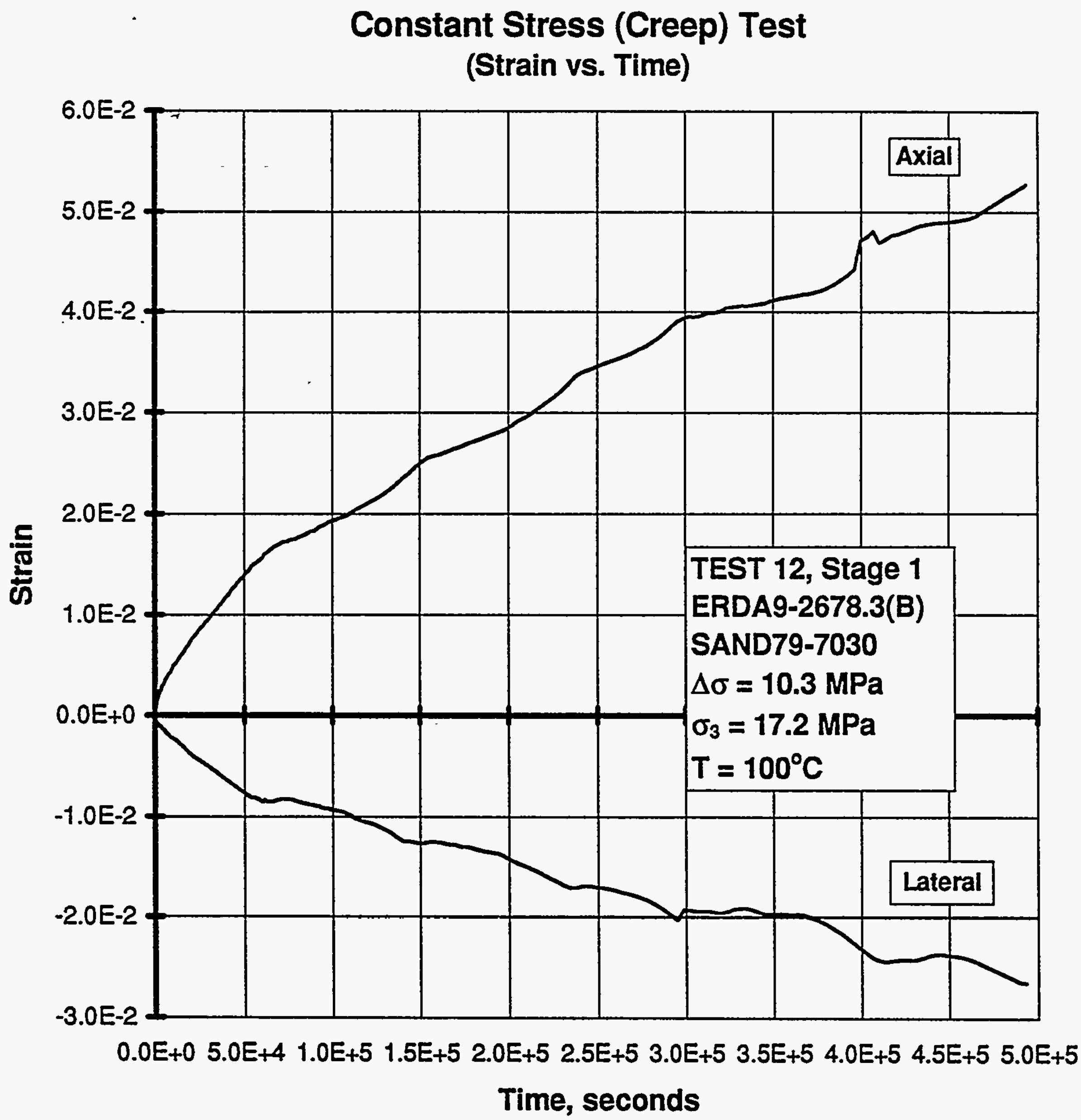

Figure B-130. Axial Strain and Lateral Strain Versus Time for a Creep Test: Specimen ERDA9-2678.3 (B); Stage 1 of 2.

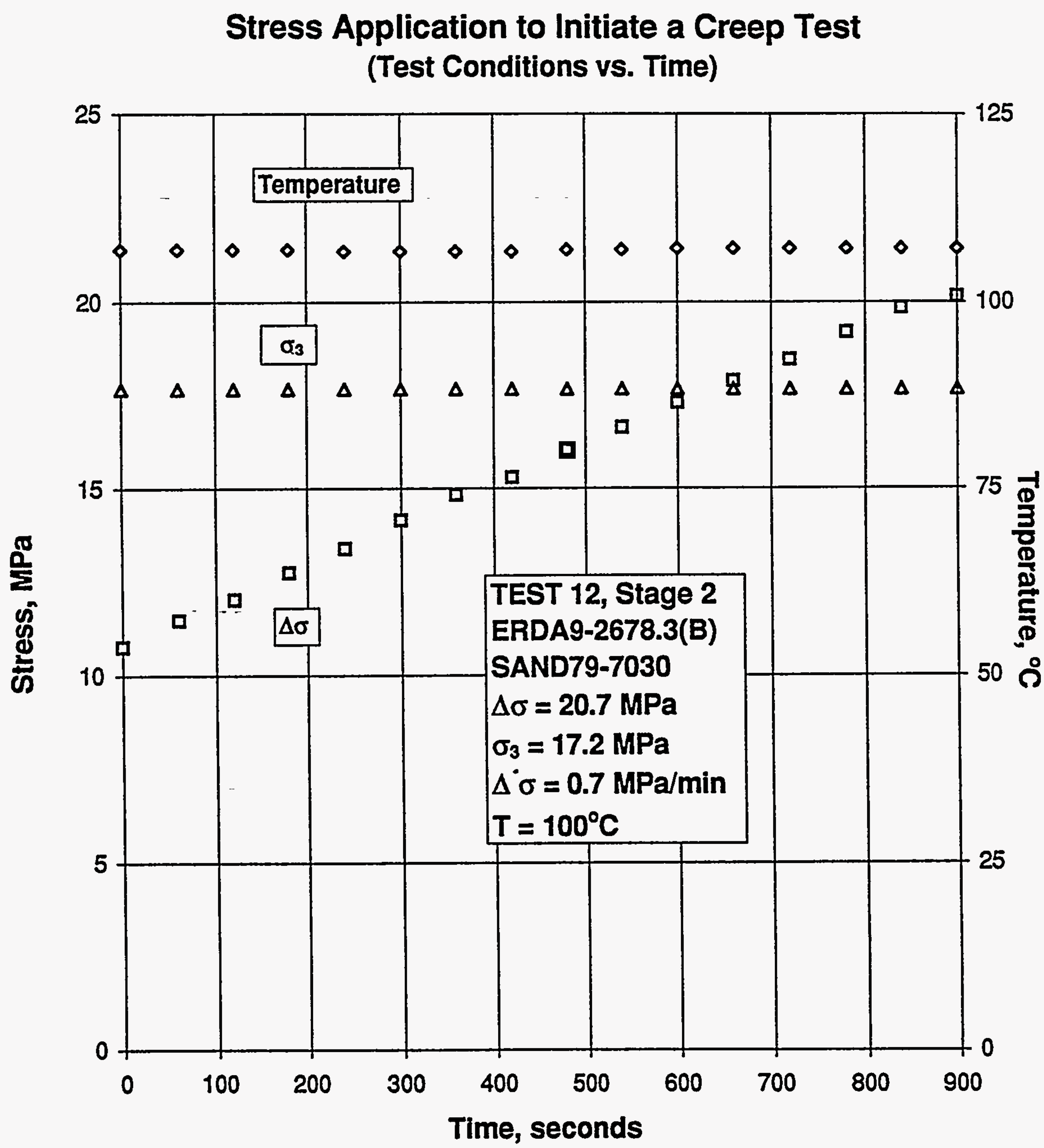

Figure B-131. Test Conditions Versus Time for Stress Application to Initiate a Creep Test: Specimen ERDA9-2678.3 (B); Stage 2 of 2.

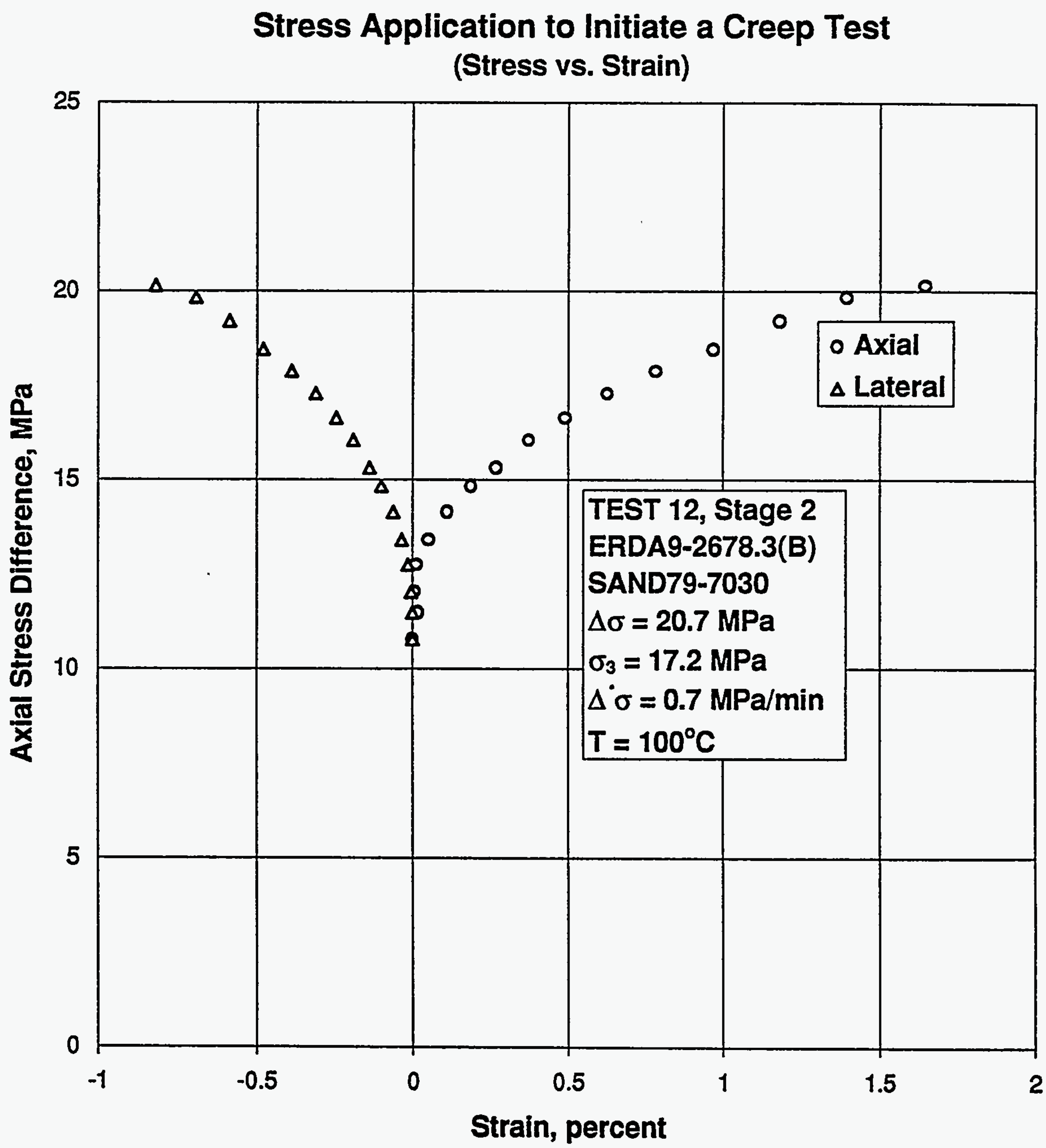

Figure B-132. Axial Stress Difference Versus Axial and Lateral Strain for Stress Application to Initiate a Creep Test: Specimen ERDA9-2678.3 (B); Stage 2 of 2.

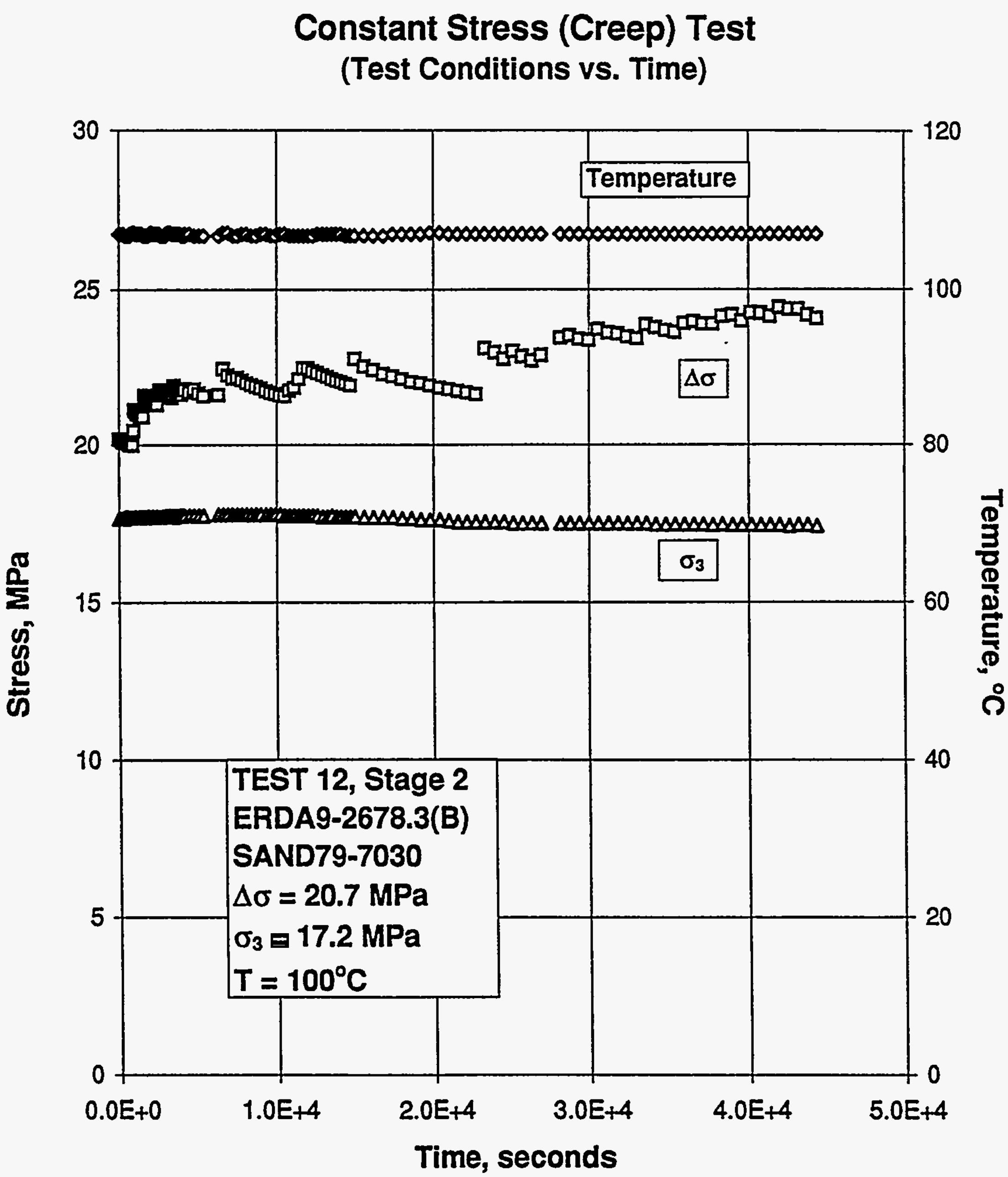

Figure B-133. Test Conditions Versus Time for a Creep Test: Specimen ERDA9-2678.3 (B); Stage 2 of 2.

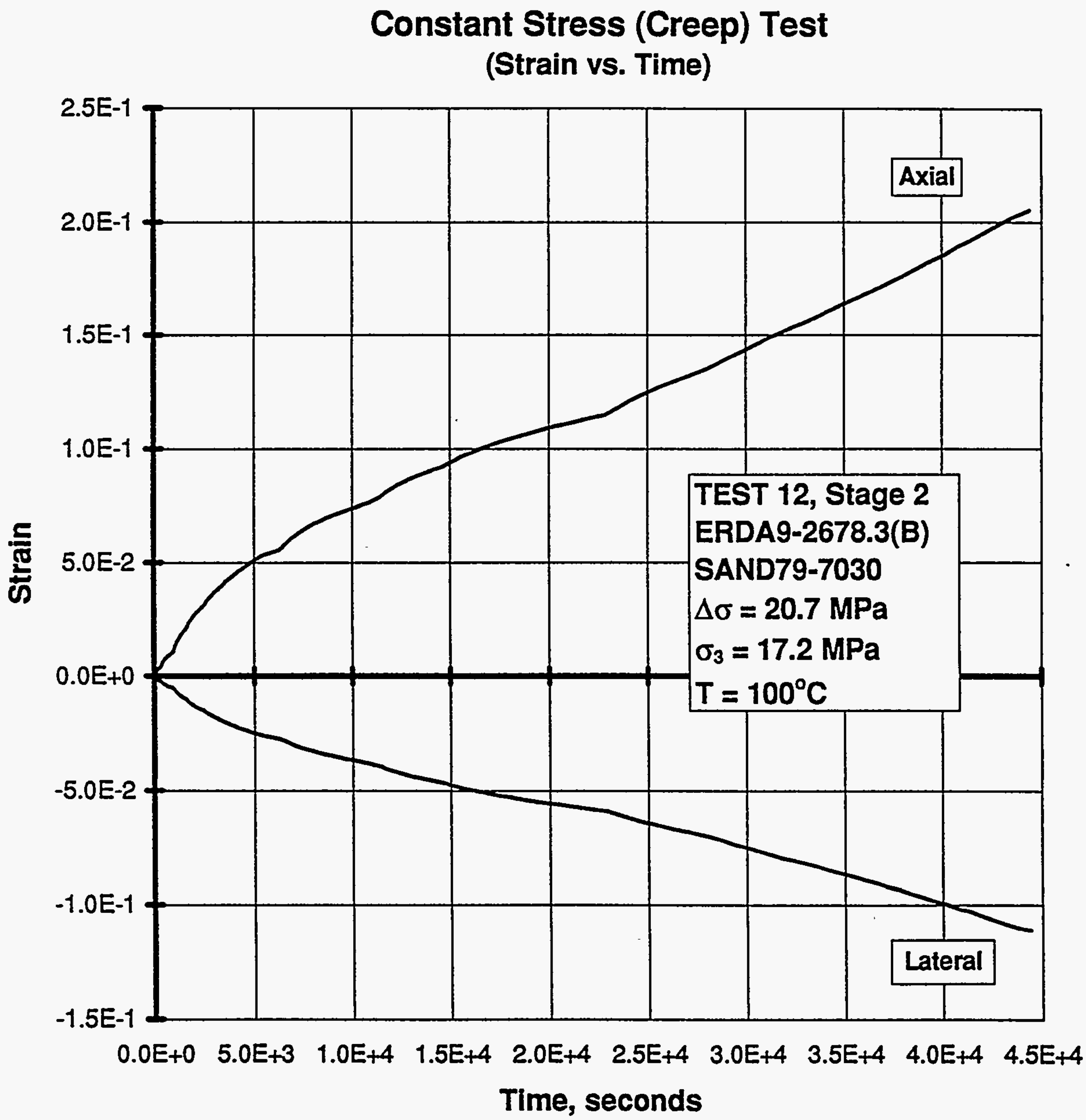

Figure B-134. Axial Strain and Lateral Strain Versus Time for a Creep Test: Specimen ERDA9-2678.3 (B); Stage 2 of 2.

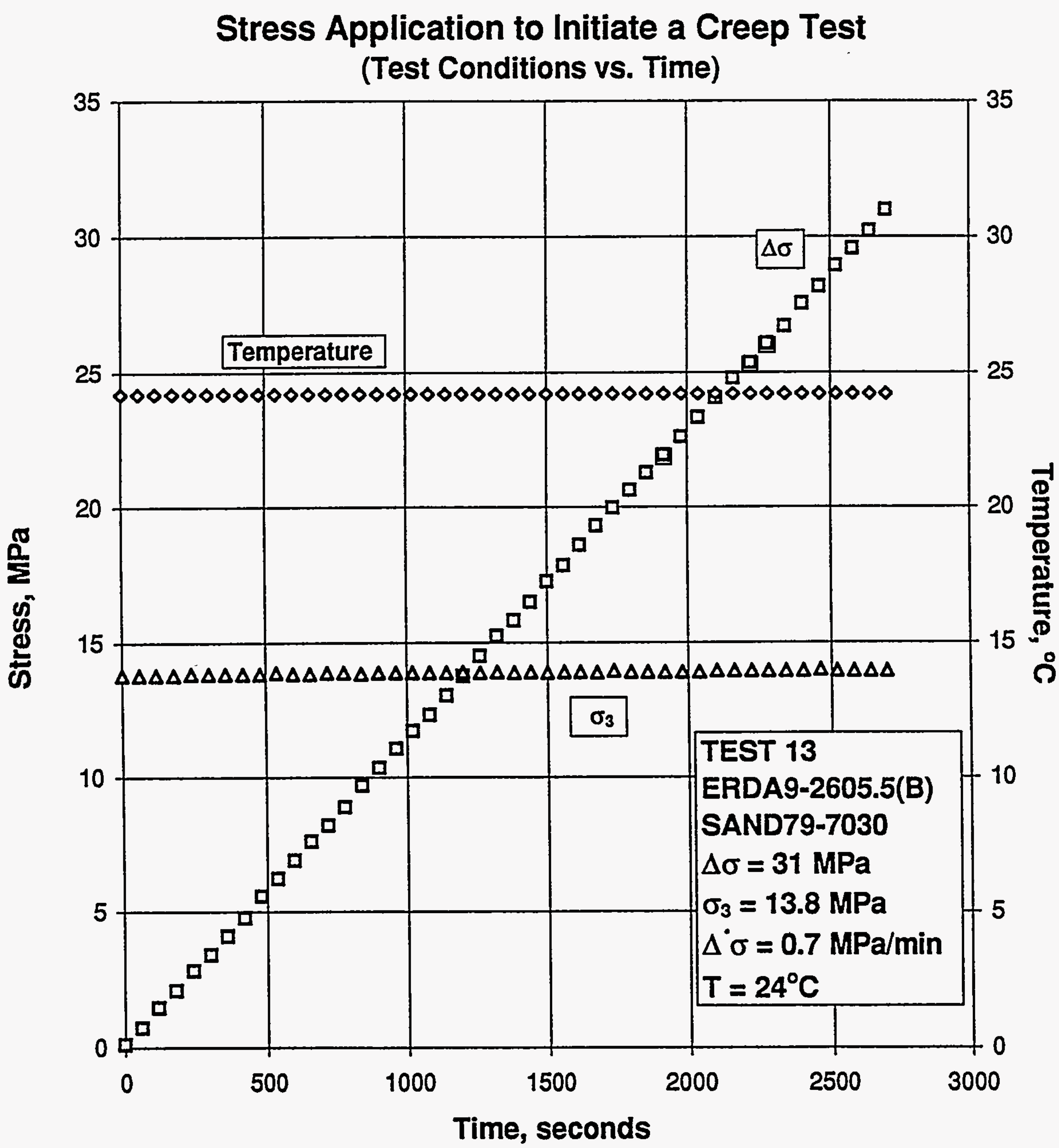

Figure B-135. Test Conditions Versus Time for Stress Application to Initiate a Creep Test: Specimen ERDA9-2605.5 (B); Stage 1 of 1.

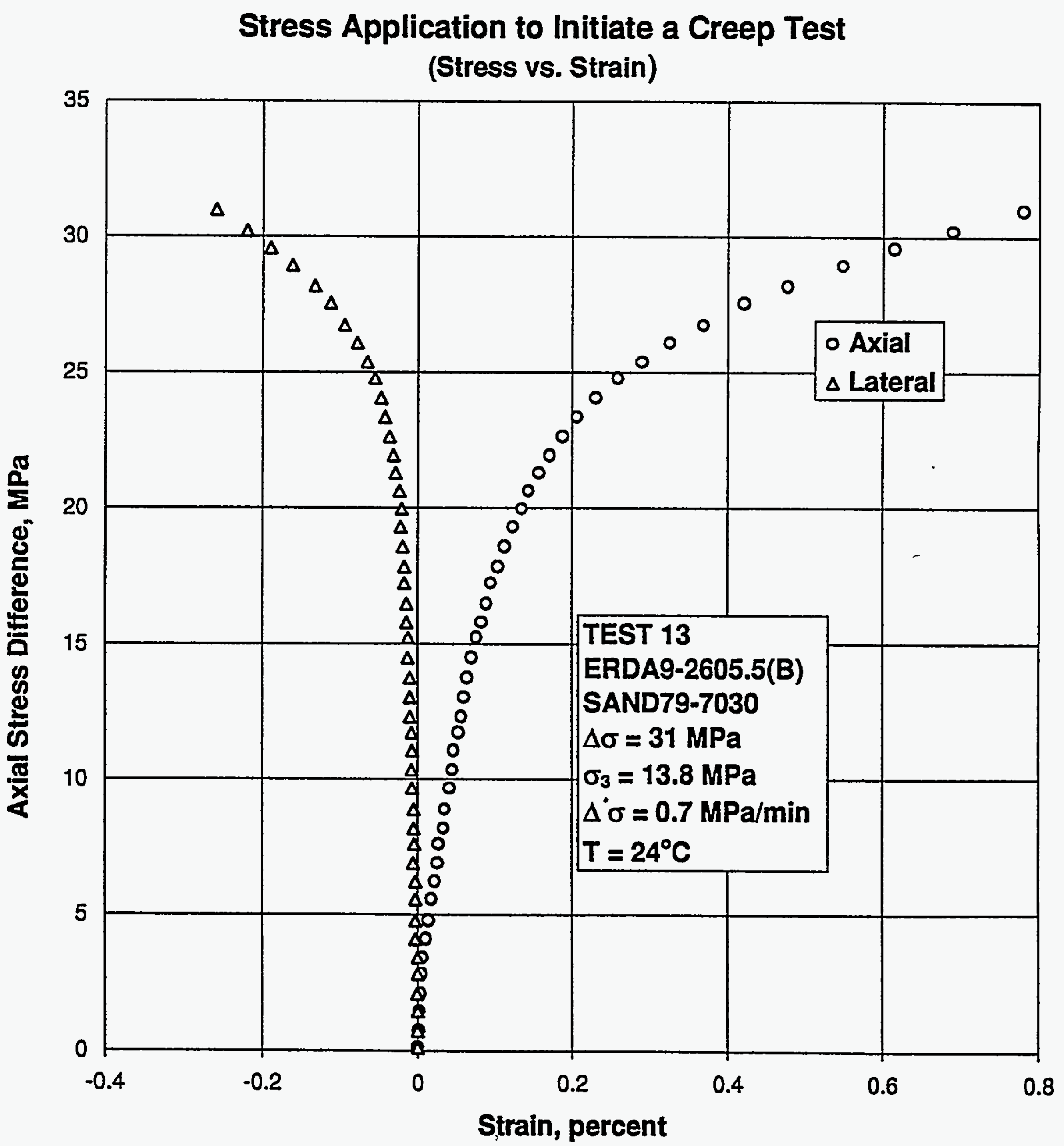

Figure B-136. Axial Stress Difference Versus Axial and Lateral Strain for Stress Application to Initiate a Creep Test: Specimen ERDA9-2605.5 (B); Stage 1 of 1.

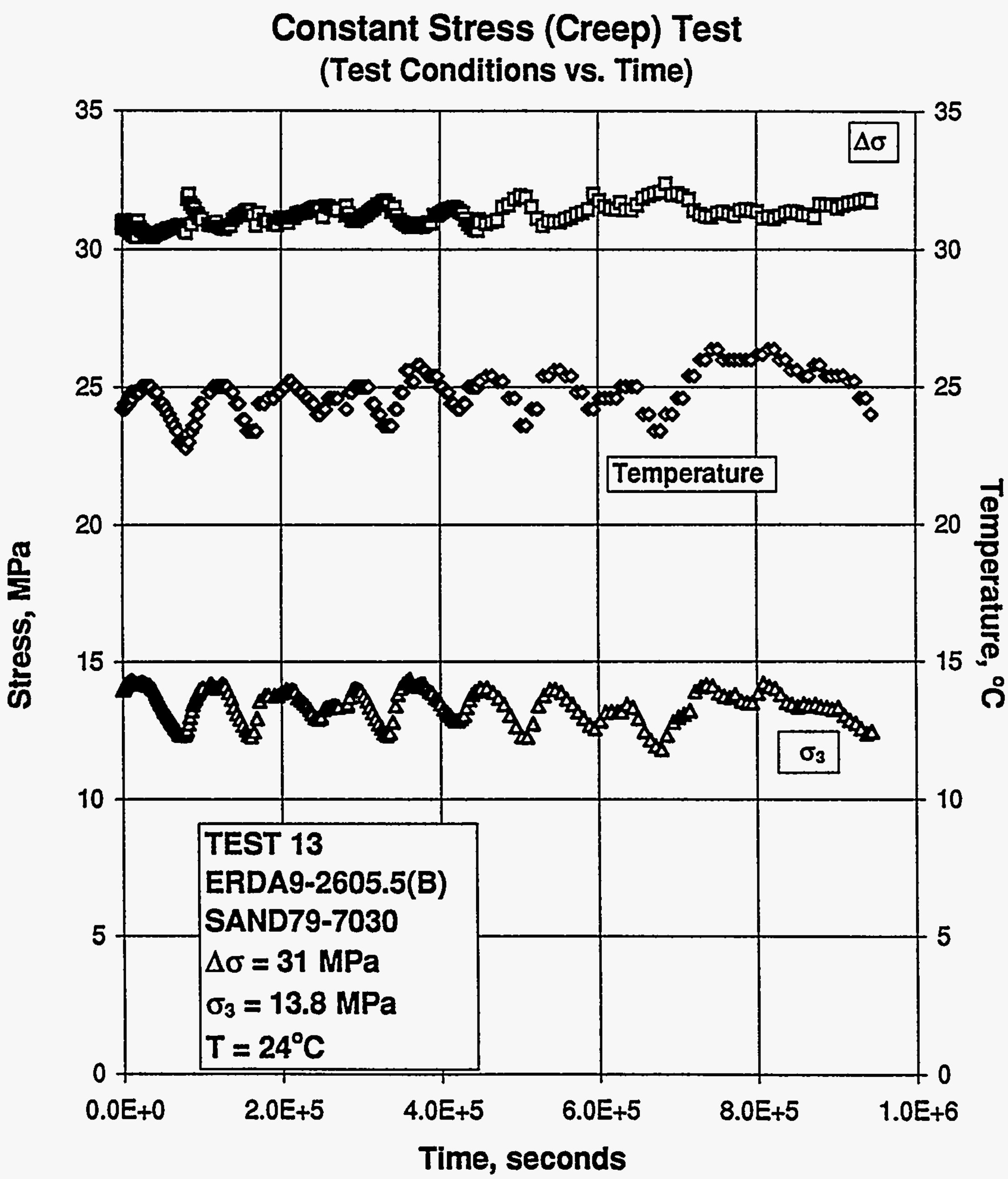

Figure B-137. Test Conditions Versus Time for a Creep Test: Specimen ERDA9-2605.5 (B); Stage 1 of 1.

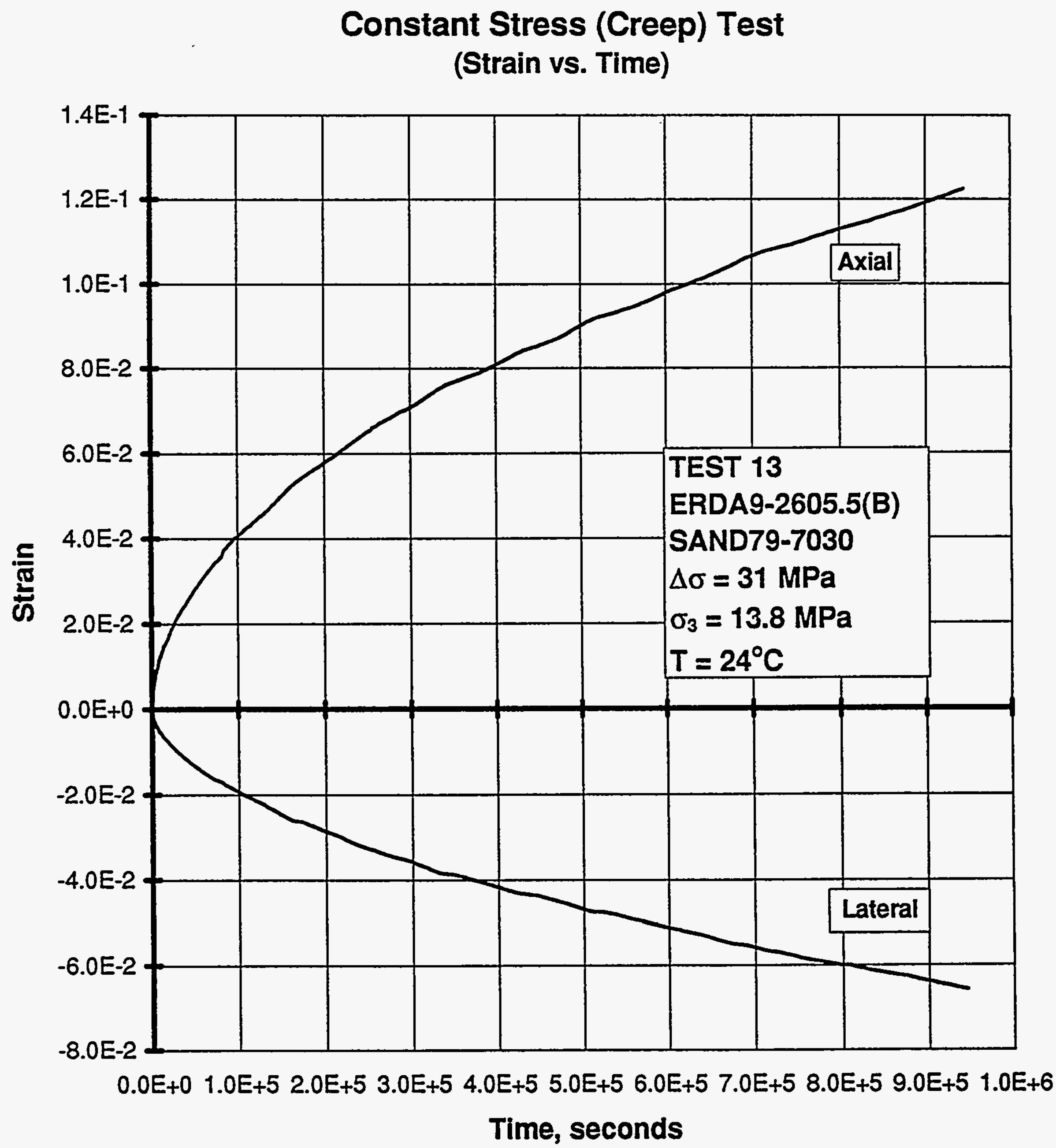

Figure B-138. Axial Strain and Lateral Strain Versus Time for a Creep Test: Specimen ERDA9-2605.5 (B); Stage 1 of 1.

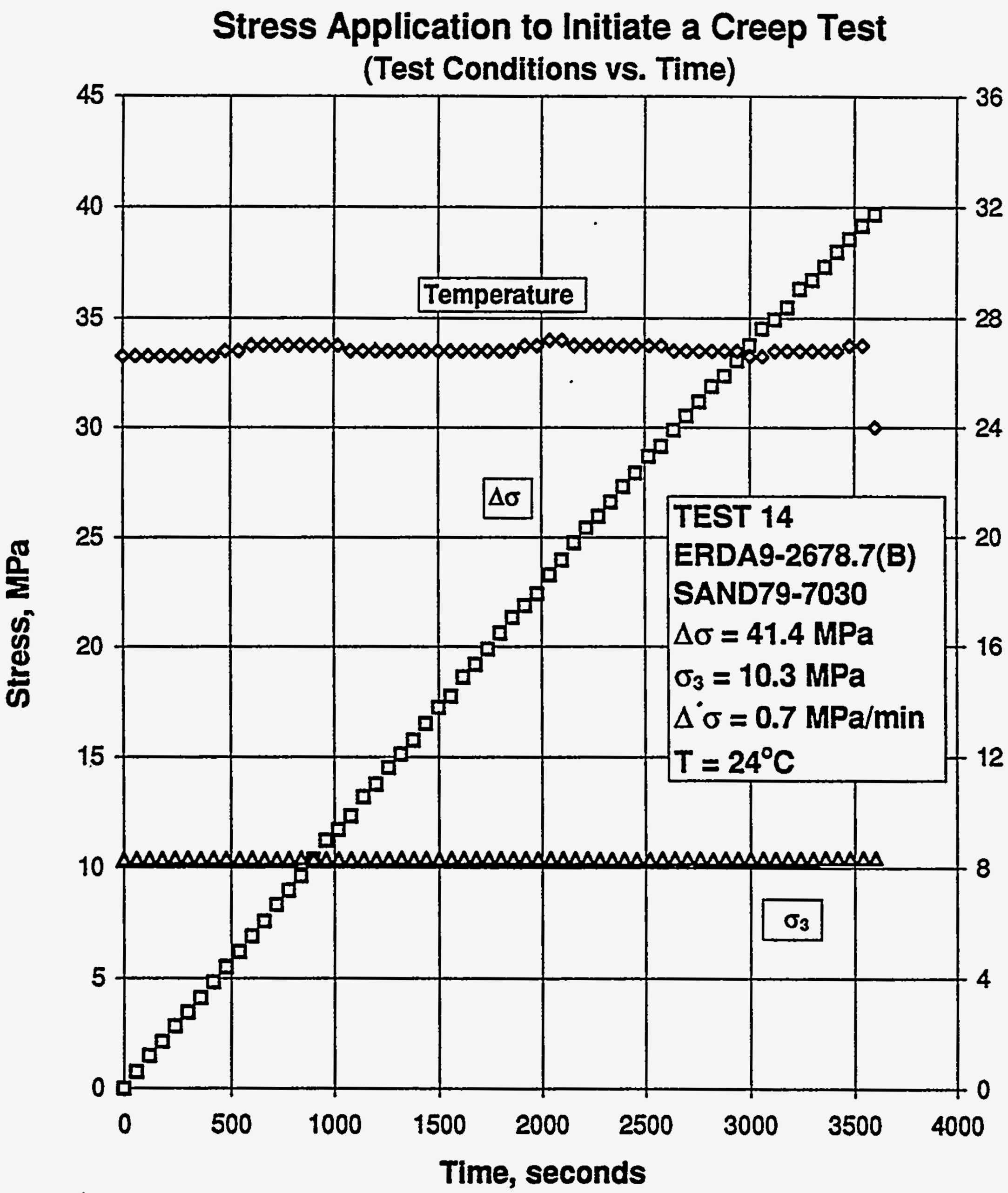

Figure B-139. Test Conditions Versus Time for Stress Application to Initiate a Creep Test: Specimen ERDA9-2678.7 (B); Stage 1 of 1.

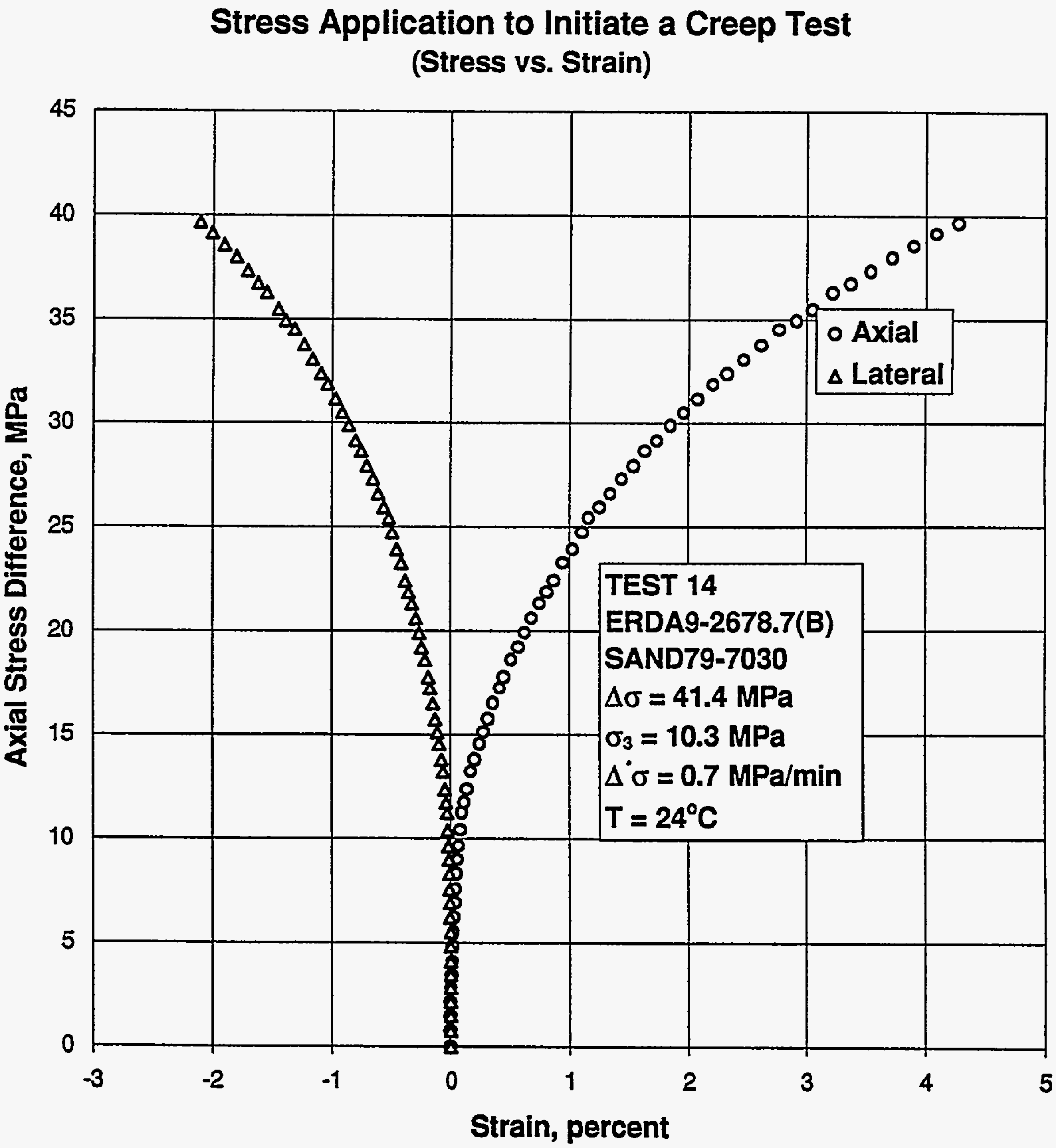

Figure B-140. Axial Stress Difference Versus Axial and Lateral Strain for Stress Application to Initiate a Creep Test: Specimen ERDA9-2678.7 (B); Stage 1 of 1.

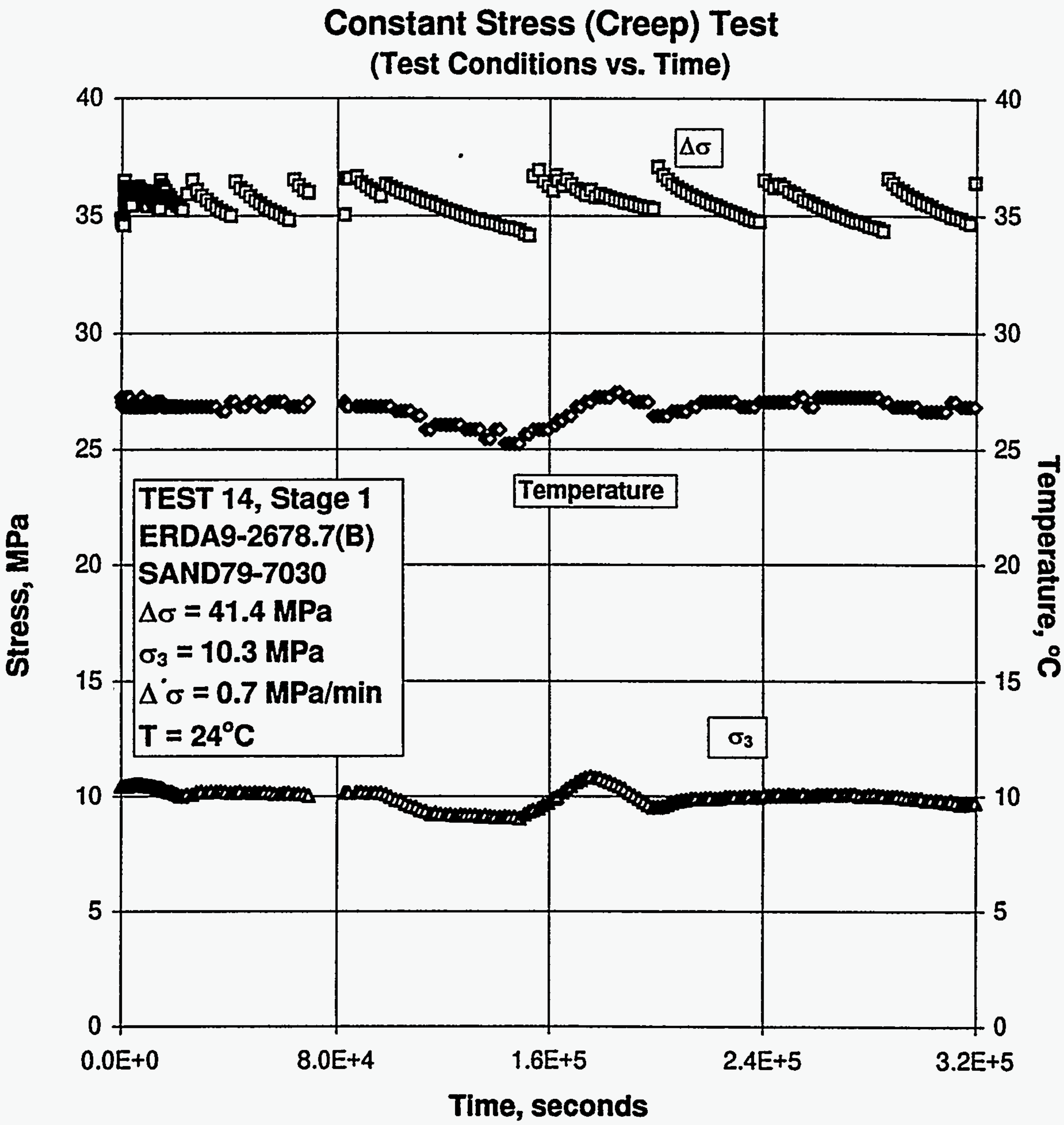

Figure B-141. Test Conditions Versus Time for a Creep Test: Specimen ERDA9-2678.7 (B); Stage 1 of 1.

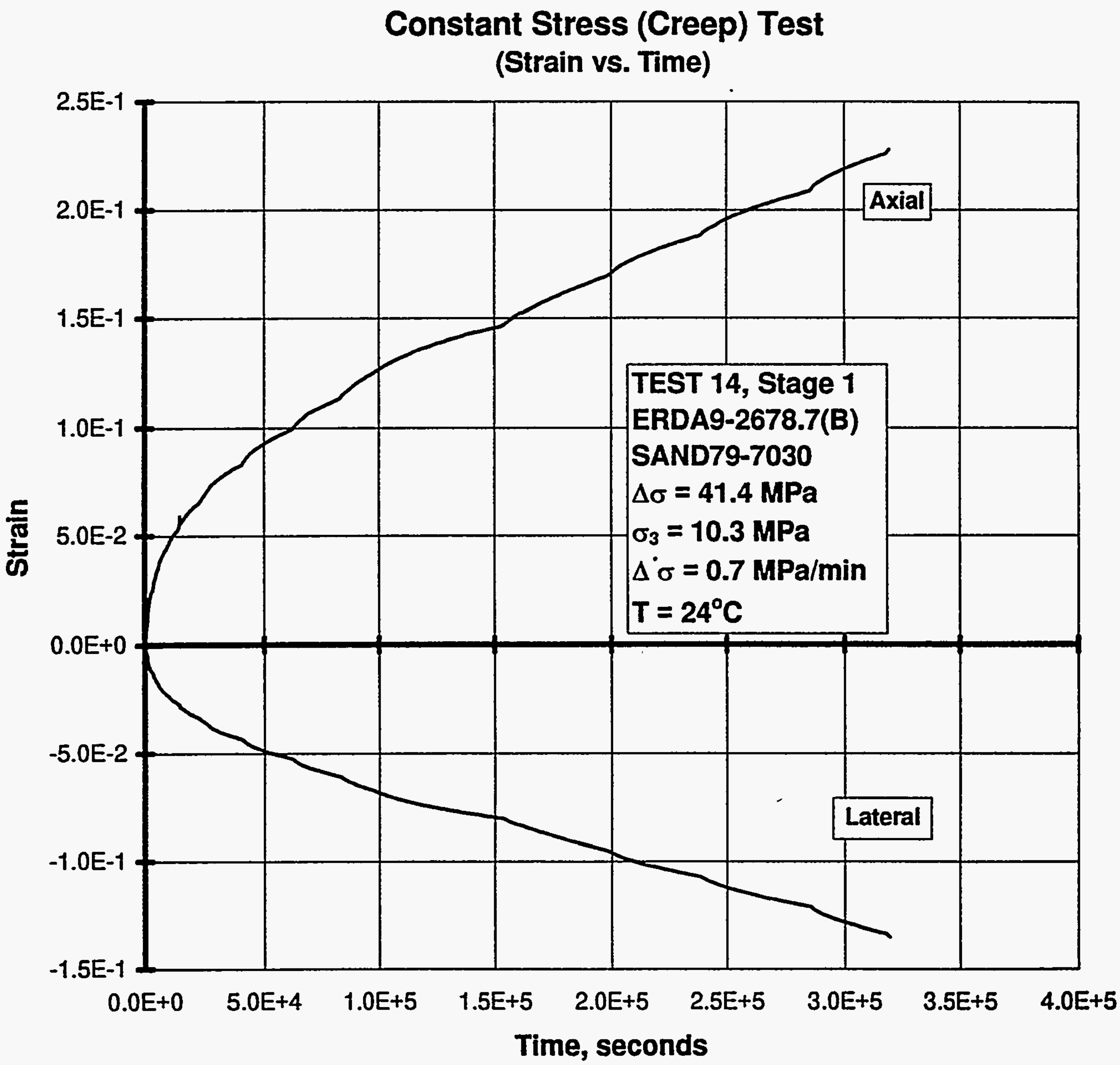

Figure B-142. Axial Strain and Lateral Strain Versus Time for a Creep Test: Specimen ERDA9-2678.7 (B); Stage 1 of 1.

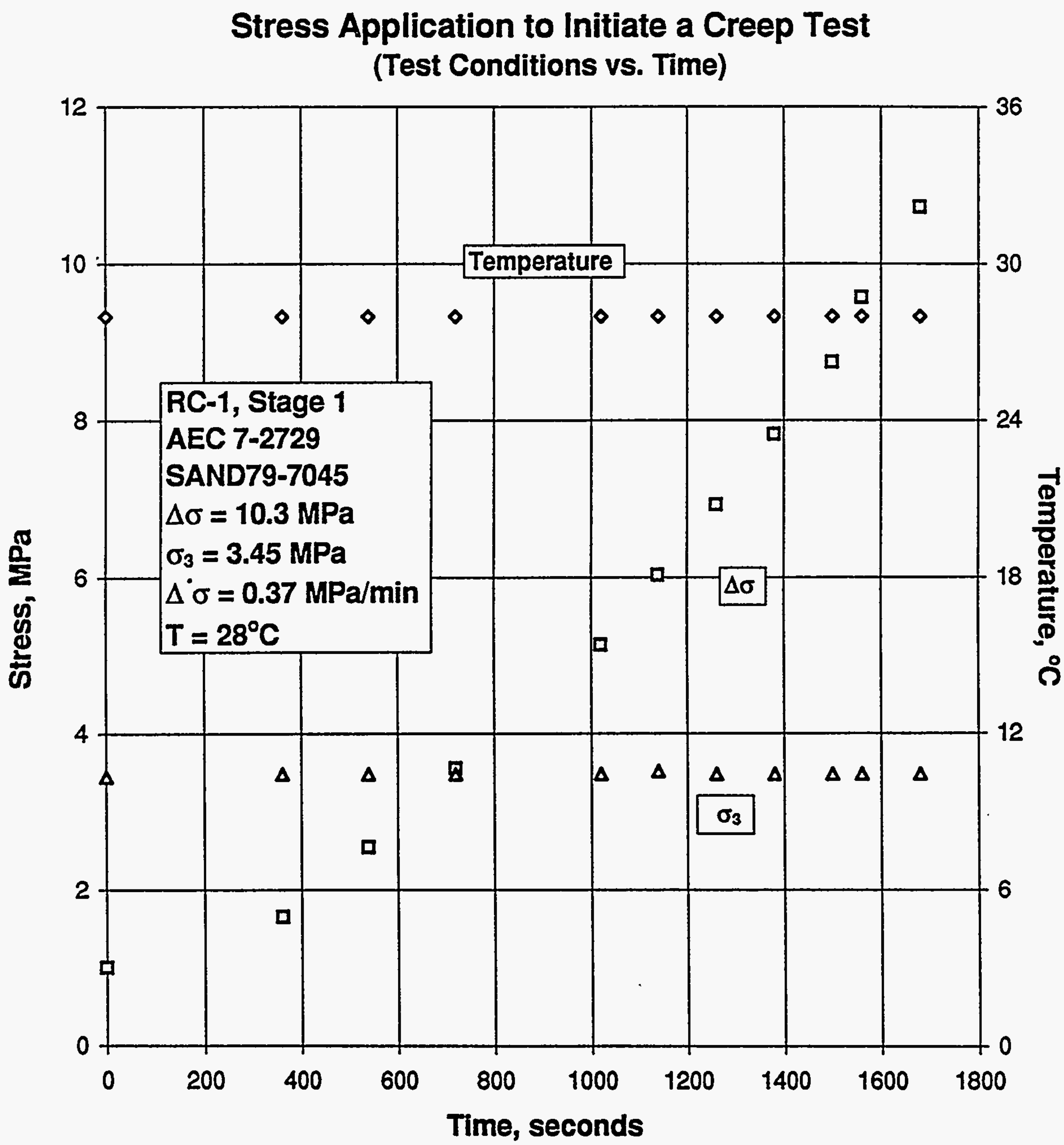

Figure B-143. Test Conditions Versus Time for Stress Application to Initiate a Creep Test: Specimen AEC7-2729; Stage 1 of 3.

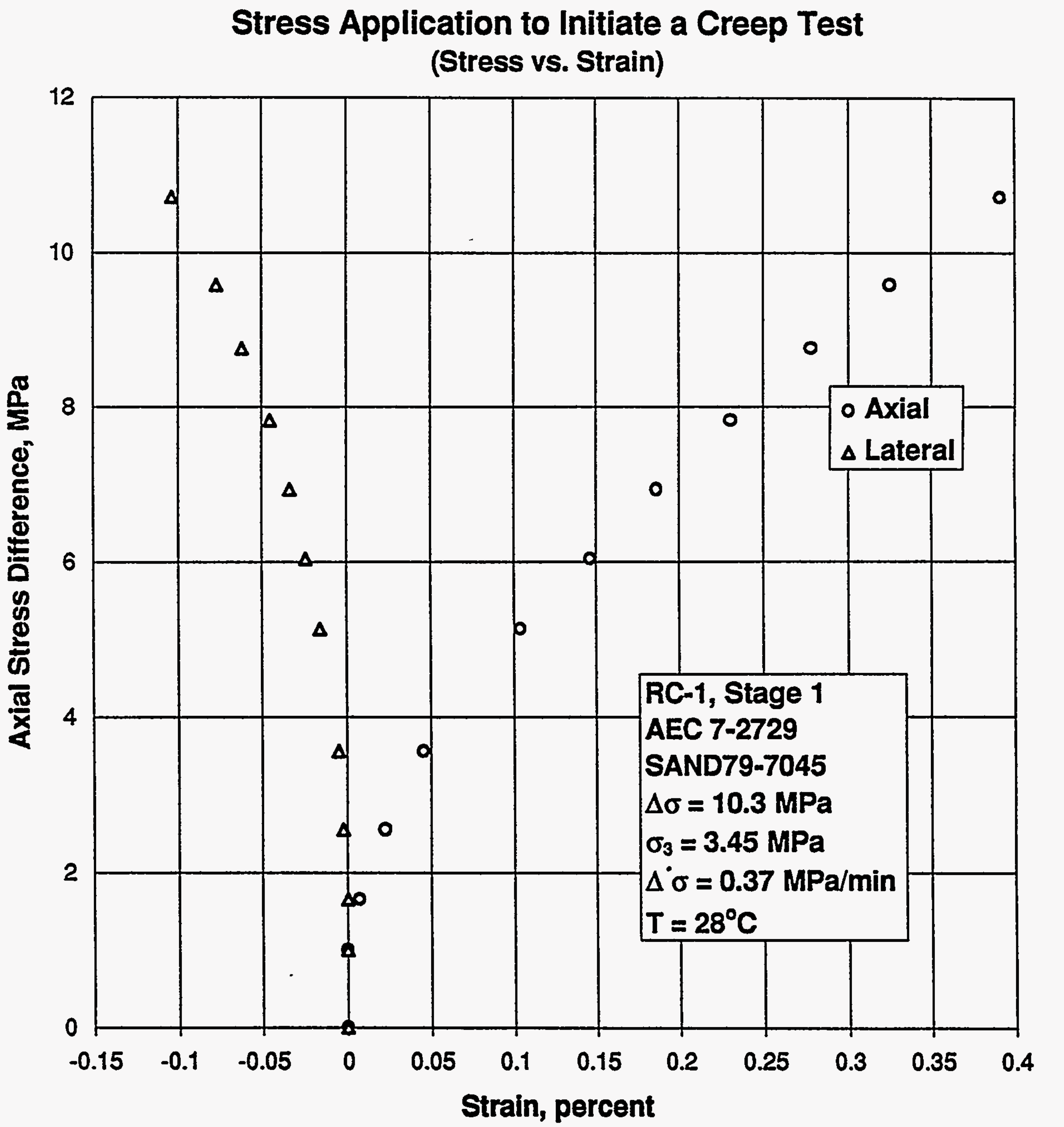

Figure B-144. Axial Stress Difference Versus Axial and Lateral Strain for Stress Application to Initiate a Creep Test: Specimen AEC7-2729; Stage 1 of 3.

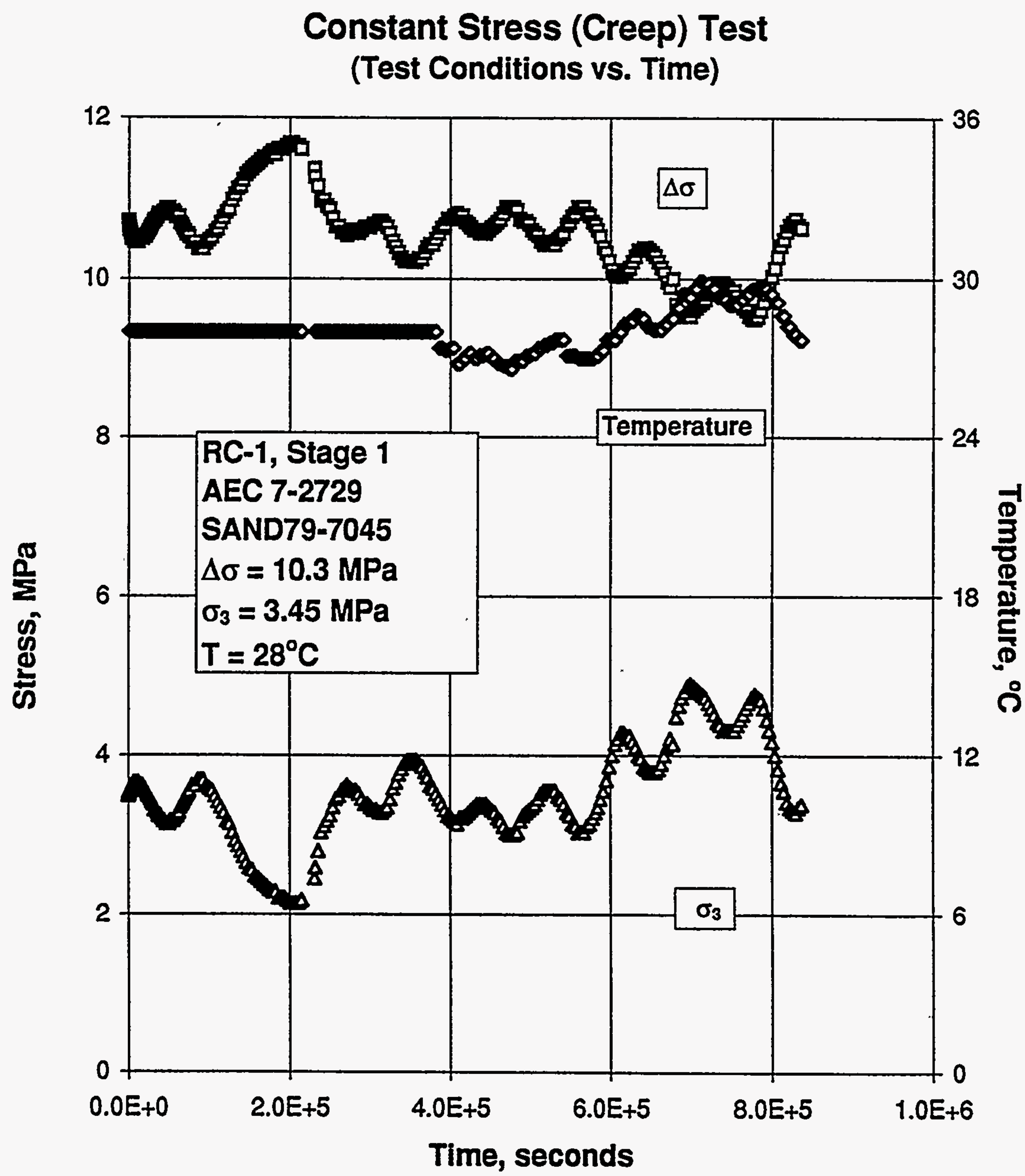

Figure B-145. Test Conditions Versus Time for a Creep Test: Specimen AEC7-2729; Stage 1 of 3.

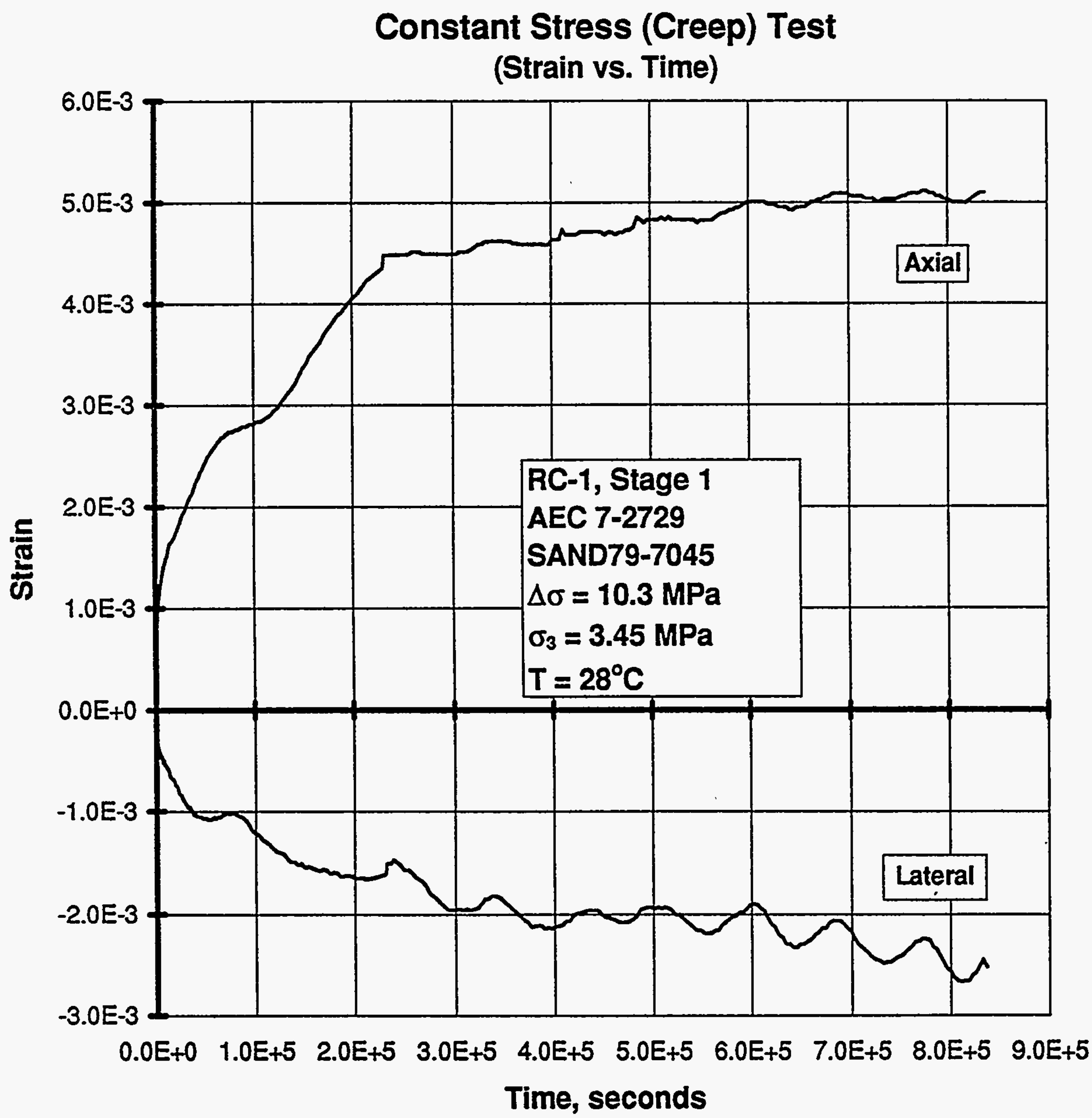

Figure B-146. Axial Strain and Lateral Strain Versus Time for a Creep Test: Specimen AEC7-2729; Stage 1 of 3.

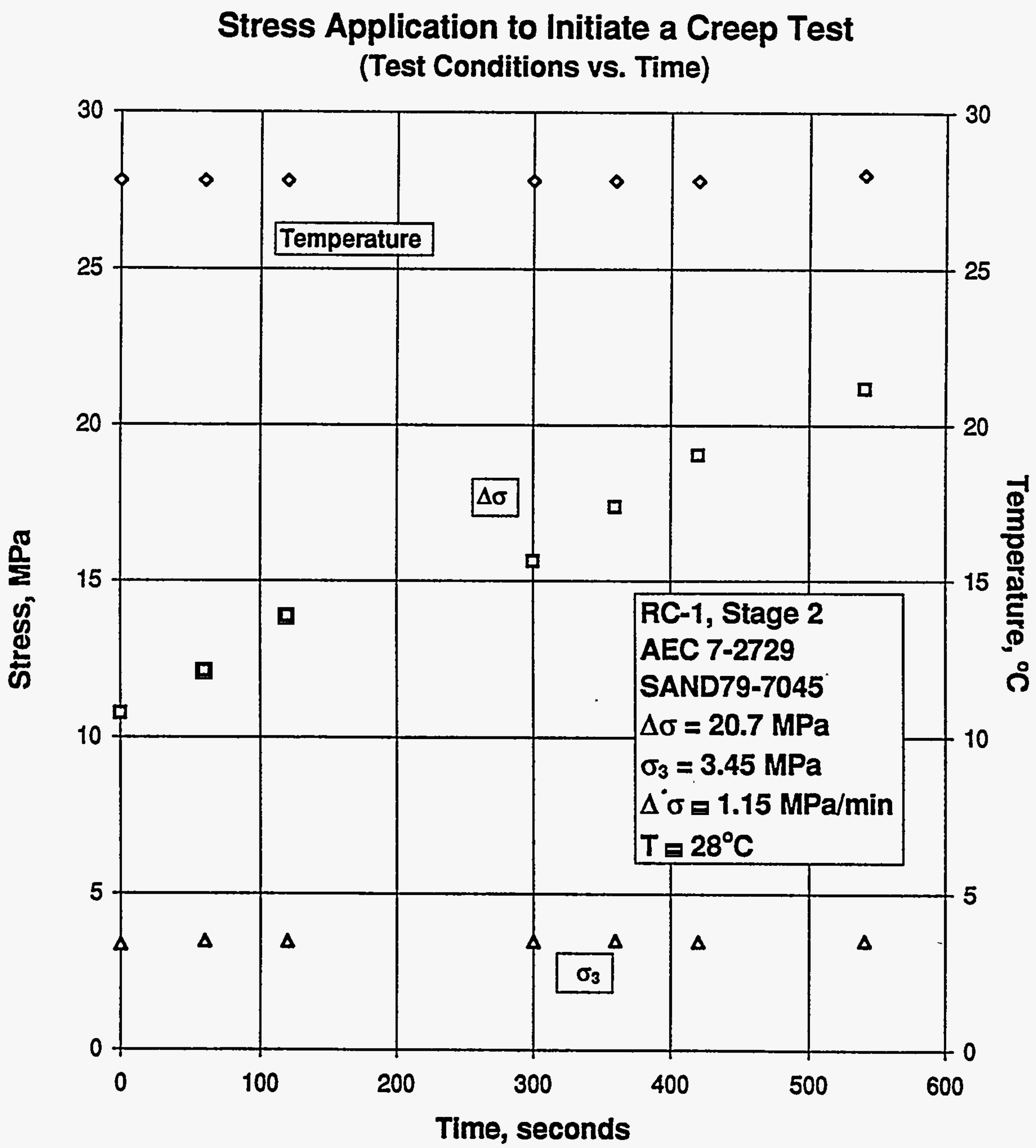

Figure B-147. Test Conditions Versus Time for Stress Application to Initiate a Creep Test: Specimen AEC7-2729; Stage 2 of 3.

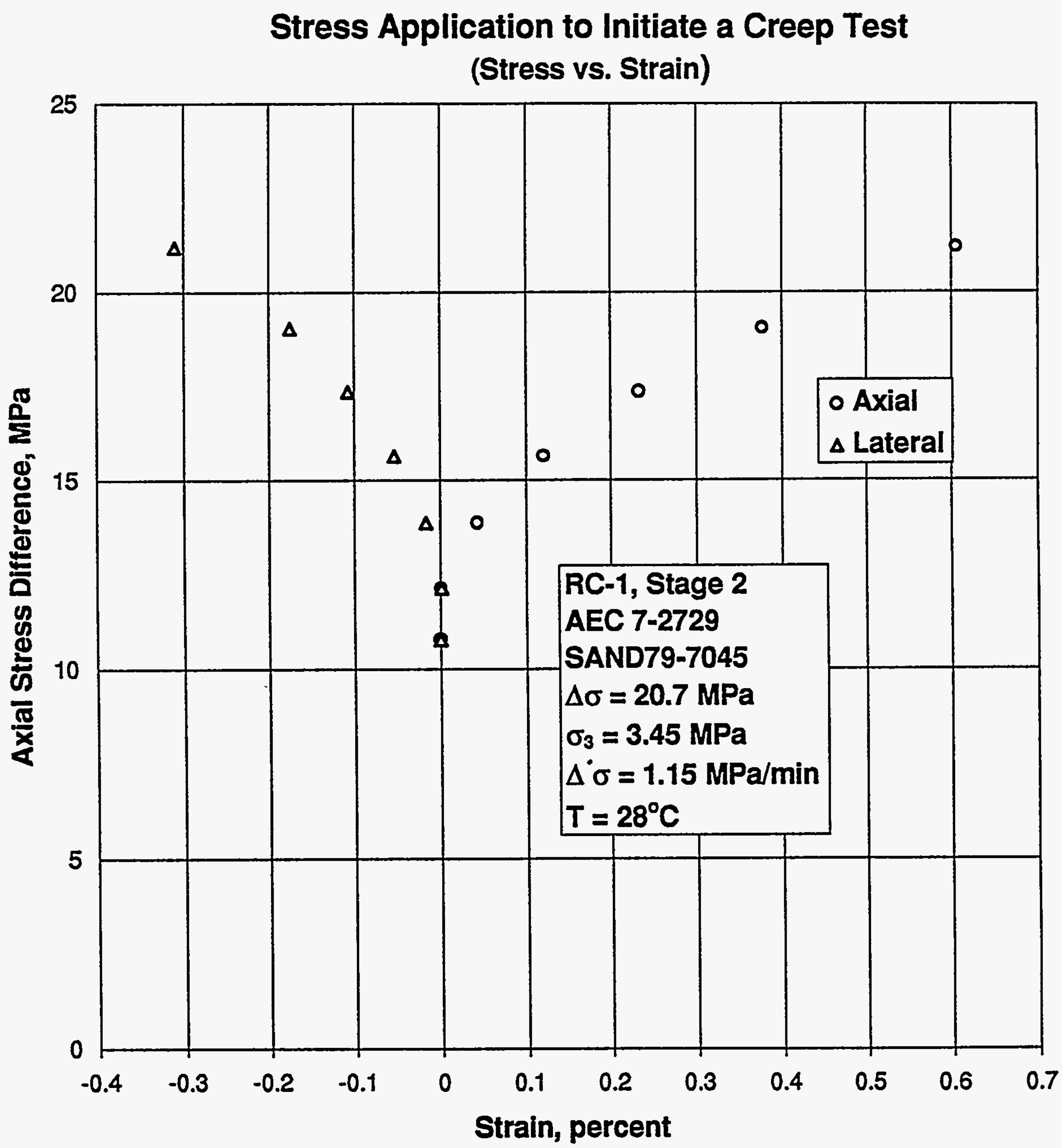

Figure B-148. Axial Stress Difference Versus Axial and Lateral Strain for Stress Application to Initiate a Creep Test: Specimen AEC7-2729; Stage 2 of 3.

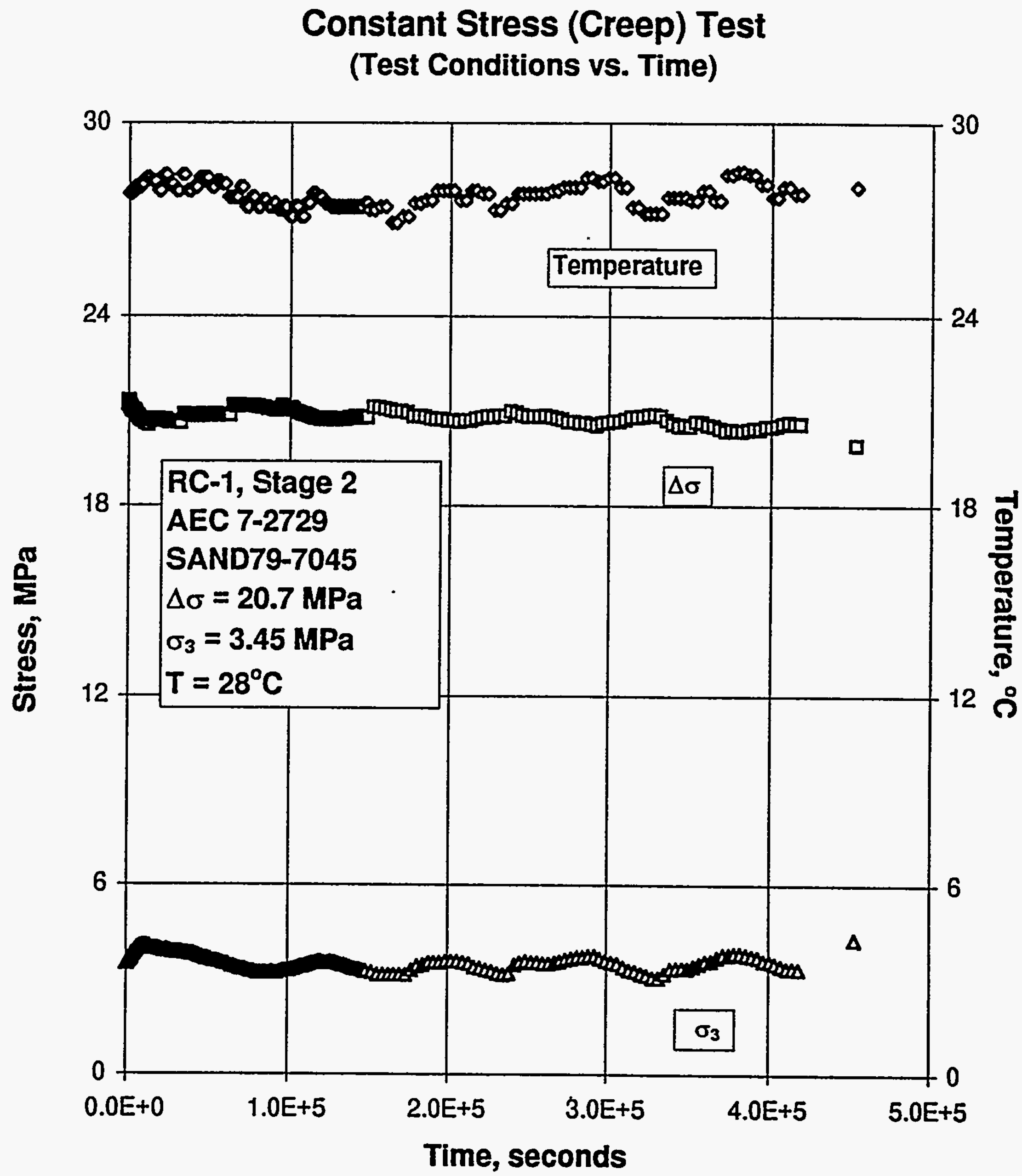

Figure B-149. Test Conditions Versus Time for a Creep Test: Specimen AEC7-2729; Stage 2 of 3.

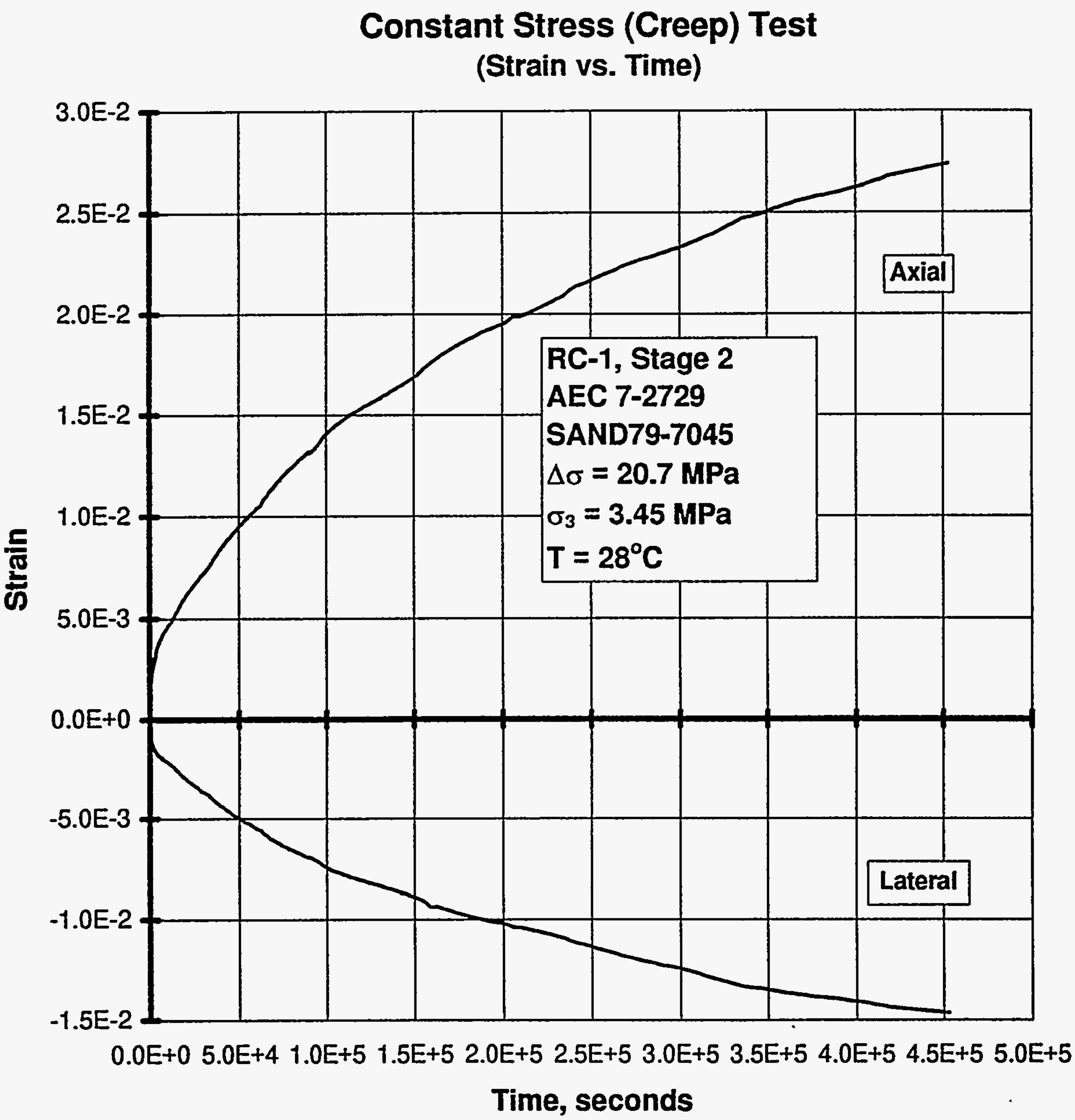

Figure B-150. Axial Strain and Lateral Strain Versus Time for a Creep Test: Specimen AEC7-2729; Stage 2 of 3.

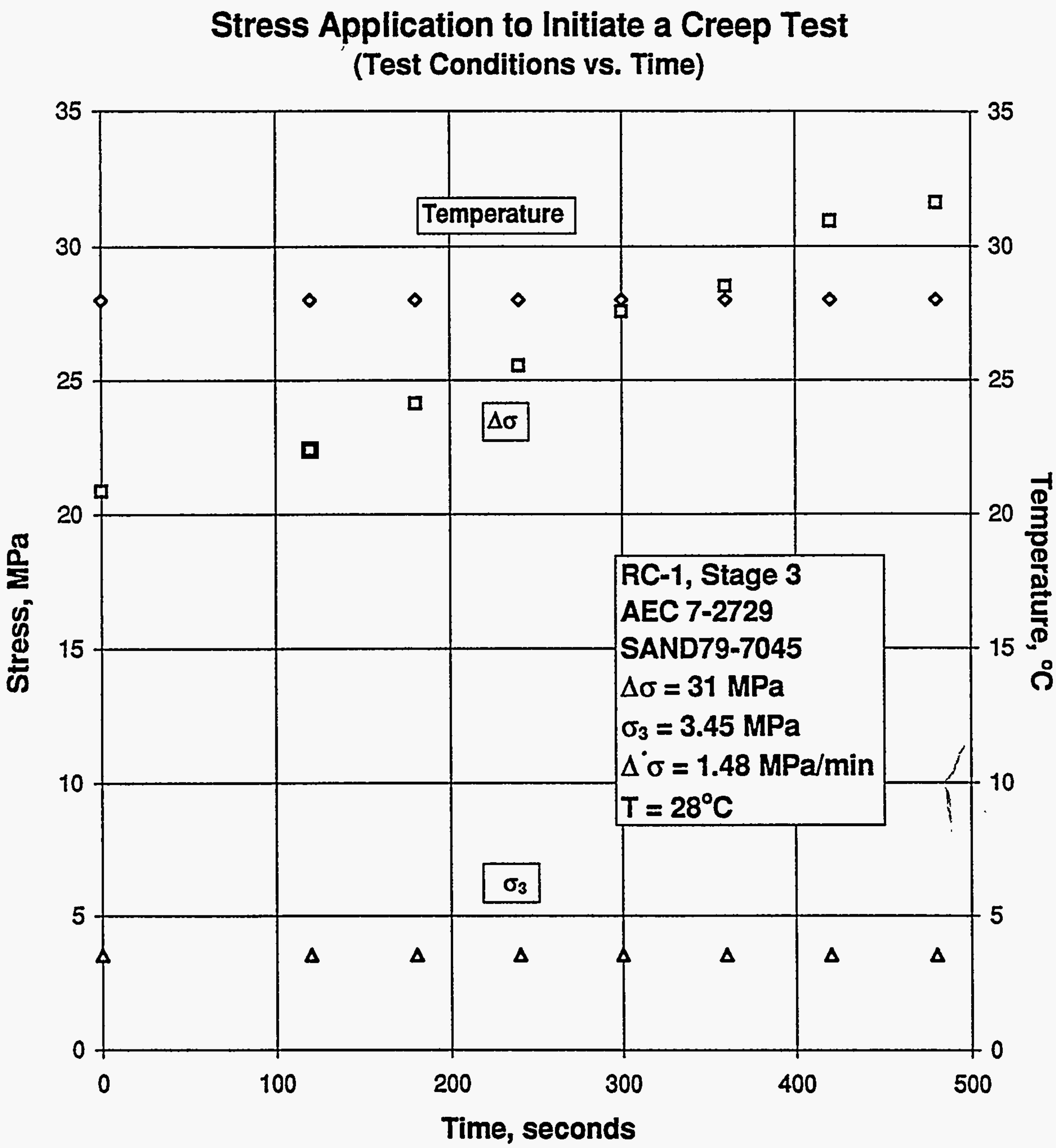

Figure B-151. Test Conditions Versus Time for Stress Application to Initiate a Creep Test: Specimen AEC7-2729; Stage 3 of 3.

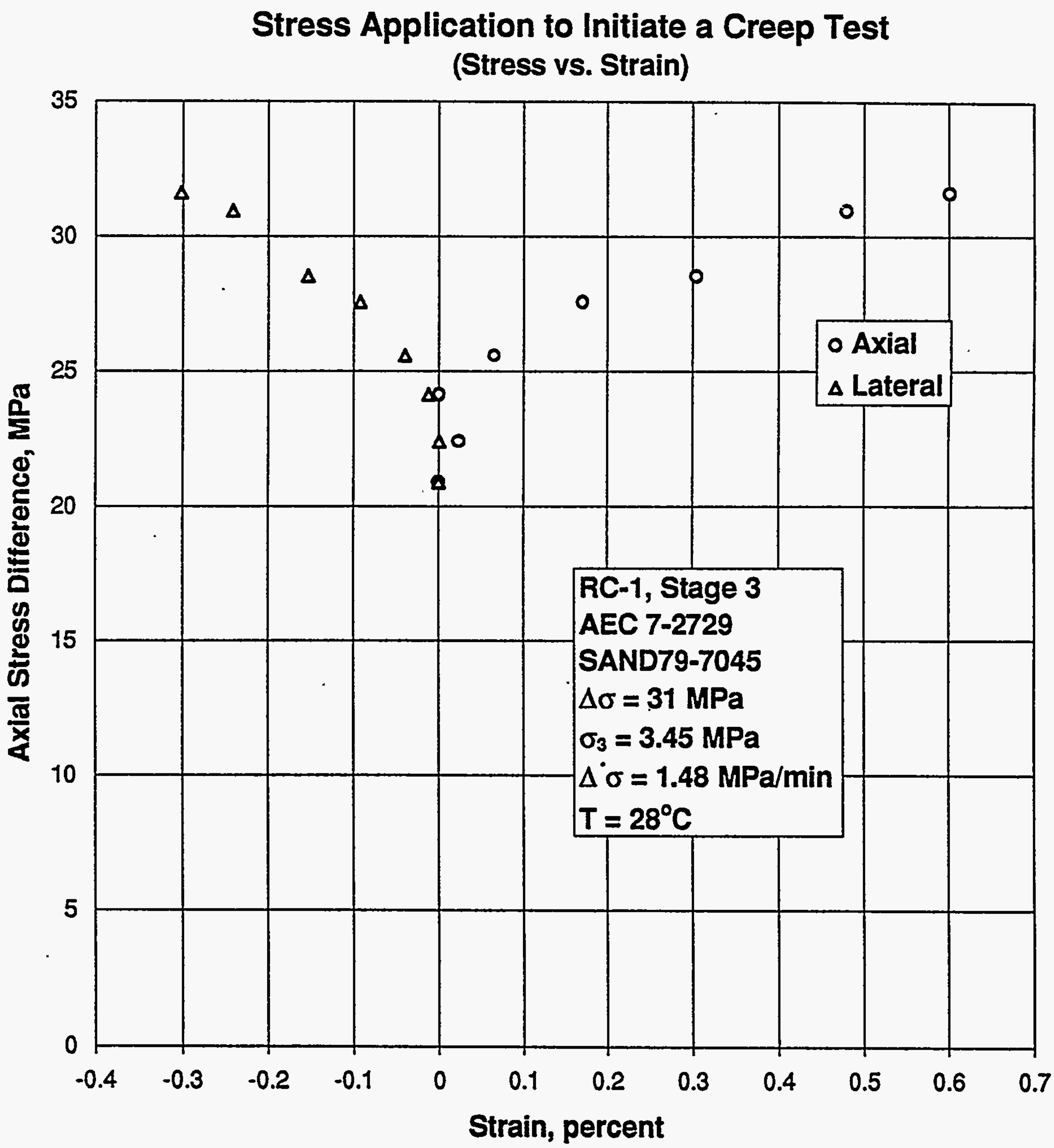

Figure B-152. Axial Stress Difference Versus Axial and Lateral Strain for Stress Application to Initiate a Creep Test: Specimen AEC7-2729; Stage 3 of 3.

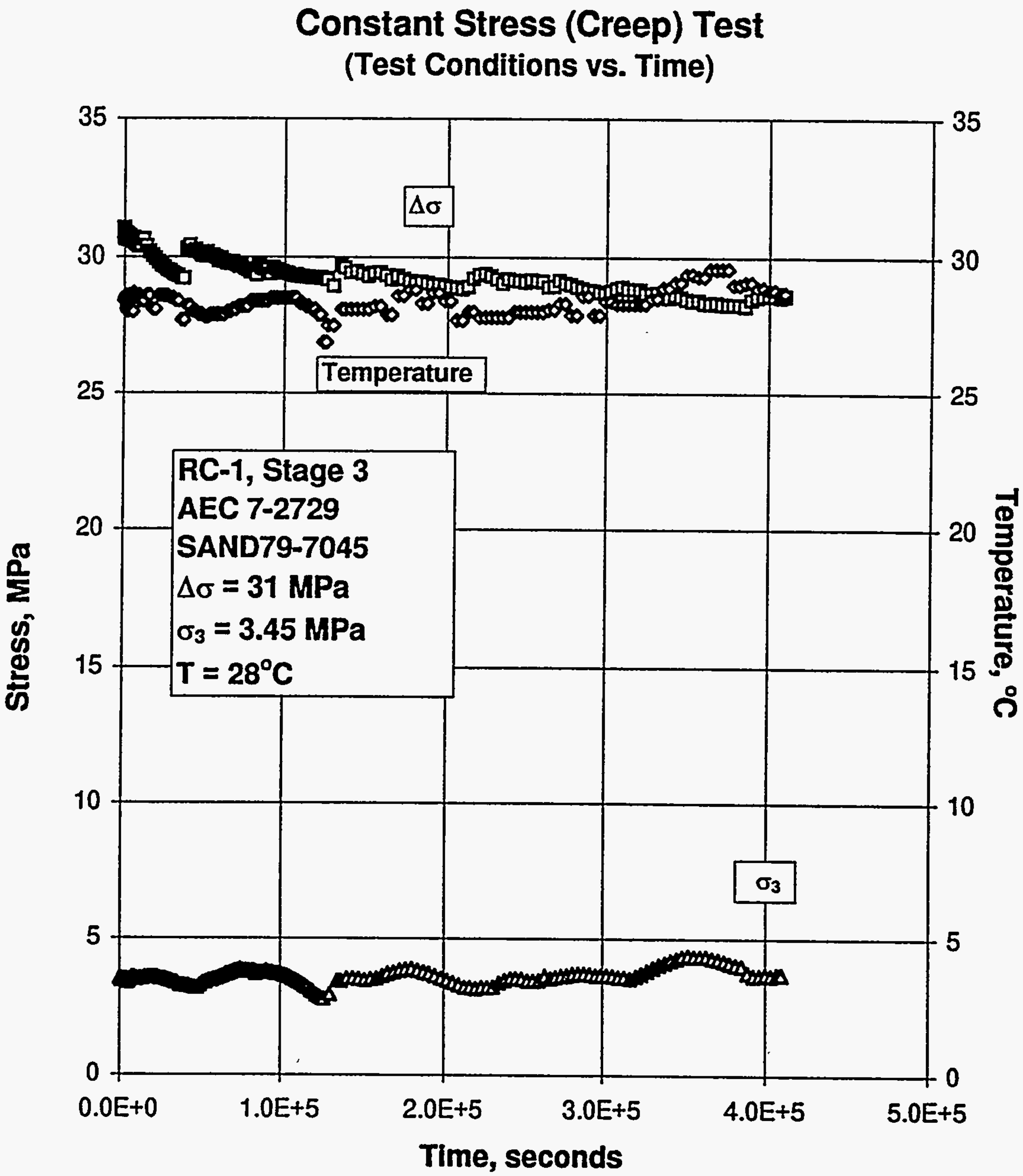

Figure B-153. Test Conditions Versus Time for a Creep Test: Specimen AEC7-2729; Stage 3 of 3.

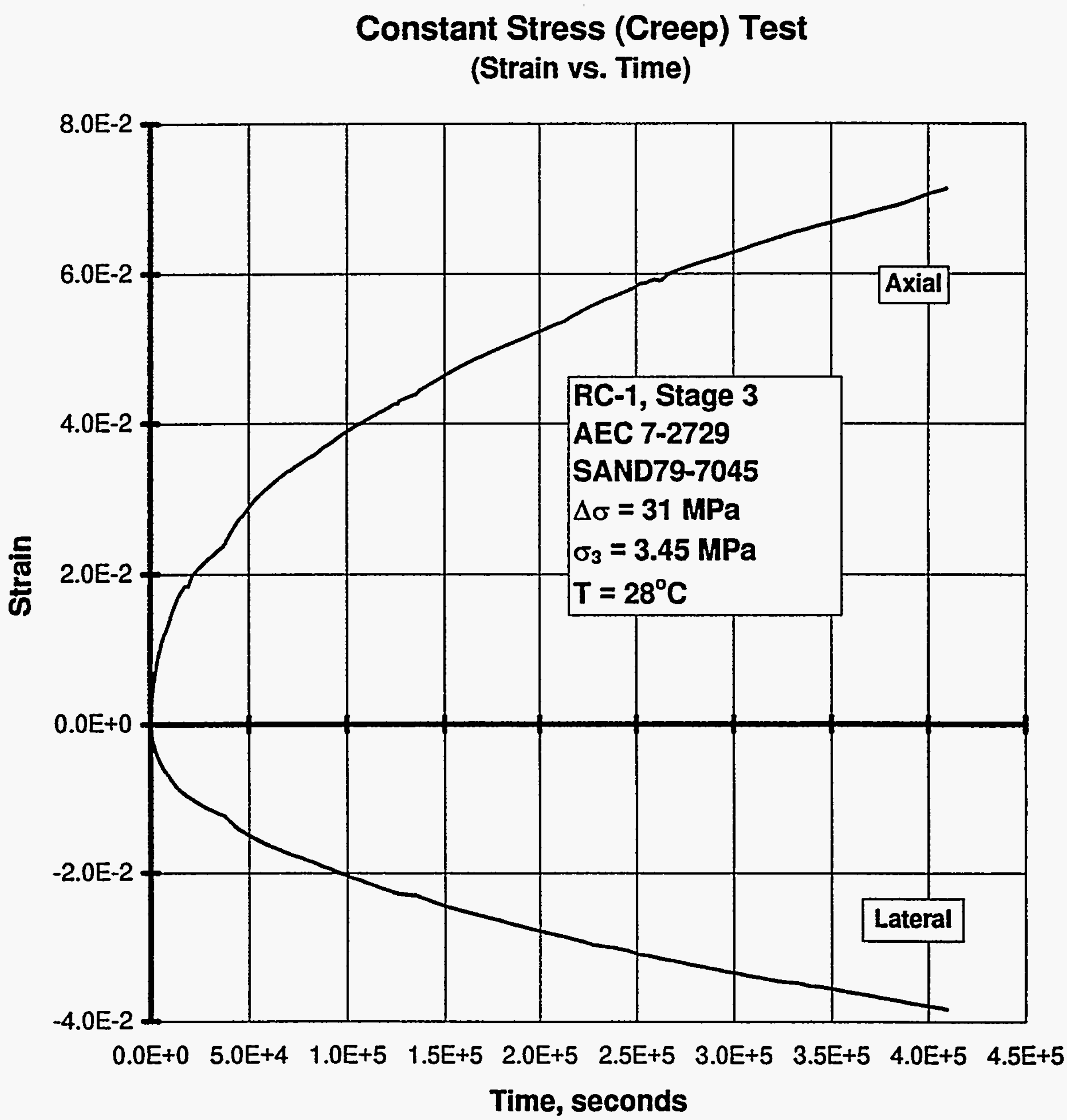

Figure B-154. Axial Strain and Lateral Strain Versus Time for a Creep Test: Specimen AEC7-2729; Stage 3 of 3.

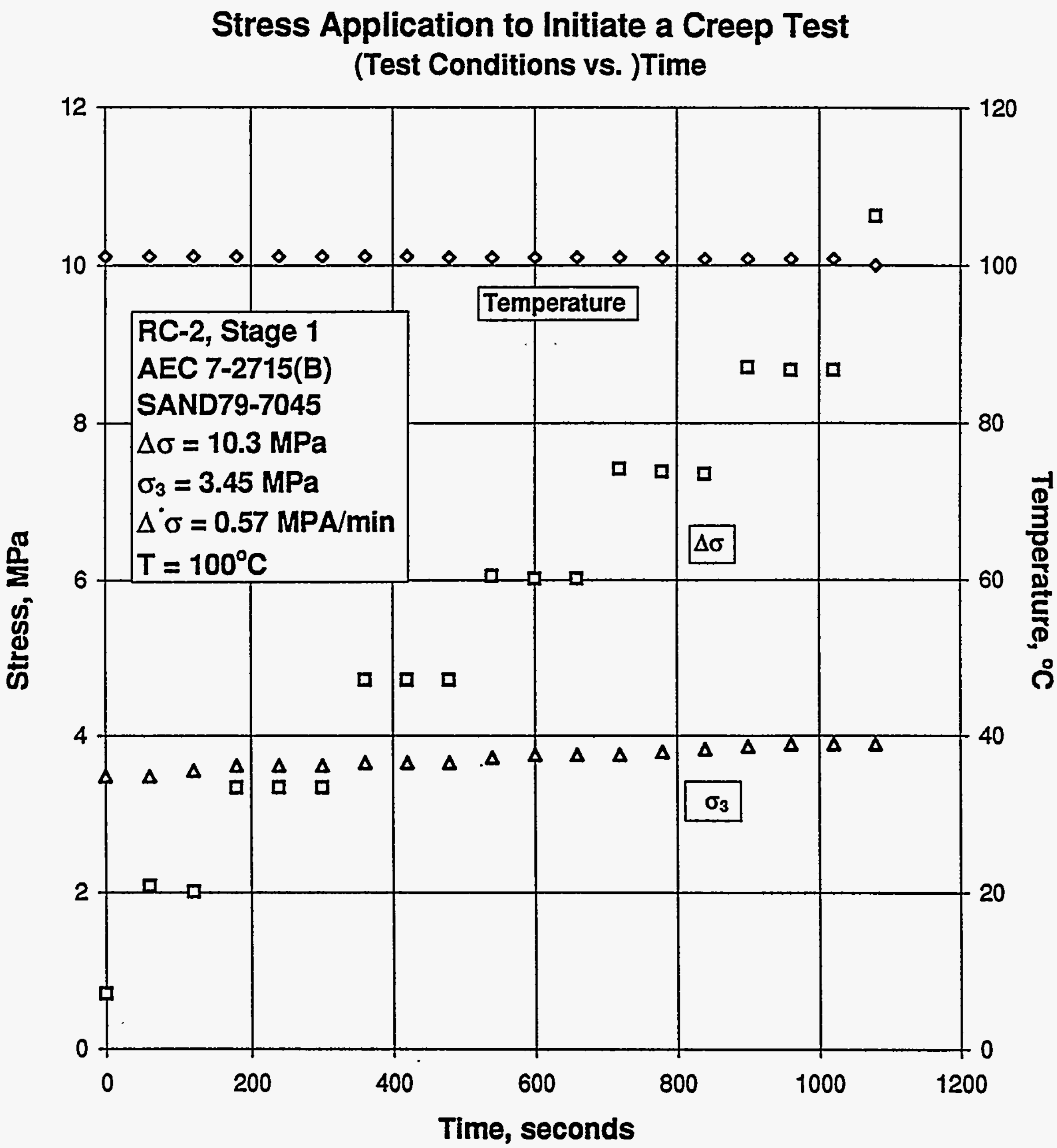

Figure B-155. Test Conditions Versus Time for Stress Application to Initiate a Creep Test: Specimen AEC7-2715 (B); Stage 1 of 2.

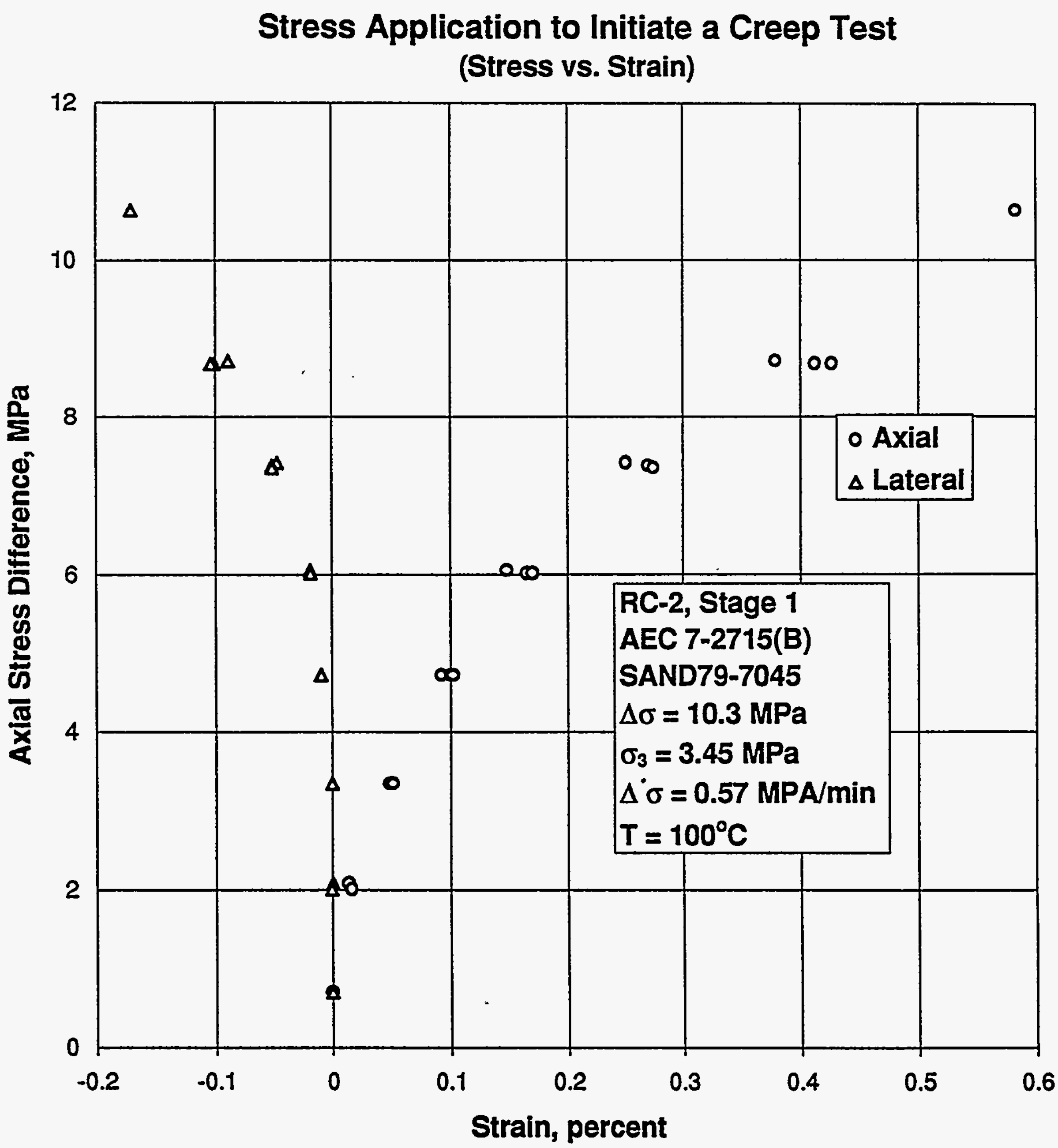

Figure B-156. Axial Stress Difference Versus Axial and Lateral Strain for Stress Application to Initiate a Creep Test: Specimen AEC7-2715 (B); Stage 1 of 2.

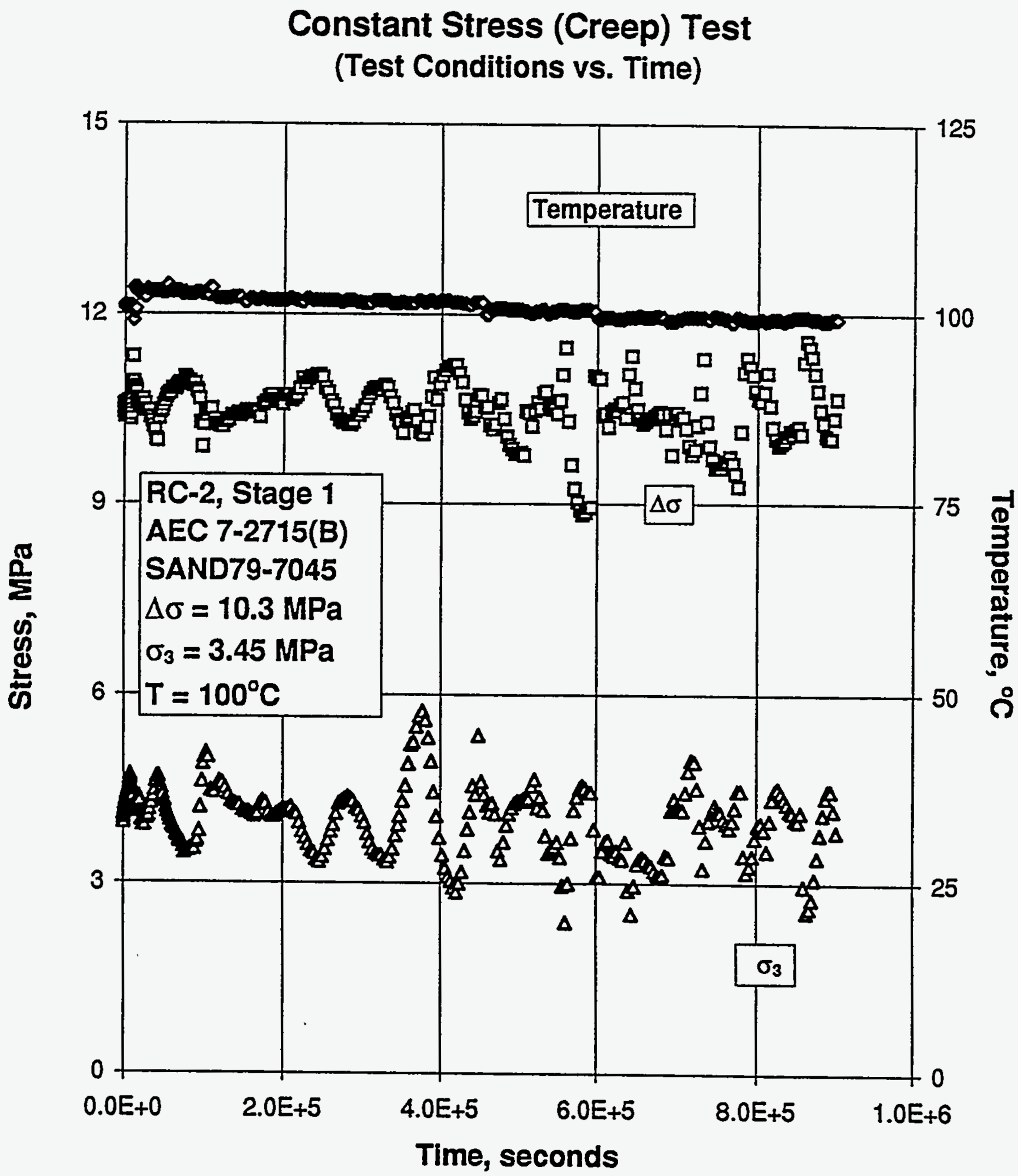

Figure B-157. Test Conditions Versus Time for a Creep Test: Specimen AEC7-2715 (B); Stage 1 of 2.

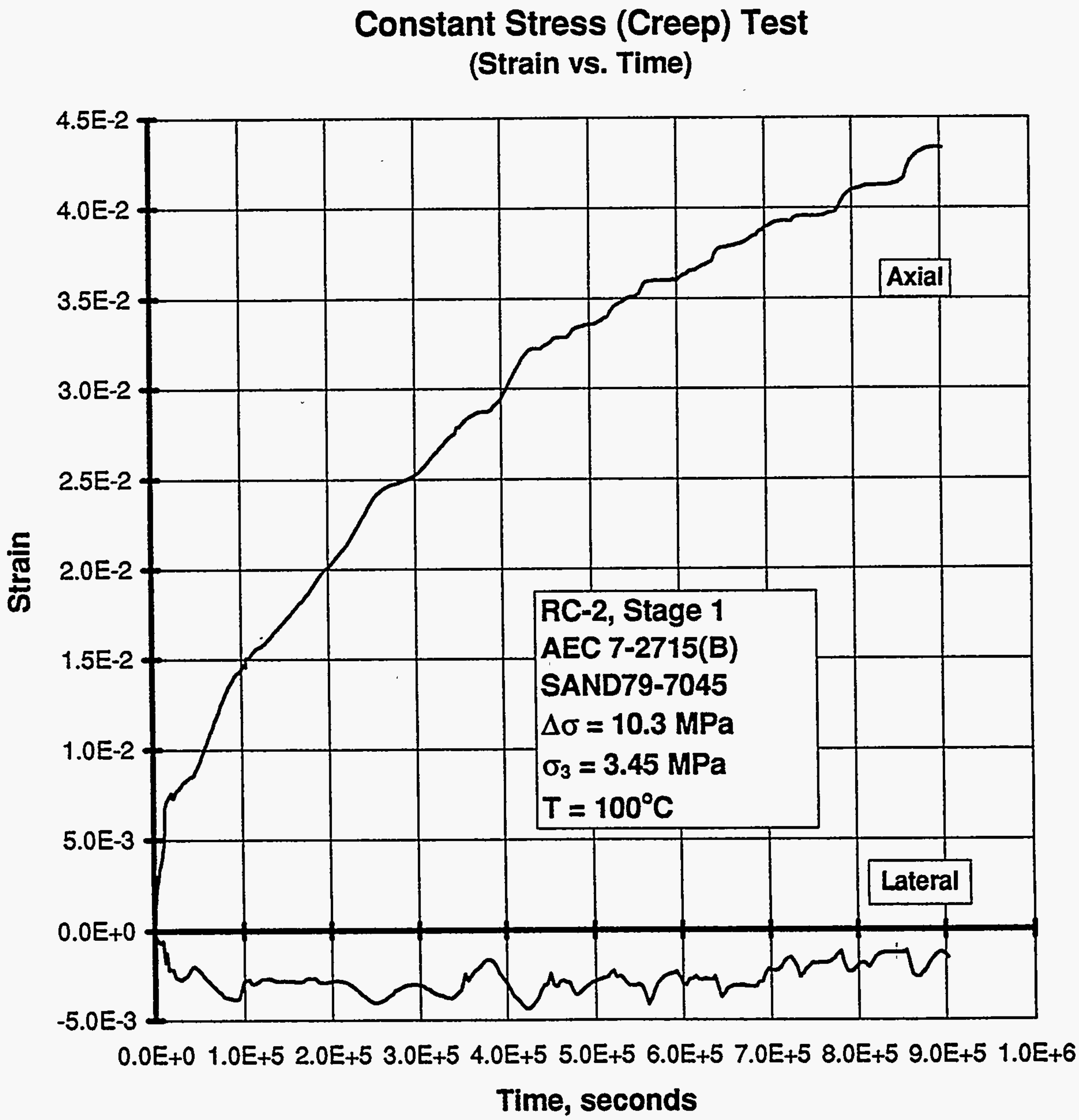

Figure B-158. Axial Strain and Lateral Strain Versus Time for a Creep Test: Specimen AEC7-2715 (B); Stage 1 of 2.

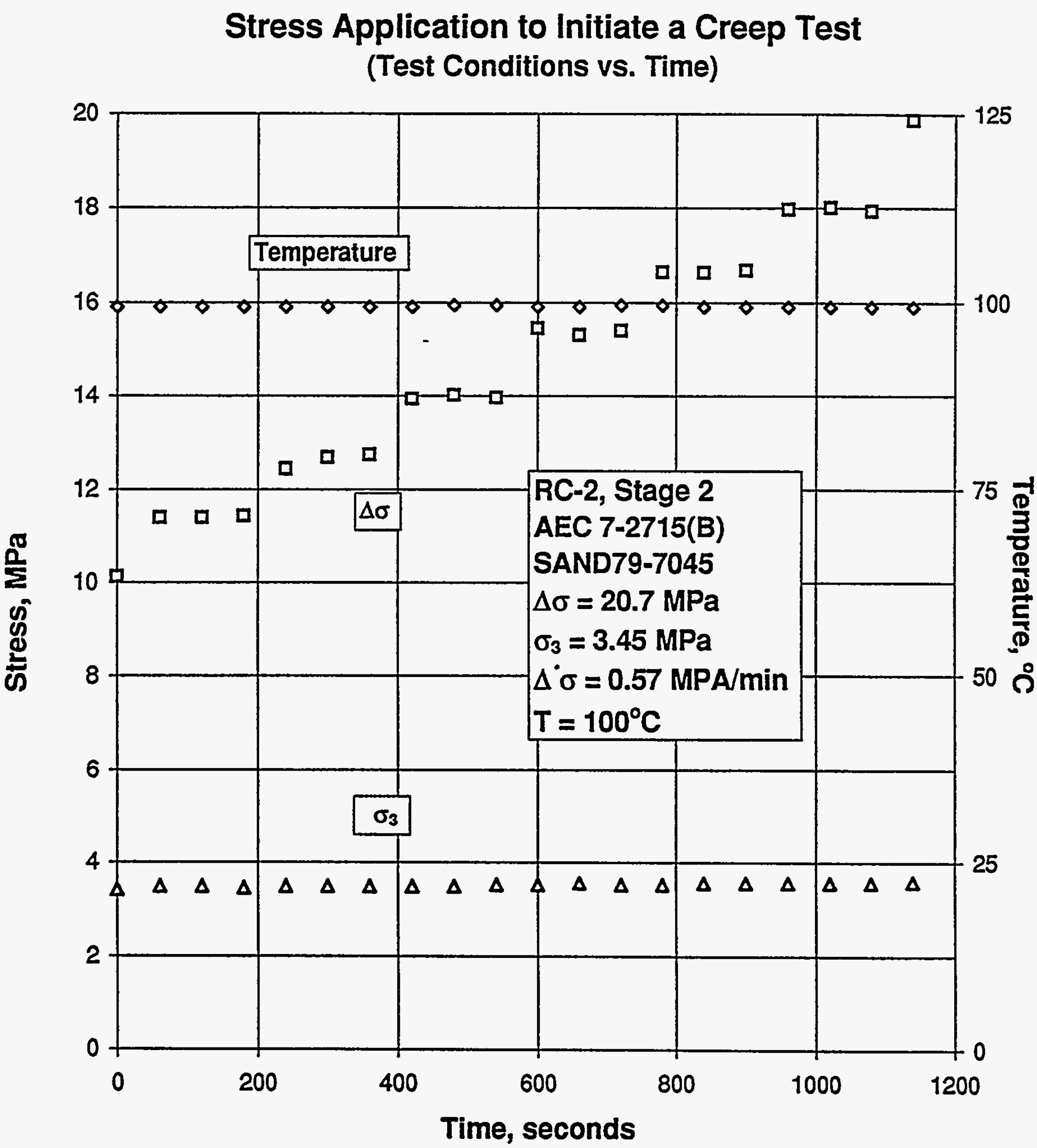

Figure B-159. Test Conditions Versus Time for Stress Application to Initiate a Creep Test: Specimen AEC7-2715 (B); Stage 2 of 2.

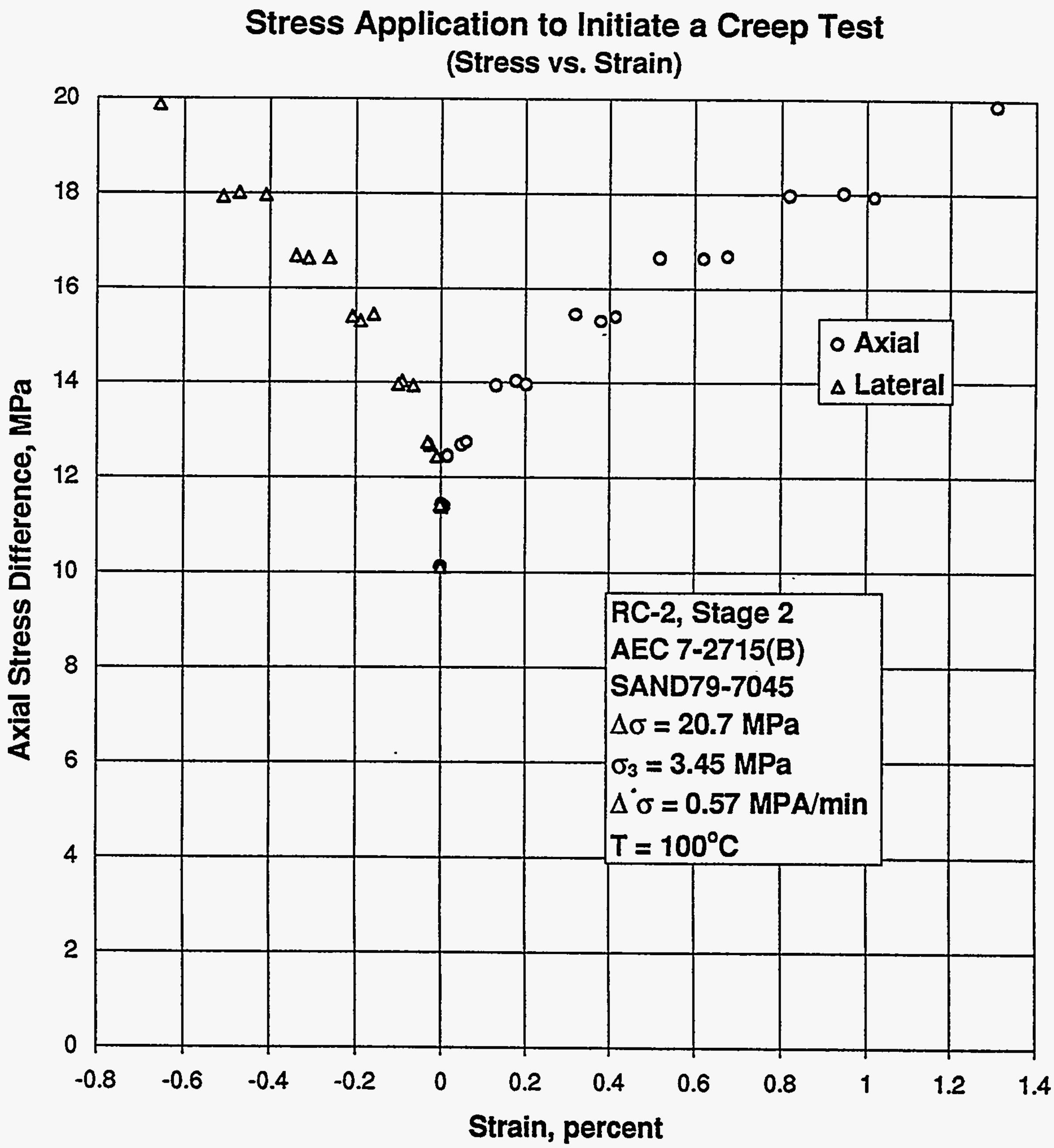

Figure B-160. Axial Stress Difference Versus Axial and Lateral Strain for Stress Application to Initiate a Creep Test: Specimen AEC7-2715 (B); Stage 2 of 2.

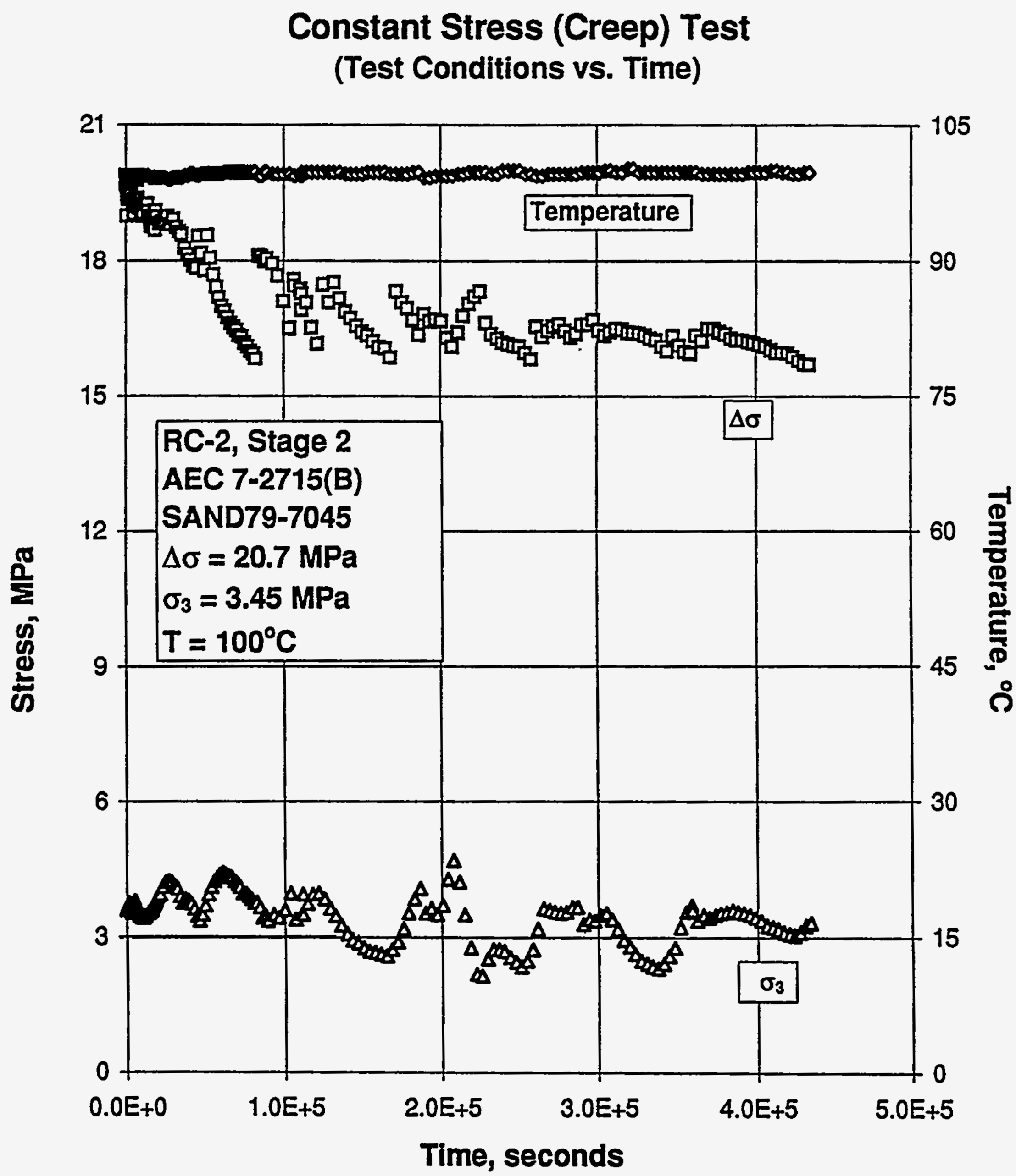

Figure B-161. Test Conditions Versus Time for a Creep Test: Specimen AEC7-2715 (B); Stage 2 of 2.

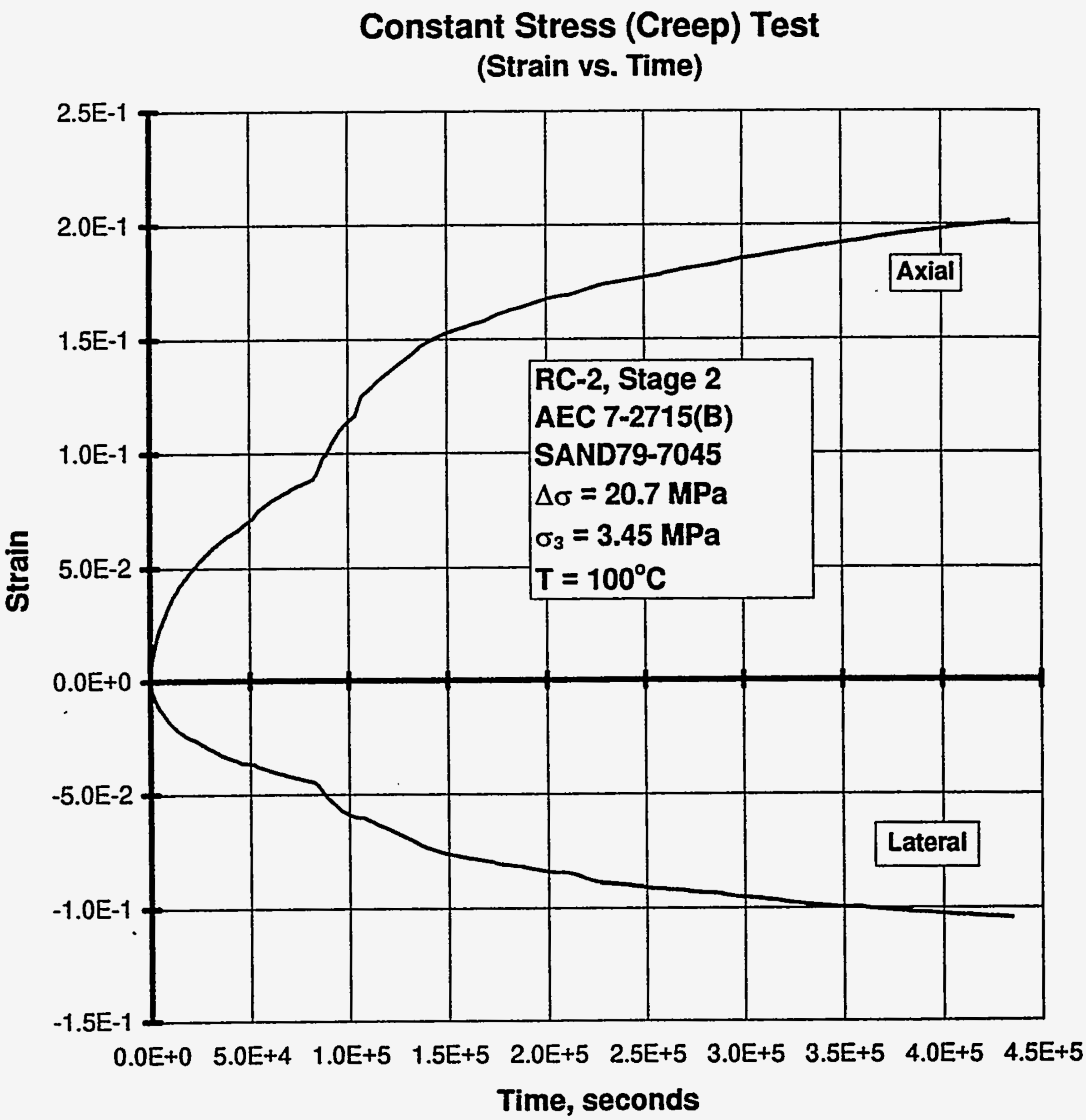

Figure B-162. Axial Strain and Lateral Strain Versus Time for a Creep Test: Specimen AEC7-2715 (B); Stage 2 of 2.

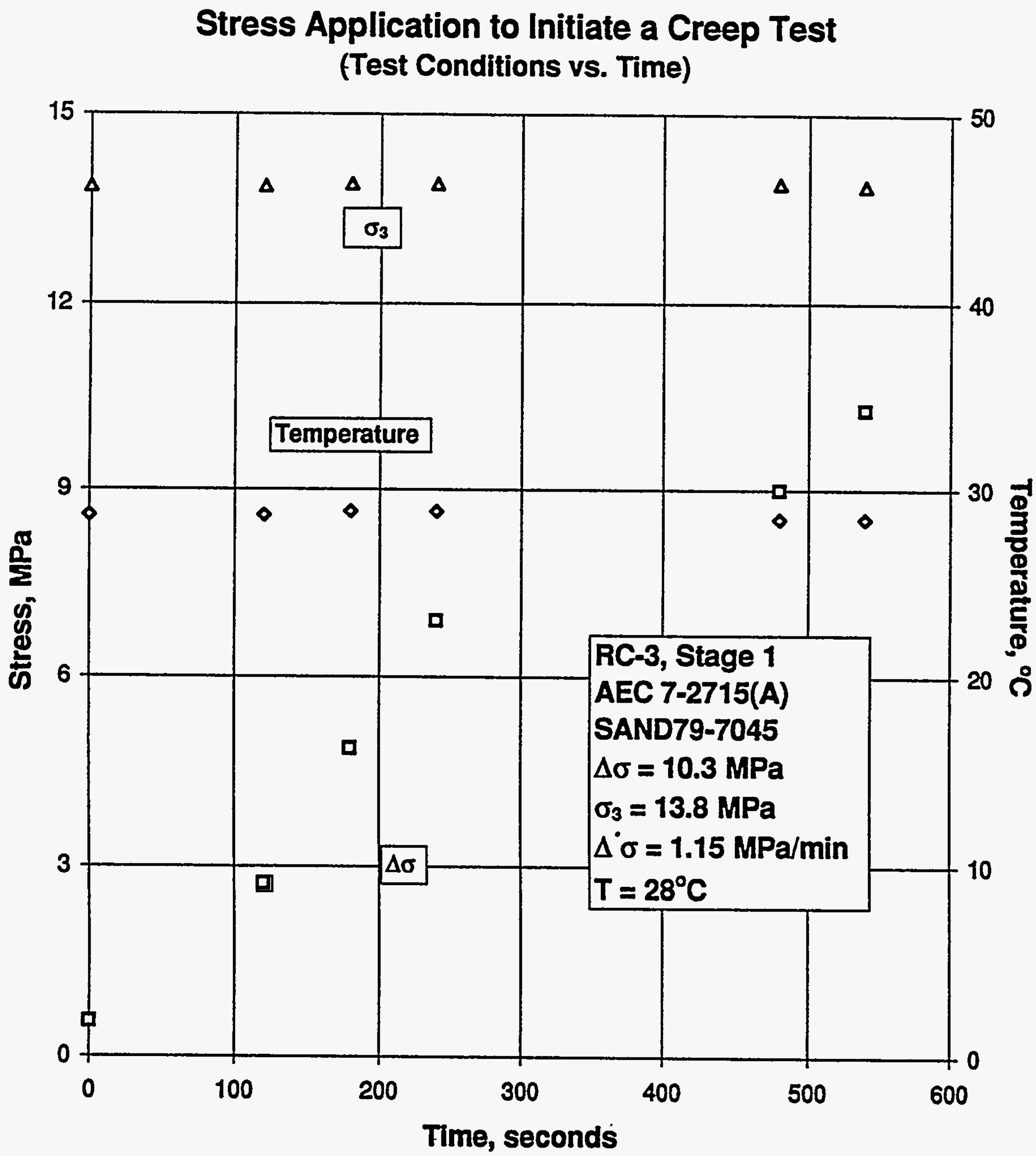

Figure B-163. Test Conditions Versus Time for Stress Application to Initiate a Creep Test: Specimen AEC7-2715 (A); Stage 1 of 3.

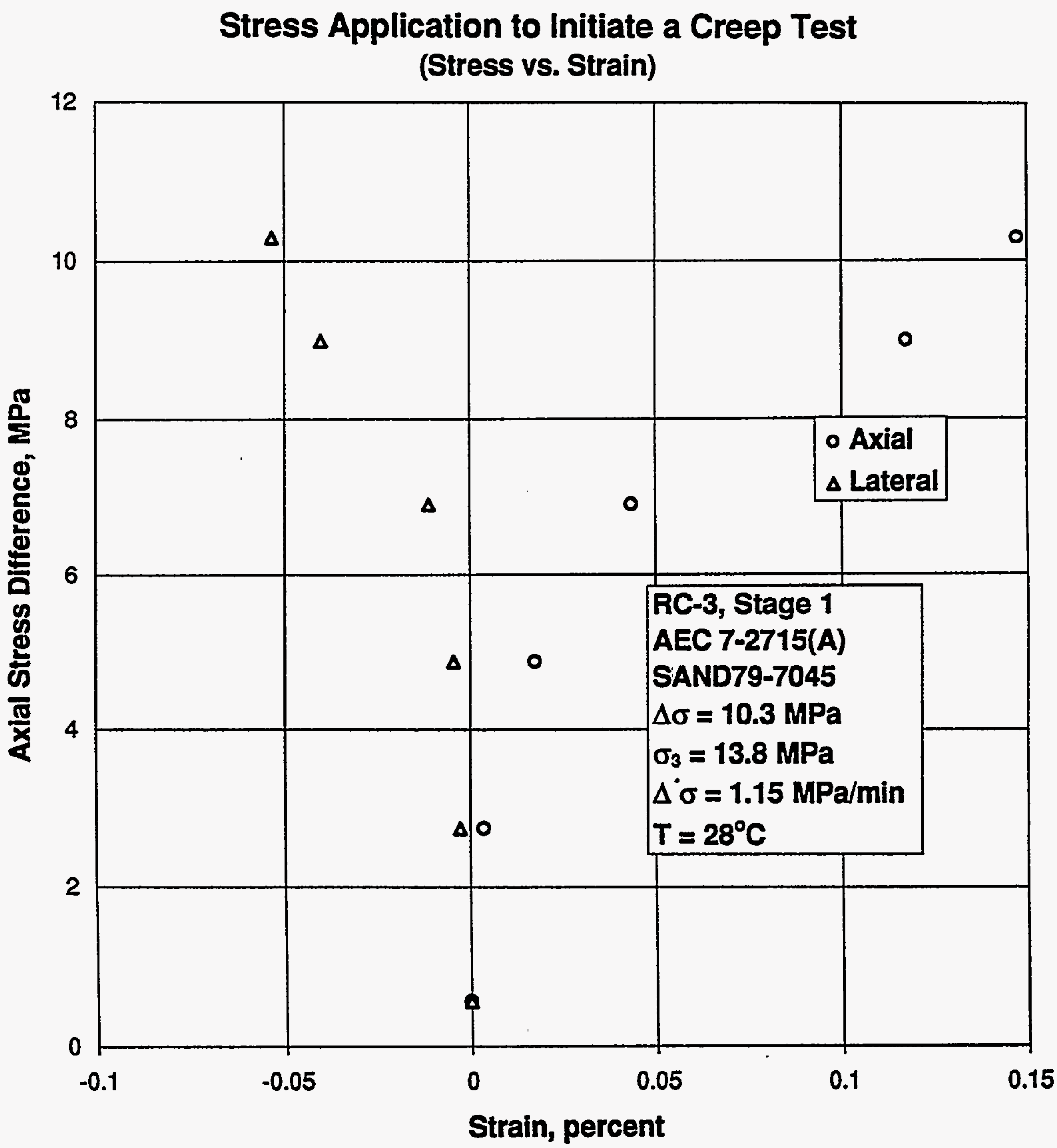

Figure B-164. Axial Stress Difference Versus Axial and Lateral Strain for Stress Application to Initiate a Creep Test: Specimen AEC7-2715 (A); Stage 1 of 3.

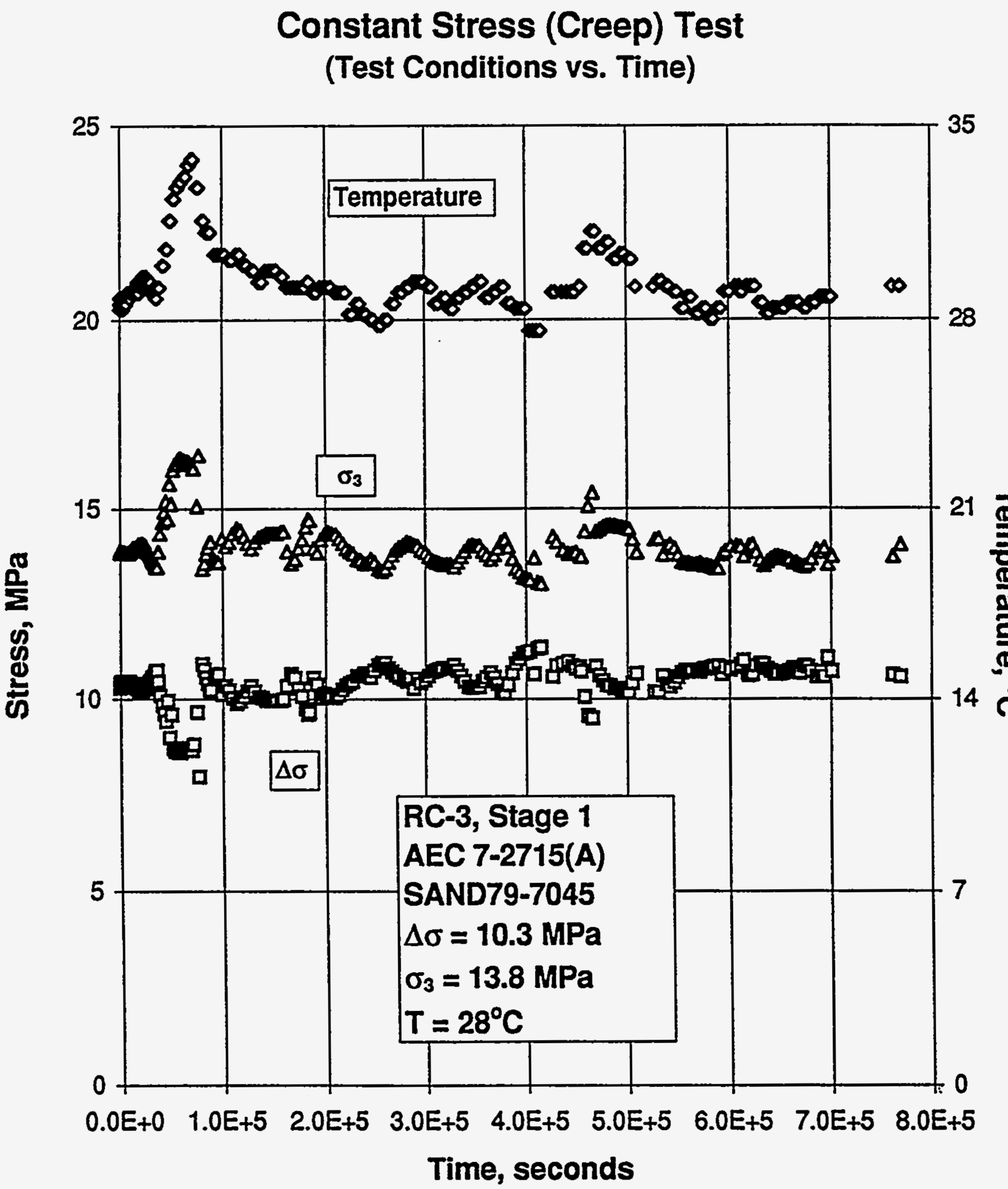

Figure B-165. Test Conditions Versus Time for a Creep Test: Specimen AEC7-2715 (A); Stage 1 of 3.

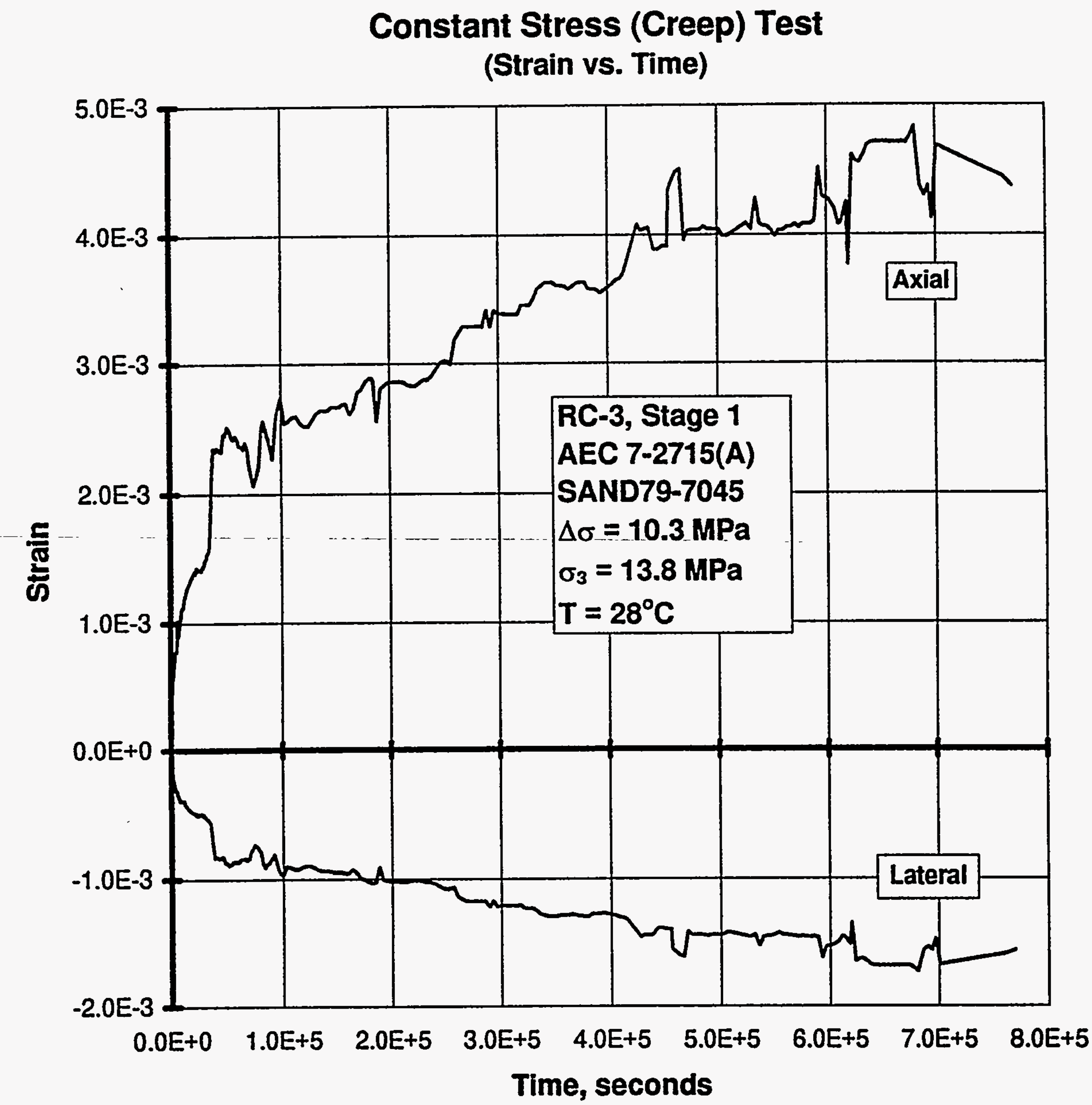

Figure B-166. Axial Strain and Lateral Strain Versus Time for a Creep Test: Specimen AEC7-2715 (A); Stage 1 of 3.

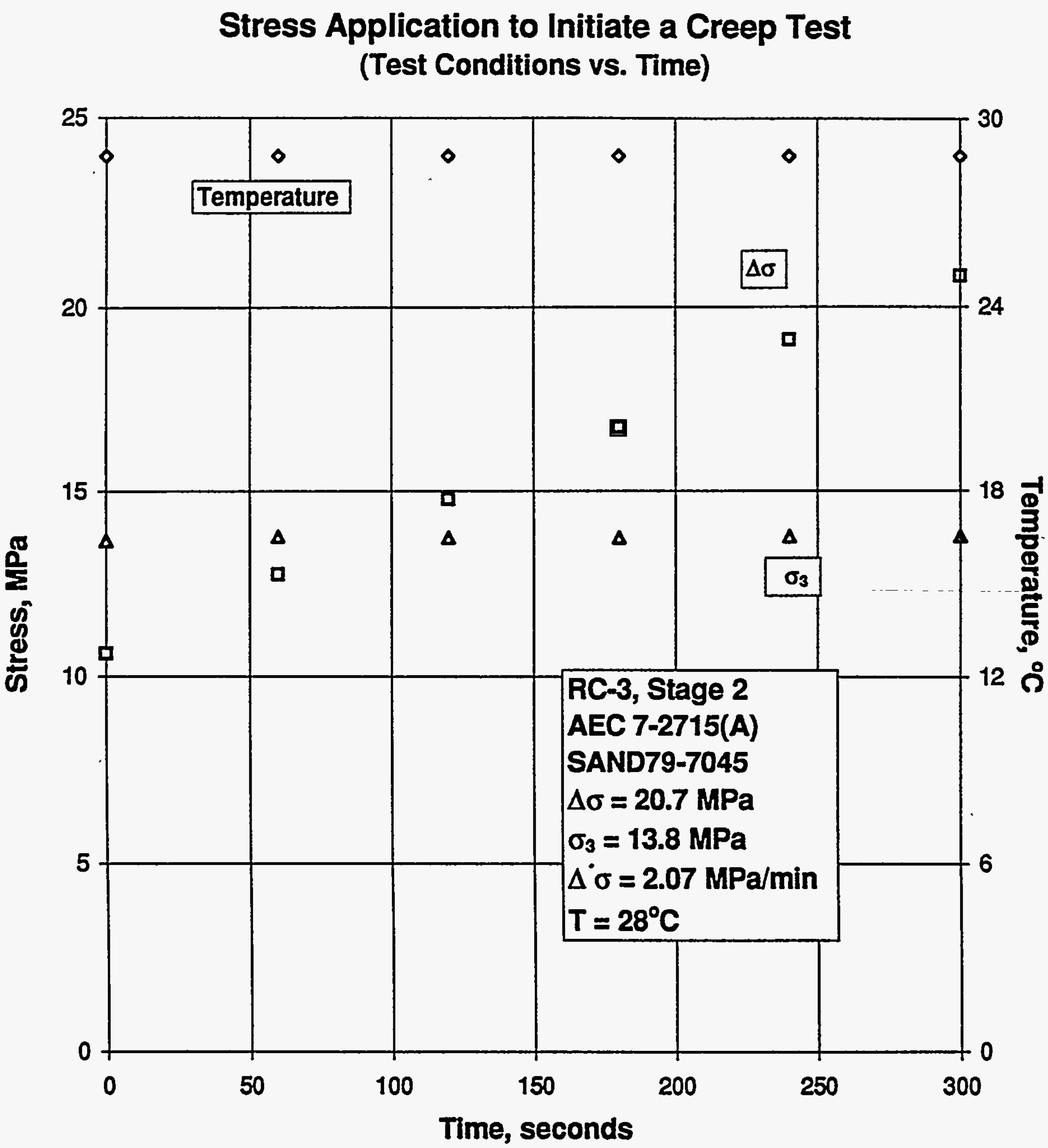

Figure B-167. Test Conditions Versus Time for Stress Application to Initiate a Creep Test: Specimen AEC7-2715 (A); Stage 2 of 3.

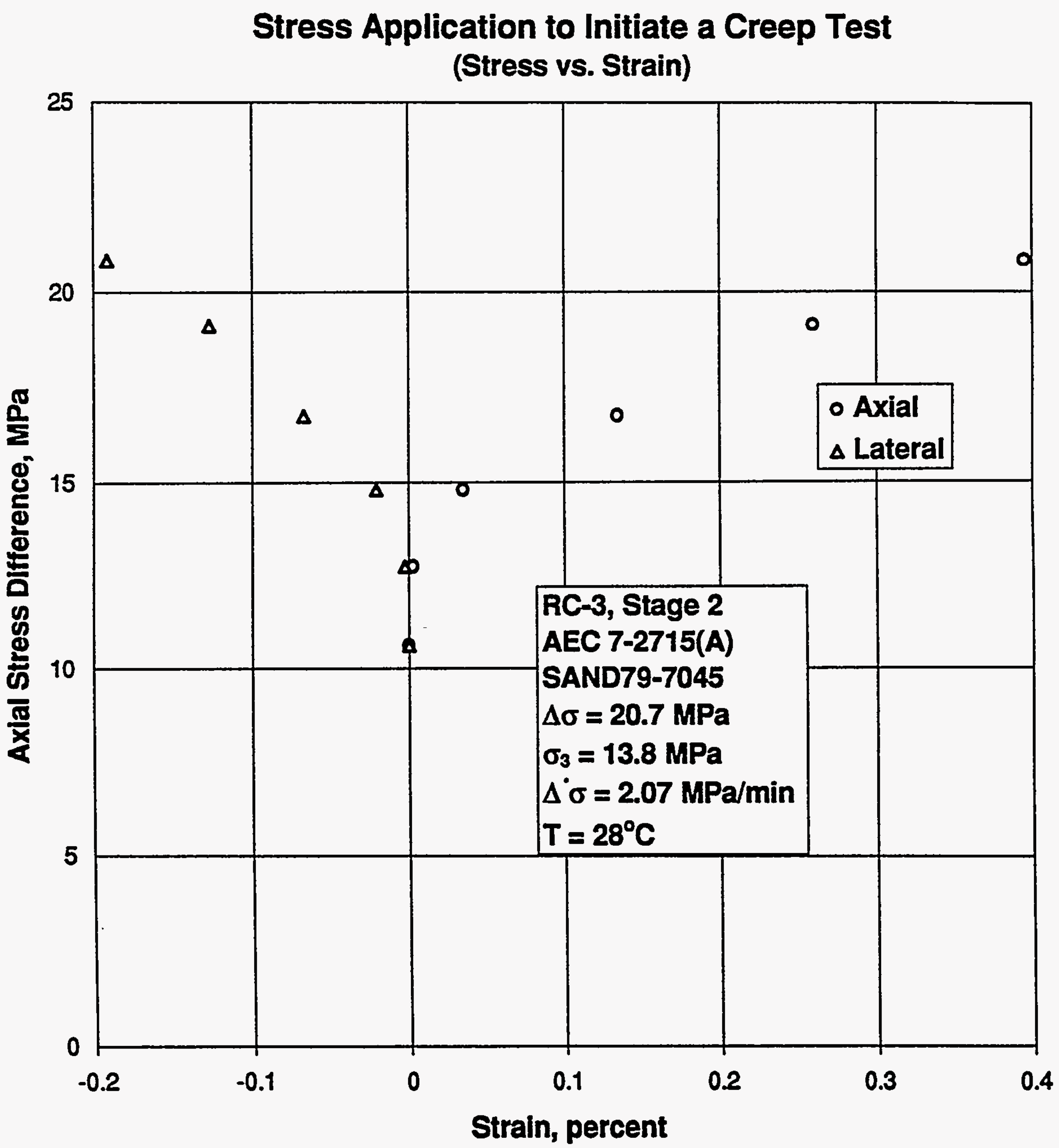

Figure B-168. Axial Stress Difference Versus Axial and Lateral Strain for Stress Application to Initiate a Creep Test: Specimen AEC7-2715 (A); Stage 2 of 3.

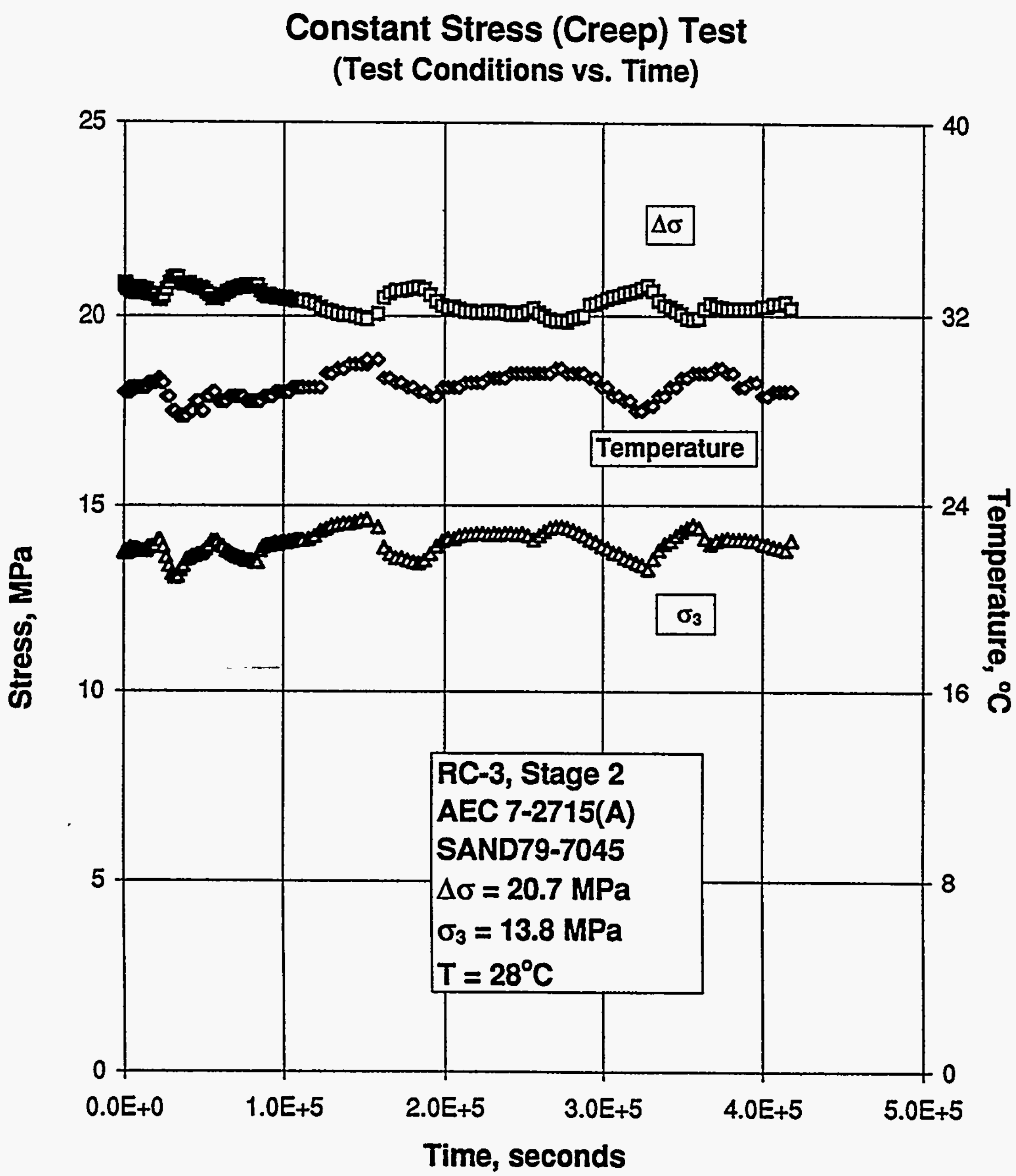

Figure B-169. Test Conditions Versus Time for a Creep Test: Specimen AEC7-2715 (A); Stage 2 of 3.

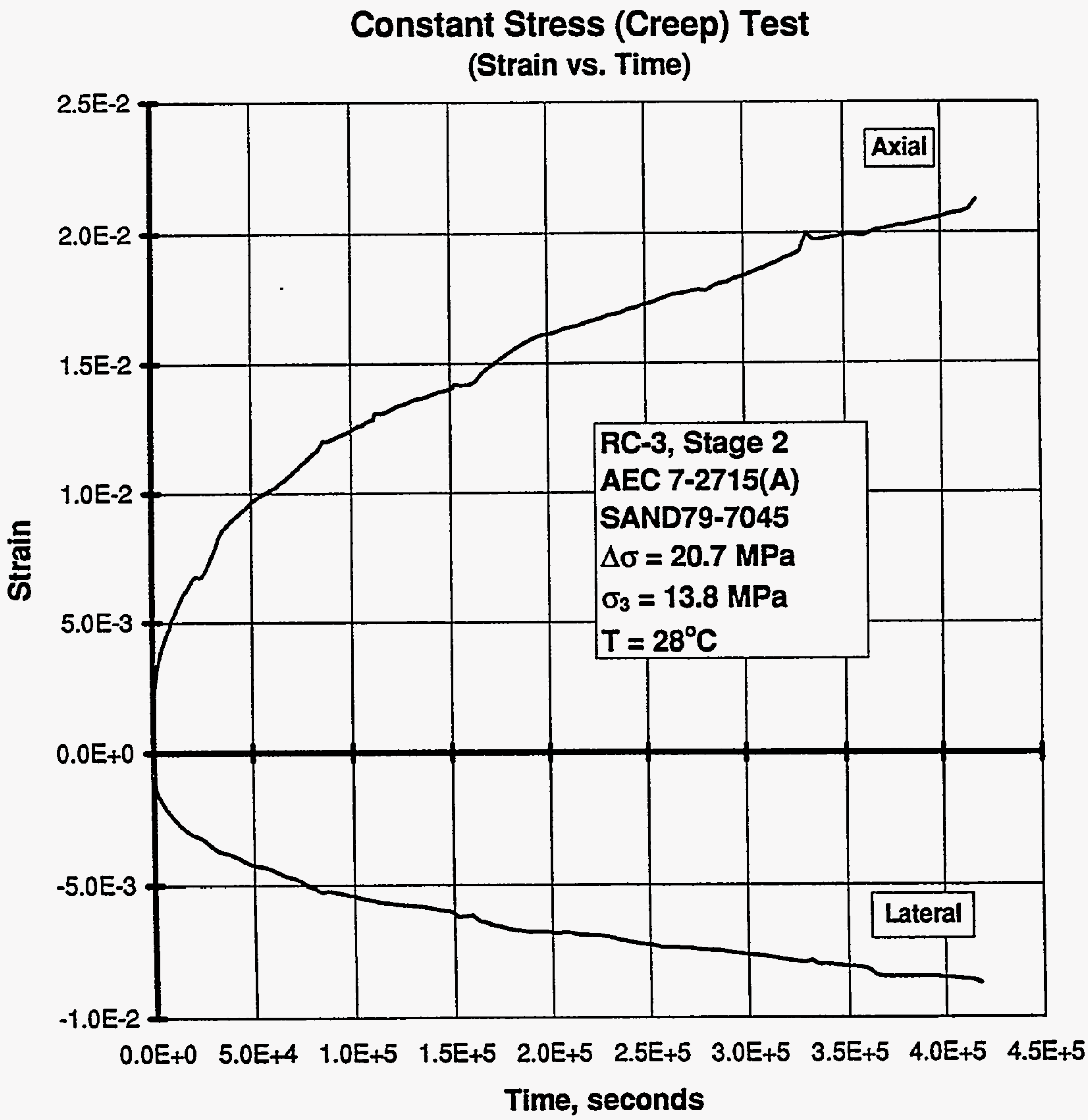

Figure B-170. Axial Strain and Lateral Strain Versus Time for a Creep Test: Specimen AEC7-2715 (A); Stage 2 of 3.

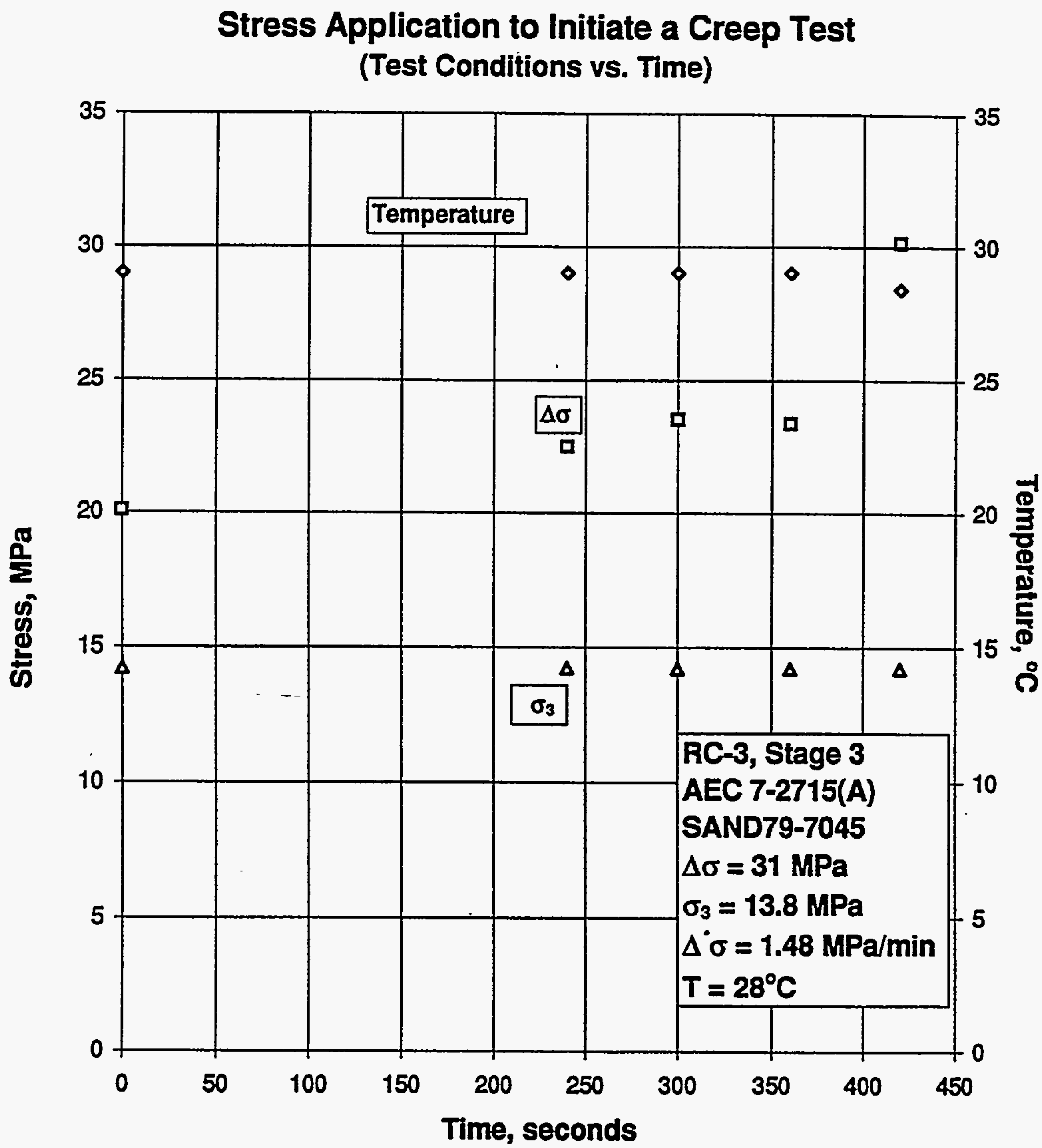

Figure B-171. Test Conditions Versus Time for Stress Application to Initiate a Creep Test: Specimen AEC7-2715 (A); Stage 3 of 3.

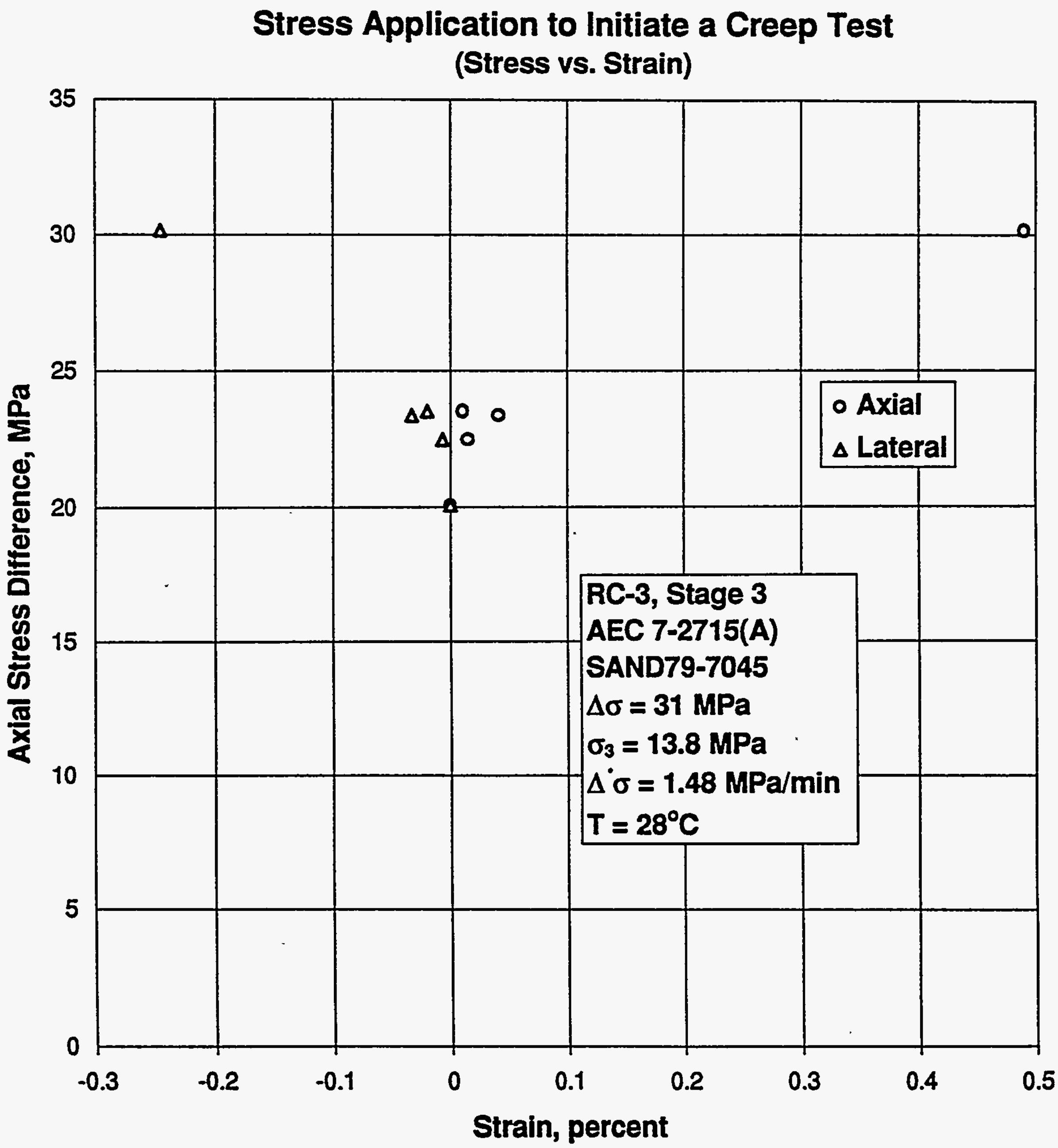

Figure B-172. Axial Stress Difference Versus Axial and Lateral Strain for Stress Application to Initiate a Creep Test: Specimen AEC7-2715 (A); Stage 3 of 3.

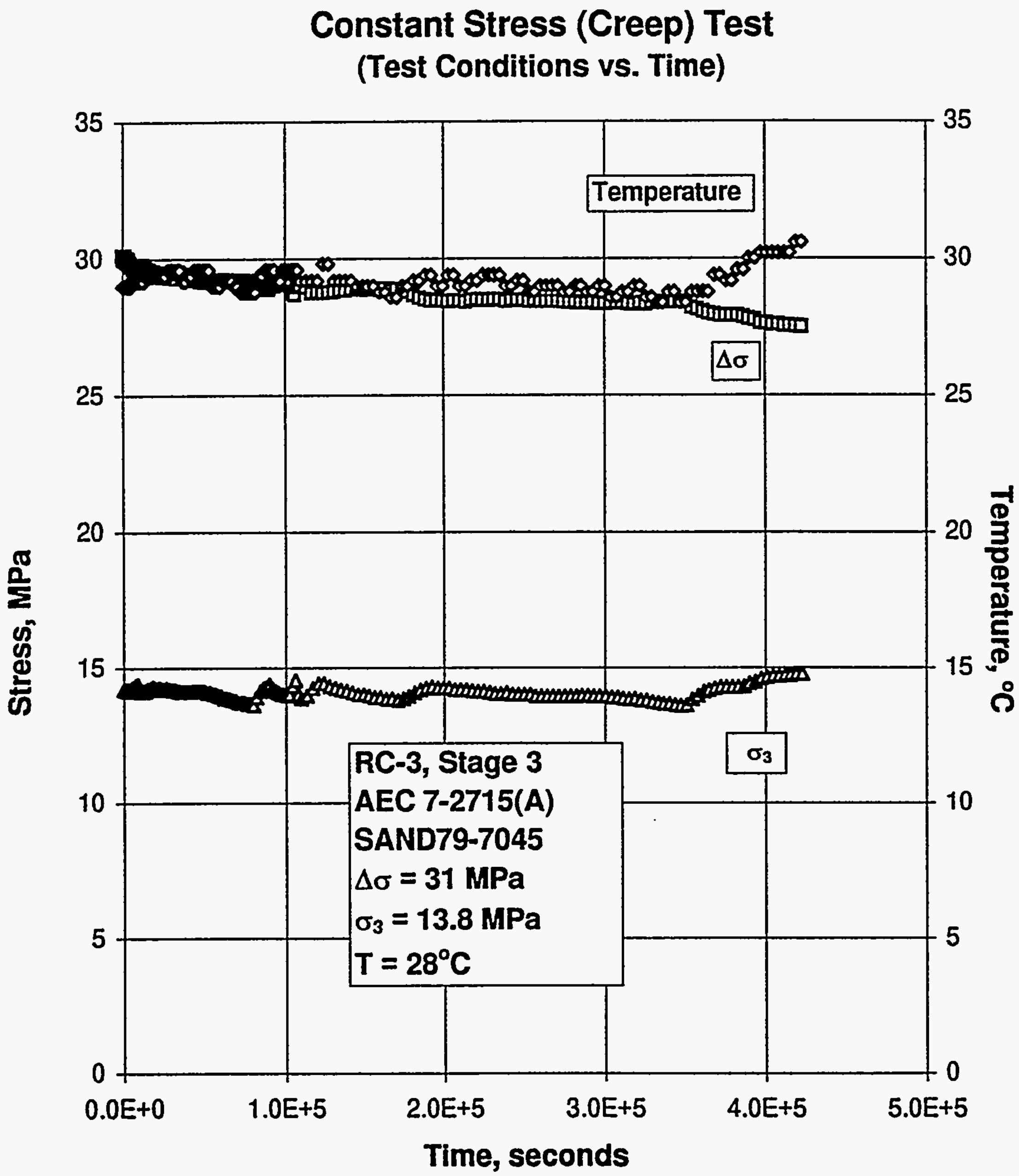

Figure B-173. Test Conditions Versus Time for a Creep Test: Specimen AEC7-2715 (A); Stage 3 of 3.

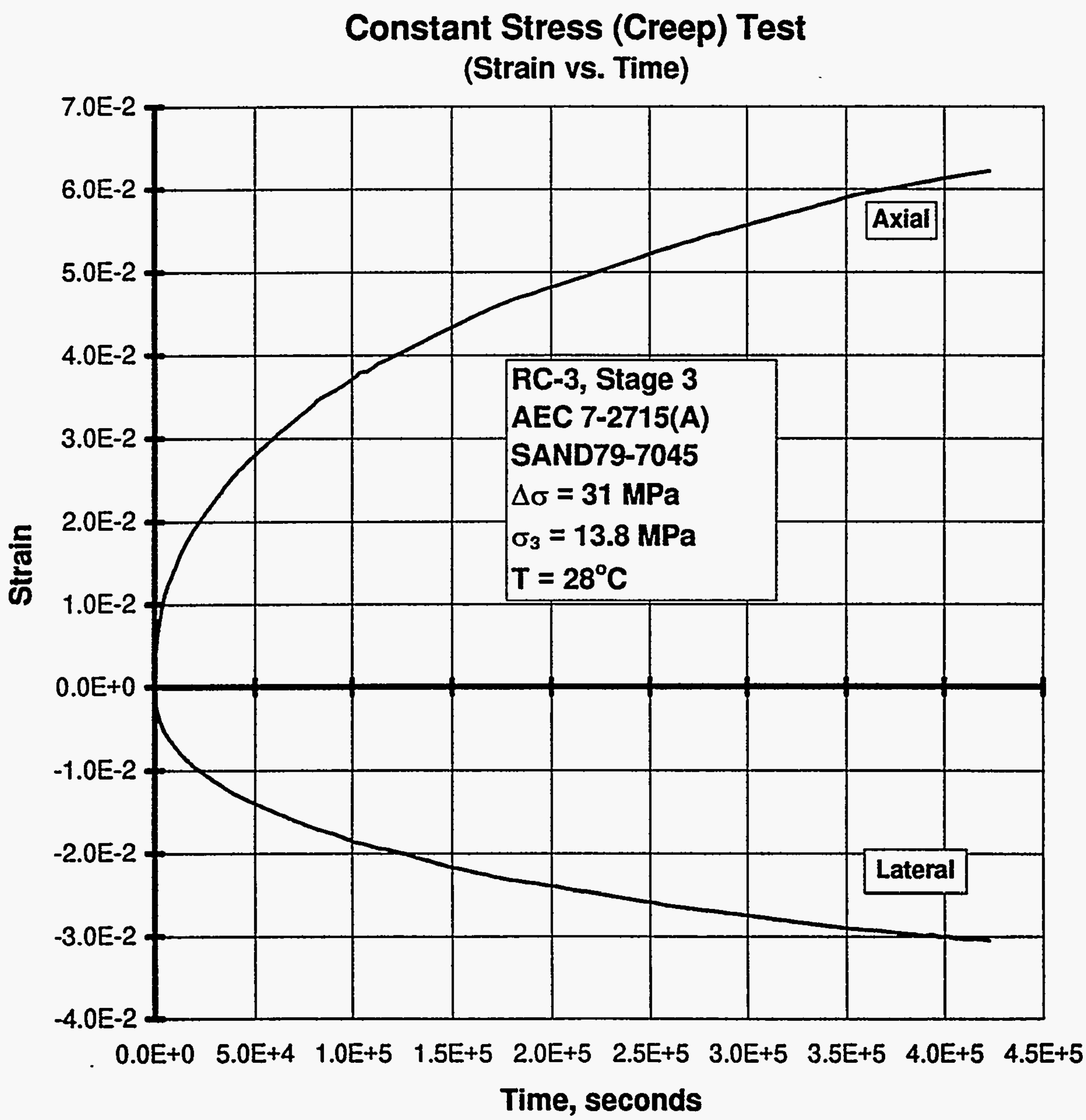

Figure B-174. Axial Strain and Lateral Strain Versus Time for a Creep Test: Specimen AEC7-2715 (A); Stage 3 of 3.

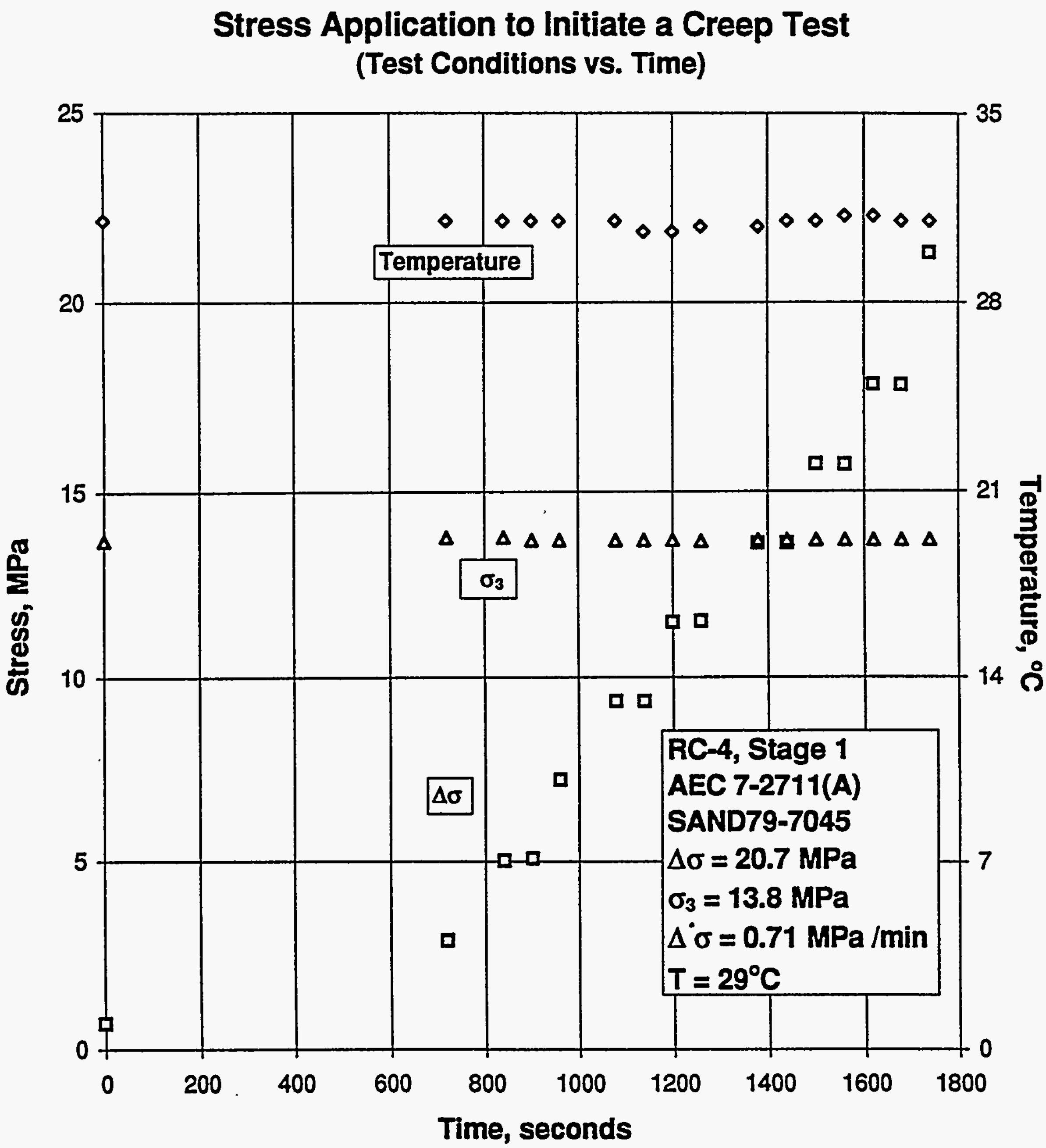

Figure B-175. Test Conditions Versus Time for Stress Application to Initiate a Creep Test: Specimen AEC7-2711 (A); Stage 1 of 2.

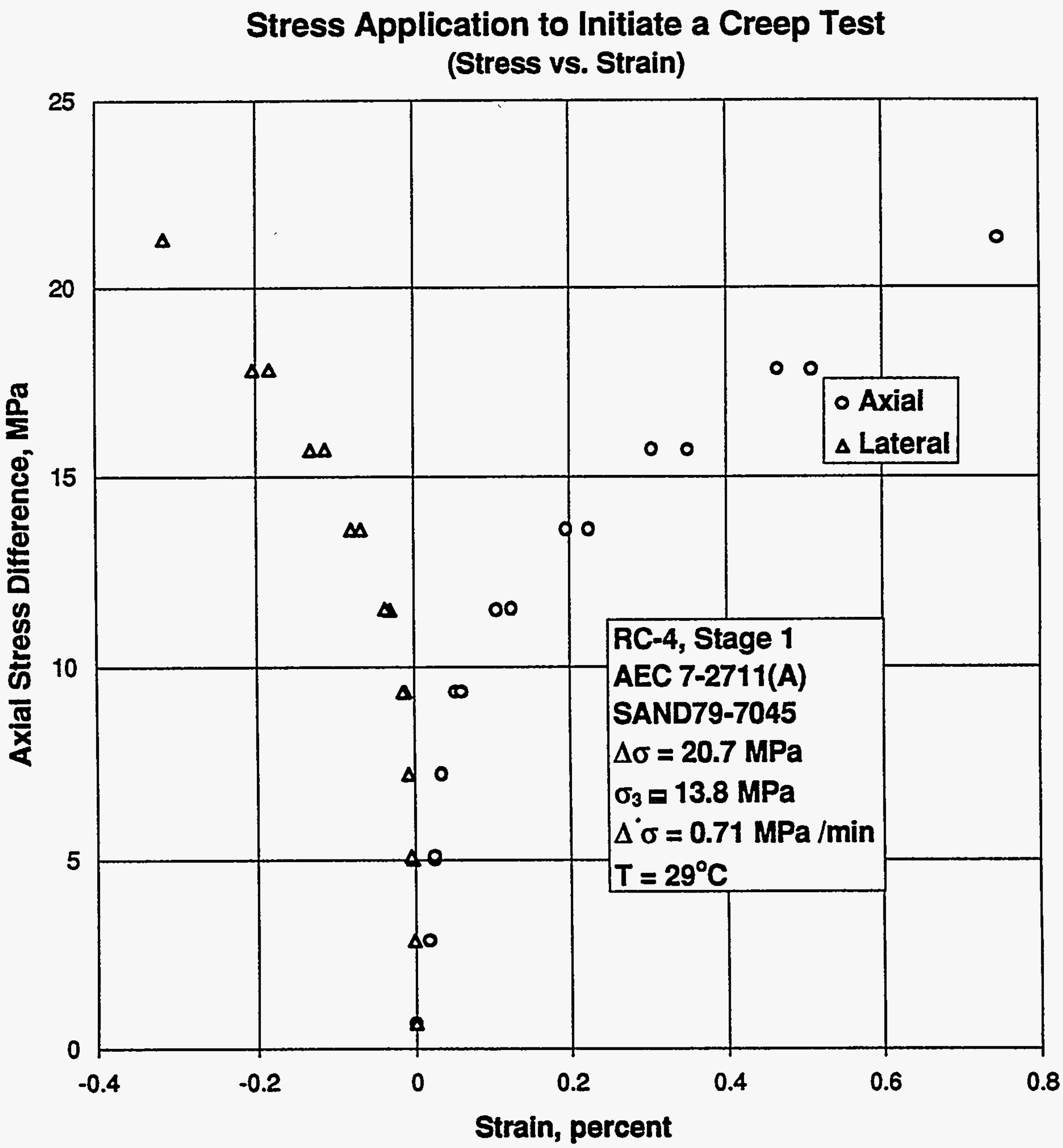

Figure B-176. Axial Stress Difference Versus Axial and Lateral Strain for Stress Application to Initiate a Creep Test: Specimen AEC7-2711 (A); Stage 1 of 2.

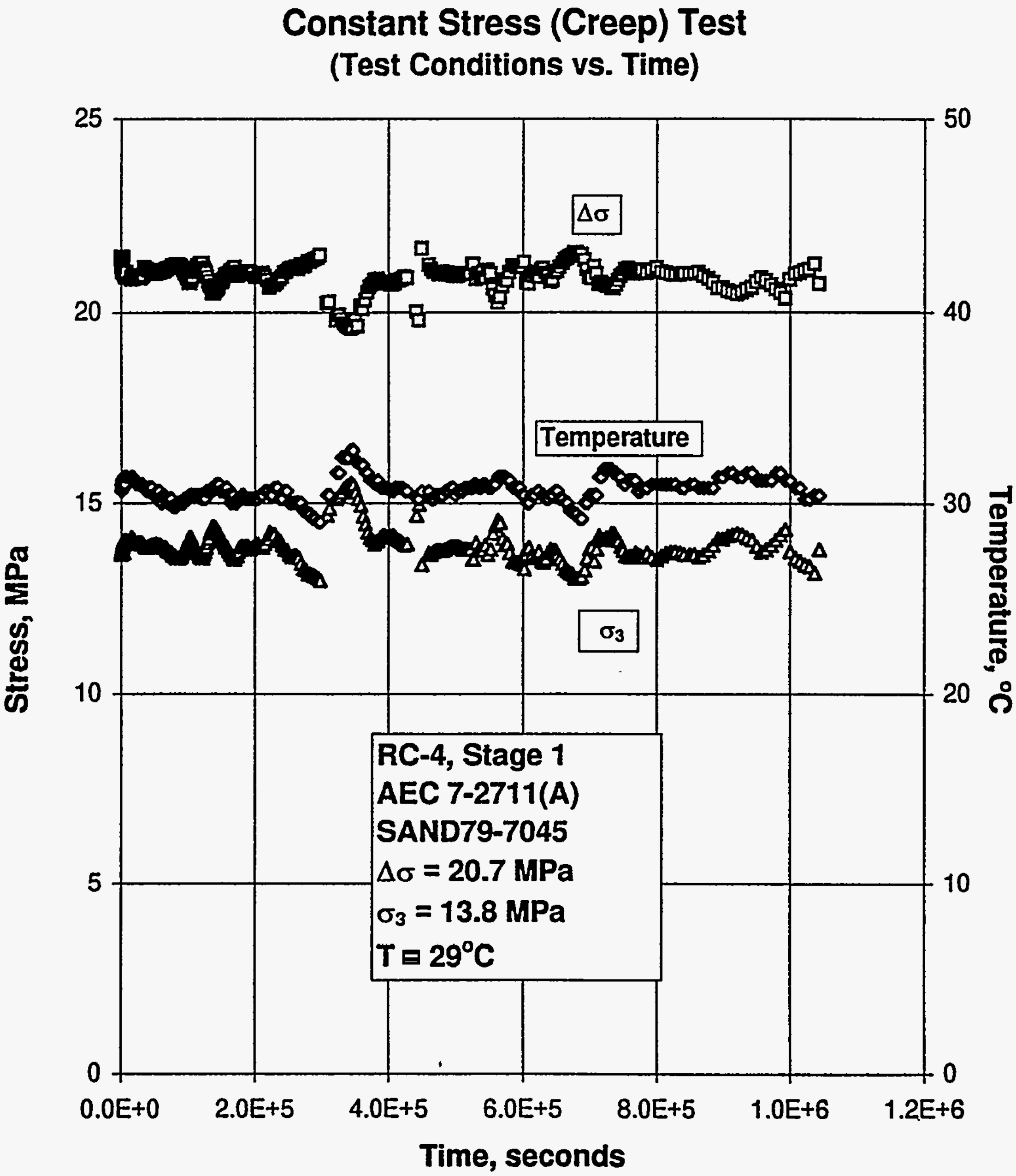

Figure B-177. Test Conditions Versus Time for a Creep Test: Specimen AEC7-2711 (A); Stage 1 of 2.

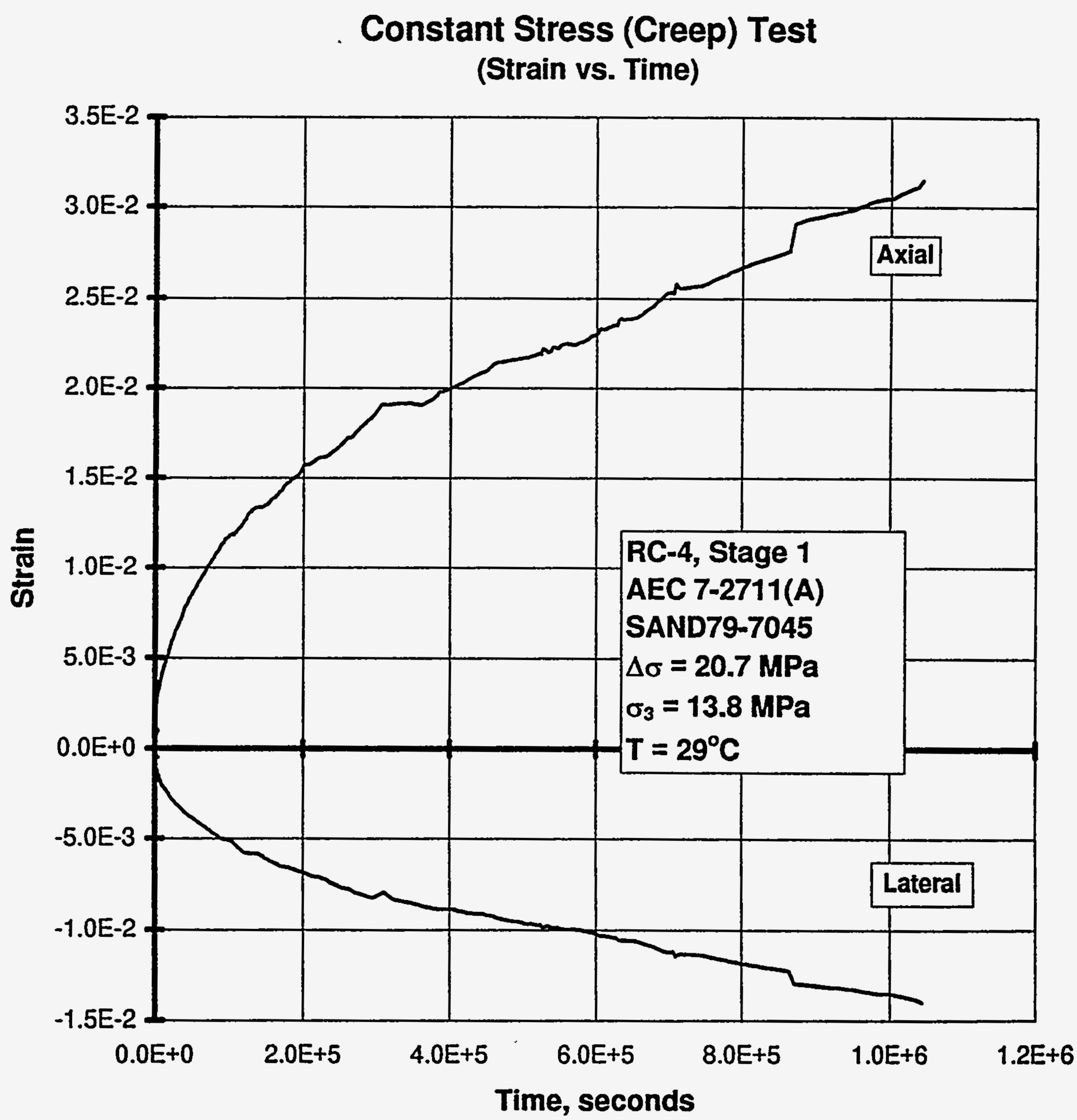

Figure B-178. Axial Strain and Lateral Strain Versus Time for a Creep Test: Specimen AEC7-2711 (A); Stage 1 of 2.

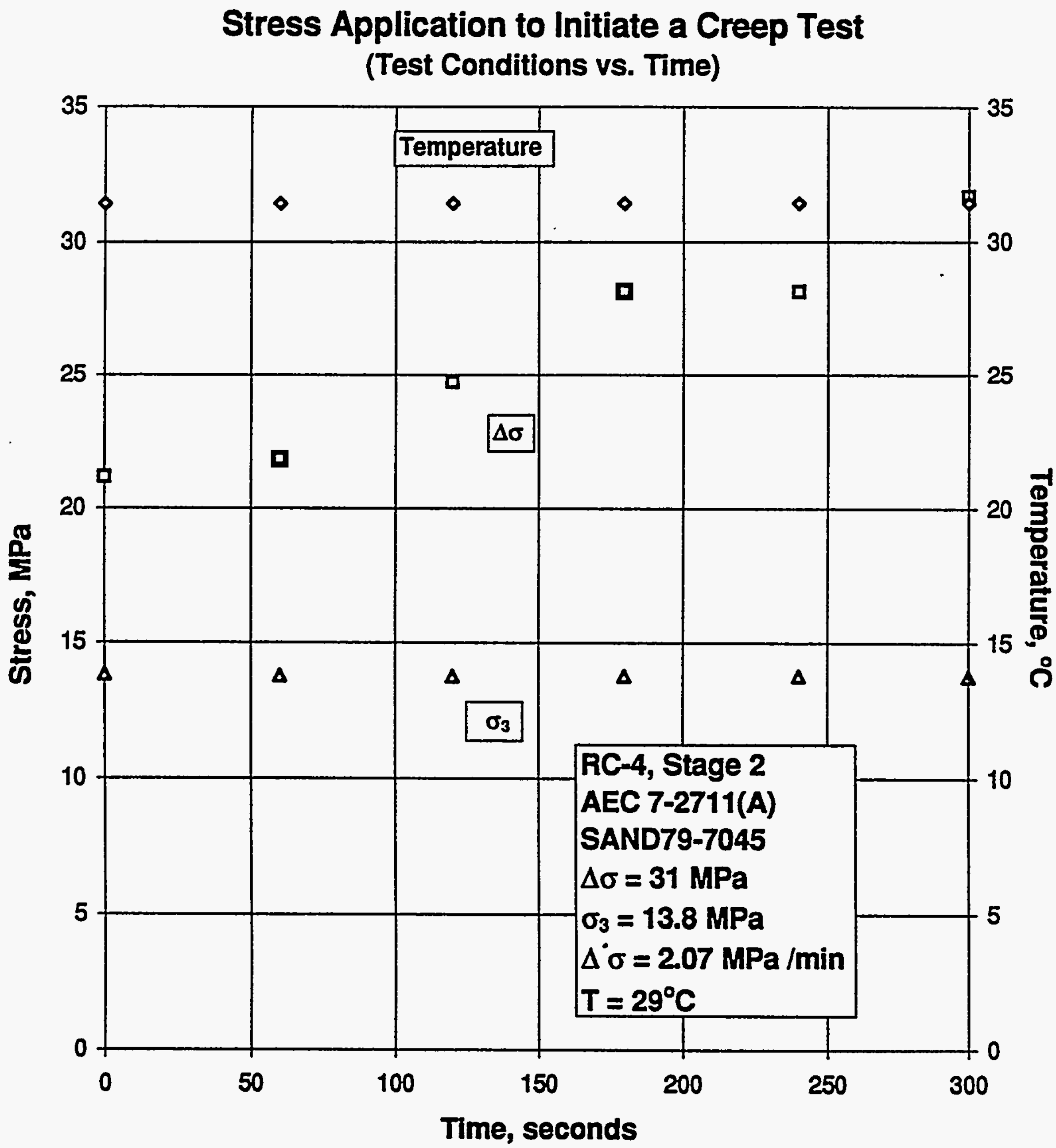

Figure B-179. Test Conditions Versus Time for Stress Application to Initiate a Creep Test: Specimen AEC7-2711 (A); Stage 2 of 2.

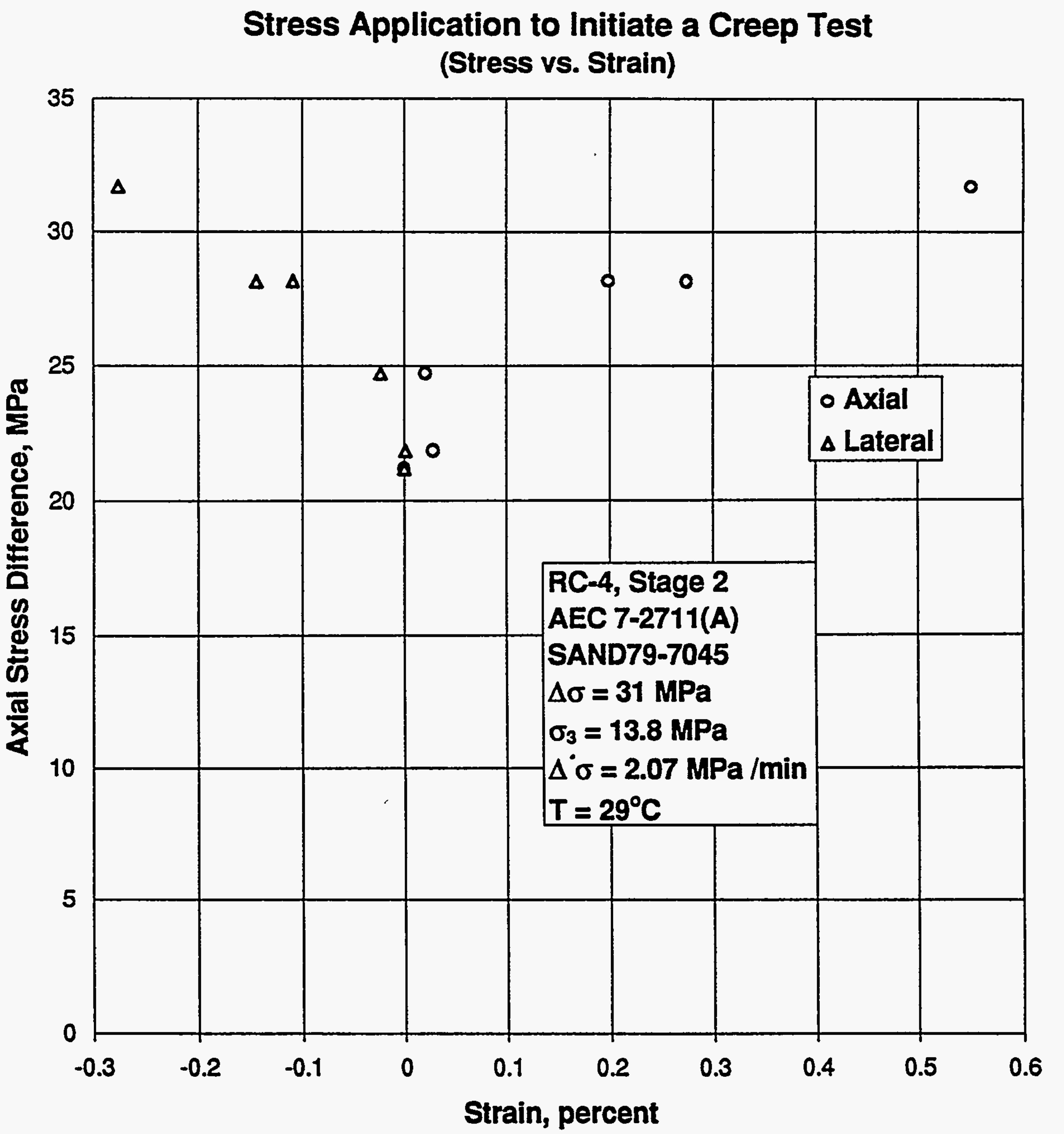

Figure B-180. Axial Stress Difference Versus Axial and Lateral Strain for Stress Application to Initiate a Creep Test: Specimen AEC7-2711 (A); Stage 2 of 2.

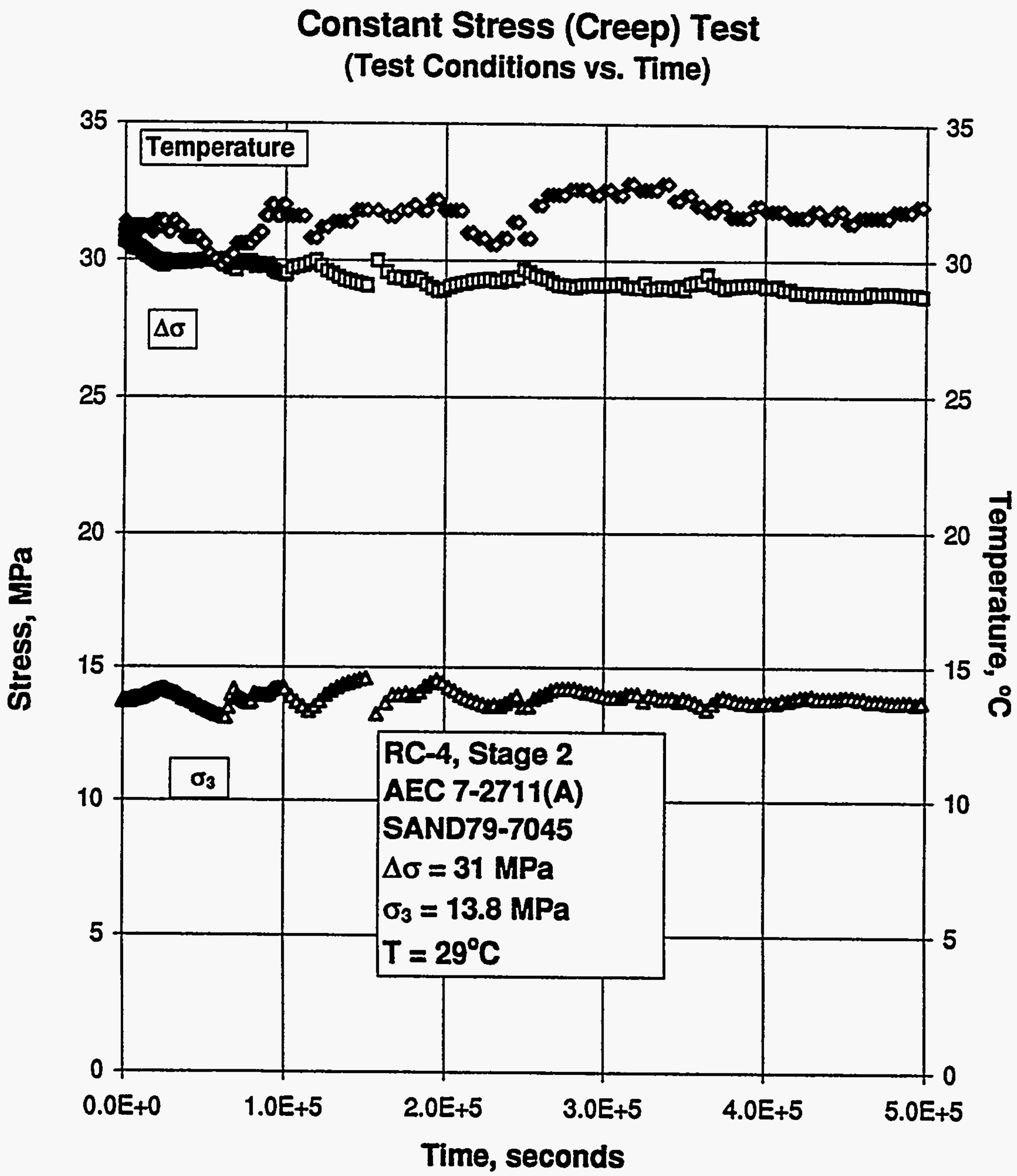

Figure B-181. Test Conditions Versus Time for a Creep Test: Specimen AEC7-2711 (A); Stage 2 of 2.

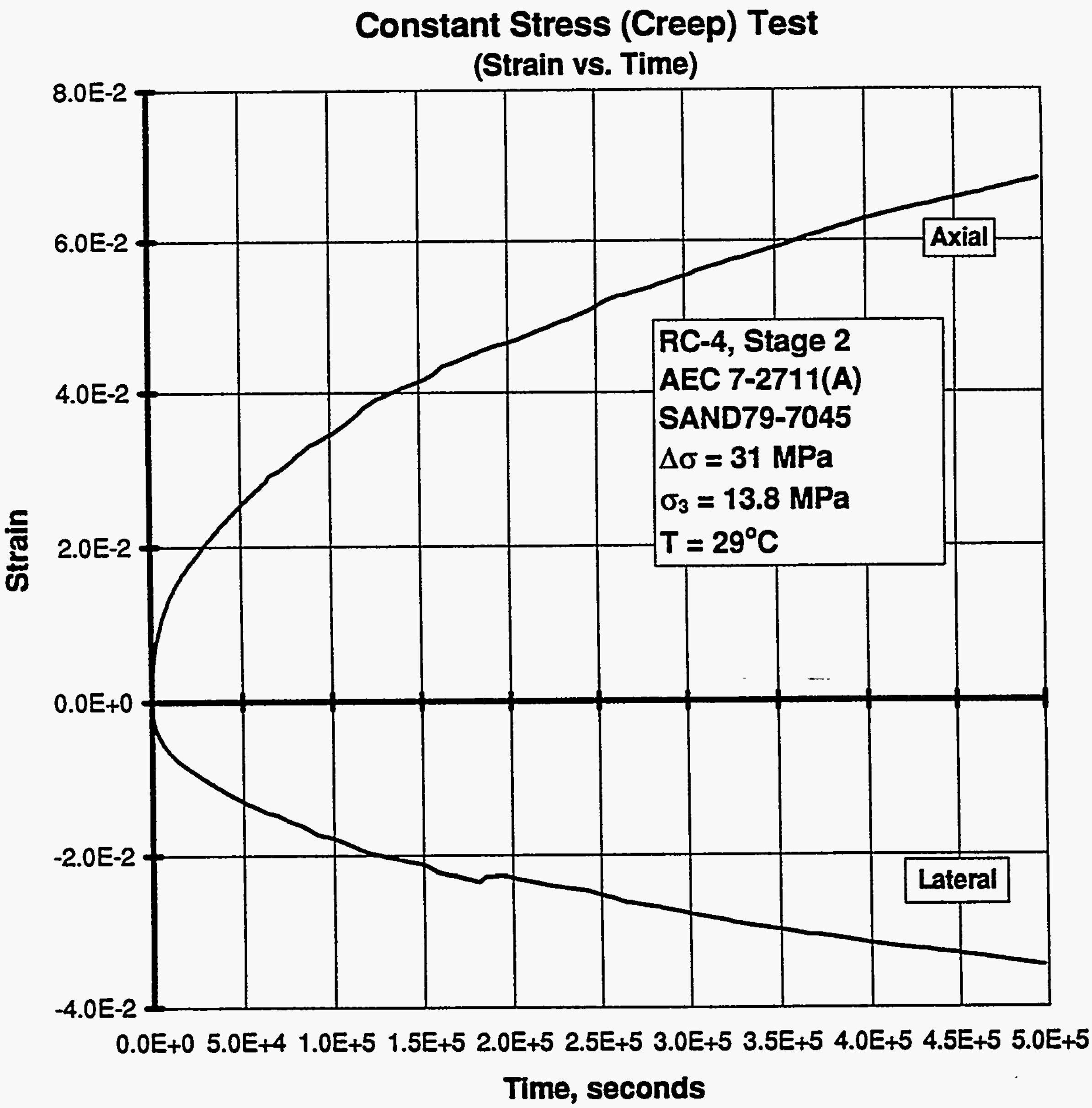

Figure B-182. Axial Strain and Lateral Strain Versus Time for a Creep Test: Specimen AEC7-2711 (A); Stage 2 of 2.

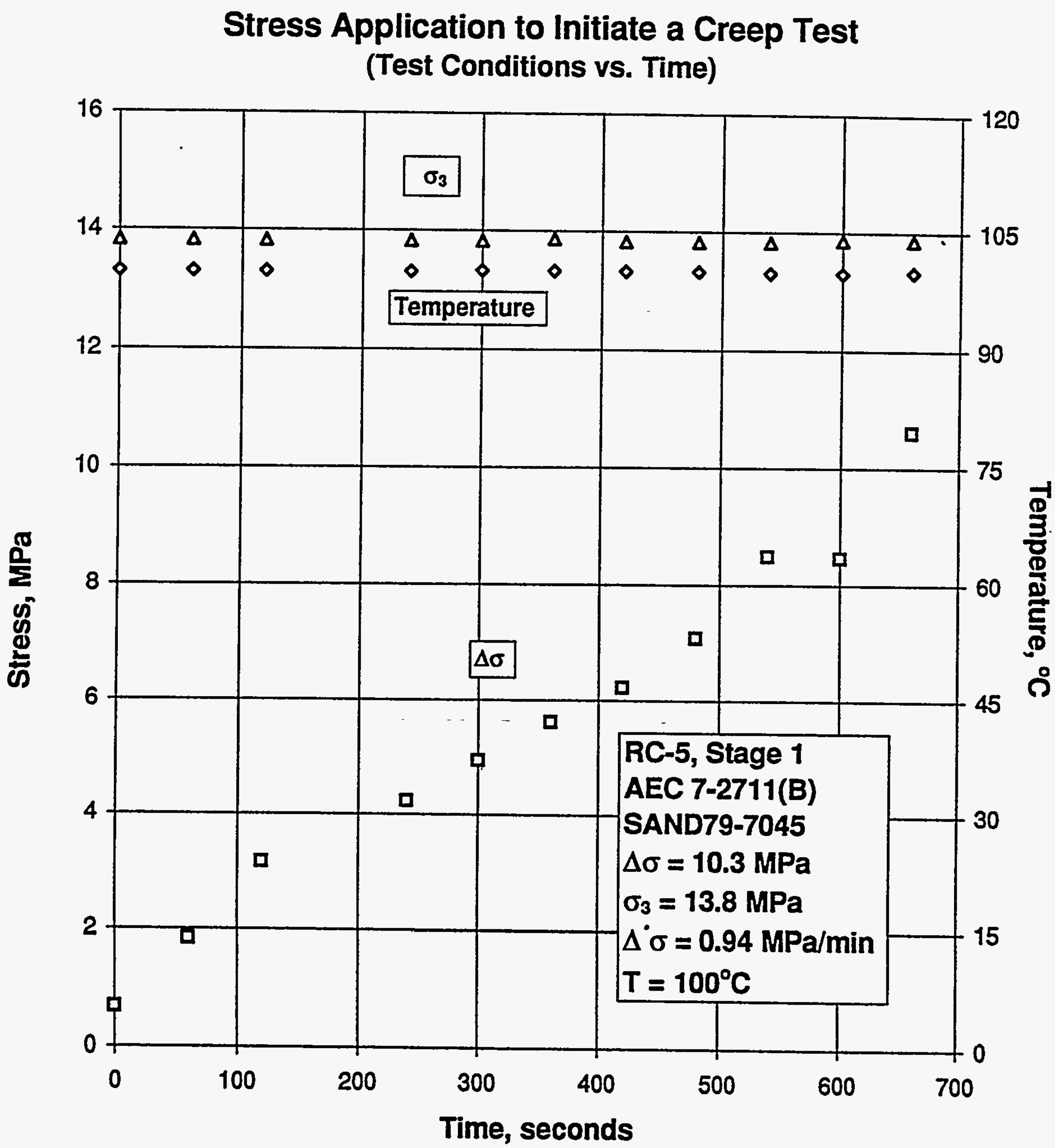

Figure B-183. Test Conditions Versus Time for Stress Application to Initiate a Creep Test: Specimen AEC7-2711 (B); Stage 1 of 2.

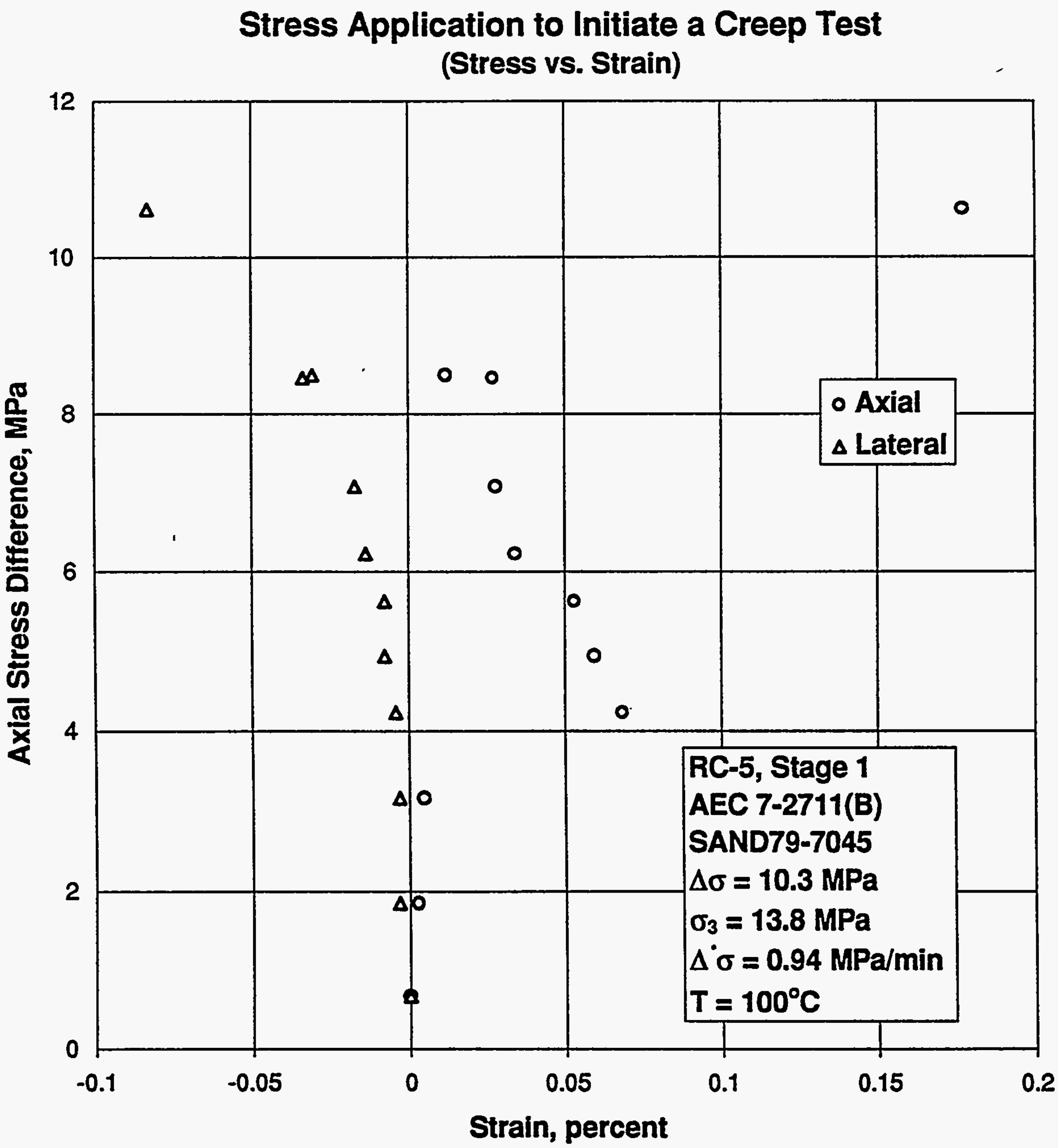

Figure B-184. Axial Stress Difference Versus Axial and Lateral Strain for Stress Application to Initiate a Creep Test: Specimen AEC7-2711 (B); Stage 1 of 2.

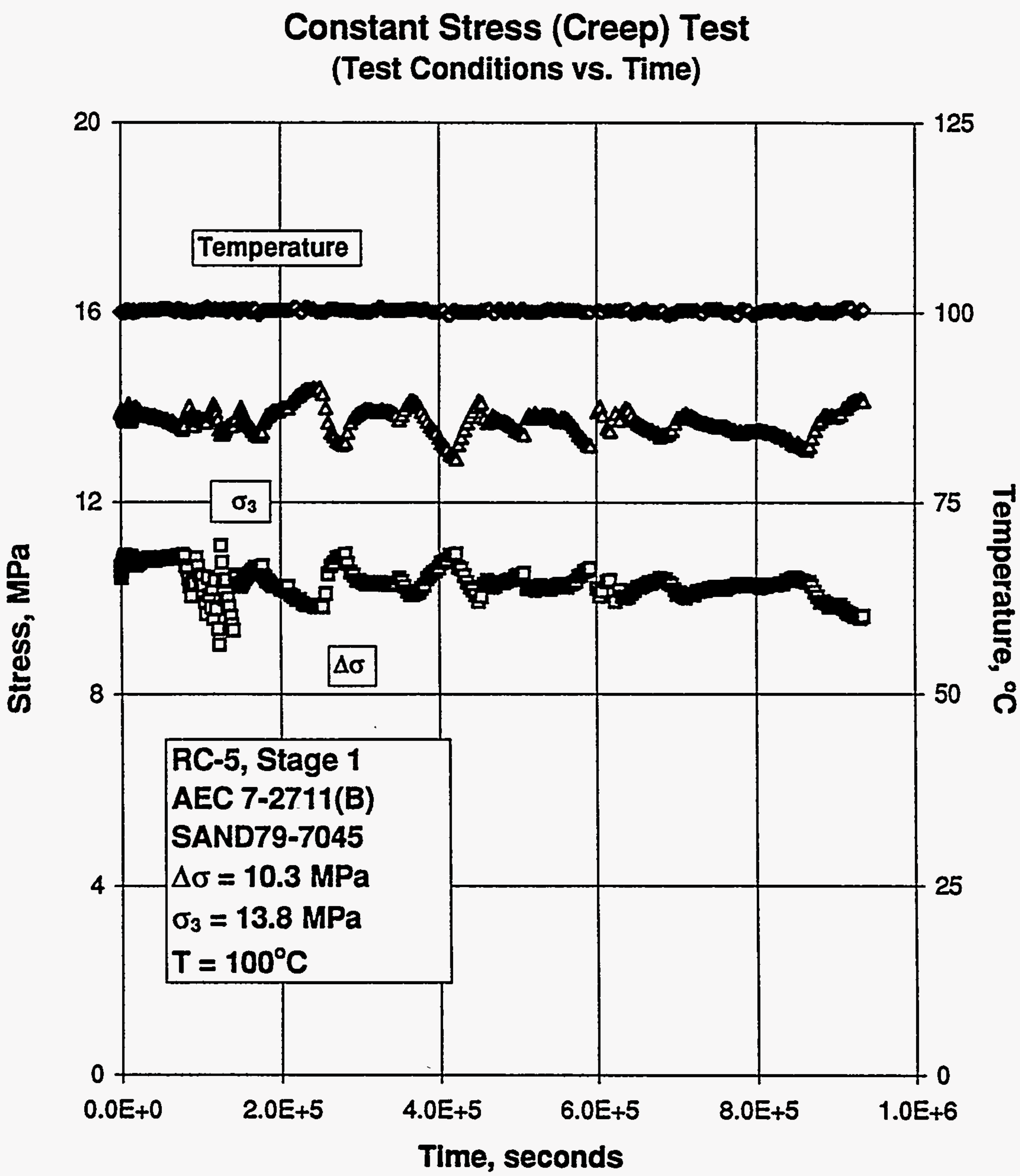

Figure B-185. Test Conditions Versus Time for a Creep Test: Specimen AEC7-2711 (B); Stage 1 of 2.

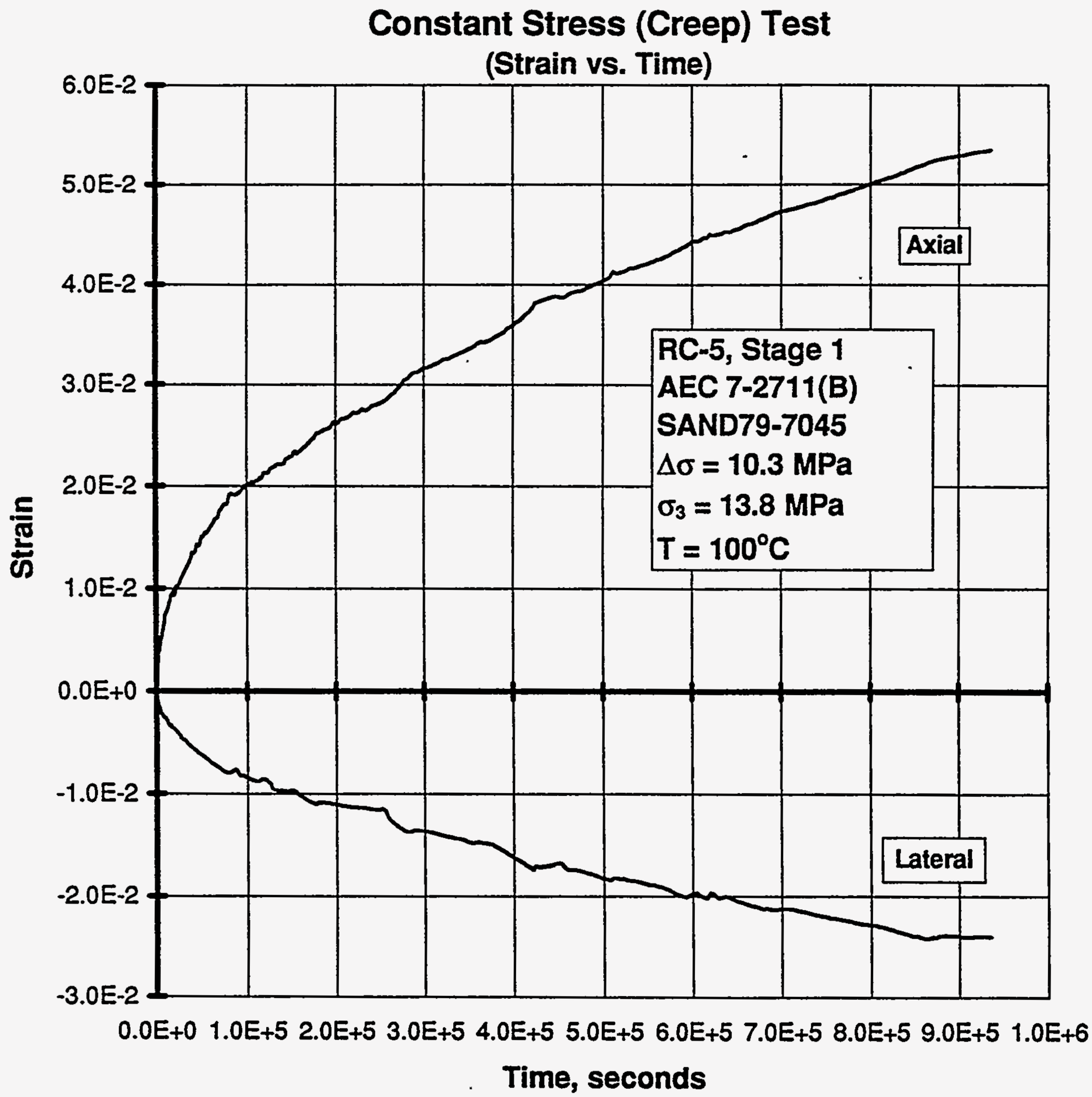

Figure B-186. Axial Strain and Lateral Strain Versus Time for a Creep Test: Specimen AEC7-2711 (B); Stage 1 of 2.

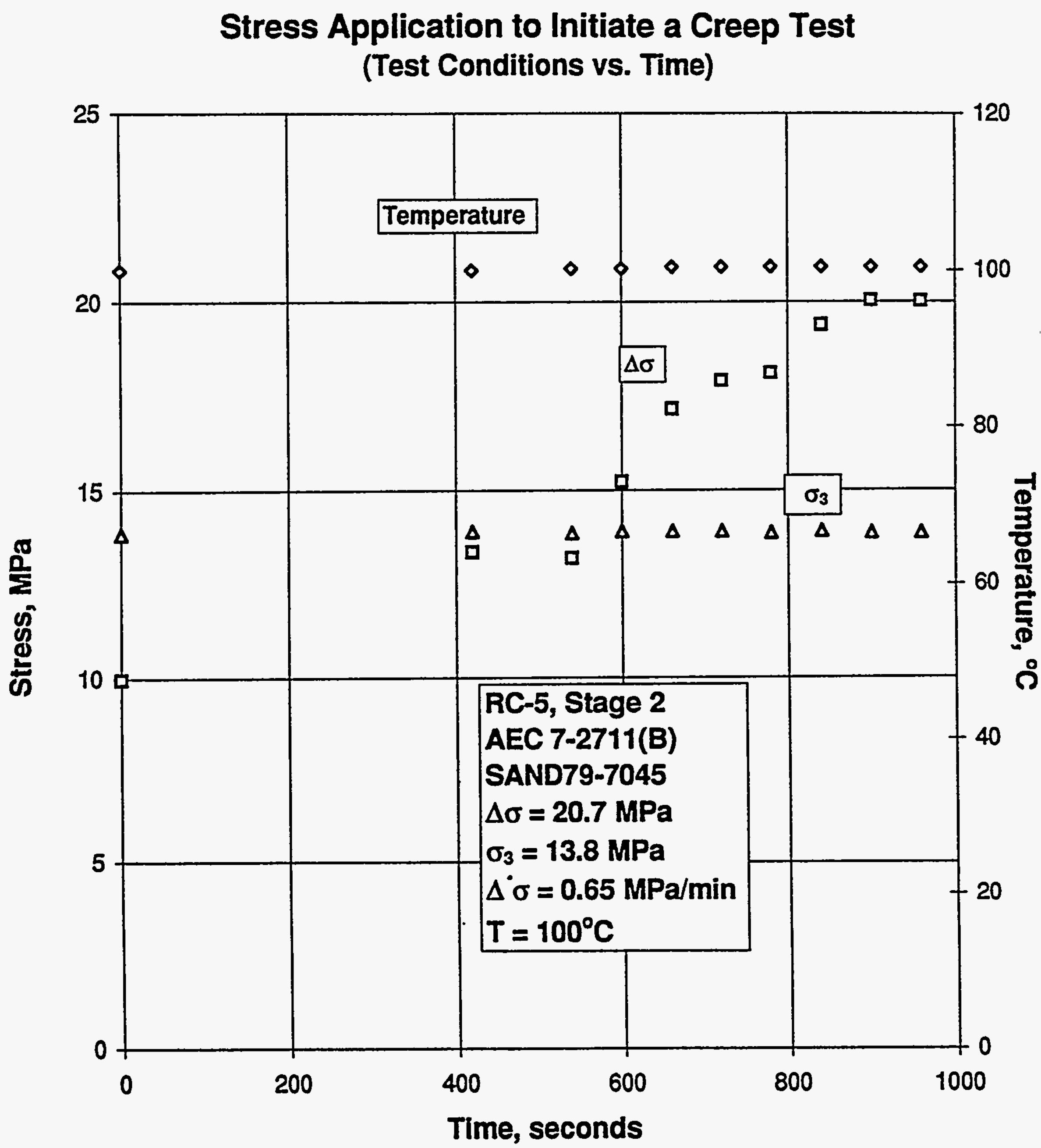

Figure B-187. Test Conditions Versus Time for Stress Application to Initiate a Creep Test: Specimen AEC7-2711 (B); Stage 2 of 2.

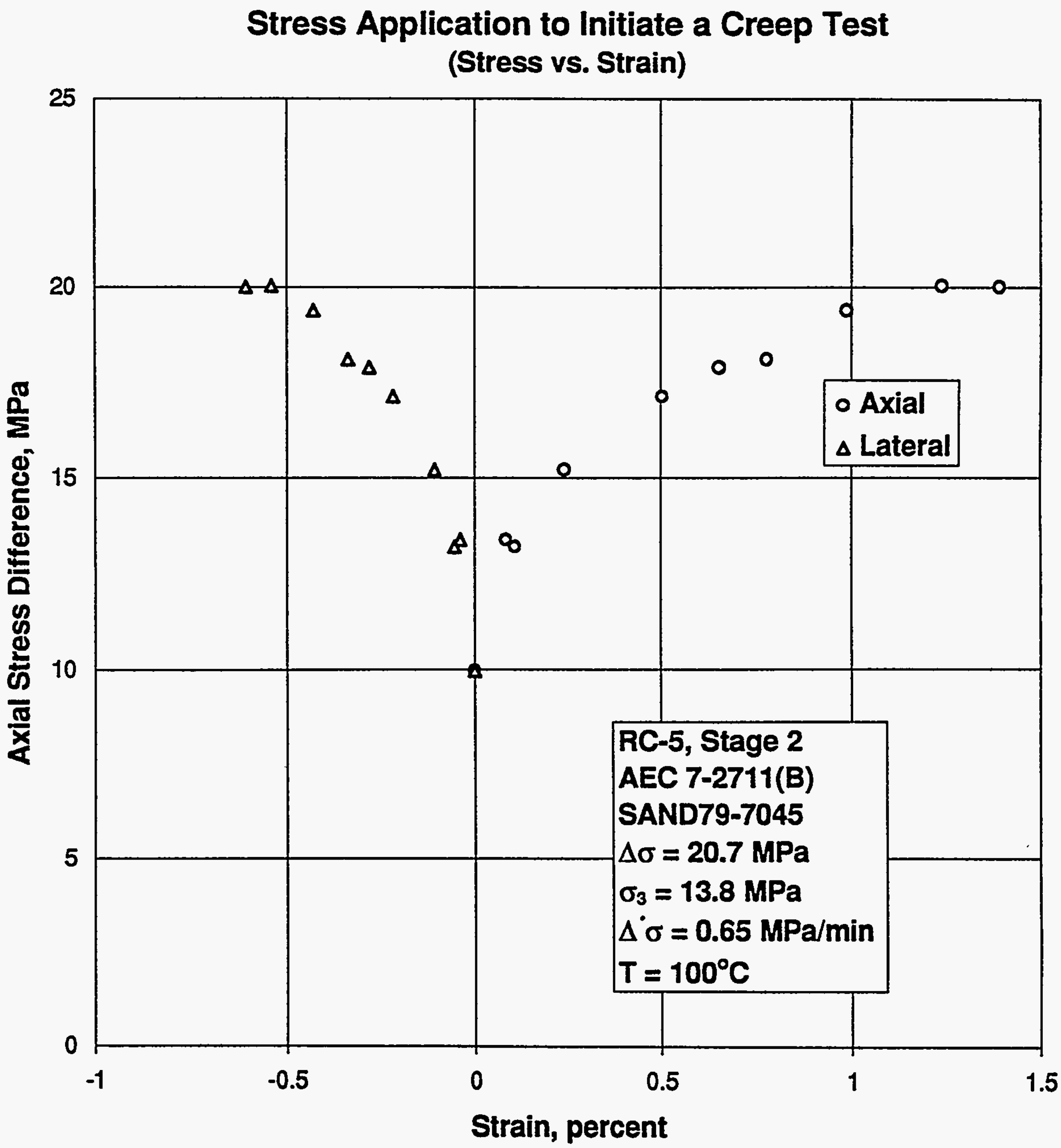

Figure B-188. Axial Stress Difference Versus Axial and Lateral Strain for Stress Application to Initiate a Creep Test: Specimen AEC7-2711 (B); Stage 2 of 2.

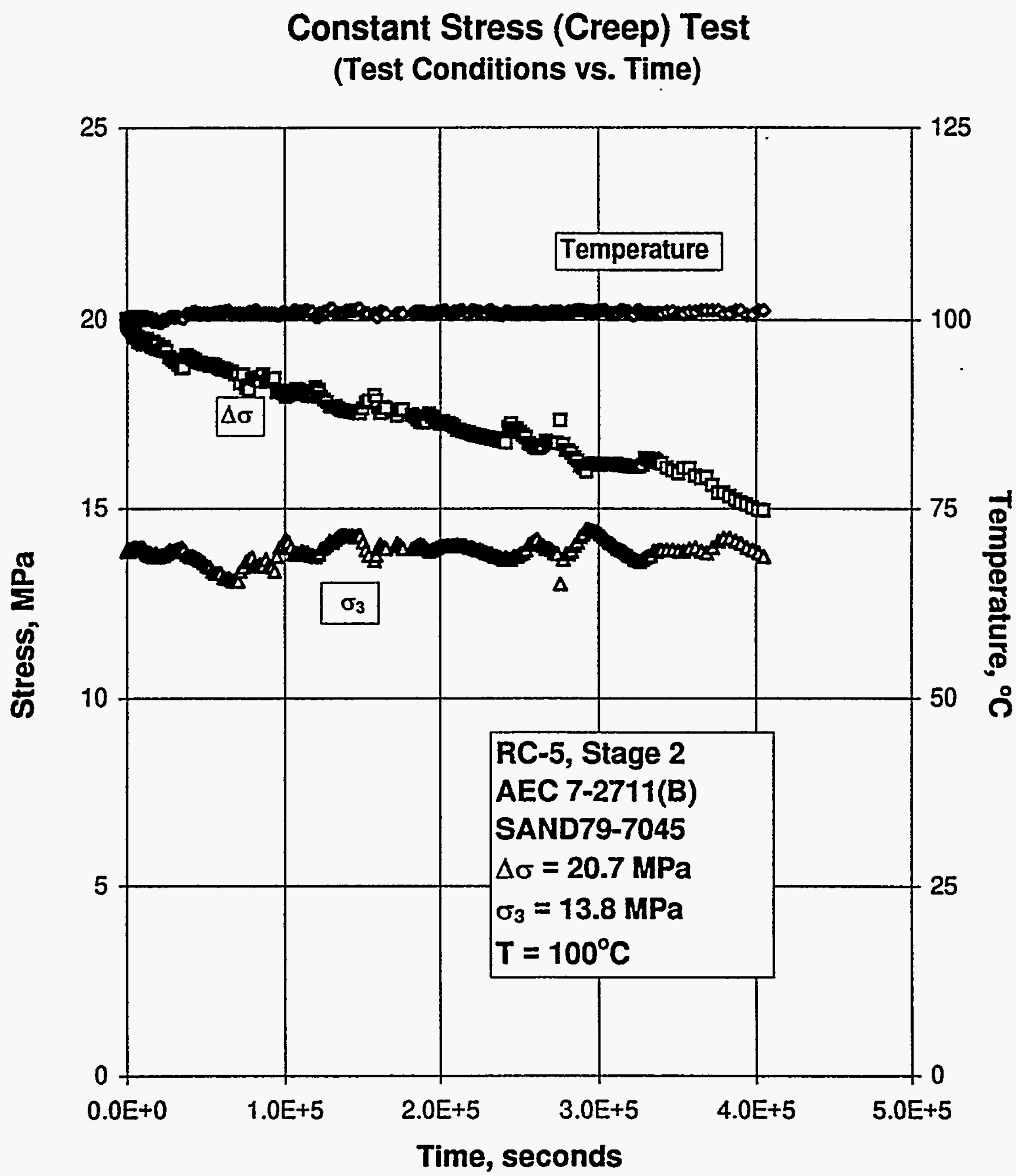

Figure B-189. Test Conditions Versus Time for a Creep Test: Specimen AEC7-2711 (B); Stage 2 of 2.

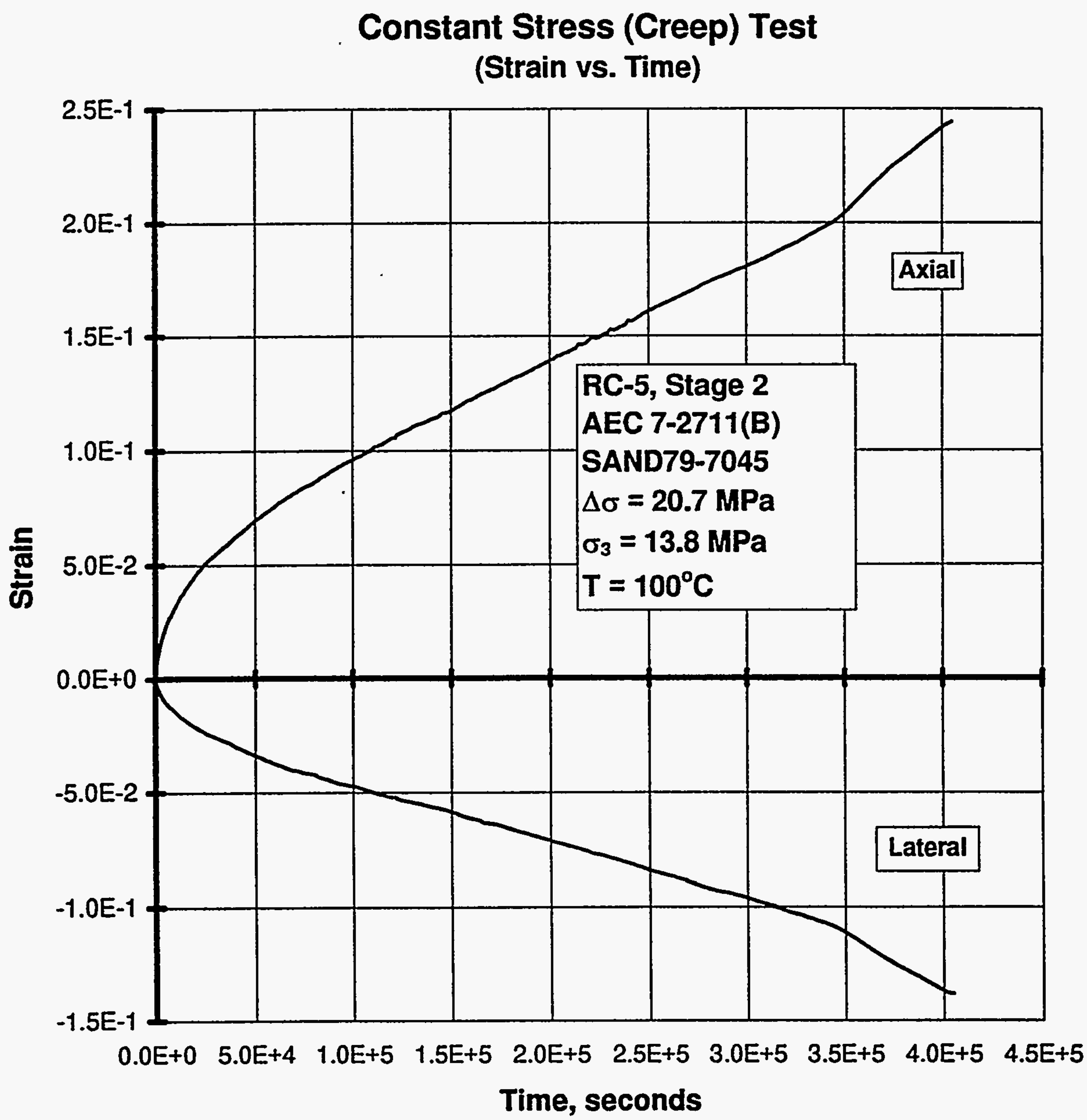

Figure B-190. Axial Strain and Lateral Strain Versus Time for a Creep Test: Specimen AEC7-2711 (B); Stage 2 of 2.

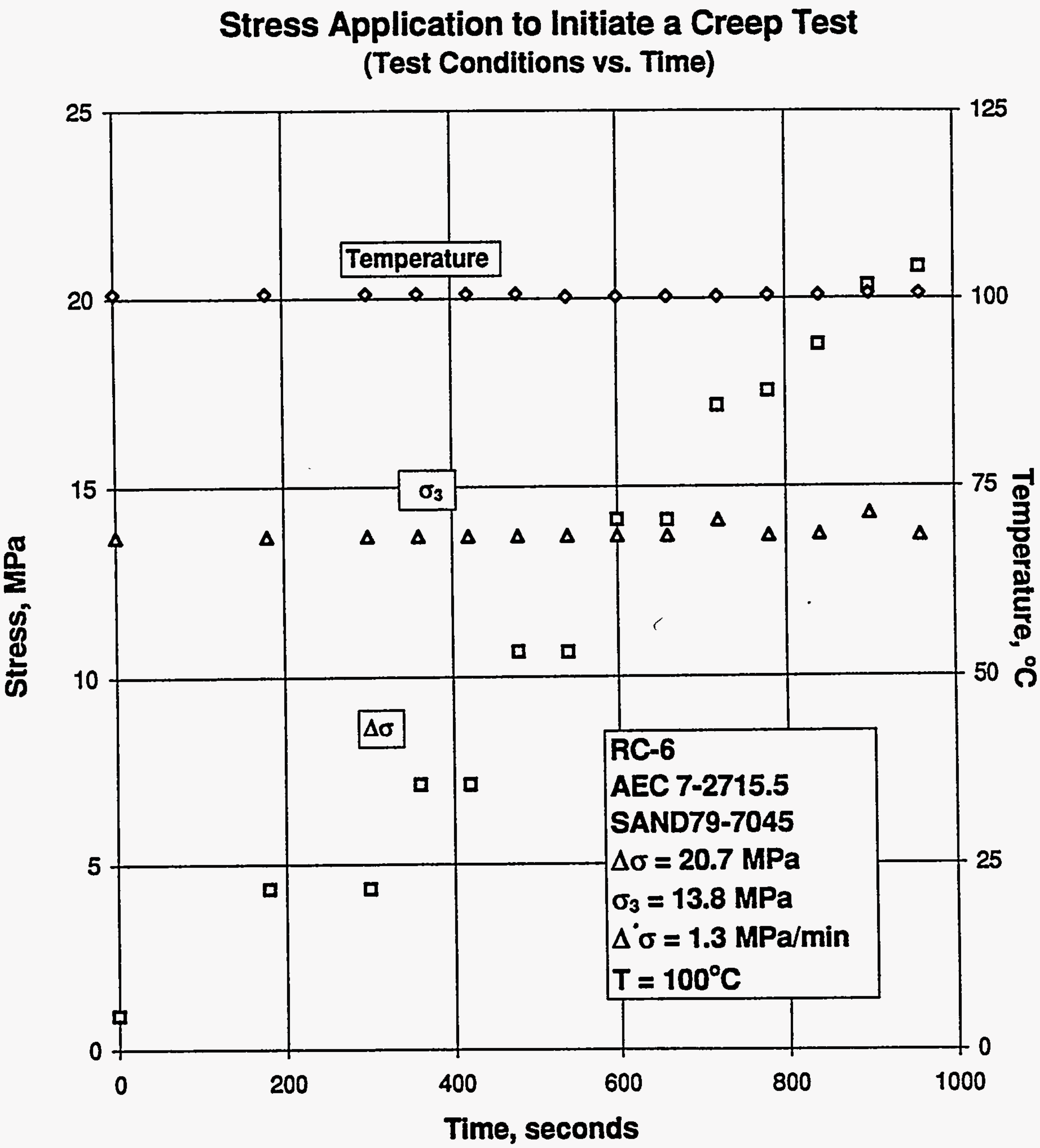

Figure B-191. Test Conditions Versus Time for Stress Application to Initiate a Creep Test: Specimen AEC7-2715.5; Stage 1 of 1.

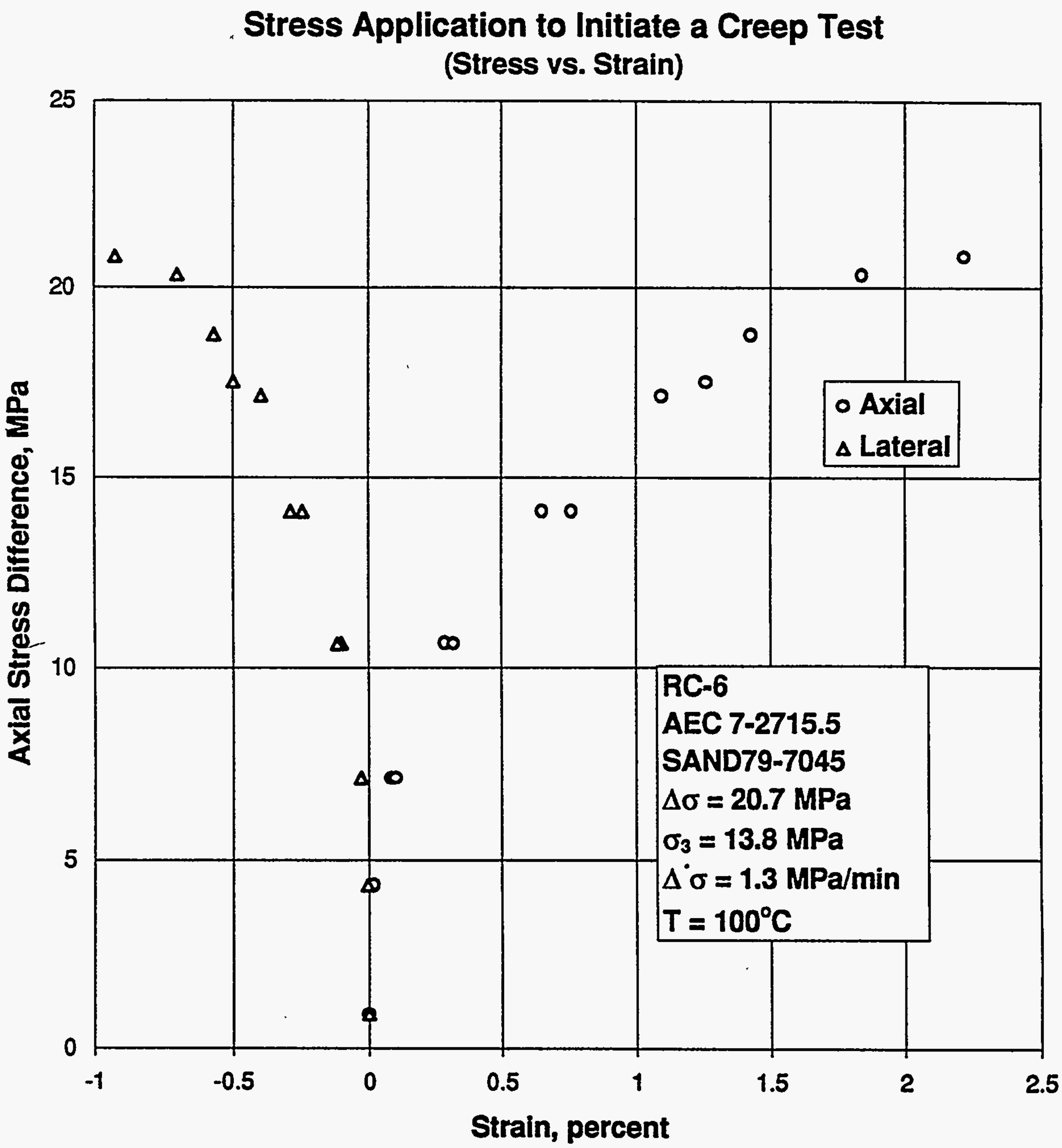

Figure B-192. Axial Stress Difference Versus Axial and Lateral Strain for Stress Application to Initiate a Creep Test: Specimen AEC7-2715.5; Stage 1 of 1.

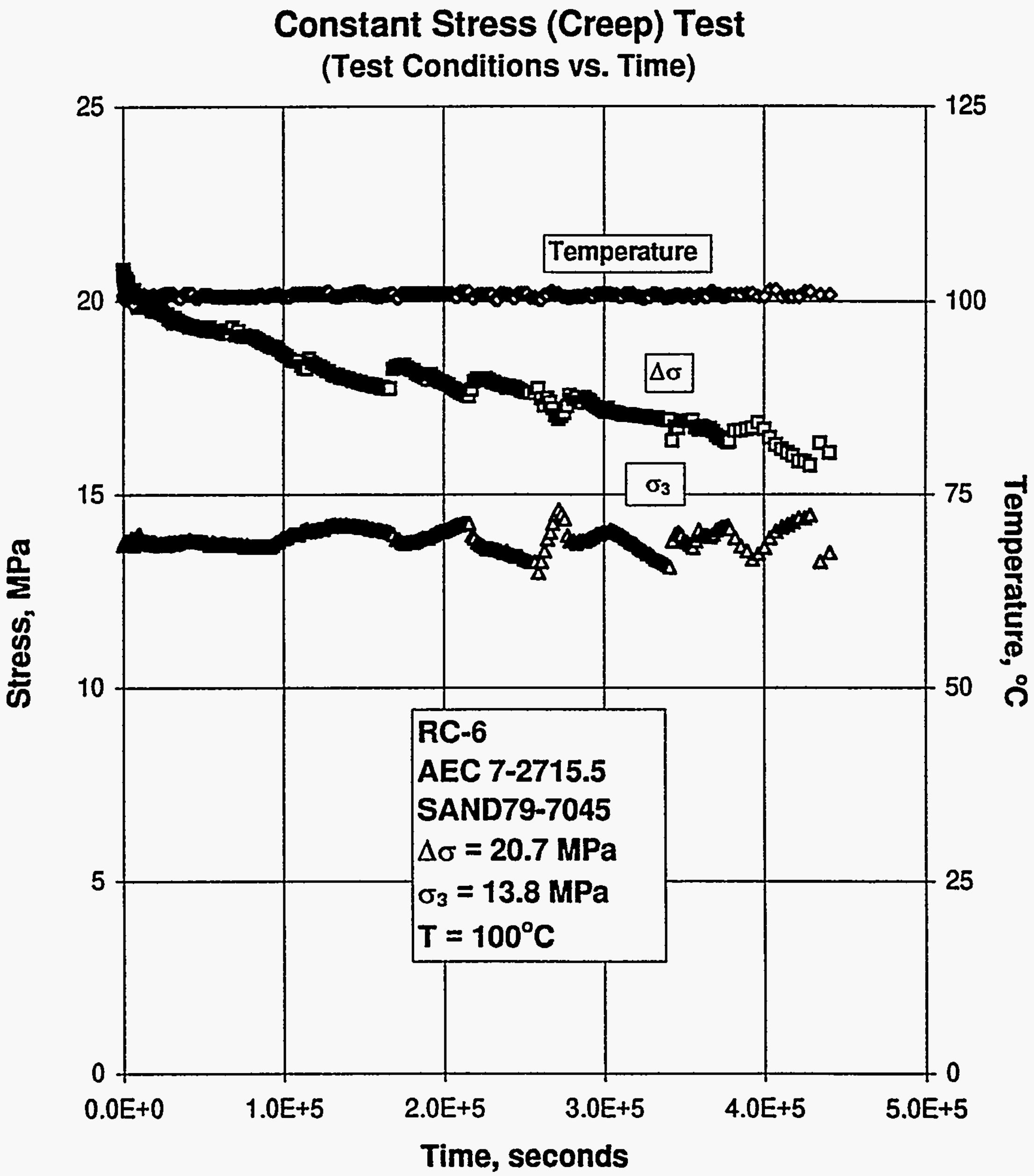

Figure B-193. Test Conditions Versus Time for a Creep Test: Specimen AEC7-2715.5; Stage 1 of 1.

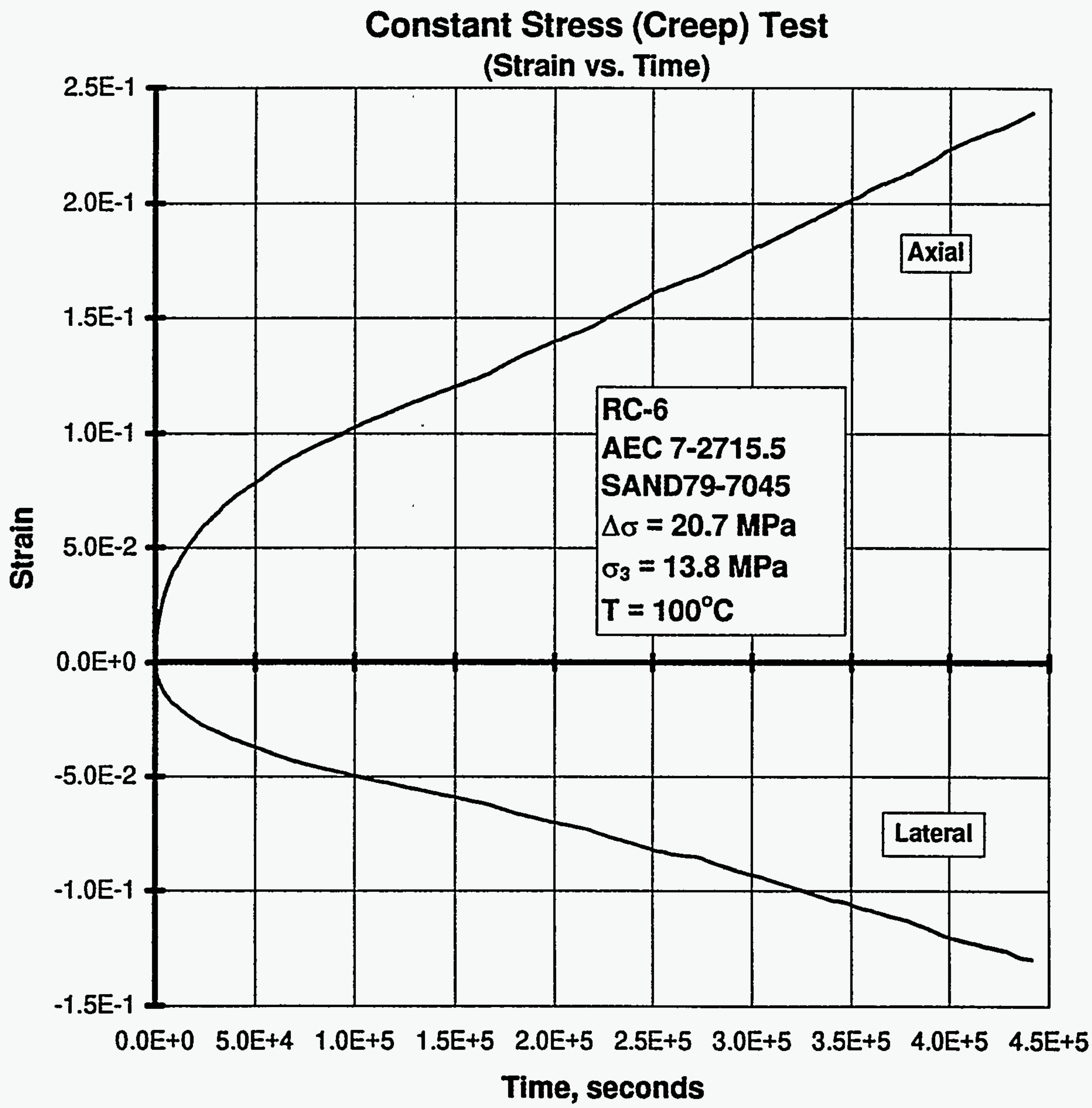

Figure B-194. Axial Strain and Lateral Strain Versus Time for a Creep Test: Specimen AEC7-2715.5; Stage 1 of 1.

APPENDIX C

CREEP TESTS ON WIPP MINE WORKINGS SPECIMENS

FIGURES

FIGURE PAGE

FIGURES (Continued)

FIGURE PAGE

FIGURES (Continued)

FIGURE PAGE

FIGURES (Continued)

FIGURES (Continued)

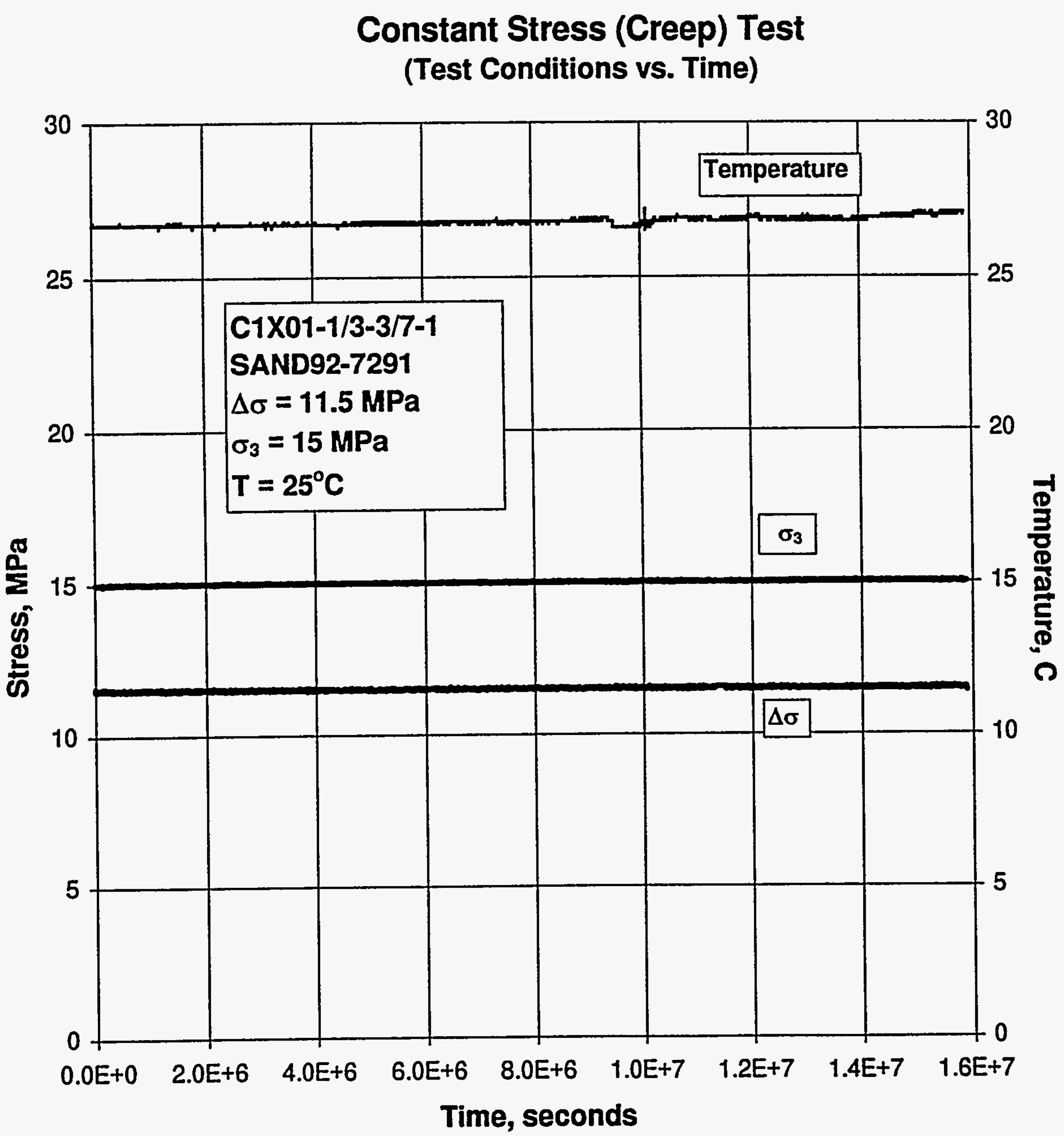

Figure C-1. Test Conditions Versus Time for a Creep Test: Specimen C1X01-1/3-3/7-1; Stage 1 of 1.

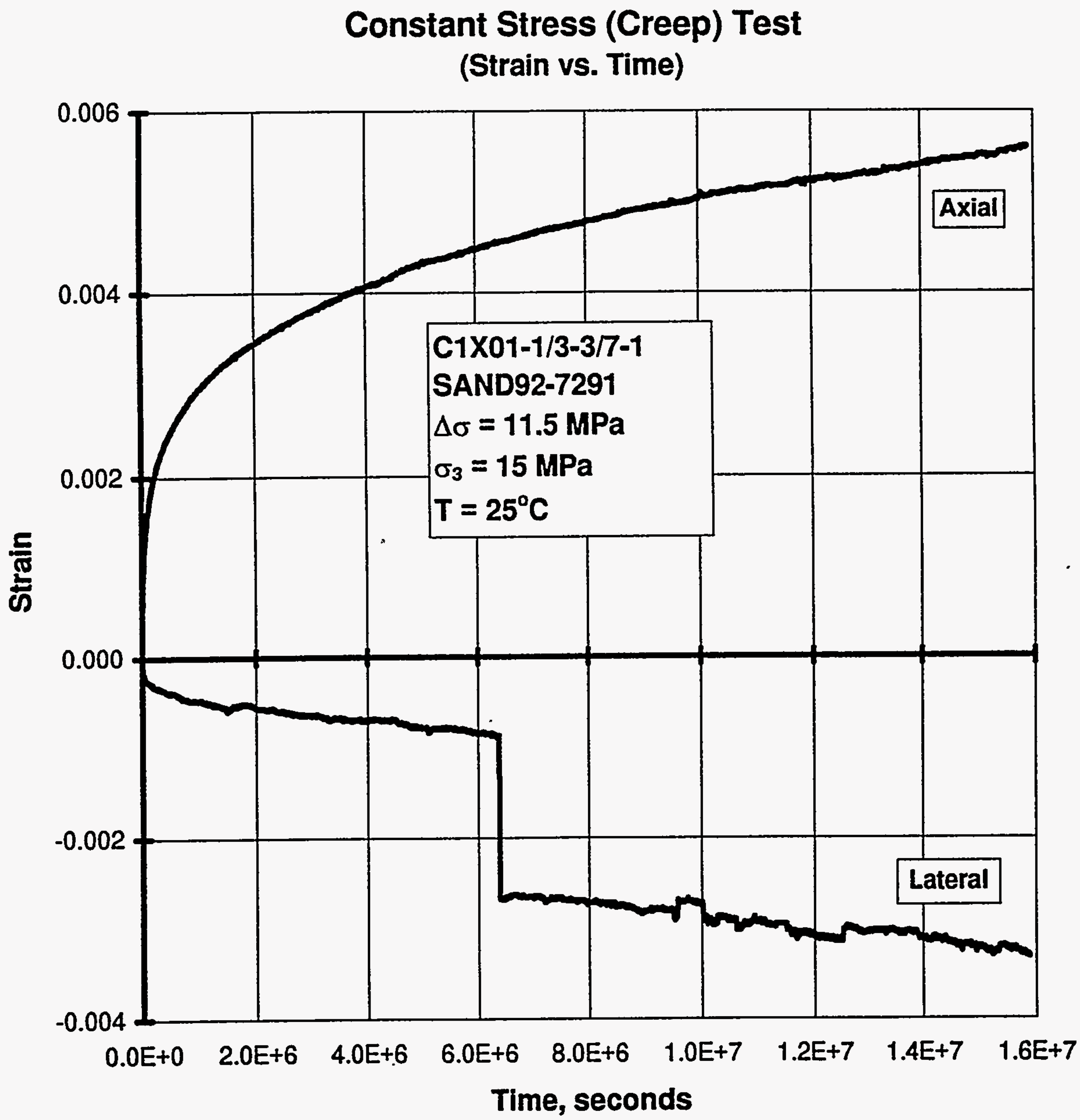

Figure C-2. Axial Strain and Lateral Strain Versus Time for a Creep Test: Specimen C1X01-1/3-3/7-1; Stage 1 of 1.

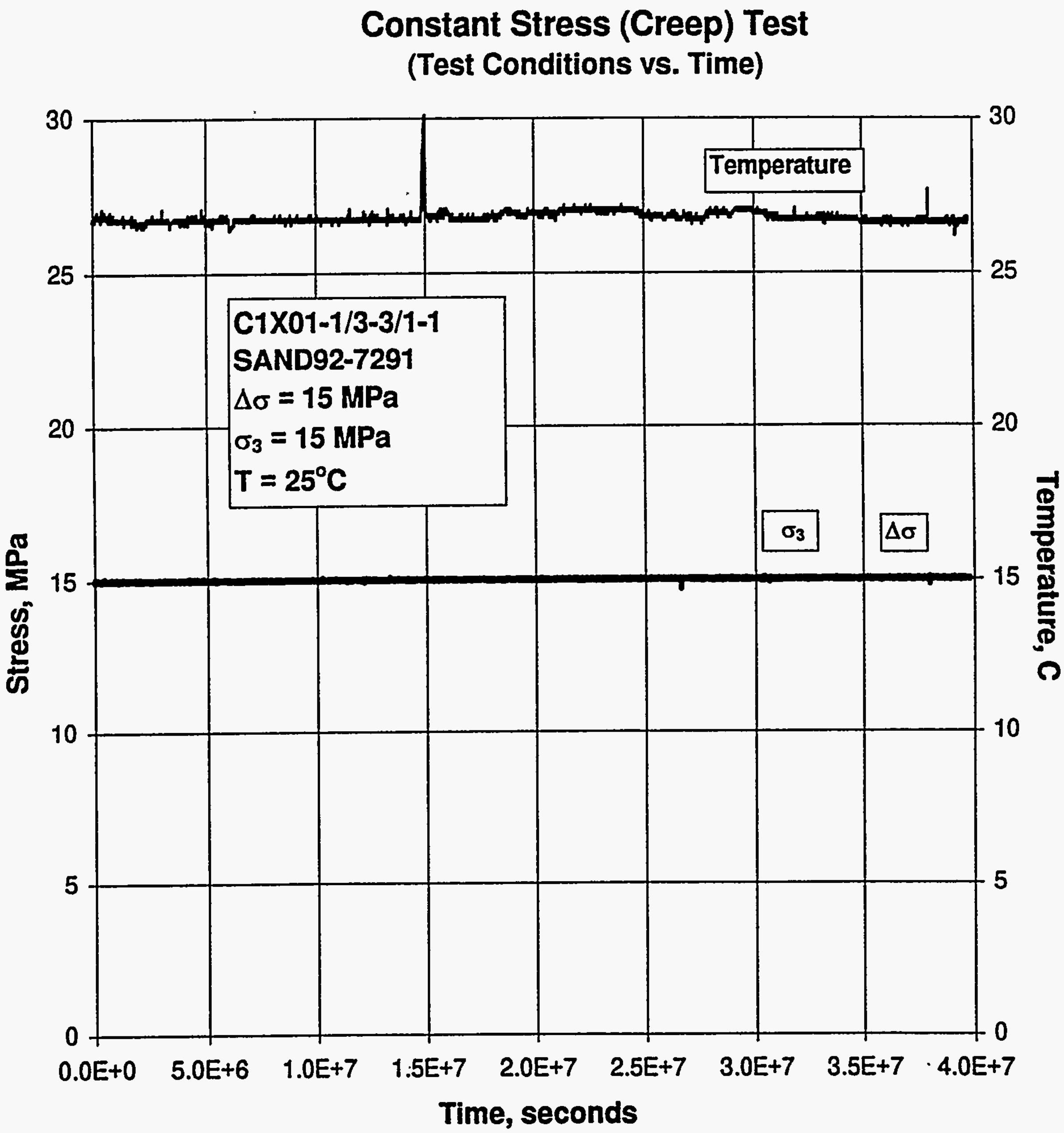

Figure C-3. Test Conditions Versus Time for a Creep Test: Specimen C1X01-1/3-3/1-1; Stage 1 of 1.

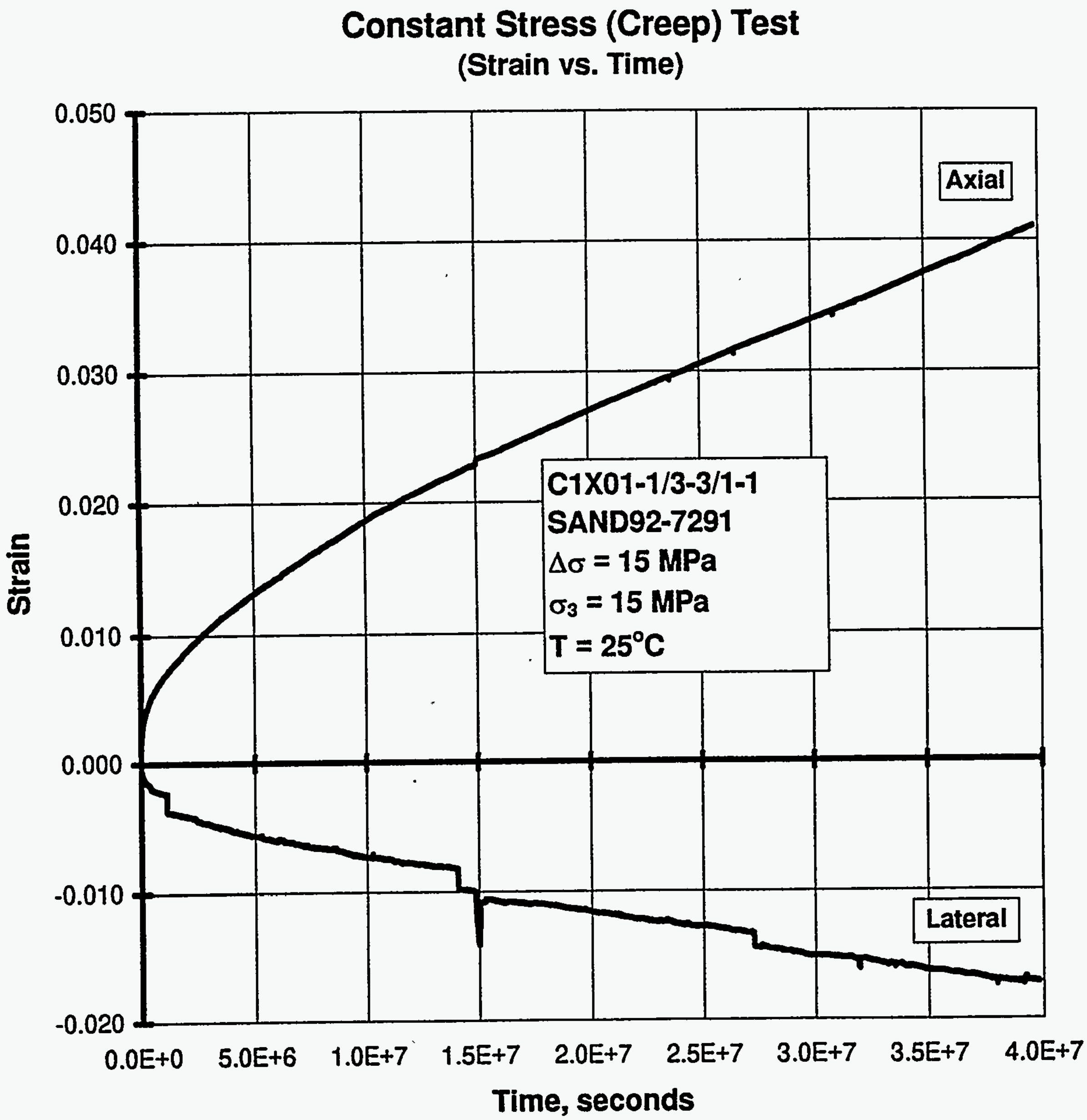

Figure C-4. Axial Strain and Lateral Strain Versus Time for a Creep Test: Specimen C1X01-1/3-3/1-1; Stage 1 of 1.

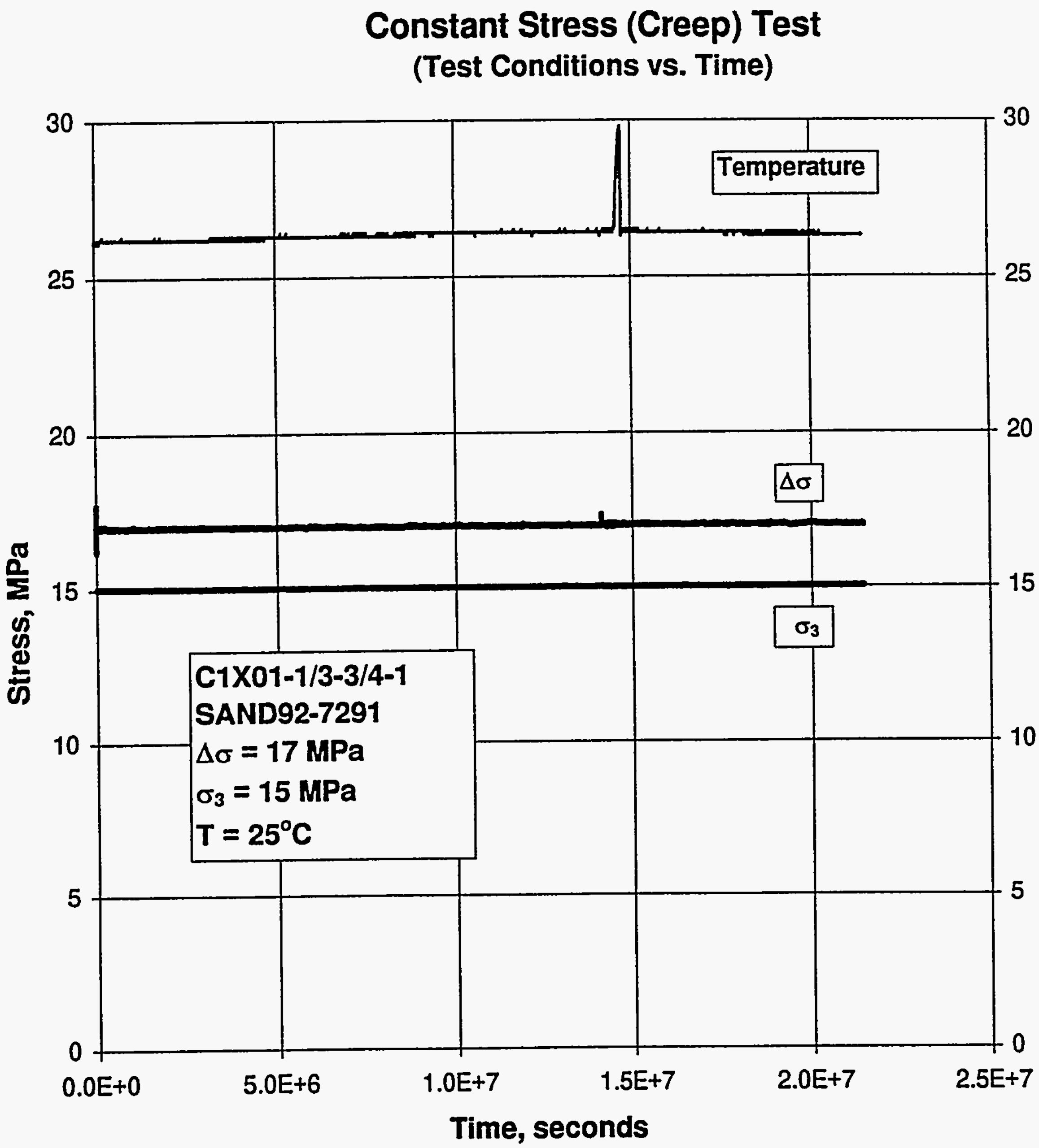

Figure C-5. Test Conditions Versus Time for a Creep Test: Specimen C1X01-1/3-3/4-1; Stage 1 of 1.

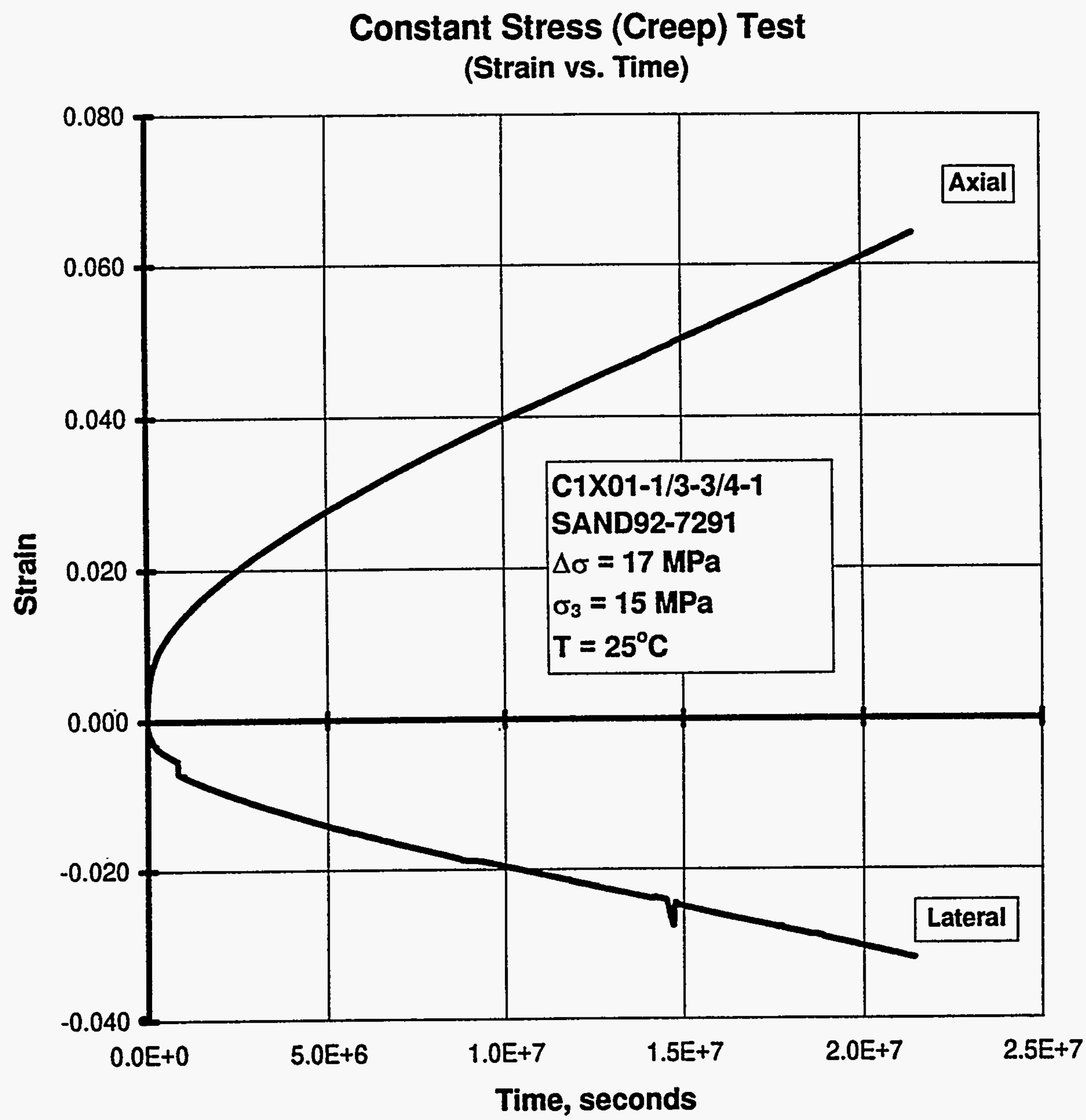

Figure C-6. Axial Strain and Lateral Strain Versus Time for a Creep Test: Specimen C1X01-1/3-3/4-1; Stage 1 of 1.

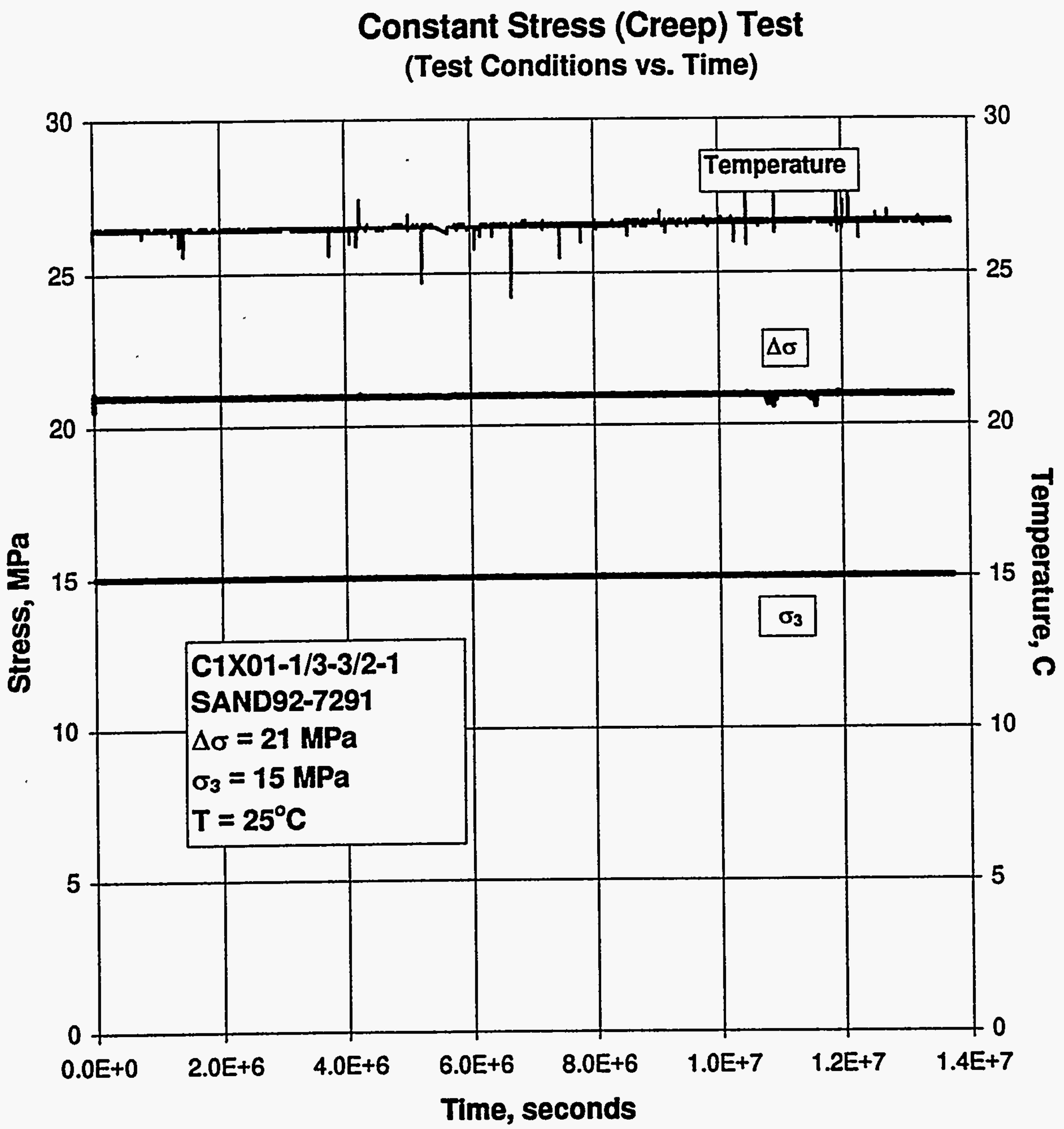

Figure C-7. Test Conditions Versus Time for a Creep Test: Specimen C1X01-1/3-3/2-1; Stage 1 of 1.

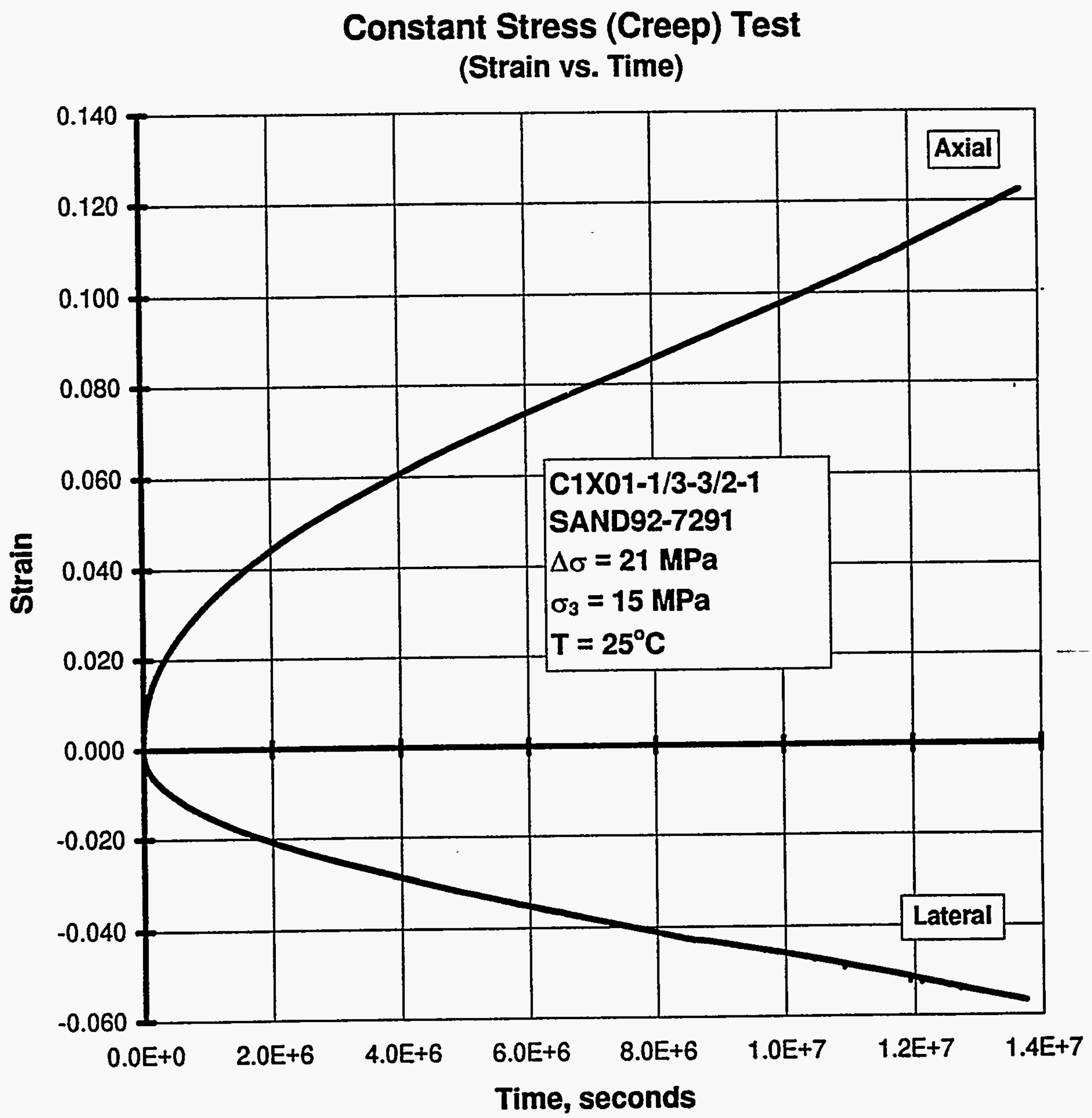

Figure C-8. Axial Strain and Lateral Strain Versus Time for a Creep Test: Specimen C1X01-1/3-3/2-1; Stage 1 of 1.

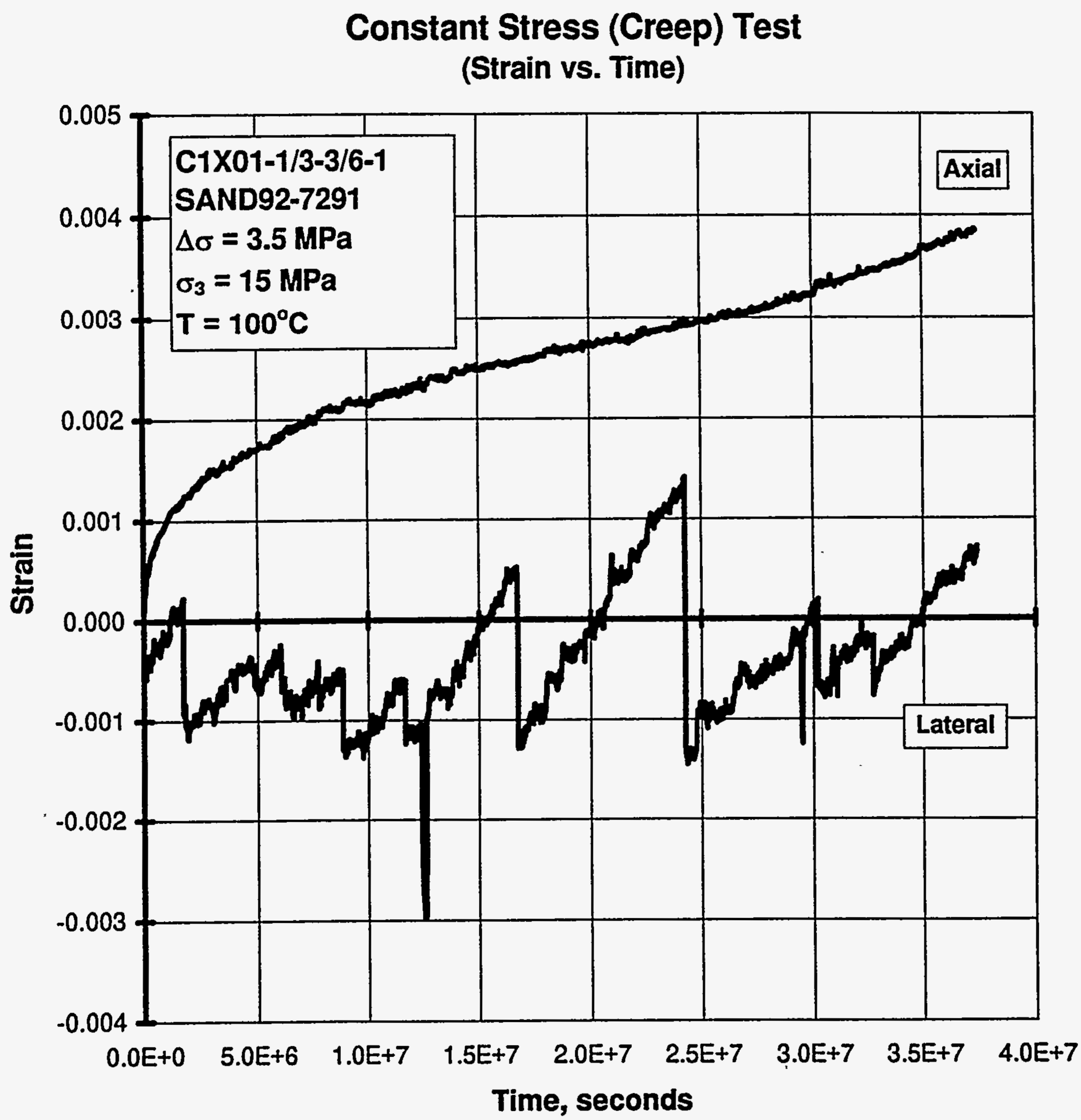

Figure C-9. Test Conditions Versus Time for a Creep Test: Specimen C1X01-1/3-3/6-1; Stage 1 of 1.

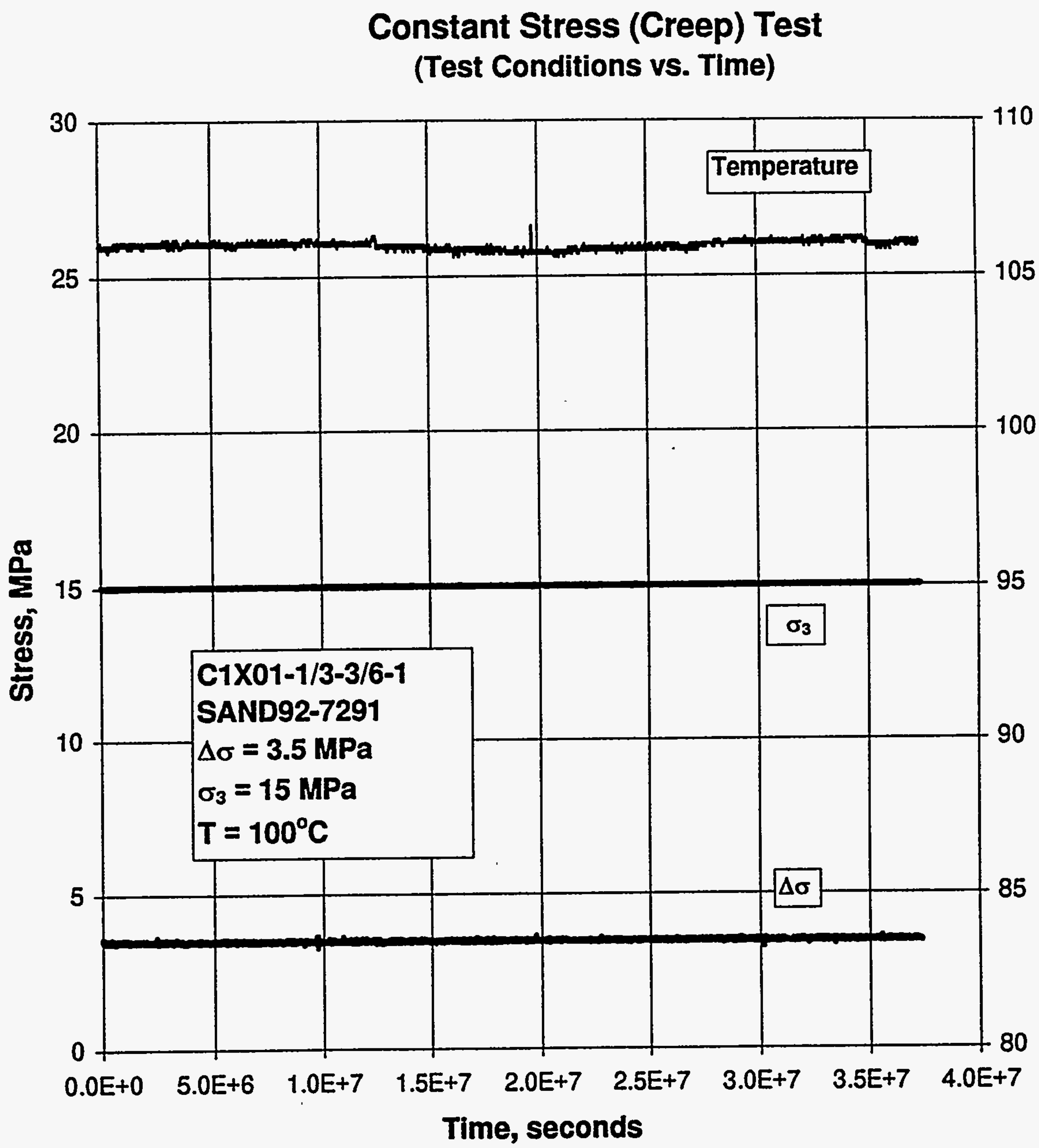

Figure C-10. Axial Strain and Lateral Strain Versus Time for a Creep Test: Specimen C1X01-1/3-3/6-1; Stage 1 of 1.

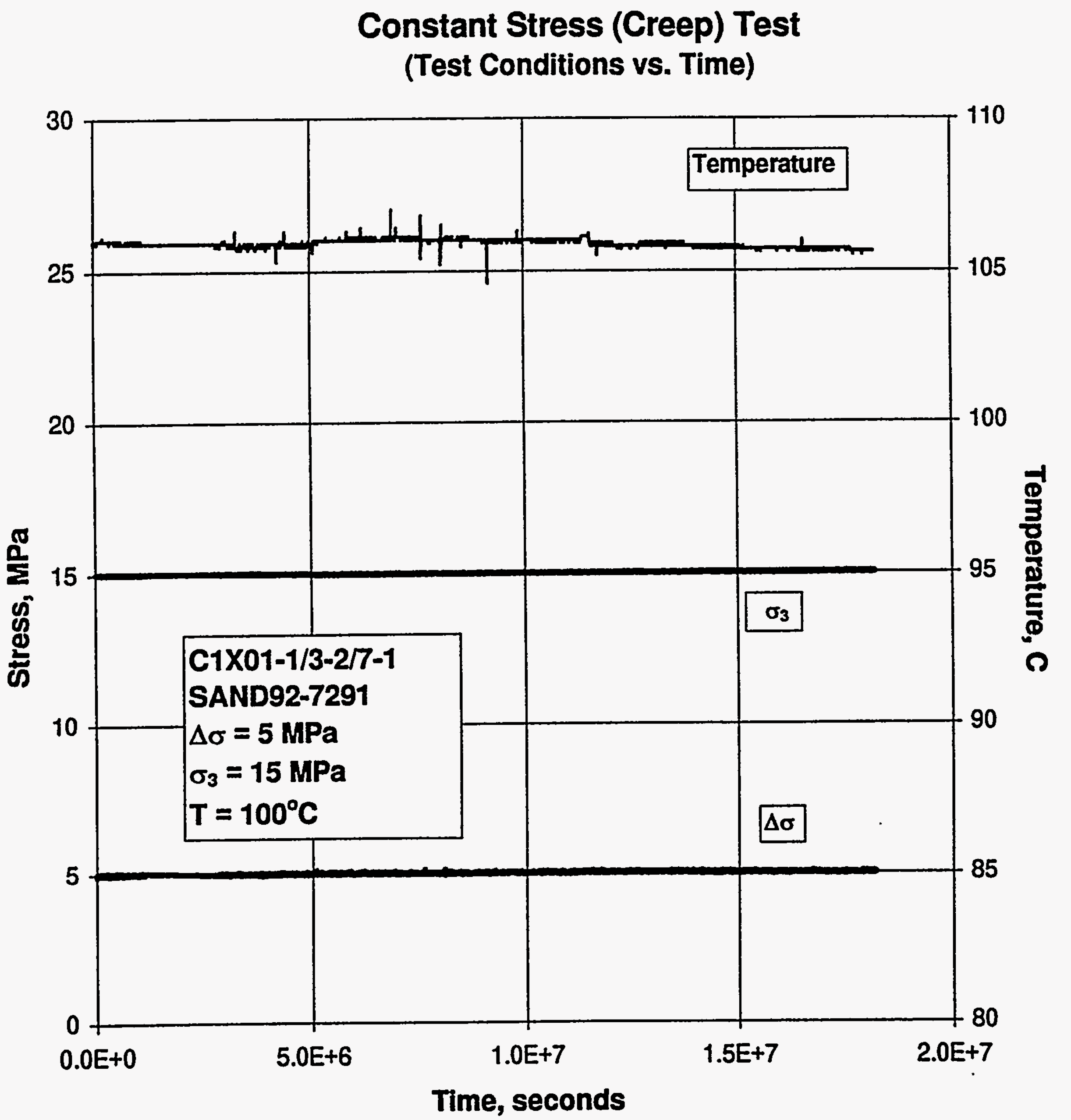

Figure C-11. Test Conditions Versus Time for a Creep Test: Specimen C1X01-1/3-2/7-1; Stage 1 of 1.

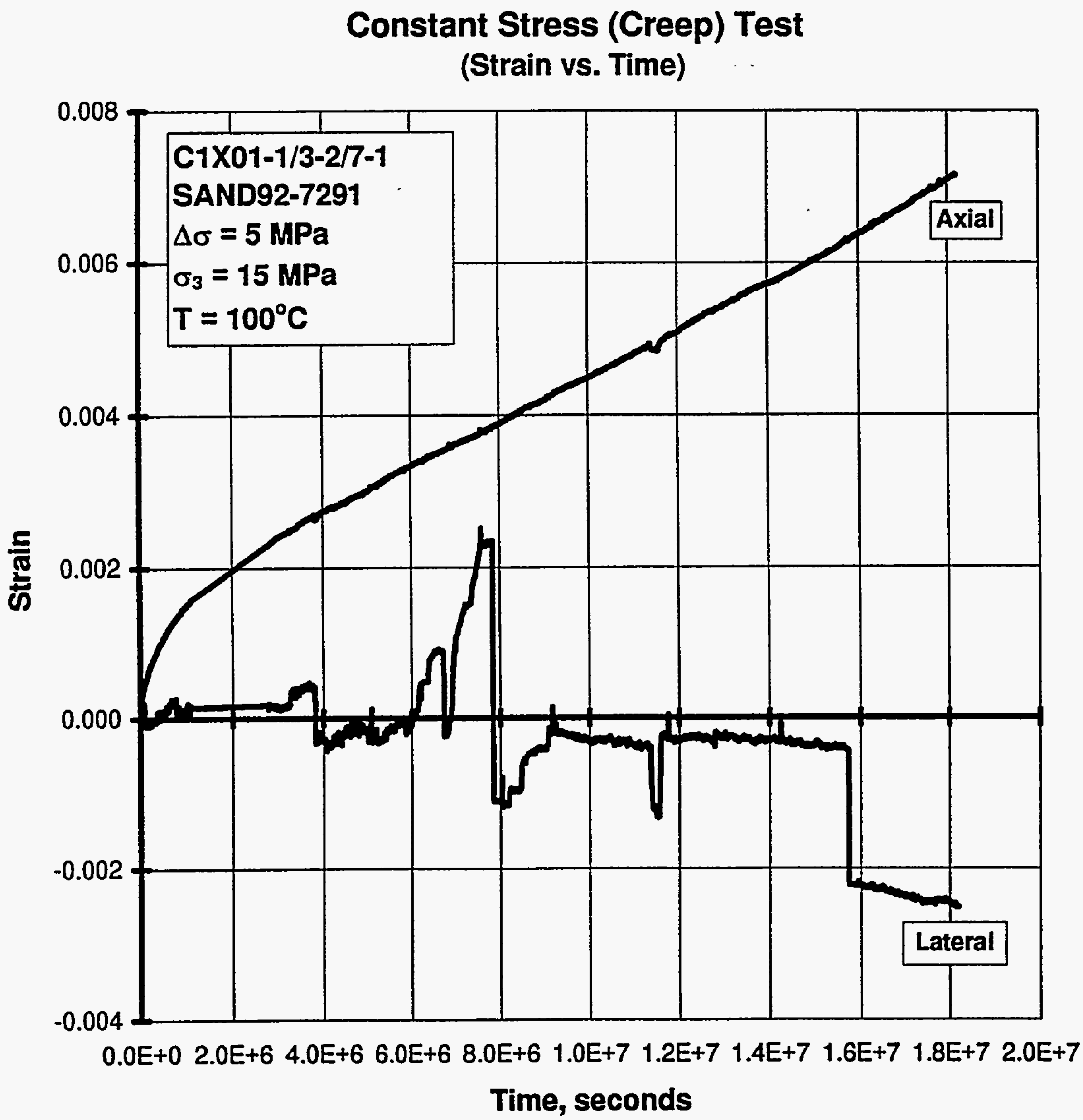

Figure C-12. Axial Strain and Lateral Strain Versus Time for a Creep Test: Specimen C1X01-1/3-2/7-1; Stage 1 of 1.

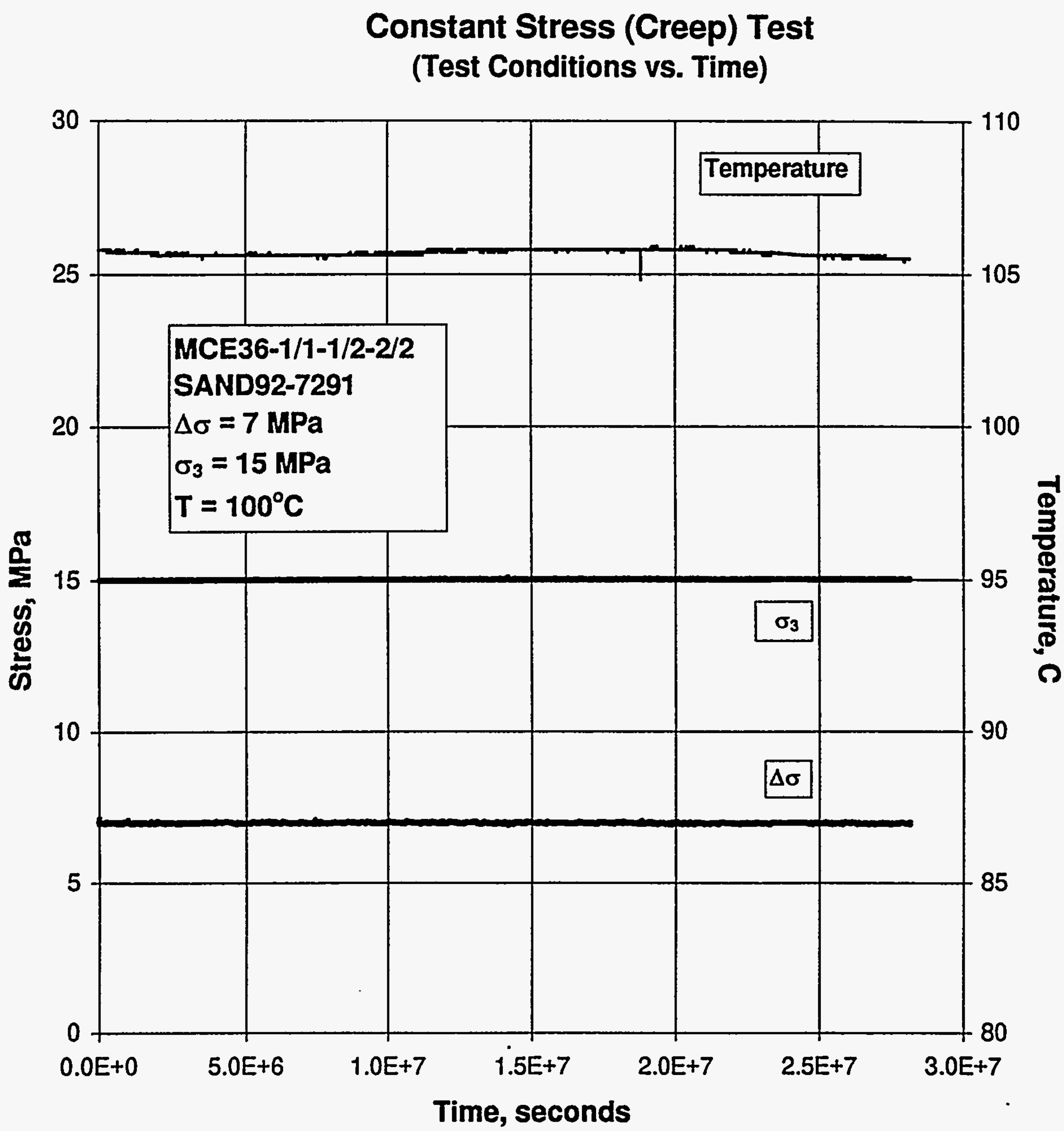

Figure C-13. Test Conditions Versus Time for a Creep Test: Specimen MCE36-1/1-1/2-2/2; Stage 1 of 1.

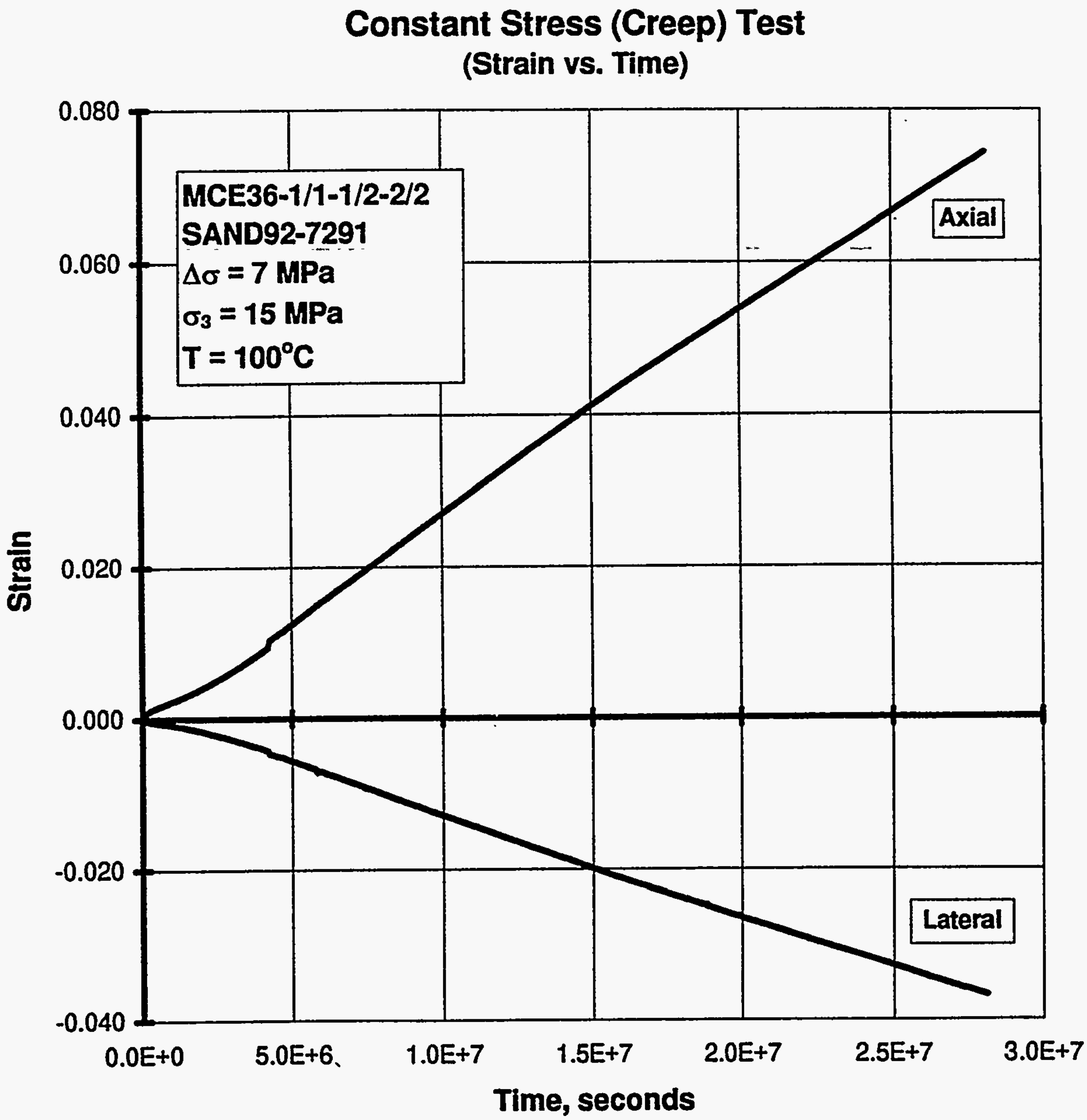

Figure C-14. Axial Strain and Lateral Strain Versus Time for a Creep Test: Specimen MCE36-1/1-1/2-2/2; Stage 1 of 1.

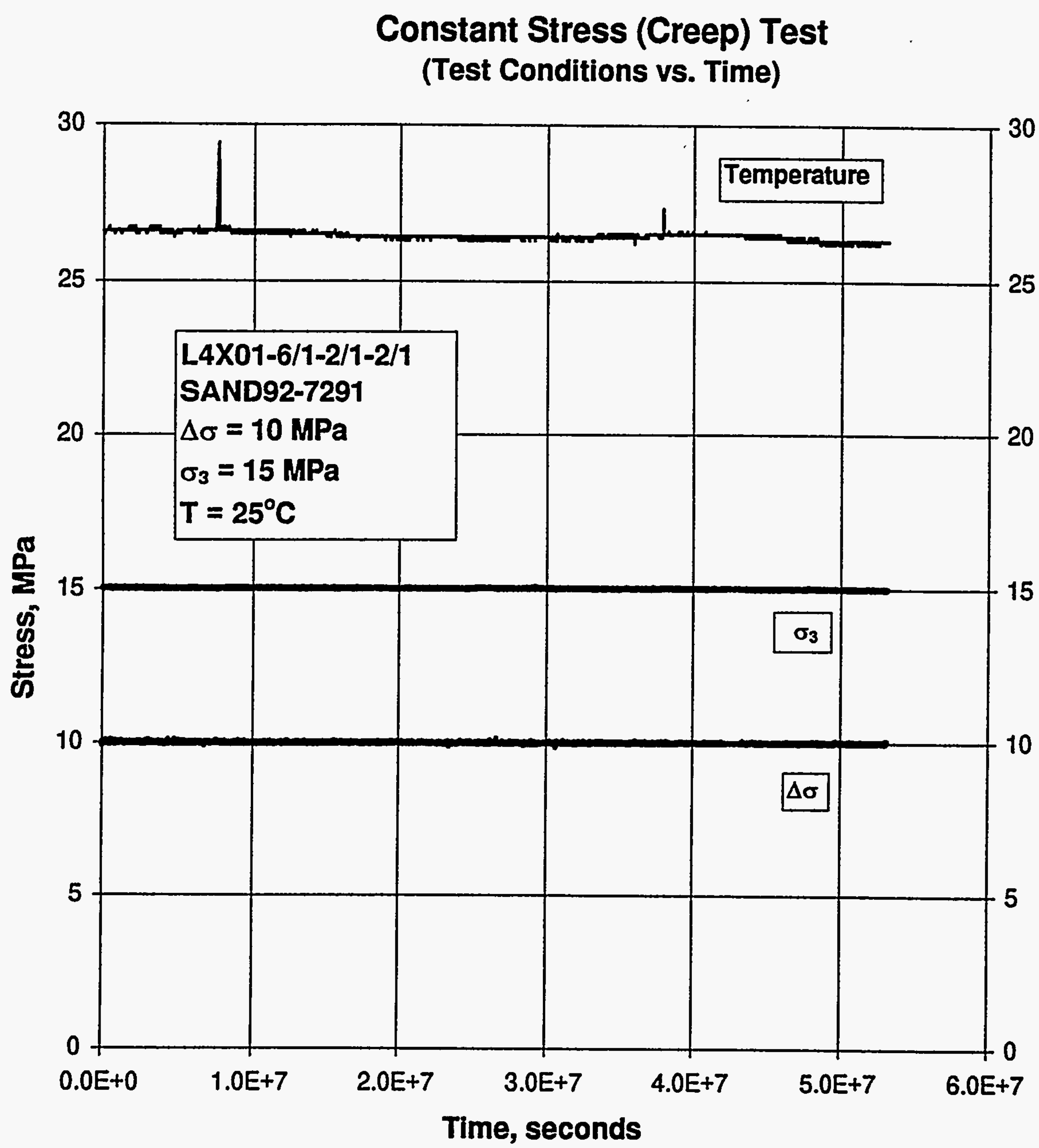

Figure C-15. Test Conditions Versus Time for a Creep Test: Specimen L4X01-6/1-2/1-2/1; Stage 1 of 1 (Argillaceous Salt).

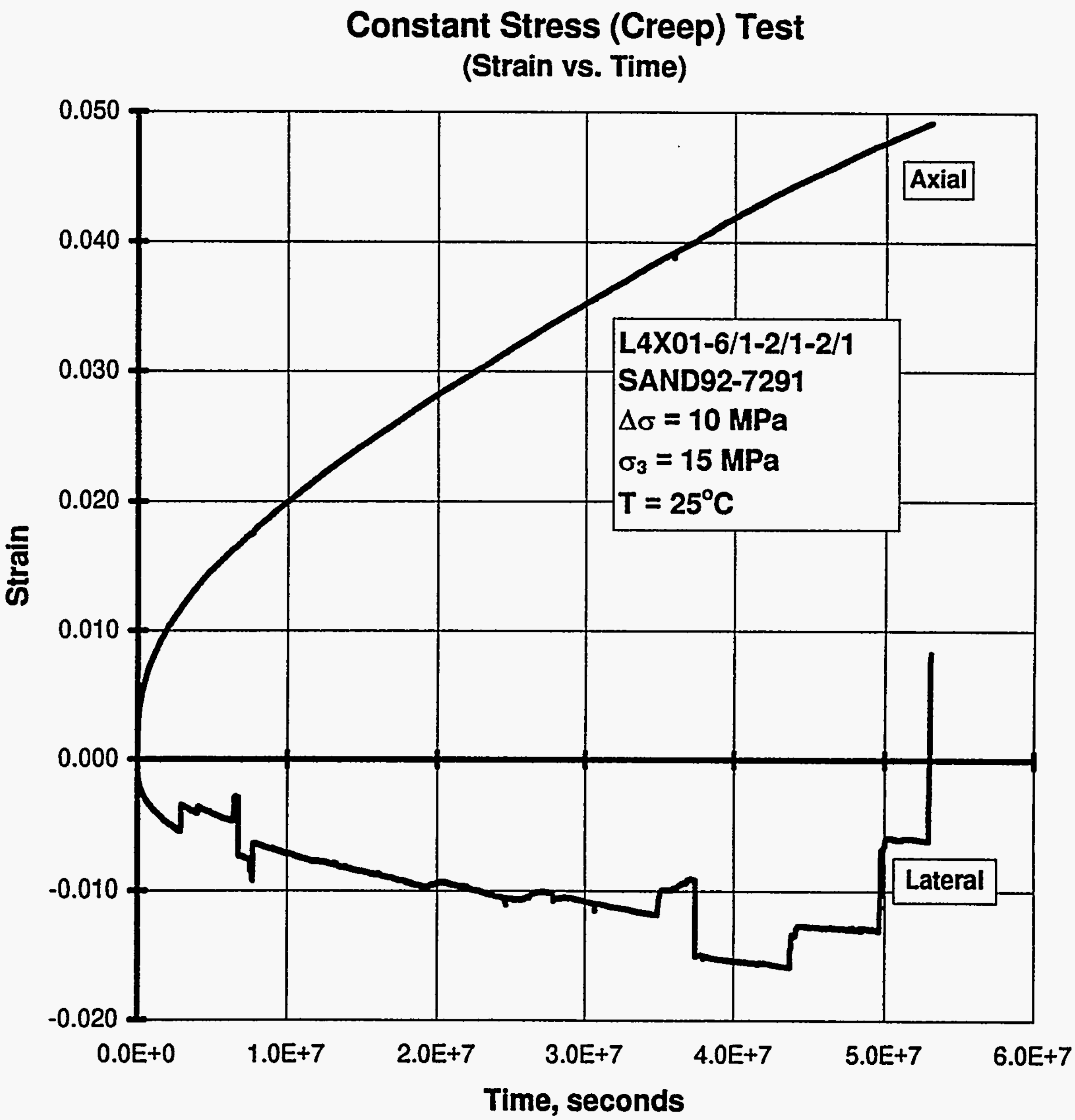

Figure C-16. Axial Strain and Lateral Strain Versus Time for a Creep Test: Specimen L4X01-6/1-2/1-2/1; Stage 1 of 1 (Argillaceous Salt).

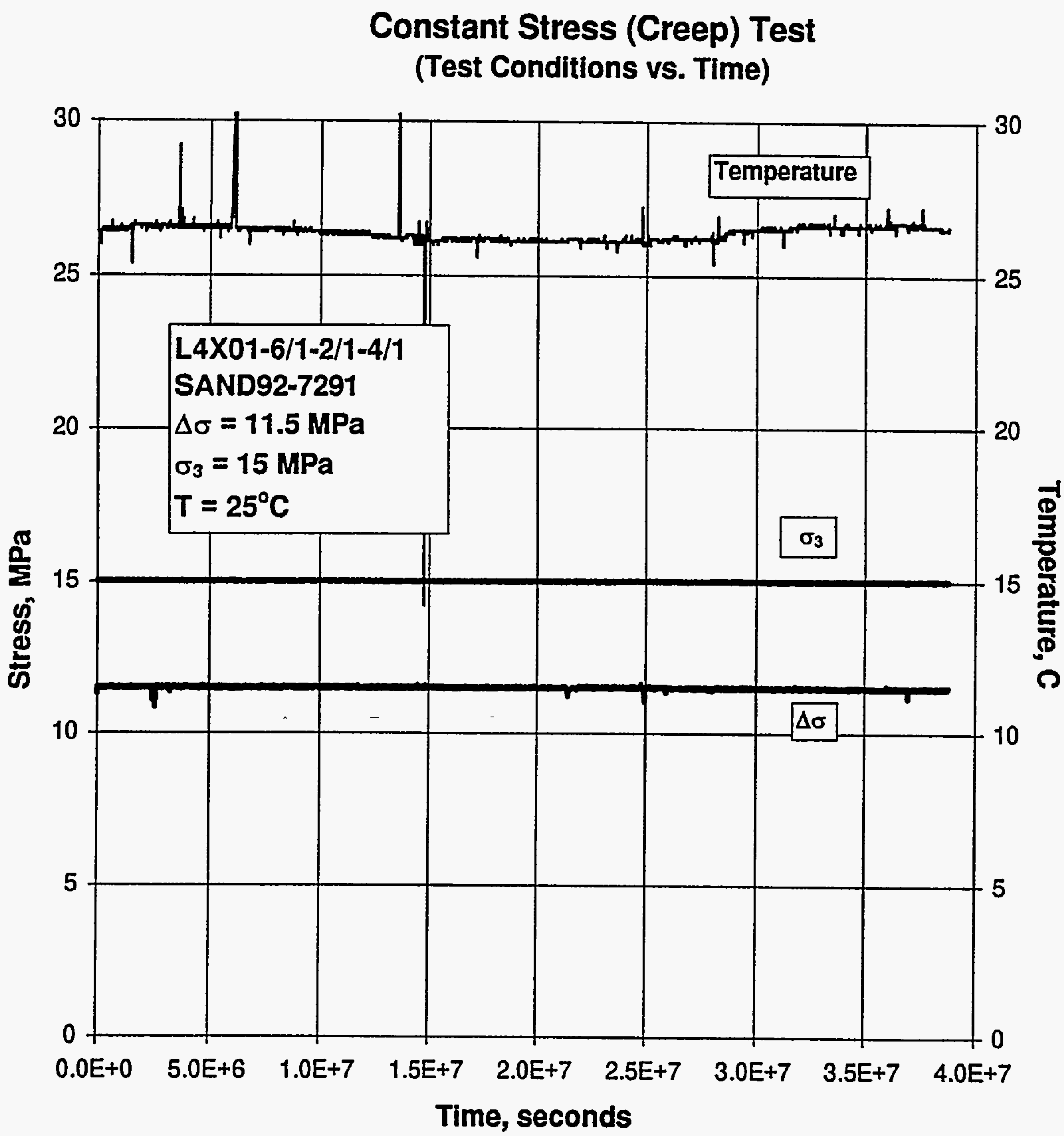

Figure C-17. Test Conditions Versus Time for a Creep Test: Specimen L4X01-6/1-2/1-4/1; Stage 1 of 1 (Argillaceous Salt).

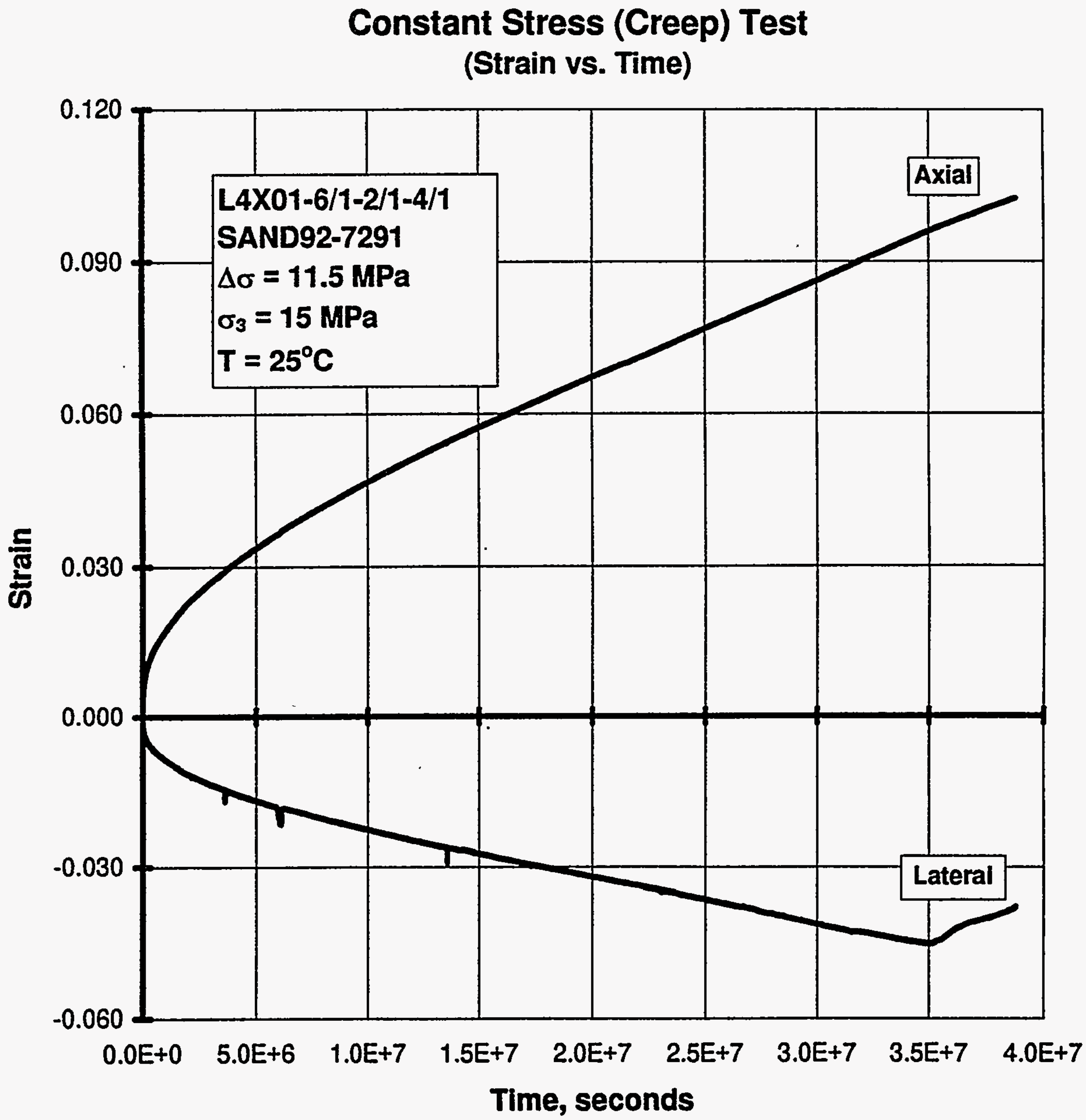

Figure C-18. Axial Strain and Lateral Strain Versus Time for a Creep Test: Specimen L4X01-6/1-2/1-4/1; Stage 1 of 1 (Argillaceous Salt).

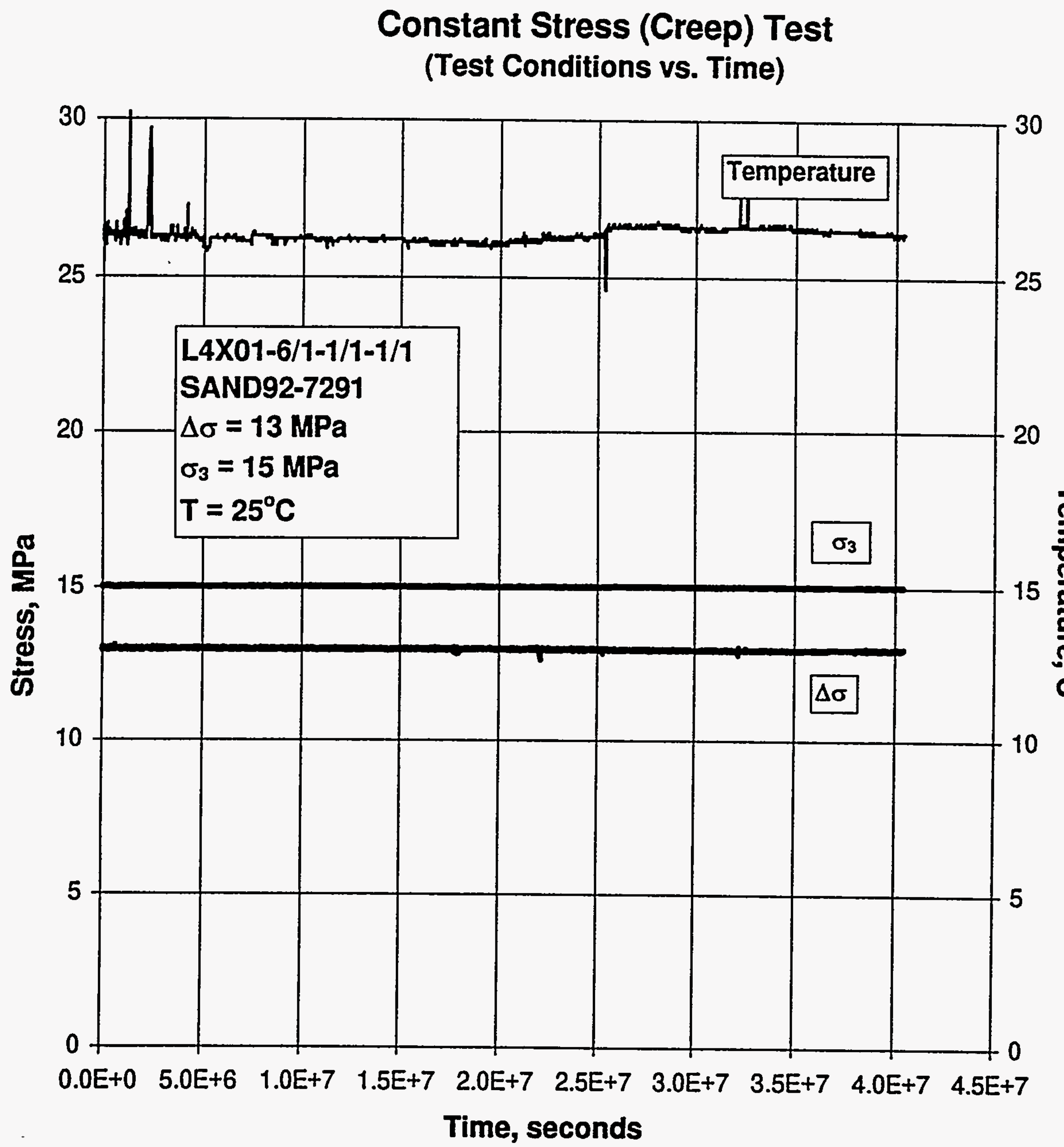

Figure C-19. Test Conditions Versus Time for a Creep Test: Specimen L4X01-6/1-1/1-1/1; Stage 1 of 1 (Argillaceous Salt).

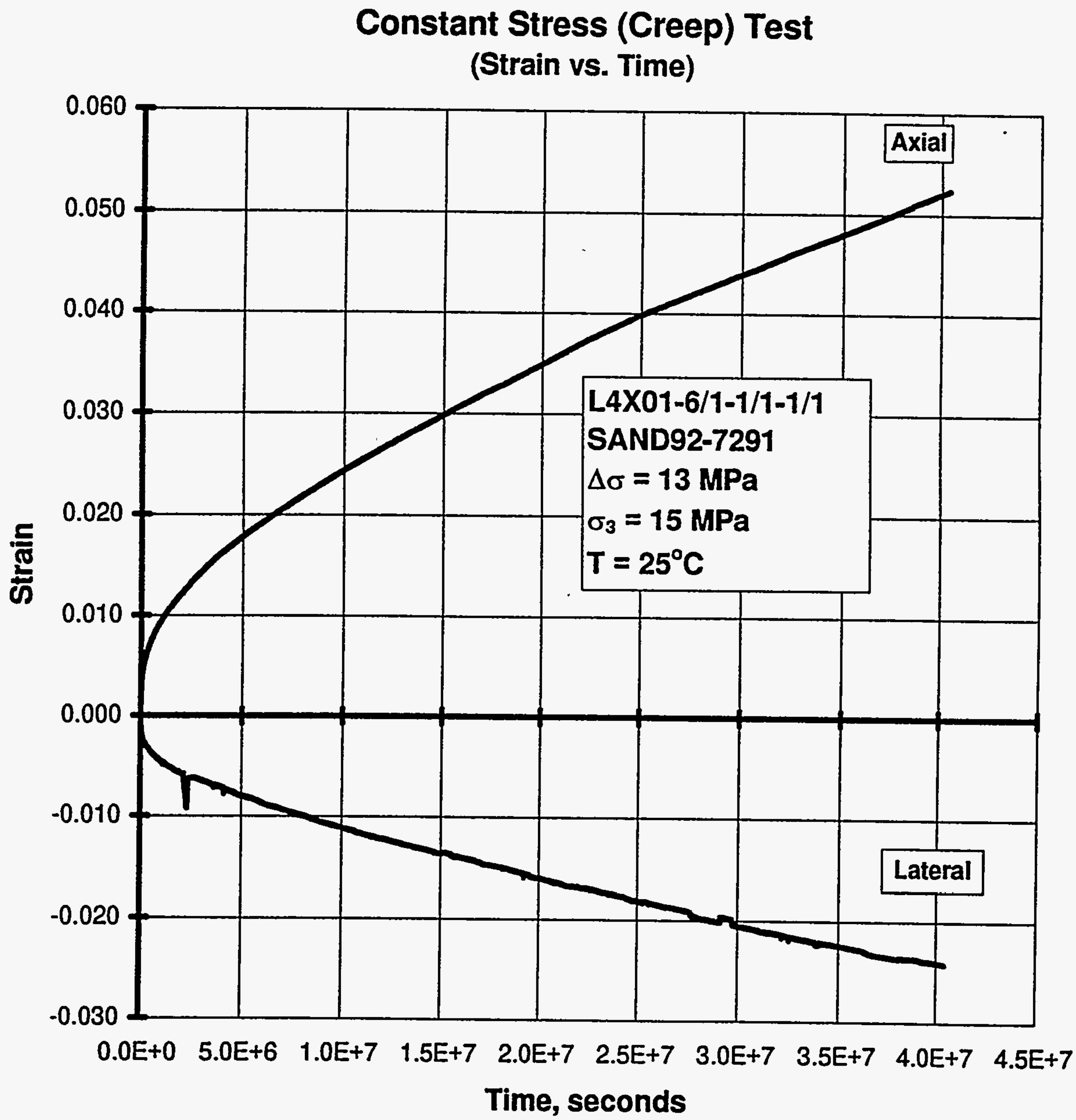

Figure C-20. Axial Strain and Lateral Strain Versus Time for a Creep Test: Specimen L4X01-6/1-1/1-1/1; Stage 1 of 1 (Argillaceous Salt).

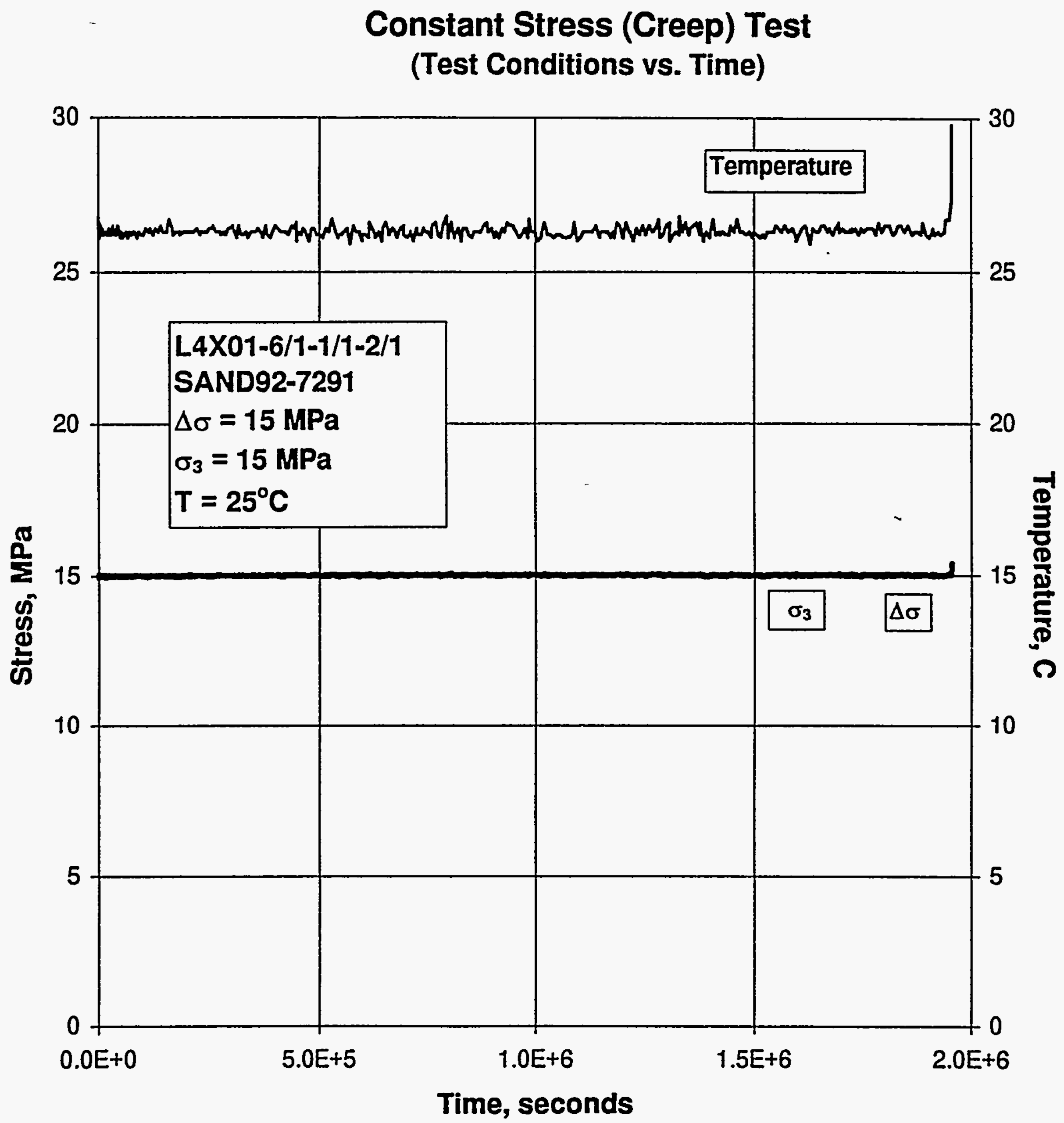

Figure C-21. Test Conditions Versus Time for a Creep Test: Specimen L4X01-6/1-1/1-2/1; Stage 1 of 1 (Argillaceous Salt).

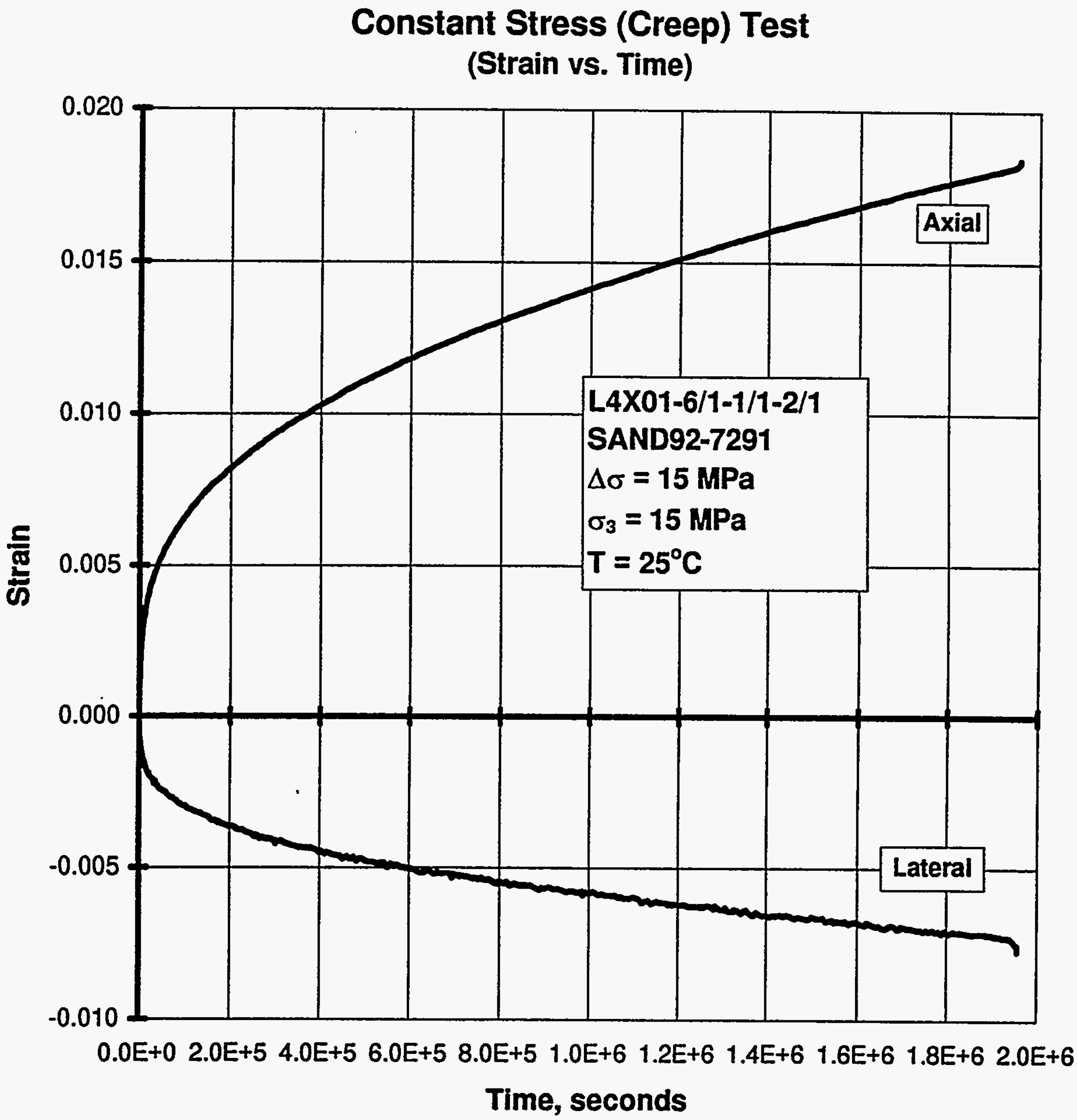

Figure C-22. Axial Strain and Lateral Strain Versus Time for a Creep Test: Specimen L4X01-6/1-1/1-2/1; Stage 1 of 1 (Argillaceous Salt).

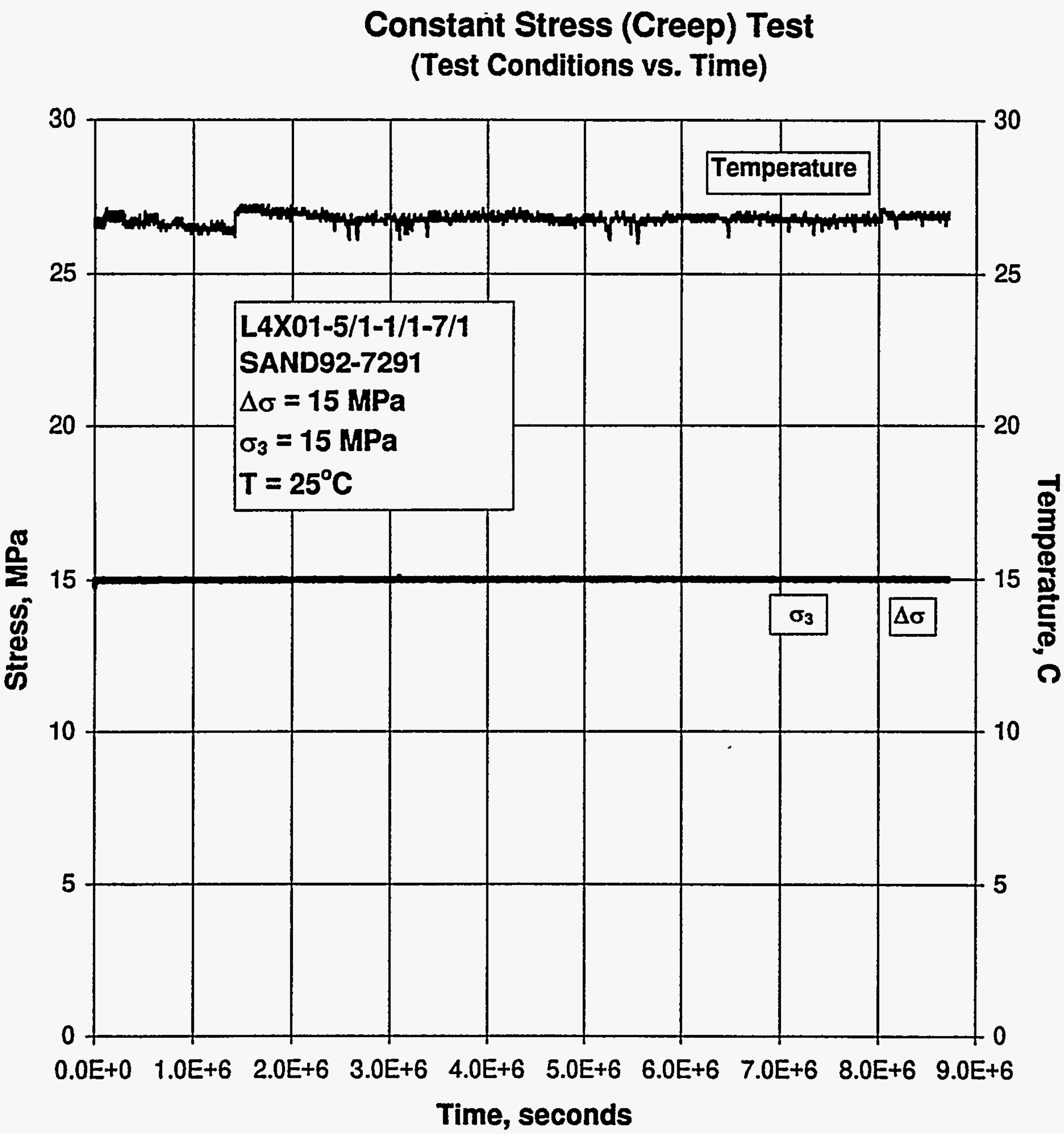

Figure C-23. Test Conditions Versus Time for a Creep Test: Specimen L4X01-5/1-1/1-7/1; Stage 1 of 1 (Argillaceous Salt).

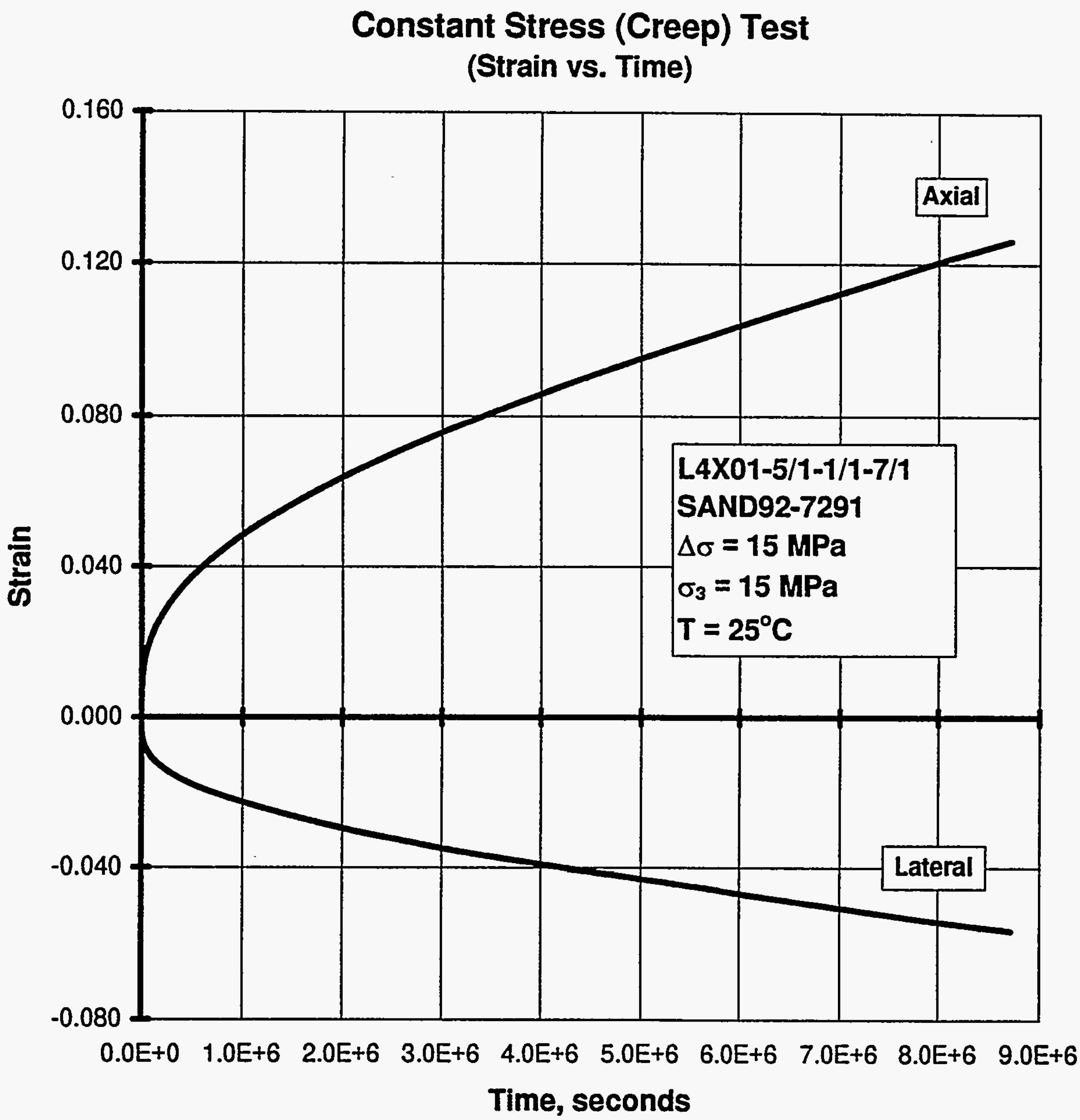

Figure C-24. Axial Strain and Lateral Strain Versus Time for a Creep Test: Specimen L4X01-5/1-1/1-7/1; Stage 1 of 1 (Argillaceous Salt).

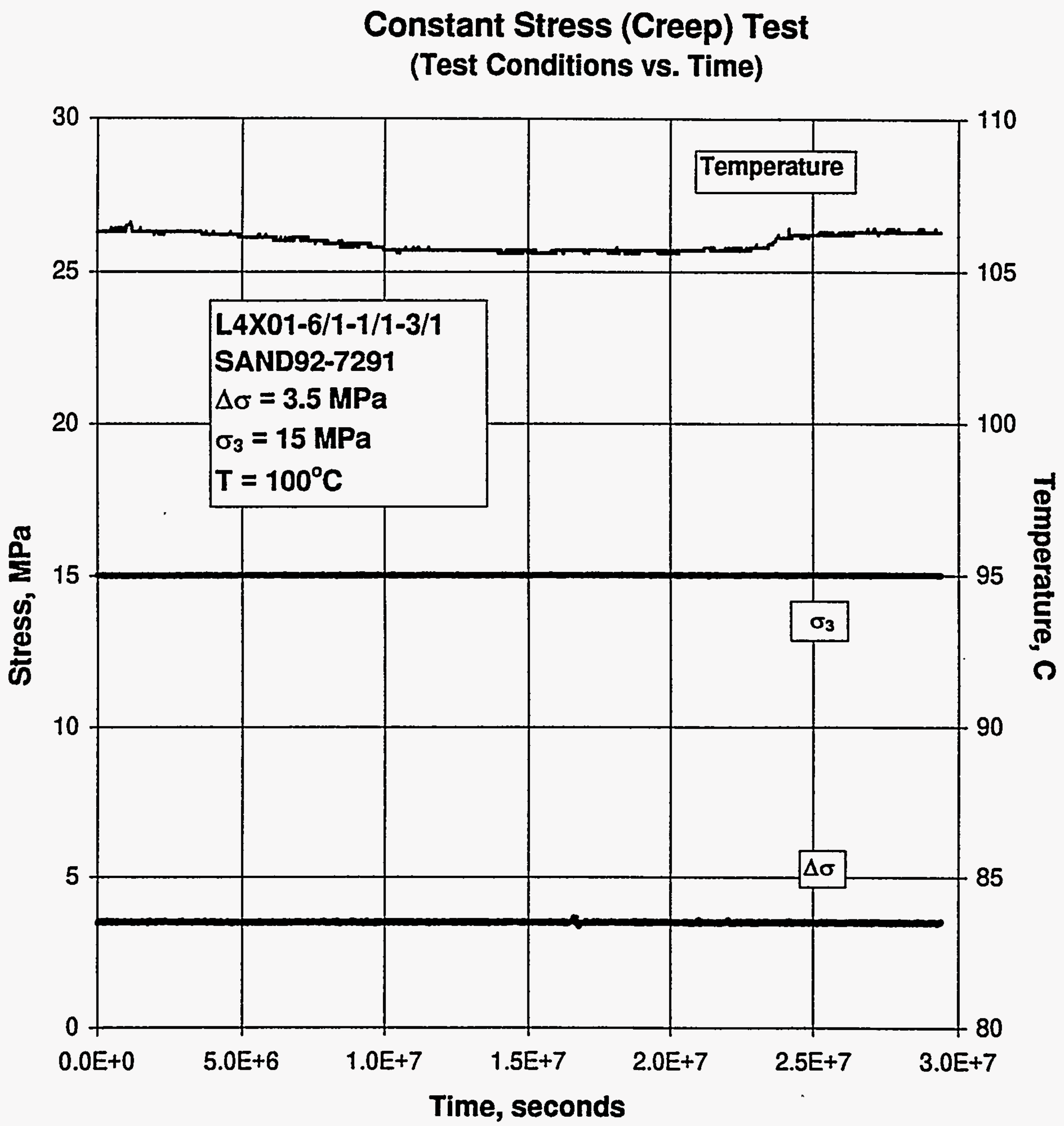

Figure C-25. Test Conditions Versus Time for a Creep Test: Specimen L4X01-6/1-1/1-3/1; Stage 1 of 1 (Argillaceous Salt).

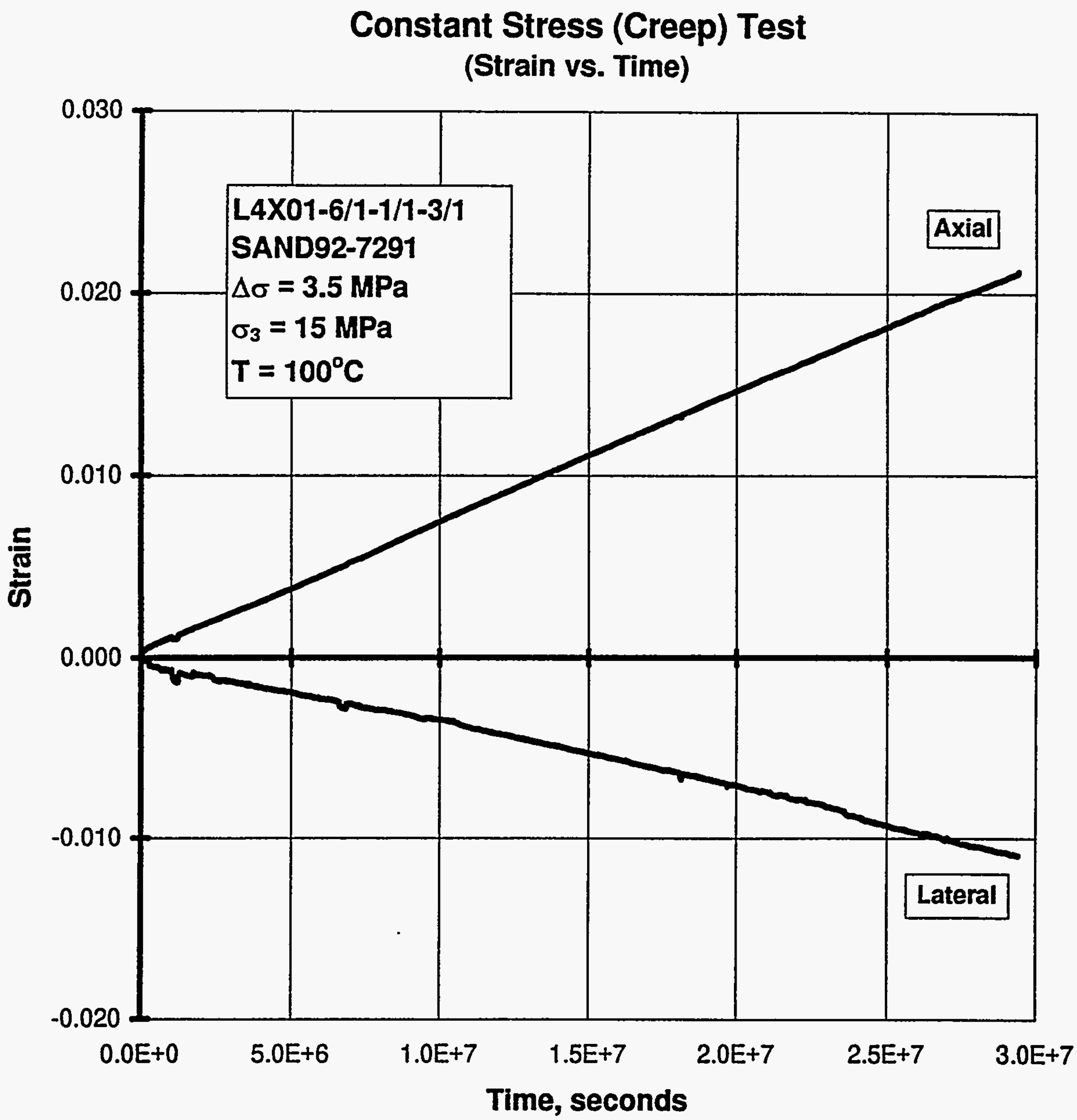

Figure C-26. Axial Strain and Lateral Strain Versus Time for a Creep Test: Specimen L4X01-6/1-1/1-3/1; Stage 1 of 1 (Argillaceous Salt).

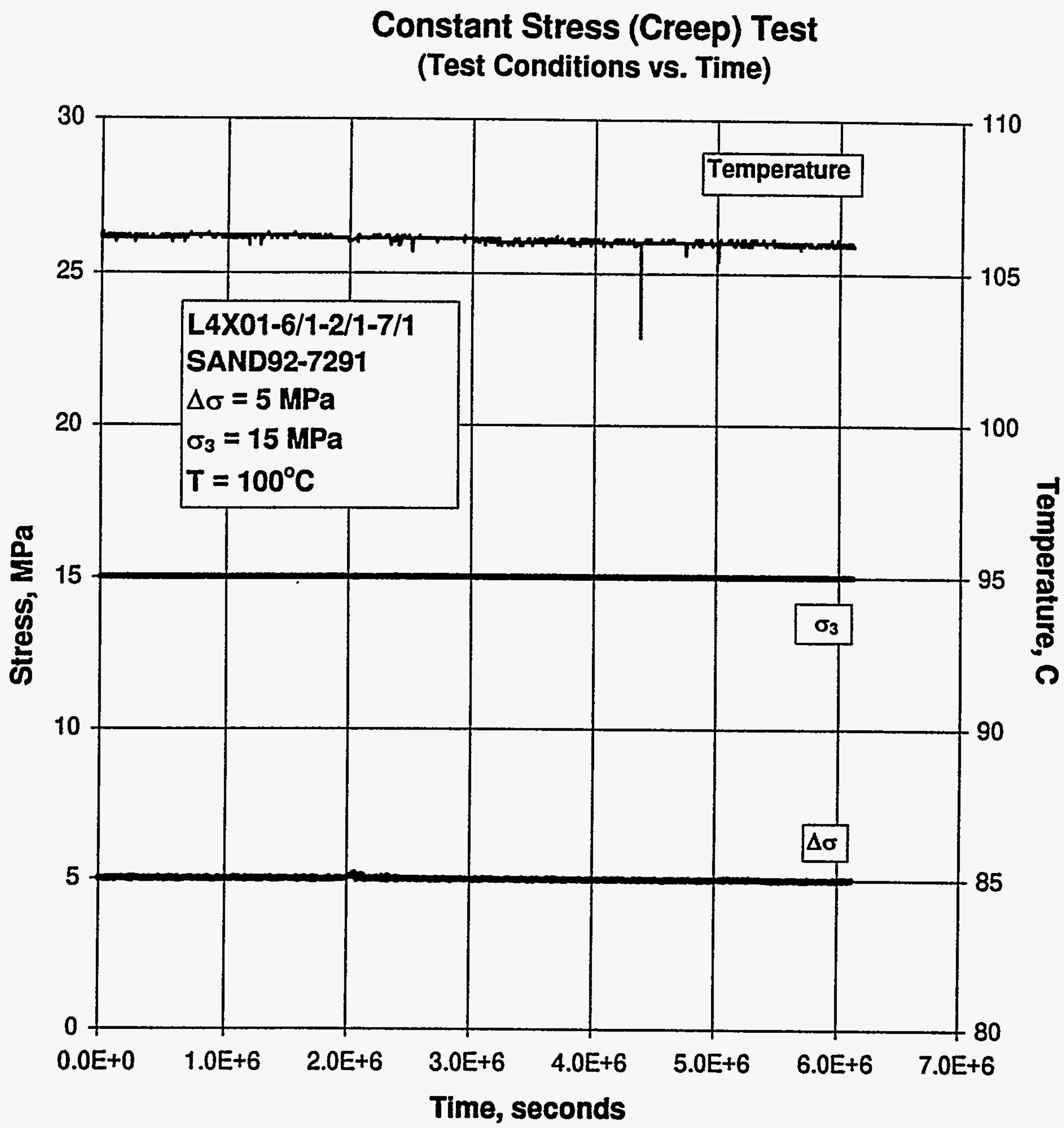

Figure C-27. Test Conditions Versus Time for a Creep Test: Specimen L4X01-6/1-2/1-7/1; Stage 1 of 1 (Argillaceous Salt).

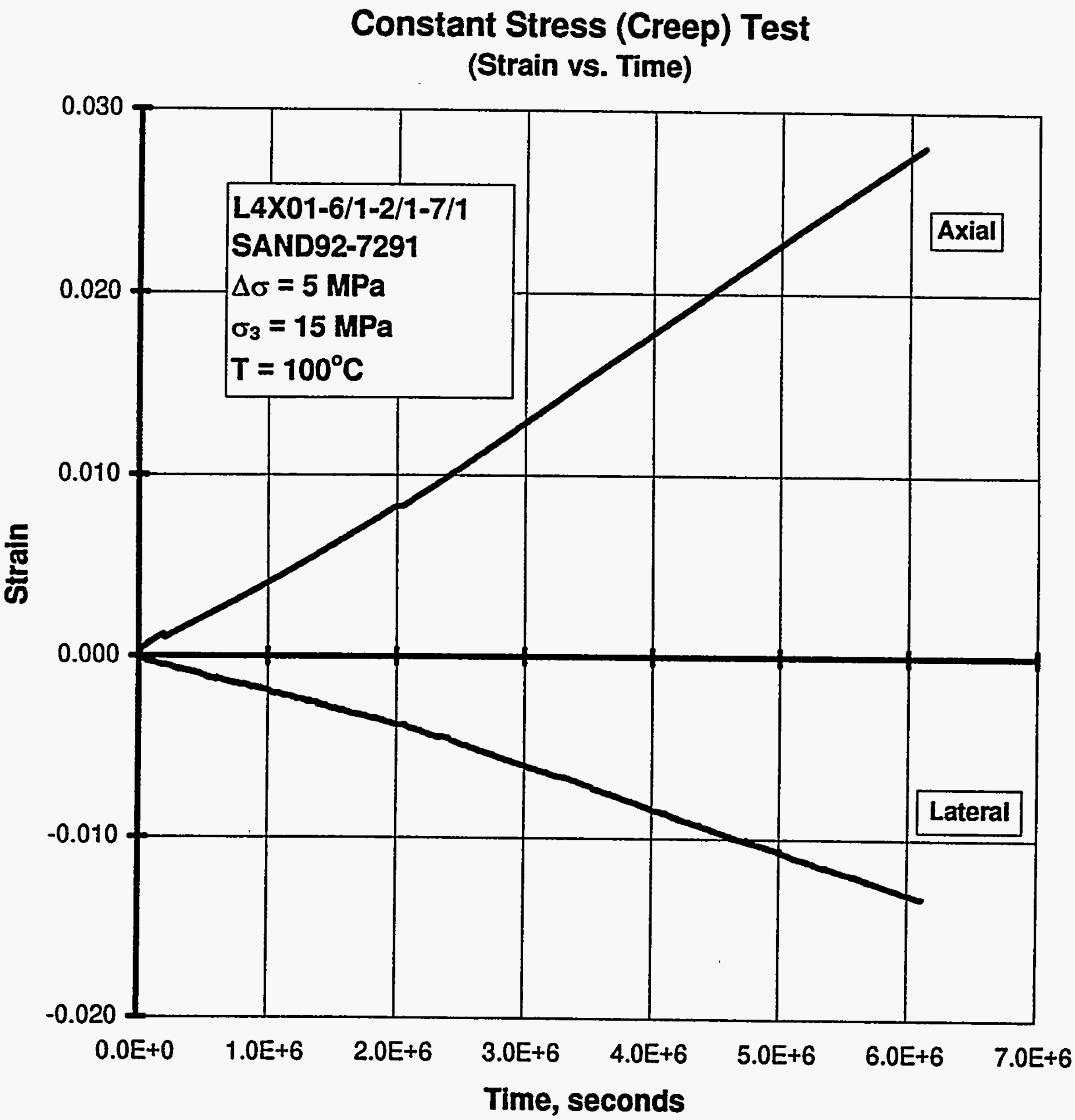

Figure C-28. Axial Strain and Lateral Strain Versus Time for a Creep Test: Specimen L4X01-6/1-2/1-7/1; Stage 1 of 1 (Argillaceous Salt).

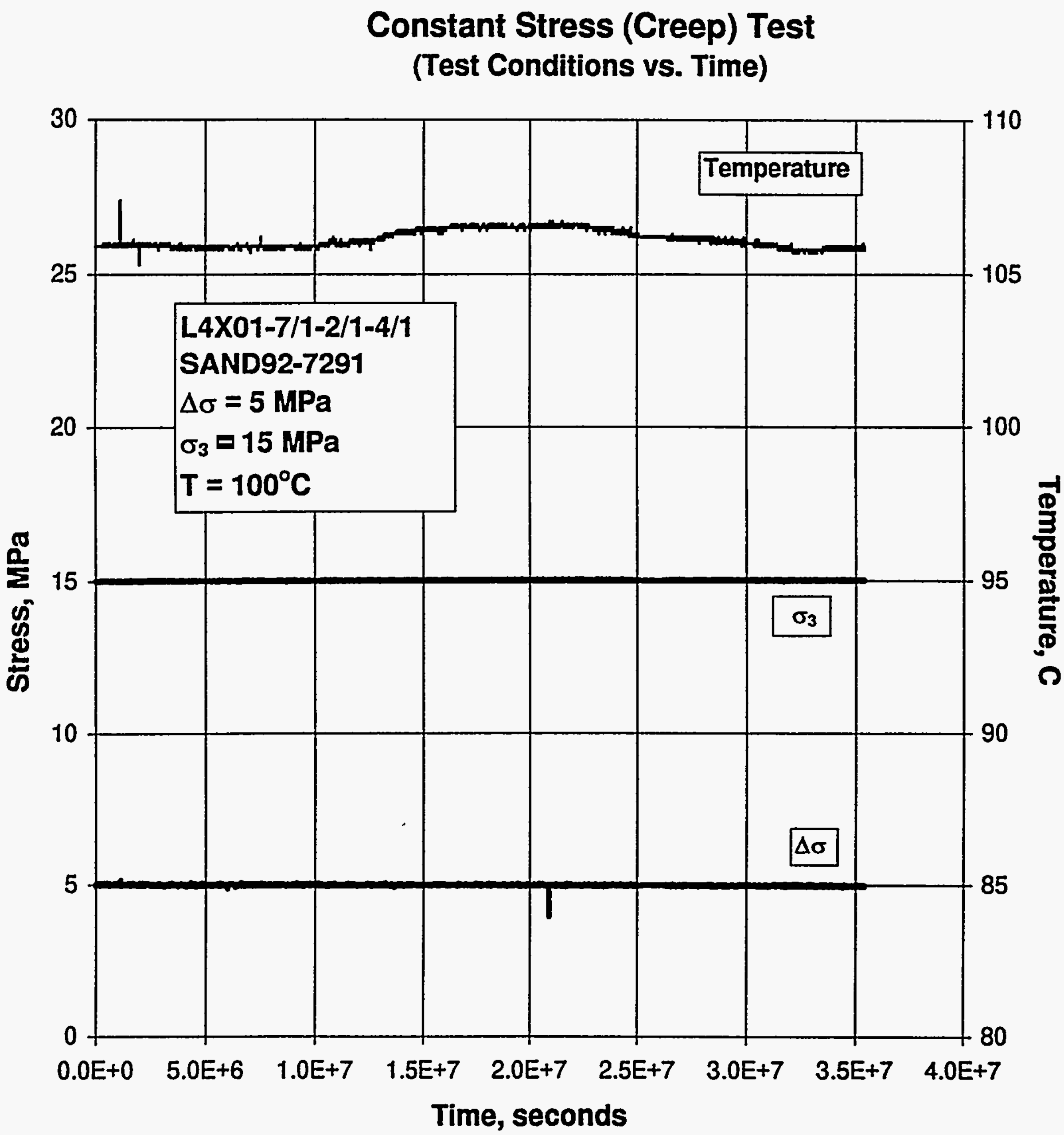

Figure C-29. Test Conditions Versus Time for a Creep Test: Specimen L4X01-7/1-2/1-4/1; Stage 1 of 1 (Argillaceous Salt).

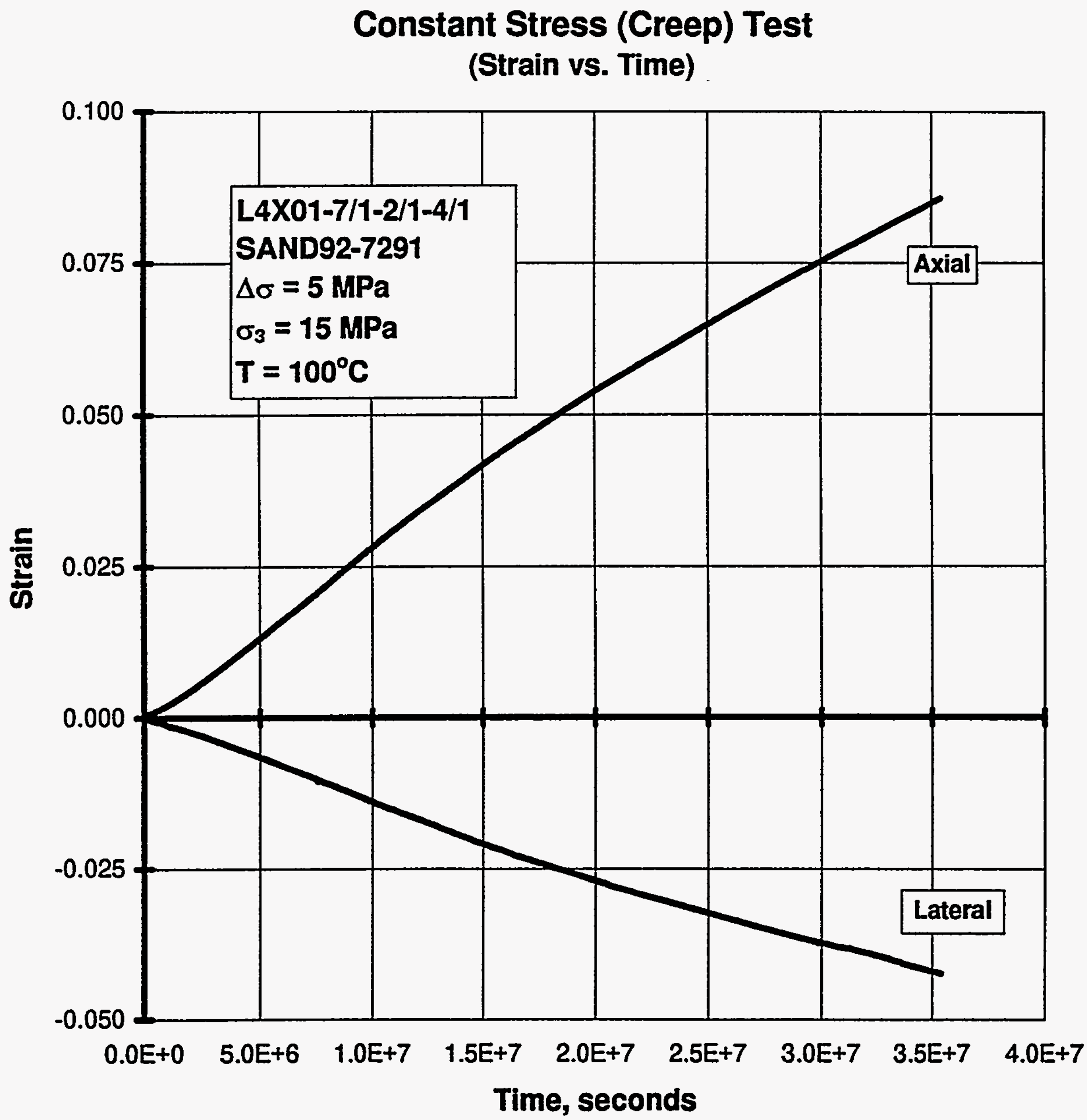

Figure C-30. Axial Strain and Lateral Strain Versus Time for a Creep Test: Specimen L4X01-7/1-2/1-4/1; Stage 1 of 1 (Argillaceous Salt).

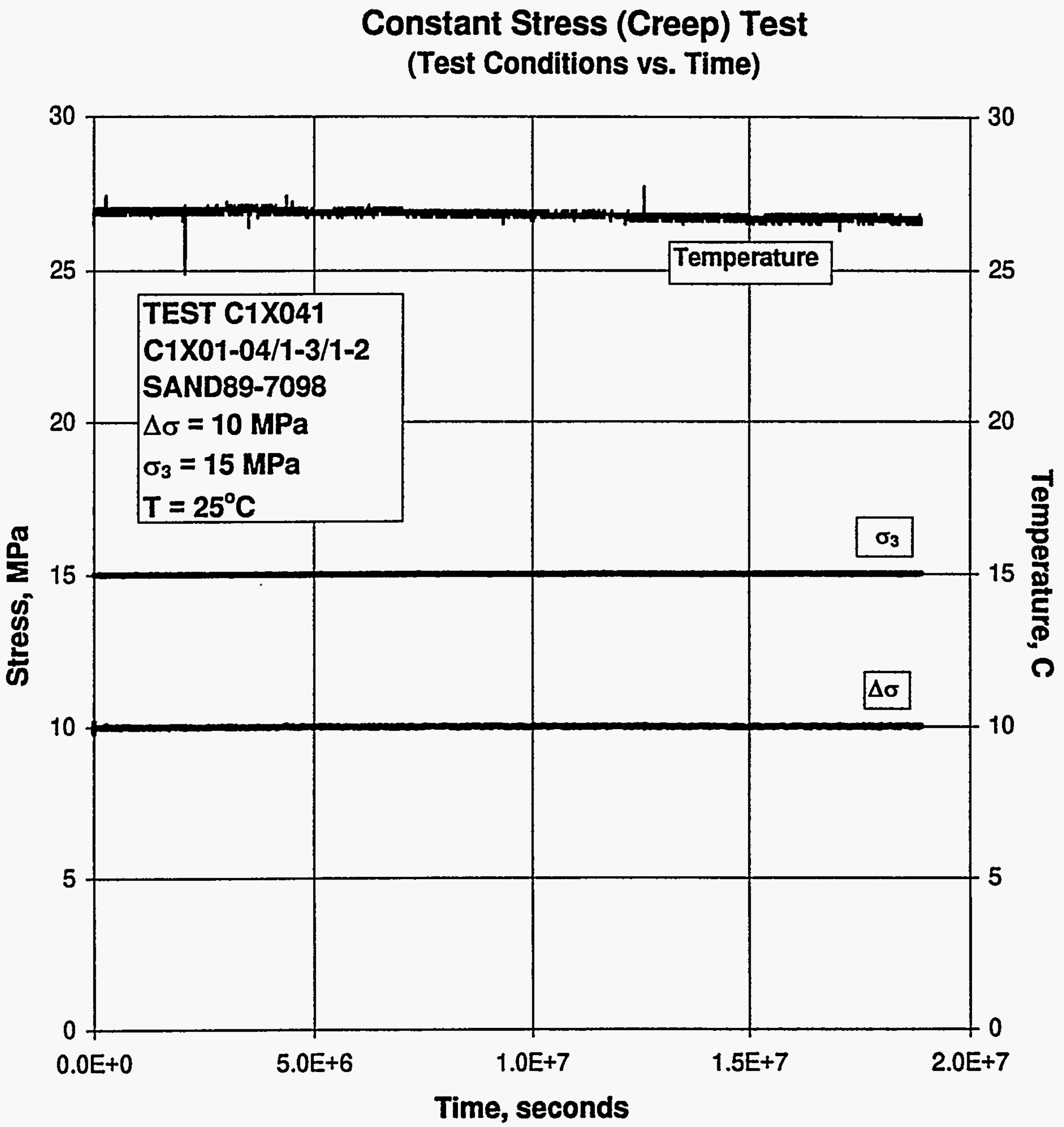

Figure C-31. Test Conditions Versus Time for a Creep Test: Specimen C1X01-04/1-3/1-2; Stage 1 of 1.

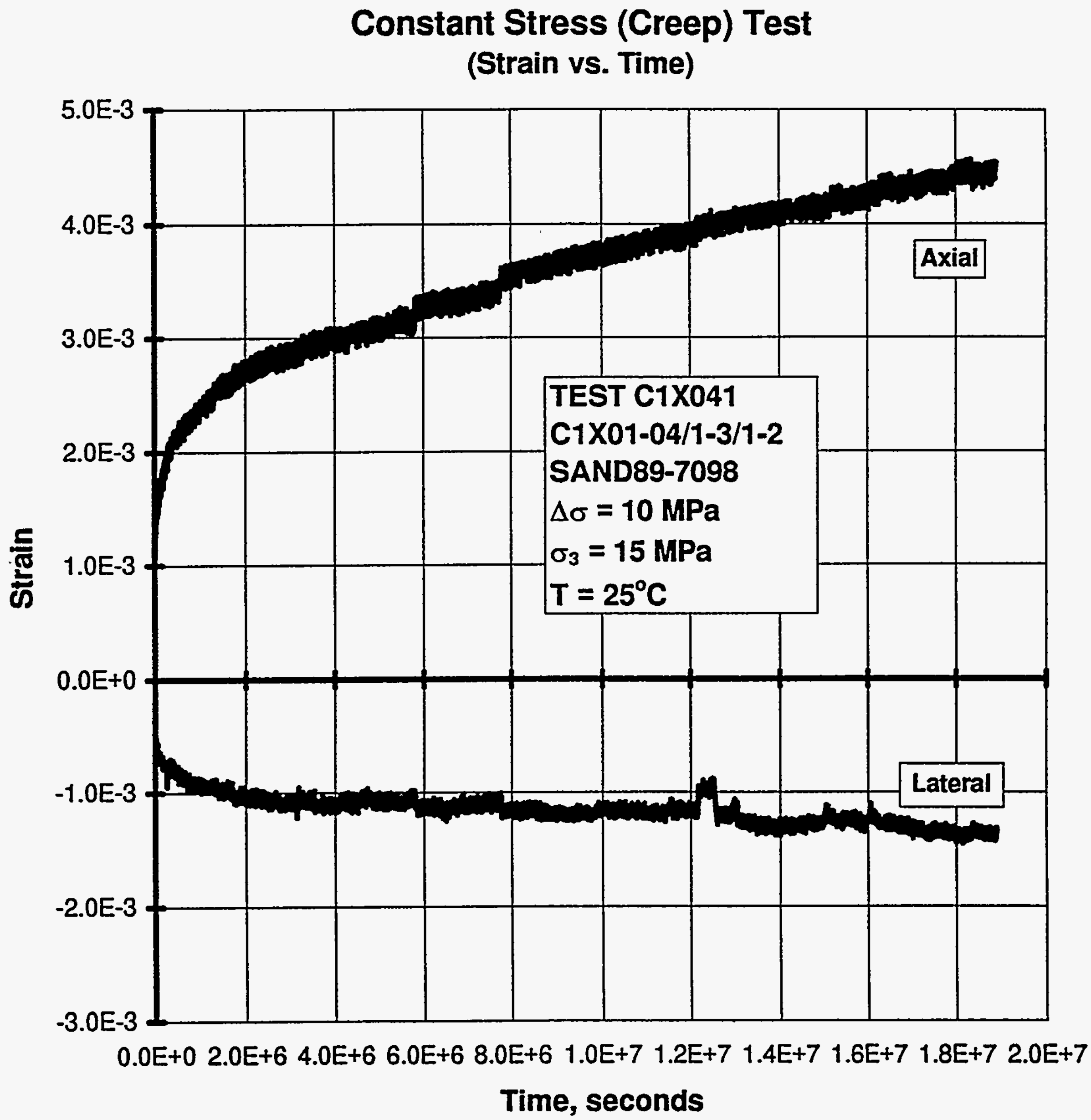

Figure C-32. Axial Strain and Lateral Strain Versus Time for a Creep Test: Specimen C1X01-04/1-3/1-2; Stage 1 of 1.

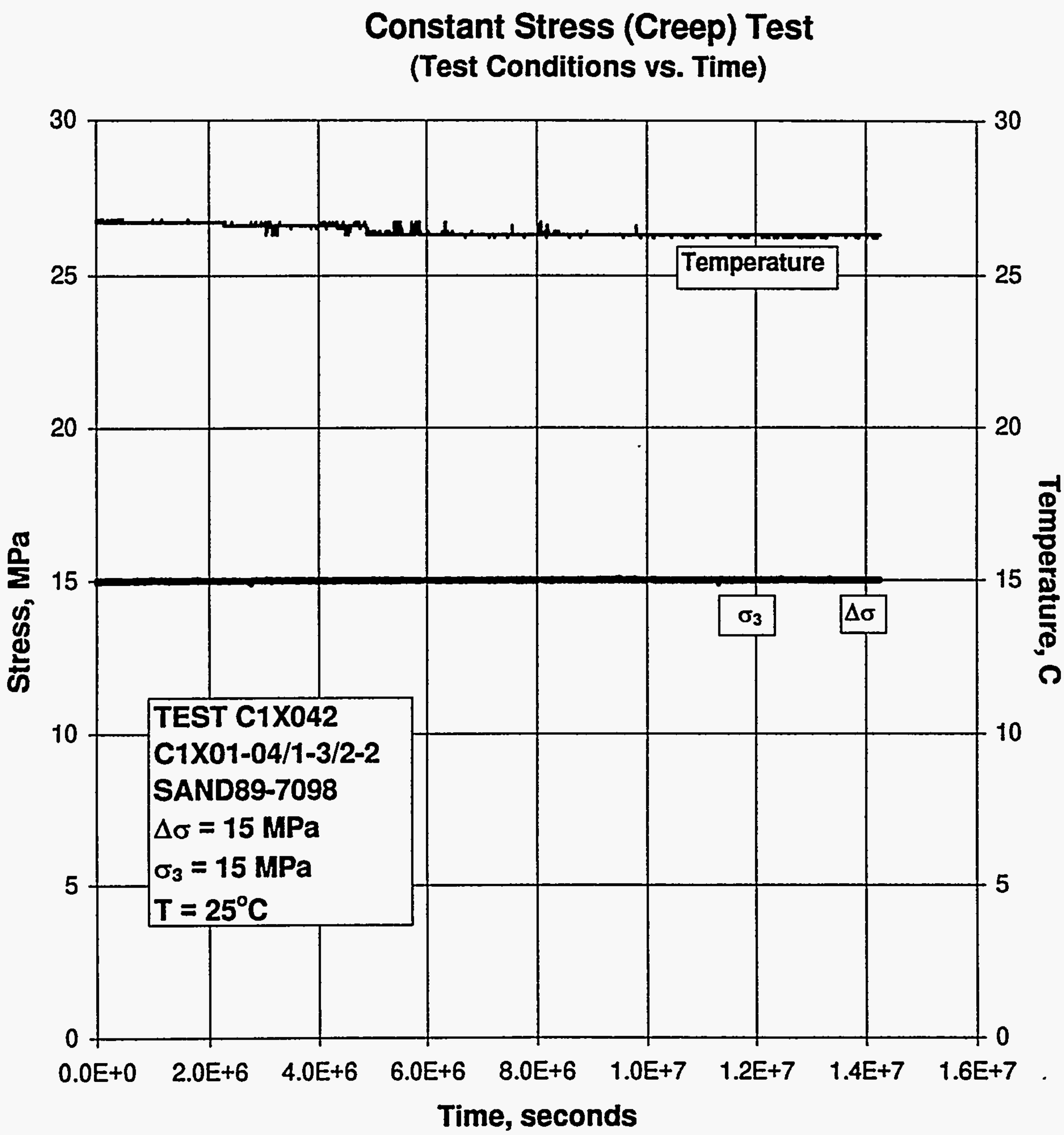

Figure C-33. Test Conditions Versus Time for a Creep Test: Specimen C1X01-04/1-3/2-2; Stage 1 of 1.

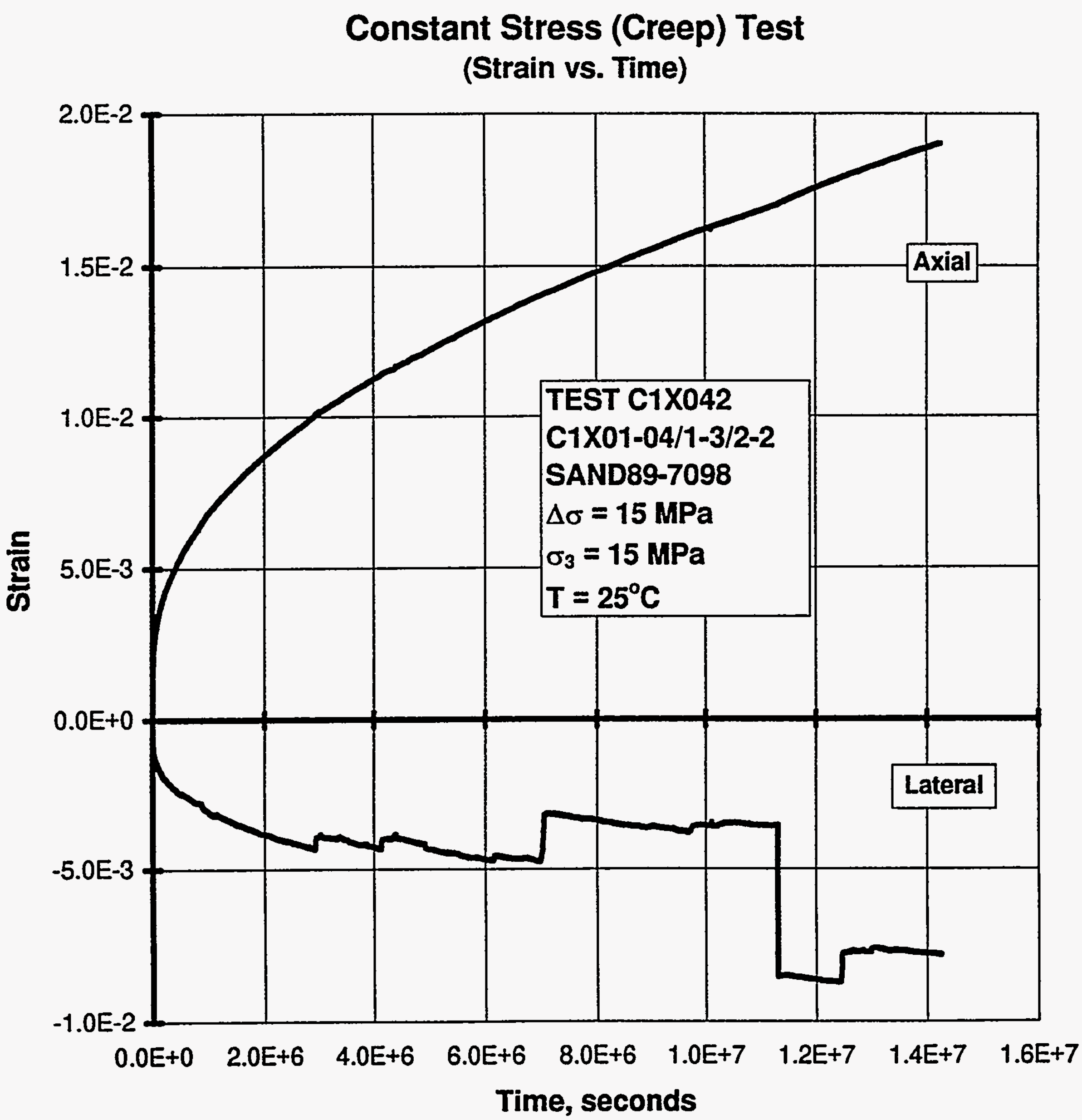

Figure C-34. Axial Strain and Lateral Strain Versus Time for a Creep Test: Specimen C1X01-04/1-3/2-2; Stage 1 of 1.

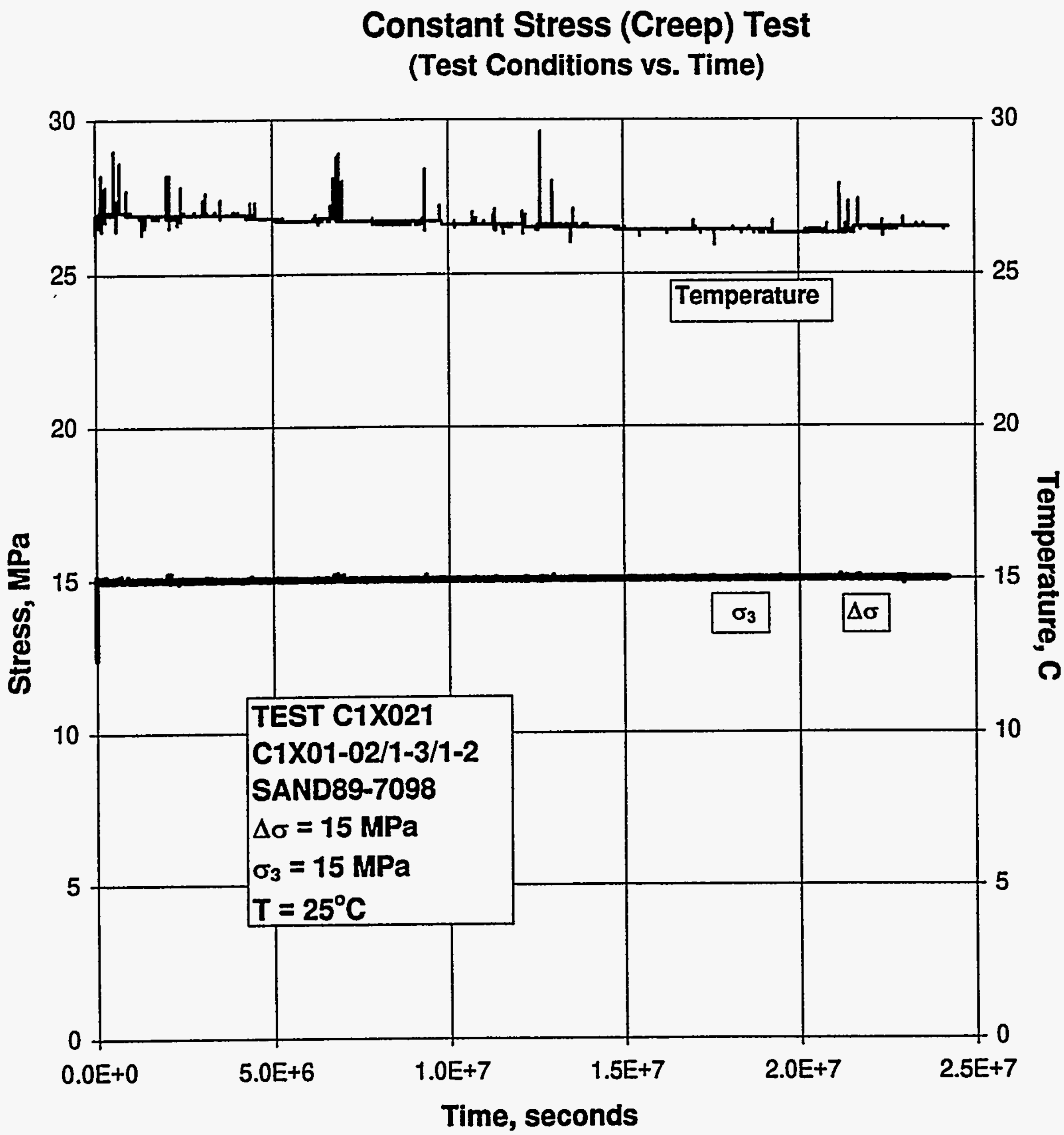

Figure C-35. Test Conditions Versus Time for a Creep Test: Specimen C1X01-02/1-3/1-2; Stage 1 of 1.

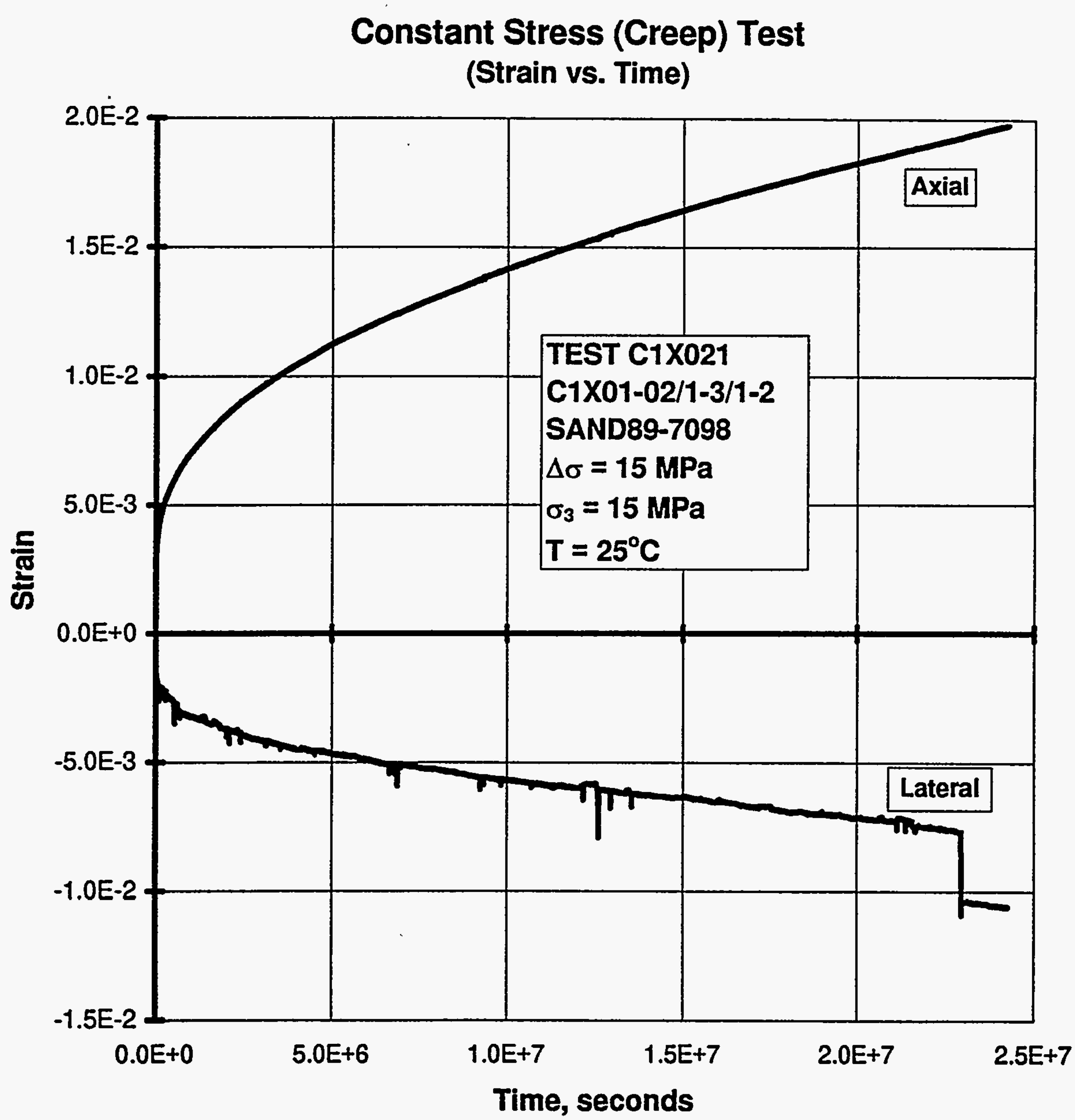

Figure C-36. Axial Strain and Lateral Strain Versus Time for a Creep Test: Specimen C1X01-02/1-3/1-2; Stage 1 of 1.

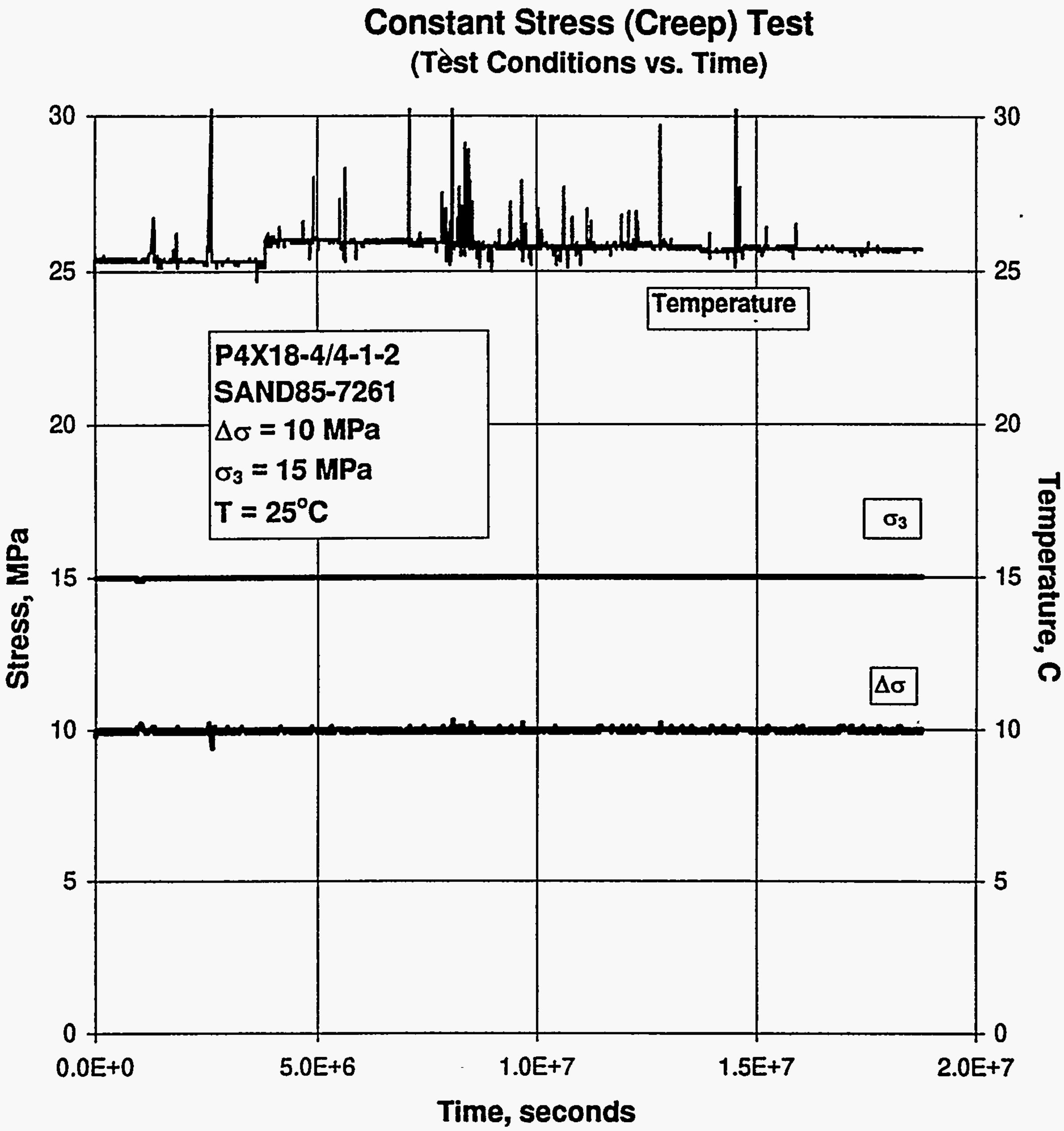

Figure C-37. Test Conditions Versus Time for a Creep Test: Specimen P4X18-4/4-1-2; Stage 1 of 1 (Argillaceous Salt).

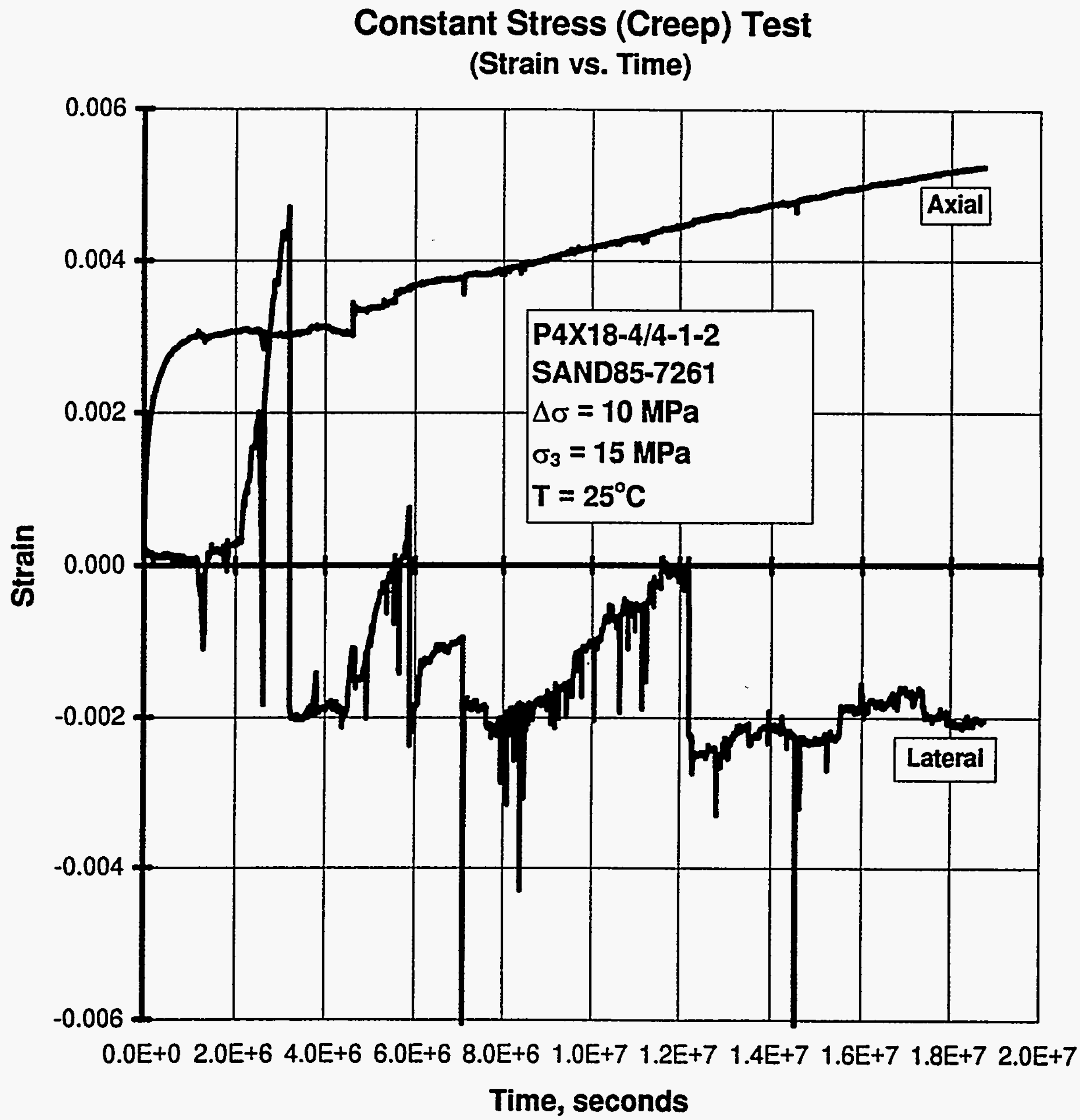

Figure C-38. Axial Strain and Lateral Strain Versus Time for a Creep Test: Specimen P4X18-4/4-1-2; Stage 1 of 1 (Argillaceous Salt).

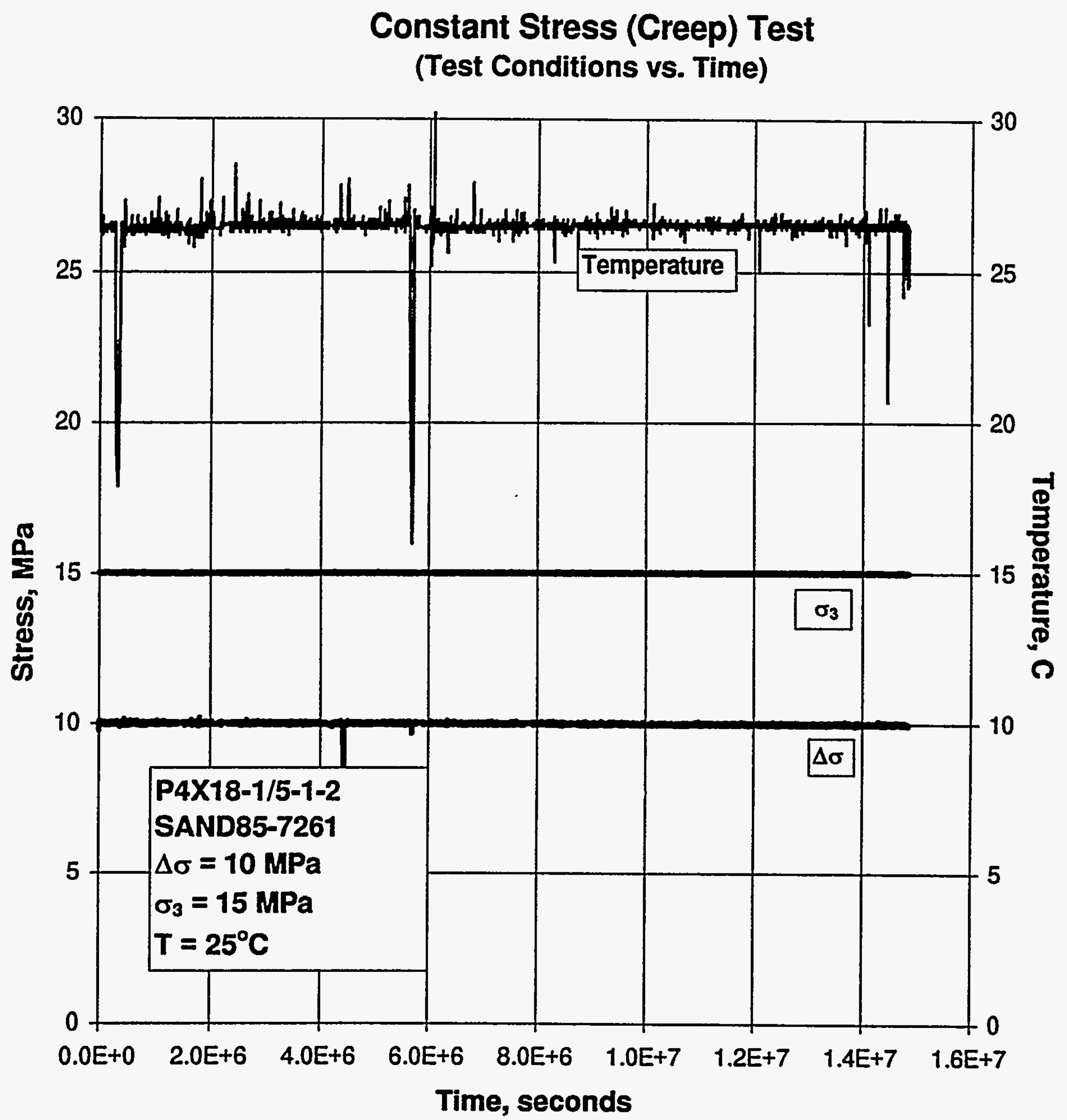

Figure C-39. Test Conditions Versus Time for a Creep Test: Specimen P4X18-1/5-1-2; Stage 1 of 1 (Argillaceous Salt).

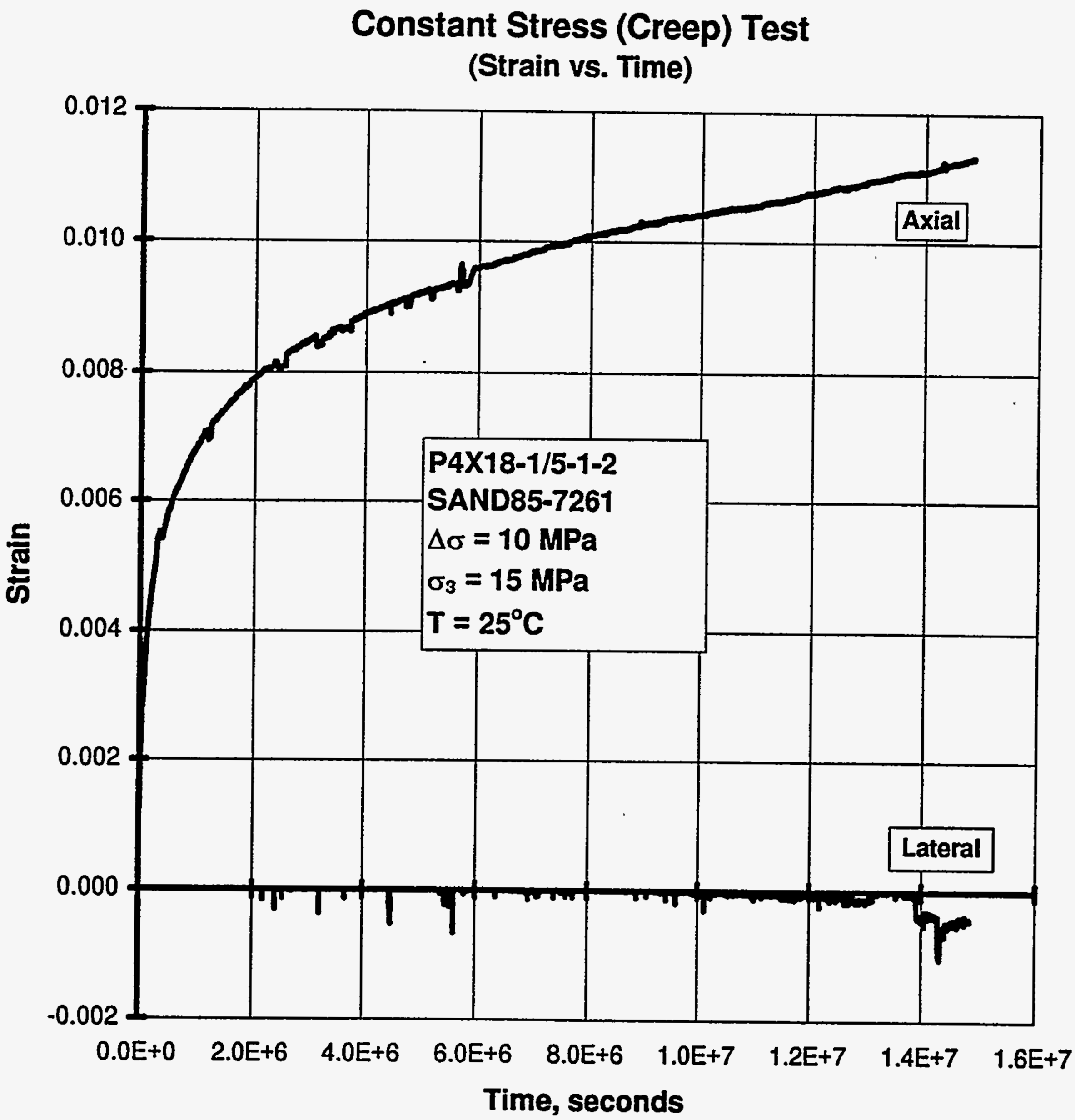

Figure C-40. Axial Strain and Lateral Strain Versus Time for a Creep Test: Specimen P4X18-1/5-1-2; Stage 1 of 1 (Argillaceous Salt).

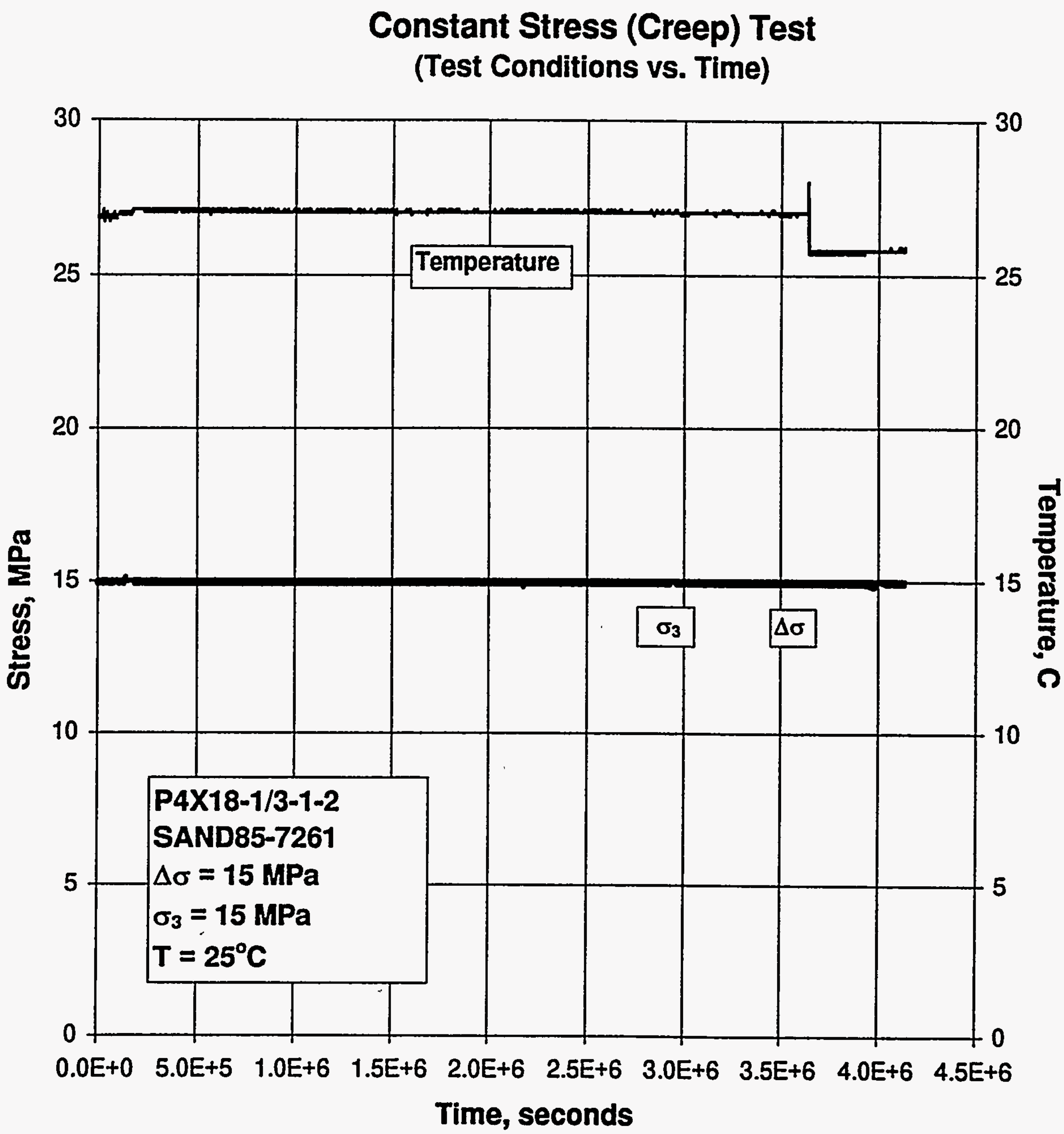

Figure C-41. Test Conditions Versus Time for a Creep Test: Specimen P4X18-1/3-1-2; Stage 1 of 1 (Argillaceous Salt).

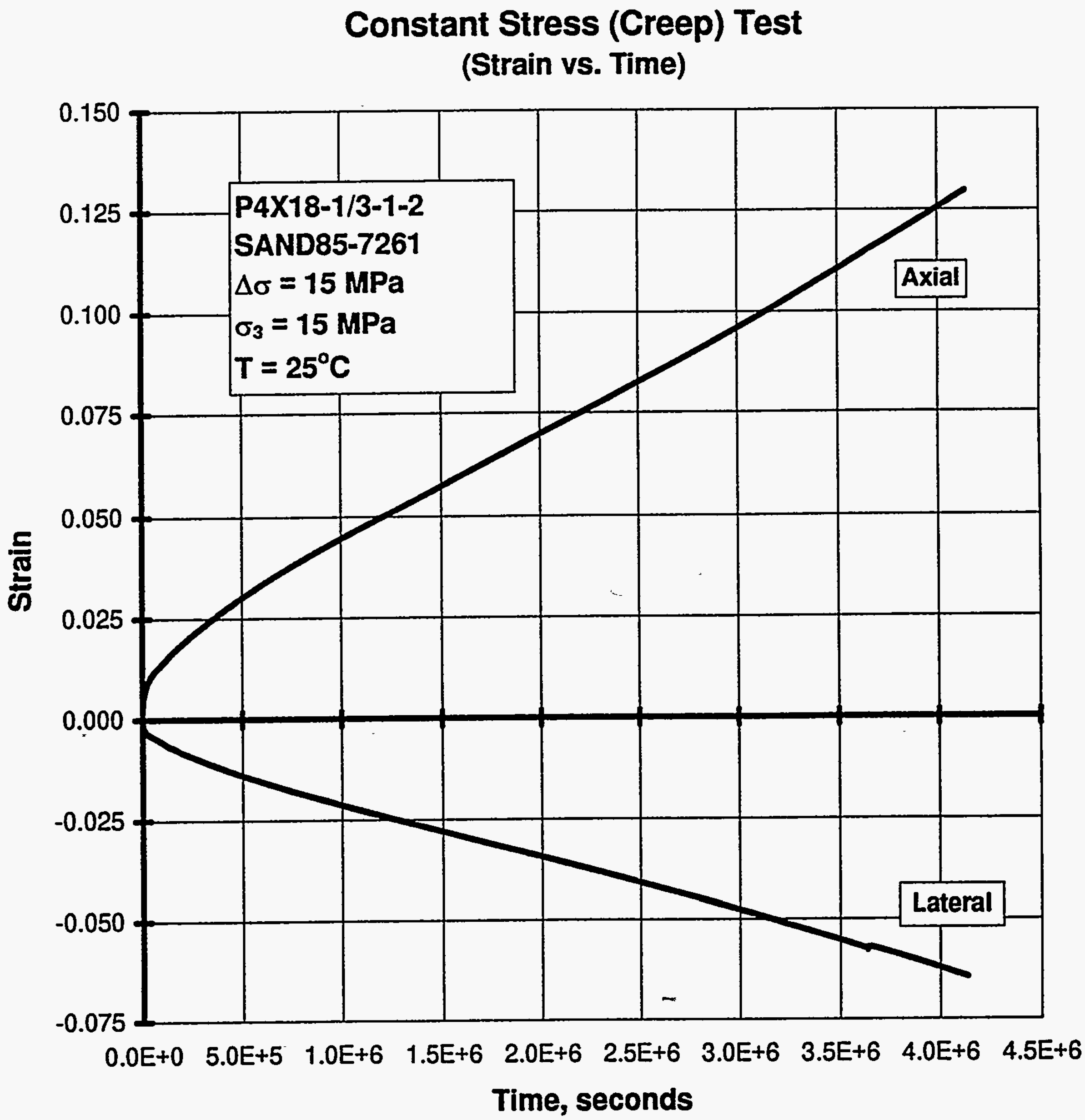

Figure C-42. Axial Strain and Lateral Strain Versus Time for a Creep Test: Specimen P4X18-1/3-1-2; Stage 1 of 1 (Argillaceous Salt. Anomalous Test Result. Localized Deformation Along Clay Seams).

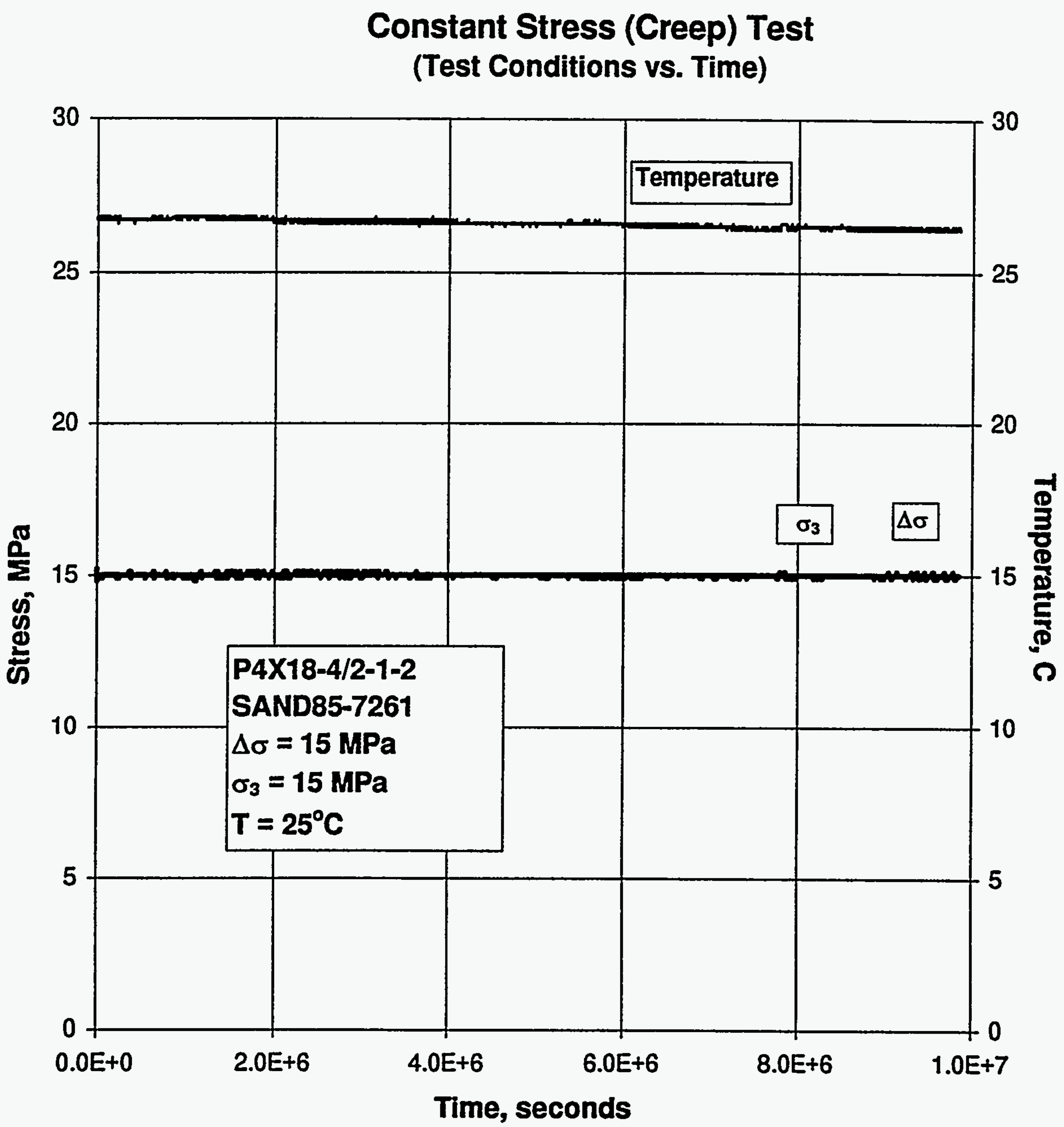

Figure C-43. Test Conditions Versus Time for a Creep Test: Specimen P4X18-4/2-1-2; Stage 1 of 1 (Argillaceous Salt).

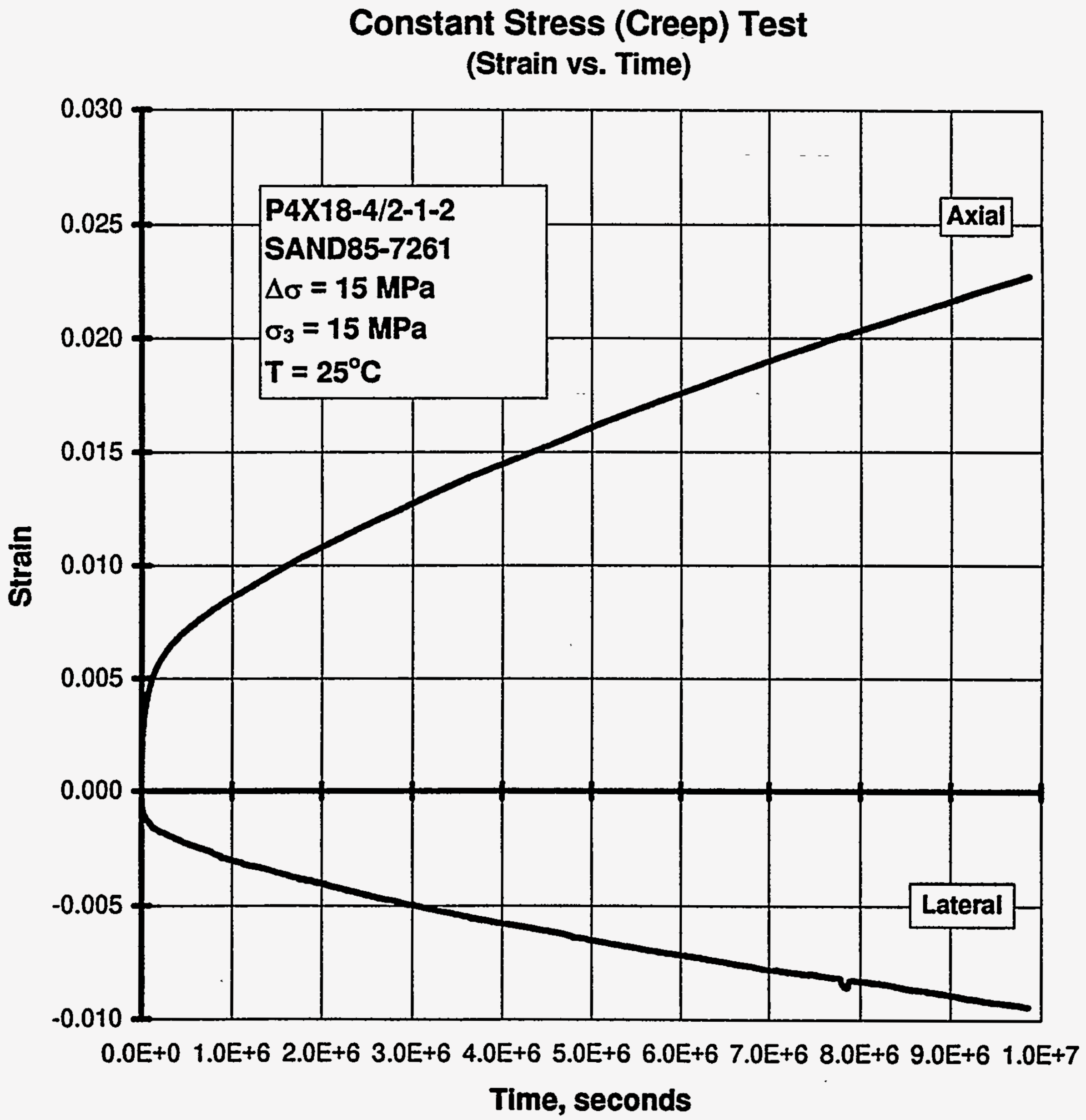

Figure C-44. Axial Strain and Lateral Strain Versus Time for a Creep Test: Specimen P4X18-4/2-1-2; Stage 1 of 1 (Argillaceous Salt).

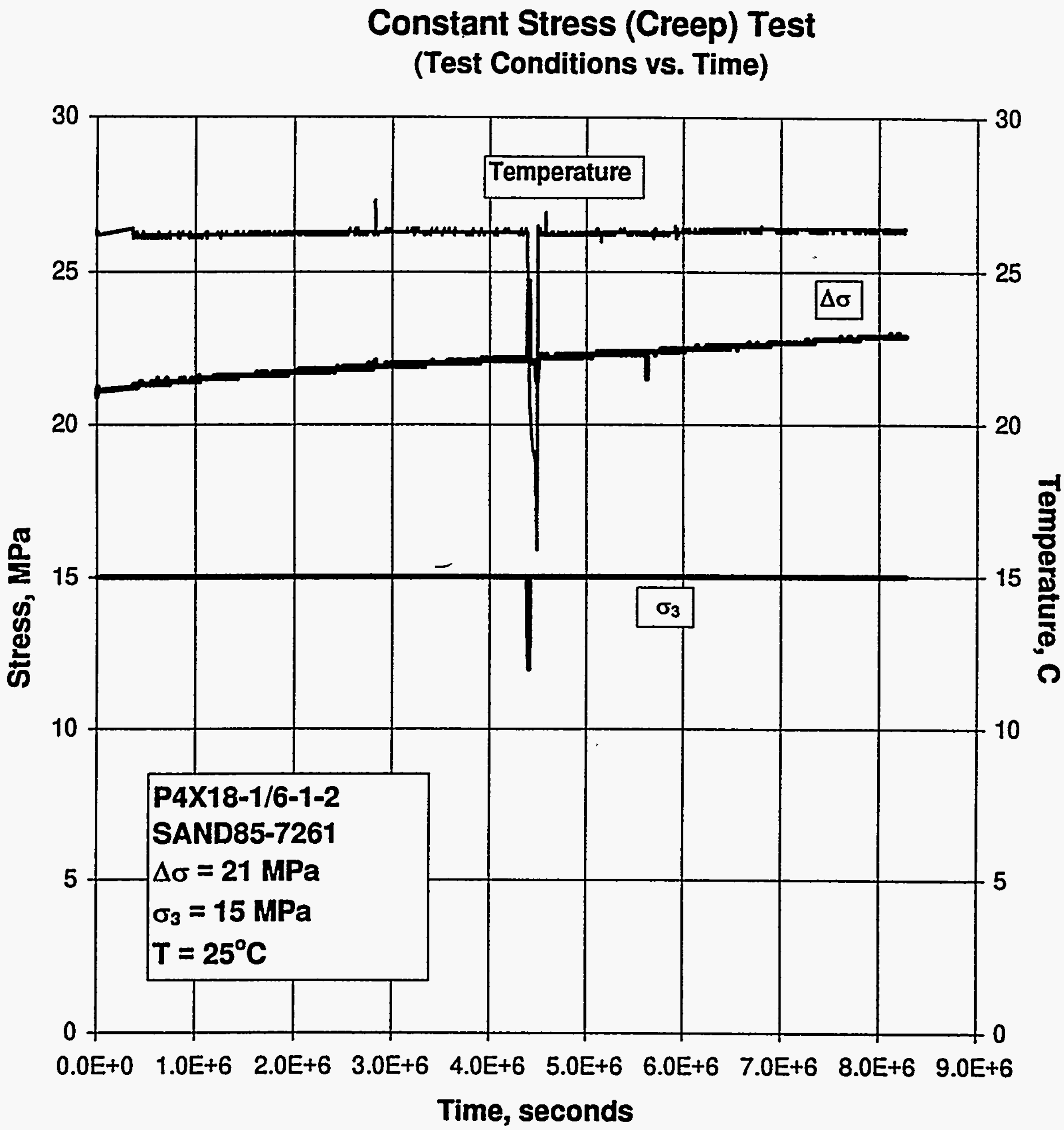

Figure C-45. Test Conditions Versus Time for a Creep Test: Specimen P4X18-1/6-1-2; Stage 1 of 1 (Argillaceous Salt).

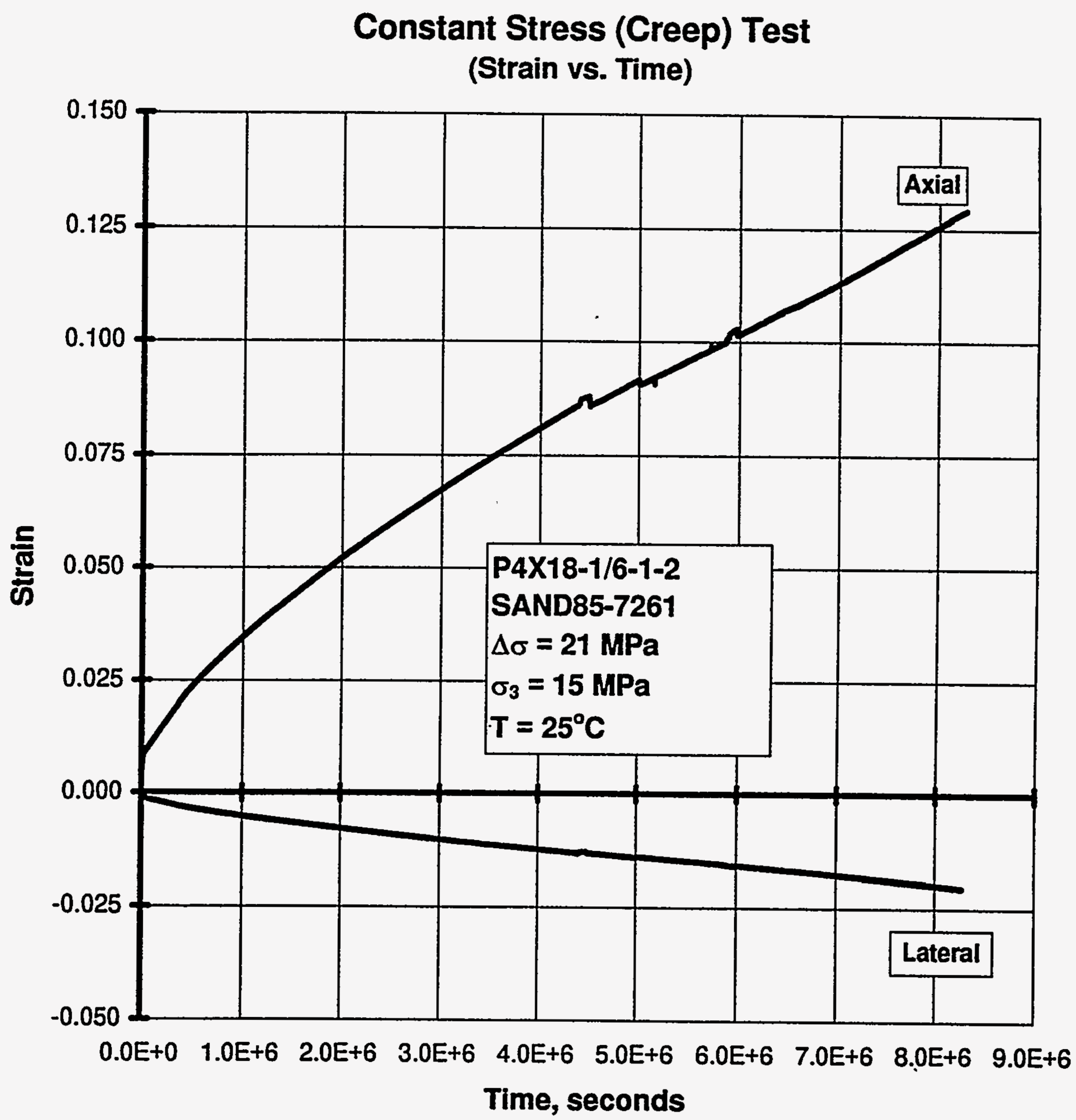

Figure C-46. Axial Strain and Lateral Strain Versus Time for a Creep Test: Specimen P4X18-1/6-1-2; Stage 1 of 1 (Argillaceous Salt).

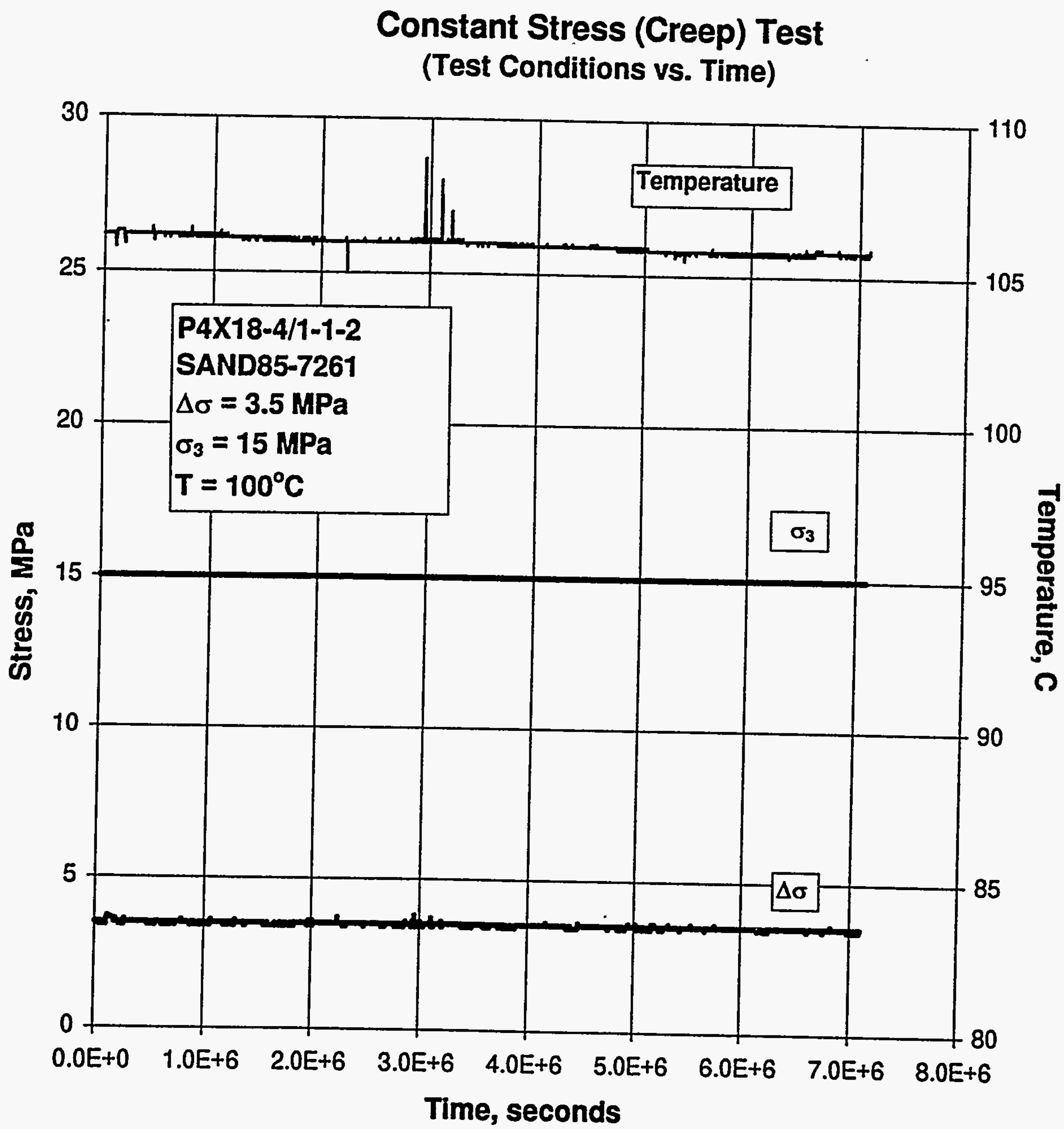

Figure C-47. Test Conditions Versus Time for a Creep Test: Specimen P4X18-4/1-1-2; Stage 1 of 1 (Argillaceous Salt).

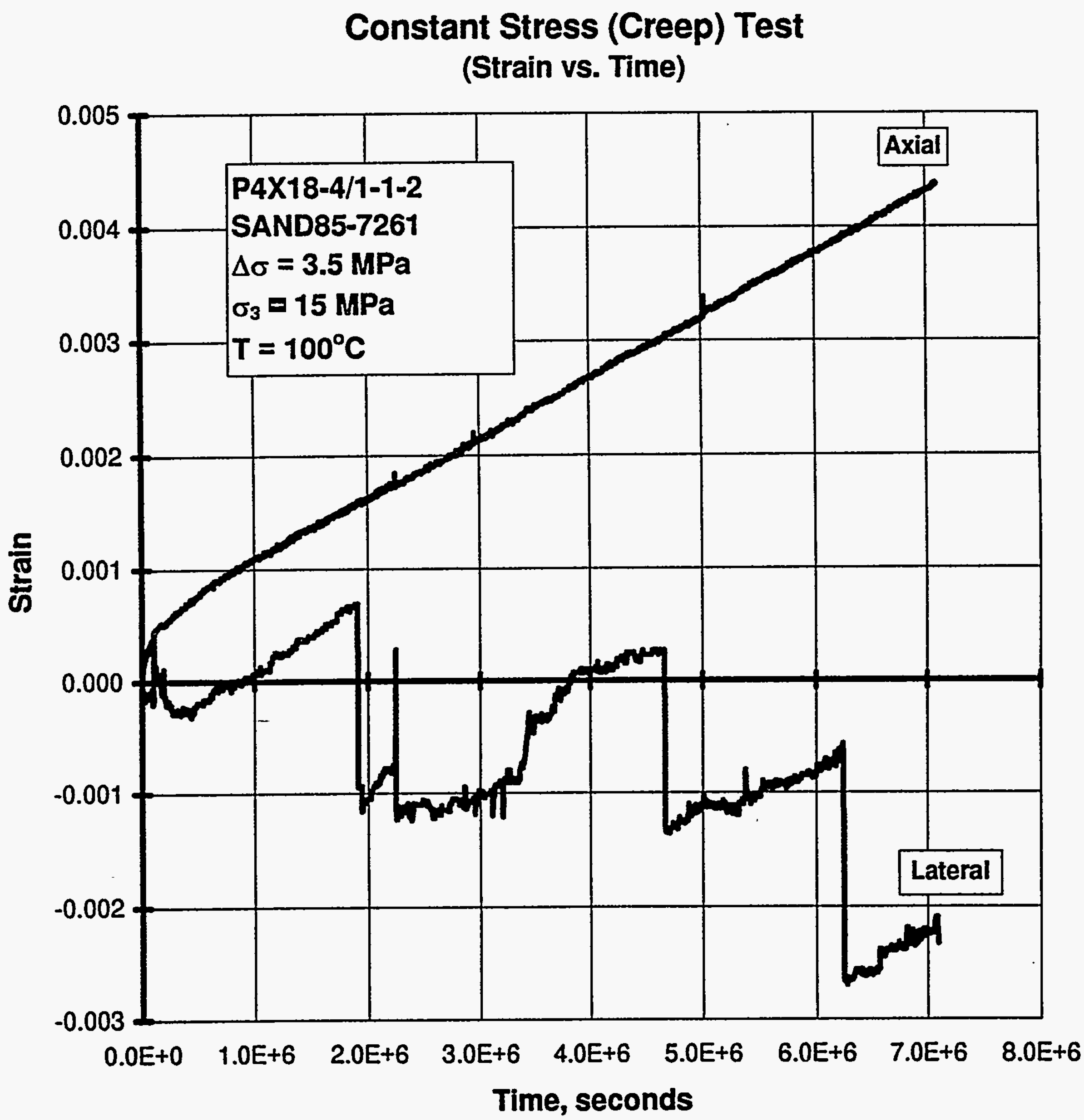

Figure C-48. Axial Strain and Lateral Strain Versus Time for a Creep Test: Specimen P4X18-4/1-1-2; Stage 1 of 1 (Argillaceous Salt).

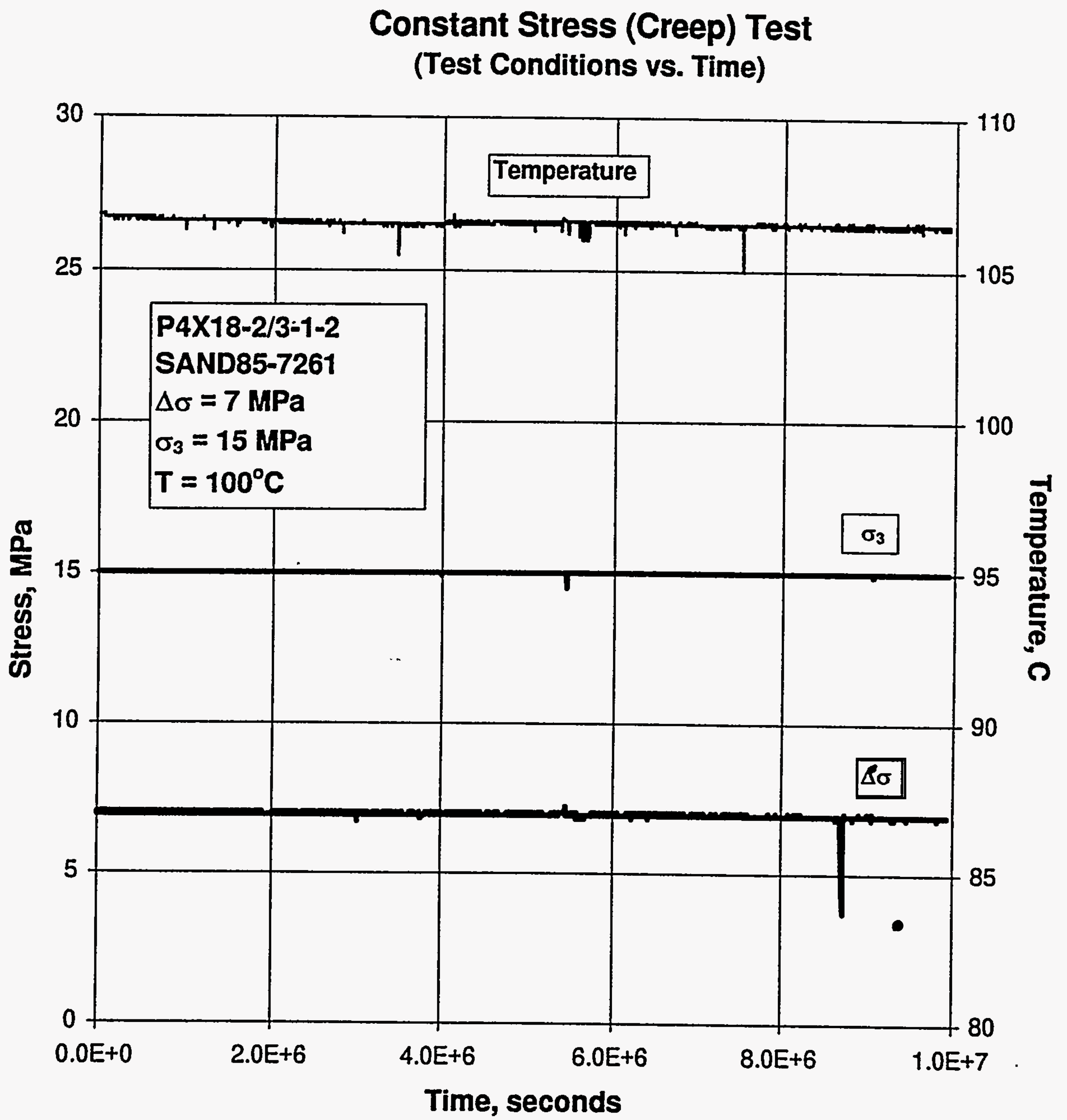

Figure C-49. Test Conditions Versus Time for a Creep Test: Specimen P4X18-2/3-1-2; Stage 1 of 1 (Argillaceous Salt).

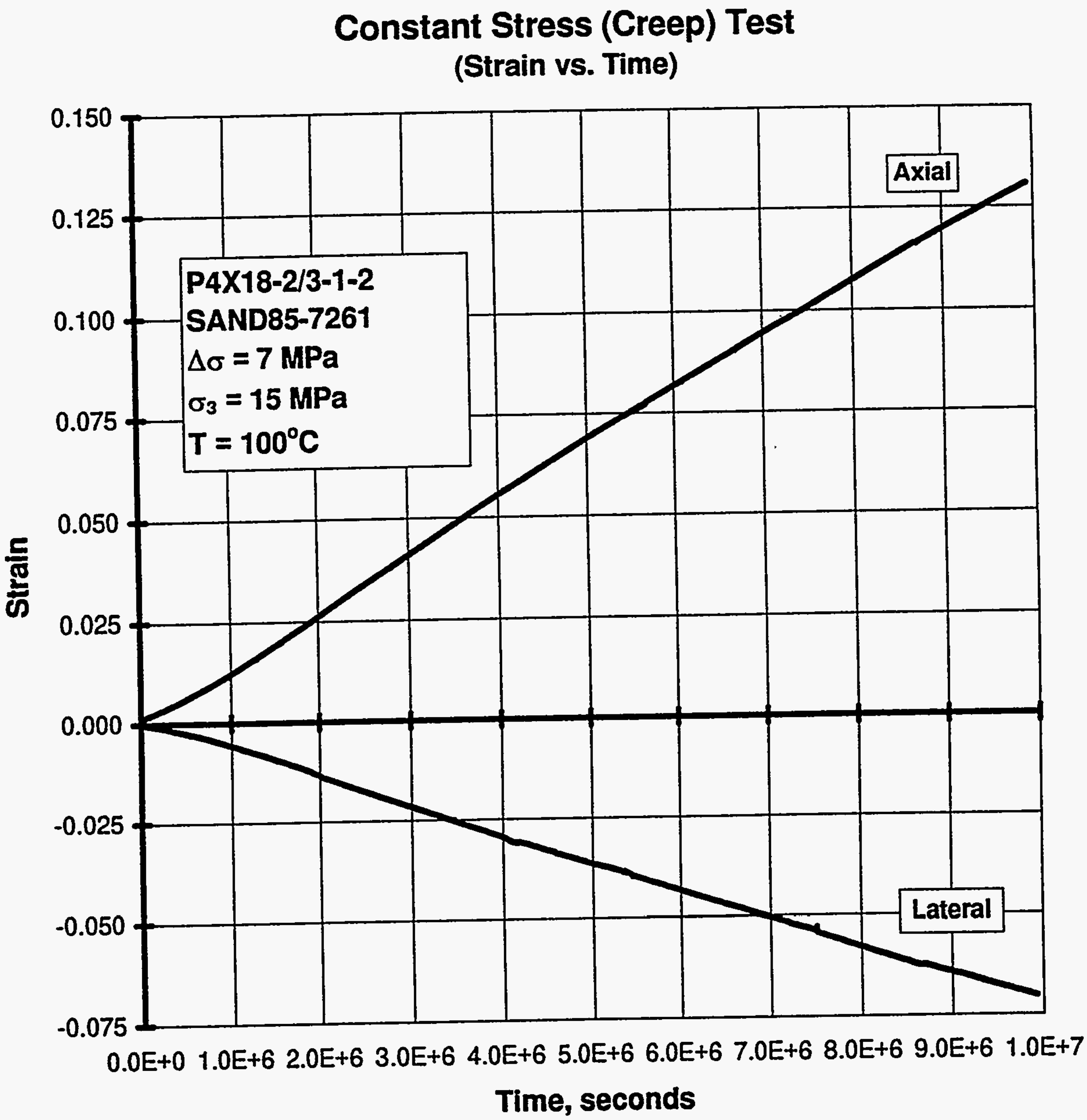

Figure C-50. Axial Strain and Lateral Strain Versus Time for a Creep Test: Specimen P4X18-2/3-1-2; Stage 1 of 1 (Argillaceous Salt. Anomalous Test Result. Possible Moisture Effects).

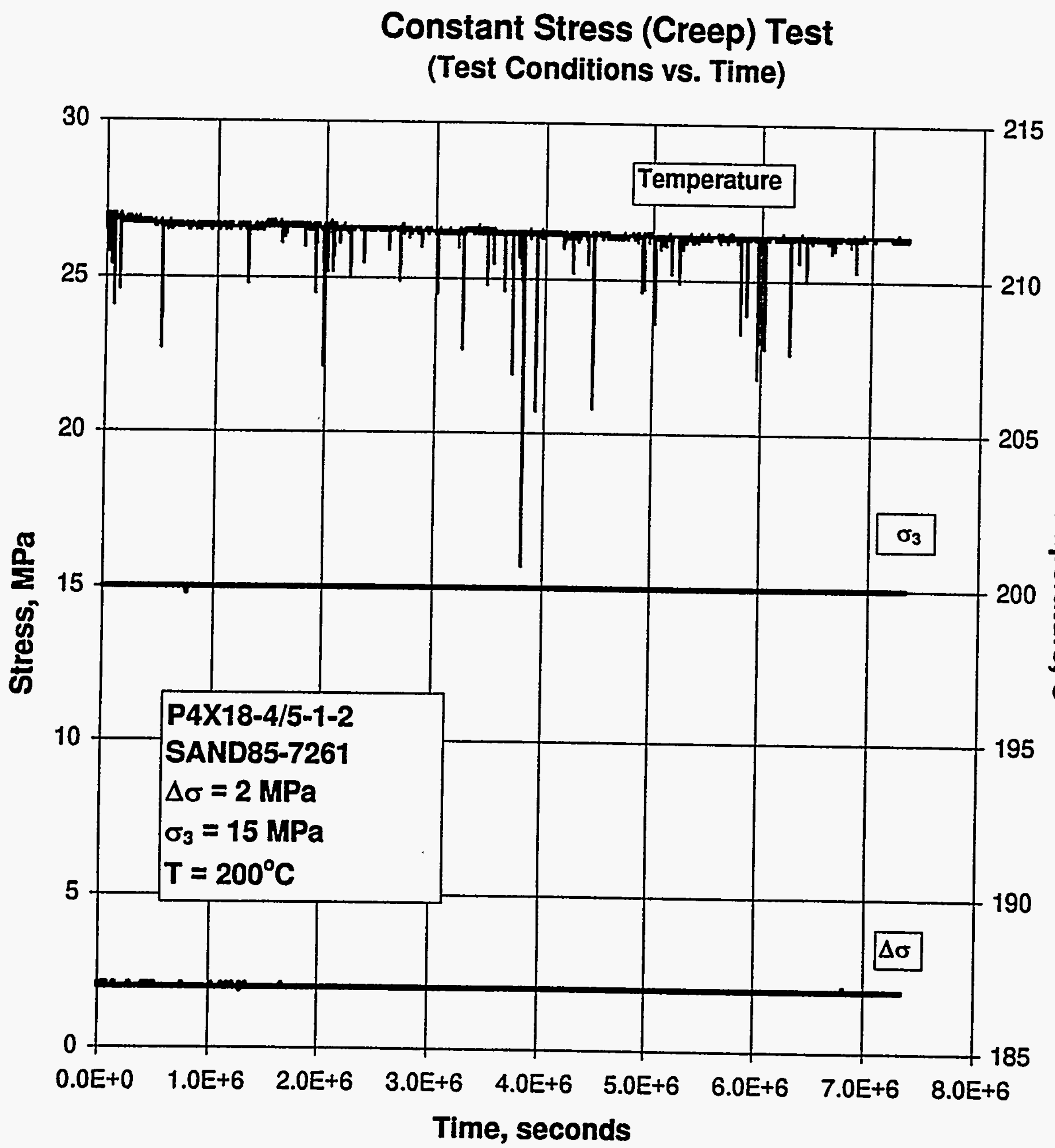

Figure C-51. Test Conditions Versus Time for a Creep Test: Specimen P4X18-4/5-1-2; Stage 1 of 1 (Argillaceous Salt).

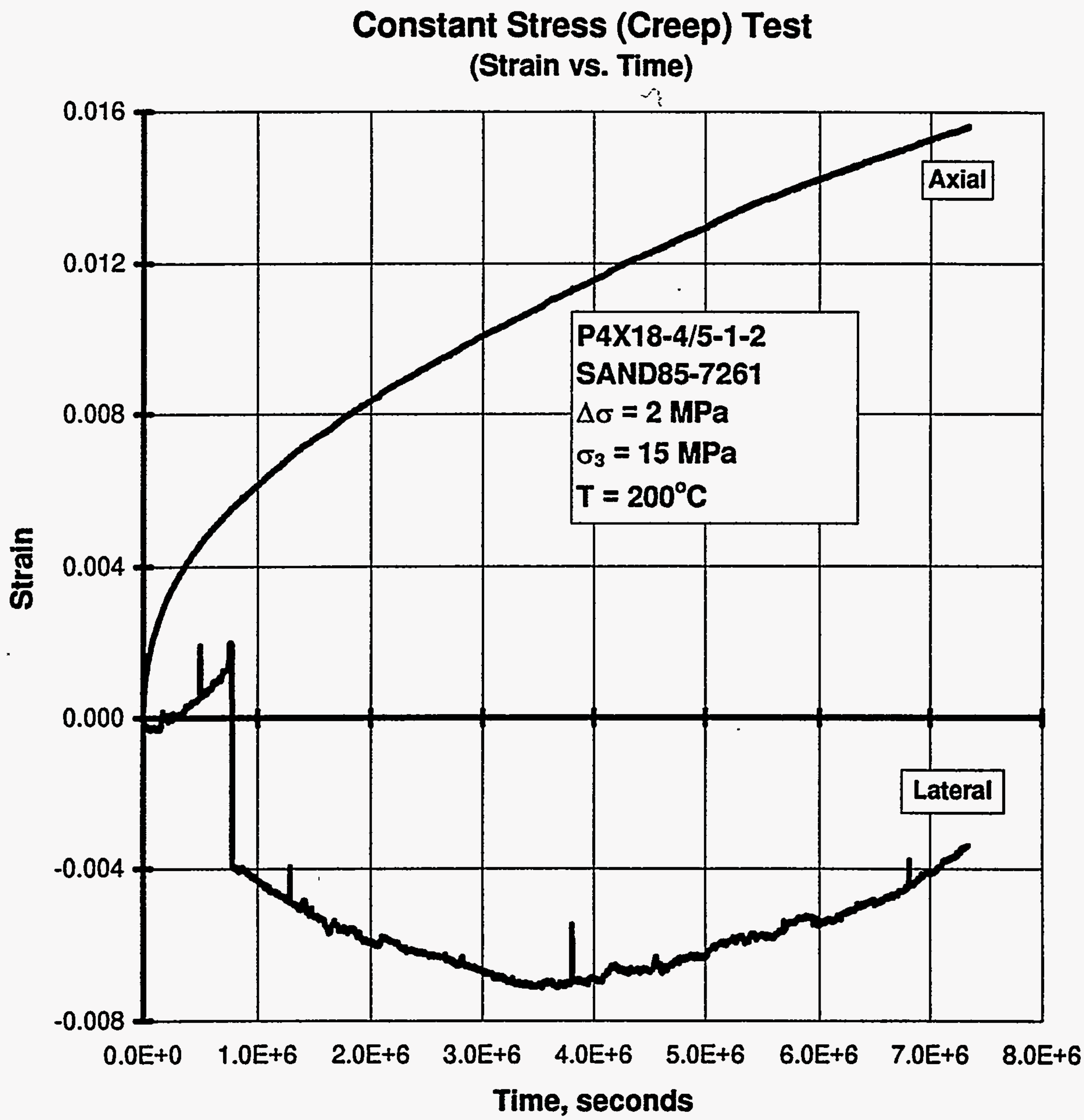

Figure C-52. Axial Strain and Lateral Strain Versus Time for a Creep Test: Specimen P4X18-4/5-1-2; Stage 1 of 1 (Argillaceous Salt).

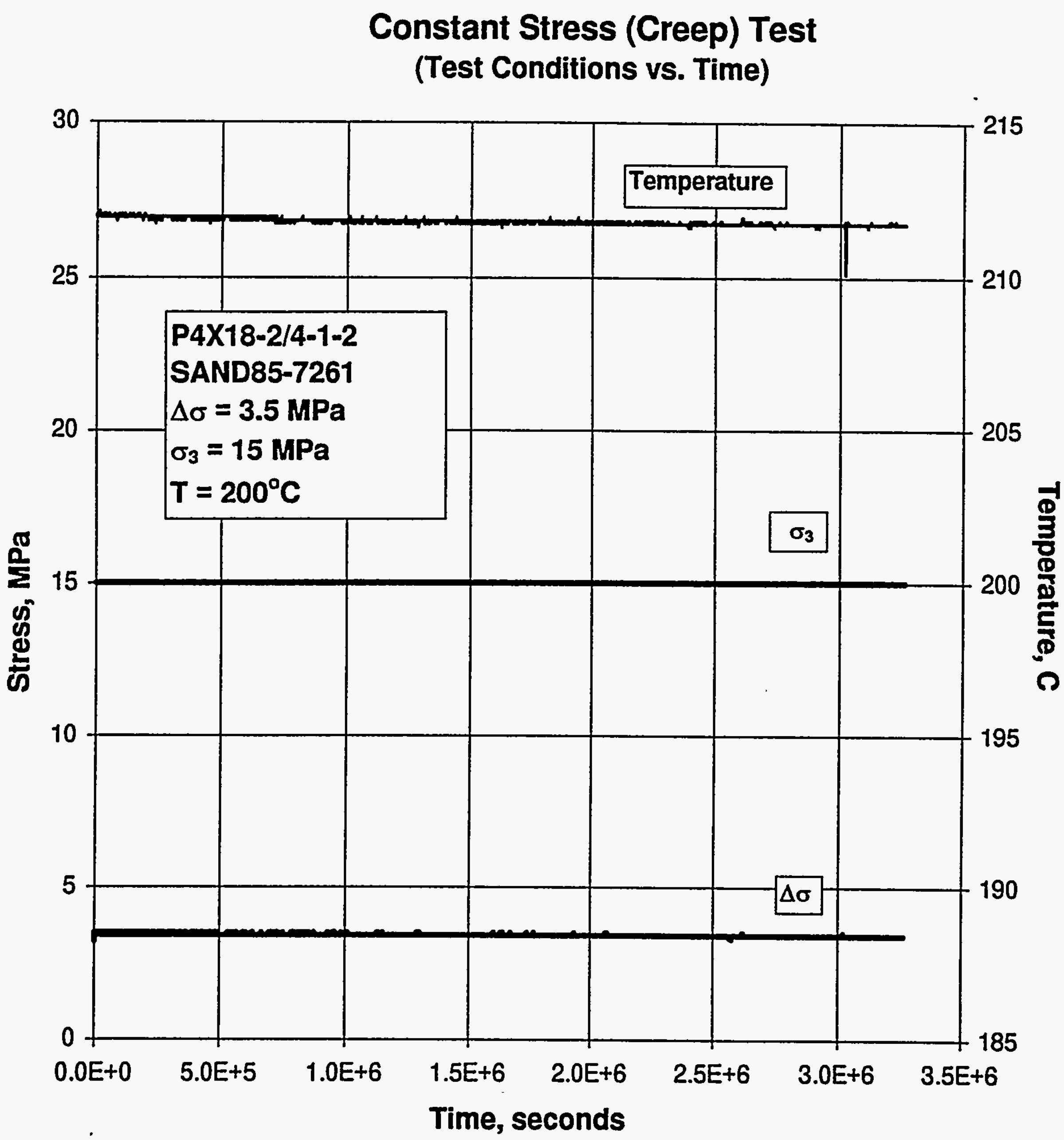

Figure C-53. Test Conditions Versus Time for a Creep Test: Specimen P4X18-2/4-1-2; Stage 1 of 1 (Argillaceous Salt).

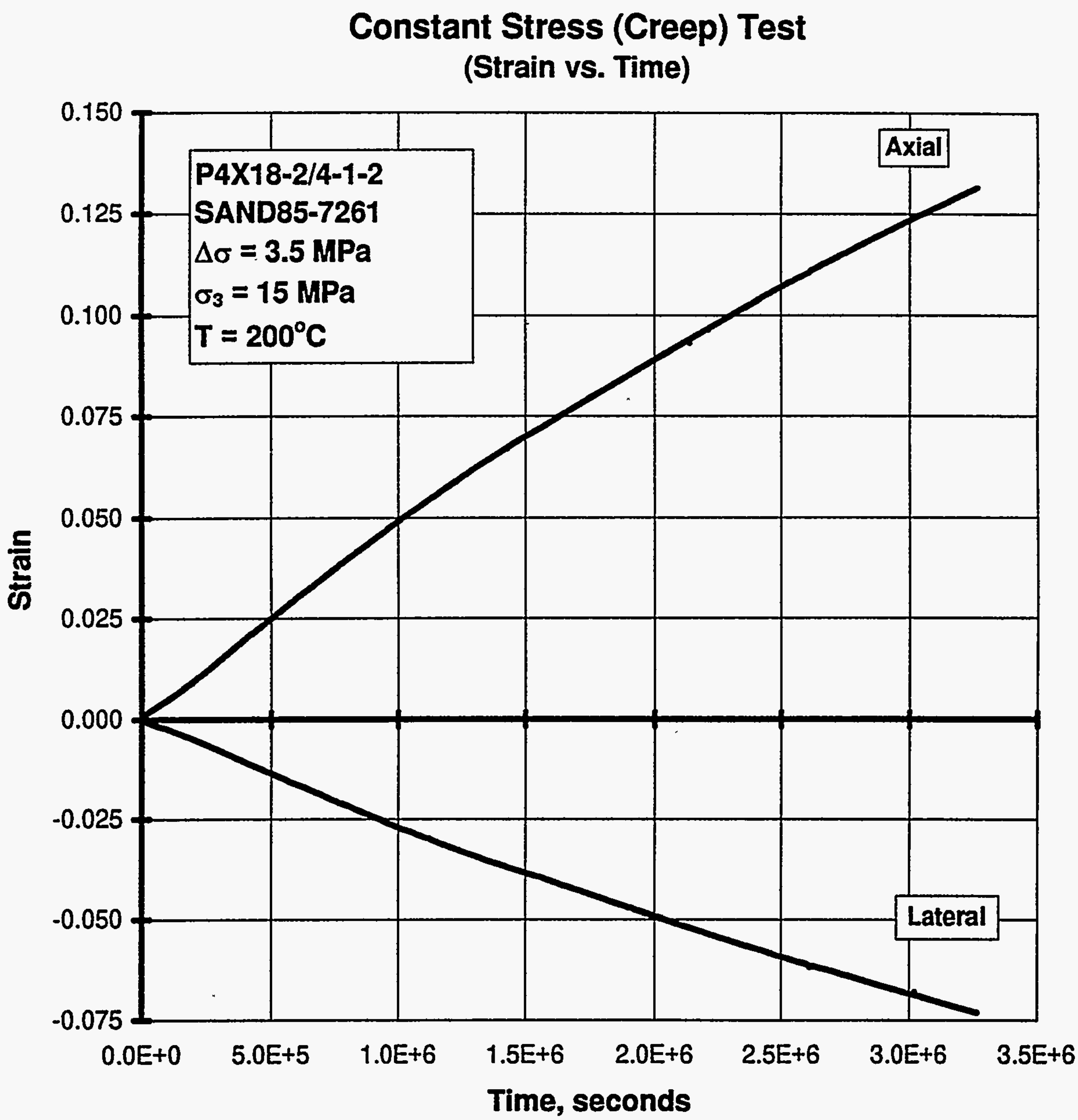

Figure C-54. Axial Strain and Lateral Strain Versus Time for a Creep Test: Specimen P4X18-2/4-1-2; Stage 1 of 1 (Argillaceous Salt. Anomalous Test Result. Possible Moisture Effects).

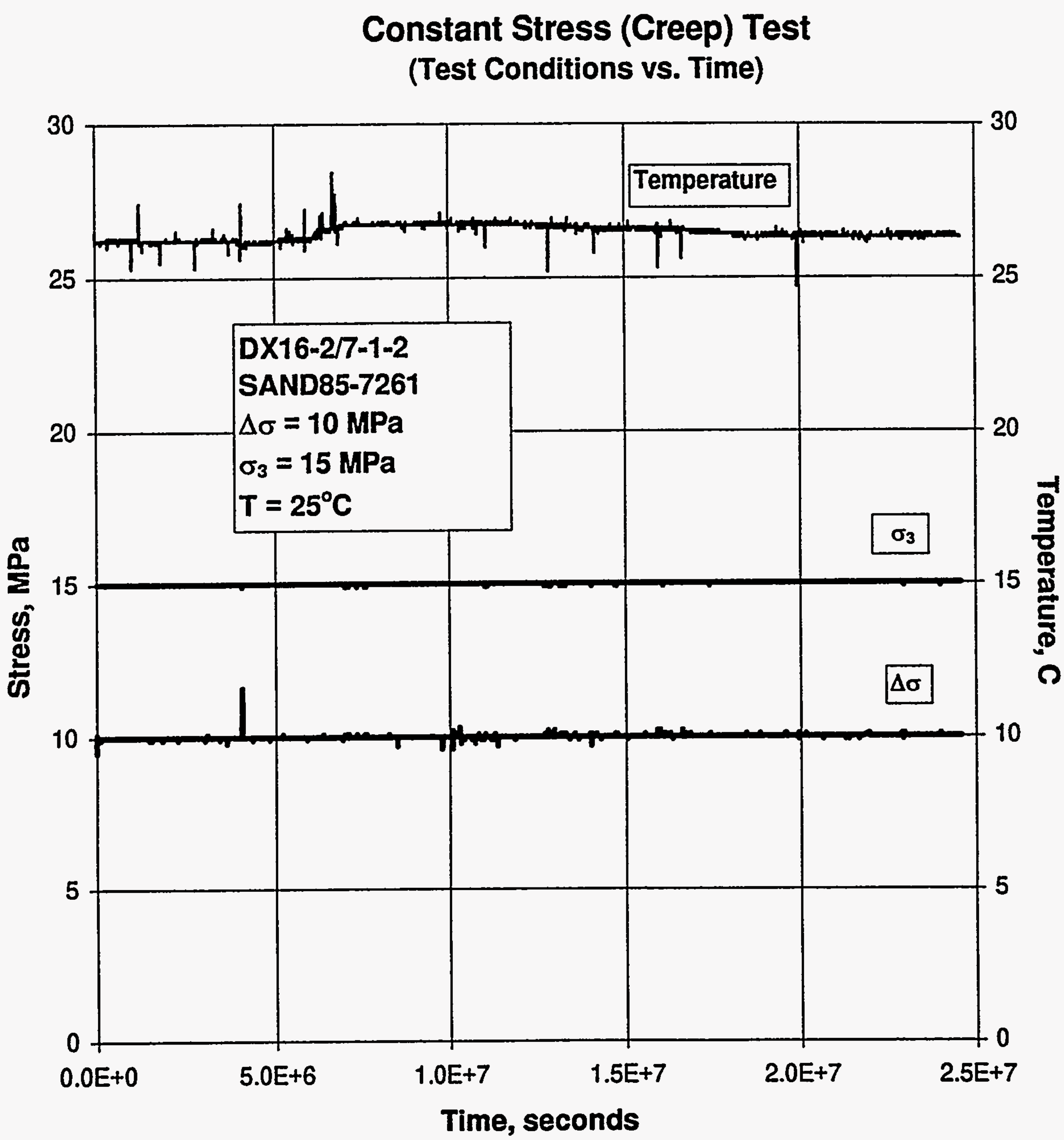

Figure C-55. Test Conditions Versus Time for a Creep Test: Specimen DX16-2/7-1-2; Stage 1 of 1.

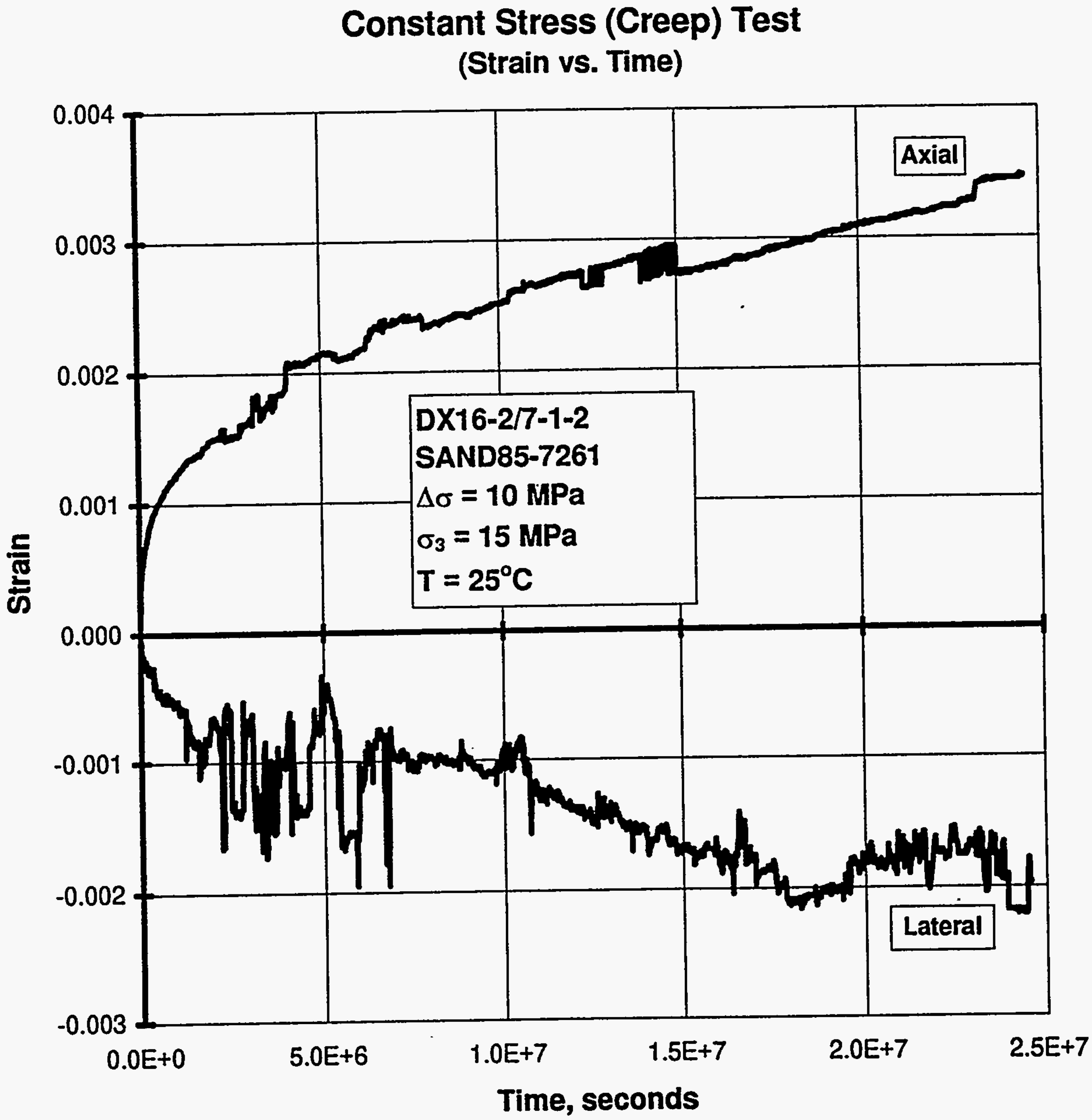

Figure C-56. Axial Strain and Lateral Strain Versus Time for a Creep Test: Specimen DX16-2/7-1-2; Stage 1 of 1.

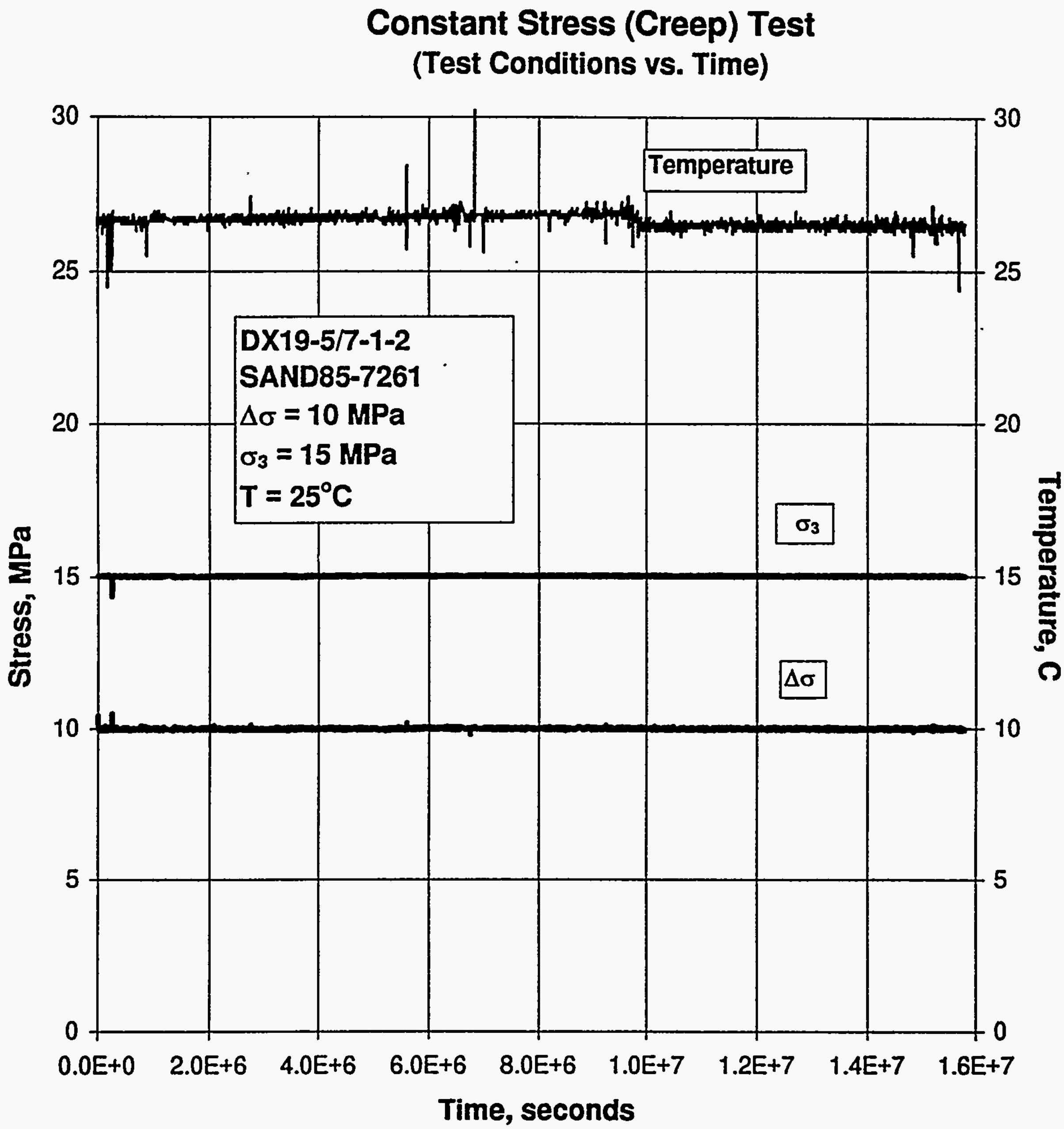

Figure C-57. Test Conditions Versus Time for a Creep Test: Specimen DX19-5/7-1-2; Stage 1 of 1.

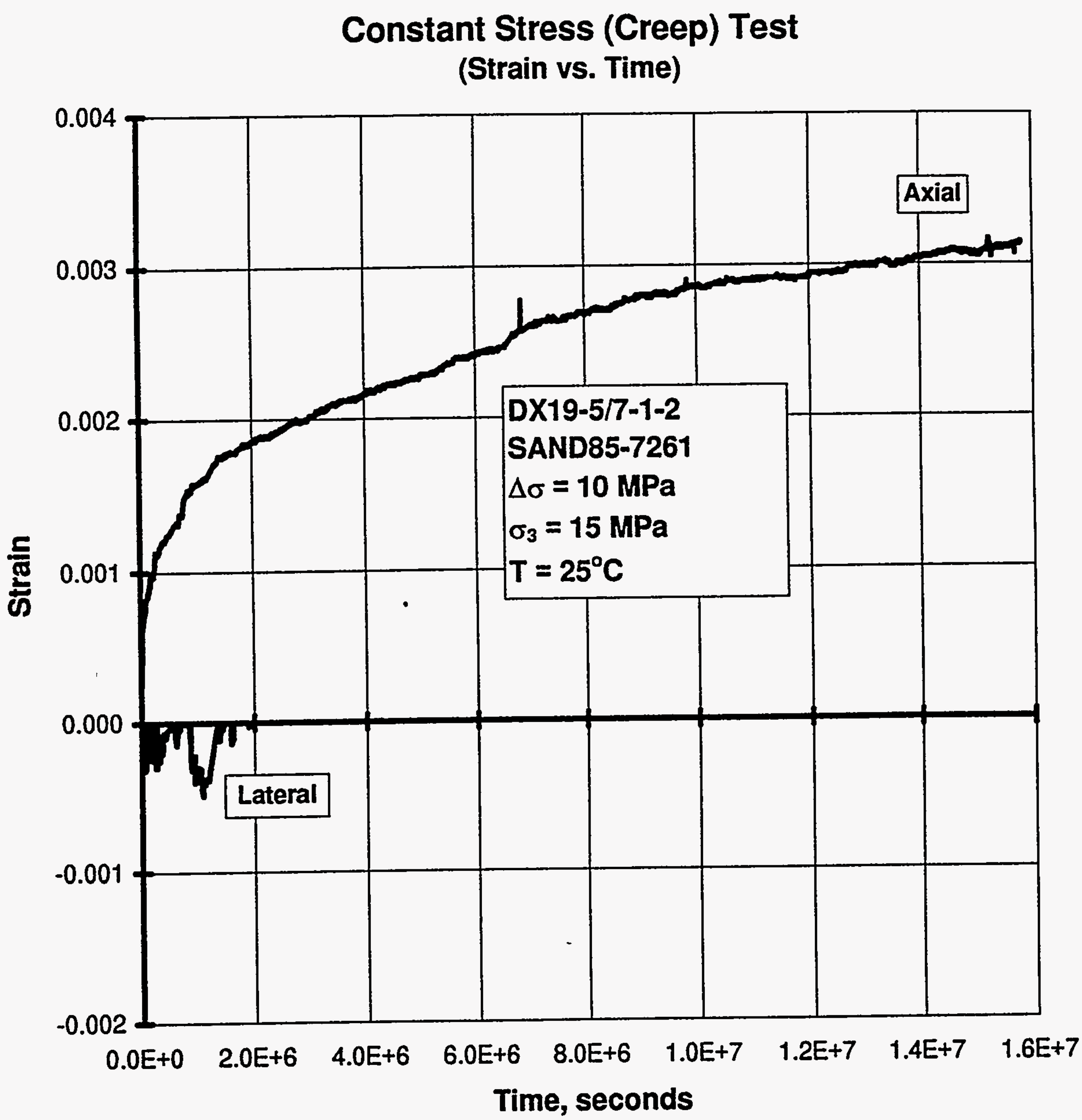

Figure C-58. Axial Strain and Lateral Strain Versus Time for a Creep Test: Specimen DX19-5/7-1-2; Stage 1 of 1.

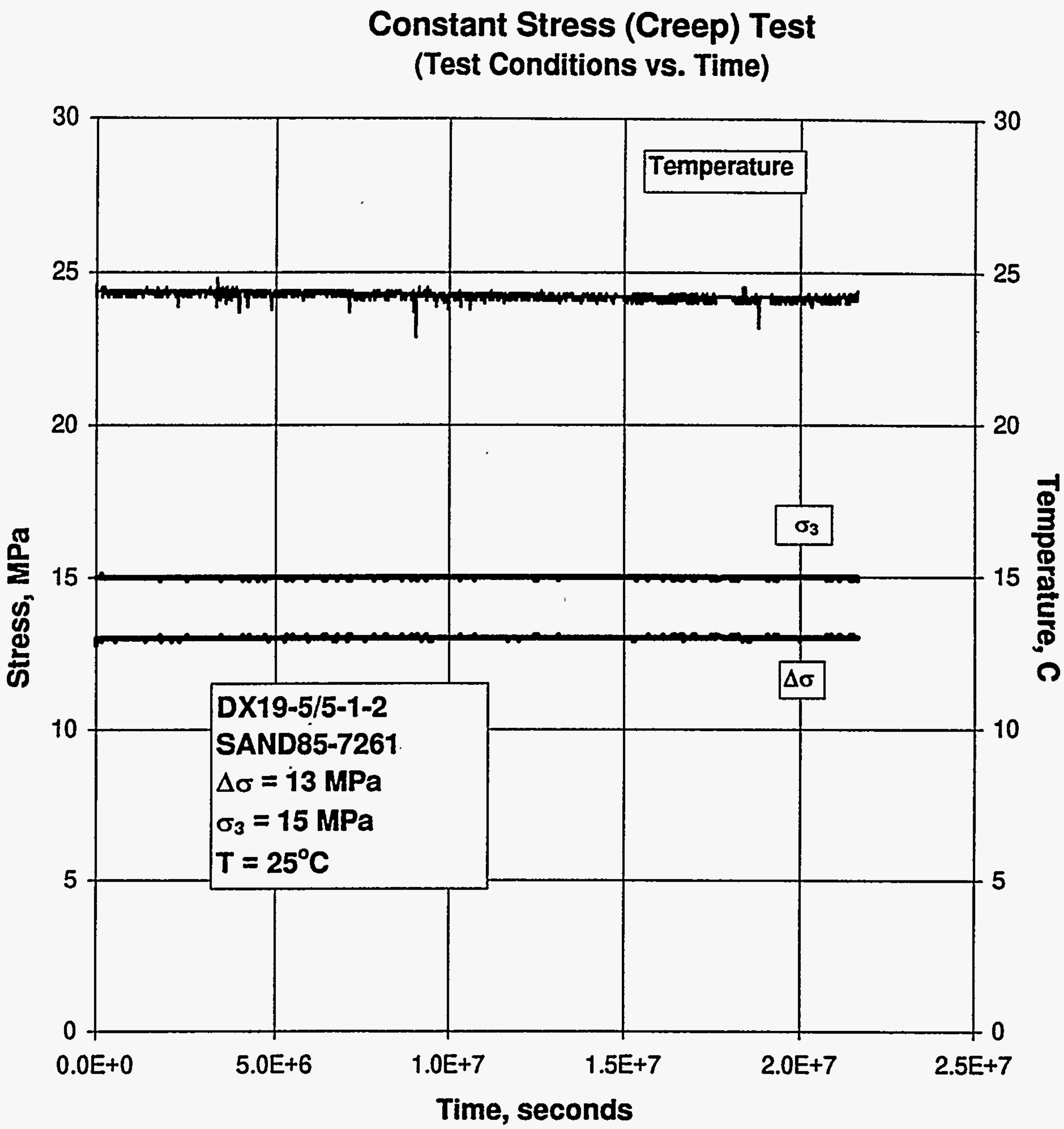

Figure C-59. Test Conditions Versus Time for a Creep Test: Specimen DX19-5/5-1-2; Stage 1 of 1.

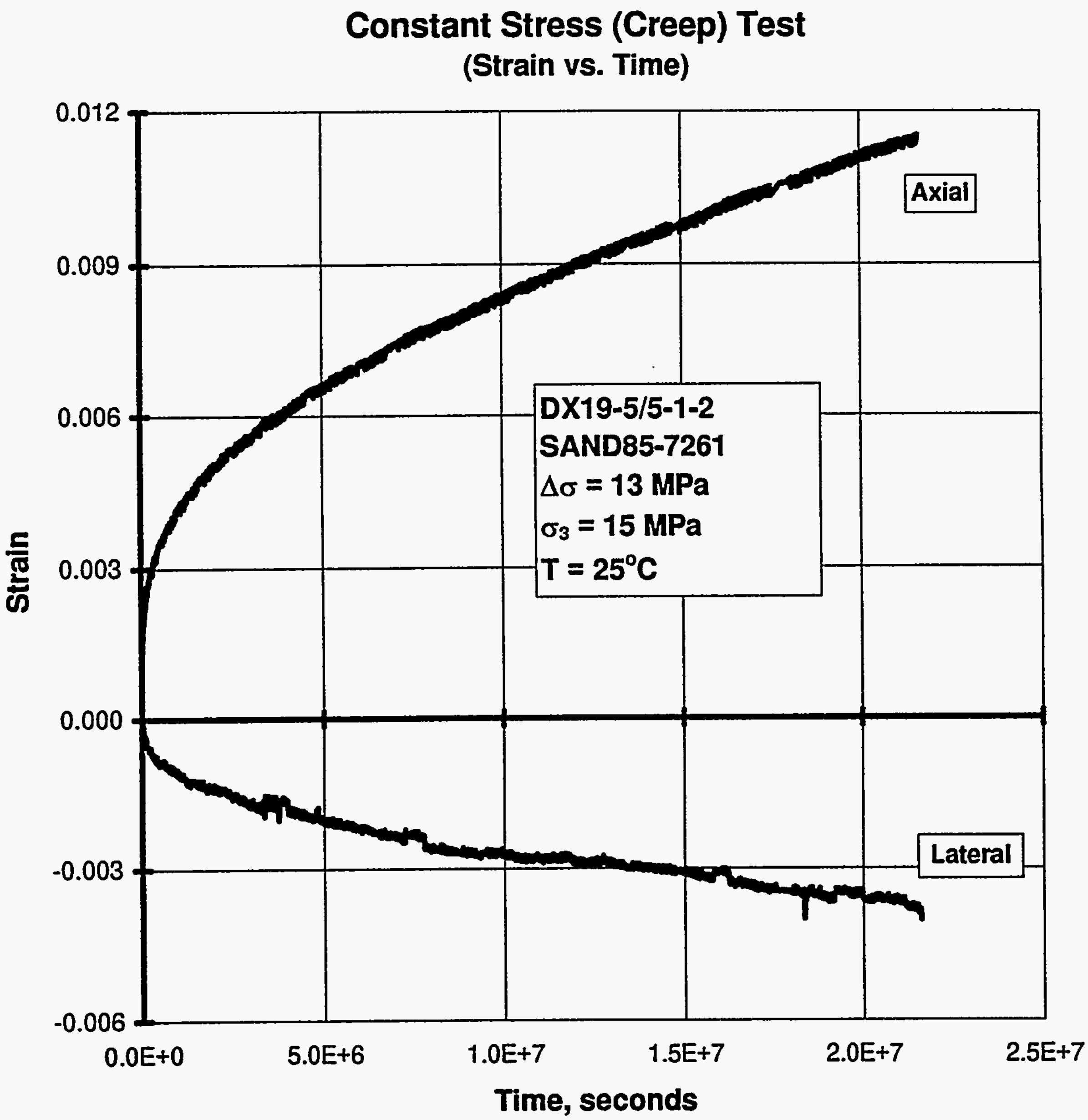

Figure C-60. Axial Strain and Lateral Strain Versus Time for a Creep Test: Specimen DX19-5/5-1-2; Stage 1 of 1.

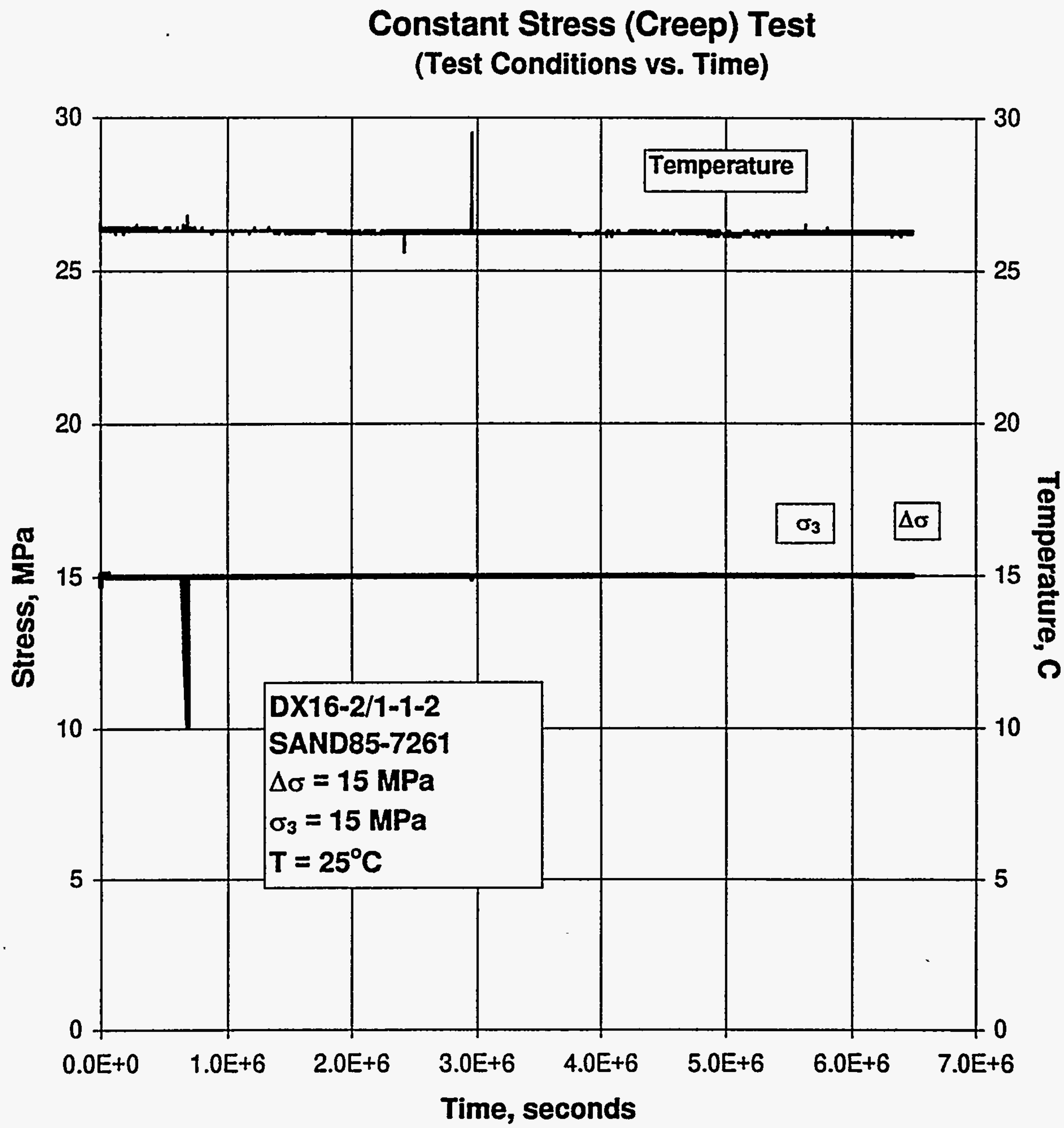

Figure C-61. Test Conditions Versus Time for a Creep Test: Specimen DX16-2/1-1-2; Stage 1 of 1.

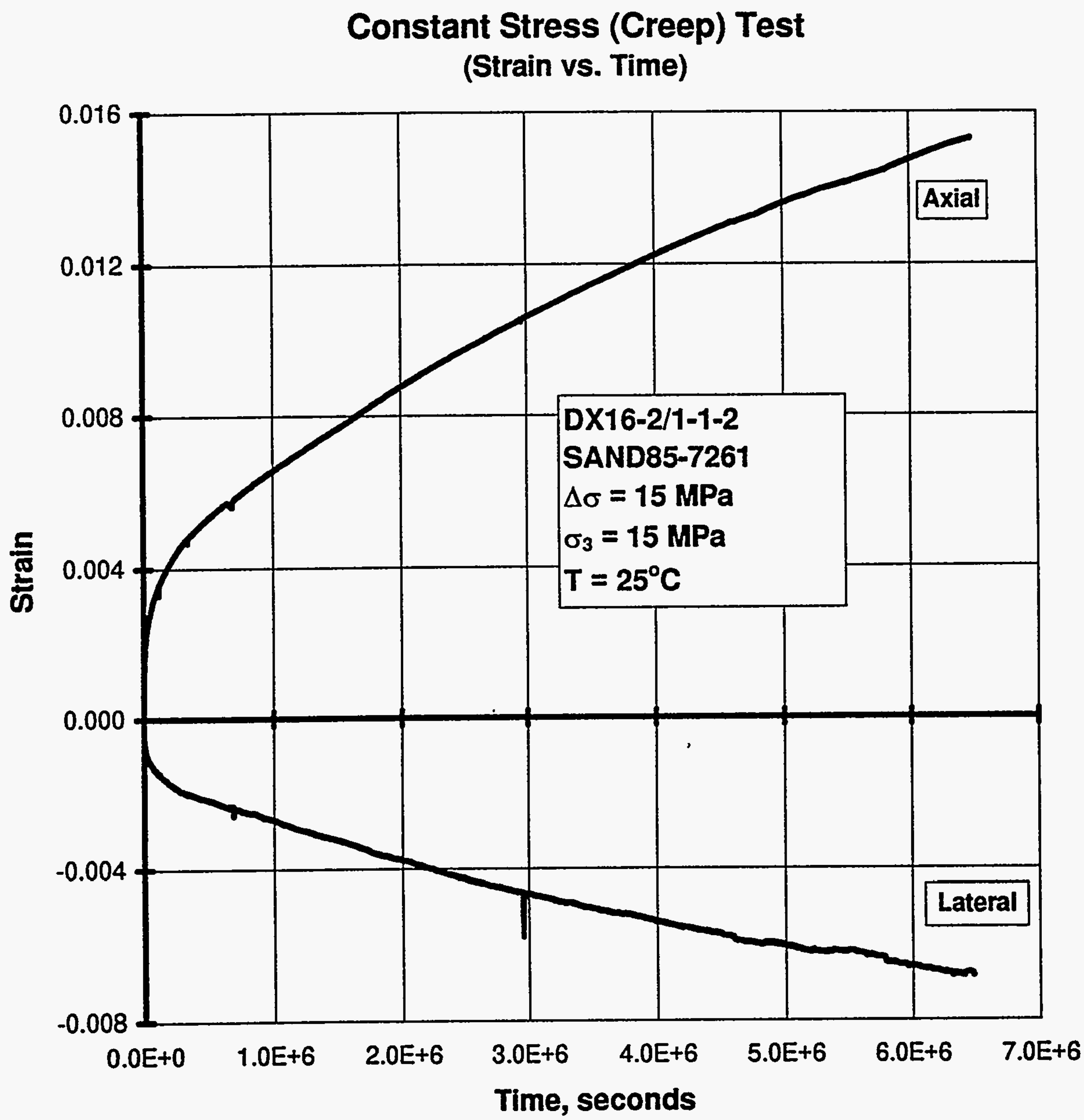

Figure C-62. Axial Strain and Lateral Strain Versus Time for a Creep Test: Specimen DX16-2/1-1-2; Stage 1 of 1.

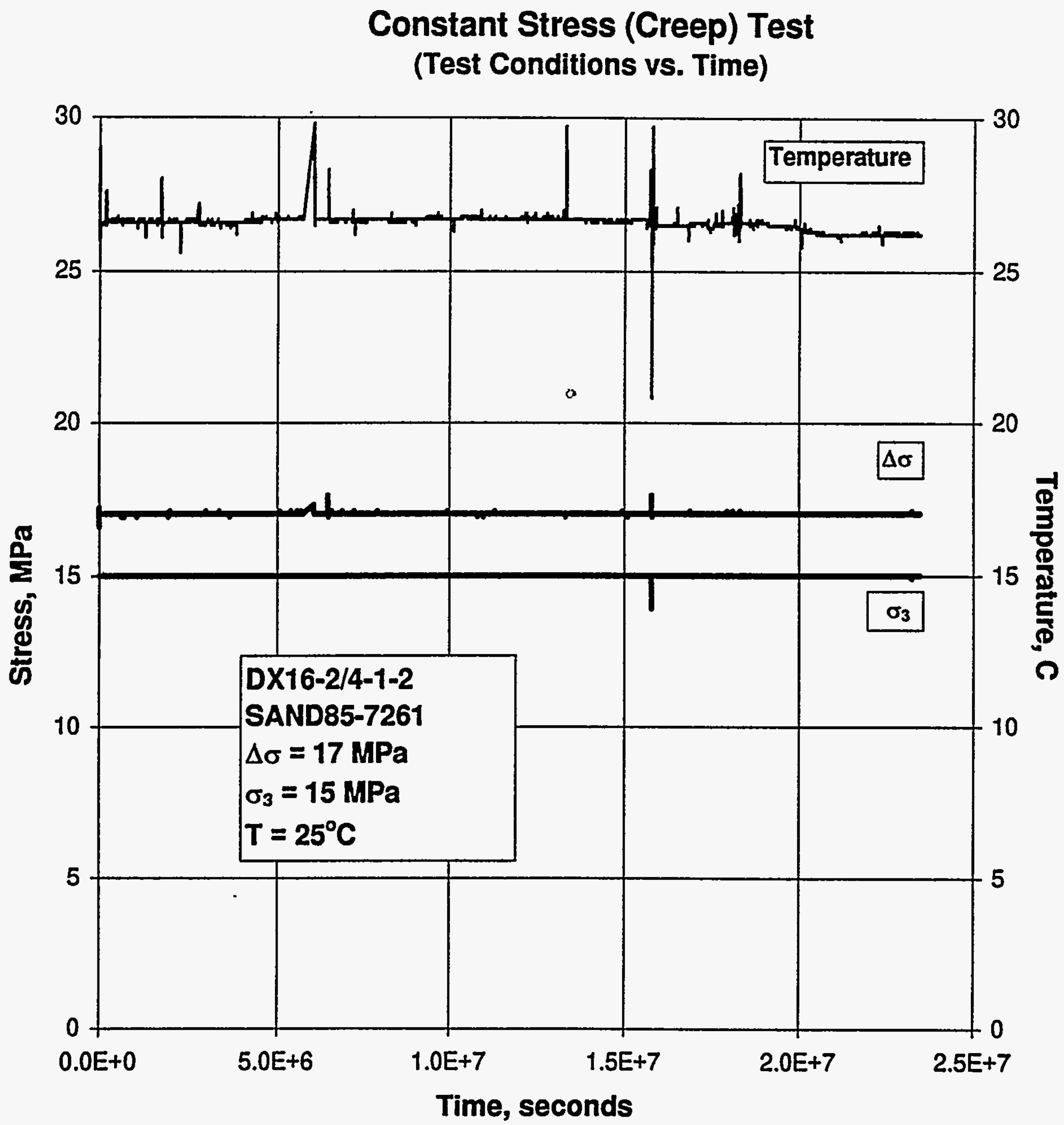

Figure C-63. Test Conditions Versus Time for a Creep Test: Specimen DX16-2/4-1-2; Stage 1 of 1.

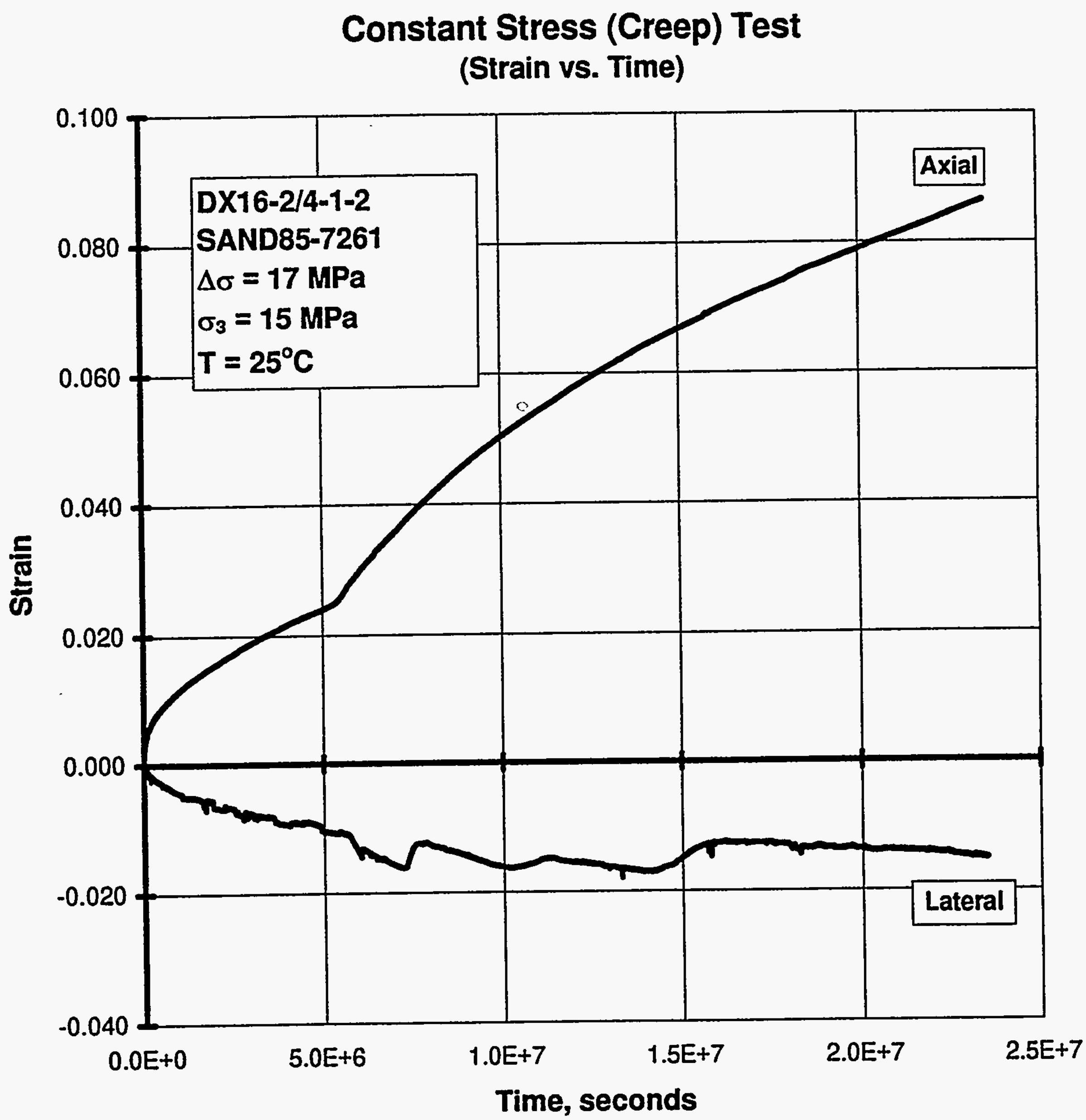

Figure C-64. Axial Strain and Lateral Strain Versus Time for a Creep Test: Specimen DX16-2/4-1-2; Stage 1 of 1 (Anomalous Test Result. Possible Machine Malfunction).

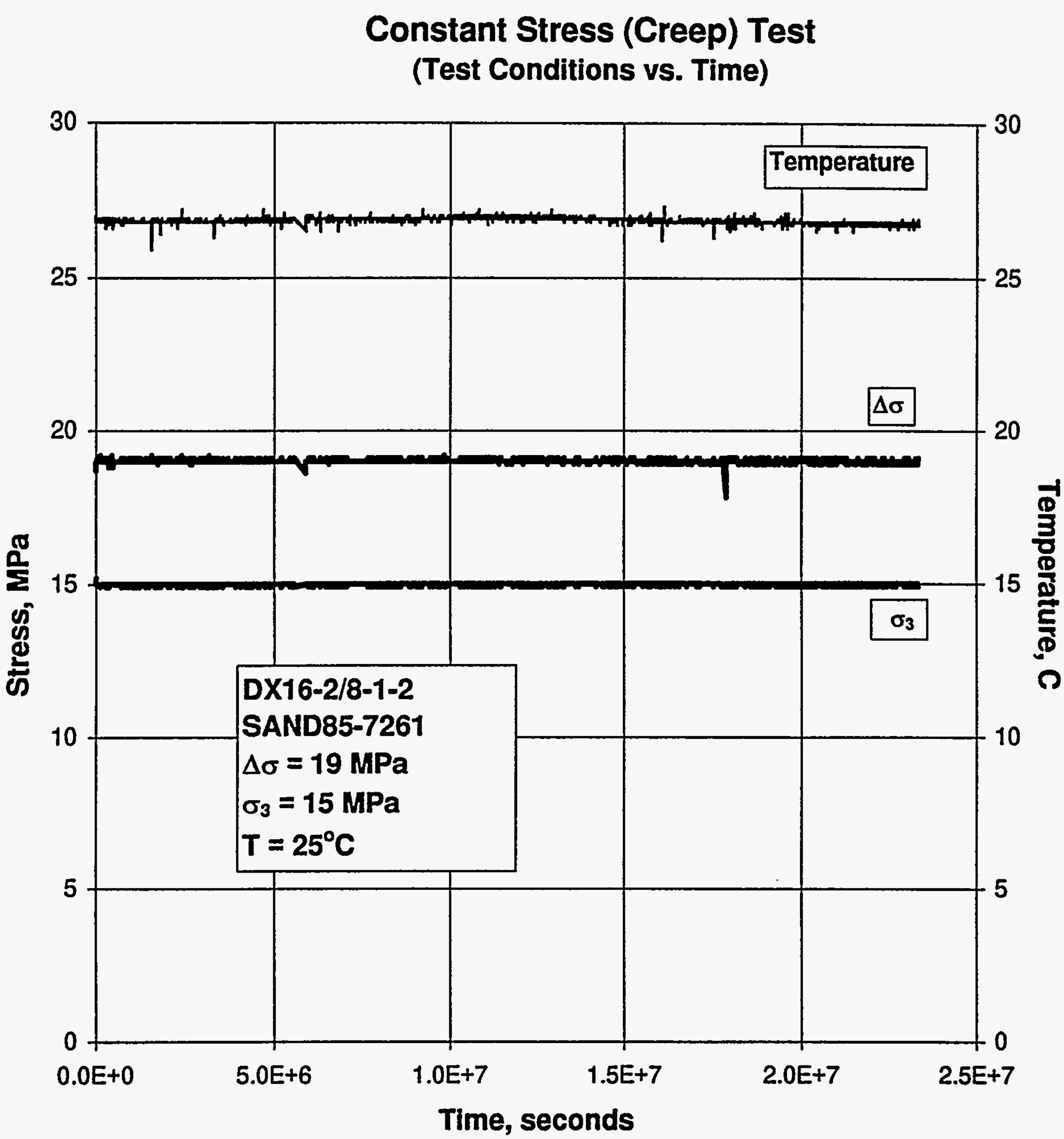

Figure C-65. Test Conditions Versus Time for a Creep Test: Specimen DX16-2/8-1-2; Stage 1 of 1.

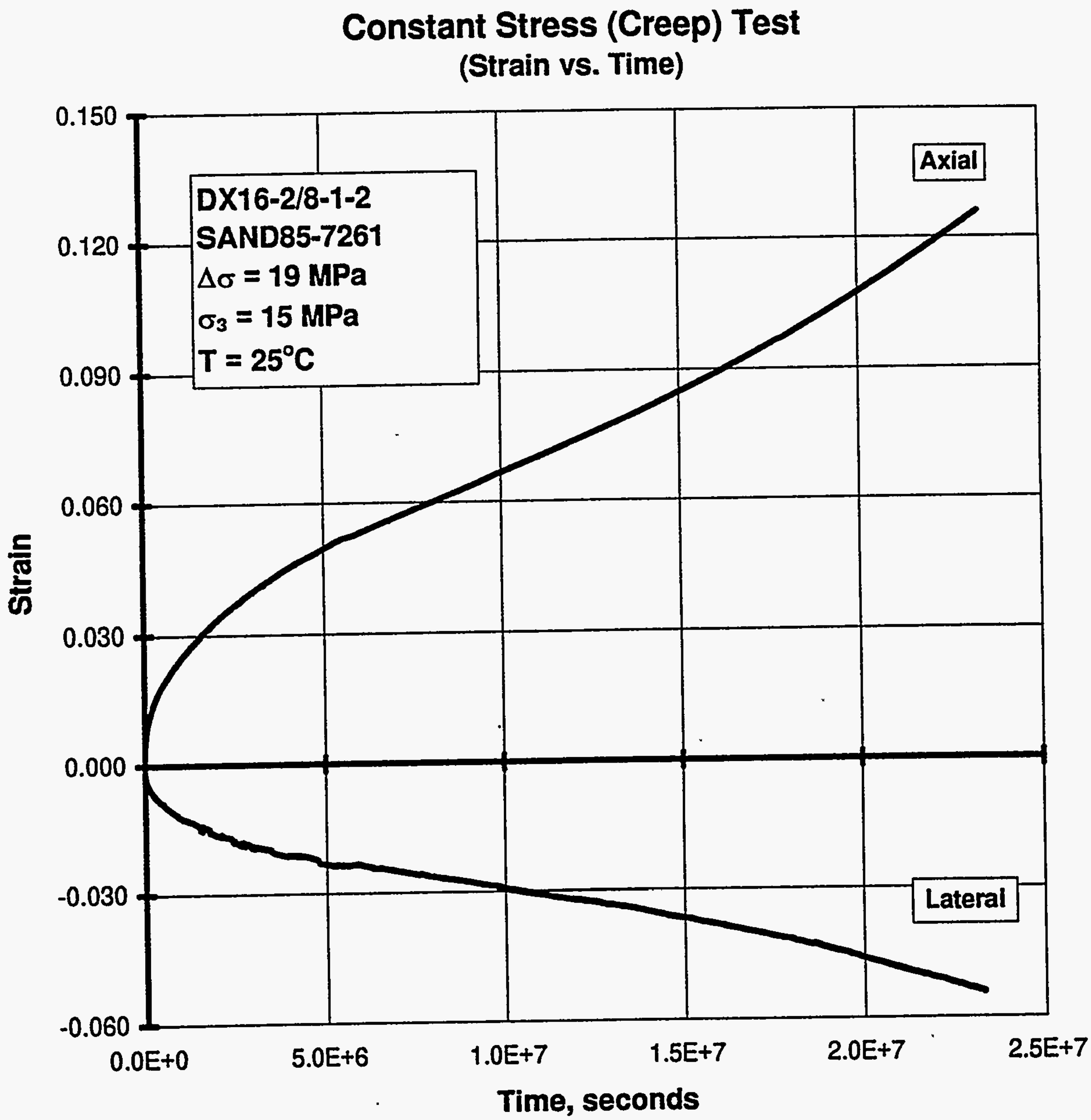

Figure C-66. Axial Strain and Lateral Strain Versus Time for a Creep Test: Specimen DX16-2/8-1-2; Stage 1 of 1.

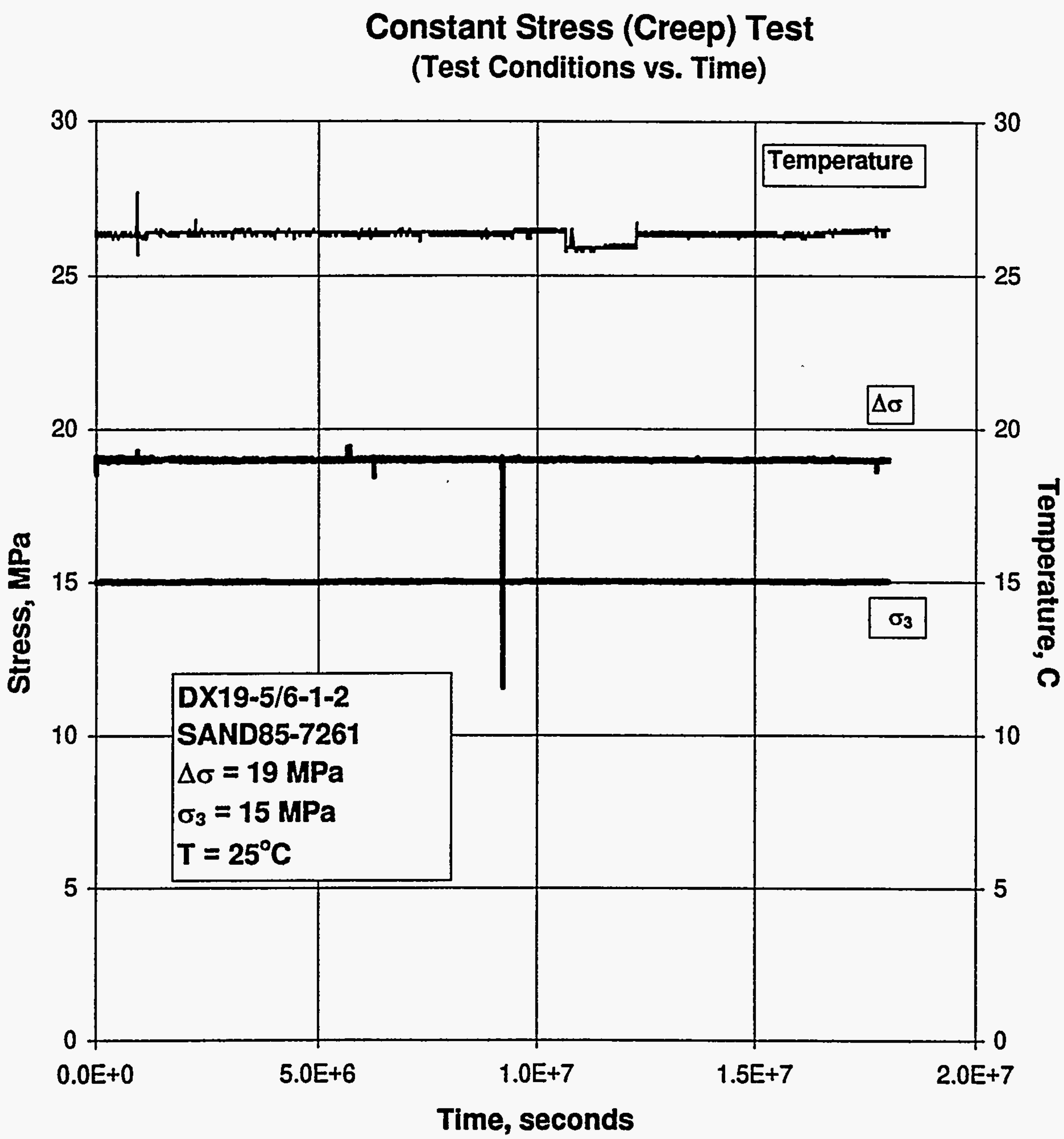

Figure C-67. Test Conditions Versus Time for a Creep Test: Specimen DX19-5/6-1-2; Stage 1 of 1.

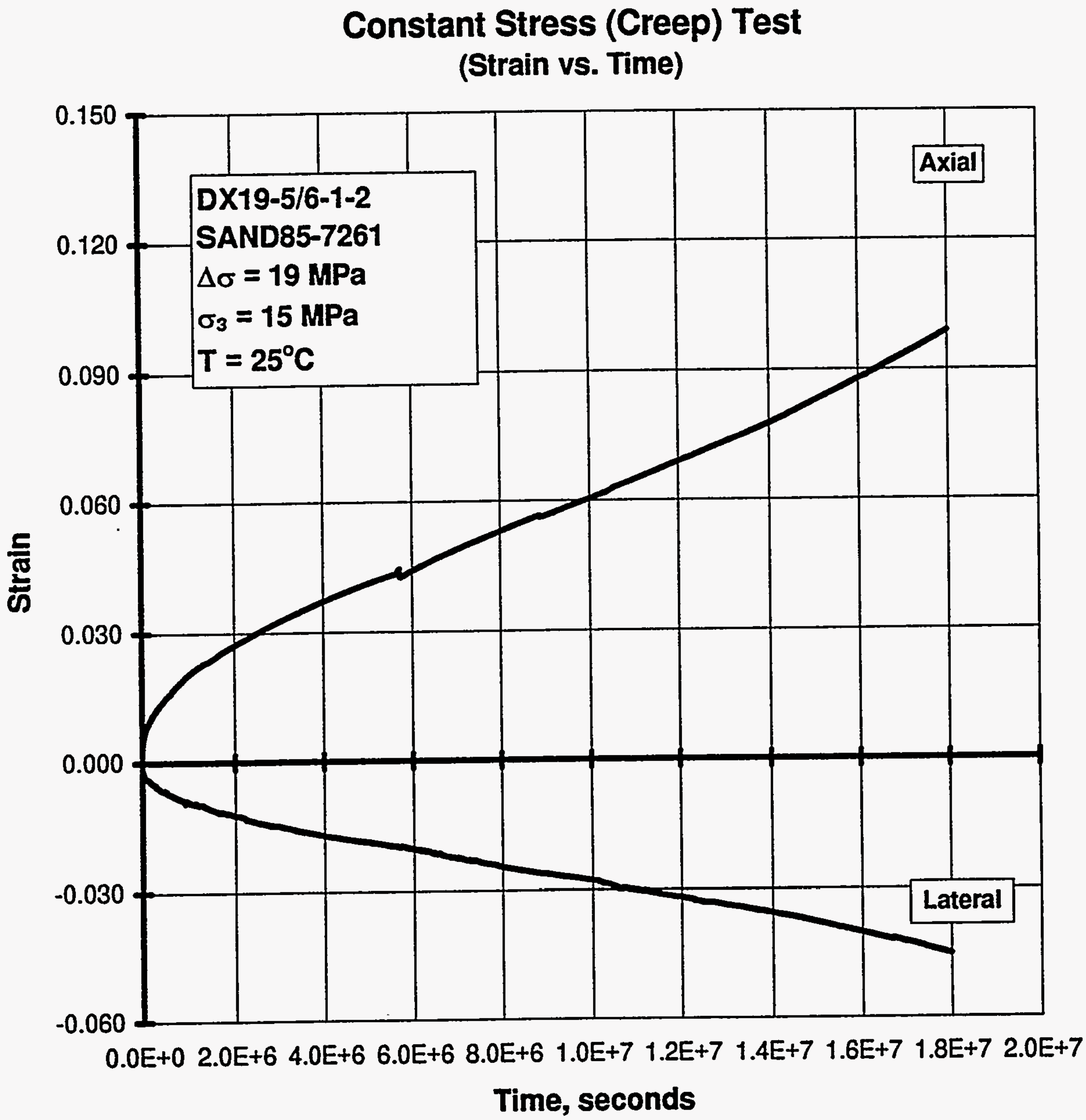

Figure C-68. Axial Strain and Lateral Strain Versus Time for a Creep Test: Specimen DX19-5/6-1-2; Stage 1 of 1.

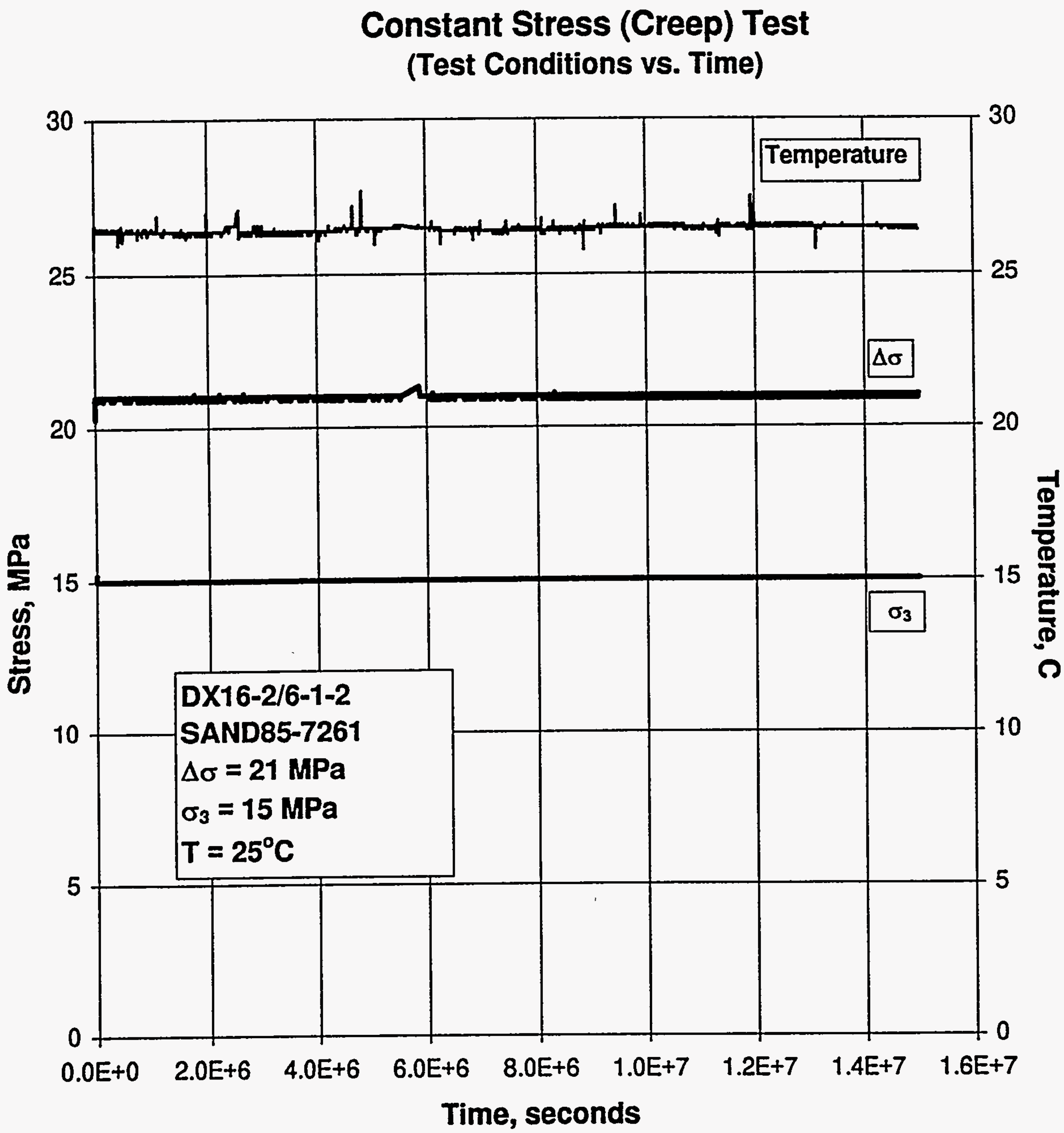

Figure C-69. Test Conditions Versus Time for a Creep Test: Specimen DX16-2/6-1-2; Stage 1 of 1.

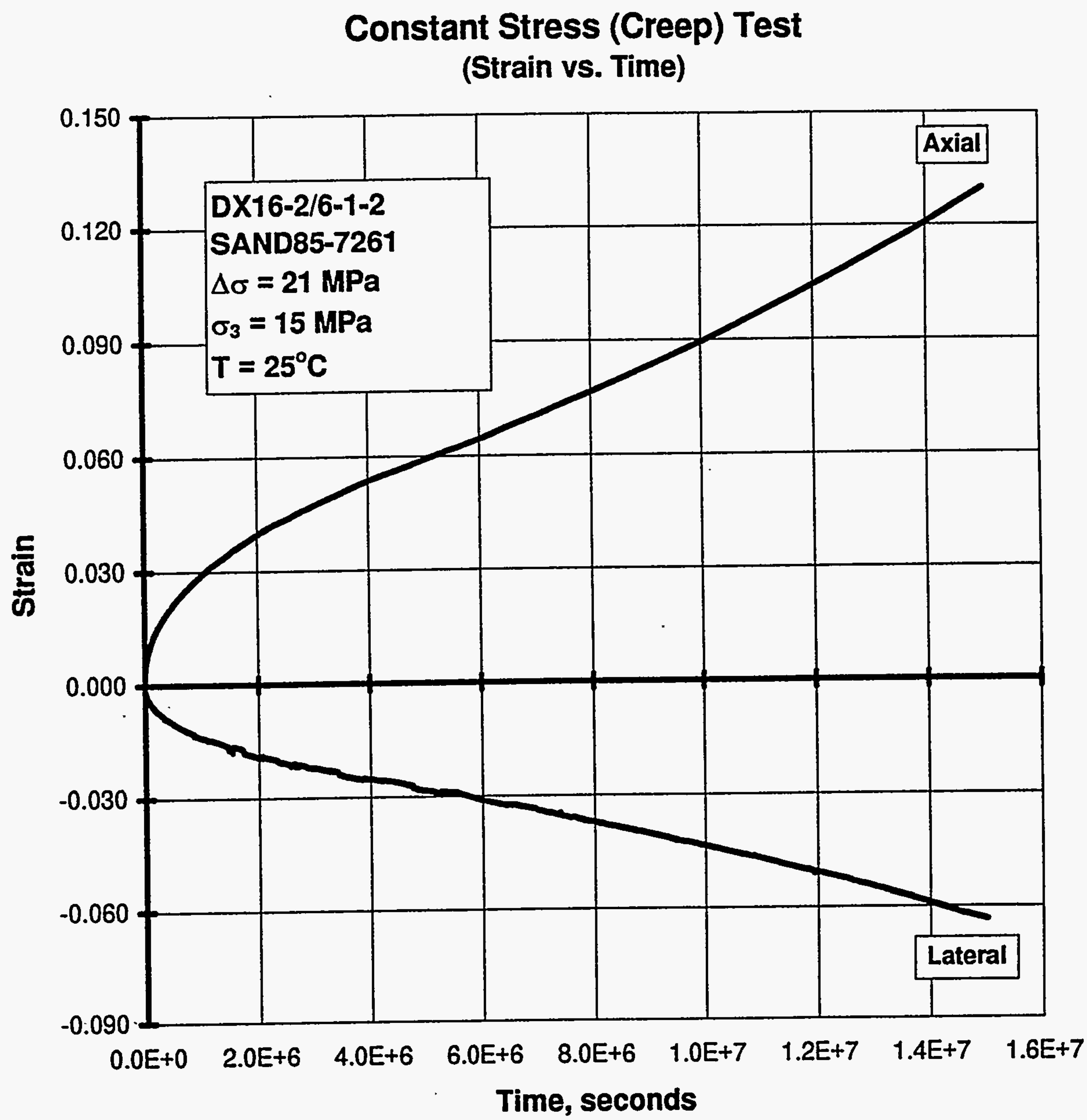

Figure C-70. Axial Strain and Lateral Strain Versus Time for a Creep Test: Specimen DX16-2/6-1-2; Stage 1 of 1 (Possible Jacket Leak Near End of Test).

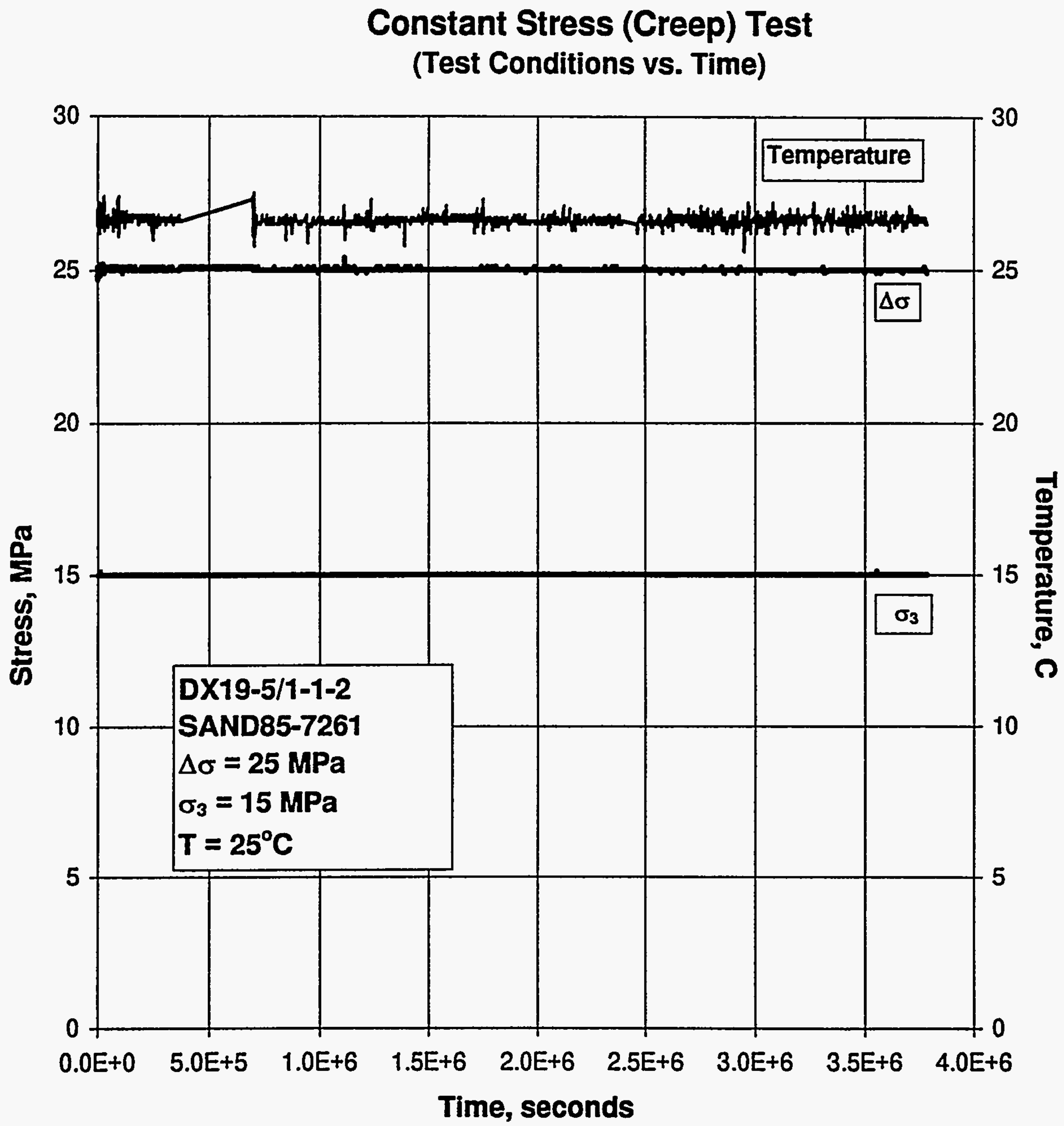

Figure C-71. Test Conditions Versus Time for a Creep Test: Specimen DX19-5/1-1-2; Stage 1 of 1.

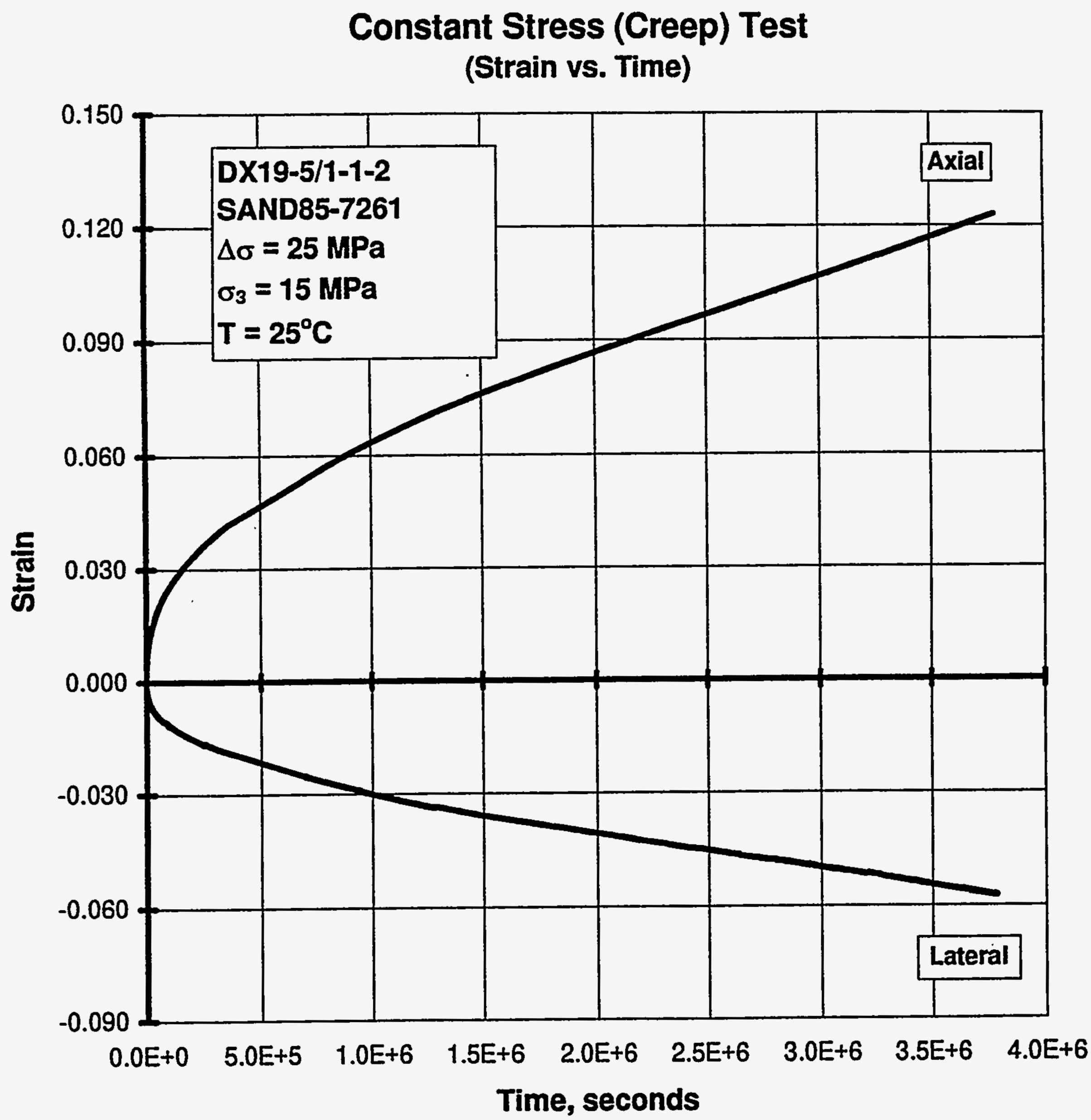

Figure C-72. Axial Strain and Lateral Strain Versus Time for a Creep Test: Specimen DX19-5/1-1-2; Stage 1 of 1.

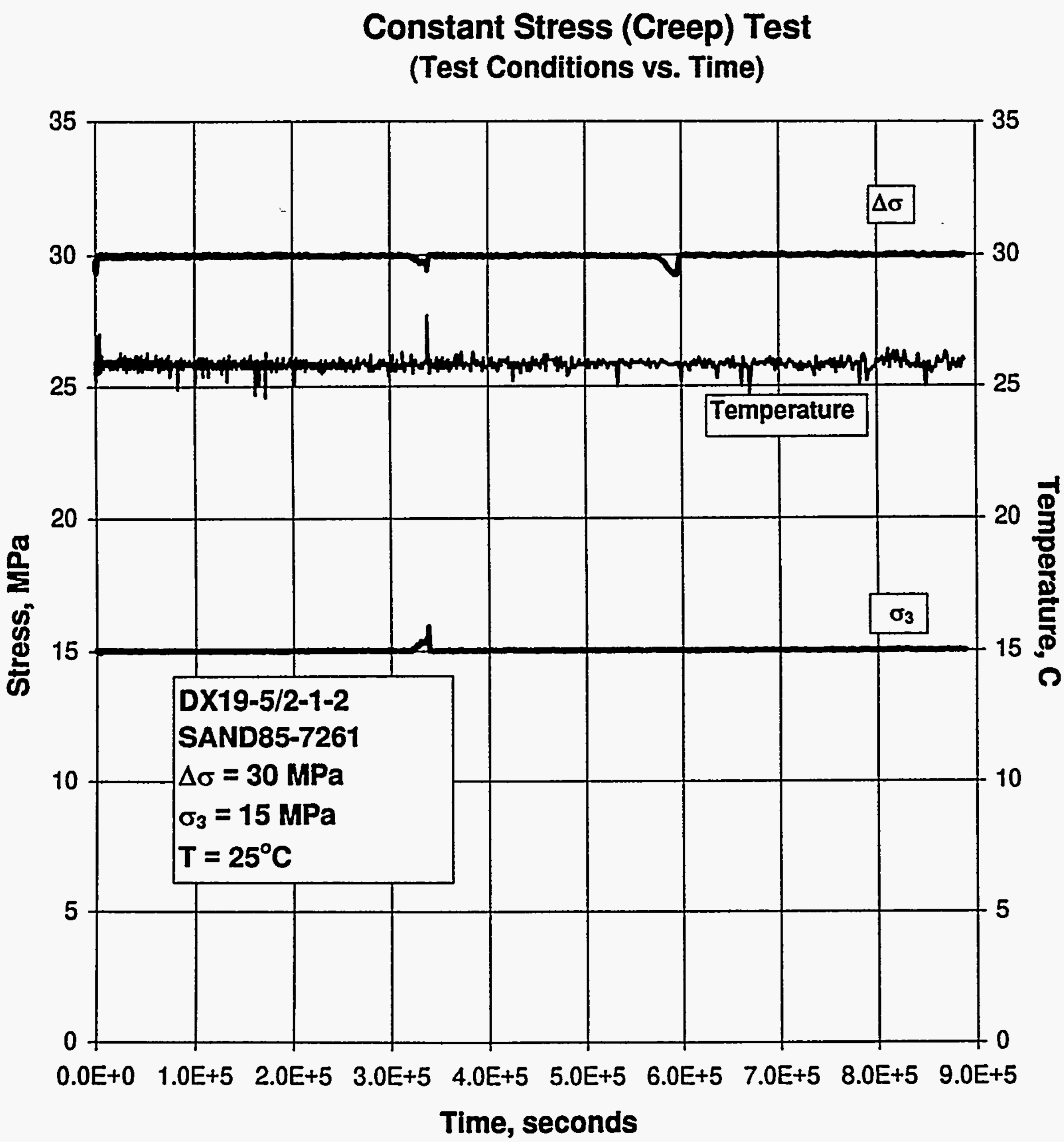

Figure C-73. Test Conditions Versus Time for a Creep Test: Specimen DX19-5/2-1-2; Stage 1 of 1.

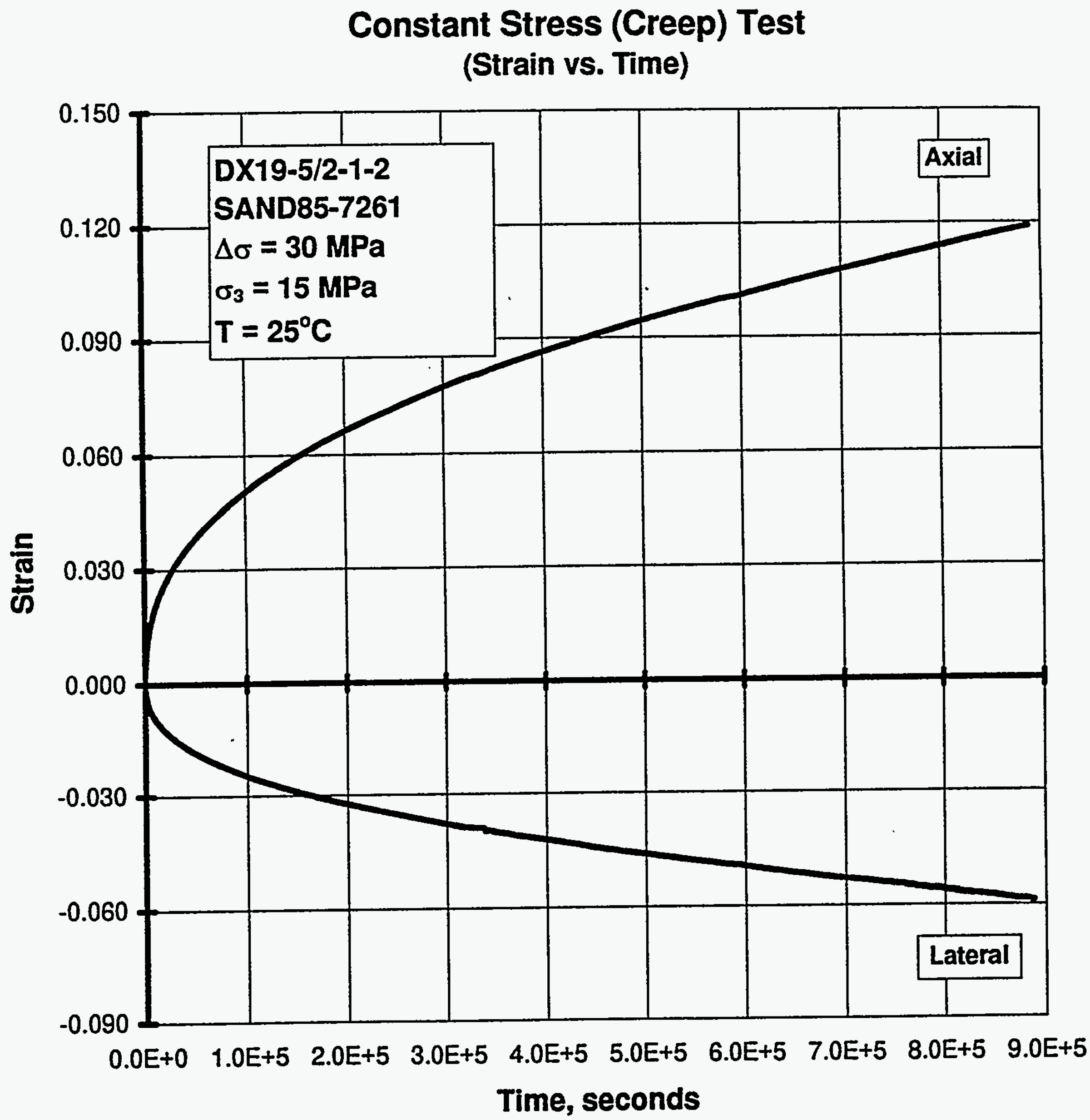

Figure C-74. Axial Strain and Lateral Strain Versus Time for a Creep Test: Specimen DX19-5/2-1-2; Stage 1 of 1.

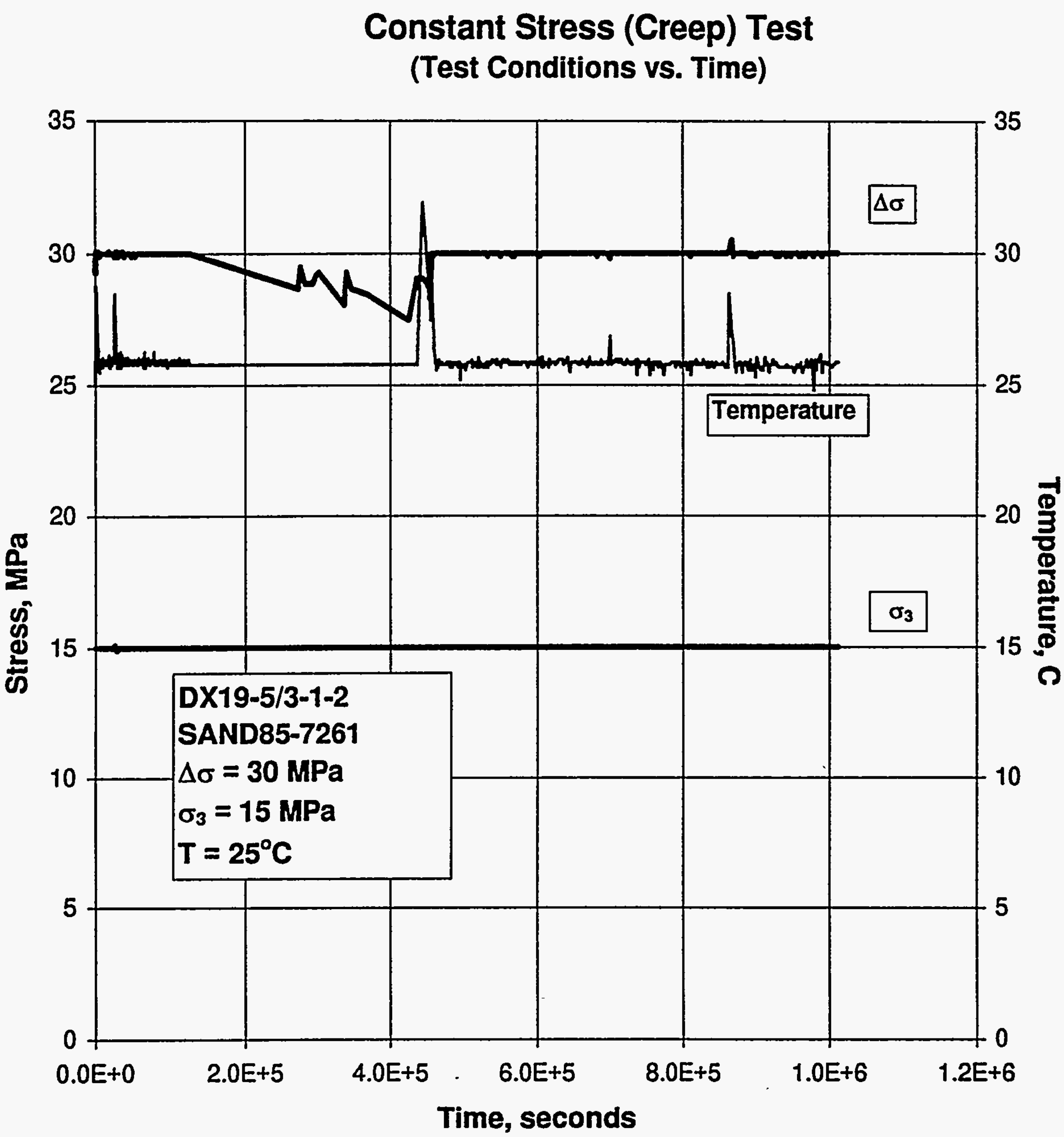

Figure C-75. Test Conditions Versus Time for a Creep Test: Specimen DX19-5/3-1-2; Stage 1 of 1.

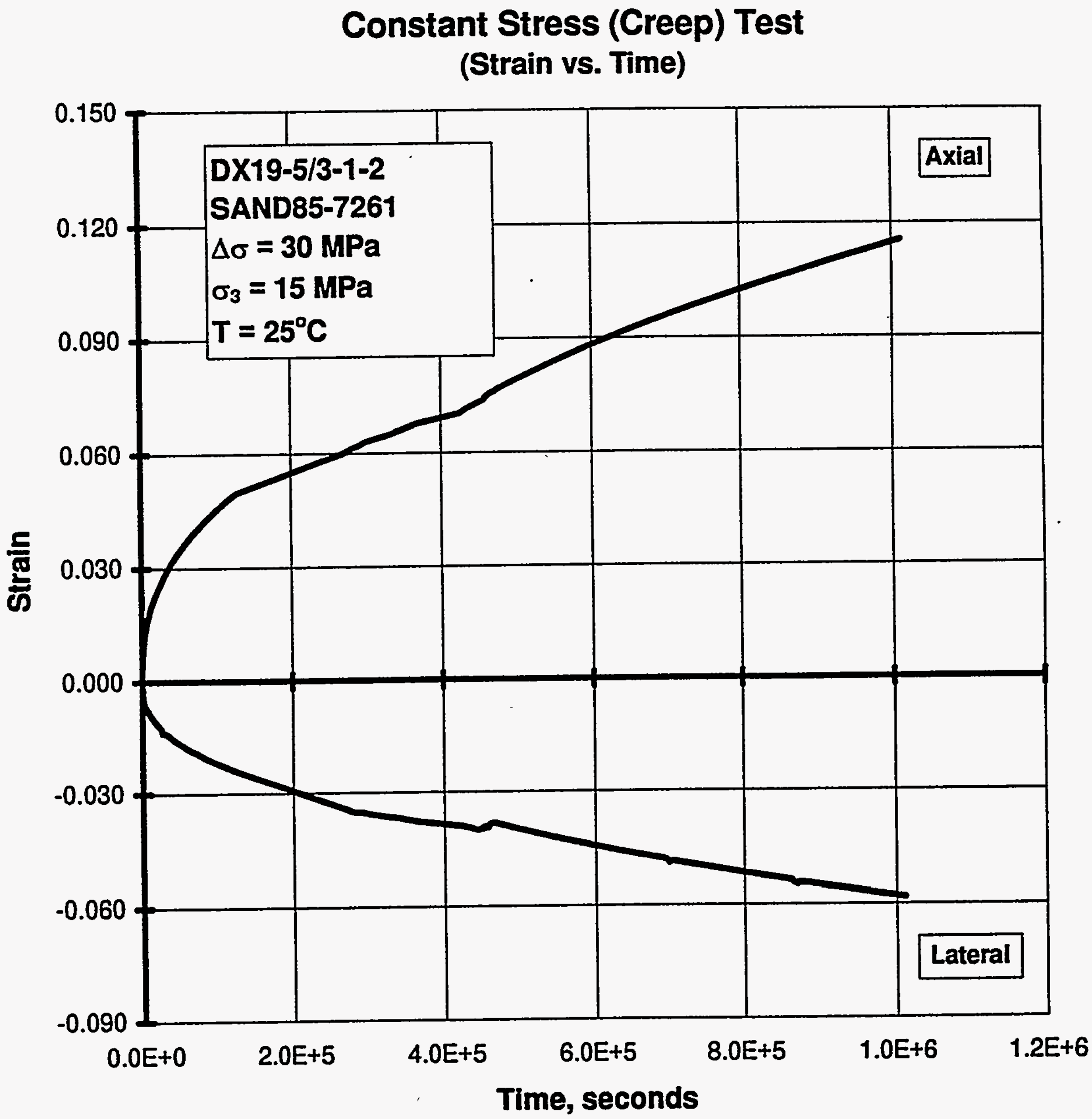

Figure C-76. Axial Strain and Lateral Strain Versus Time for a Creep Test: Specimen DX19-5/3-1-2; Stage 1 of 1.

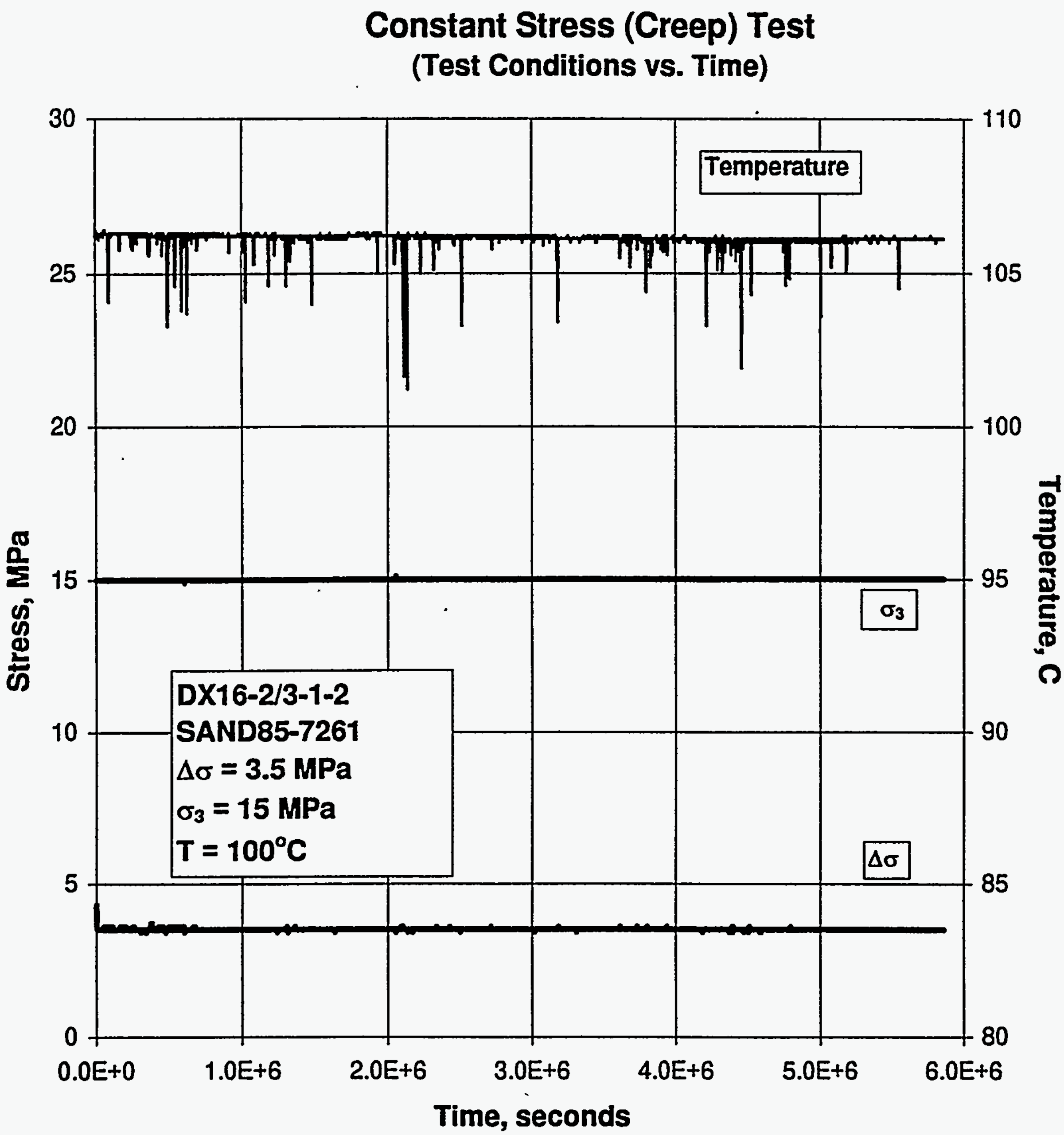

Figure C-77. Test Conditions Versus Time for a Creep Test: Specimen DX16-2/3-1-2; Stage 1 of 1.

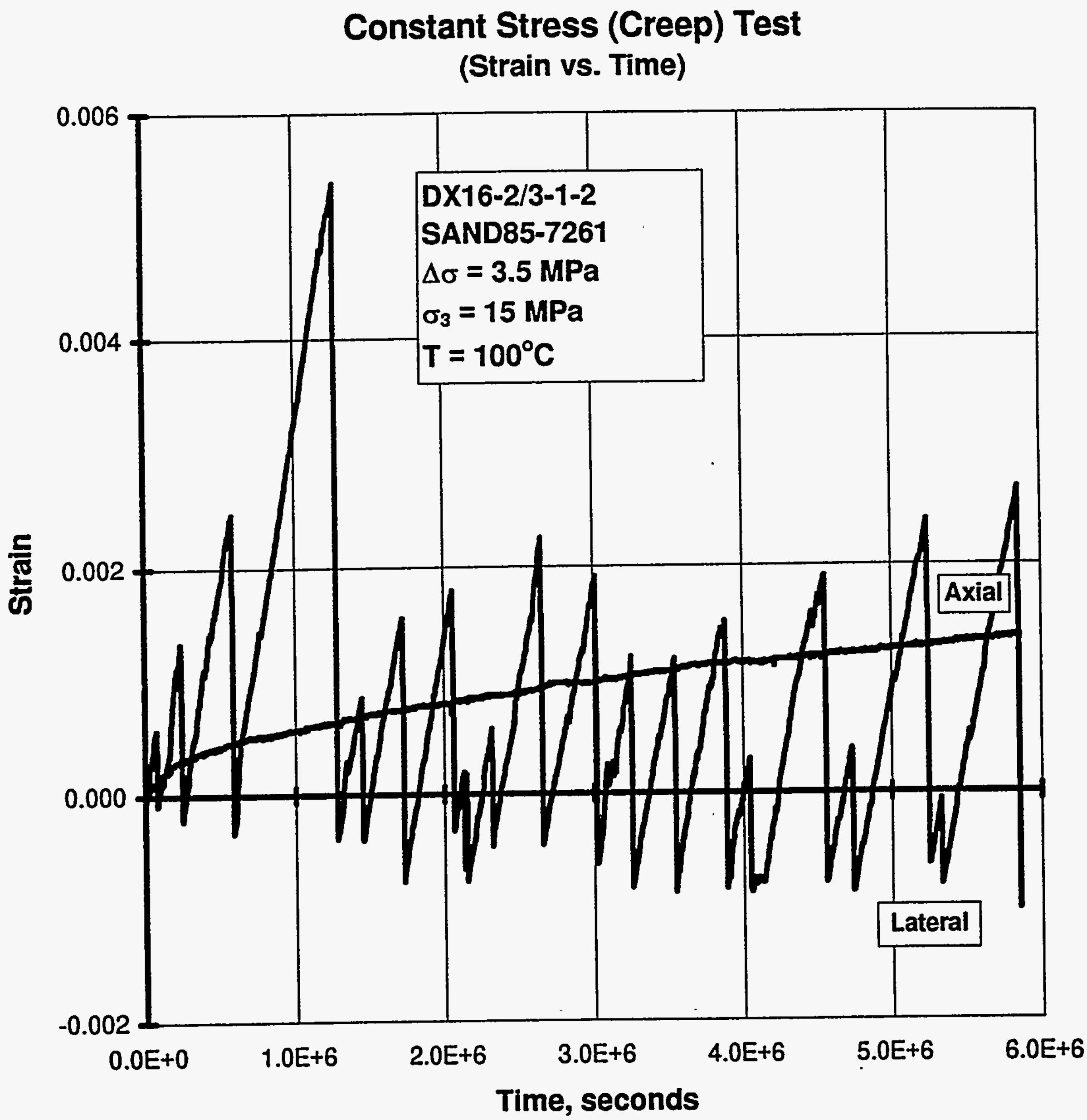

Figure C-78. Axial Strain and Lateral Strain Versus Time for a Creep Test: Specimen DX16-2/3-1-2; Stage 1 of 1.

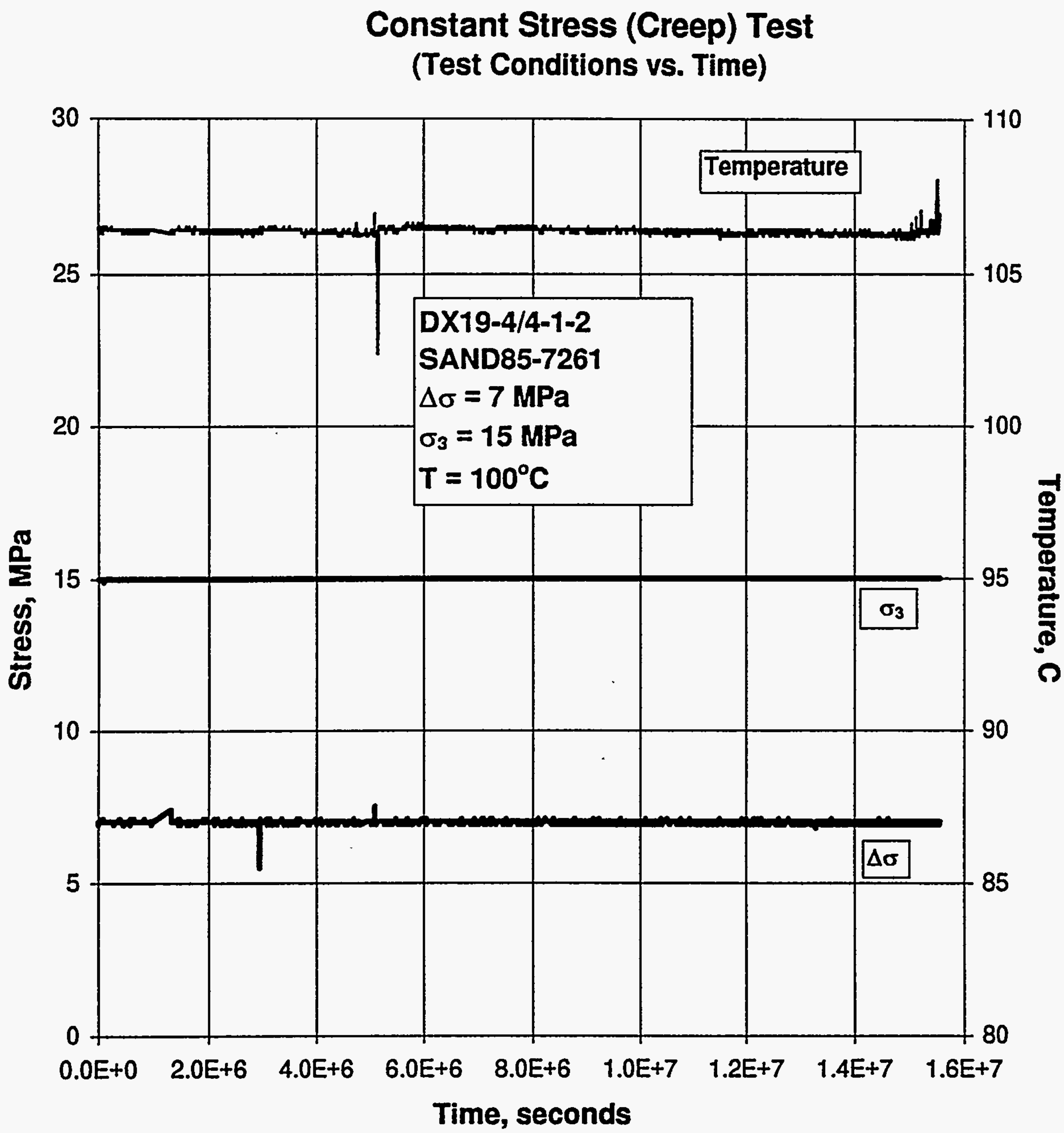

Figure C-79. Test Conditions Versus Time for a Creep Test: Specimen DX19-4/4-1-2; Stage 1 of 1.

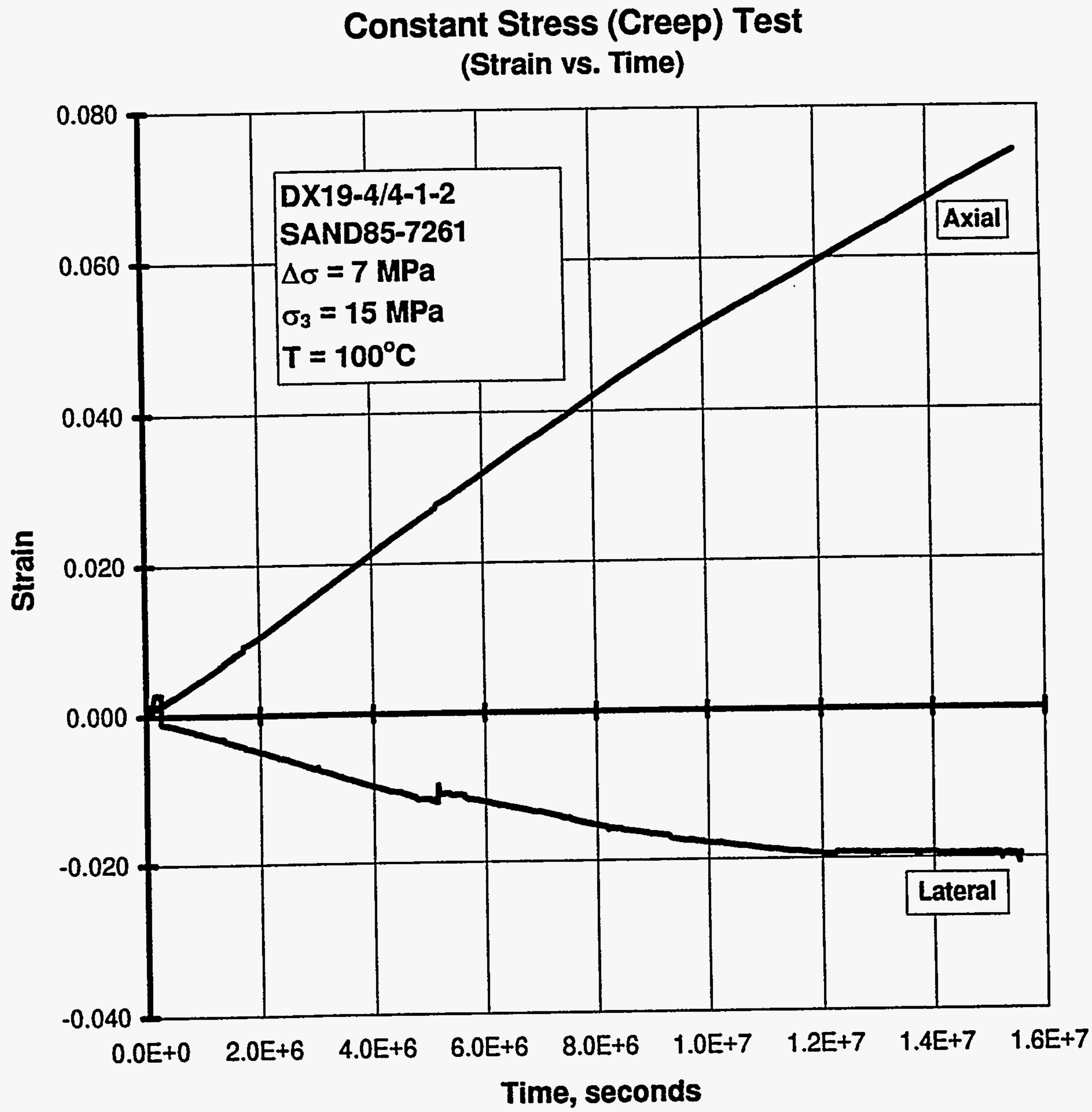

Figure C-80. Axial Strain and Lateral Strain Versus Time for a Creep Test: Specimen DX19-4/4-1-2; Stage 1 of 1 (Anomalous Test Result. Unknown Cause).

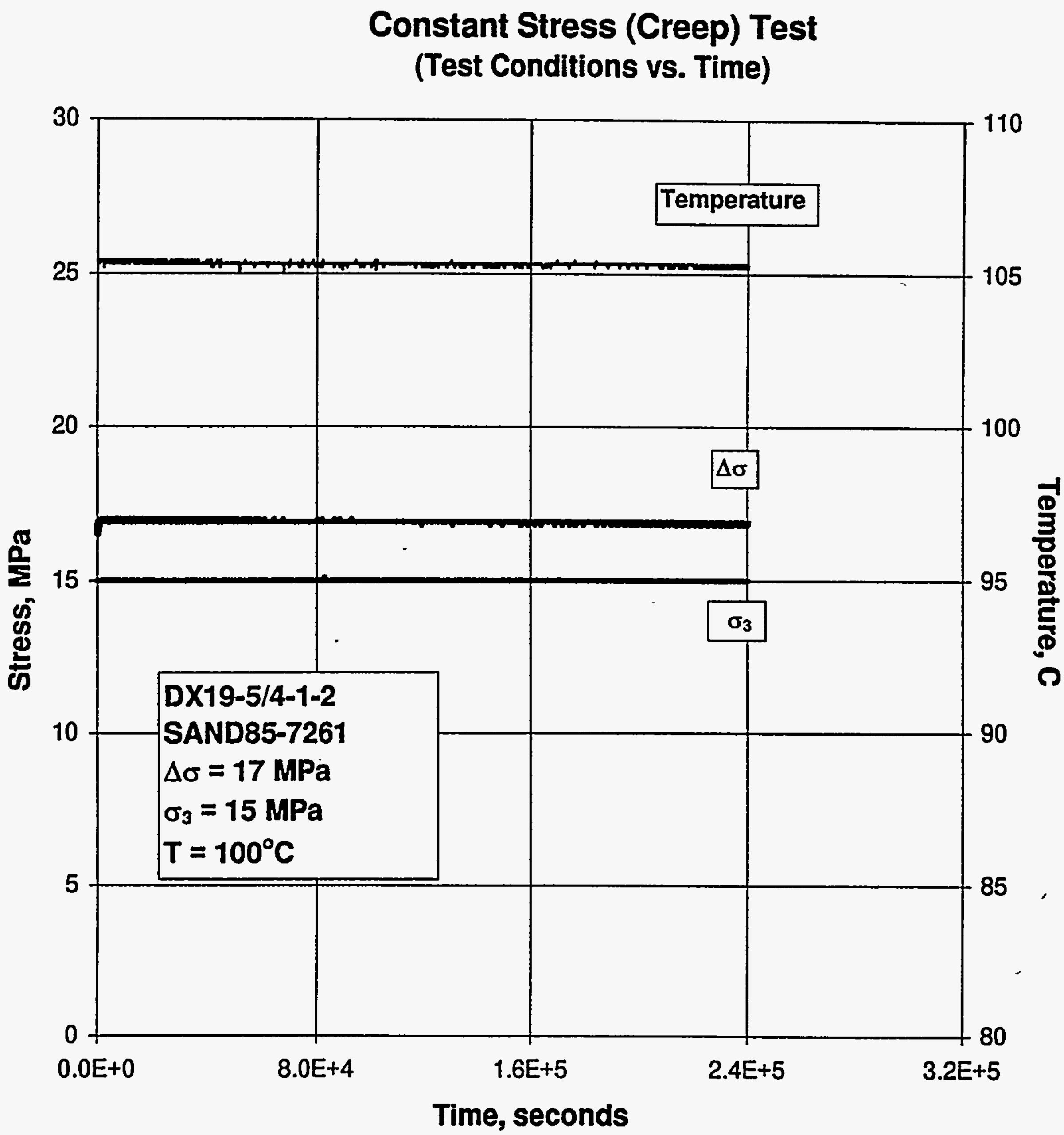

Figure C-81. Test Conditions Versus Time for a Creep Test: Specimen DX19-5/4-1-2; Stage 1 of 1.

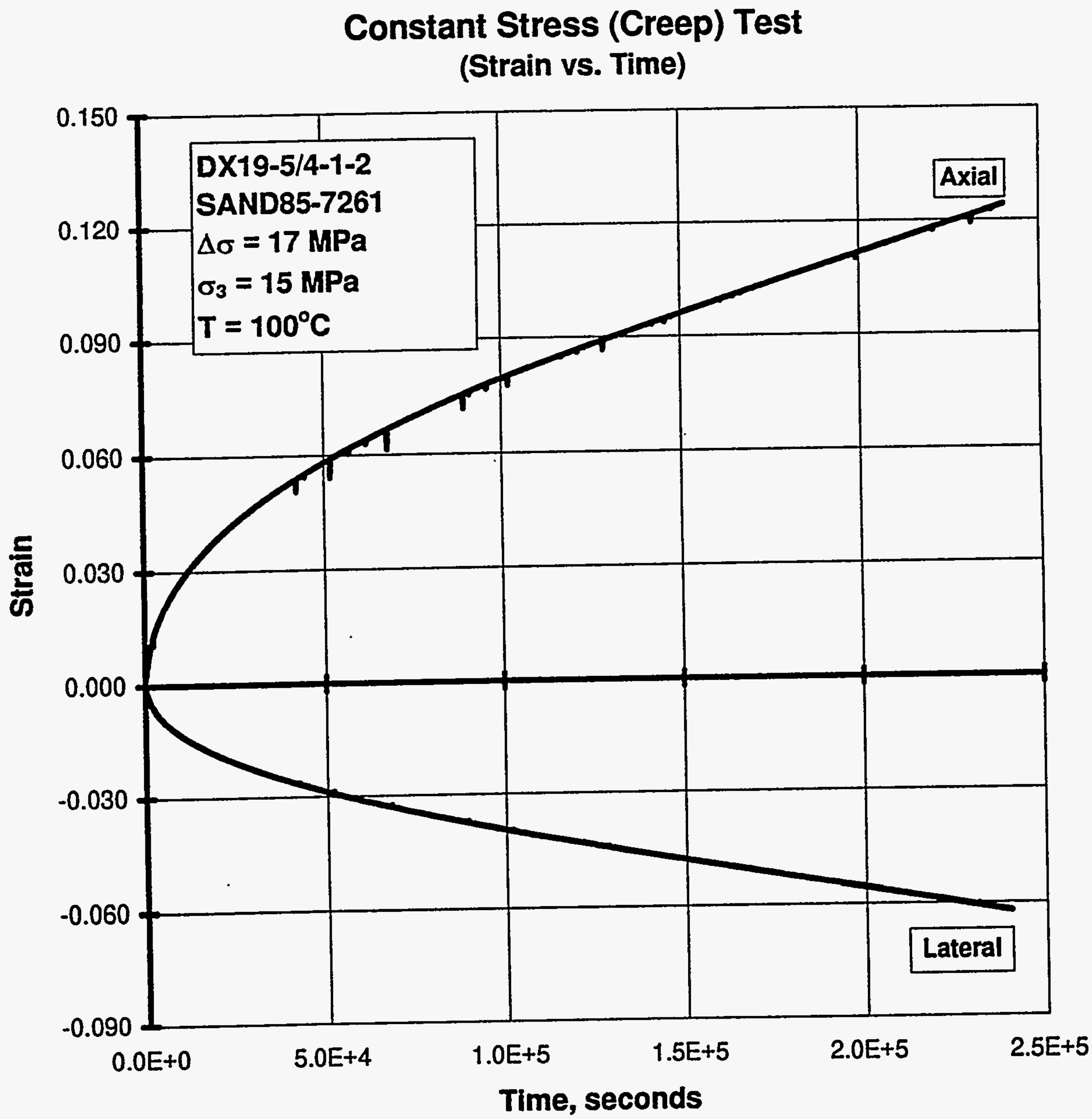

Figure C-82. Axial Strain and Lateral Strain Versus Time for a Creep Test: Specimen DX19-5/4-1-2; Stage 1 of 1.

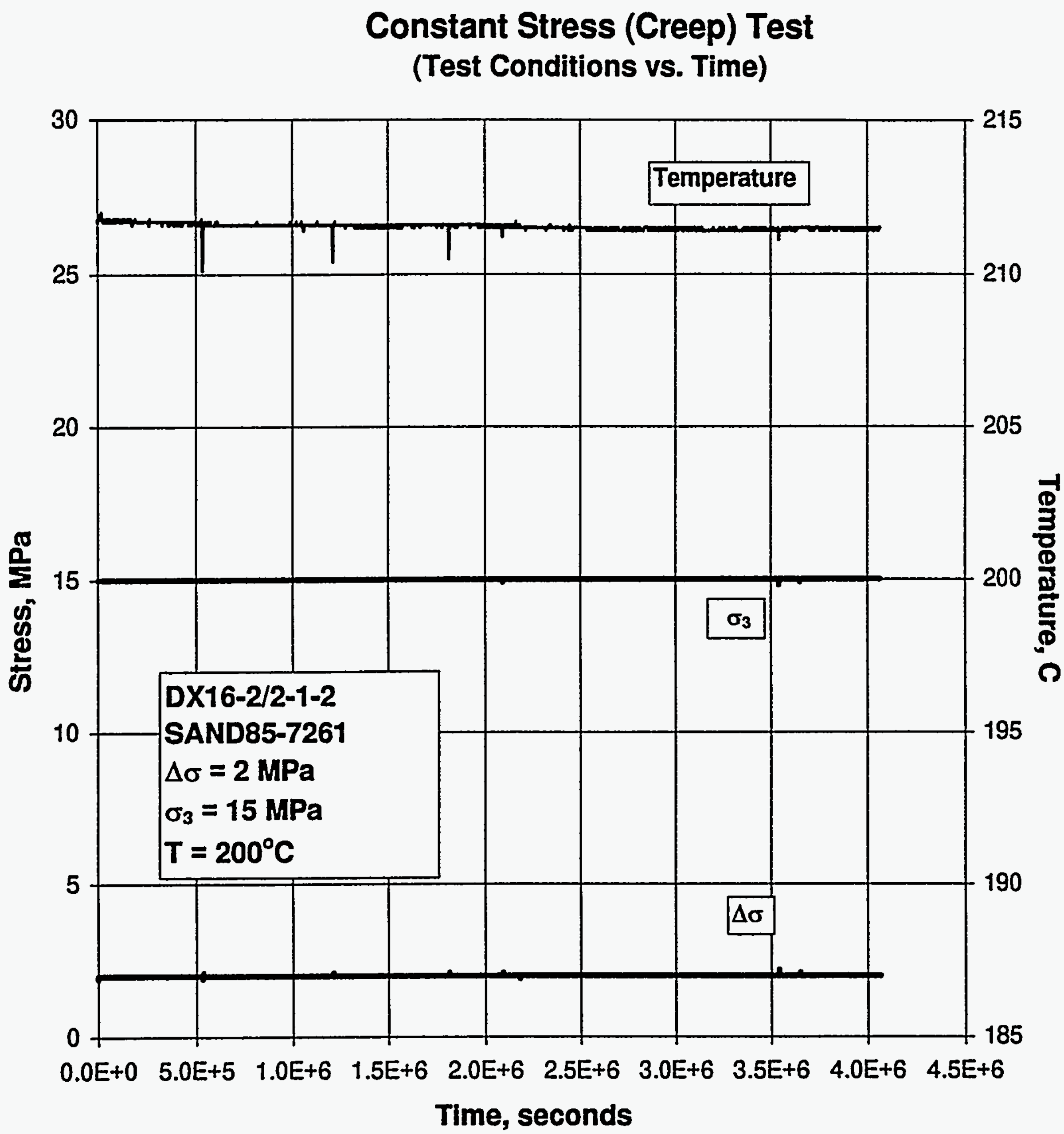

Figure C-83. Test Conditions Versus Time for a Creep Test: Specimen DX16-2/2-1-2; Stage 1 of 1.

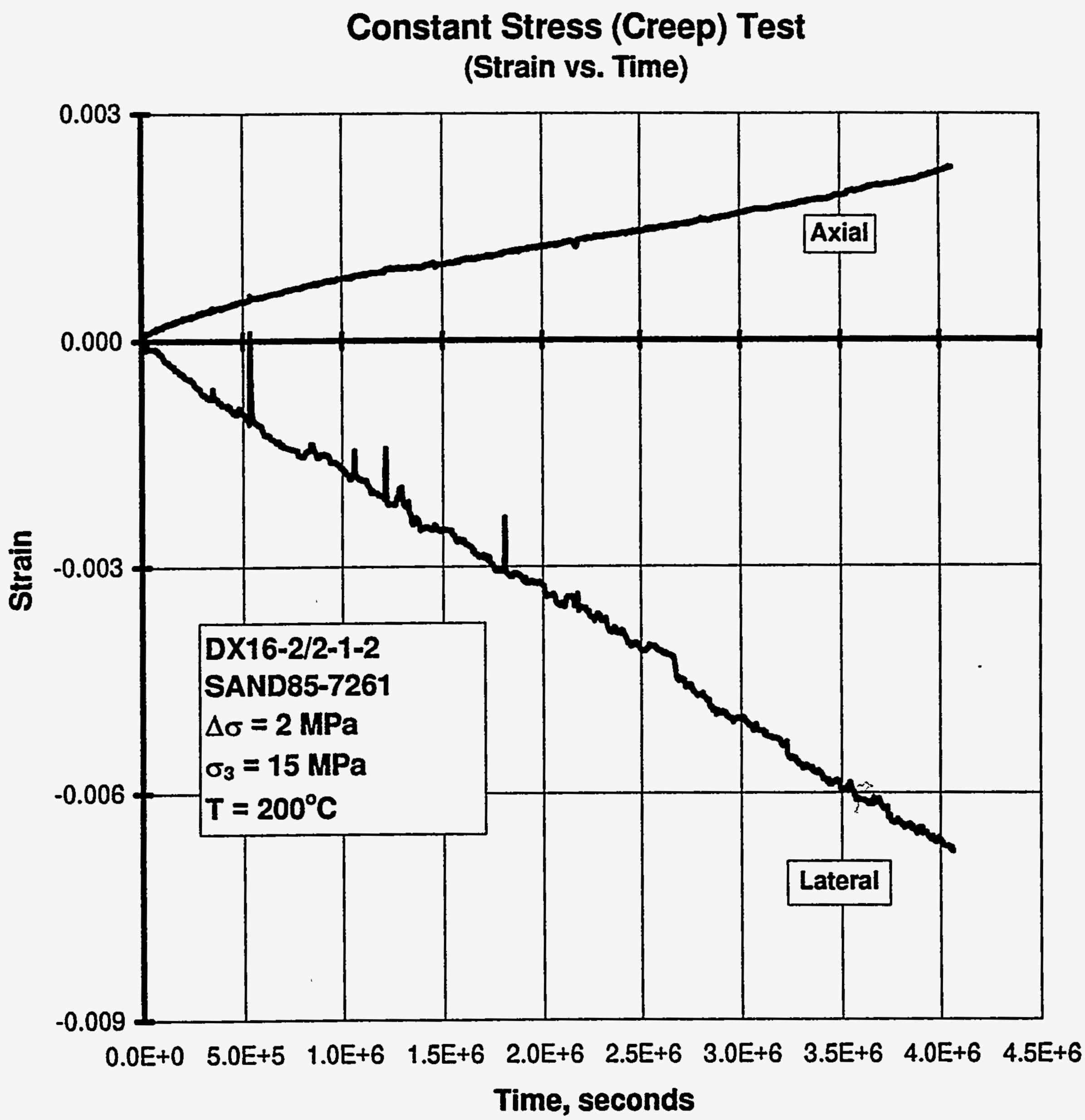

Figure C-84. Axial Strain and Lateral Strain Versus Time for a Creep Test: Specimen DX16-2/2-1-2; Stage 1 of 1 (Anomalous Test Result. Unknown Cause).

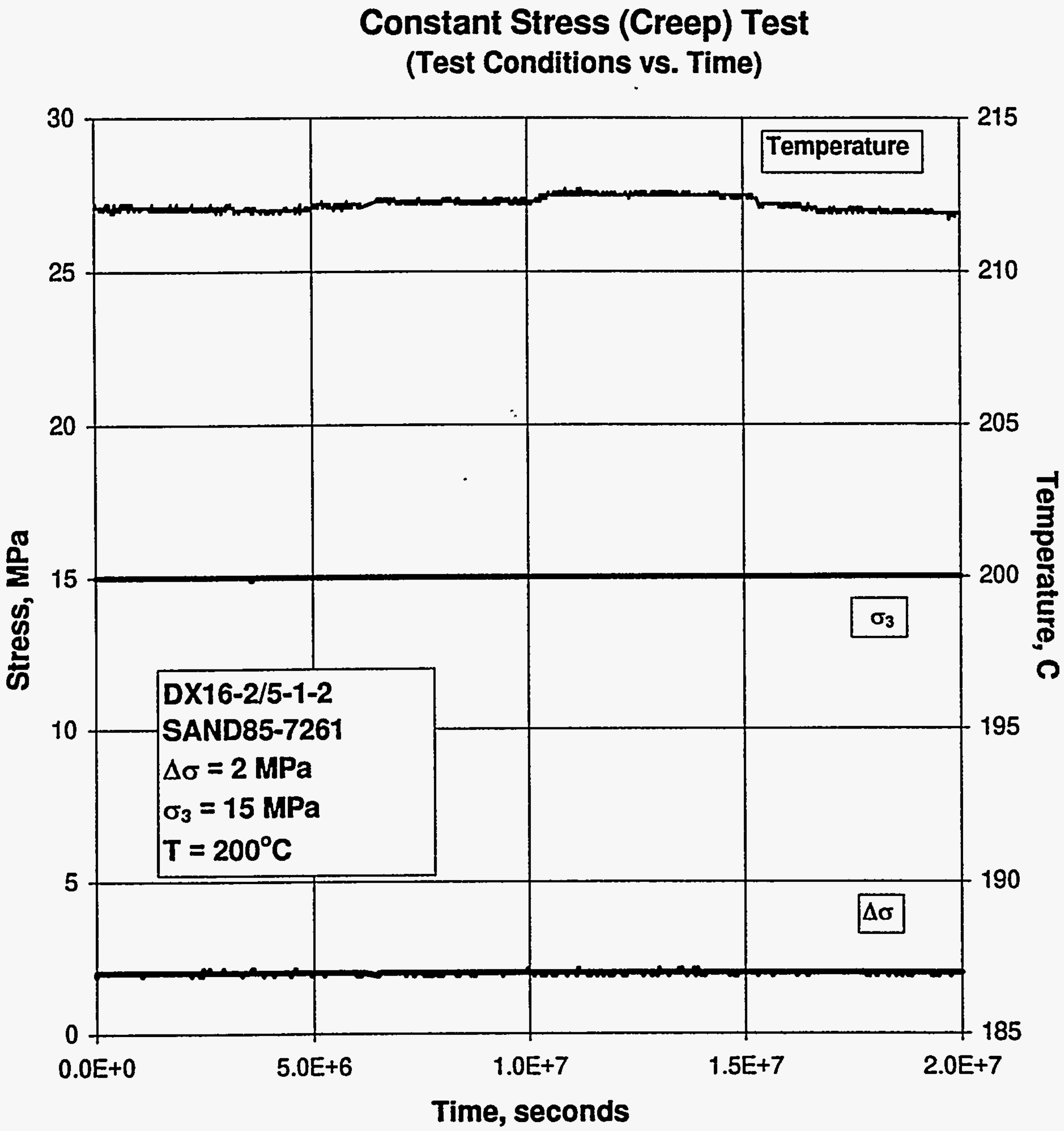

Figure C-85. Test Conditions Versus Time for a Creep Test: Specimen DX16-2/5-1-2; Stage 1 of 1.

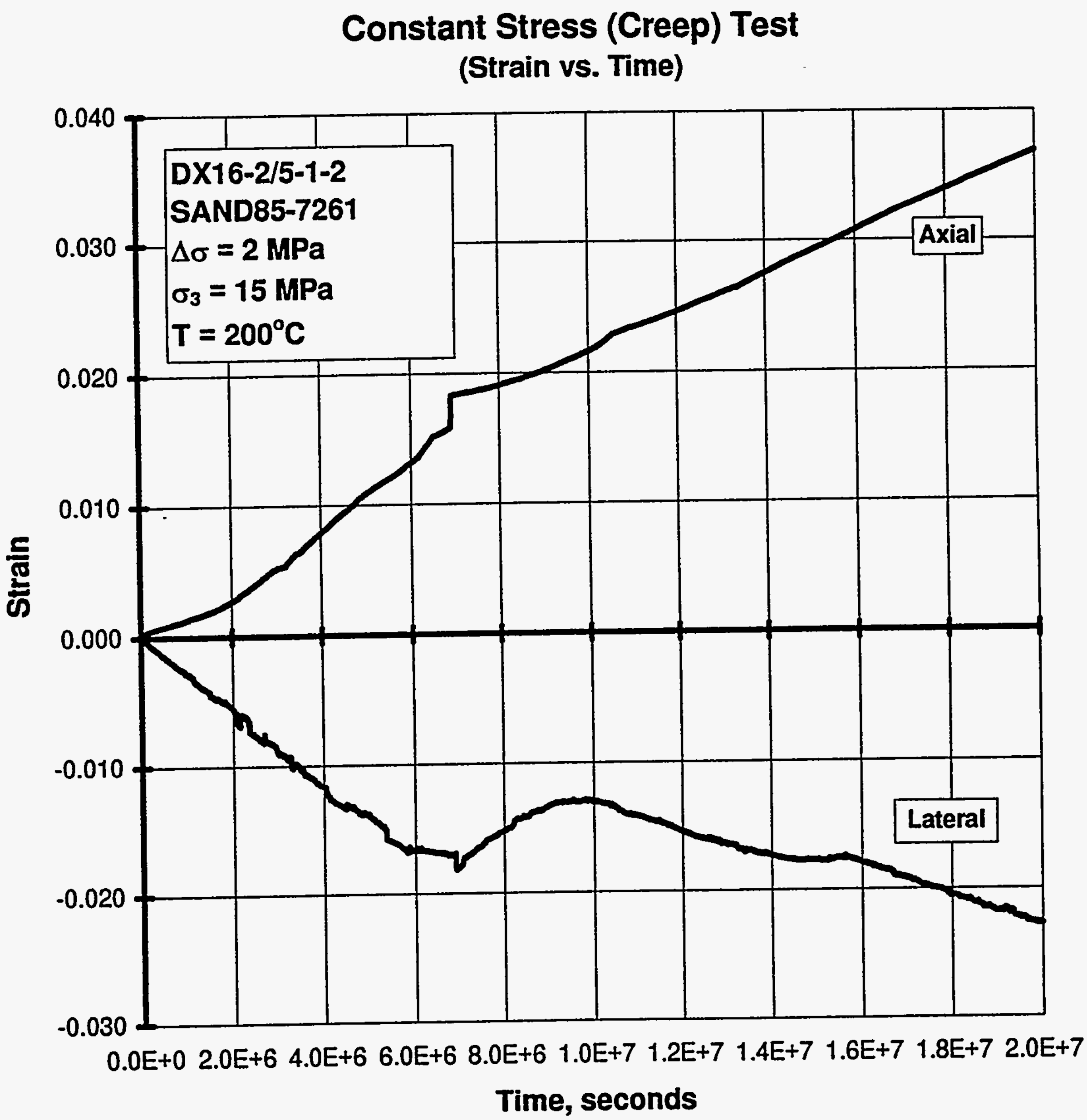

Figure C-86. Axial Strain and Lateral Strain Versus Time for a Creep Test: Specimen DX16-2/5-1-2; Stage 1 of 1 (Anomalous Test Result. Unknown Cause).

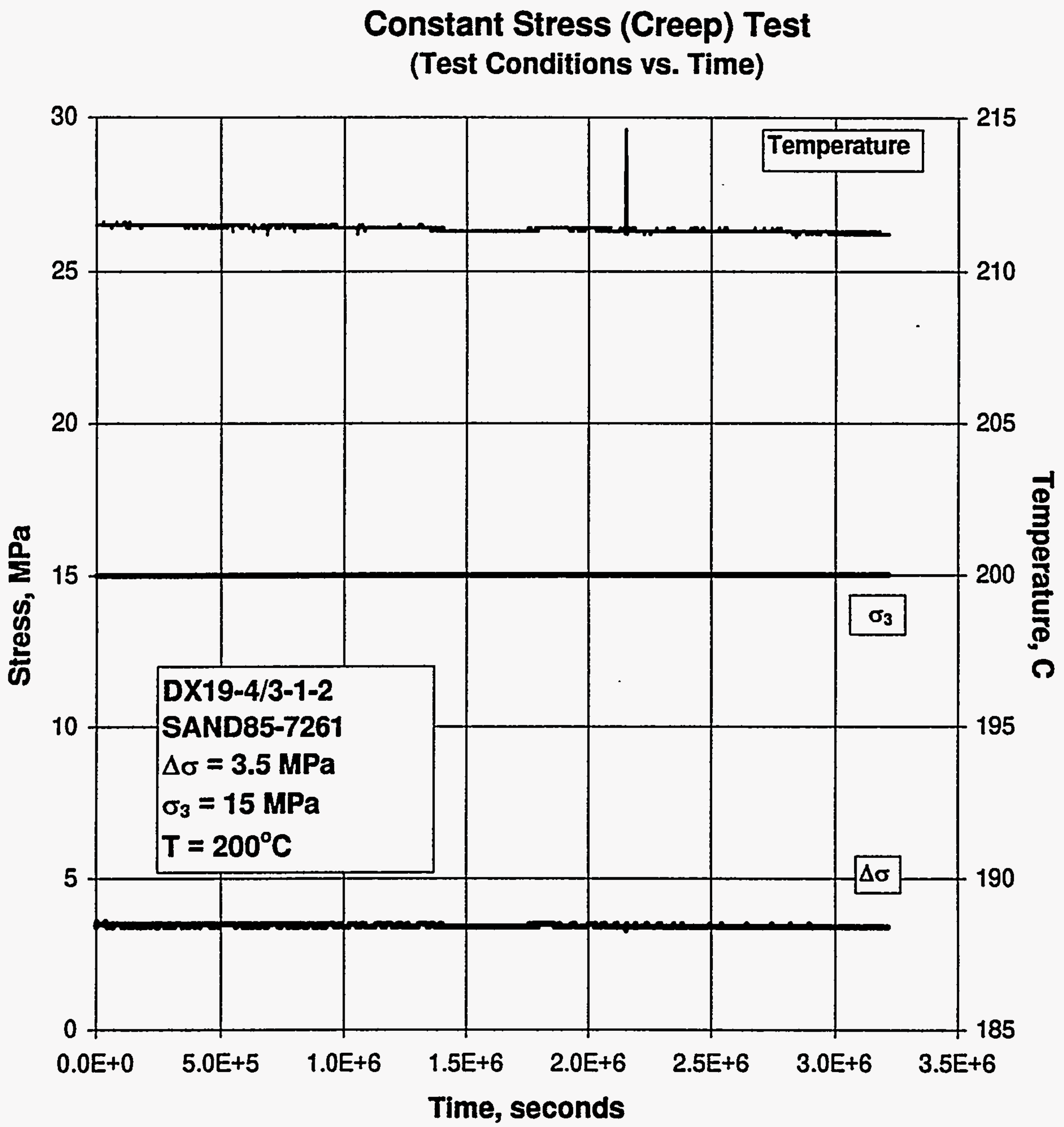

Figure C-87. Test Conditions Versus Time for a Creep Test: Specimen DX19-4/3-1-2; Stage 1 of 1.

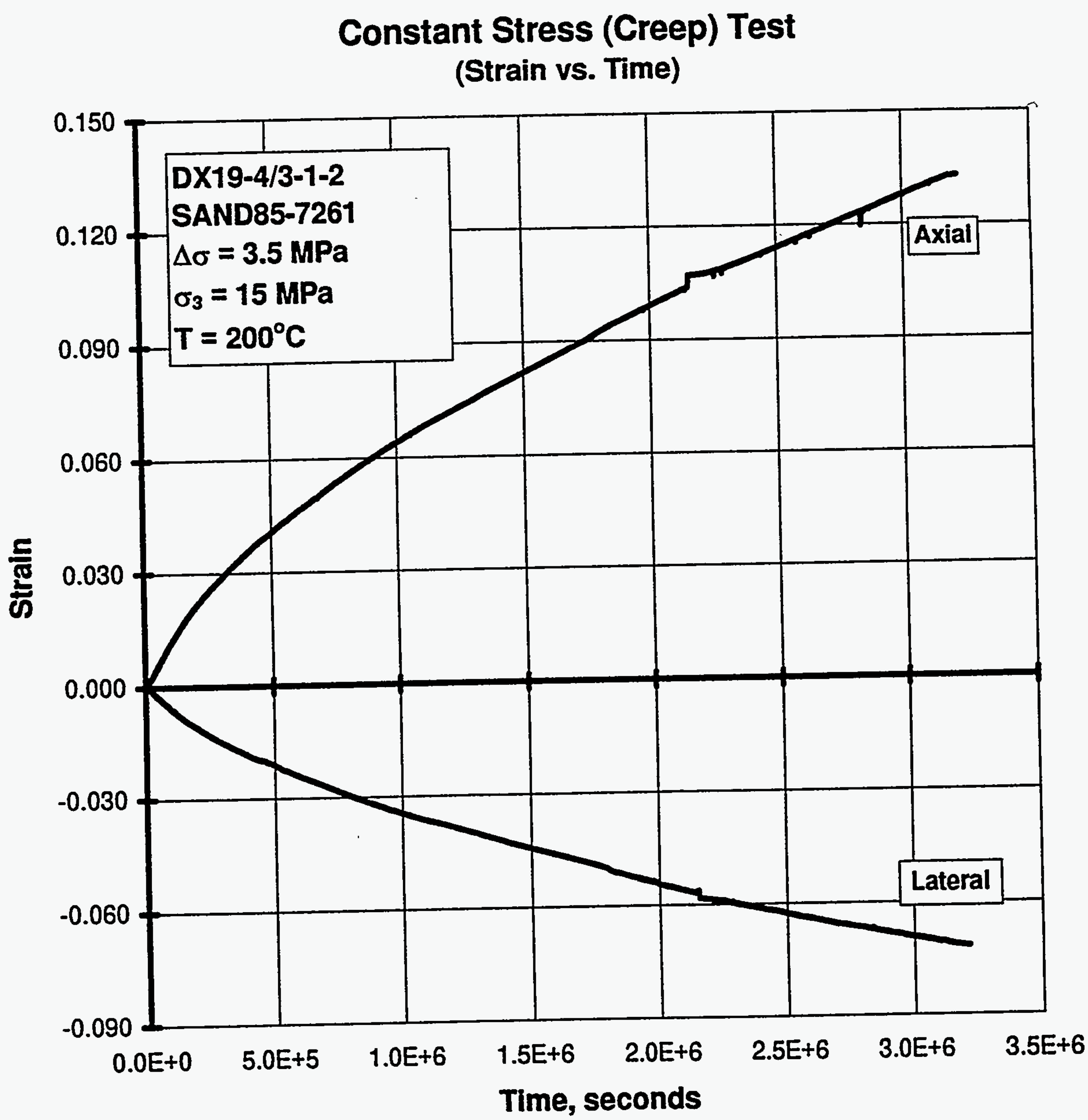

Figure C-88. Axial Strain and Lateral Strain Versus Time for a Creep Test: Specimen DX19-4/3-1-2; Stage 1 of 1.

APPENDIX D

MULTIAXIAL TESTS ON AVERY ISLAND SALT

FIGURES

FIGURE **PAGE**

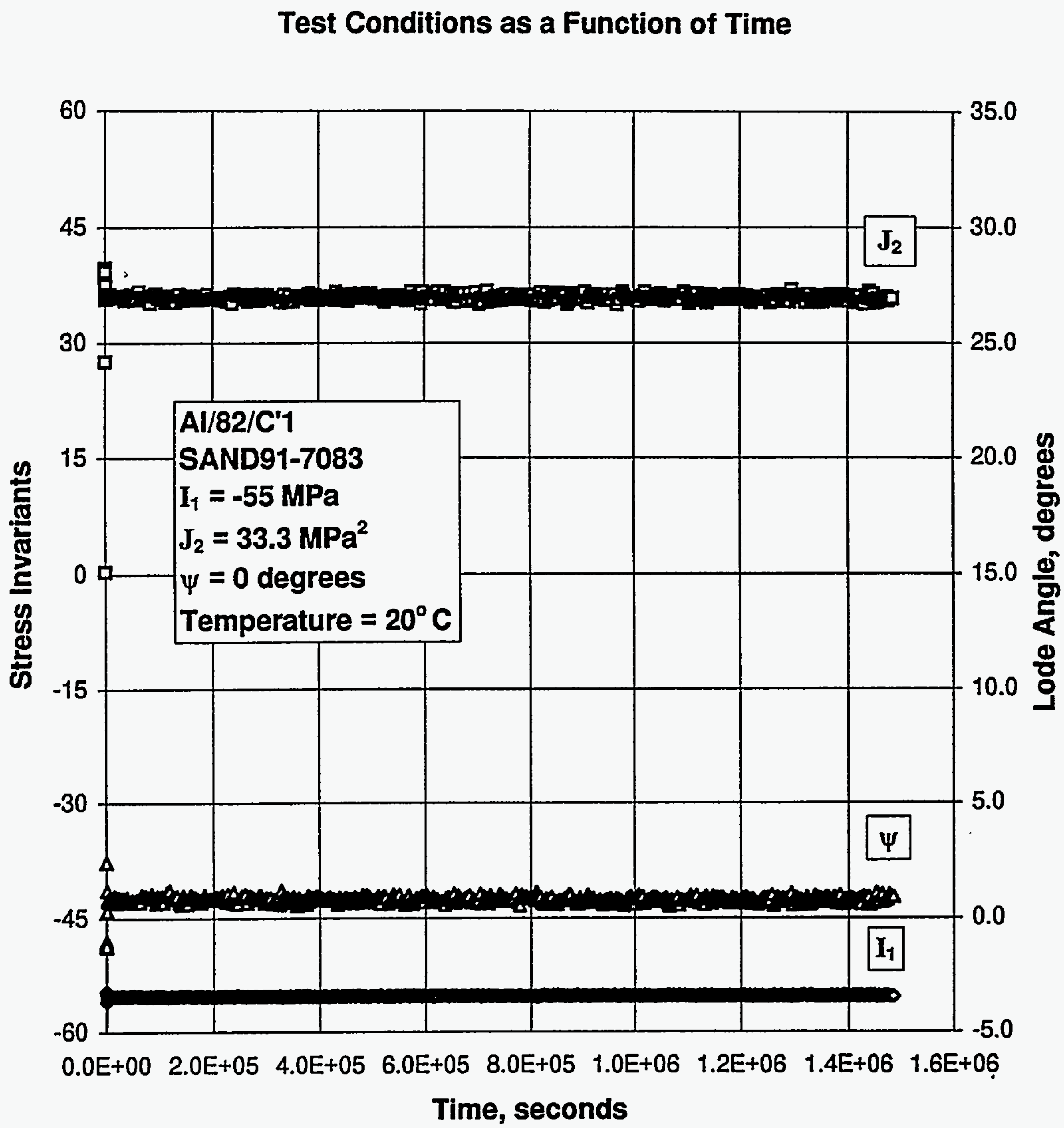

Figure D-1. Test Conditions Versus Time for a Multiaxial Creep Test: Specimen AI/82/C'1.

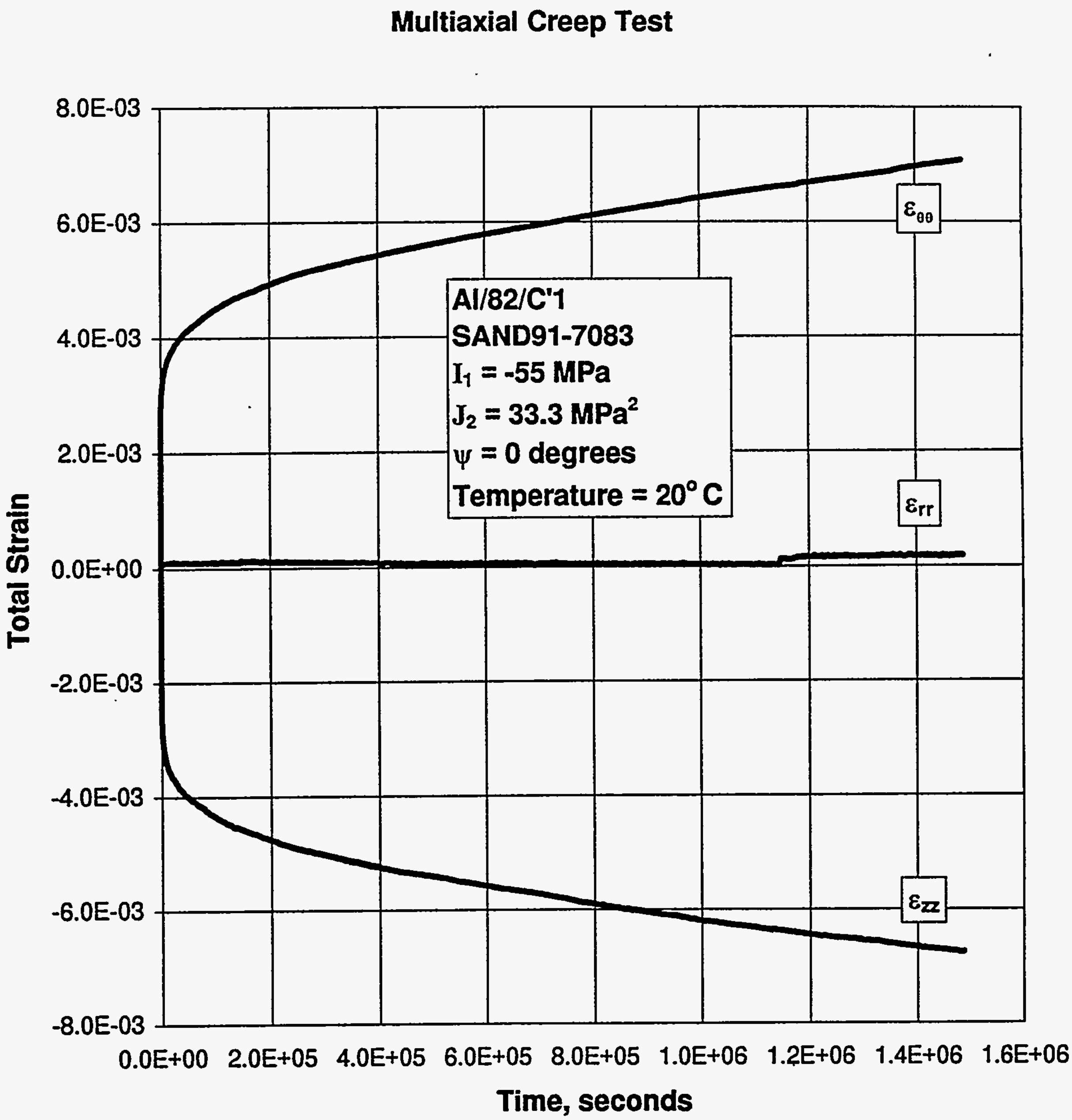

Figure D-2. Principal Strains Versus Time for a Multiaxial Creep Test: Specimen AI/82/C'1.

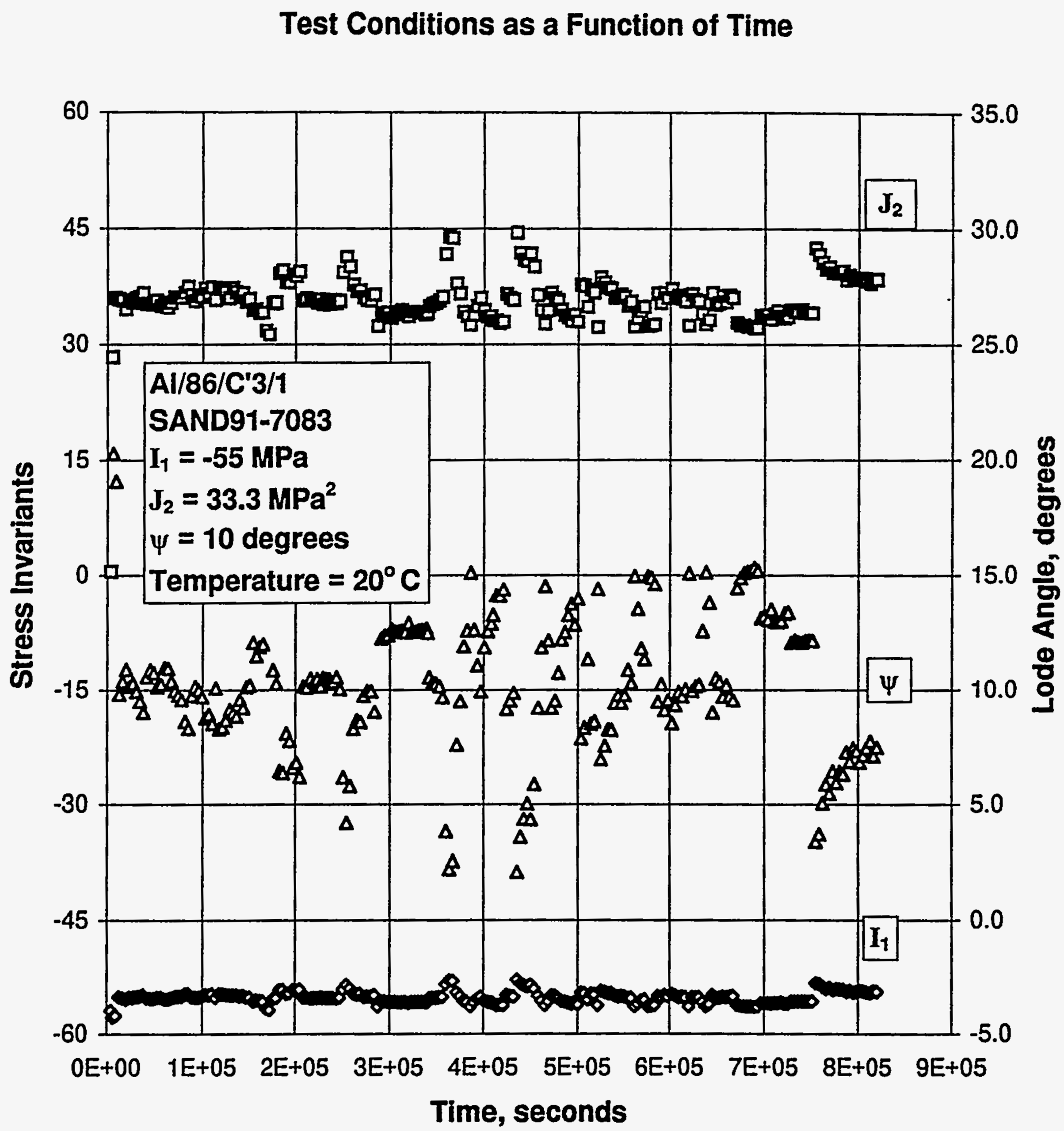

Figure D-3. Test Conditions Versus Time for a Multiaxial Creep Test: Specimen AI/86/C'3/1.

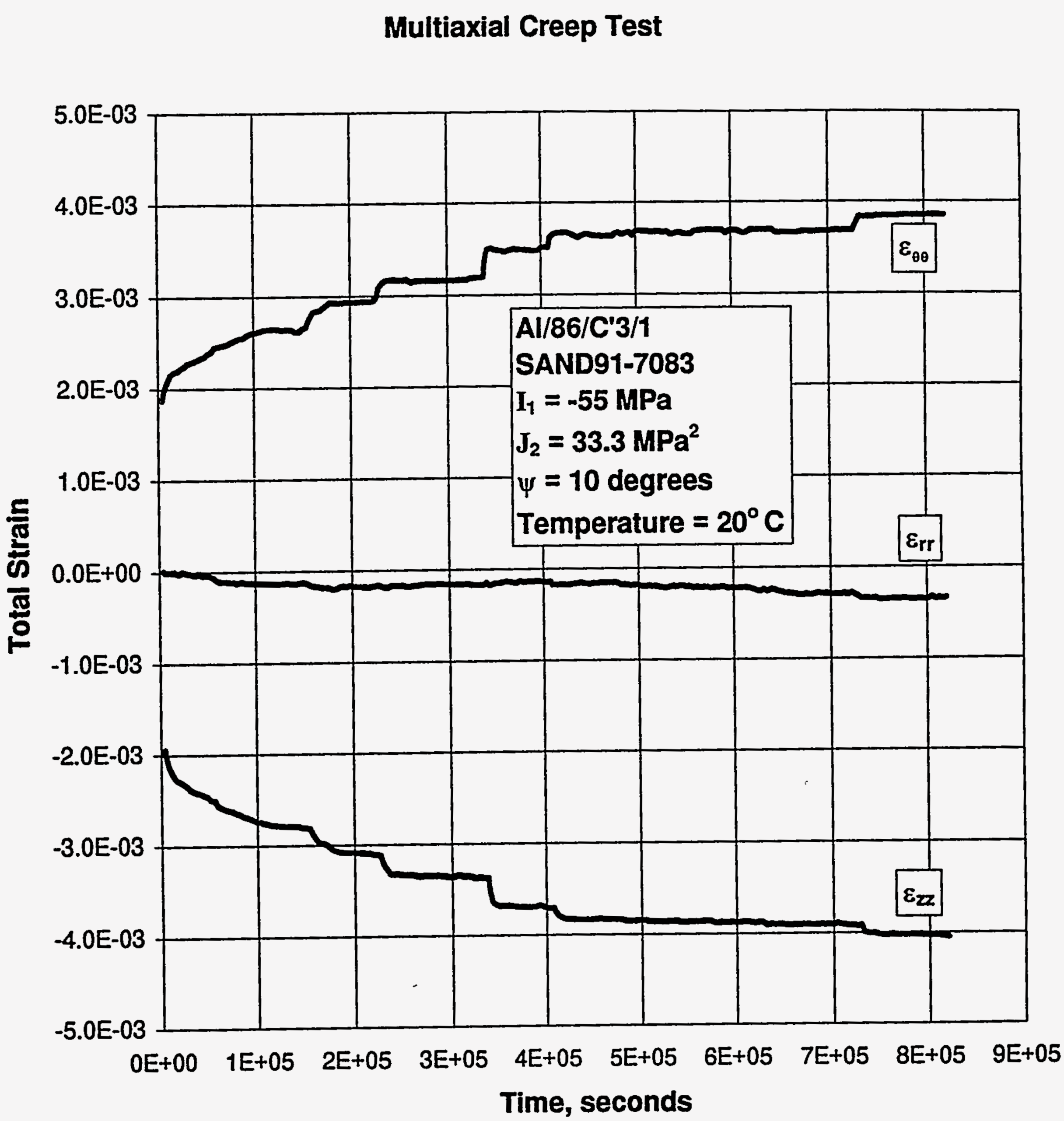

Figure D-4. Principal Strains Versus Time for a Multiaxial Creep Test: Specimen AI/86/C'3/1.

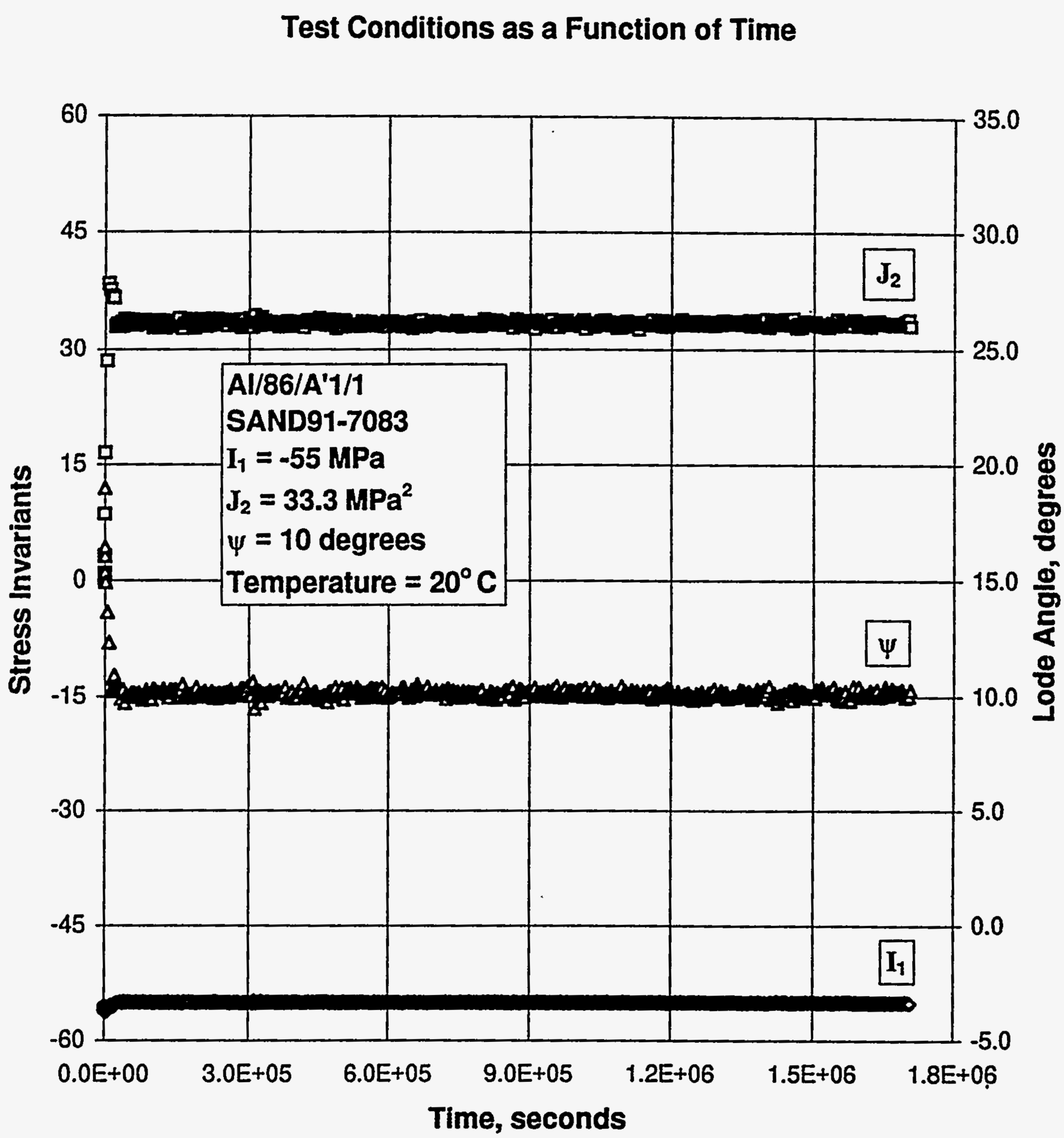

Figure D-5. Test Conditions Versus Time for a Multiaxial Creep Test: Specimen AI/86/A'1/1.

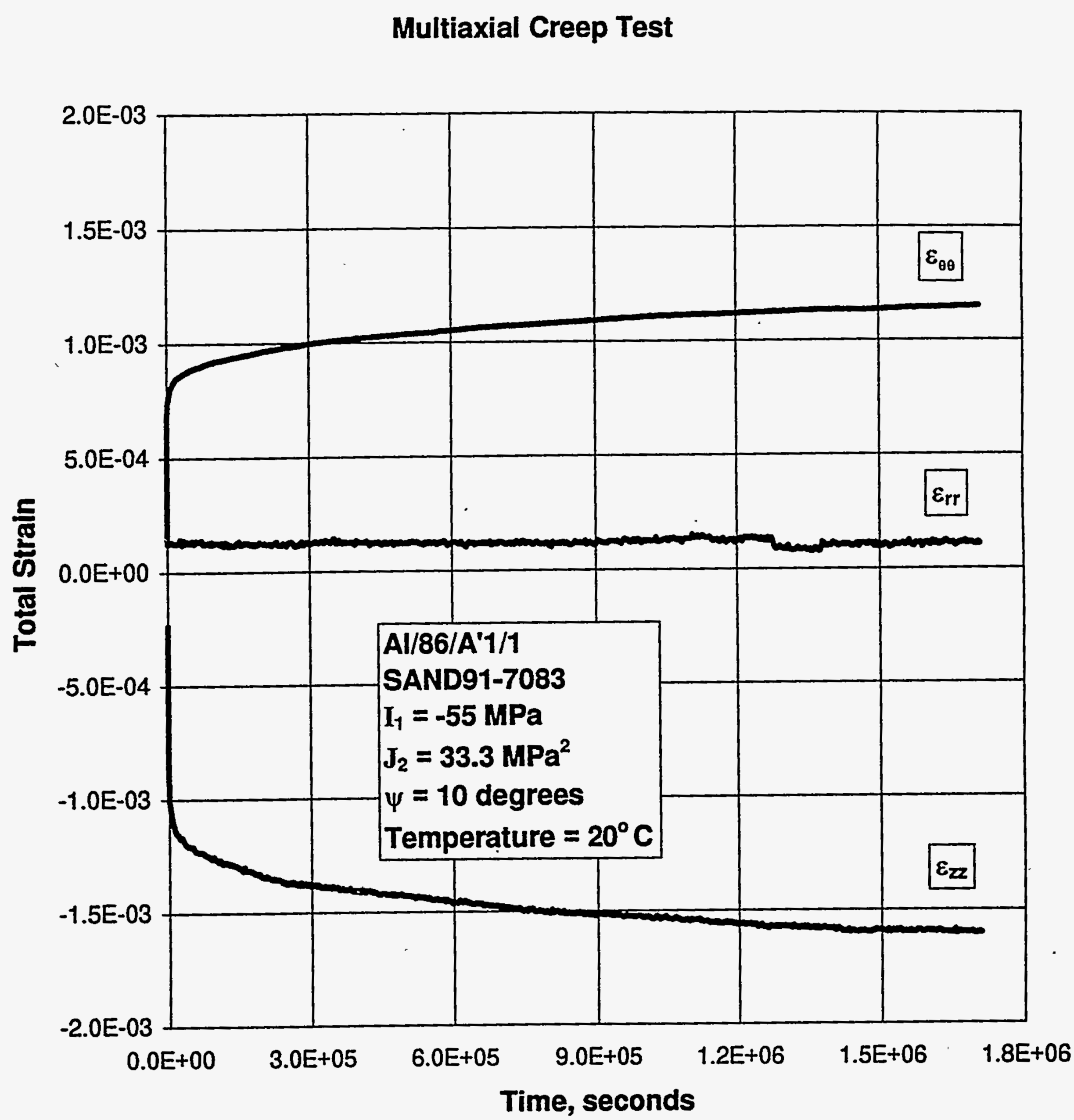

Figure D-6. Principal Strains Versus Time for a Multiaxial Creep Test: Specimen AI/86/A'1/1.

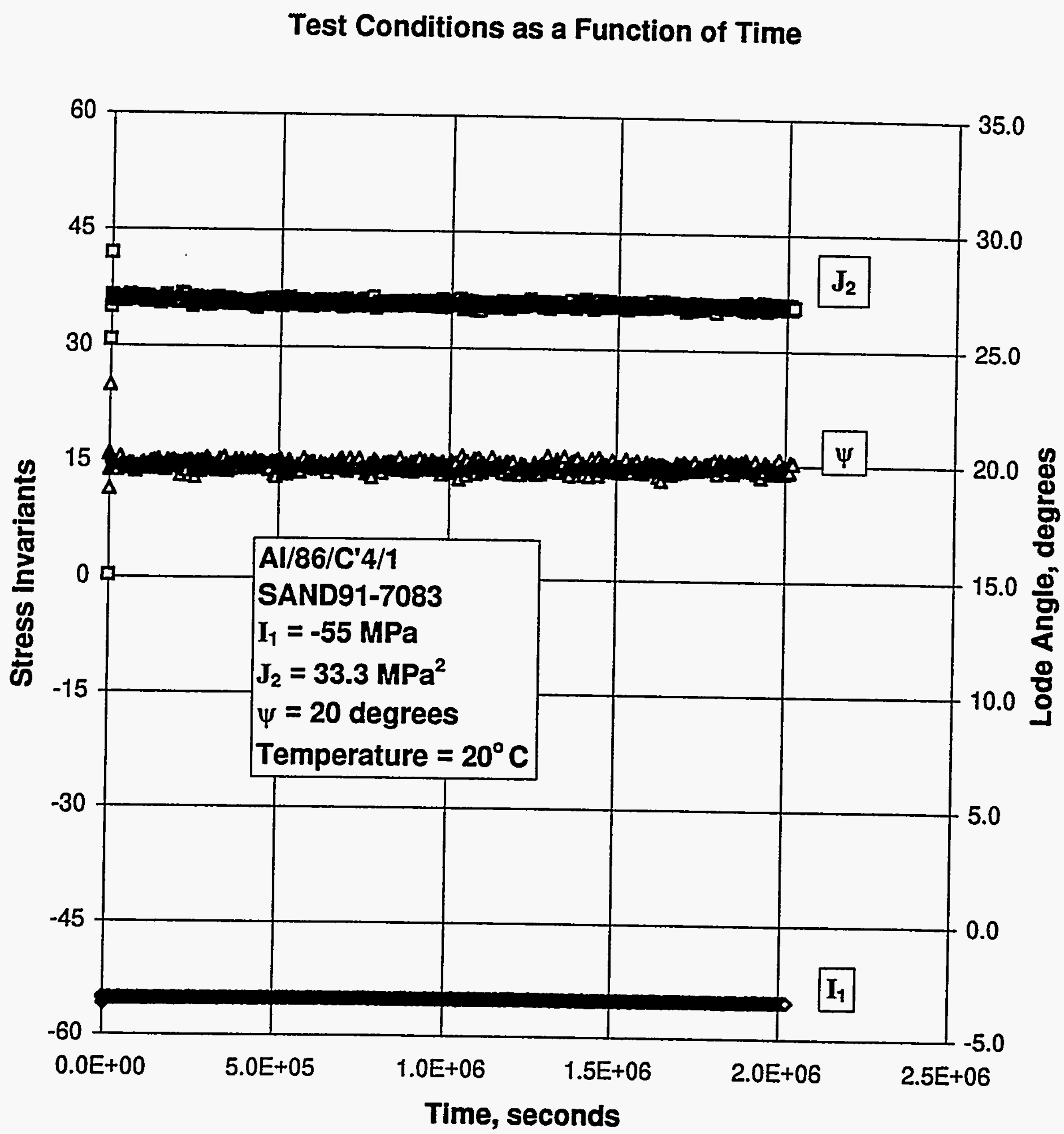

Figure D-7. Test Conditions Versus Time for a Multiaxial Creep Test: Specimen AI/86/C'4/1.

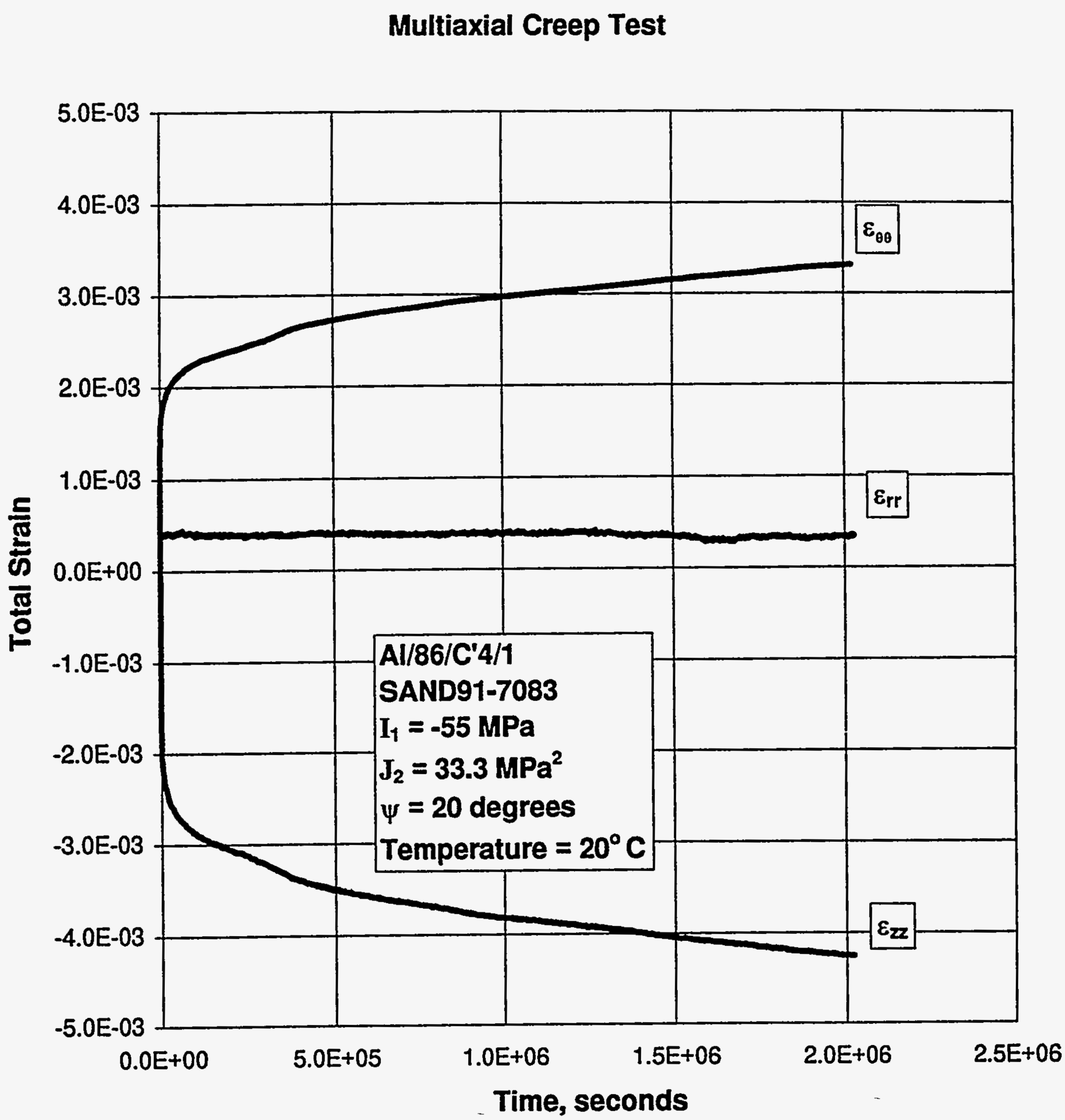

Figure D-8. Principal Strains Versus Time for a Multiaxial Creep Test: Specimen AI/86/C'4/1.

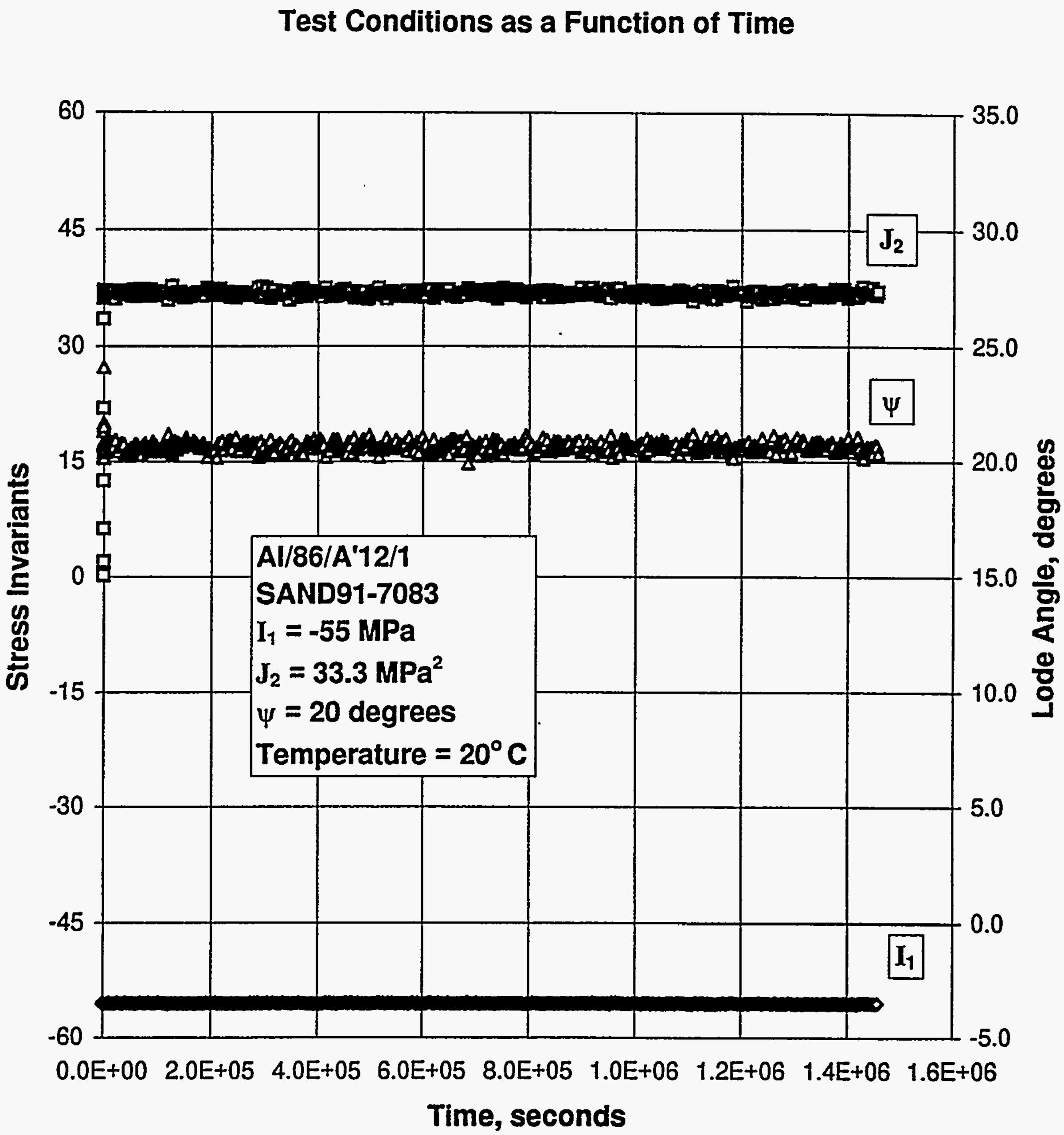

Figure D-9. Test Conditions Versus Time for a Multiaxial Creep Test: Specimen AI/86/A′12/1.

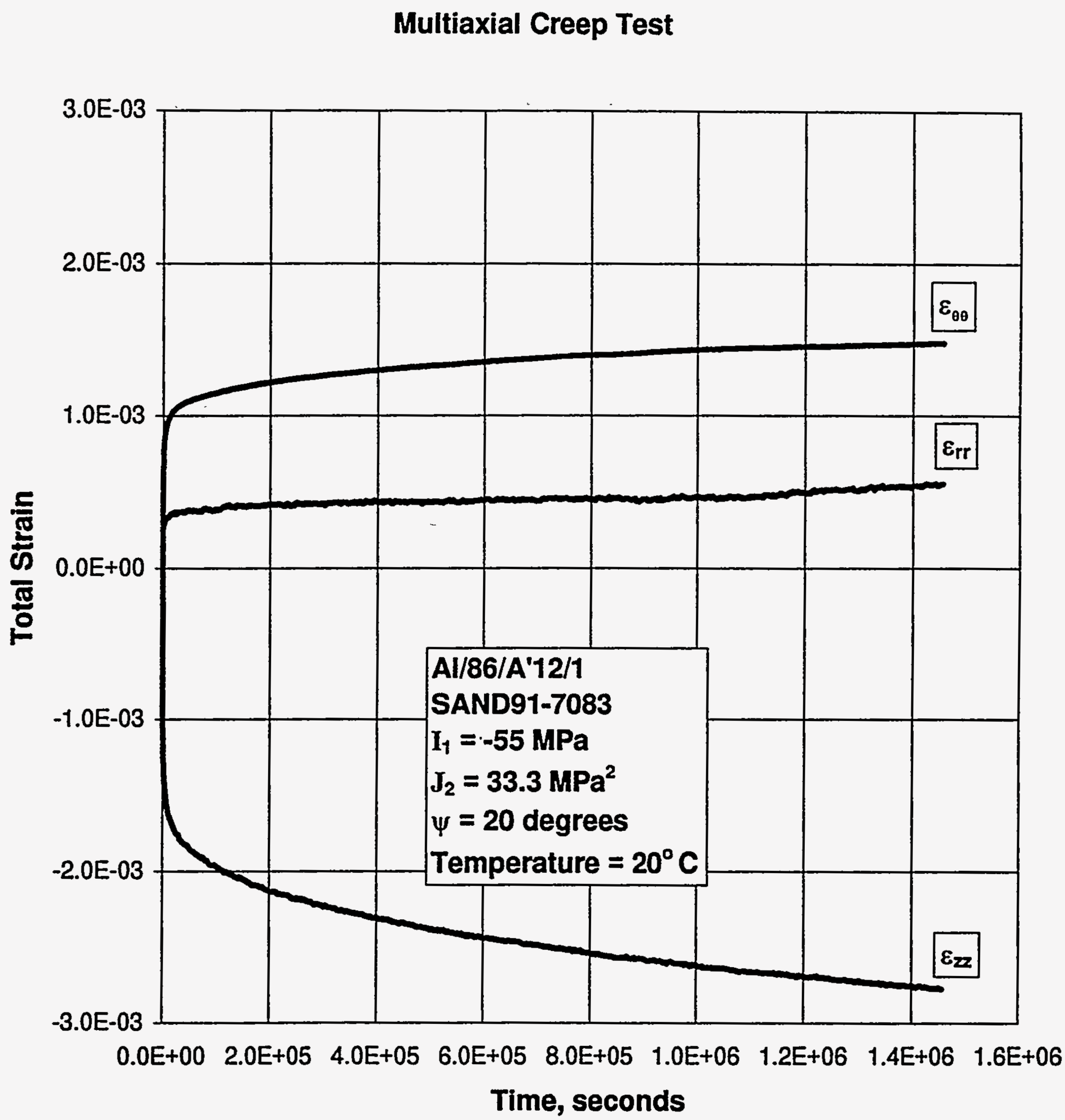

Figure D-10. Principal Strains Versus Time for a Multiaxial Creep Test: Specimen AI/86/A'12/1.

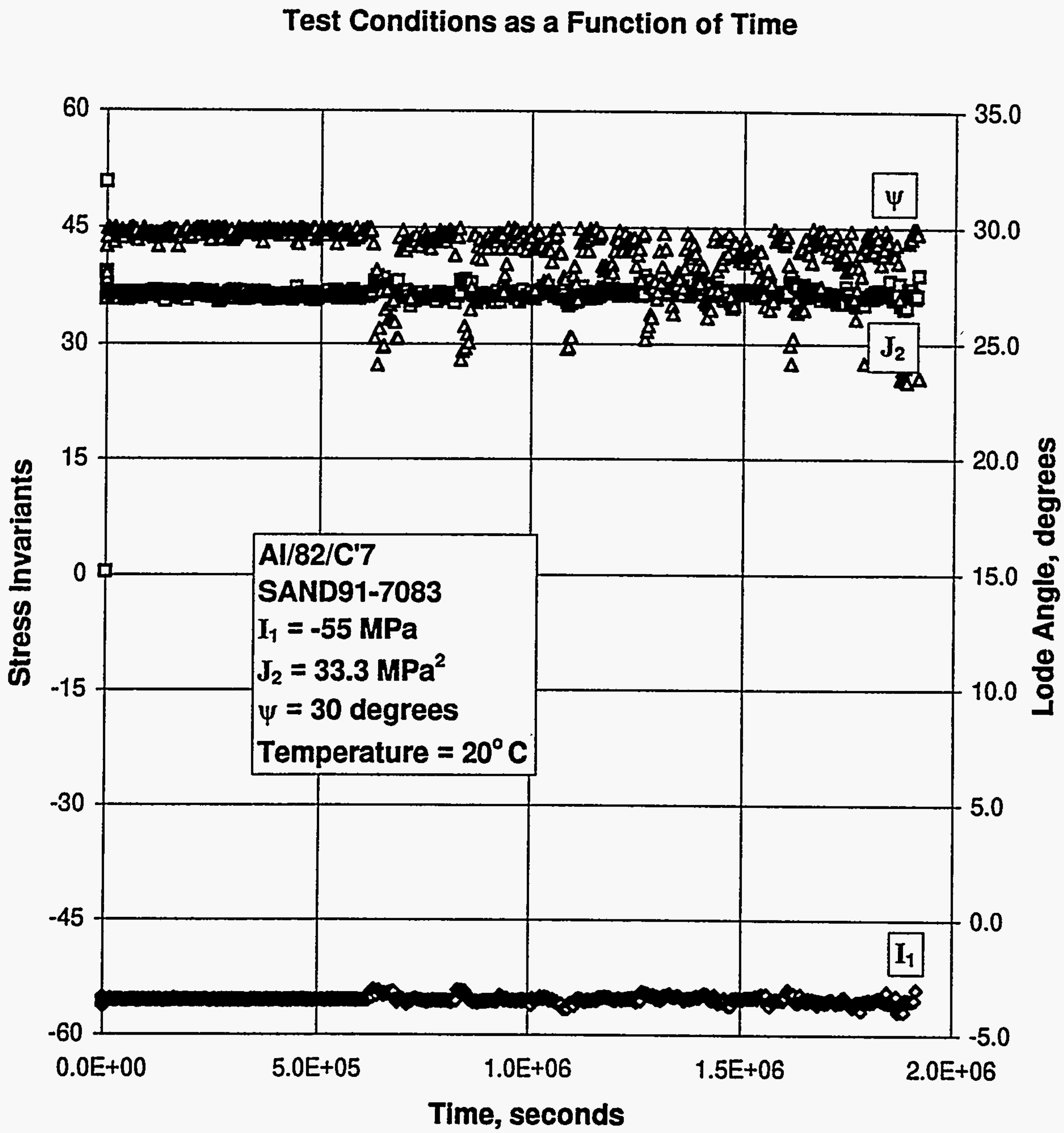

Figure D-11. Test Conditions Versus Time for a Multiaxial Creep Test: Specimen AI/82/C'7.

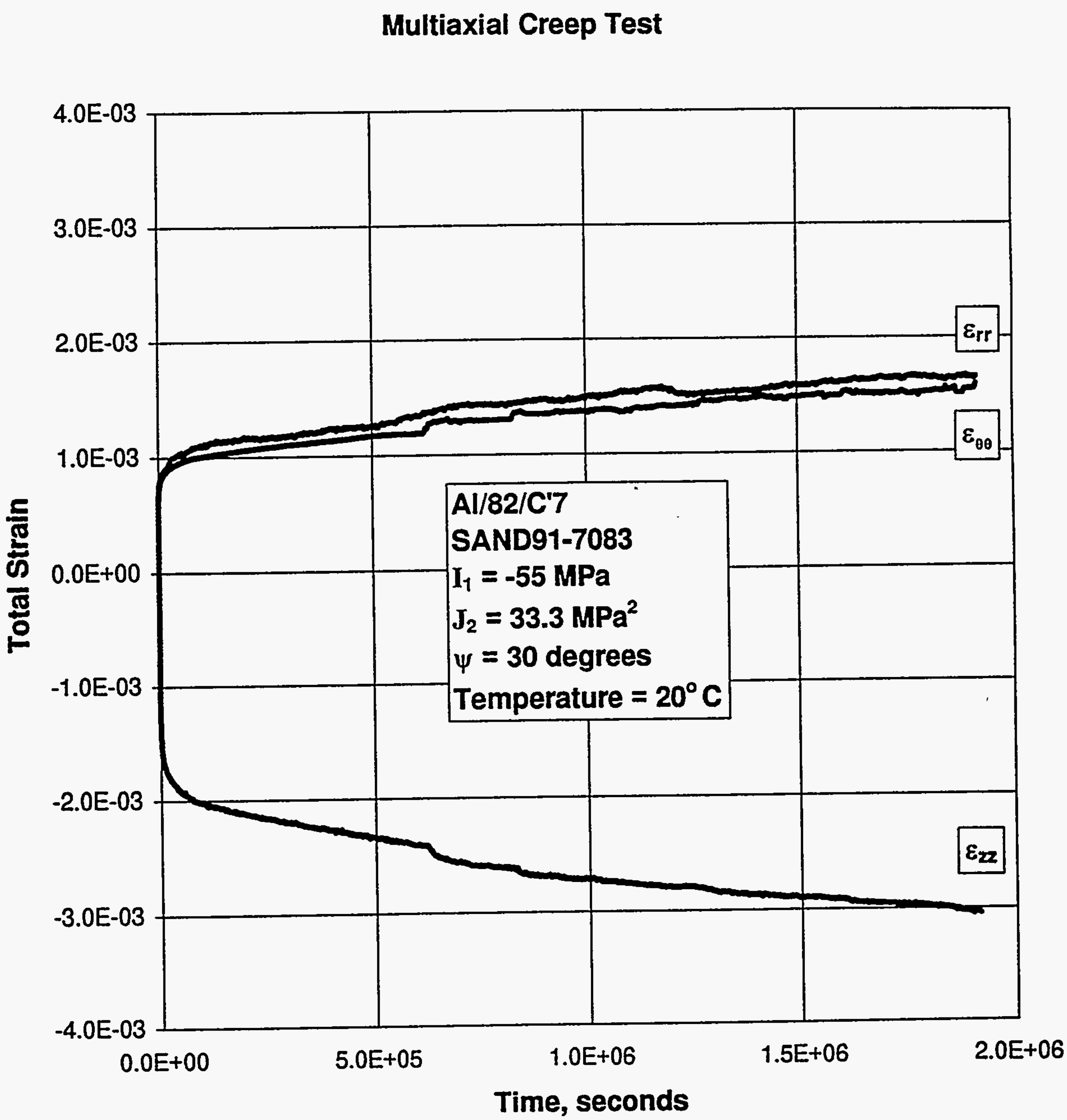

Figure D-12. Principal Strains Versus Time for a Multiaxial Creep Test: Specimen AI/82/C'7.

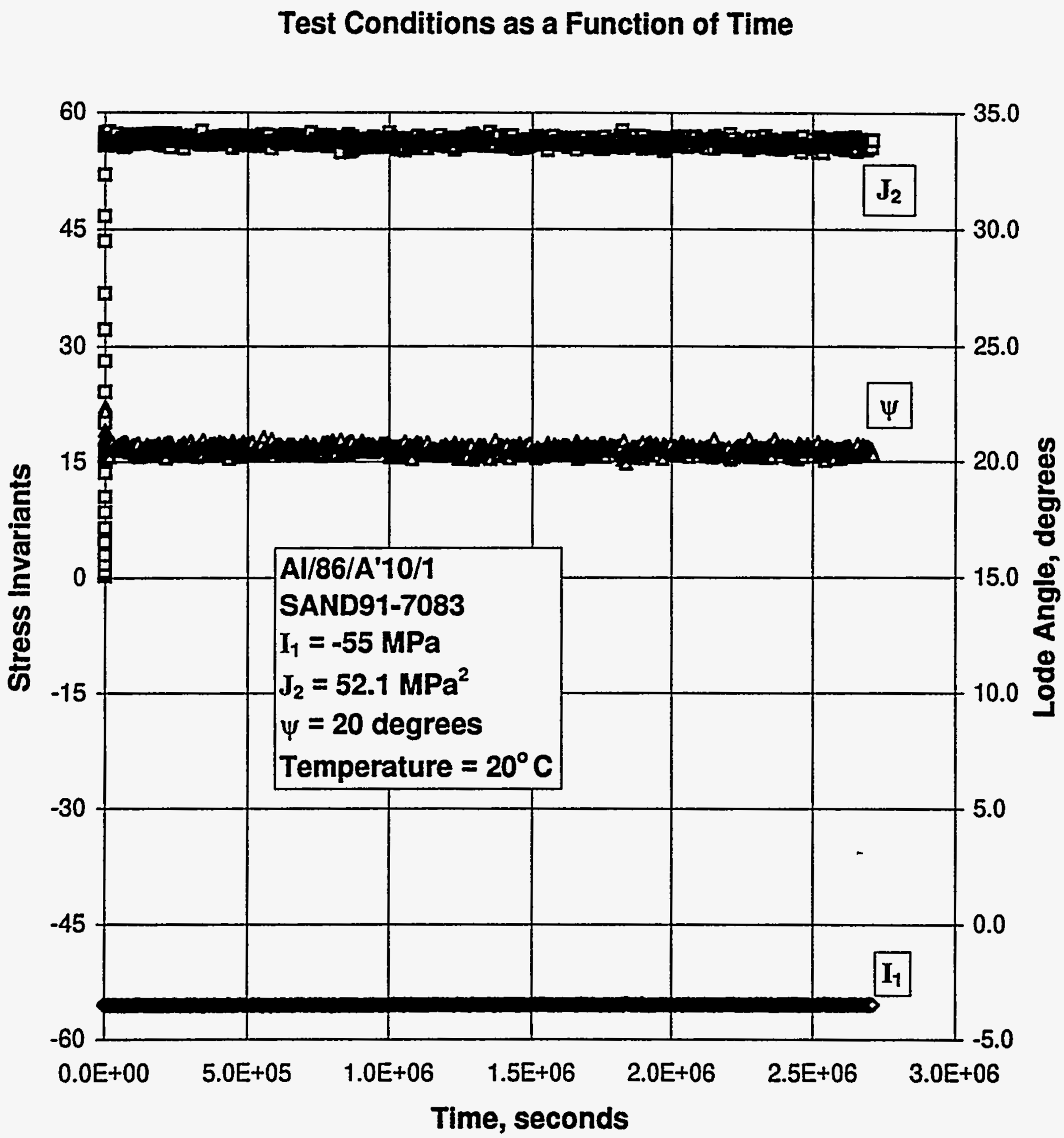

Figure D-13. Test Conditions Versus Time for a Multiaxial Creep Test: Specimen Al/86/A'10/1.

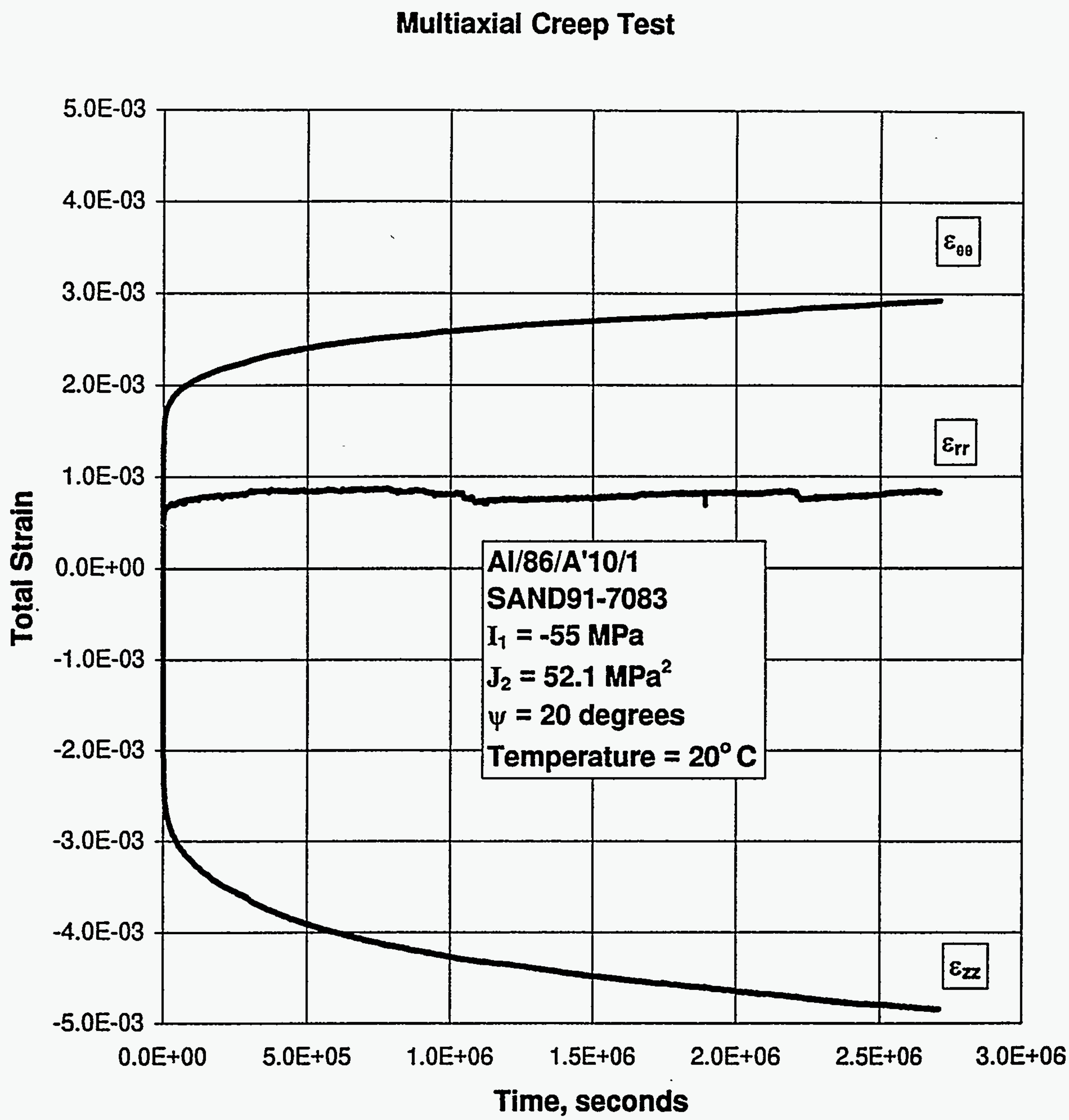

Figure D-14. Principal Strains Versus Time for a Multiaxial Creep Test: Specimen AI/86/A'10/1.

APPENDIX E

DAMAGE RECOVERY TESTS

FIGURES

FIGURES (Continued)

FIGURES (Continued)

FIGURES (Continued)

FIGURES (Continued)

FIGURES (Continued)

FIGURES (Continued)

Figure **Page**

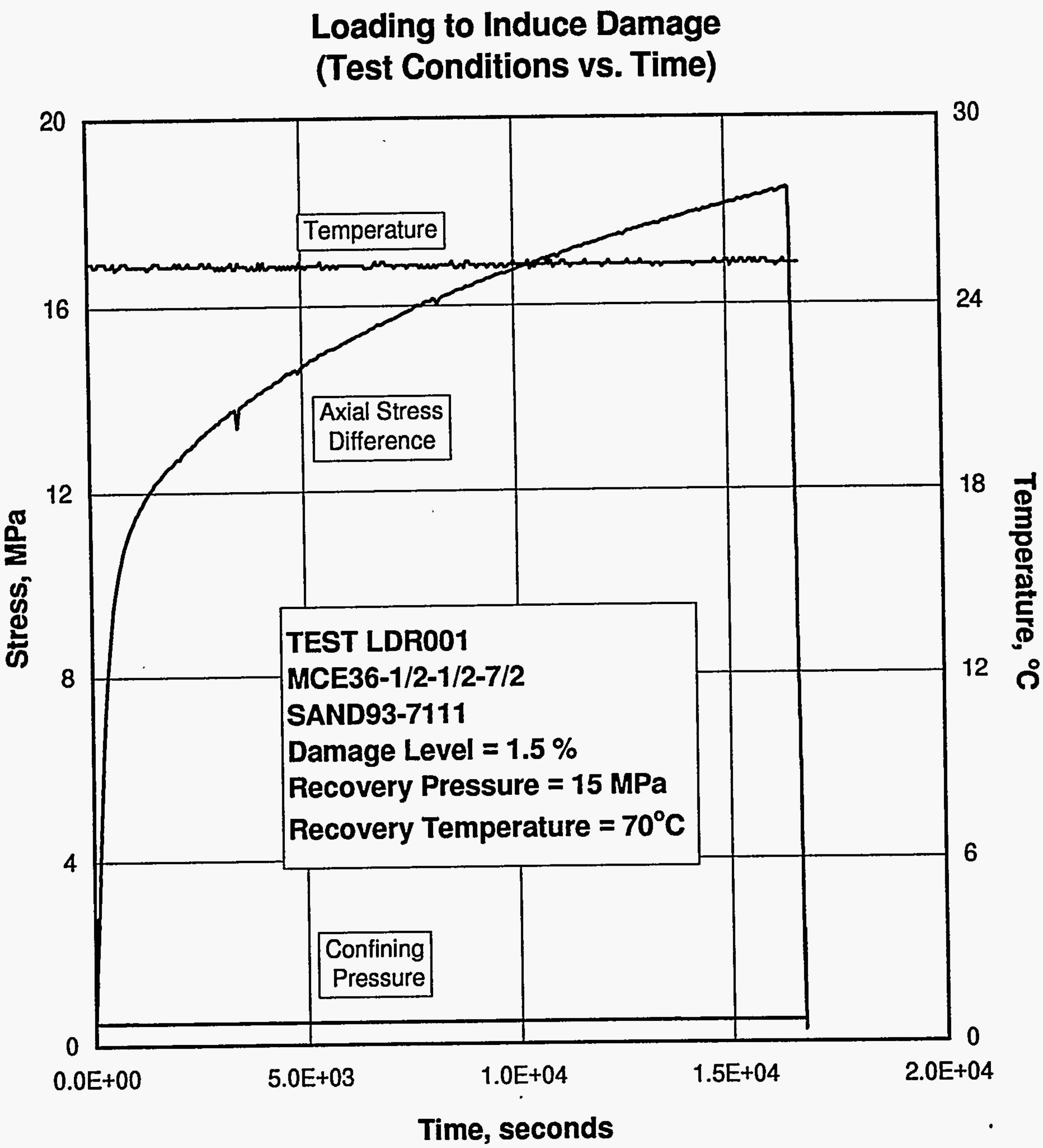

Figure E-1. Test Conditions as a Function of Time During the Quasi-Static Loading to Induce Damage in Specimen MCE36-1/2-1/2-7/2.

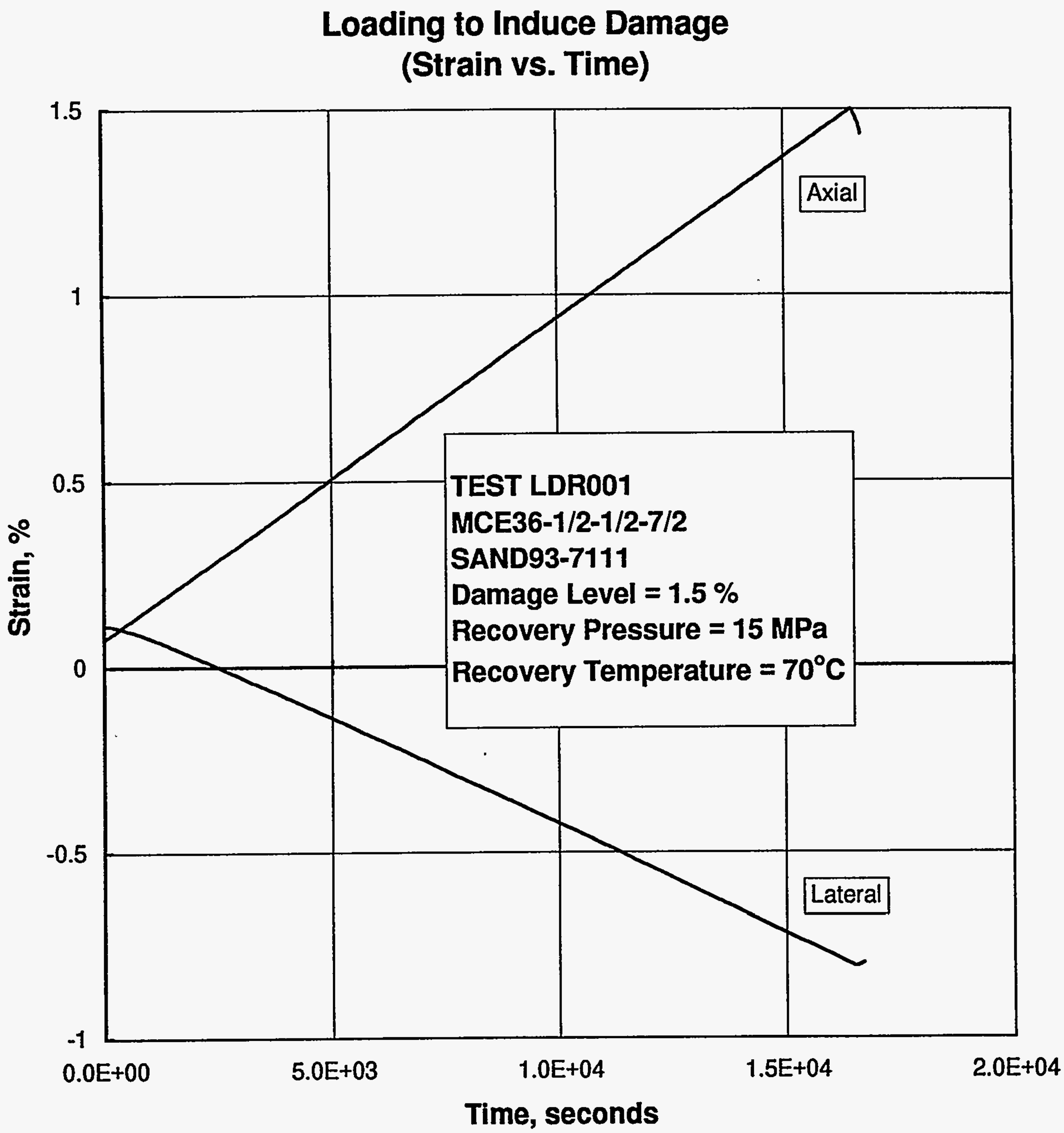

Figure E-2. Axial and Lateral Strain as a Function of Time During the Quasi-Static Loading to Induce Damage in Specimen MCE36-1/2-1/2-7/2.

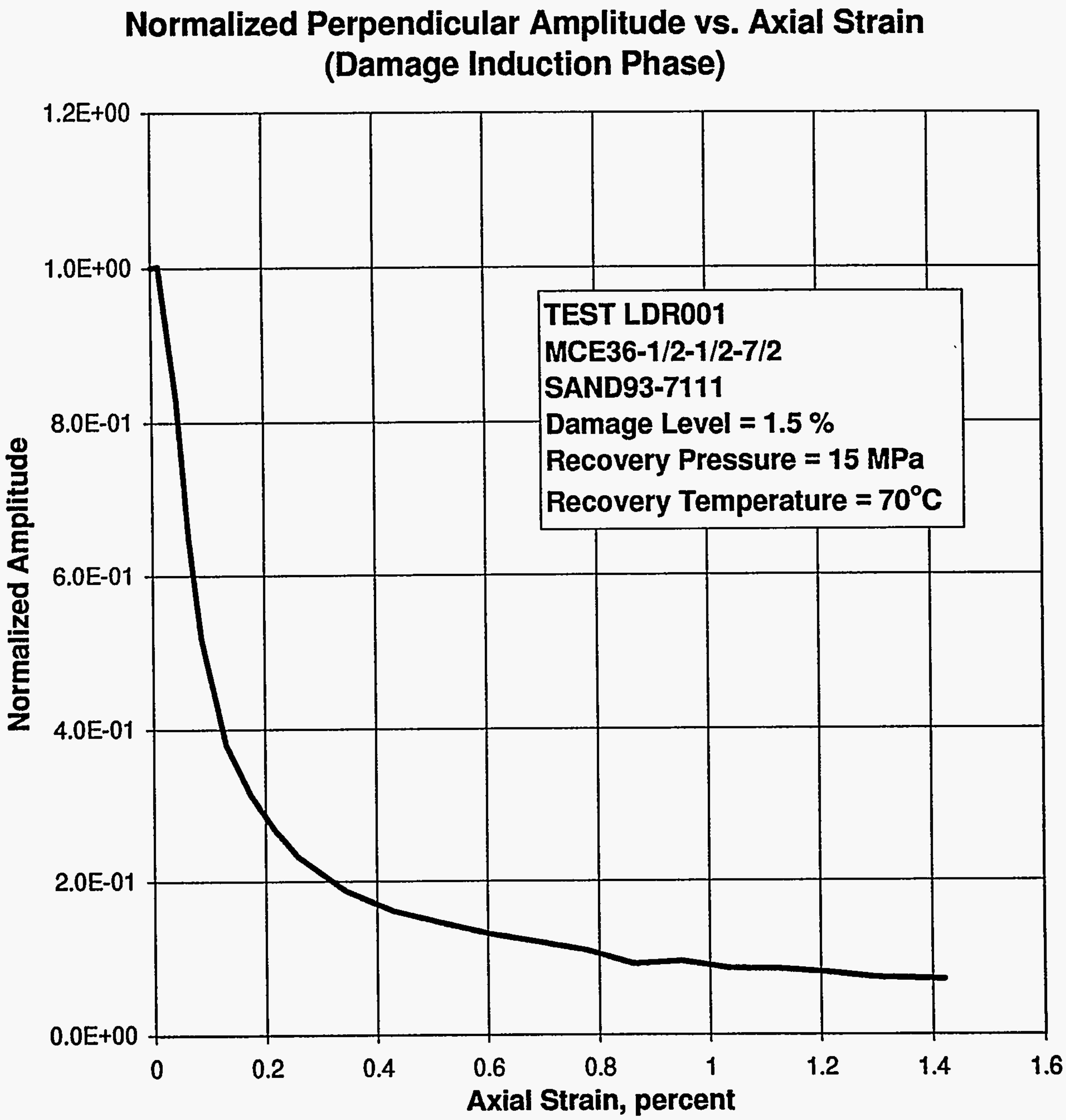

Figure E-3. Normalized Perpendicular Amplitude as a Function of Axial Strain During the Quasi-Static Loading to Induce Damage in Specimen MCE36-1/2-1/2-7/2.

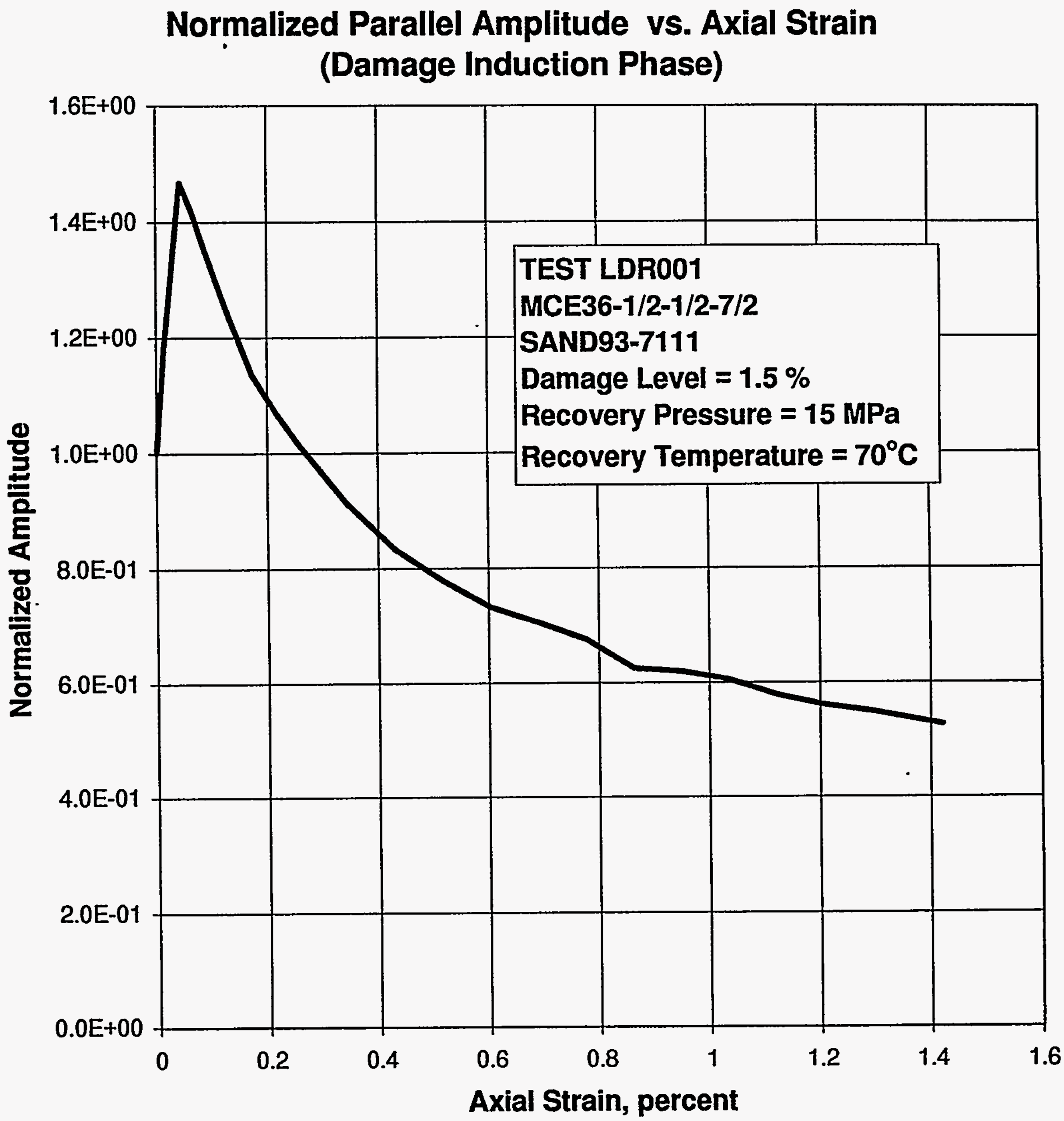

Figure E-4. Normalized Parallel Amplitude as a Function of Axial Strain During the Quasi-Static Loading to Induce Damage in Specimen MCE36-1/2-1/2-7/2.

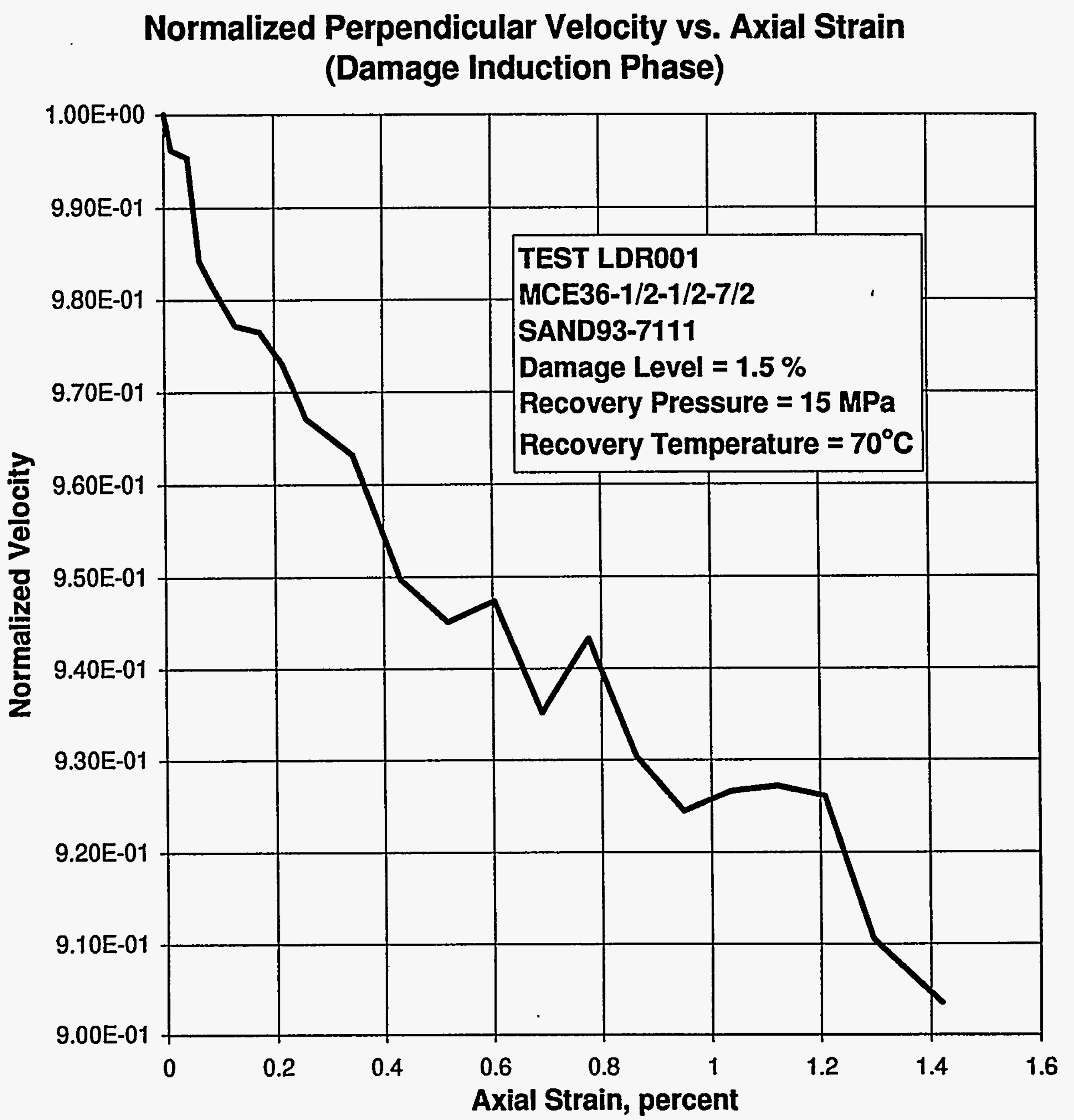

Figure E-5. Normalized Perpendicular Velocity as a Function of Axial Strain During the Quasi-Static Loading to Induce Damage in Specimen MCE36-1/2-1/2-7/2.

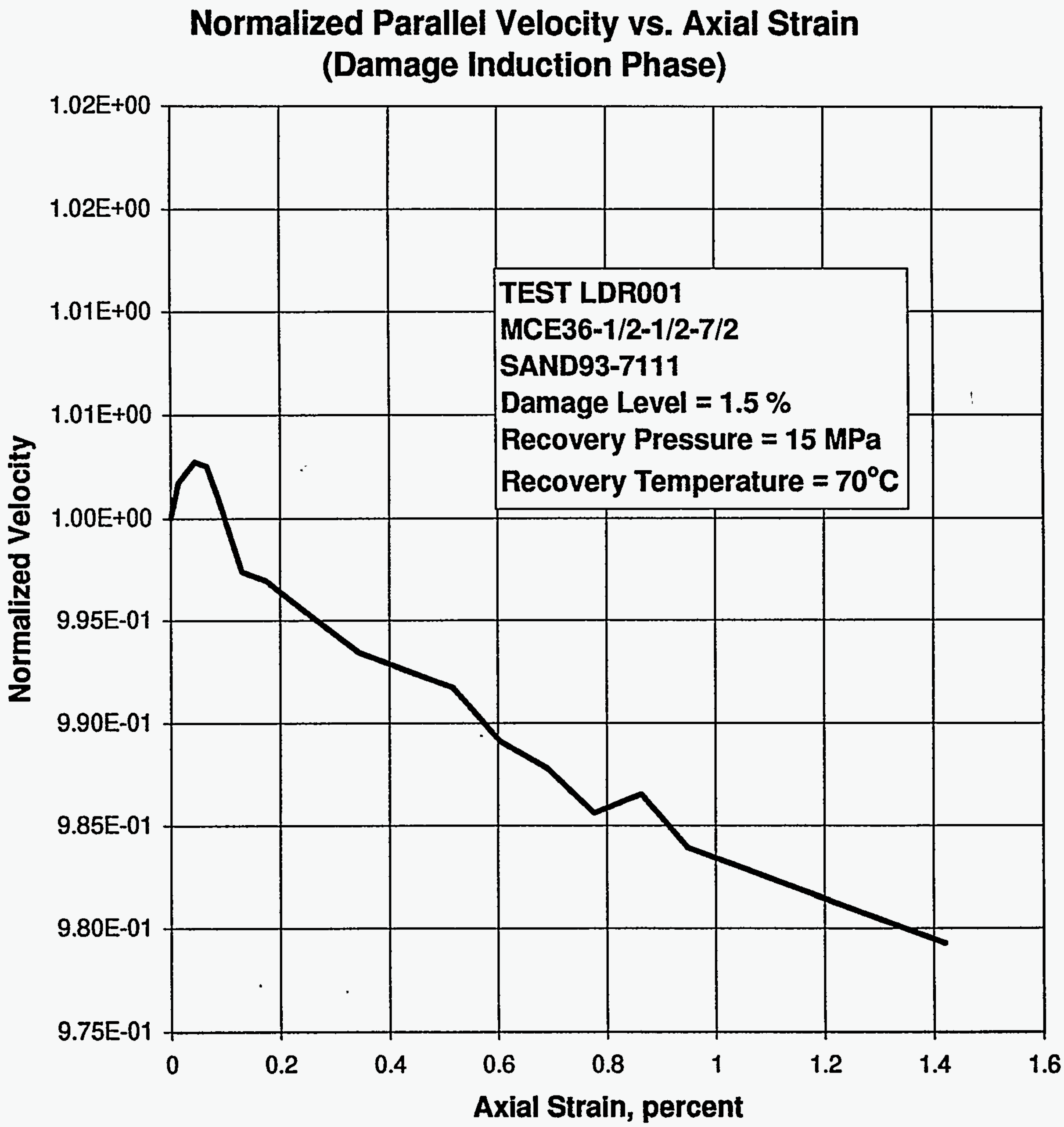

Figure E-6. Normalized Parallel Velocity as a Function of Axial Strain During the Quasi-Static Loading to Induce Damage in Specimen MCE36-1/2-1/2-7/2.

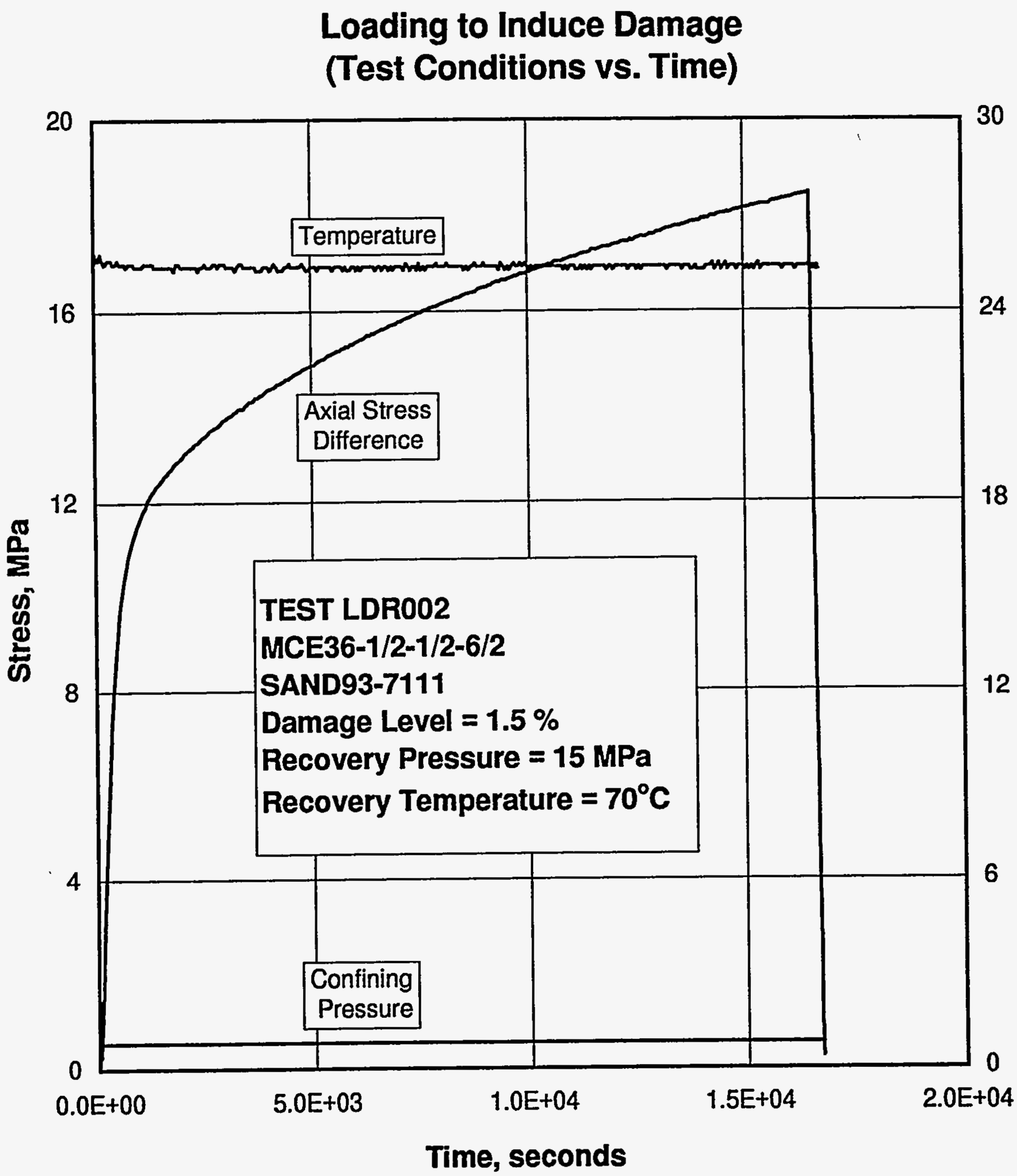

Figure E-7. Test Conditions as a Function of Time During the Quasi-Static Loading to Induce Damage in Specimen MCE36-1/2-1/2-6/2.

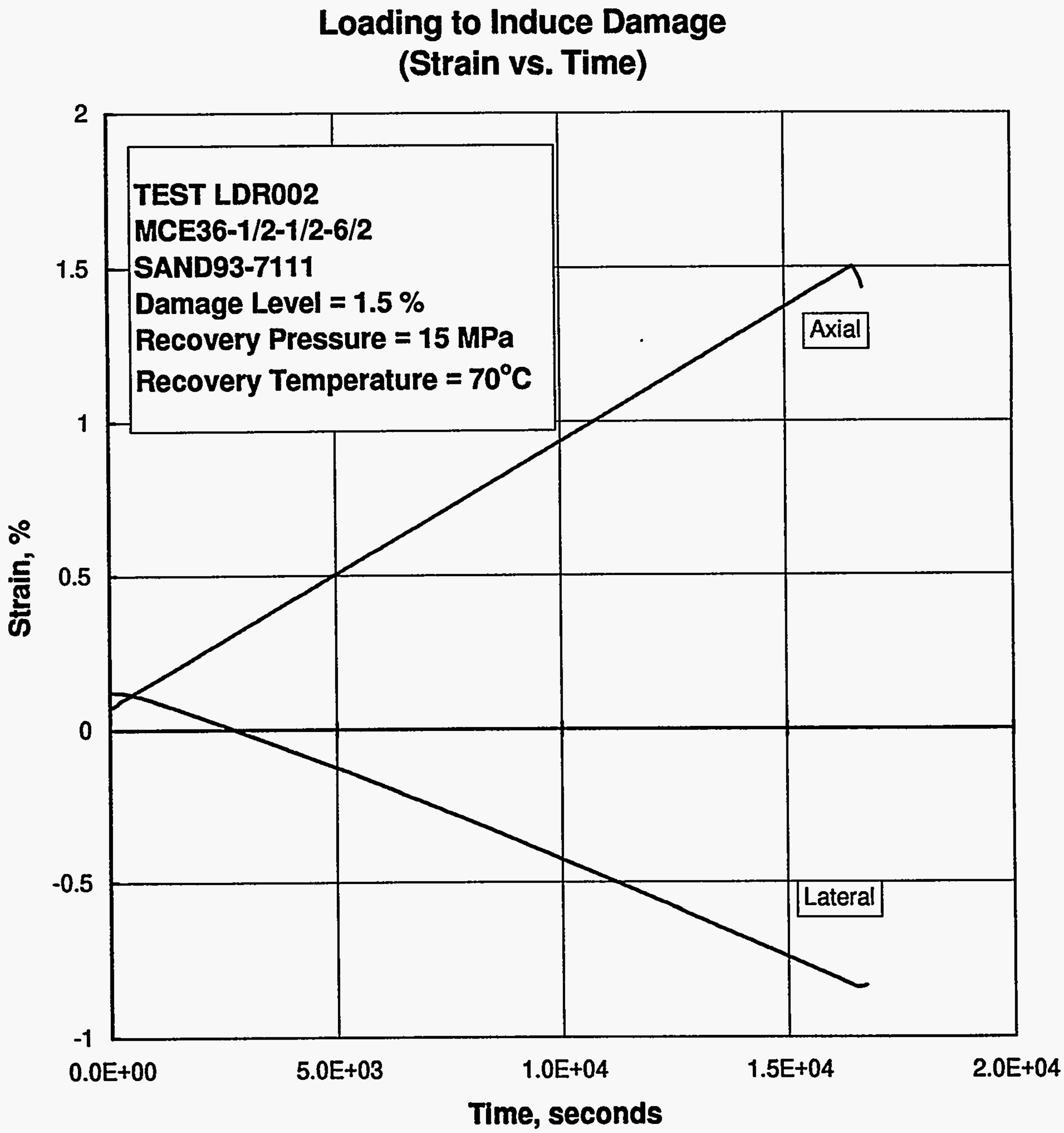

Figure E-8. Axial and Lateral Strain as a Function of Time During the Quasi-Static Loading to Induce Damage in Specimen MCE36-1/2-1/2-6/2.

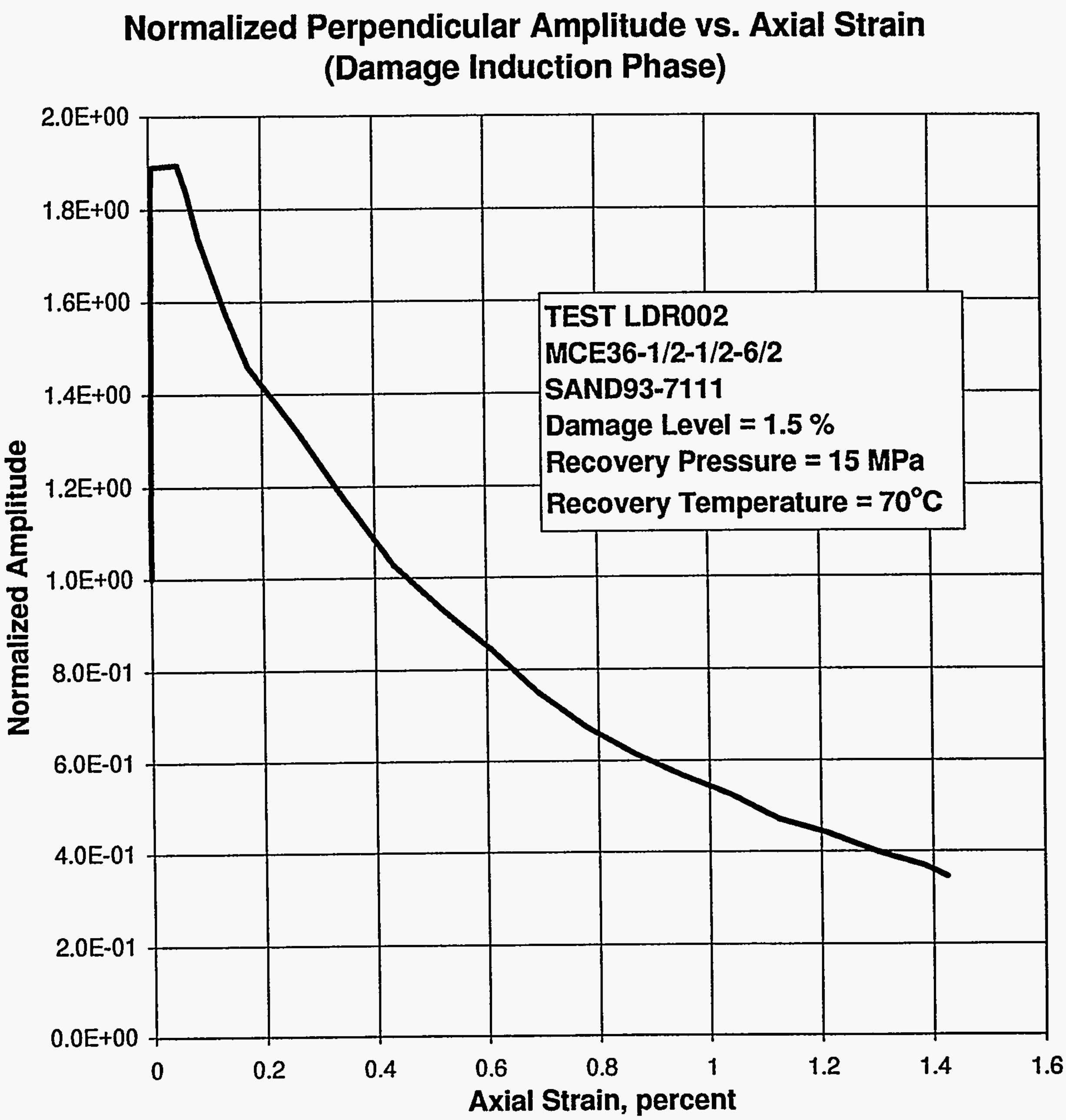

Figure E-9. Normalized Perpendicular Amplitude as a Function of Axial Strain During the Quasi-Static Loading to Induce Damage in Specimen MCE36-1/2-1/2-6/2.

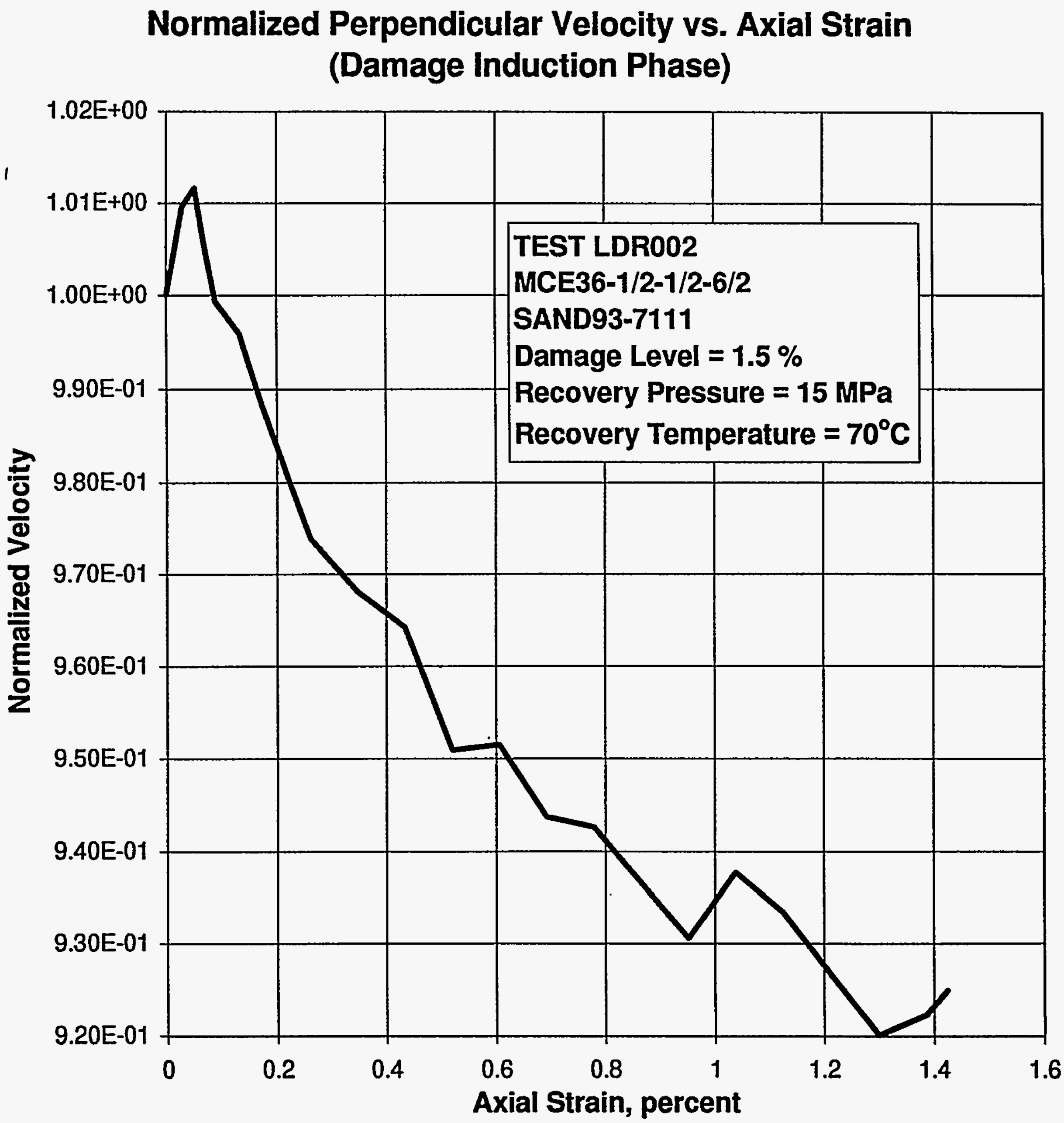

Figure E-10. Normalized Perpendicular Velocity as a Function of Axial Strain During the Quasi-Static Loading to Induce Damage in Specimen MCE36-1/2-1/2-6/2.

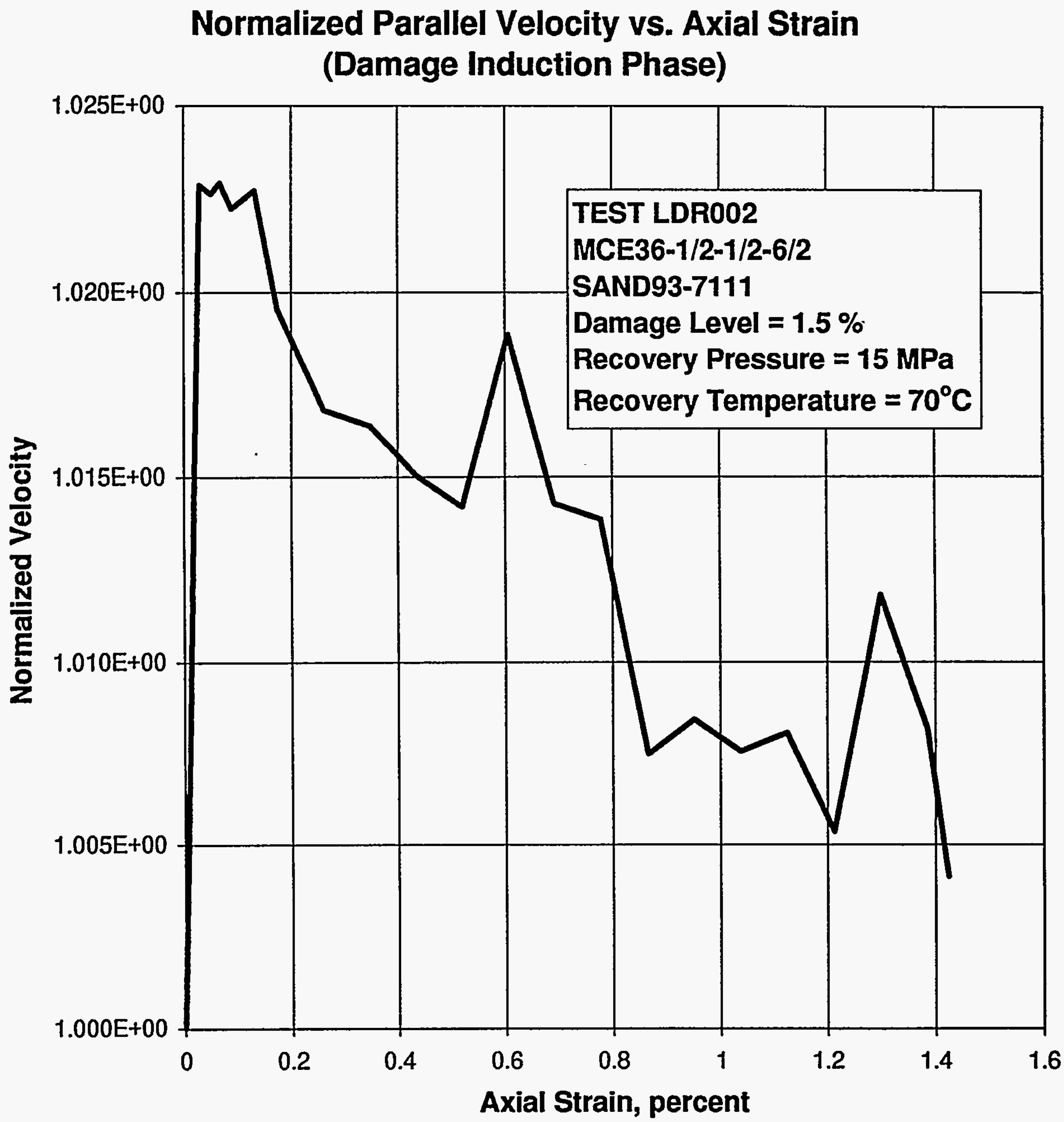

Figure E-11. Normalized Parallel Velocity as a Function of Axial Strain During the Quasi-Static Loading to Induce Damage in Specimen MCE36-1/2-1/2-6/2.

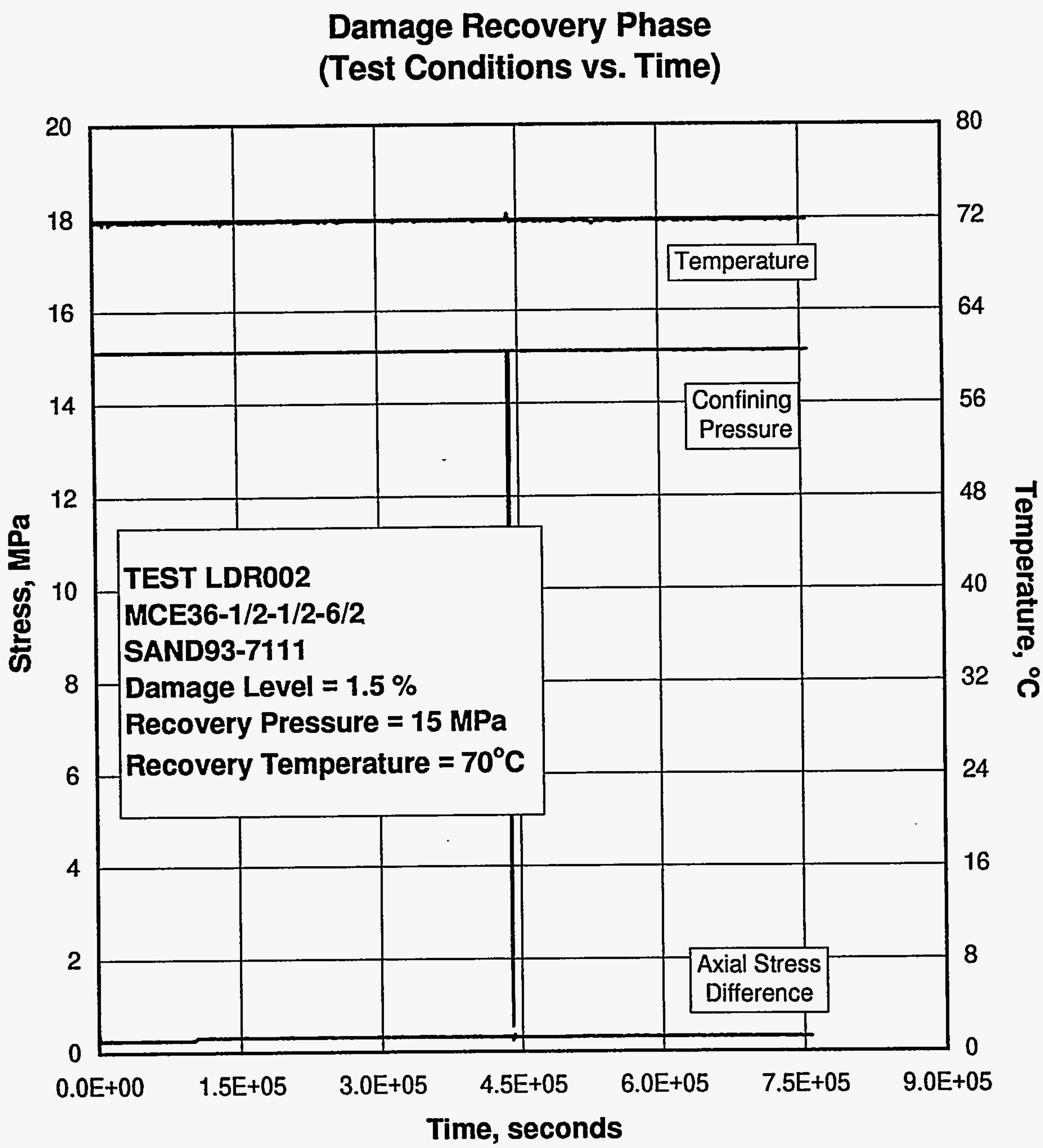

Figure E-12. Test Conditions as a Function of Time During the Hydrostatic Loading to Recover Damage in Specimen MCE36-1/2-1/2-6/2.

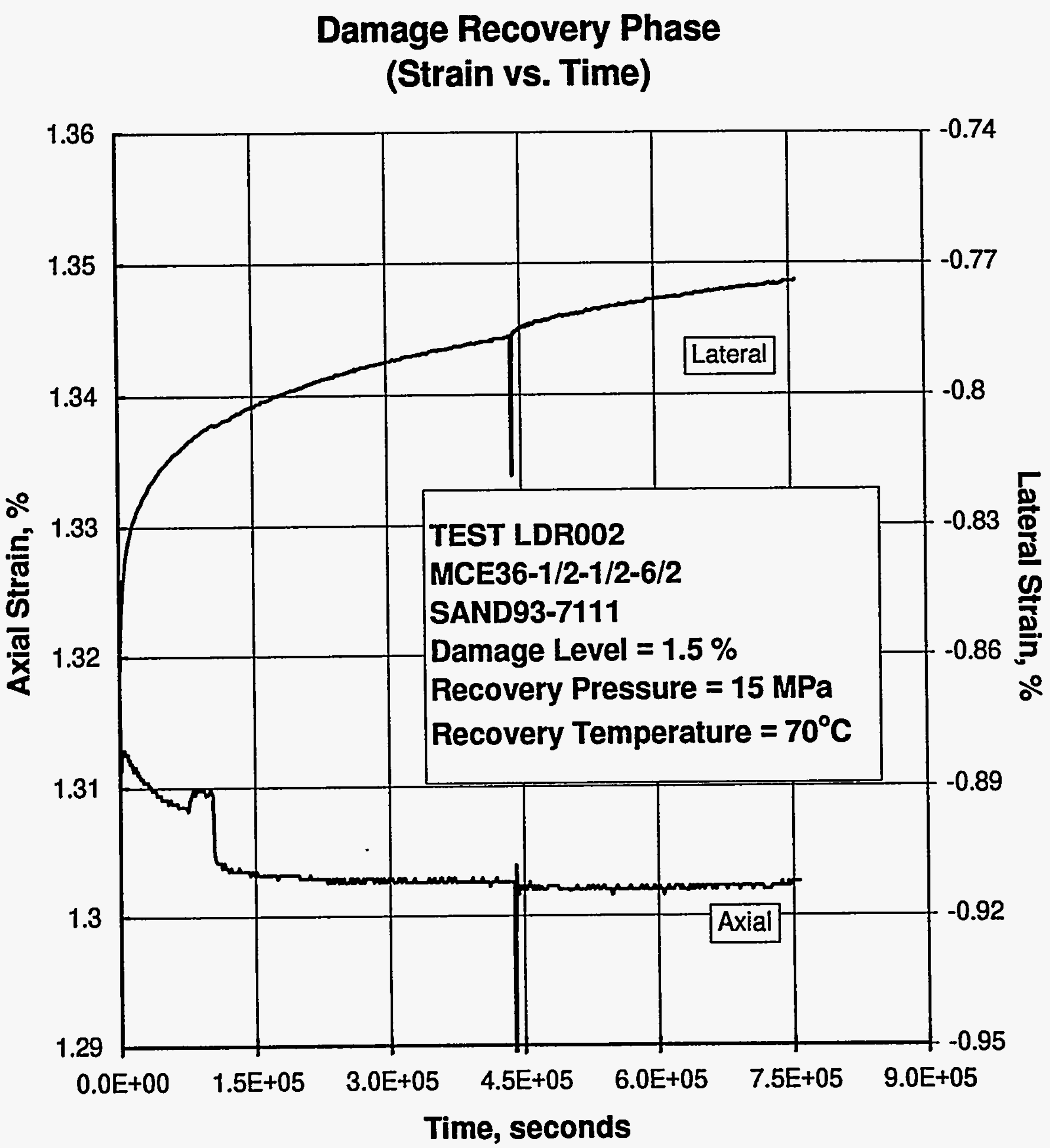

Figure E-13. Axial and Lateral Strain as a Function of Time During the Hydrostatic Loading to Recover Damage in Specimen MCE36-1/2-1/2-6/2.

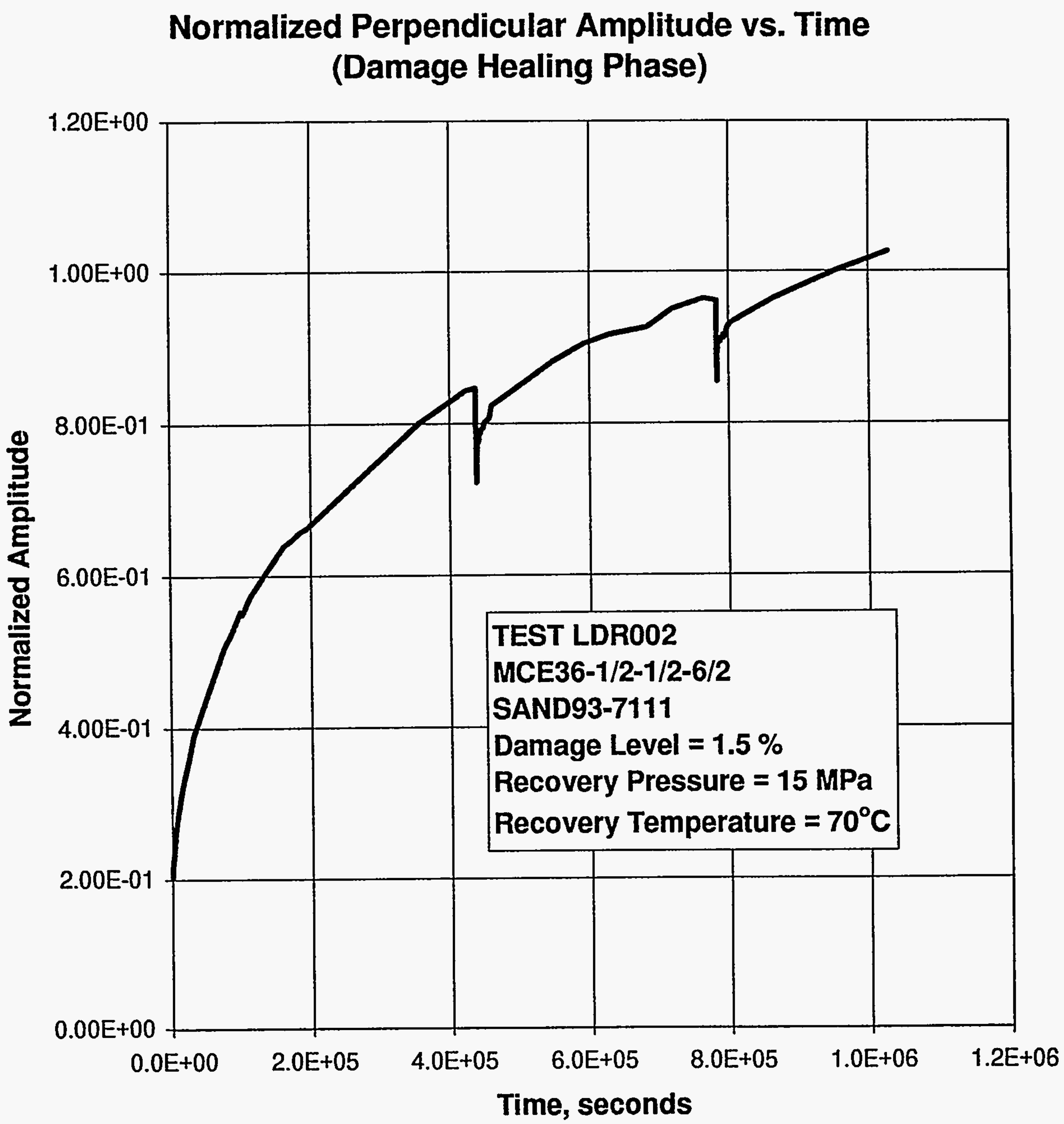

Figure E-14. Normalized Perpendicular Amplitude as a Function of Time During the Hydrostatic Loading to Recover Damage in Specimen MCE36-1/2-1/2-6/2.

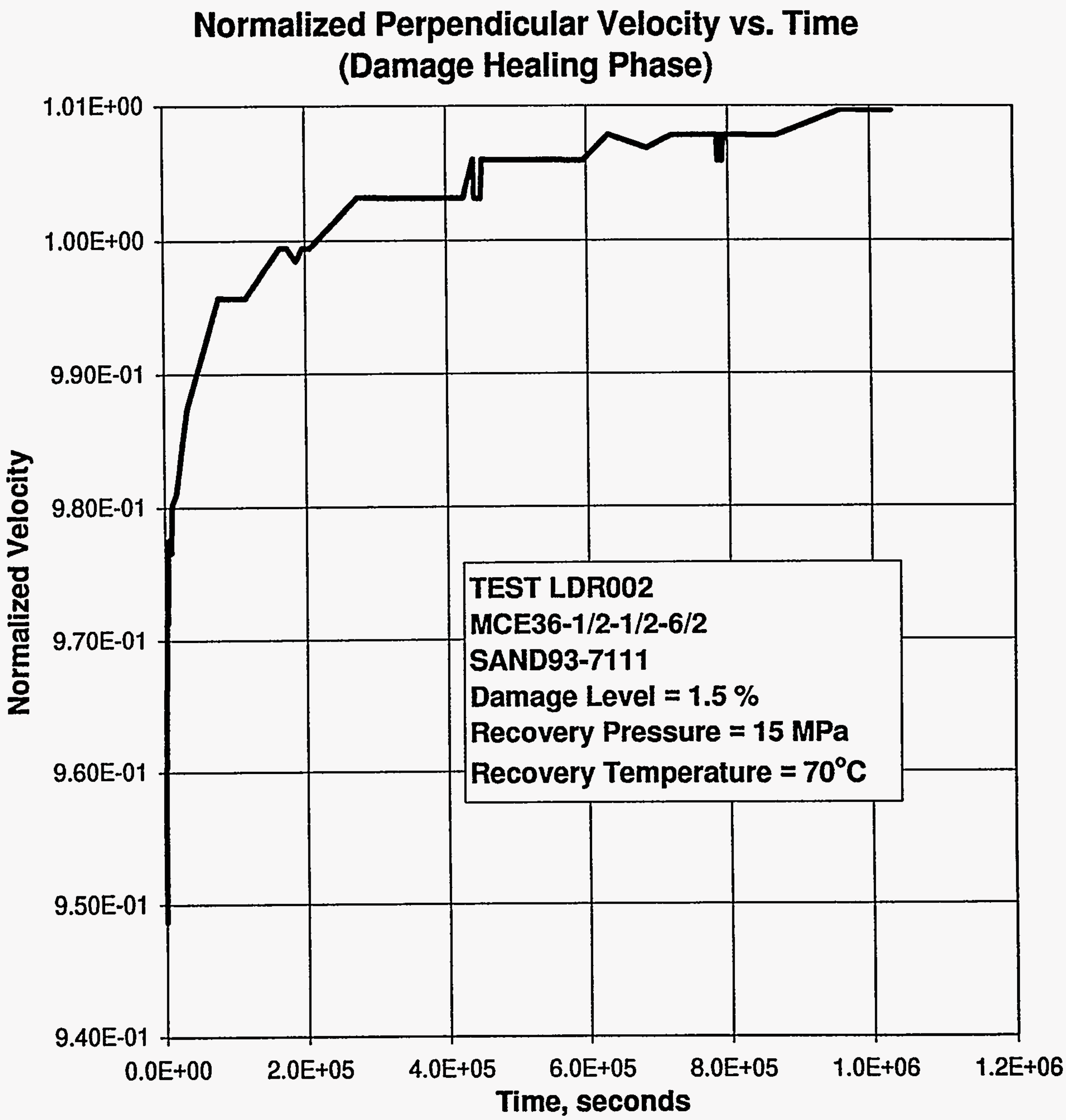

Figure E-15. Normalized Perpendicular Velocity as a Function of Time During the Hydrostatic Loading to Recover Damage in Specimen MCE36-1/2-1/2-6/2.

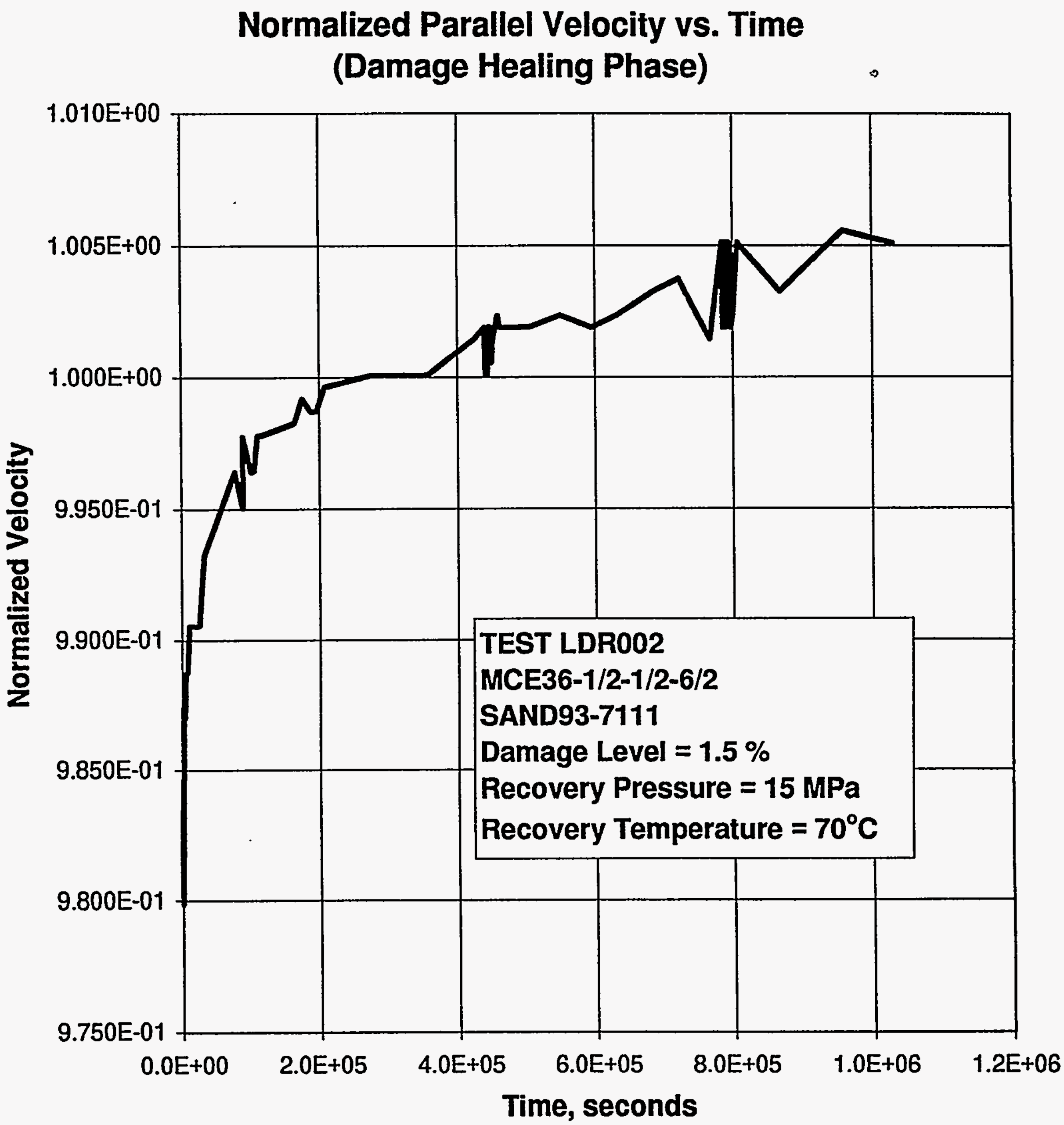

Figure E-16. Normalized Parallel Velocity as a Function of Time During the Hydrostatic Loading to Recover Damage in Specimen MCE36-1/2-1/2-6/2.

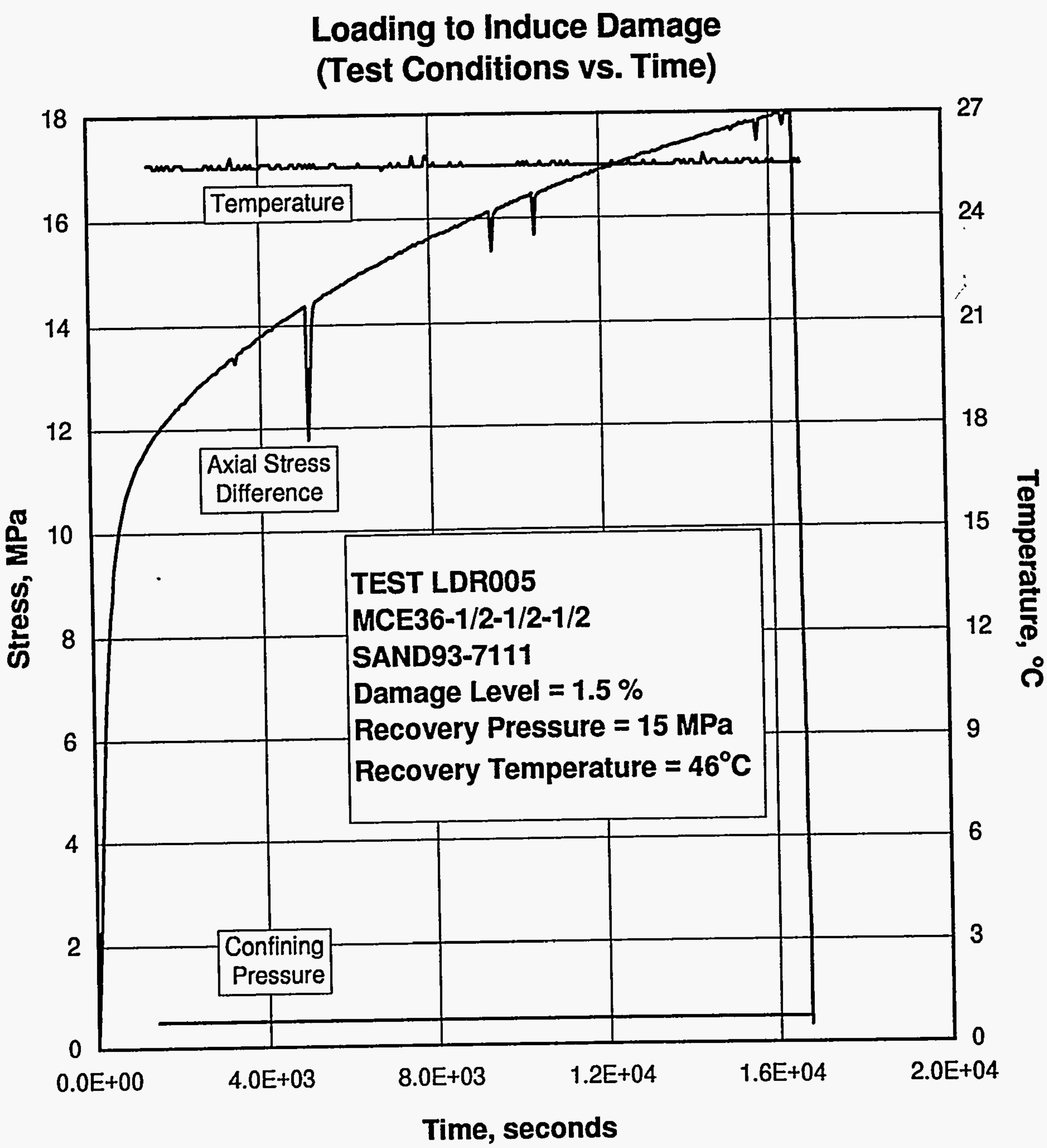

Figure E-17. Test Conditions as a Function of Time During the Quasi-Static Loading to Induce Damage in Specimen MCE36-1/2-1/2-1/2.

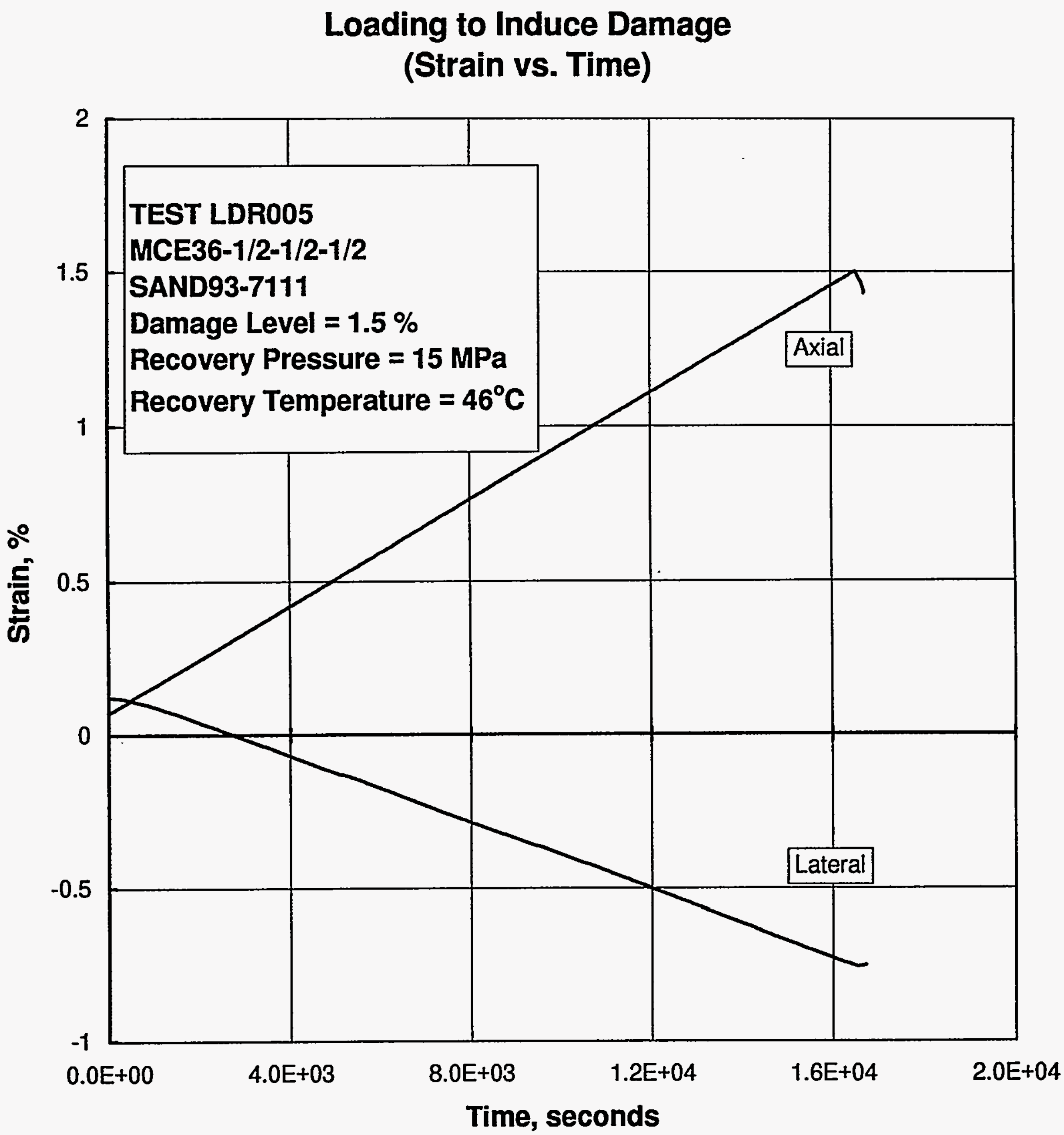

Figure E-18. Axial and Lateral Strain as a Function of Time During the Quasi-Static Loading to Induce Damage in Specimen MCE36-1/2-1/2-1/2.

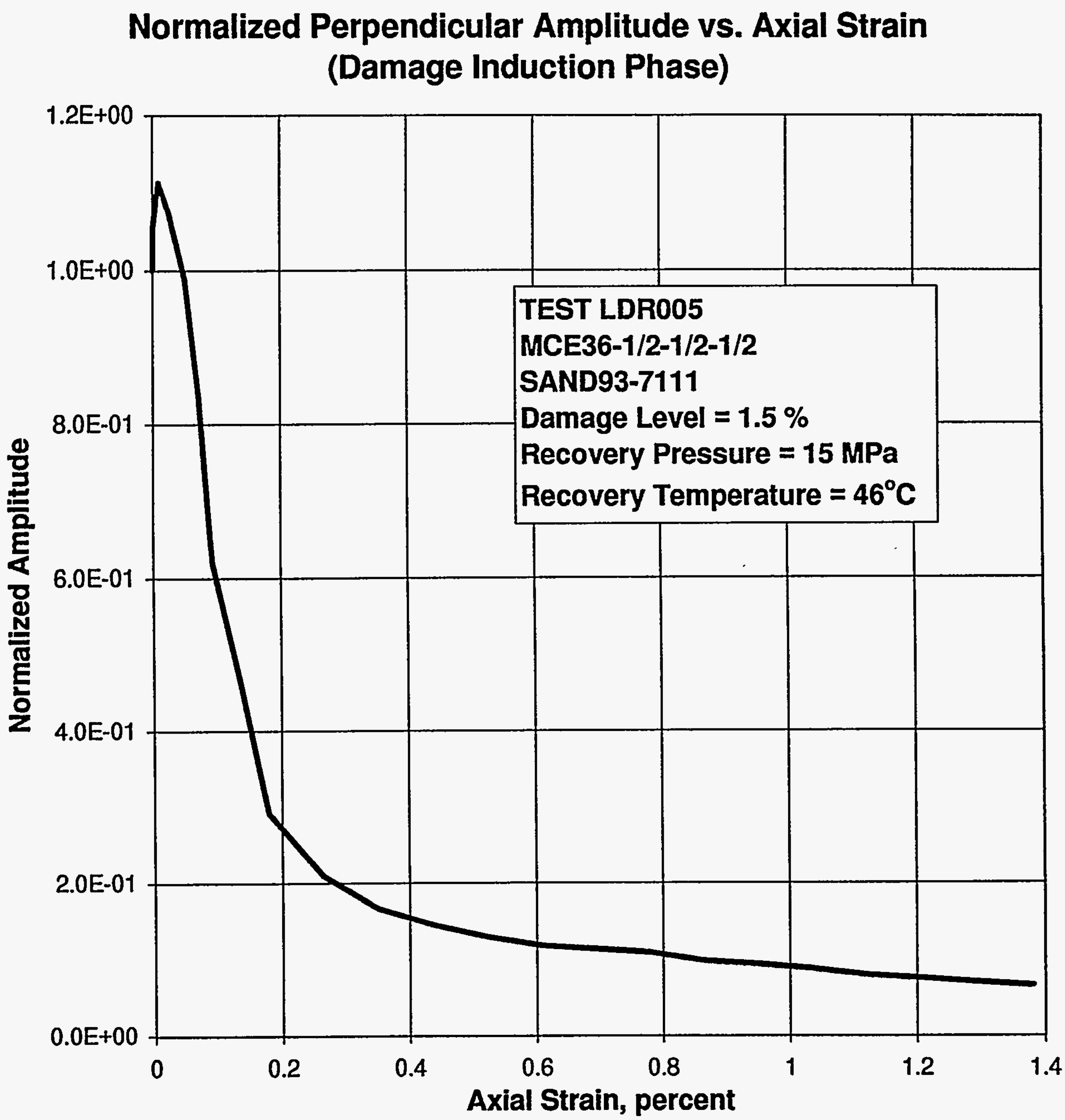

Figure E-19. Normalized Perpendicular Amplitude as a Function of Axial Strain During the Quasi-Static Loading to Induce Damage in Specimen MCE36-1/2-1/2-1/2.

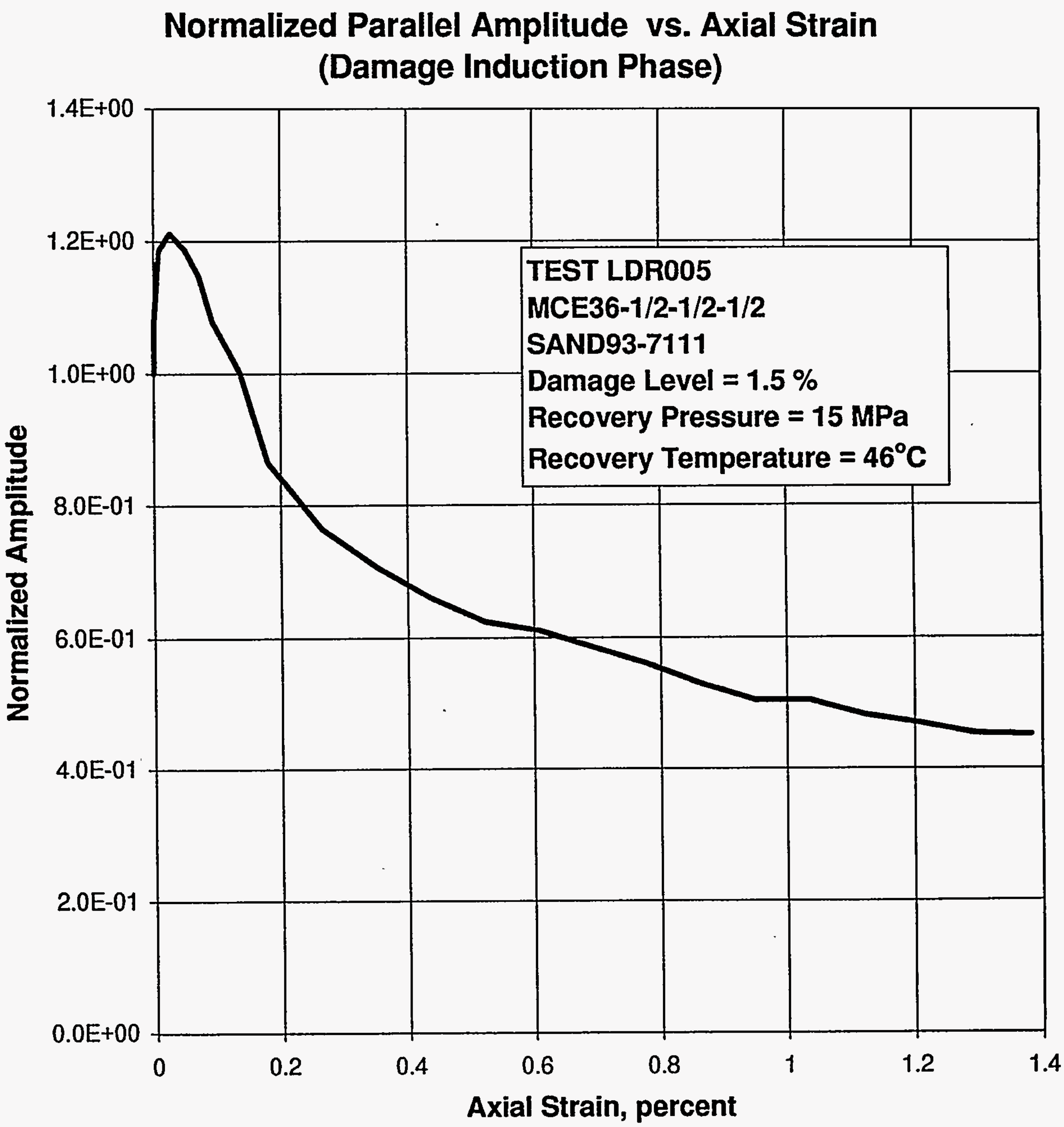

Figure E-20. Normalized Parallel Amplitude as a Function of Axial Strain During the Quasi-Static Loading to Induce Damage in Specimen MCE36-1/2-1/2-1/2.

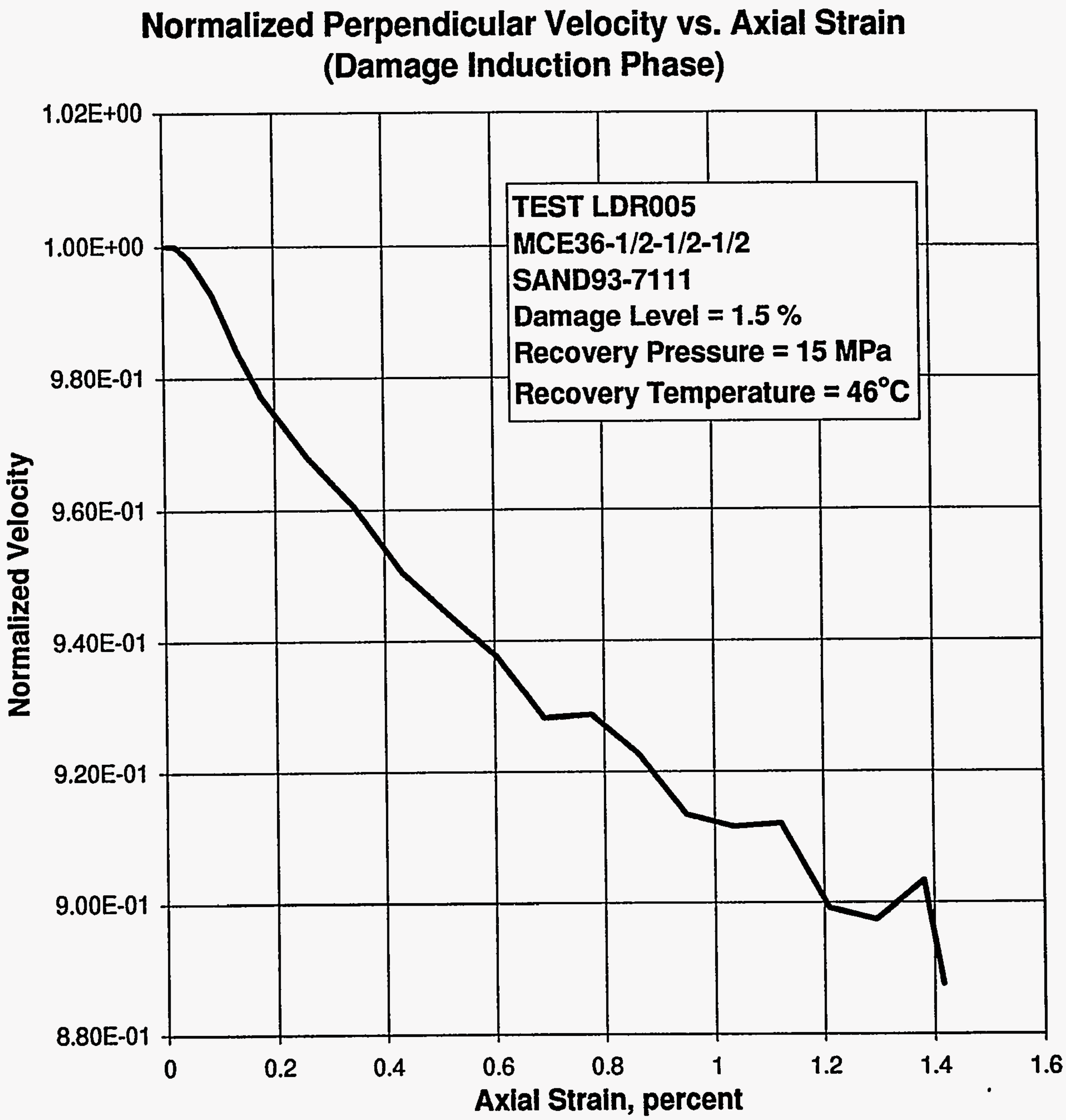

Figure E-21. Normalized Perpendicular Velocity as a Function of Axial Strain During the Quasi-Static Loading to Induce Damage in Specimen MCE36-1/2-1/2-1/2.

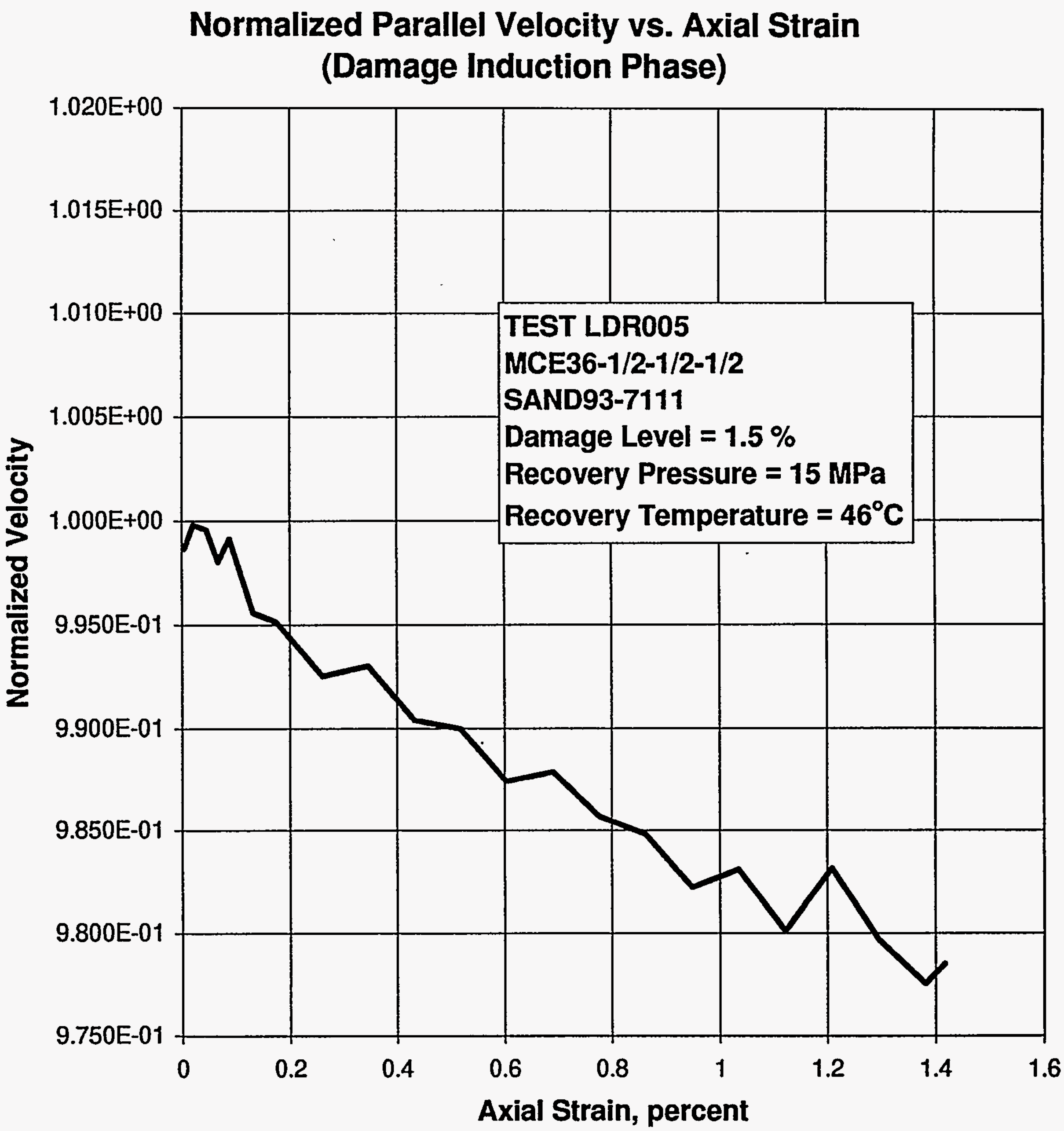

Figure E-22. Normalized Parallel Velocity as a Function of Axial Strain During the Quasi-Static Loading to Induce Damage in Specimen MCE36-1/2-1/2-1/2.

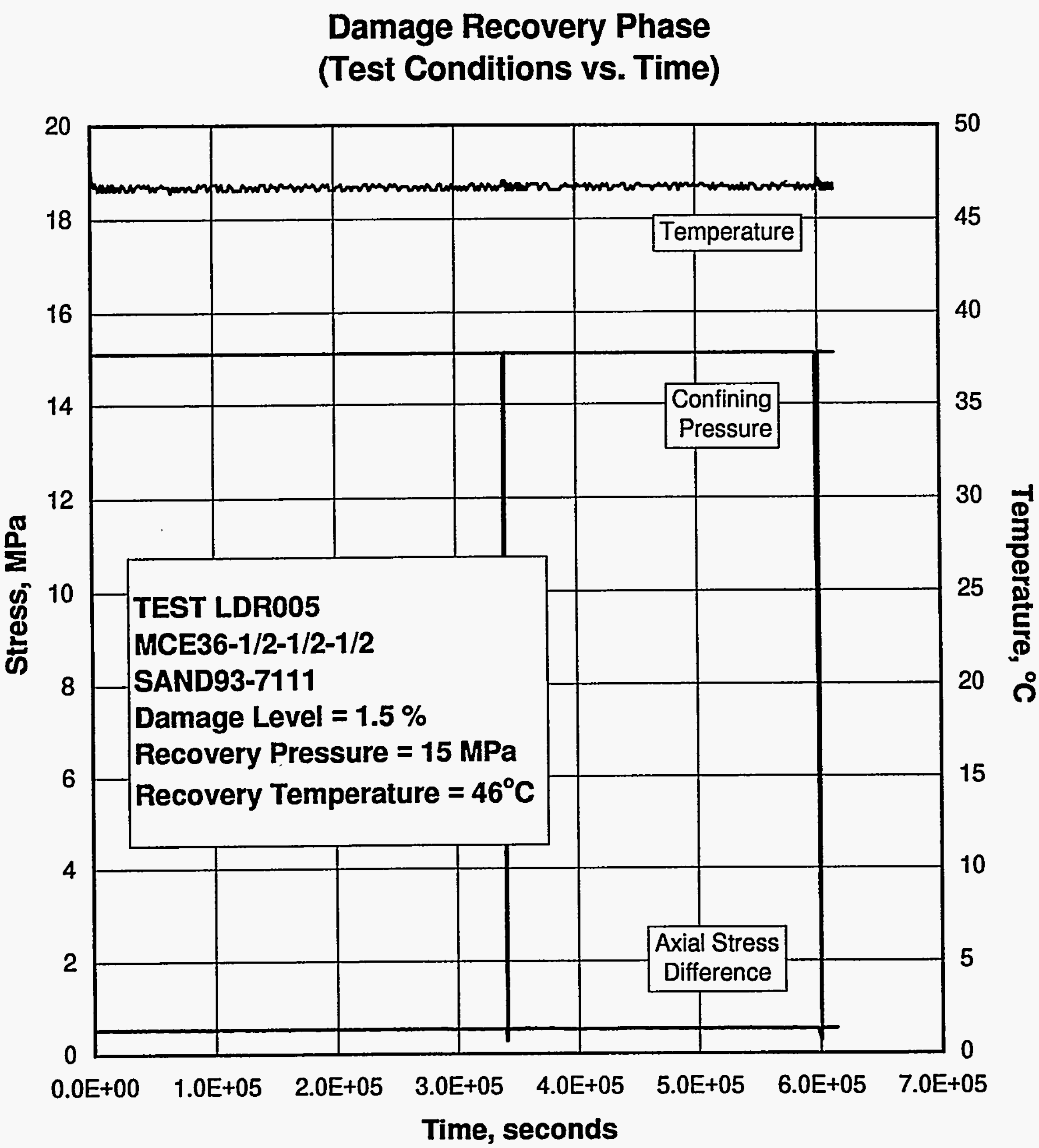

Figure E-23. Test Conditions as a Function of Time During the Hydrostatic Loading to Recover Damage in Specimen MCE36-1/2-1/2-1/2.

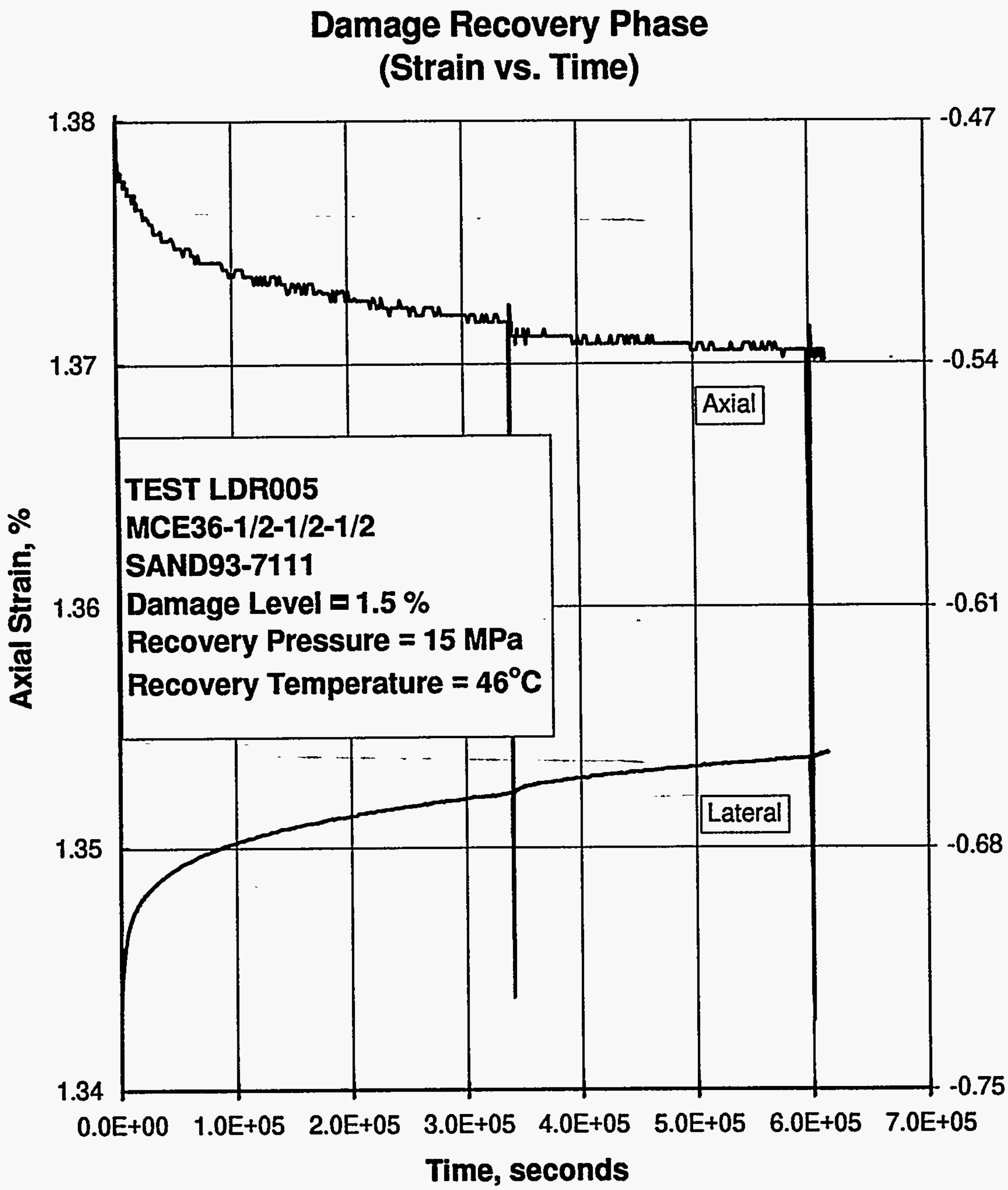

Figure E-24. Axial and Lateral Strain as a Function of Time During the Hydrostatic Loading to Recover Damage in Specimen MCE36-1/2-1/2-1/2.

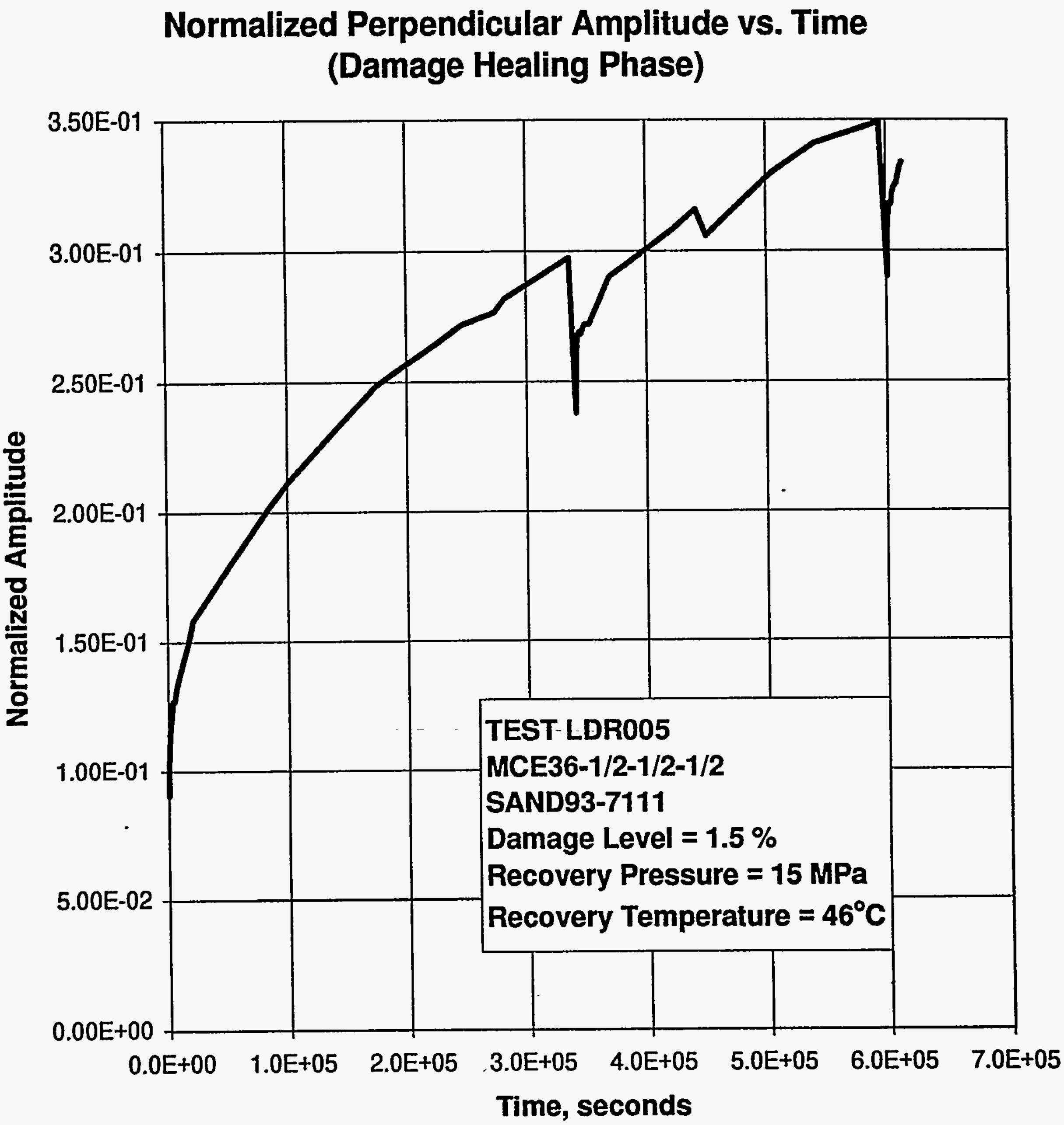

Figure E-25. Normalized Perpendicular Amplitude as a Function of Time During the Hydrostatic Loading to Recover Damage in Specimen MCE36-1/2-1/2-1/2.

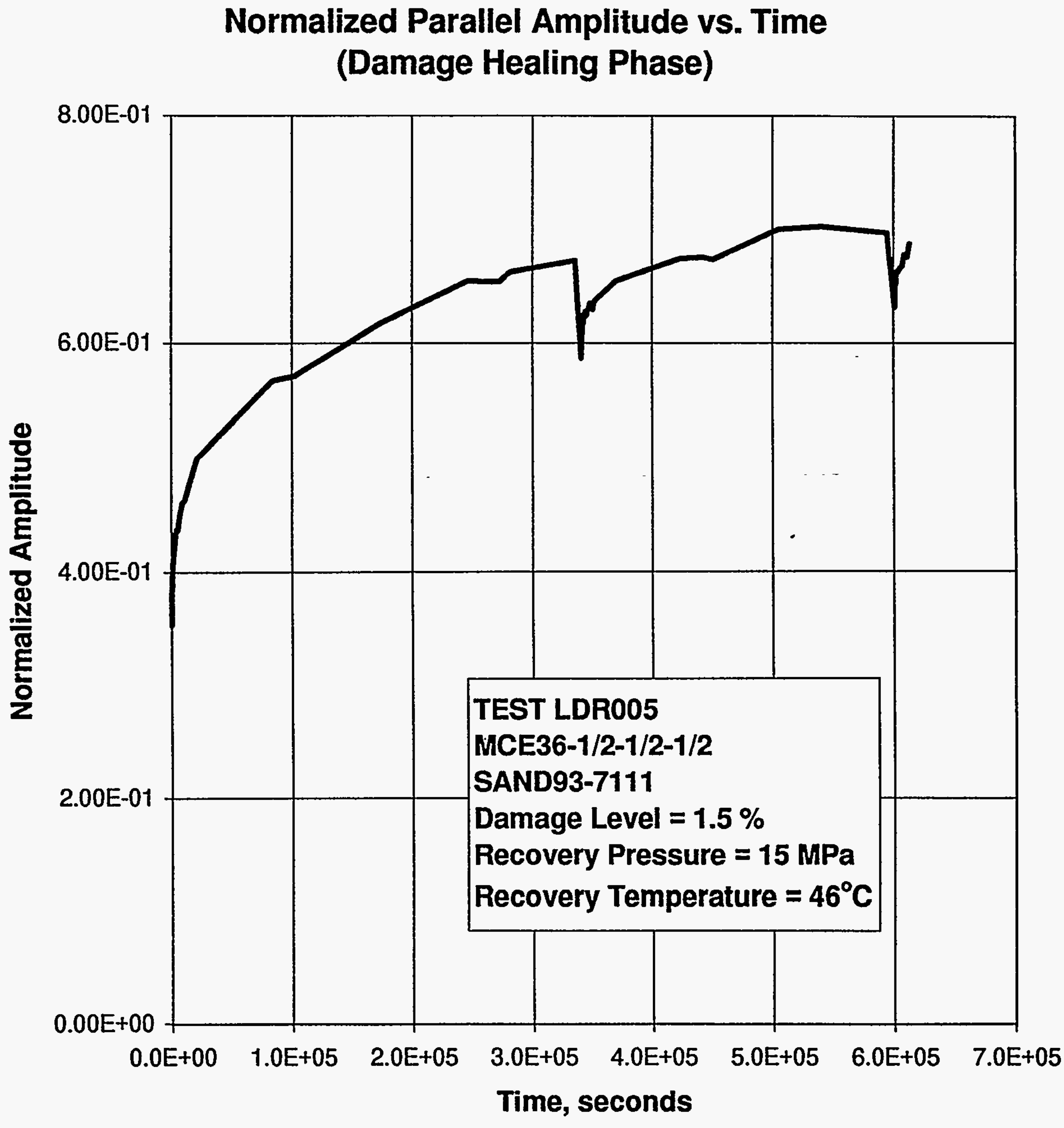

Figure E-26. Normalized Parallel Amplitude as a Function of Time During the Hydrostatic Loading to Recover Damage in Specimen MCE36-1/2-1/2-1/2.

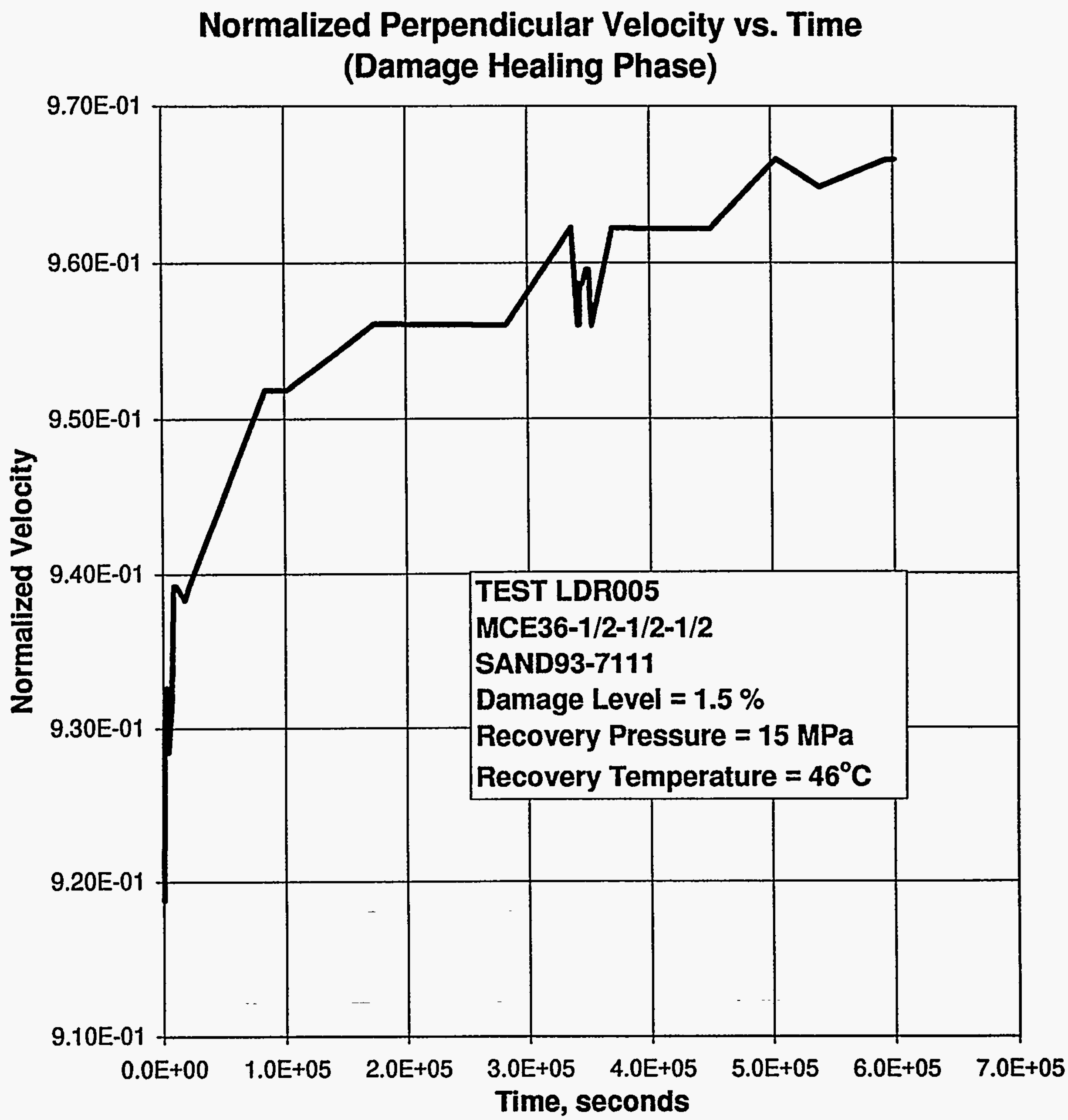

Figure E-27. Normalized Perpendicular Velocity as a Function of Time During the Hydrostatic Loading to Recover Damage in Specimen MCE36-1/2-1/2-1/2.

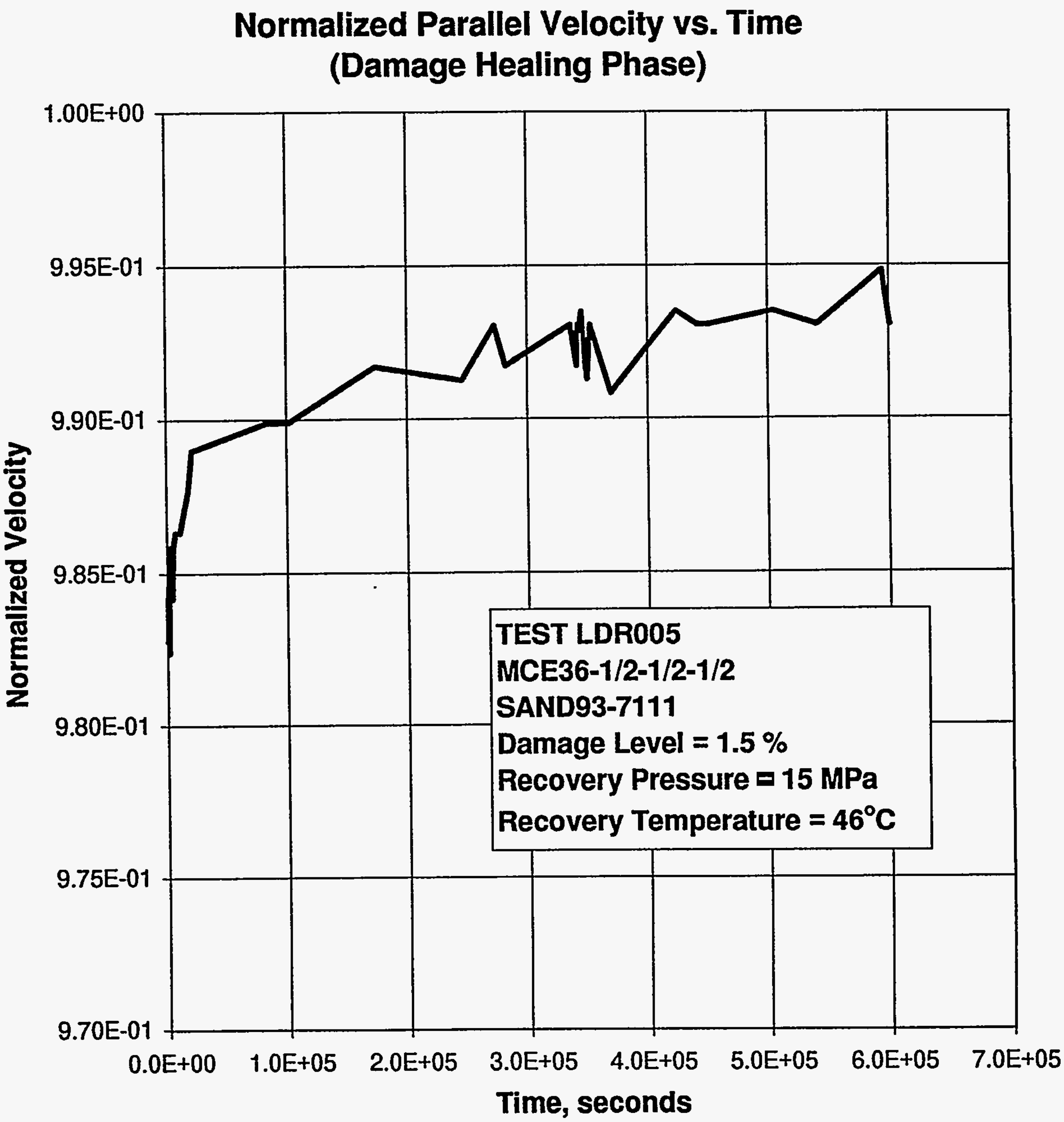

Figure E-28. Normalized Parallel Velocity as a Function of Time During the Hydrostatic Loading to Recover Damage in Specimen MCE36-1/2-1/2-1/2.

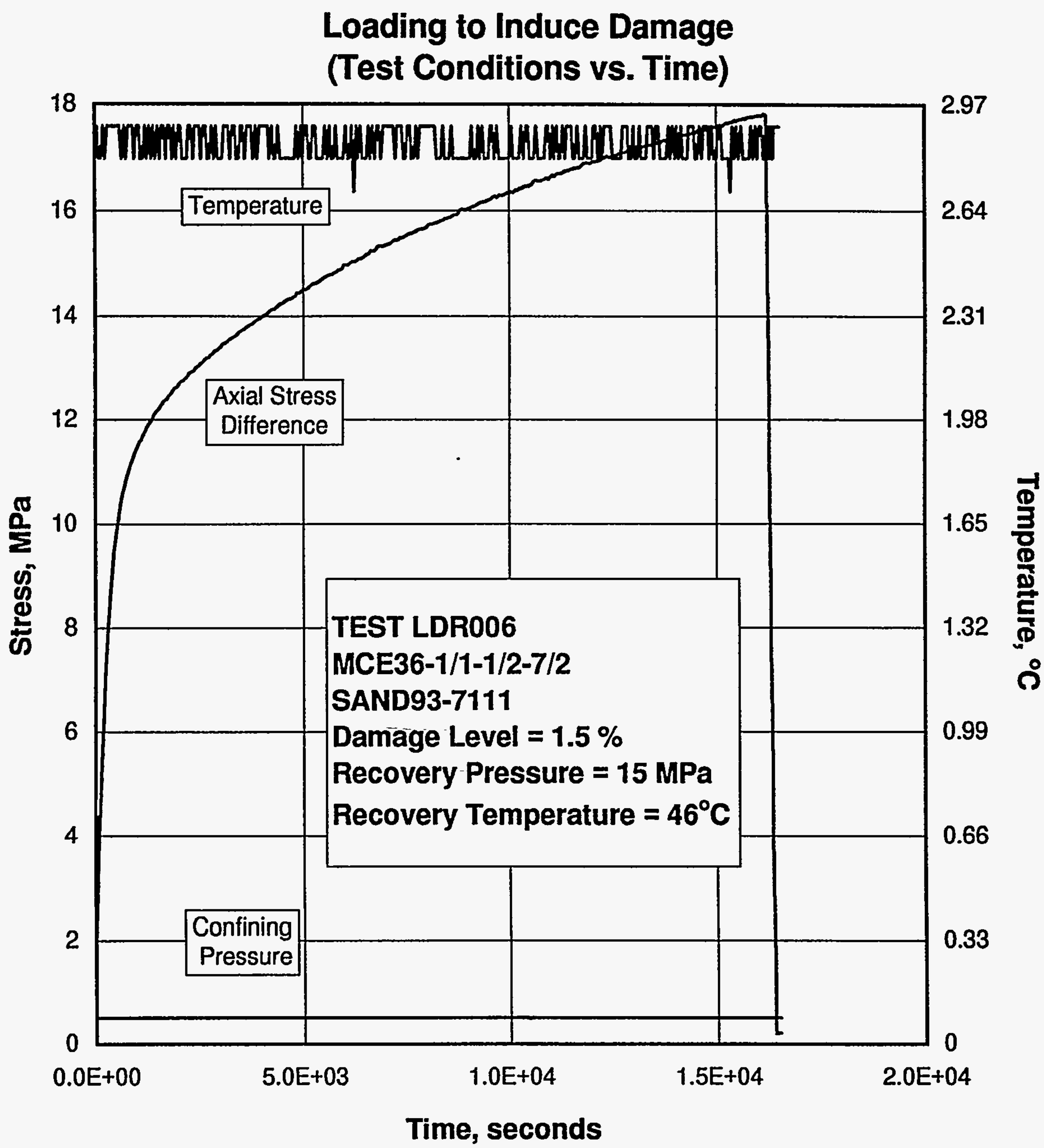

Figure E-29. Test Conditions as a Function of Time During the Quasi-Static Loading to Induce Damage in Specimen MCE36-1/1-1/2-7/2.

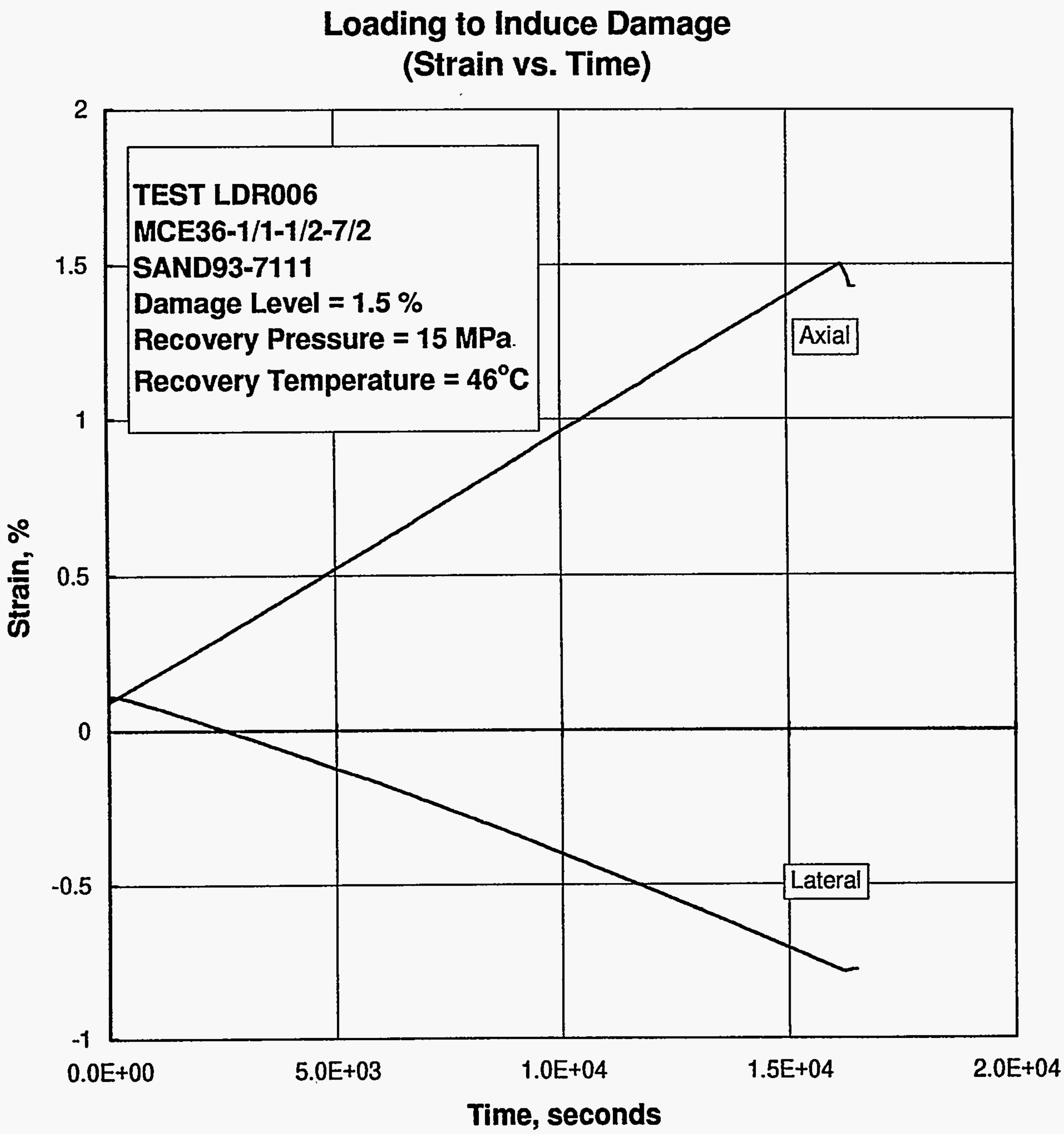

Figure E-30. Axial and Lateral Strain as a Function of Time During the Quasi-Static Loading to Induce Damage in Specimen MCE36-1/1-1/2-7/2.

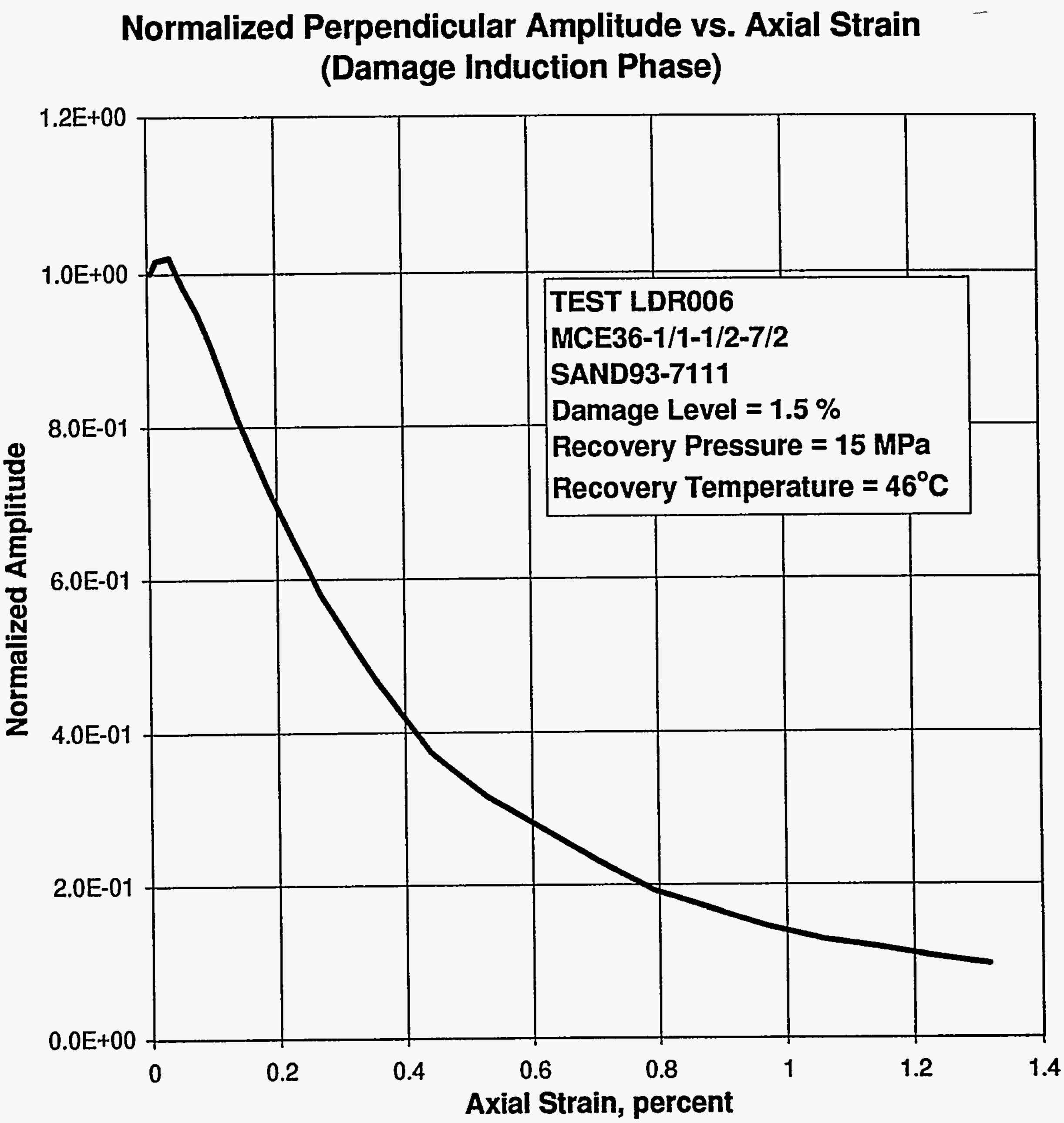

Figure E-31. Normalized Perpendicular Amplitude as a Function of Axial Strain During the Quasi-Static Loading to Induce Damage in Specimen MCE36-1/1-1/2-7/2.

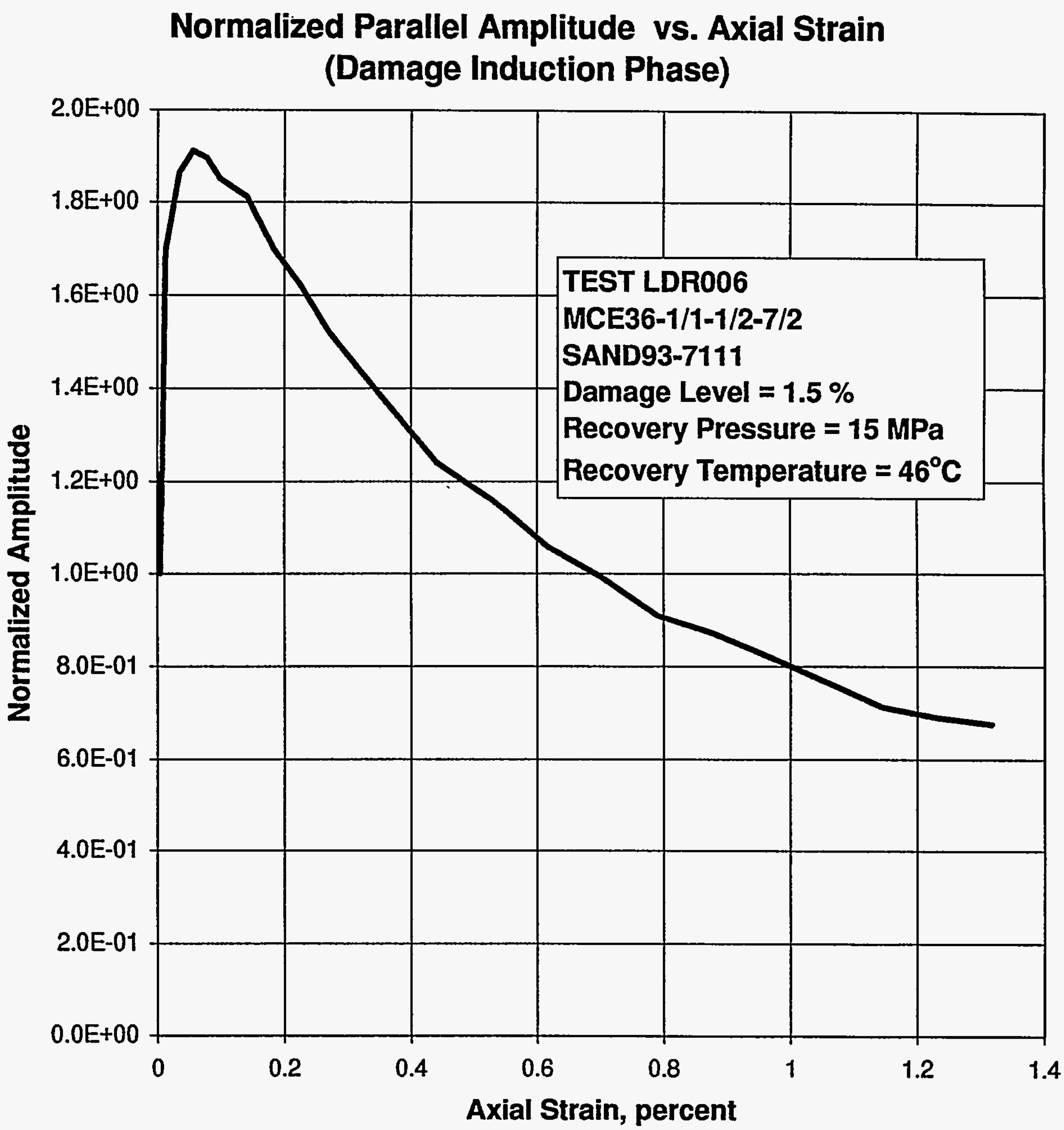

Figure E-32. Normalized Parallel Amplitude as a Function of Axial Strain During the Quasi-Static Loading to Induce Damage in Specimen MCE36-1/1-1/2-7/2.

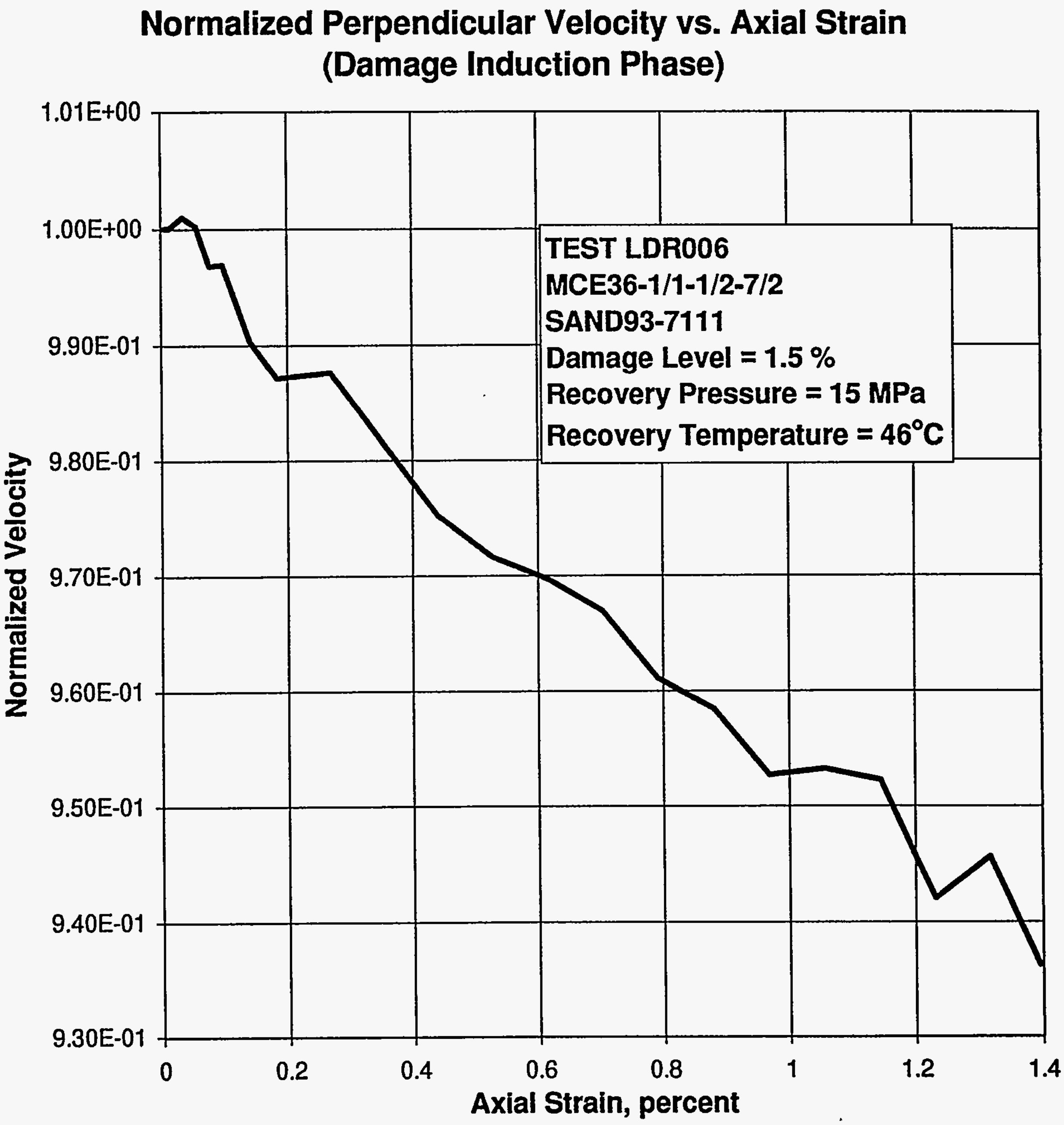

Figure E-33. Normalized Perpendicular Velocity as a Function of Axial Strain During the Quasi-Static Loading to Induce Damage in Specimen MCE36-1/1-1/2-7/2.

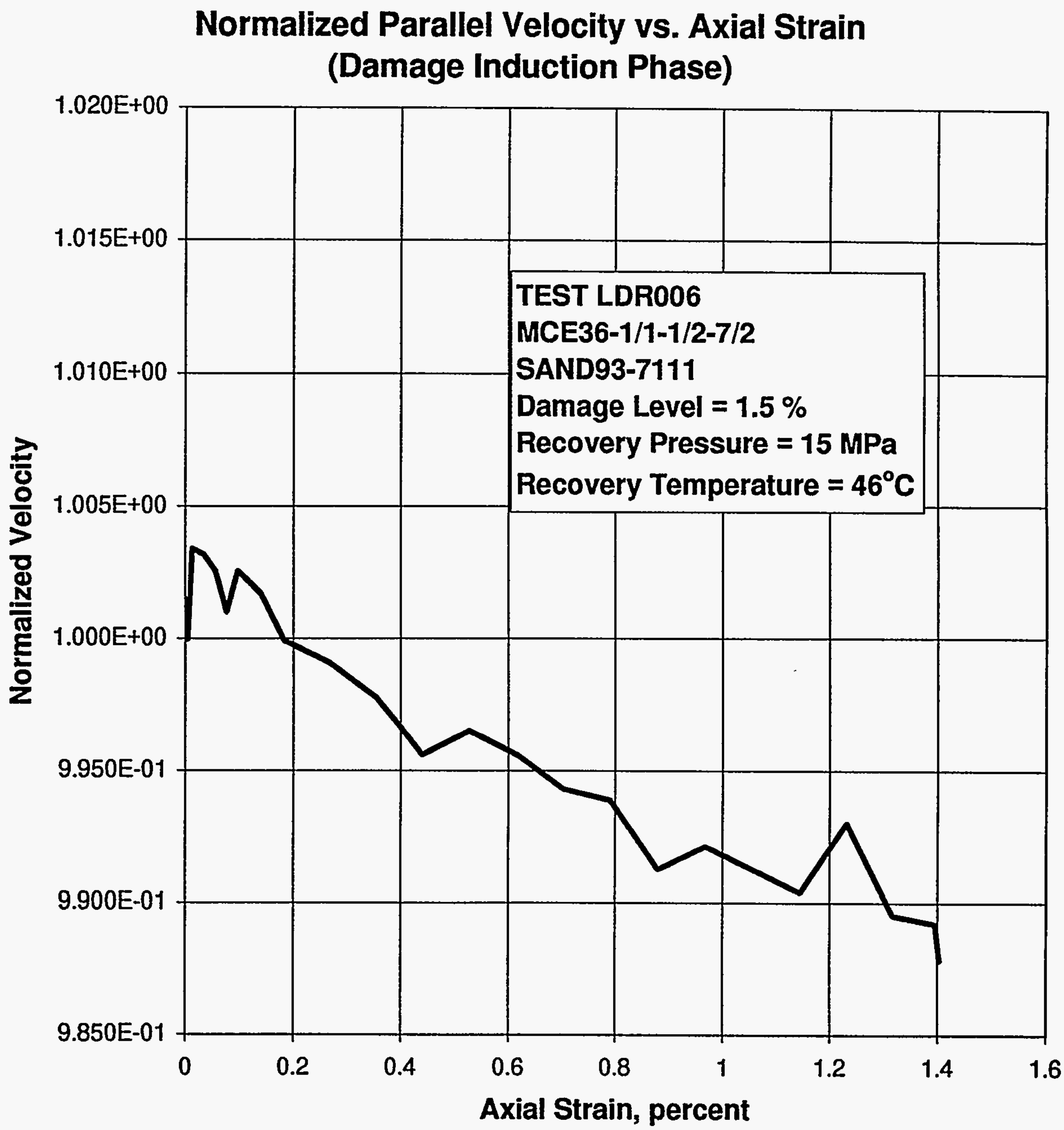

Figure E-34. Normalized Parallel Velocity as a Function of Axial Strain During the Quasi-Static Loading to Induce Damage in Specimen MCE36-1/1-1/2-7/2.

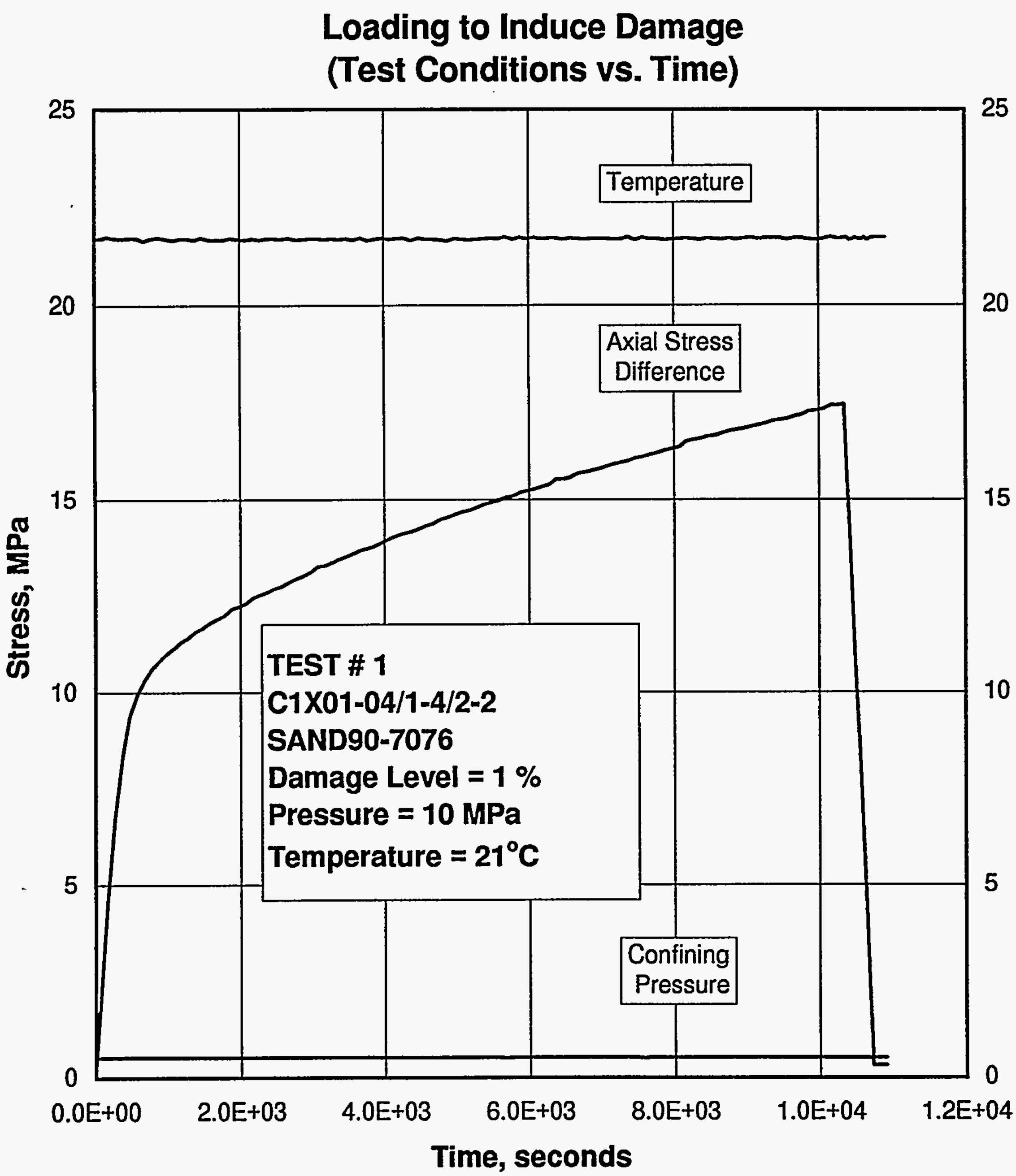

Figure E-35. Test Conditions as a Function of Time During the Quasi-Static Loading to Induce Damage in Specimen C1X01-04/1-4/2-2.

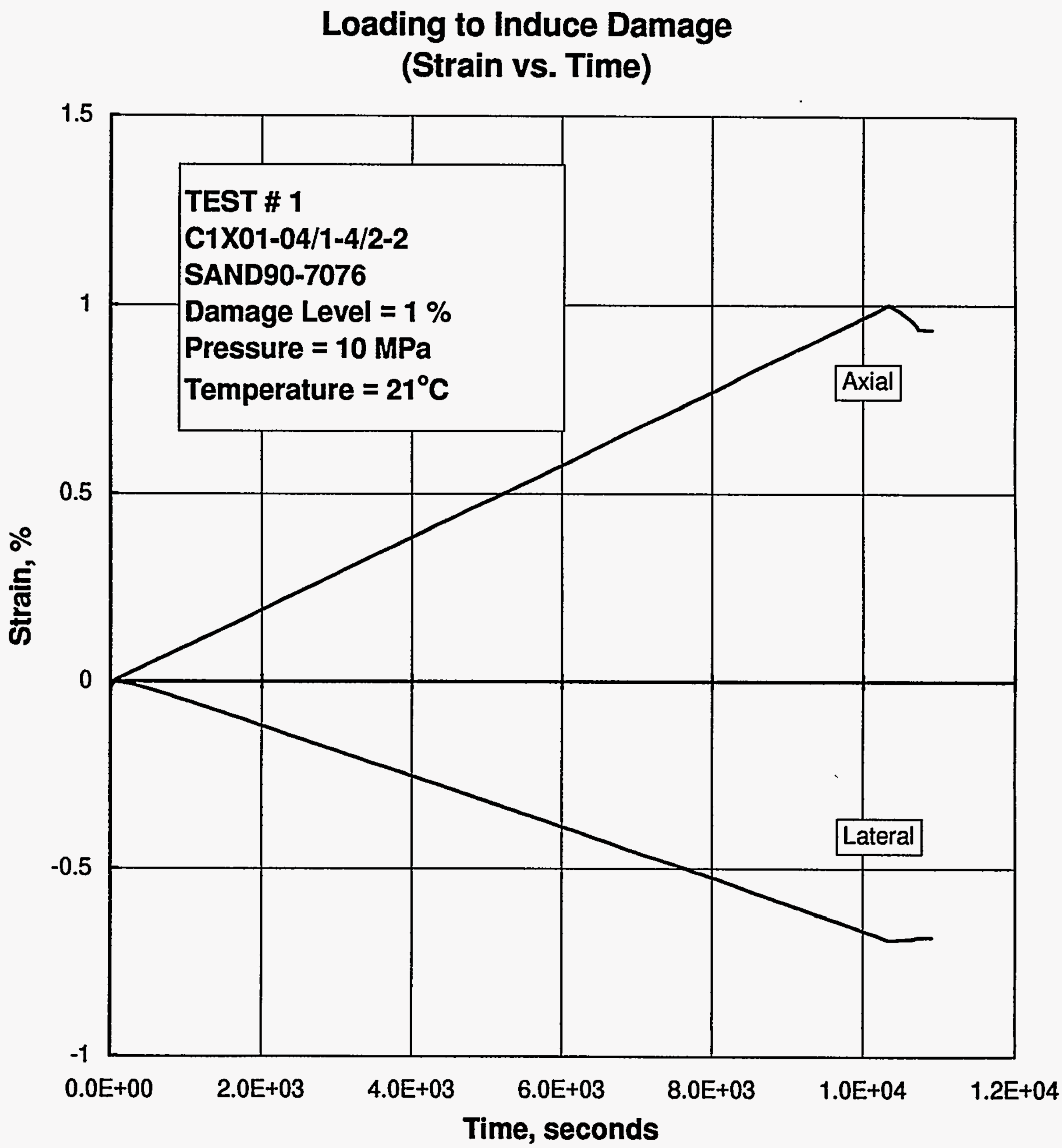

Figure E-36. Axial and Lateral Strain as a Function of Time During the Quasi-Static Loading to Induce Damage in Specimen C1X01-04/1-4/2-2.

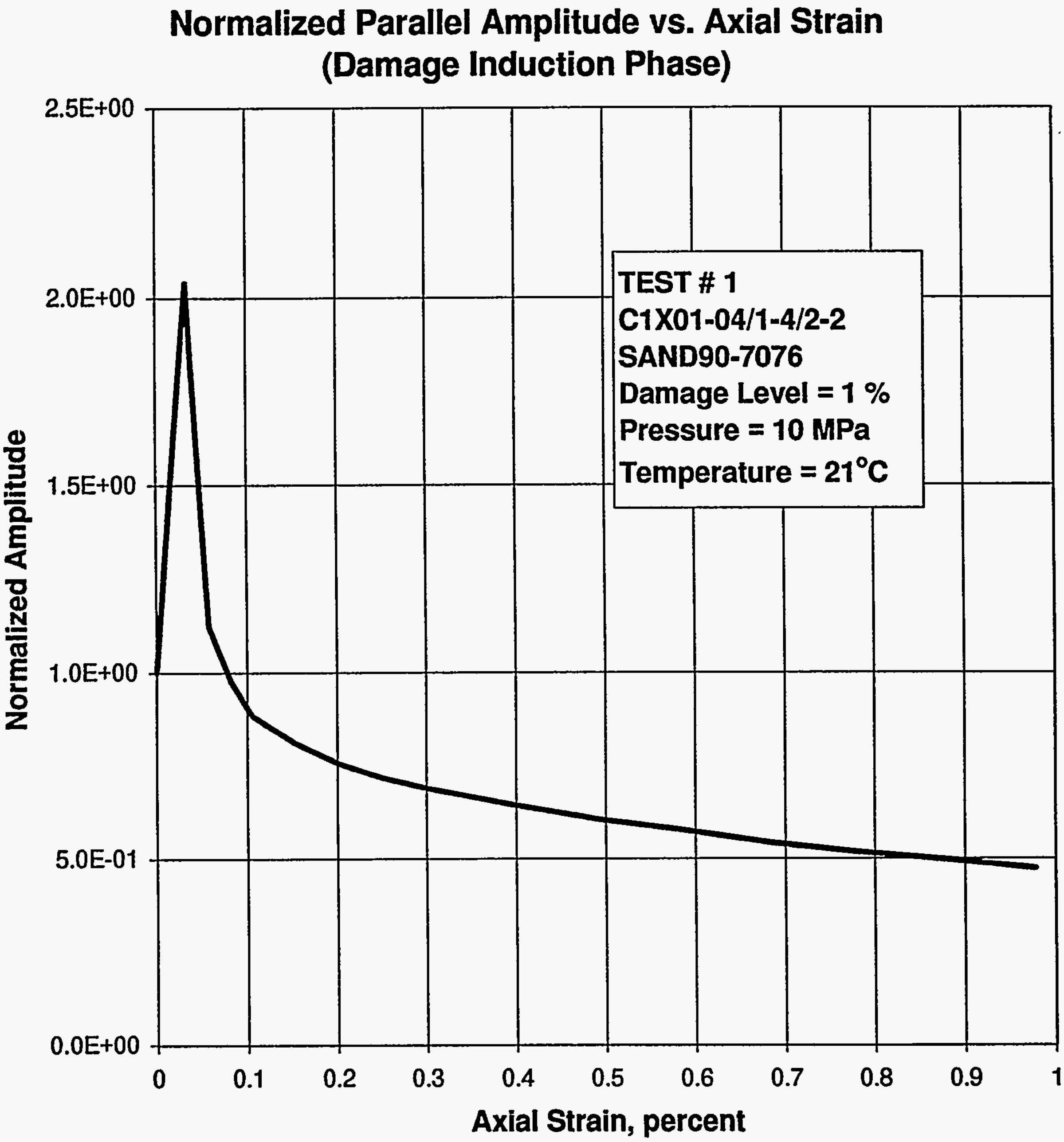

Figure E-37. Normalized Perpendicular Amplitude as a Function of Axial Strain During the Quasi-Static Loading to Induce Damage in Specimen C1X01-04/1-4/2-2.

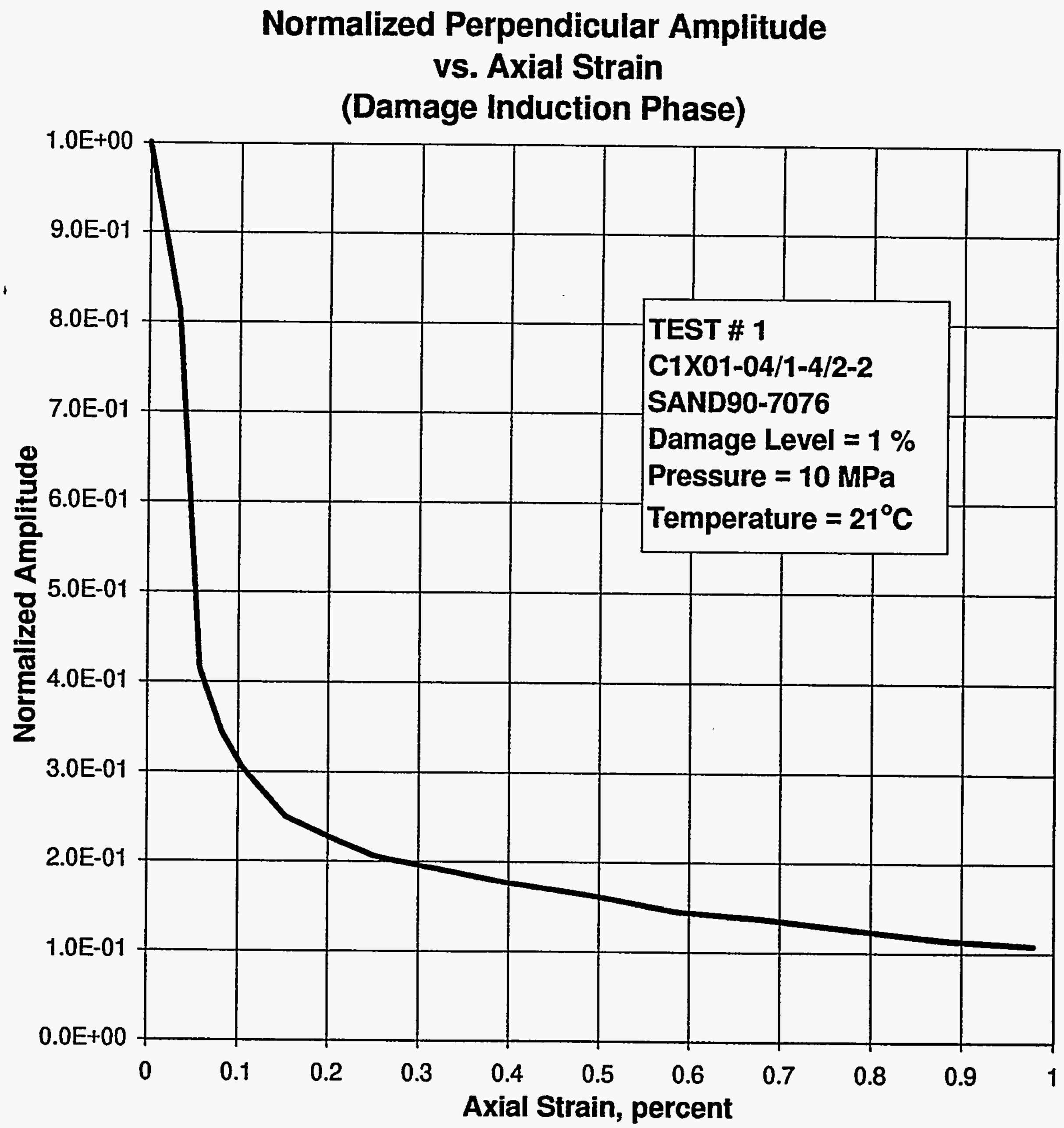

Figure E-38. Normalized Parallel Amplitude as a Function of Axial Strain During the Quasi-Static Loading to Induce Damage in Specimen C1X01-04/1-4/2-2.

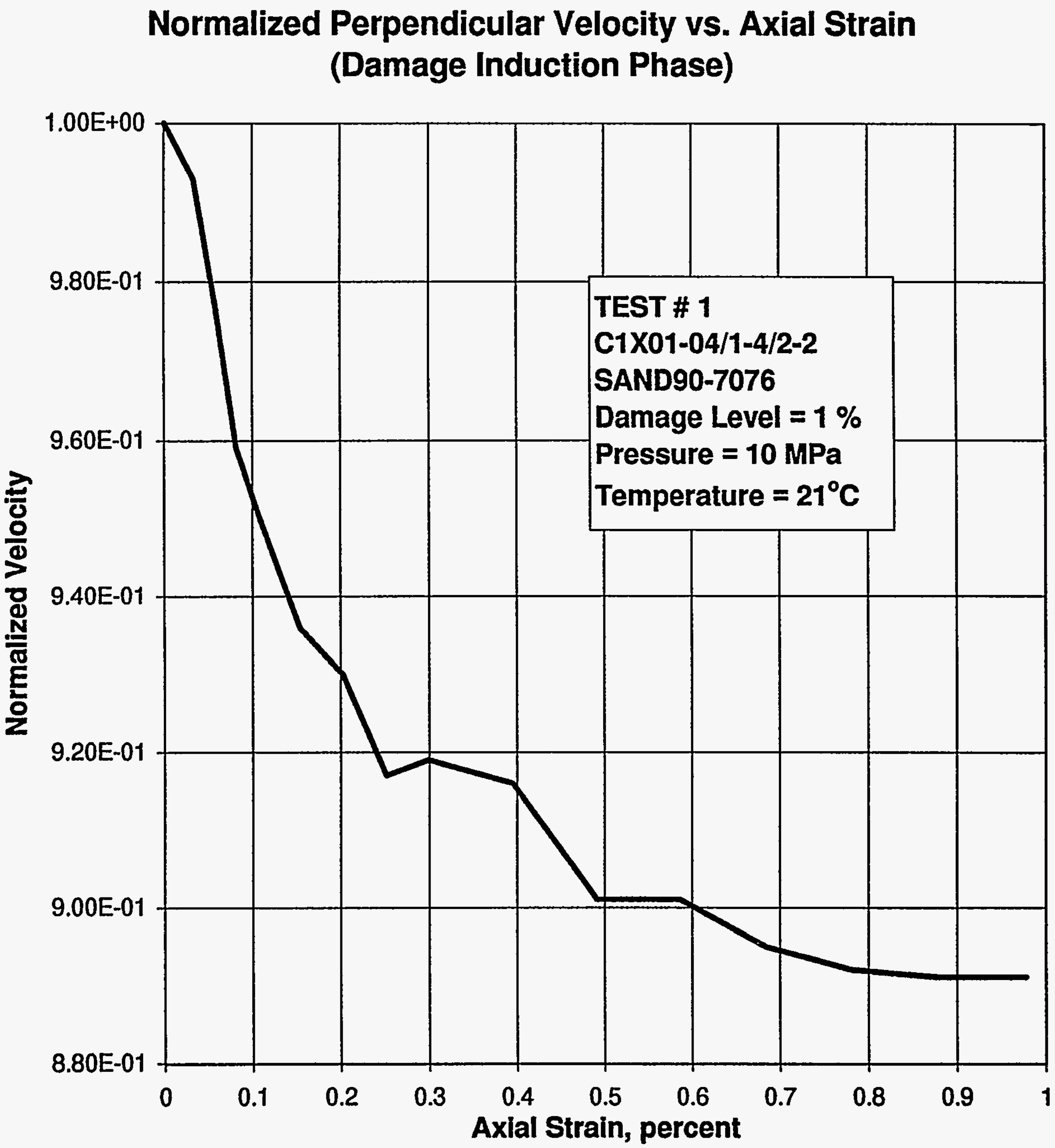

Figure E-39. Normalized Perpendicular Velocity as a Function of Axial Strain During the Quasi-Static Loading to Induce Damage in Specimen C1X01-04/1-4/2-2.

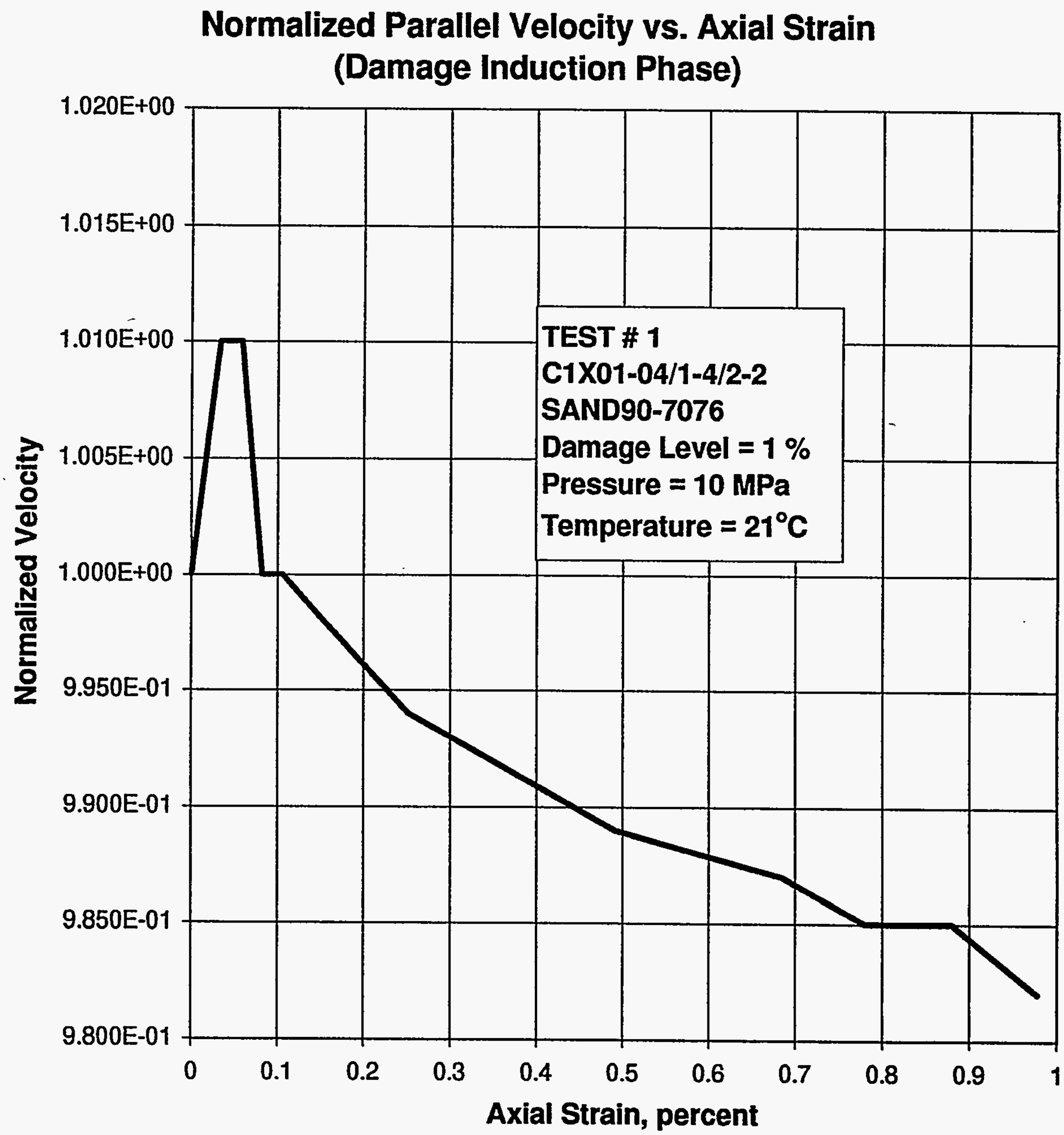

Figure E-40. Normalized Parallel Velocity as a Function of Axial Strain During the Quasi-Static Loading to Induce Damage in Specimen C1X01-04/1-4/2-2.

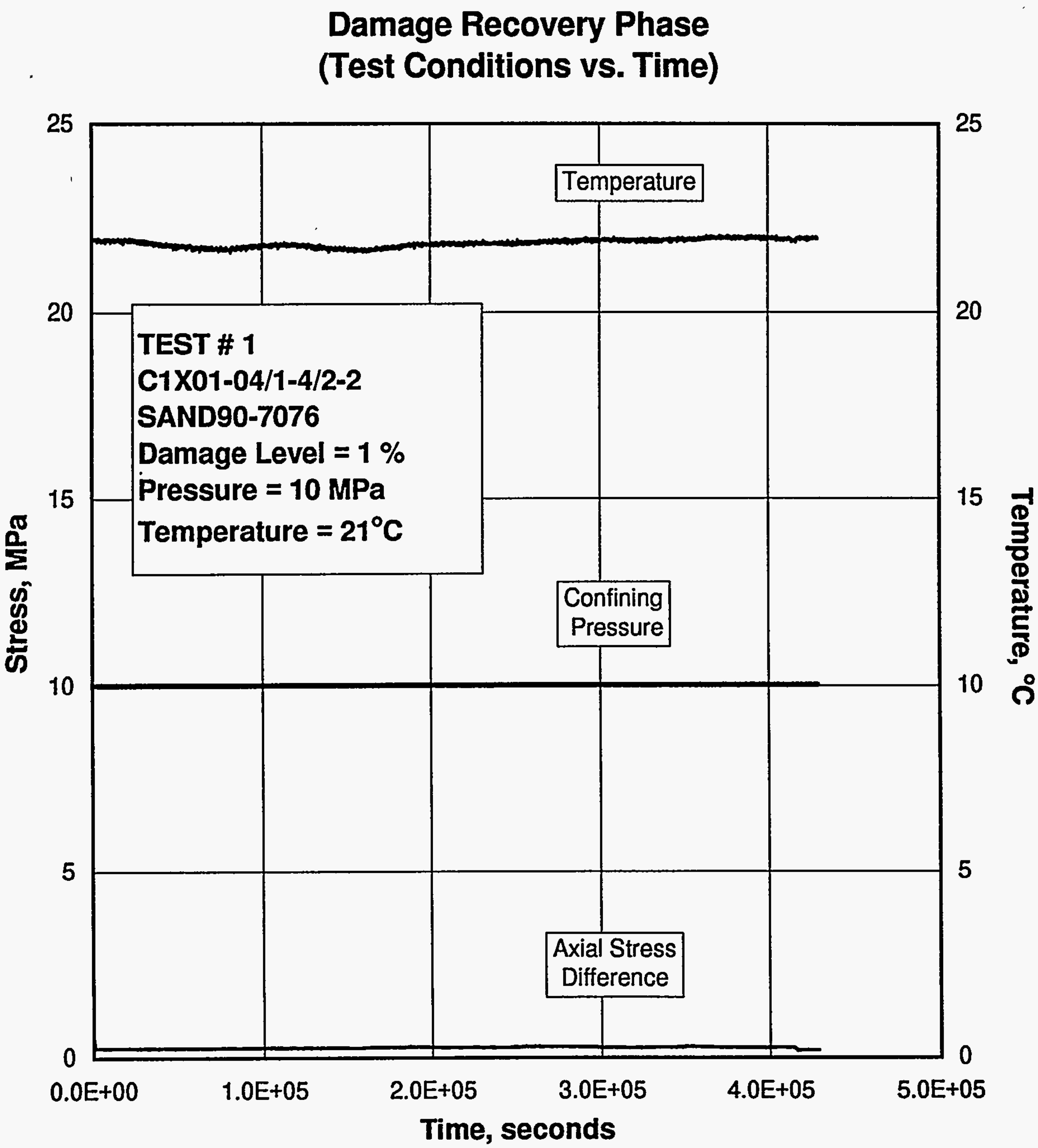

Figure E-41. Test Conditions as a Function of Time During the Hydrostatic Loading to Recover Damage in Specimen C1X01-04/1-4/2-2.

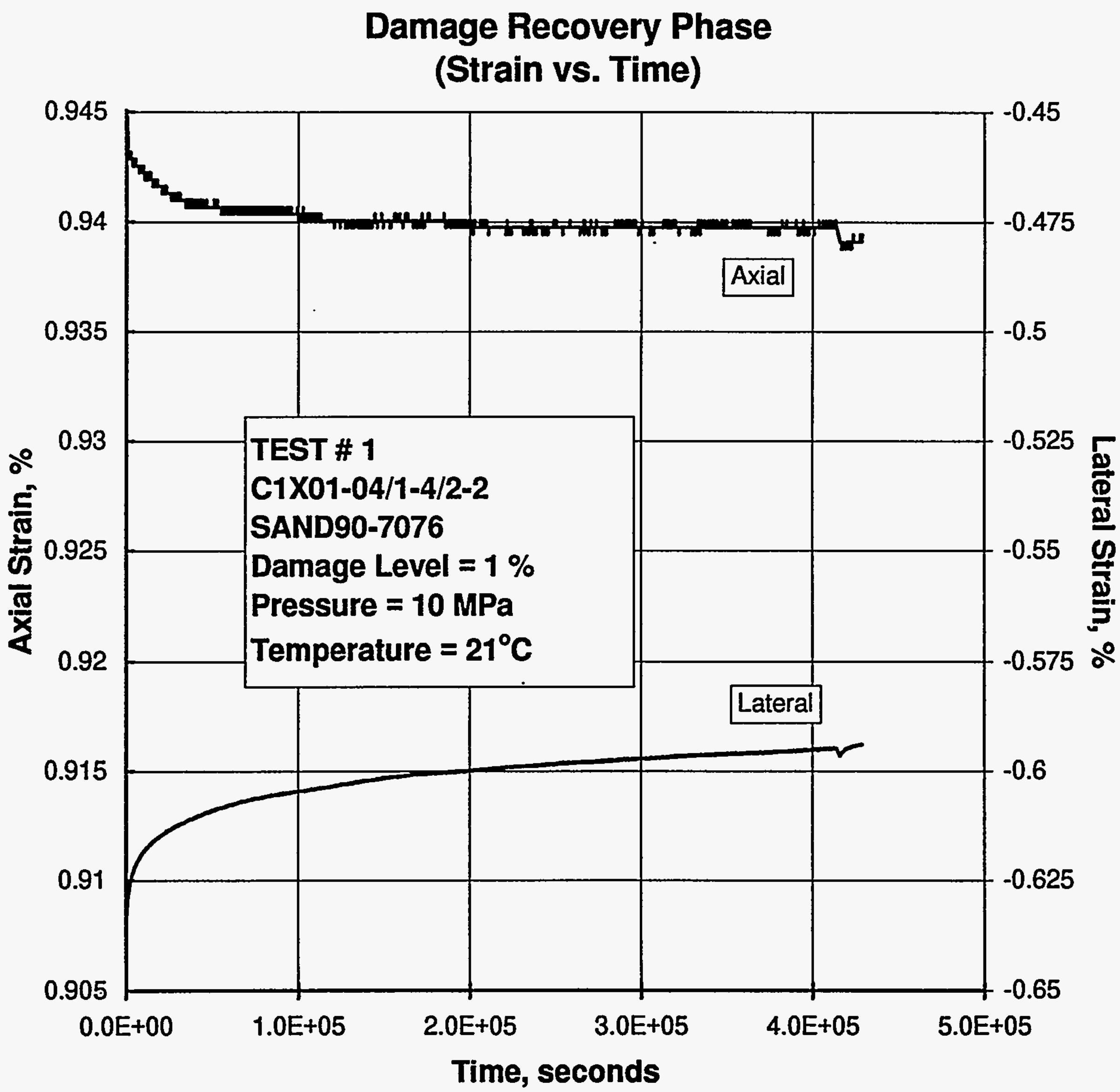

Figure E-42. Axial and Lateral Strain as a Function of Time During the Hydrostatic Loading to Recover Damage in Specimen C1X01-04/1-4/2-2.

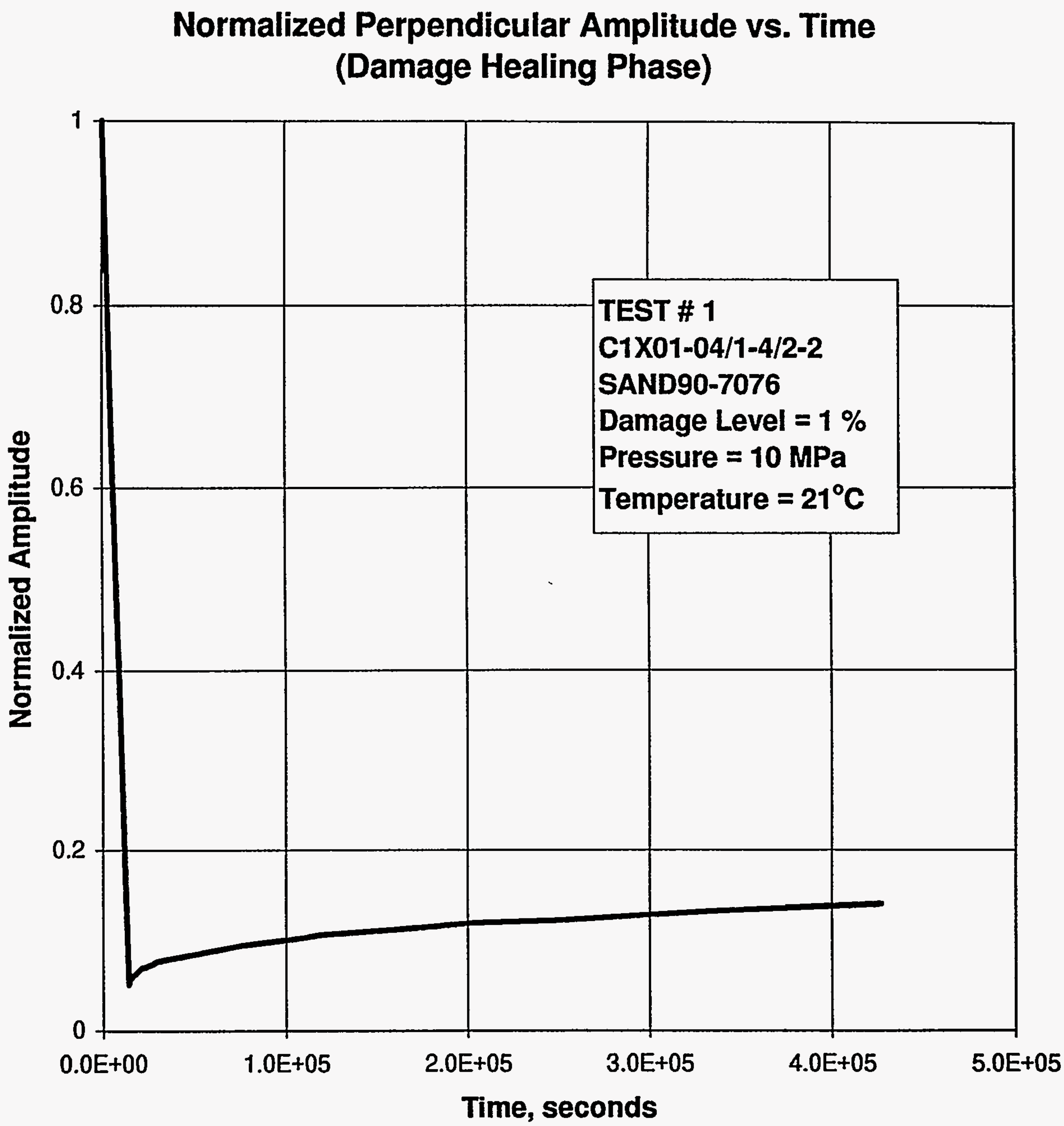

Figure E-43. Normalized Perpendicular Amplitude as a Function of Time During the Hydrostatic Loading to Recover Damage in Specimen C1X01-04/1-4/2-2.

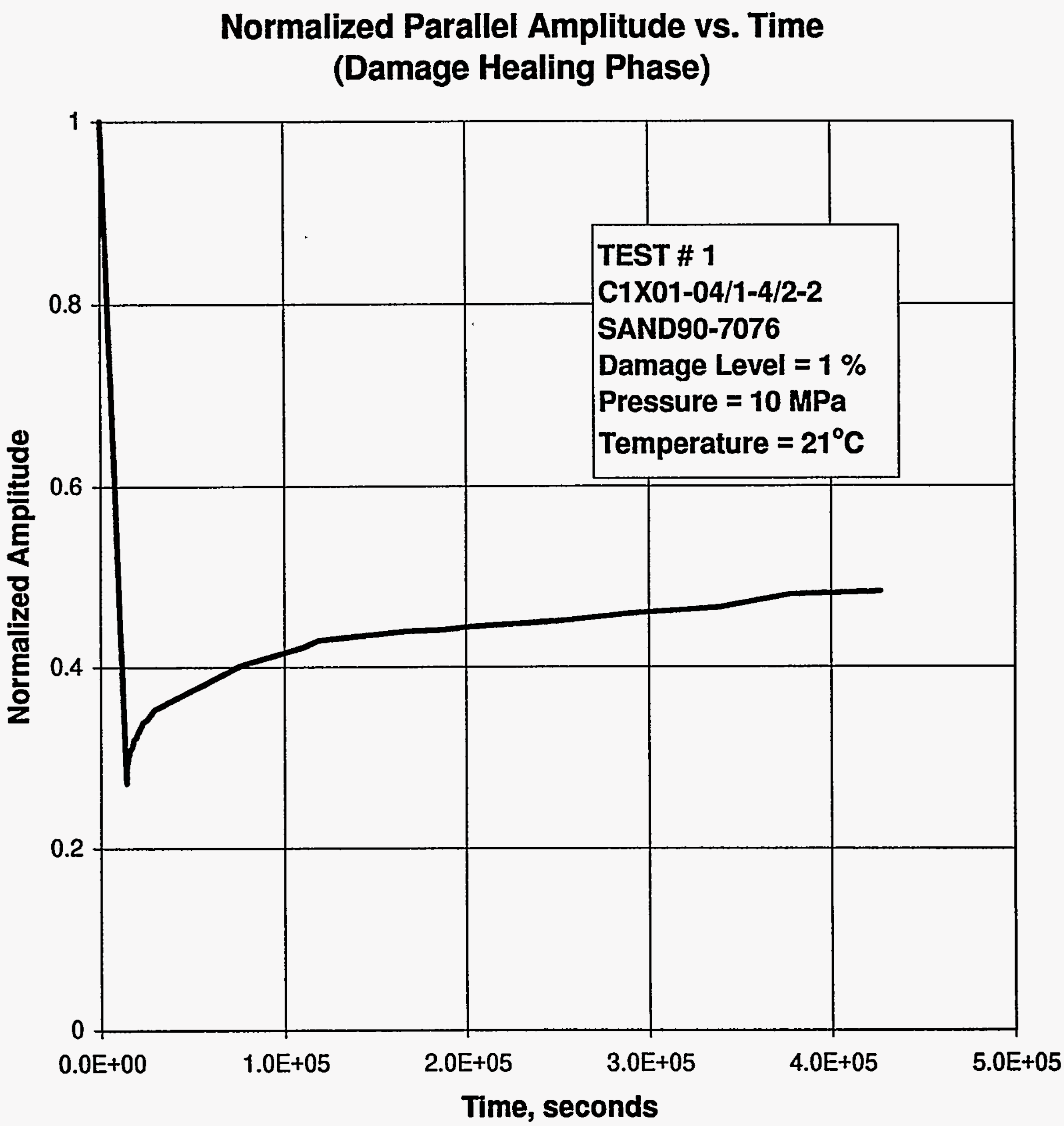

Figure E-44. Normalized Parallel Amplitude as a Function of Time During the Hydrostatic Loading to Recover Damage in Specimen C1X01-04/1-4/2-2.

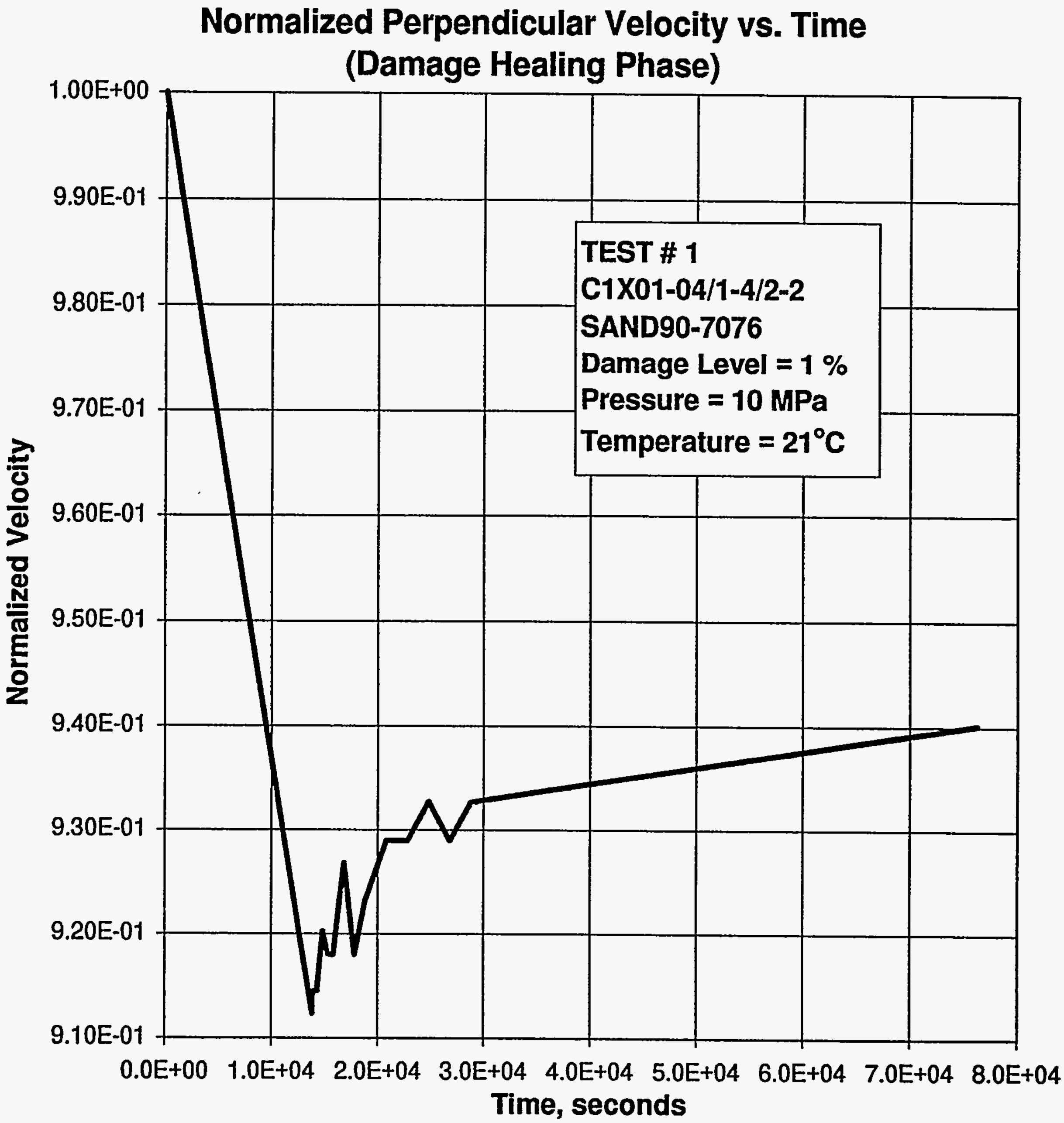

Figure E-45. Normalized Perpendicular Velocity as a Function of Time During the Hydrostatic Loading to Recover Damage in Specimen C1X01-04/1-4/2-2.

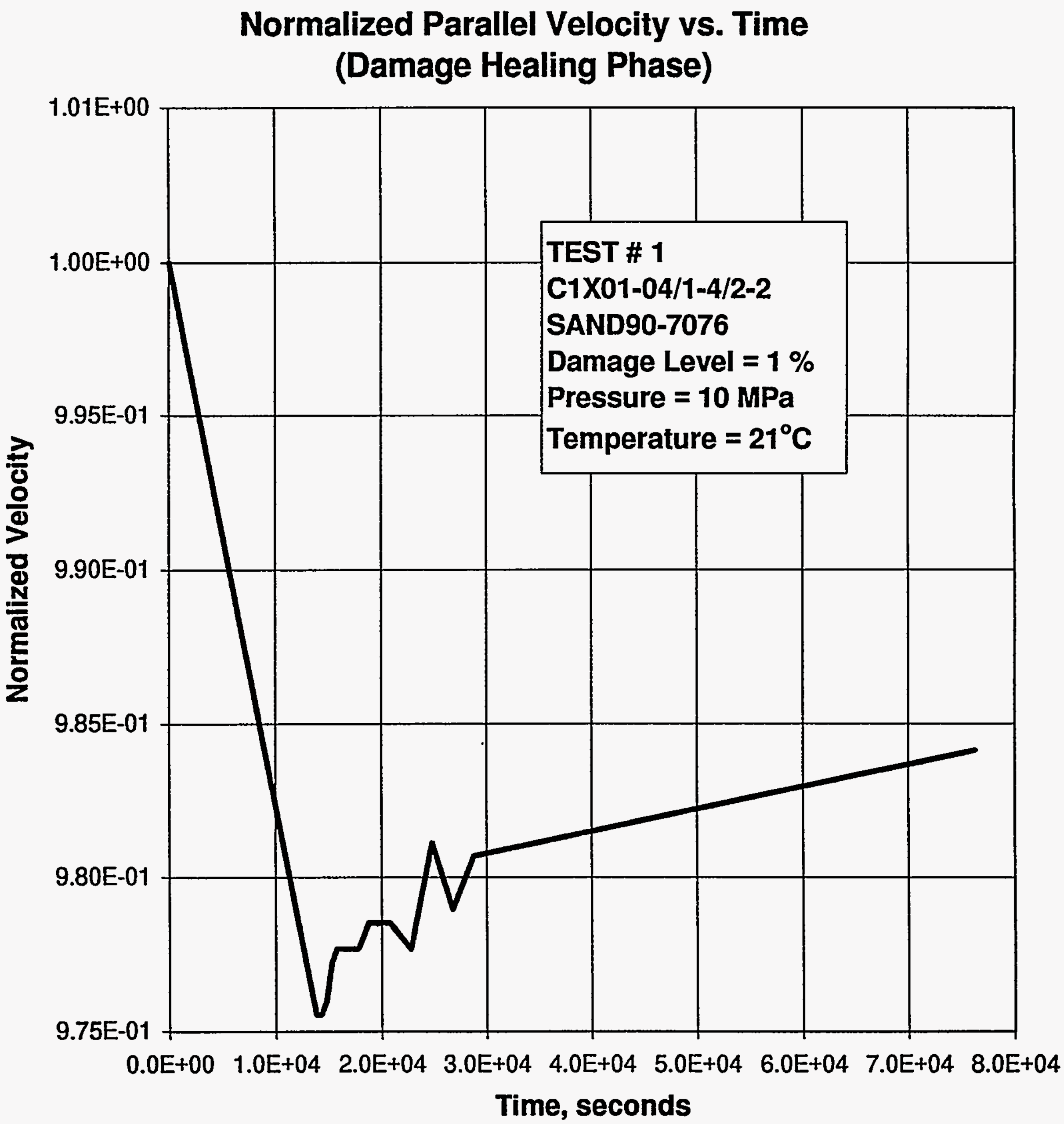

Figure E-46. Normalized Parallel Velocity as a Function of Time During the Hydrostatic Loading to Recover Damage in Specimen C1X01-04/1-4/2-2.

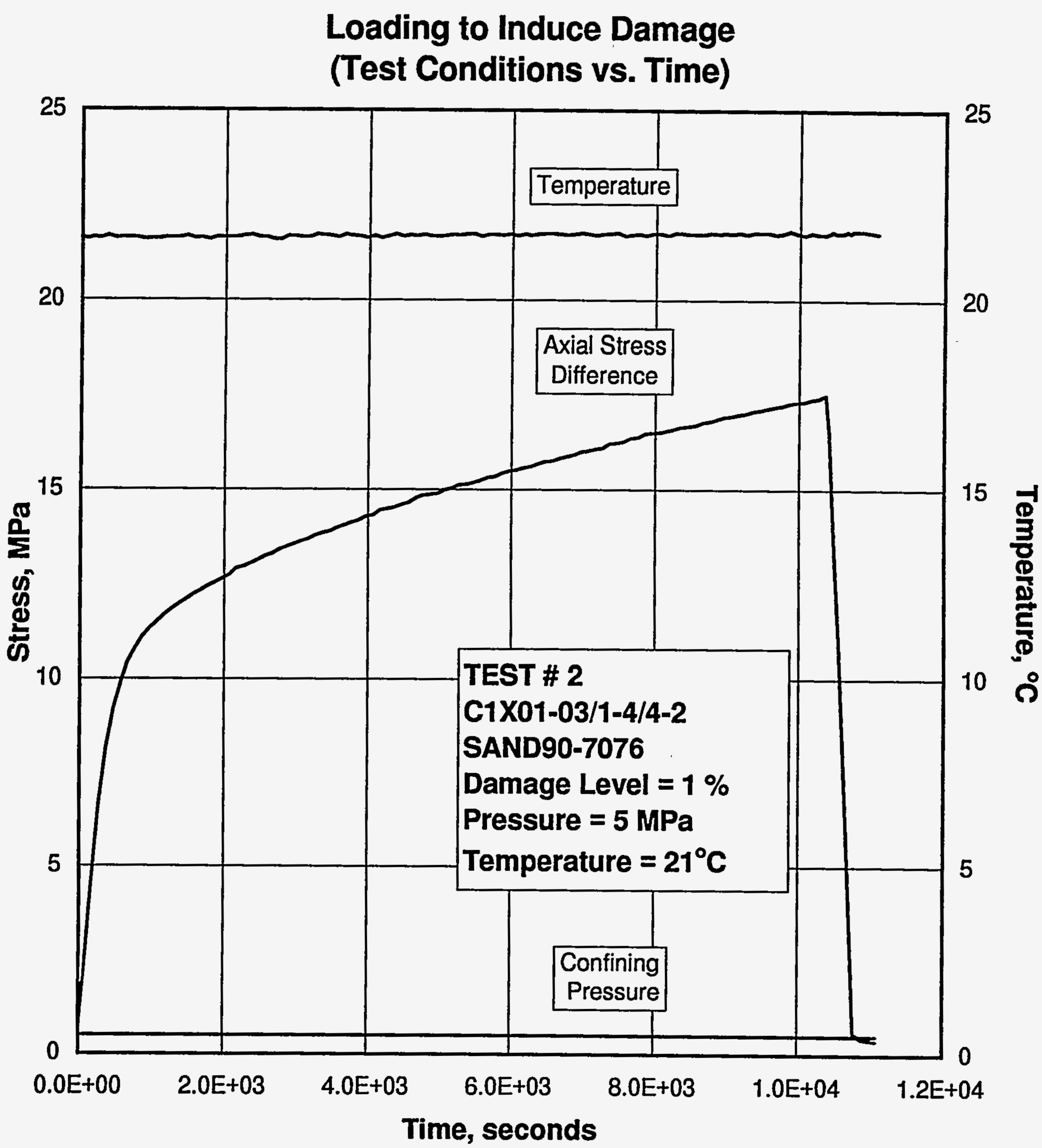

Figure E-47. Test Conditions as a Function of Time During the Quasi-Static Loading to Induce Damage in Specimen C1X01-03/1-4/4-2.

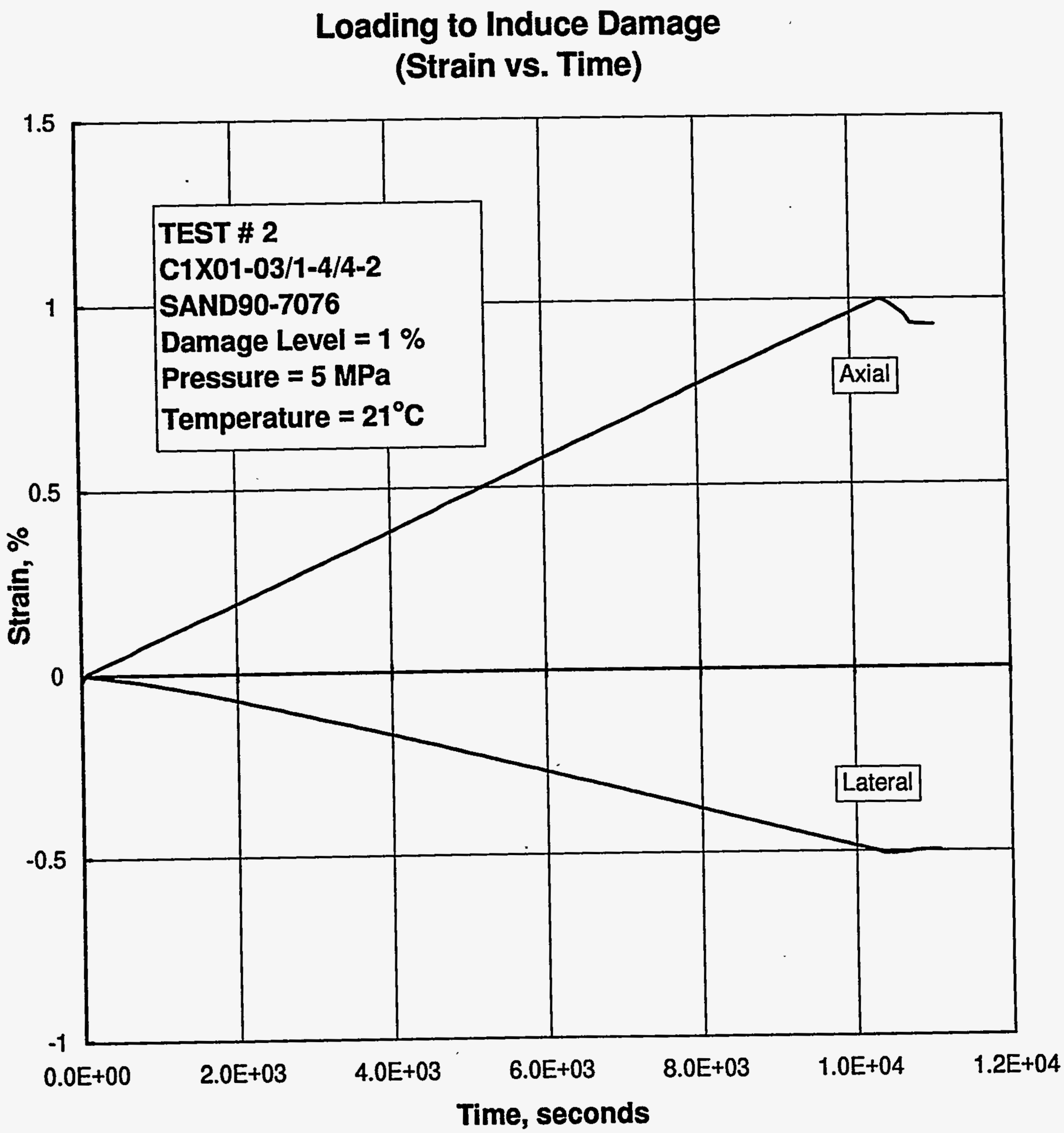

Figure E-48. Axial and Lateral Strain as a Function of Time During the Quasi-Static Loading to Induce Damage in Specimen C1X01-03/1-4/4-2.

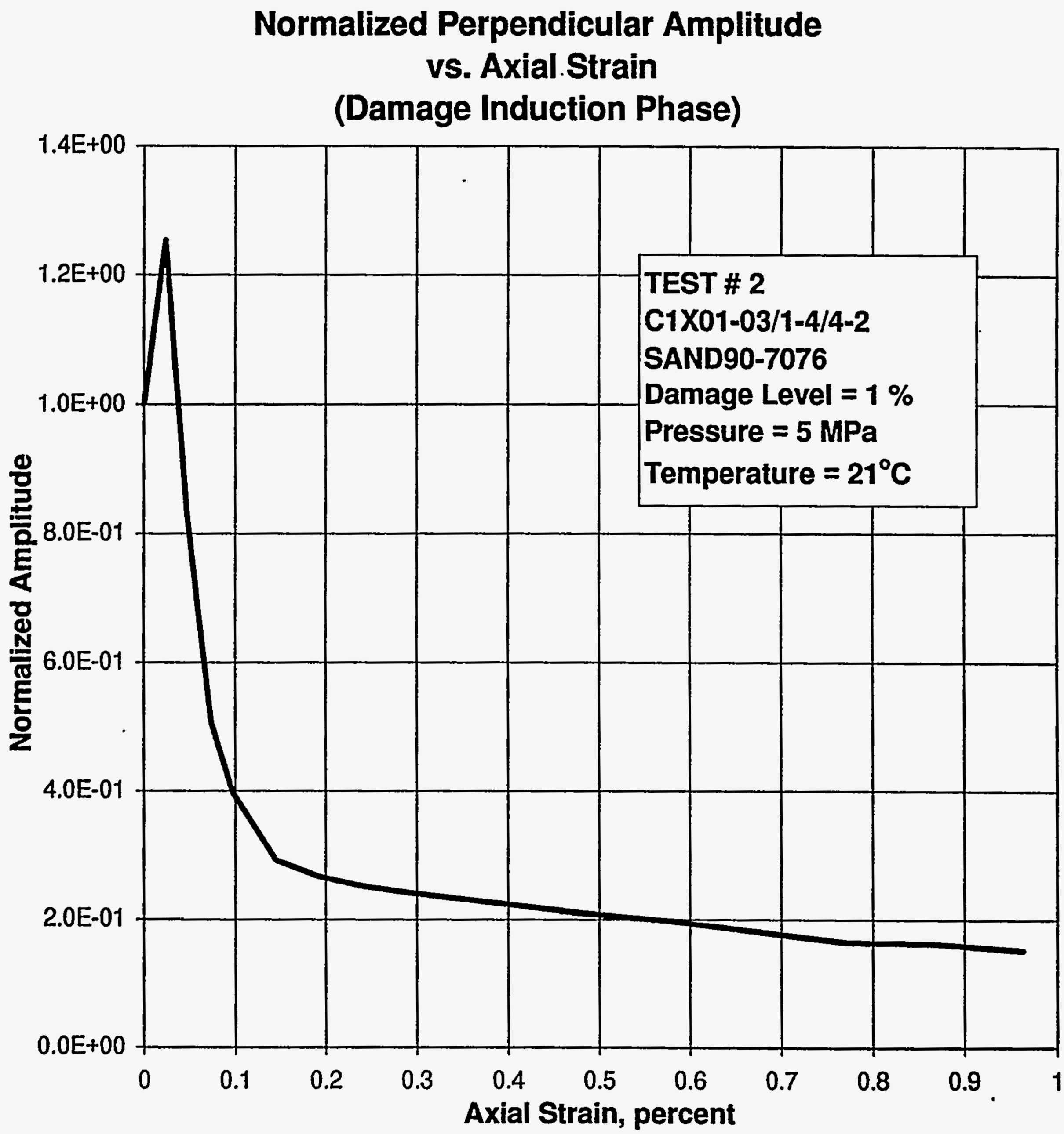

Figure E-49. Normalized Perpendicular Amplitude as a Function of Axial Strain During the Quasi-Static Loading to Induce Damage in Specimen C1X01-03/1-4/4-2.

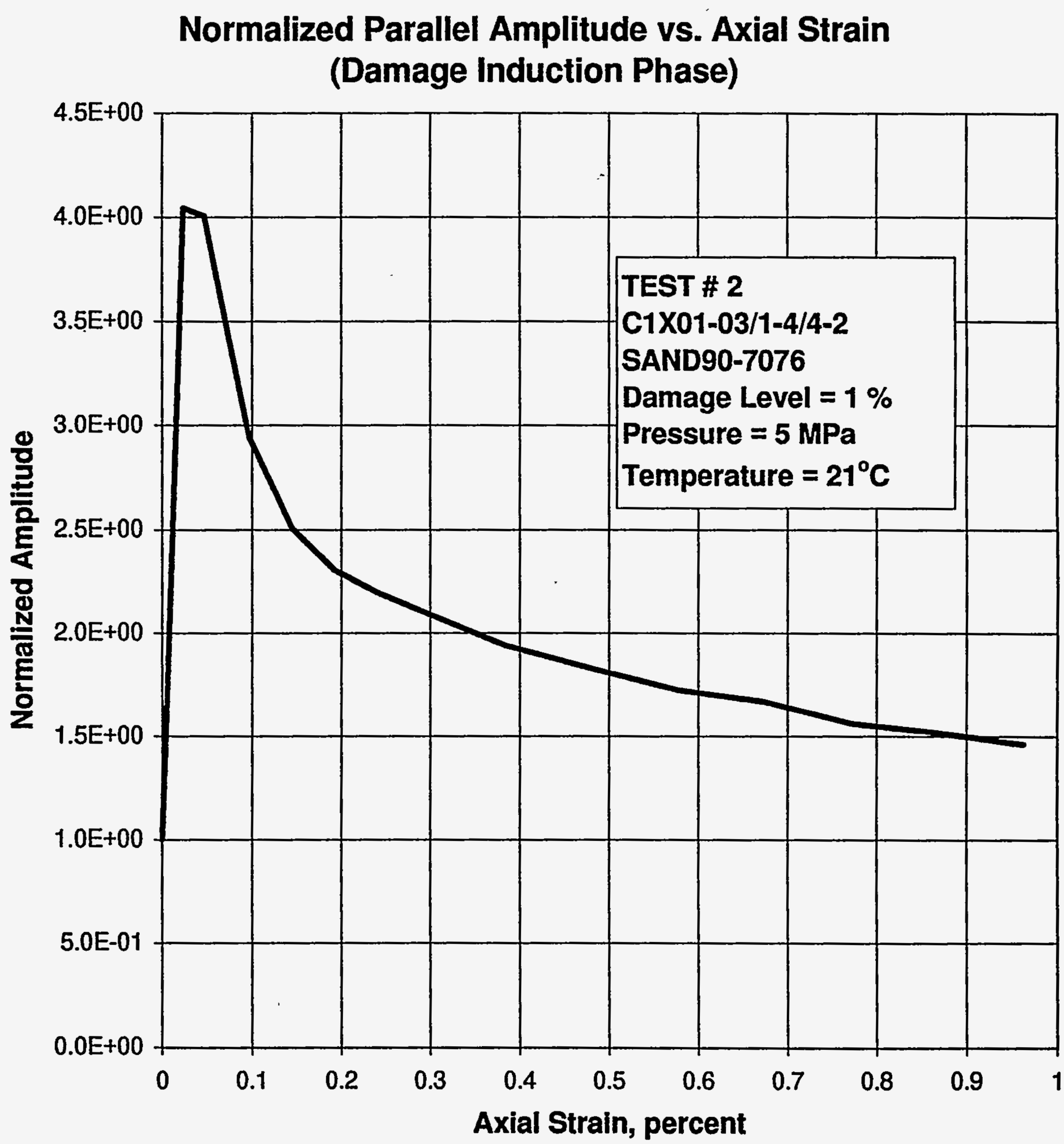

Figure E-50. Normalized Parallel Amplitude as a Function of Axial Strain During the Quasi-Static Loading to Induce Damage in Specimen C1X01-03/1-4/4-2.

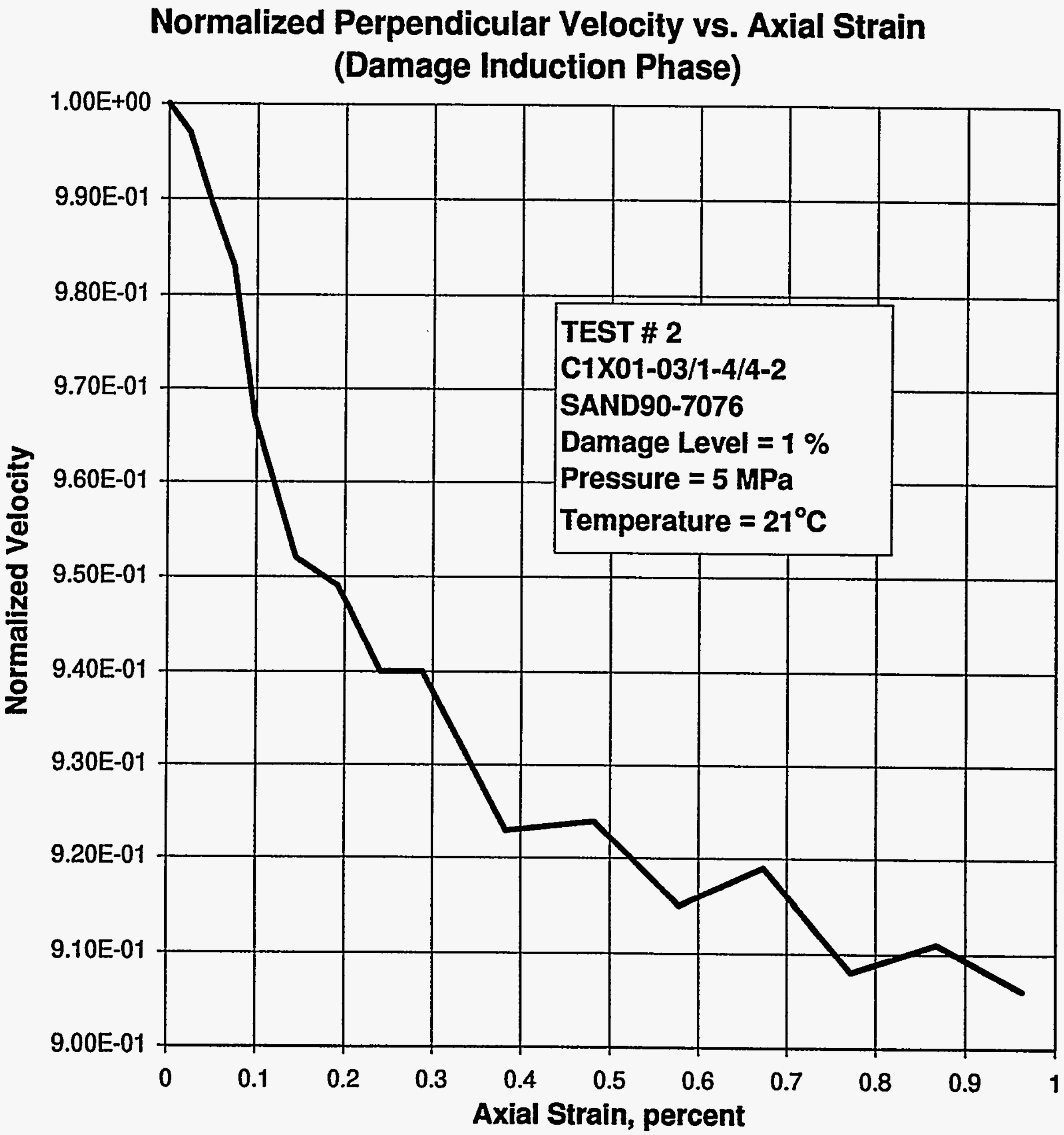

Figure E-51. Normalized Perpendicular Velocity as a Function of Axial Strain During the Quasi-Static Loading to Induce Damage in Specimen C1X01-03/1-4/4-2.

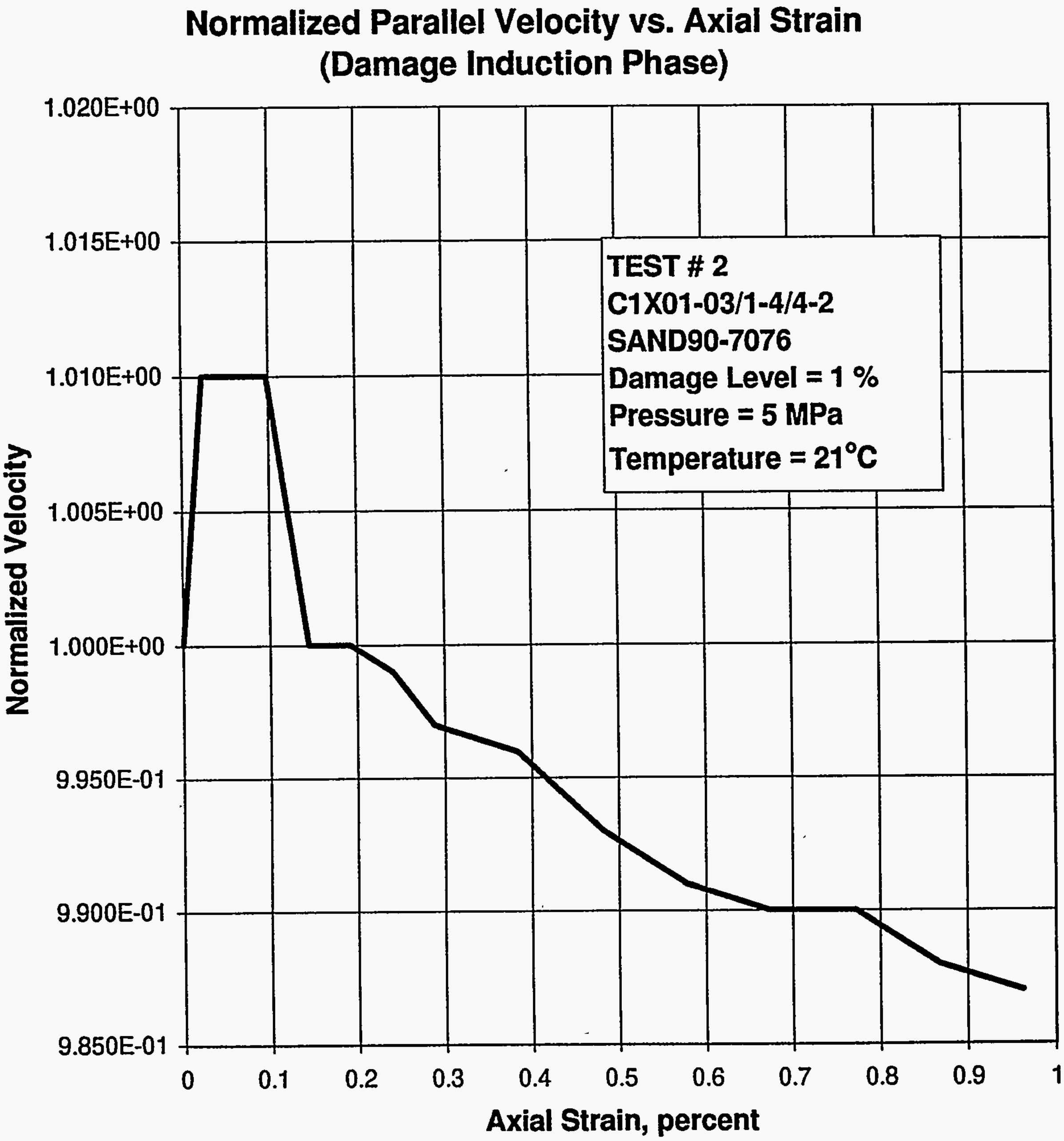

Figure E-52. Normalized Parallel Velocity as a Function of Axial Strain During the Quasi-Static Loading to Induce Damage in Specimen C1X01-03/1-4/4-2.

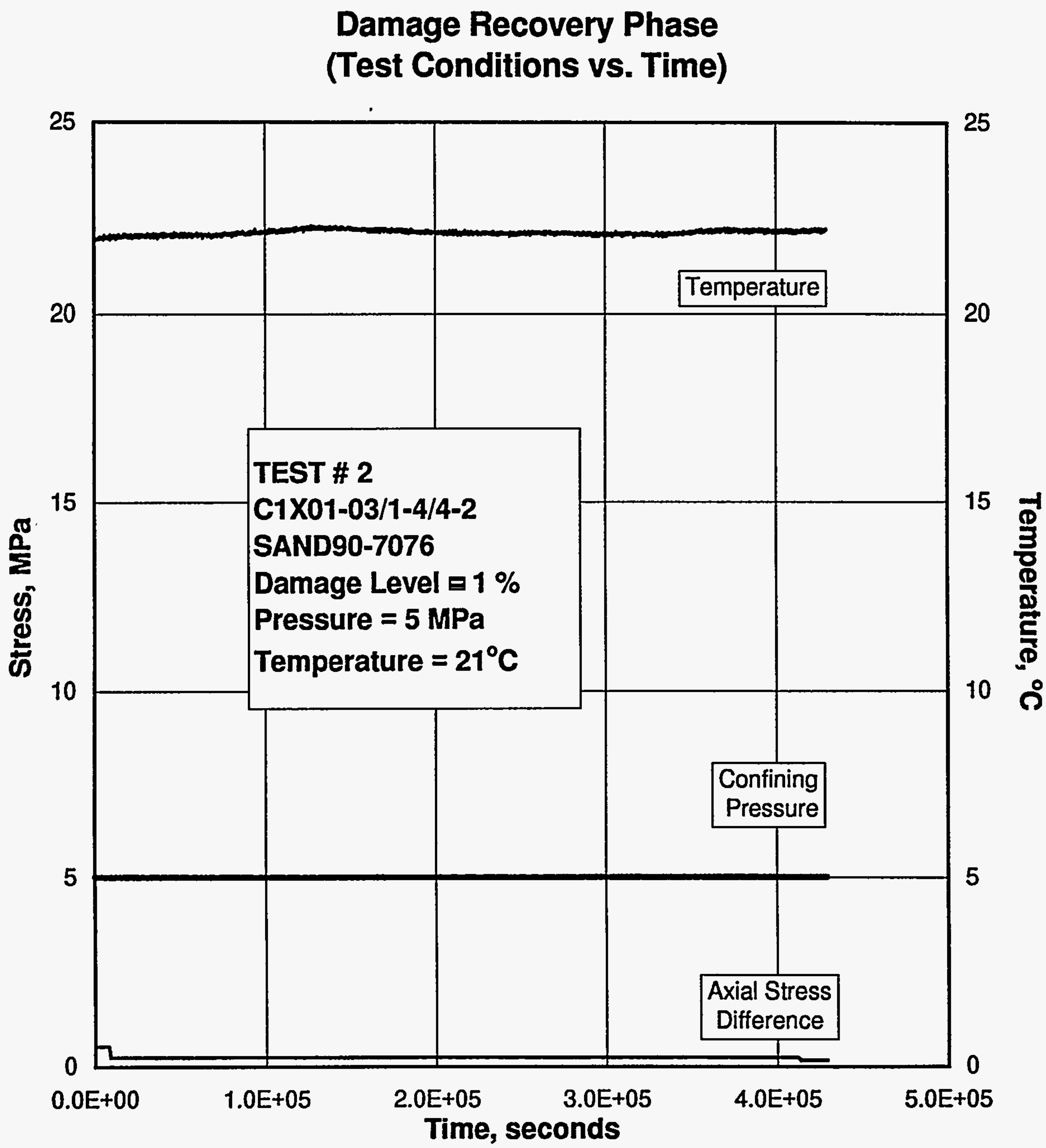

Figure E-53. Test Conditions as a Function of Time During the Hydrostatic Loading to Recover Damage in Specimen C1X01-03/1-4/4-2.

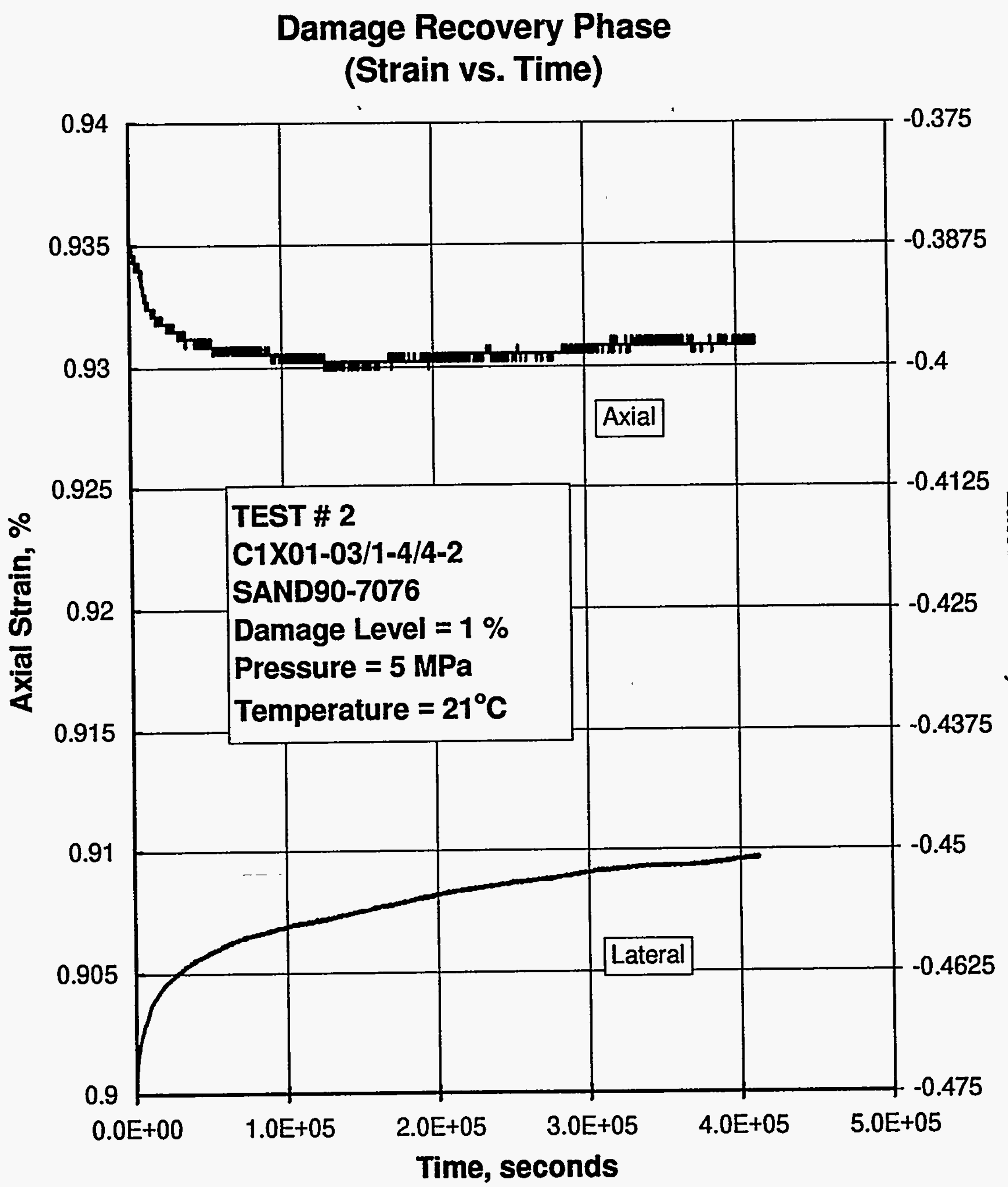

Figure E-54. Axial and Lateral Strain as a Function of Time During the Hydrostatic Loading to Recover Damage in Specimen C1X01-03/1-4/4-2.

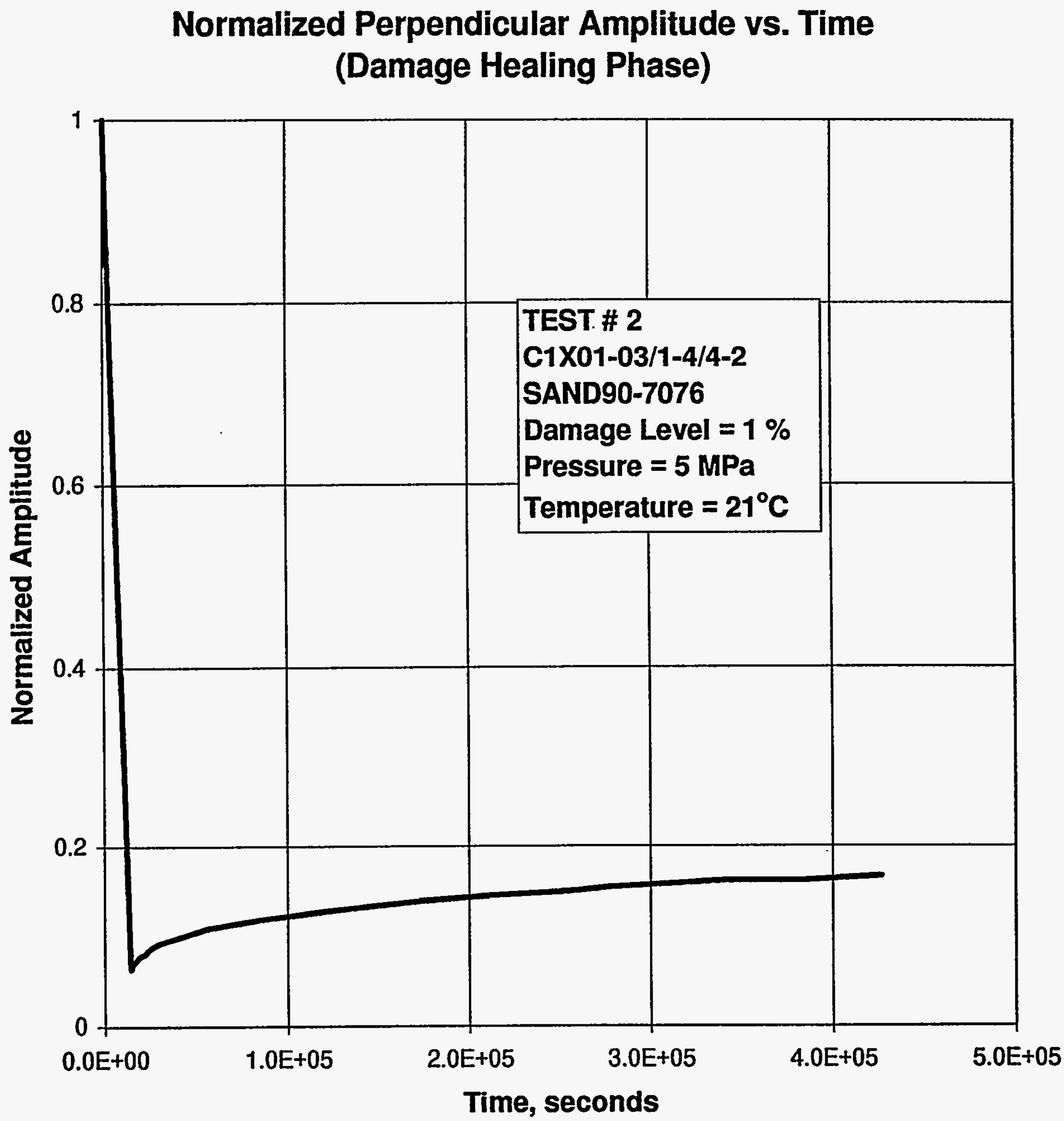

Figure E-55. Normalized Perpendicular Amplitude as a Function of Time During the Hydrostatic Loading to Recover Damage in Specimen C1X01-03/1-4/4-2.

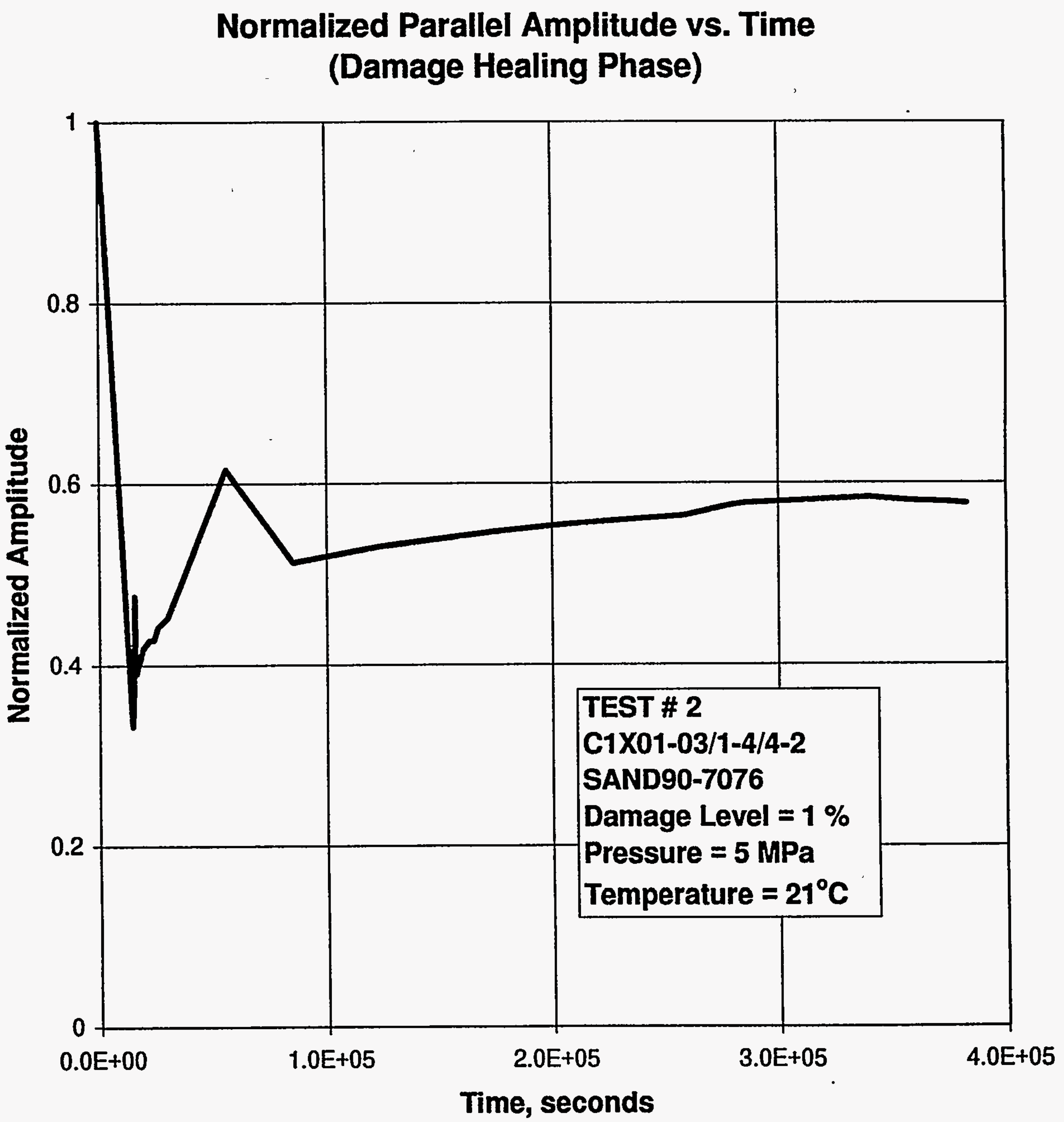

Figure E-56. Normalized Parallel Amplitude as a Function of Time During the Hydrostatic Loading to Recover Damage in Specimen C1X01-03/1-4/4-2.

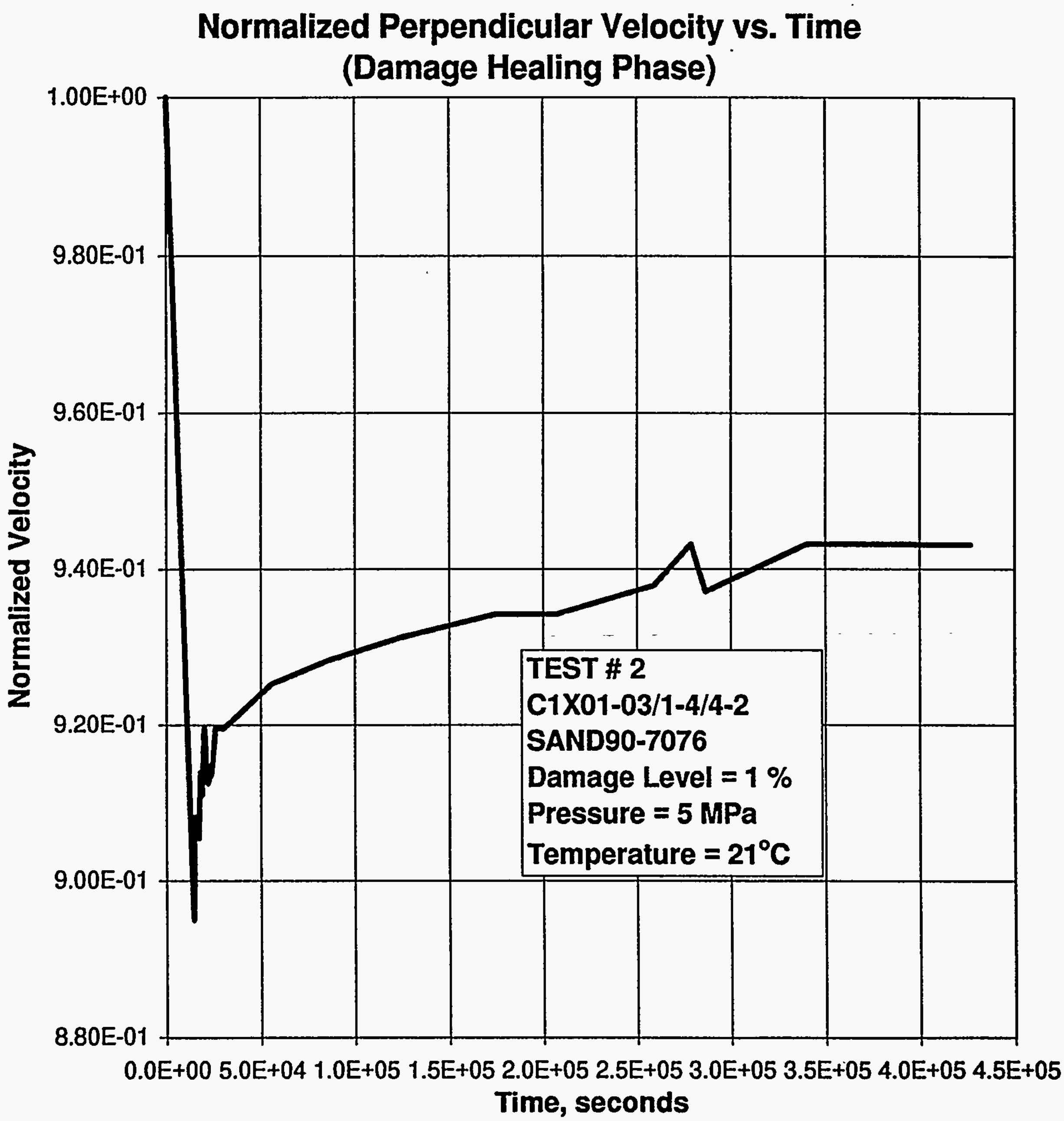

Figure E-57. Normalized Perpendicular Velocity as a Function of Time During the Hydrostatic Loading to Recover Damage in Specimen C1X01-03/1-4/4-2.

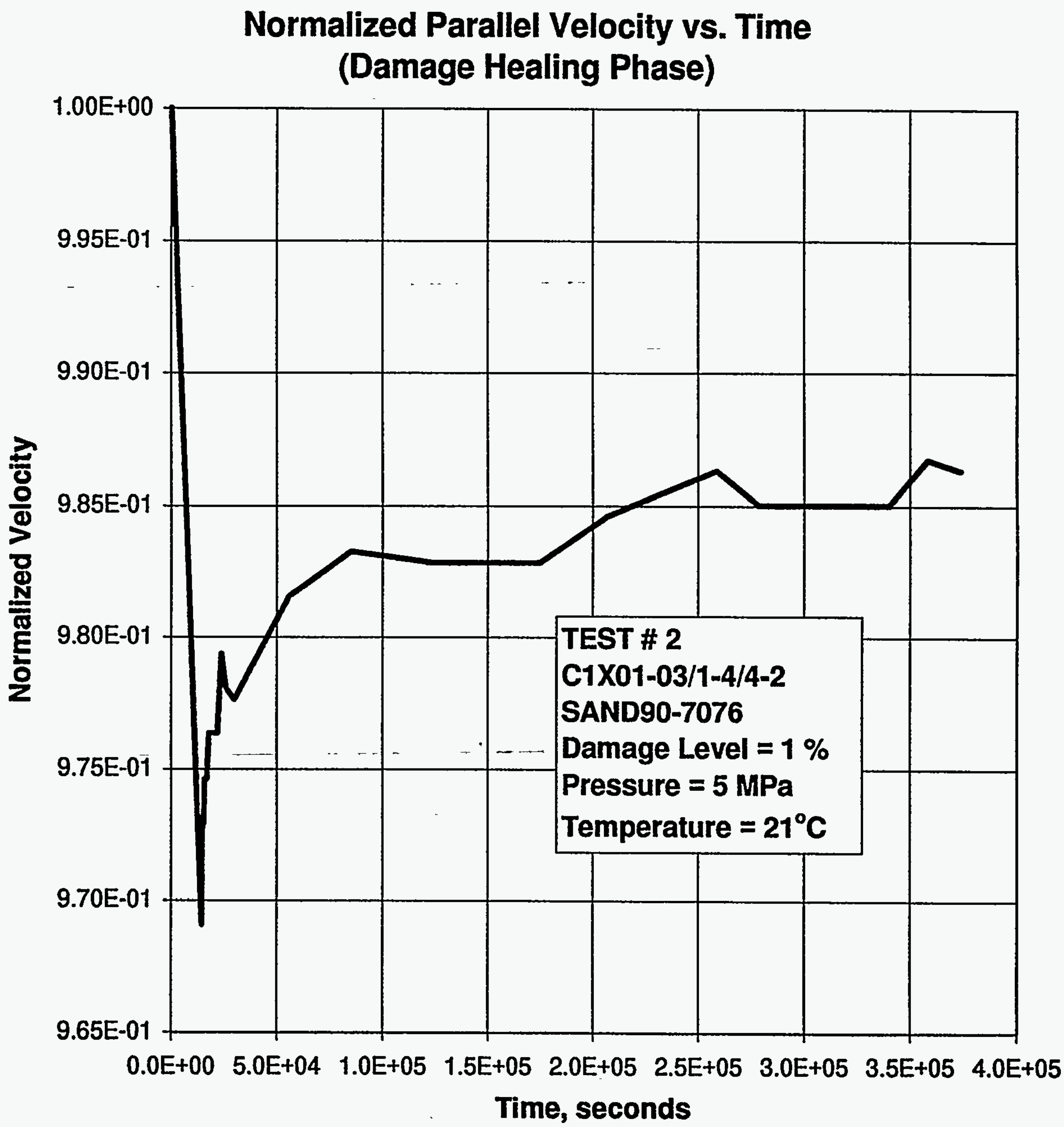

Figure E-58. Normalized Parallel Velocity as a Function of Time During the Hydrostatic Loading to Recover Damage in Specimen C1X01-03/1-4/4-2.

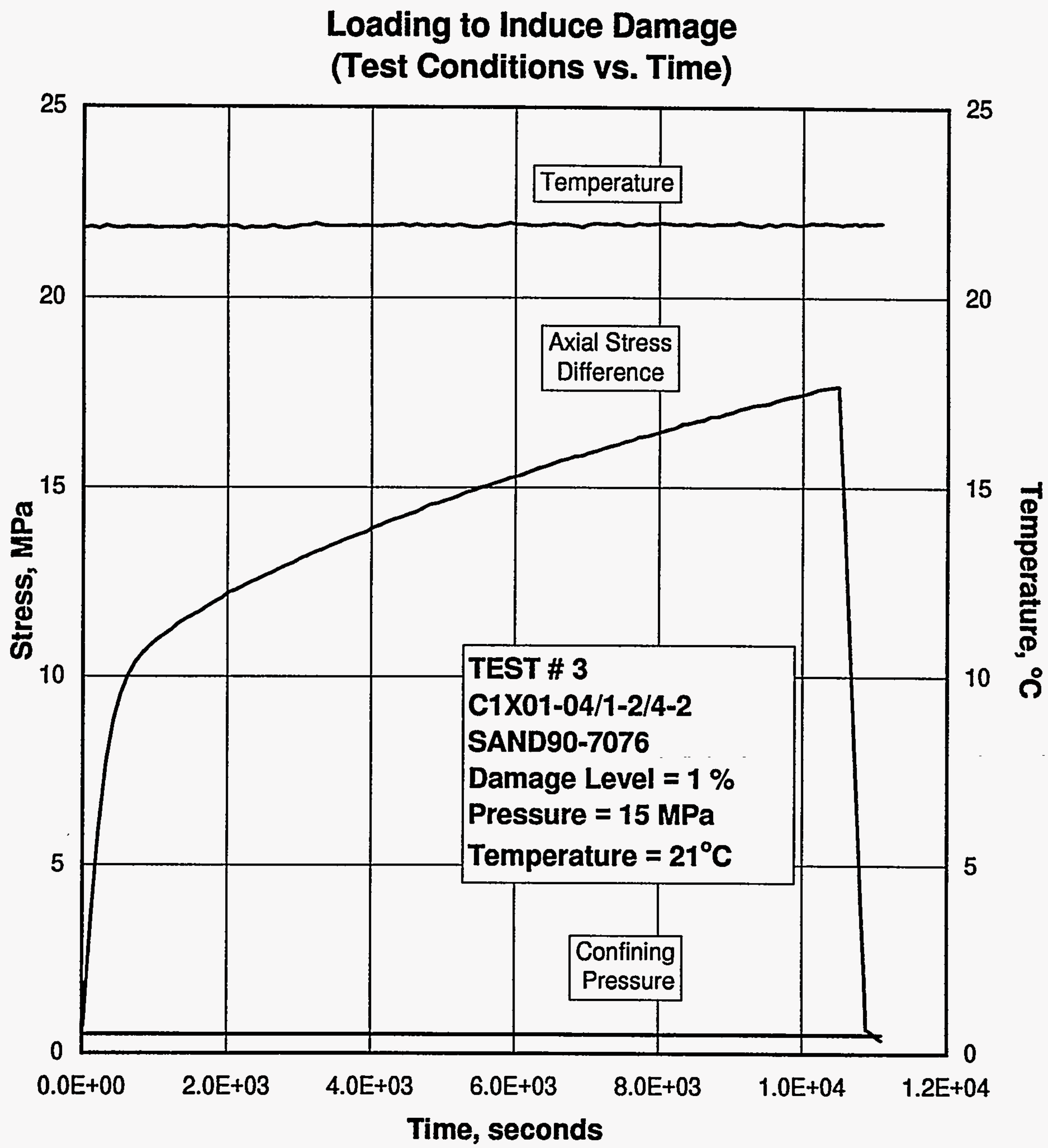

Figure E-59. Test Conditions as a Function of Time During the Quasi-Static Loading to Induce Damage in Specimen C1X01-04/1-2/4-2.

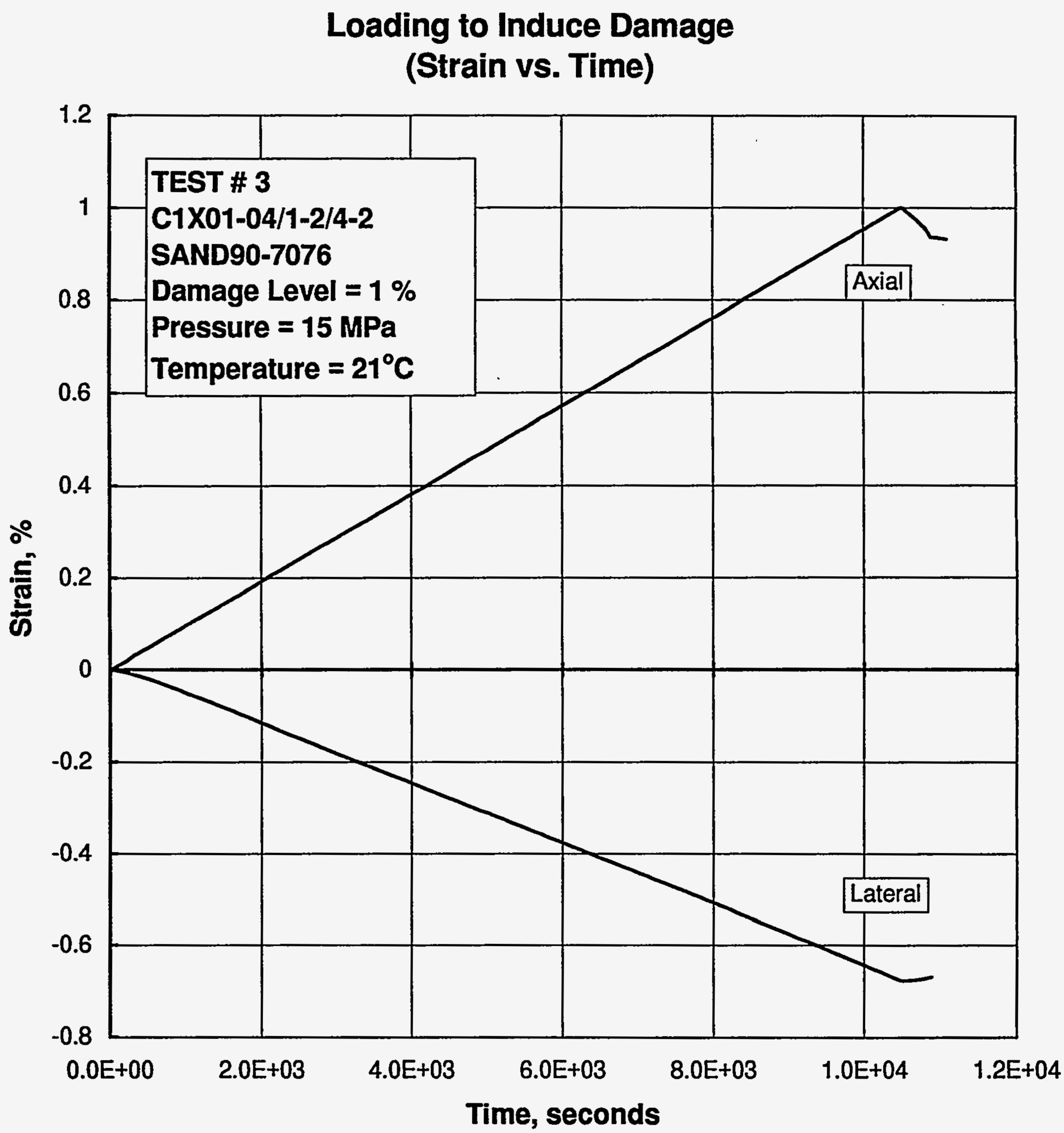

Figure E-60. Axial and Lateral Strain as a Function of Time During the Quasi-Static Loading to Induce Damage in Specimen C1X01-04/1-2/4-2.

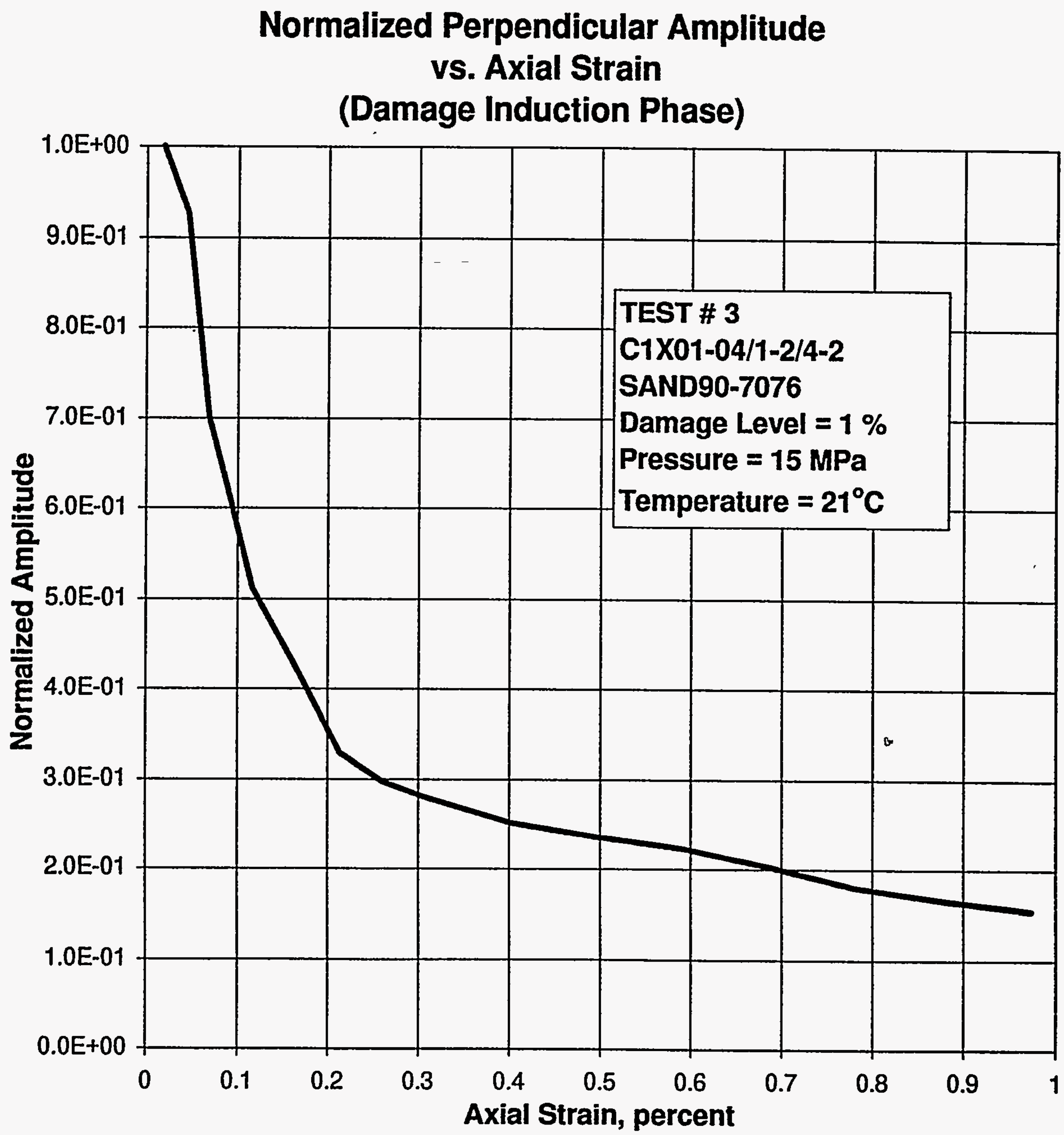

Figure E-61. Normalized Perpendicular Amplitude as a Function of Axial Strain During the Quasi-Static Loading to Induce Damage in Specimen C1X01-04/1-2/4-2.

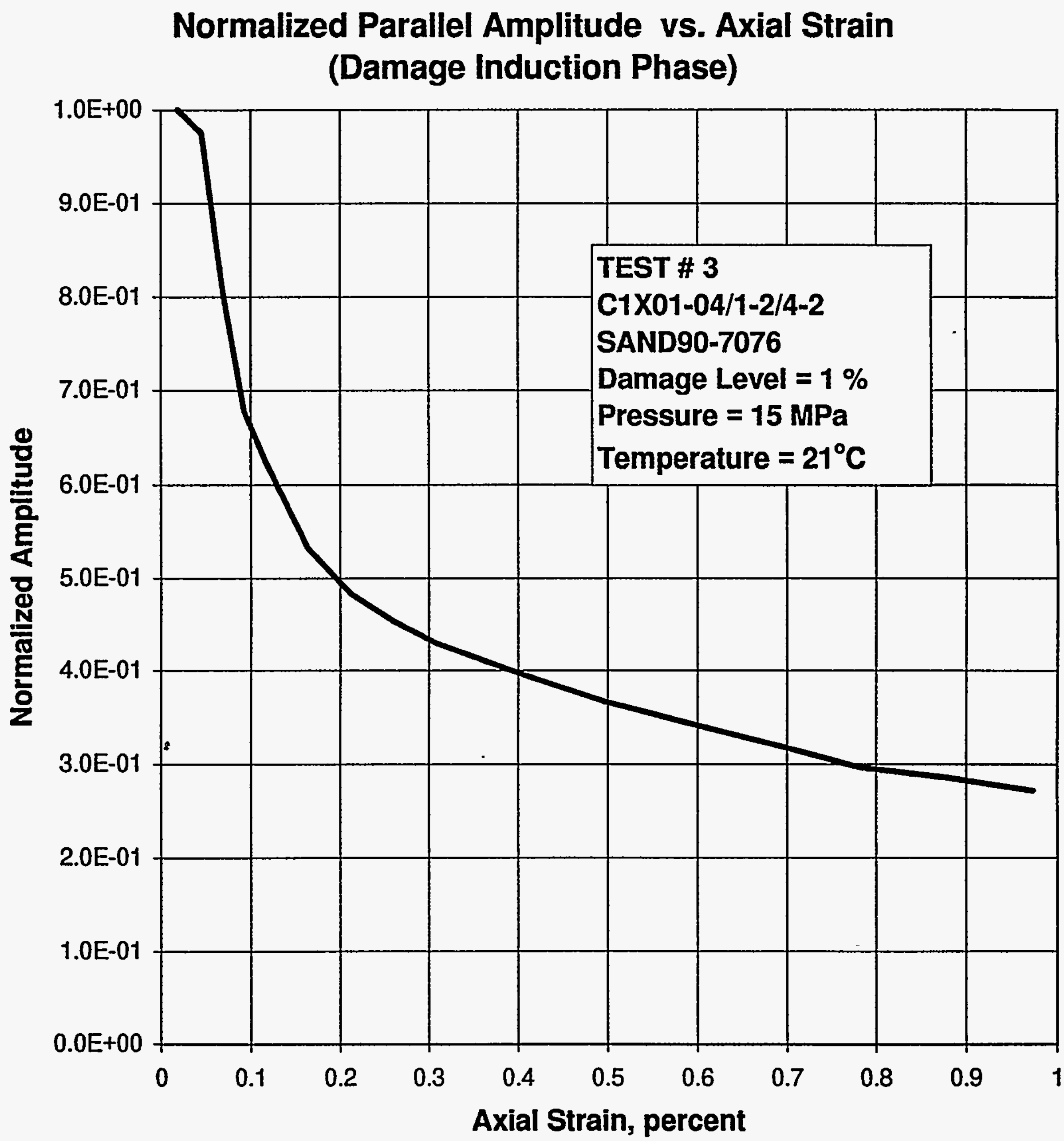

Figure E-62. Normalized Parallel Amplitude as a Function of Axial Strain During the Quasi-Static Loading to Induce Damage in Specimen C1X01-04/1-2/4-2.

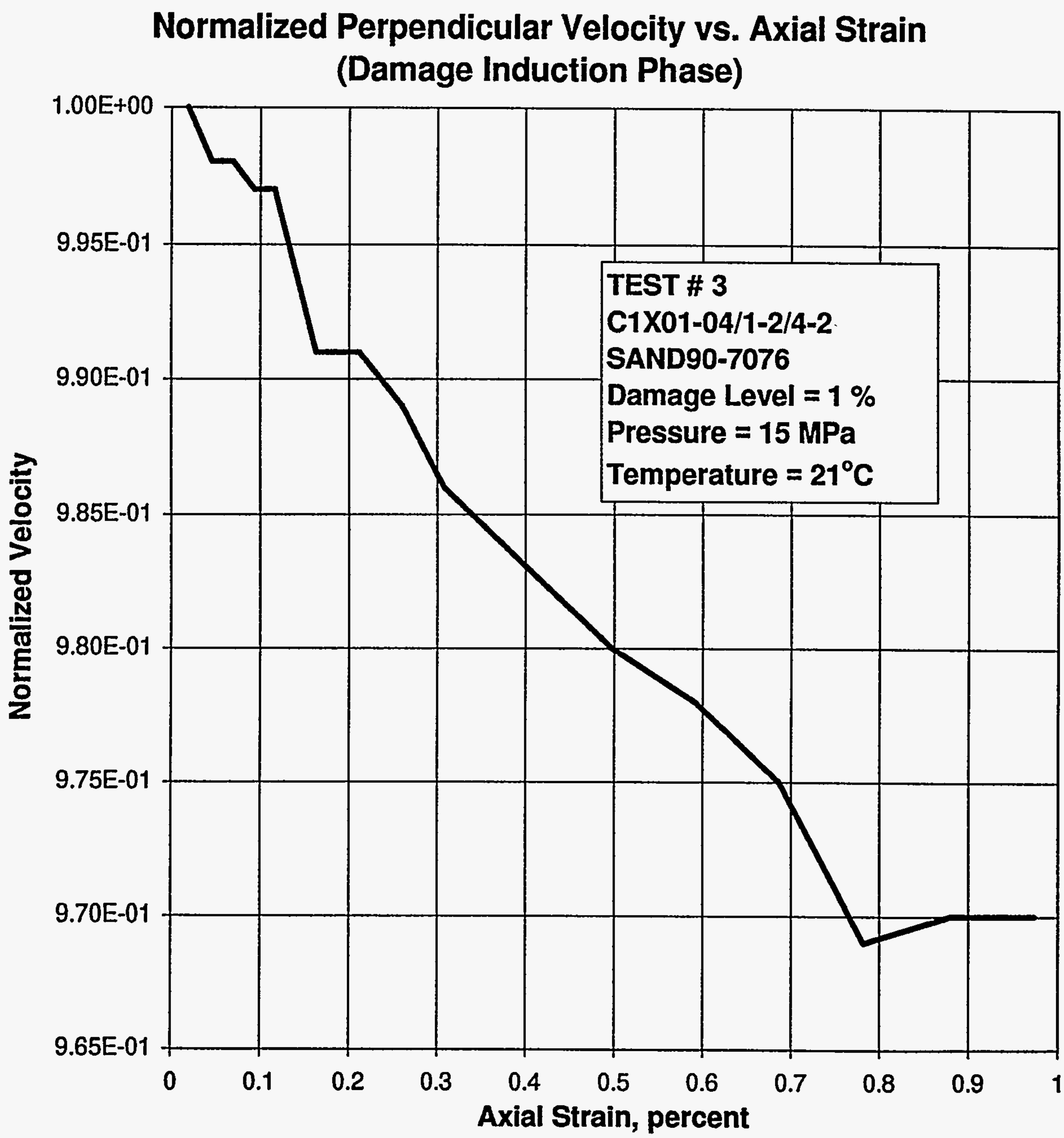

Figure E-63. Normalized Perpendicular Velocity as a Function of Axial Strain During the Quasi-Static Loading to Induce Damage in Specimen C1X01-04/1-2/4-2.

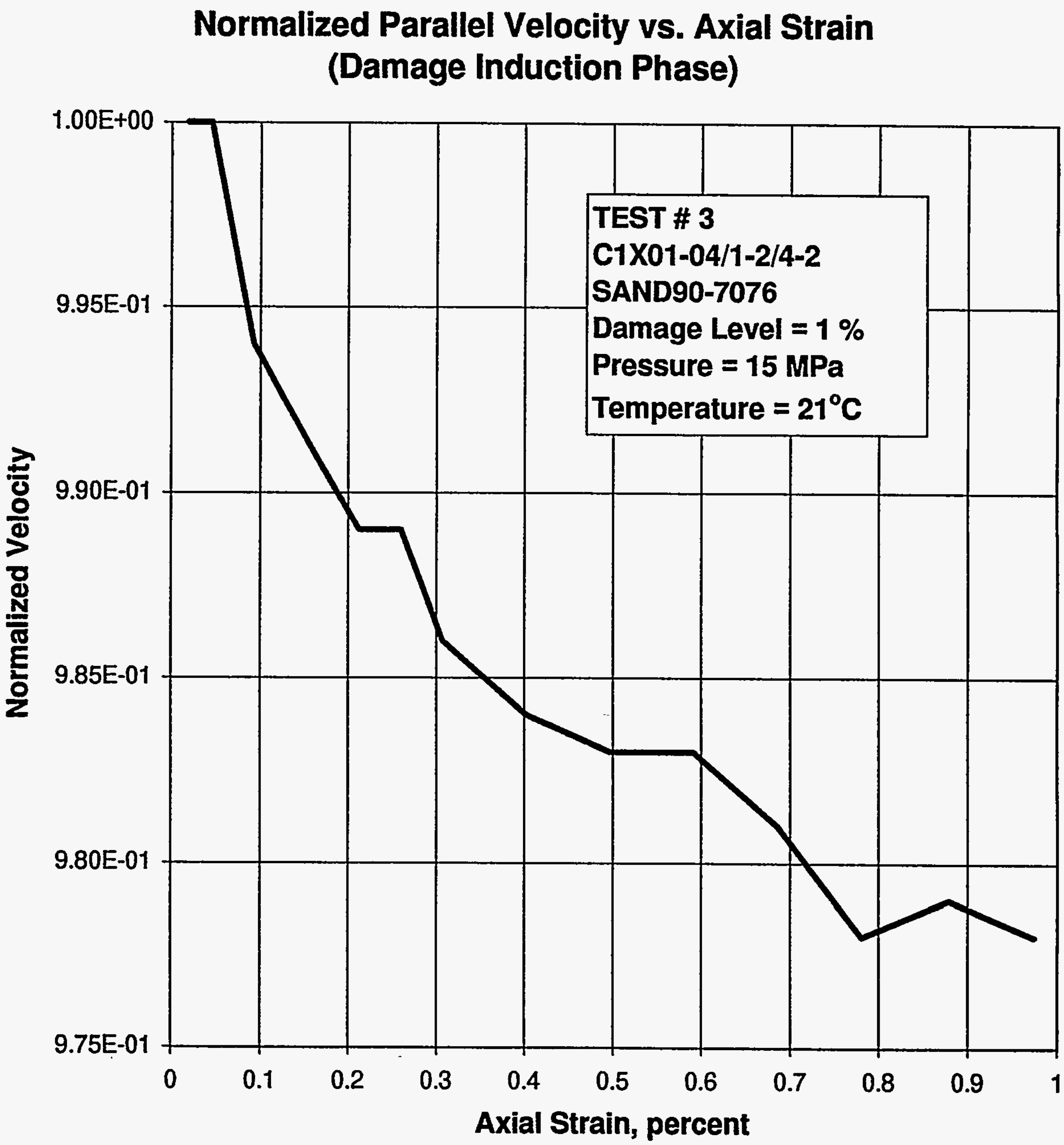

Figure E-64. Normalized Parallel Velocity as a Function of Axial Strain During the Quasi-Static Loading to Induce Damage in Specimen C1X01-04/1-2/4-2.

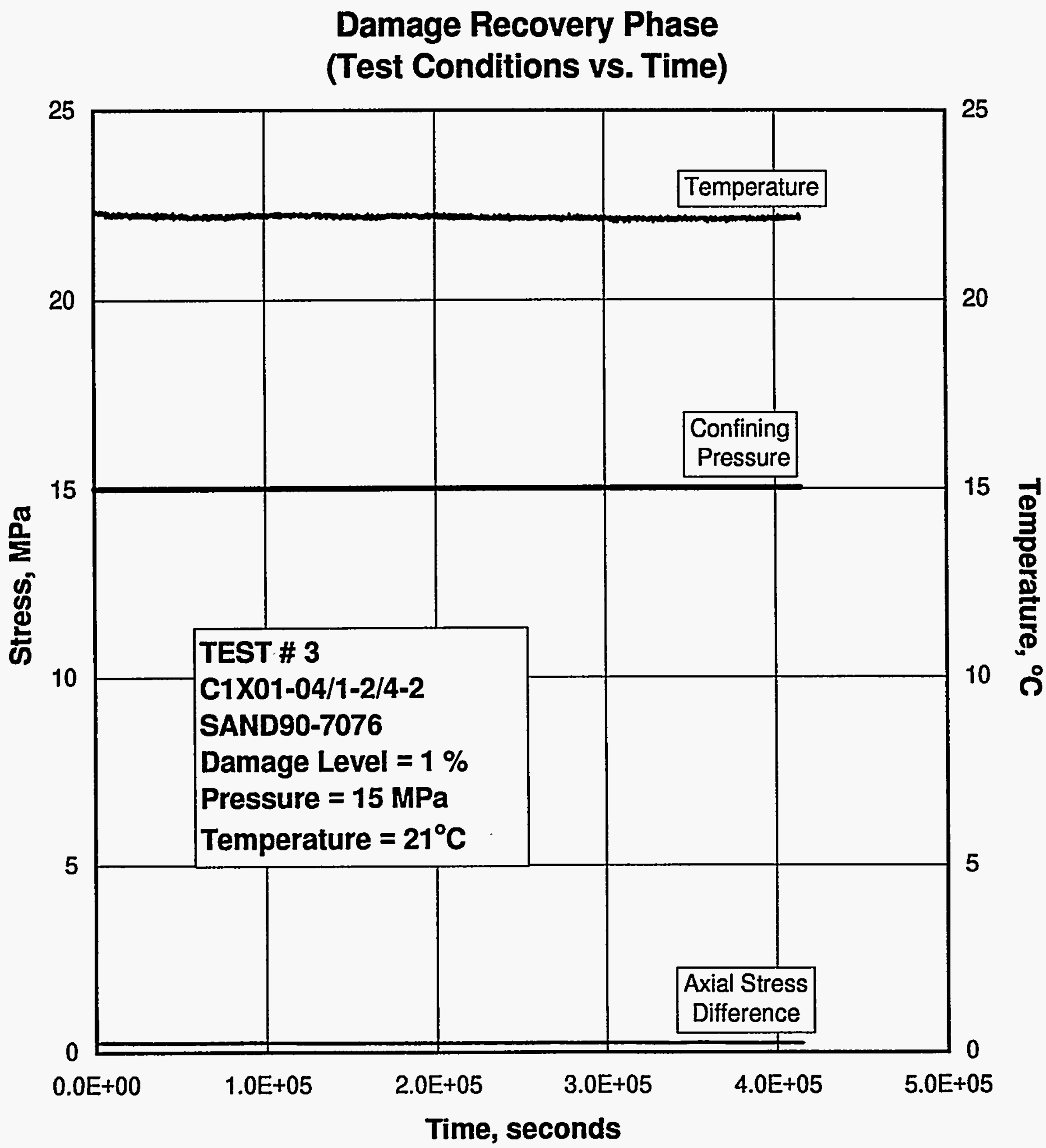

Figure E-65. Test Conditions as a Function of Time During the Hydrostatic Loading to Recover Damage in Specimen C1X01-04/1-2/4-2.

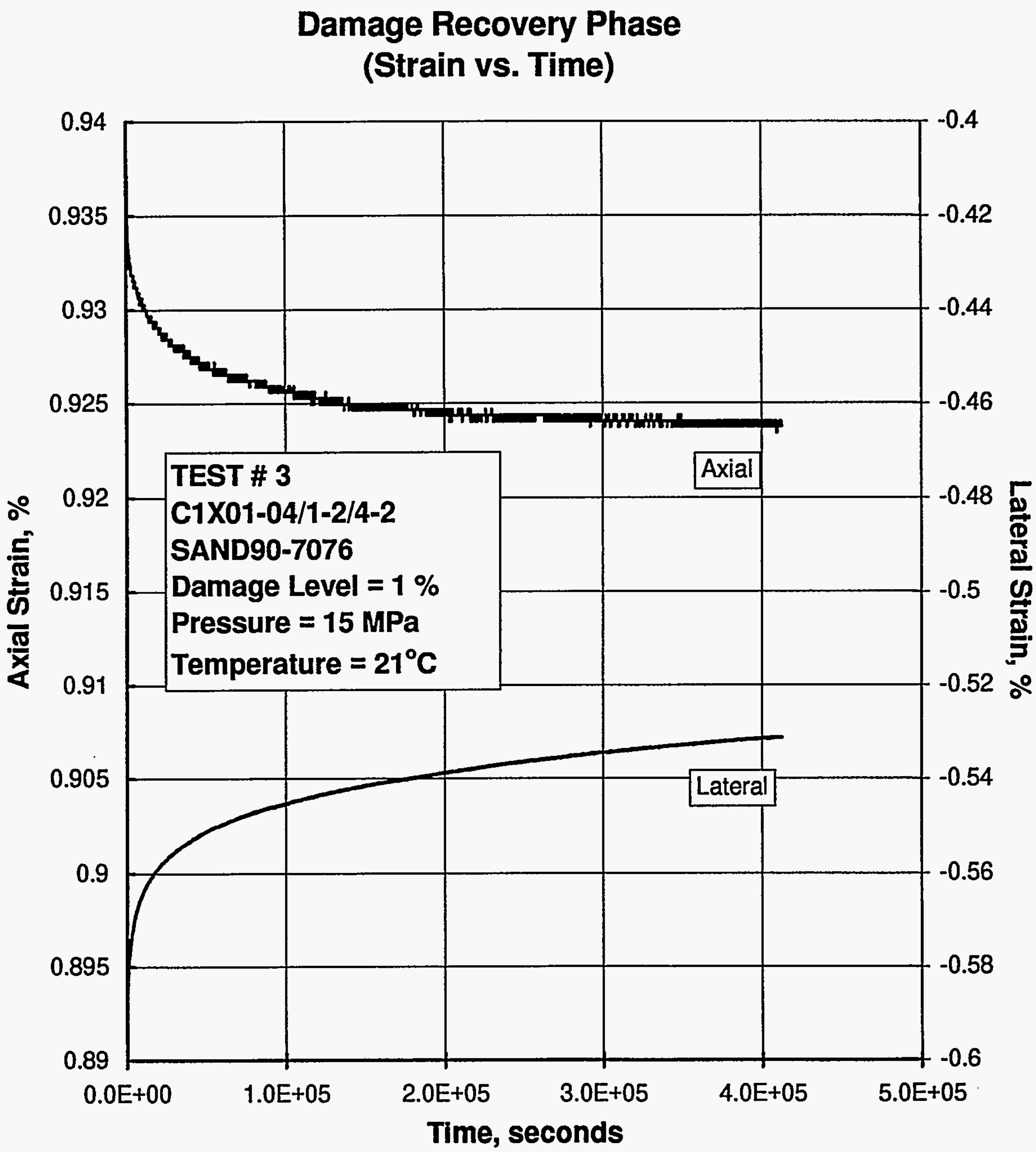

Figure E-66. Axial and Lateral Strain as a Function of Time During the Hydrostatic Loading to Recover Damage in Specimen C1X01-04/1-2/4-2.

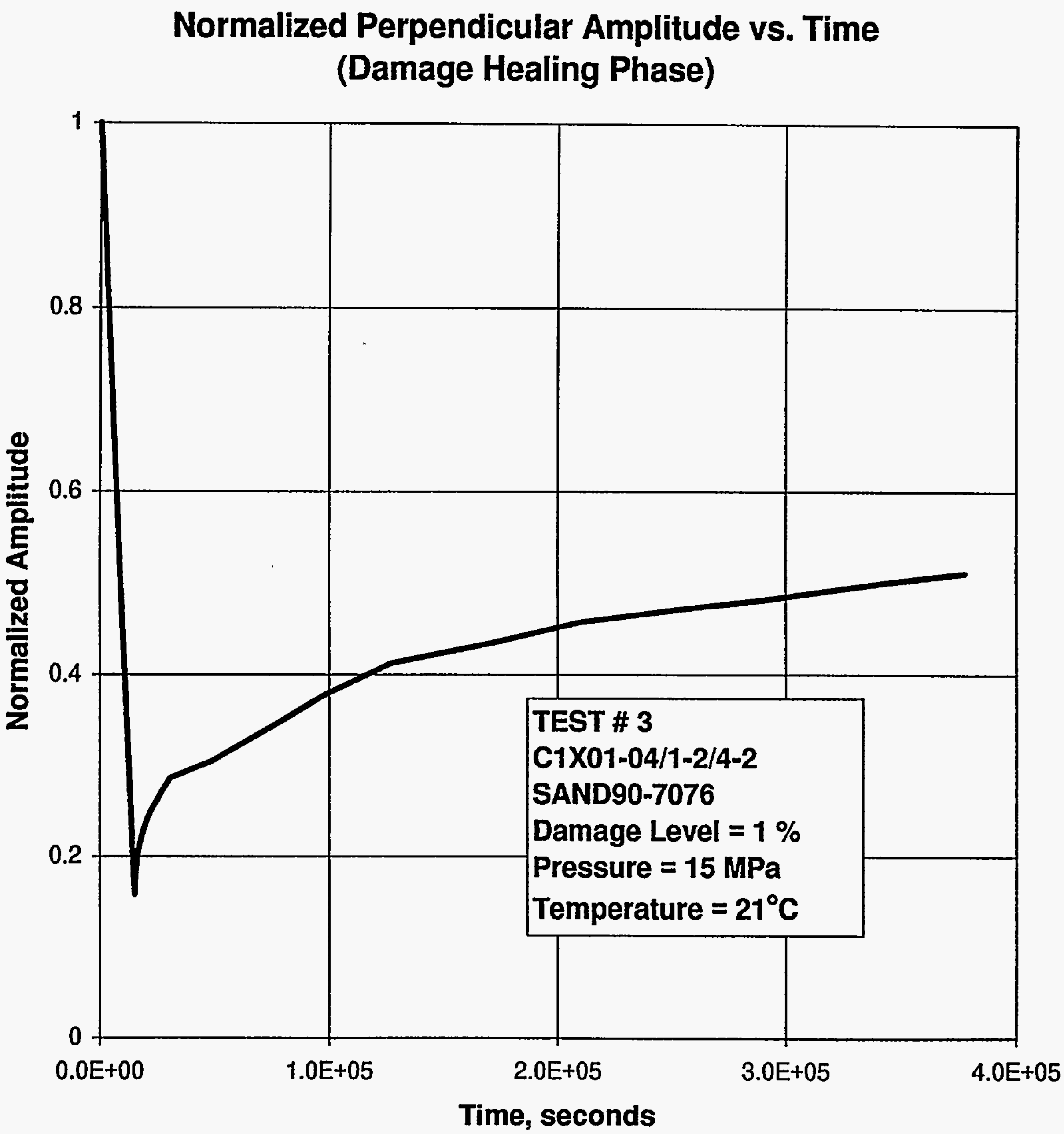

Figure E-67. Normalized Perpendicular Amplitude as a Function of Time During the Hydrostatic Loading to Recover Damage in Specimen C1X01-04/1-2/4-2.

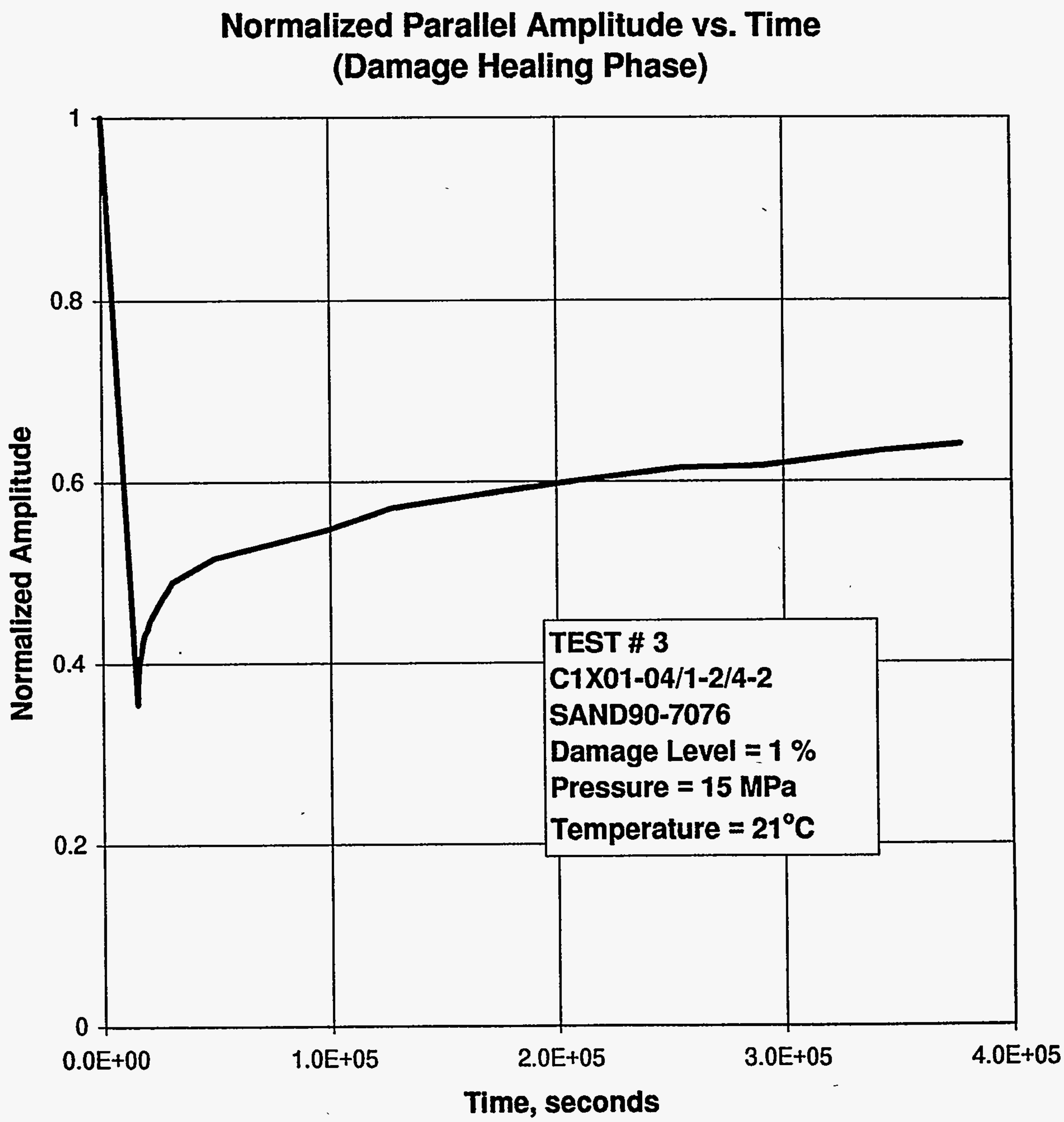

Figure E-68. Normalized Parallel Amplitude as a Function of Time During the Hydrostatic Loading to Recover Damage in Specimen C1X01-04/1-2/4-2.

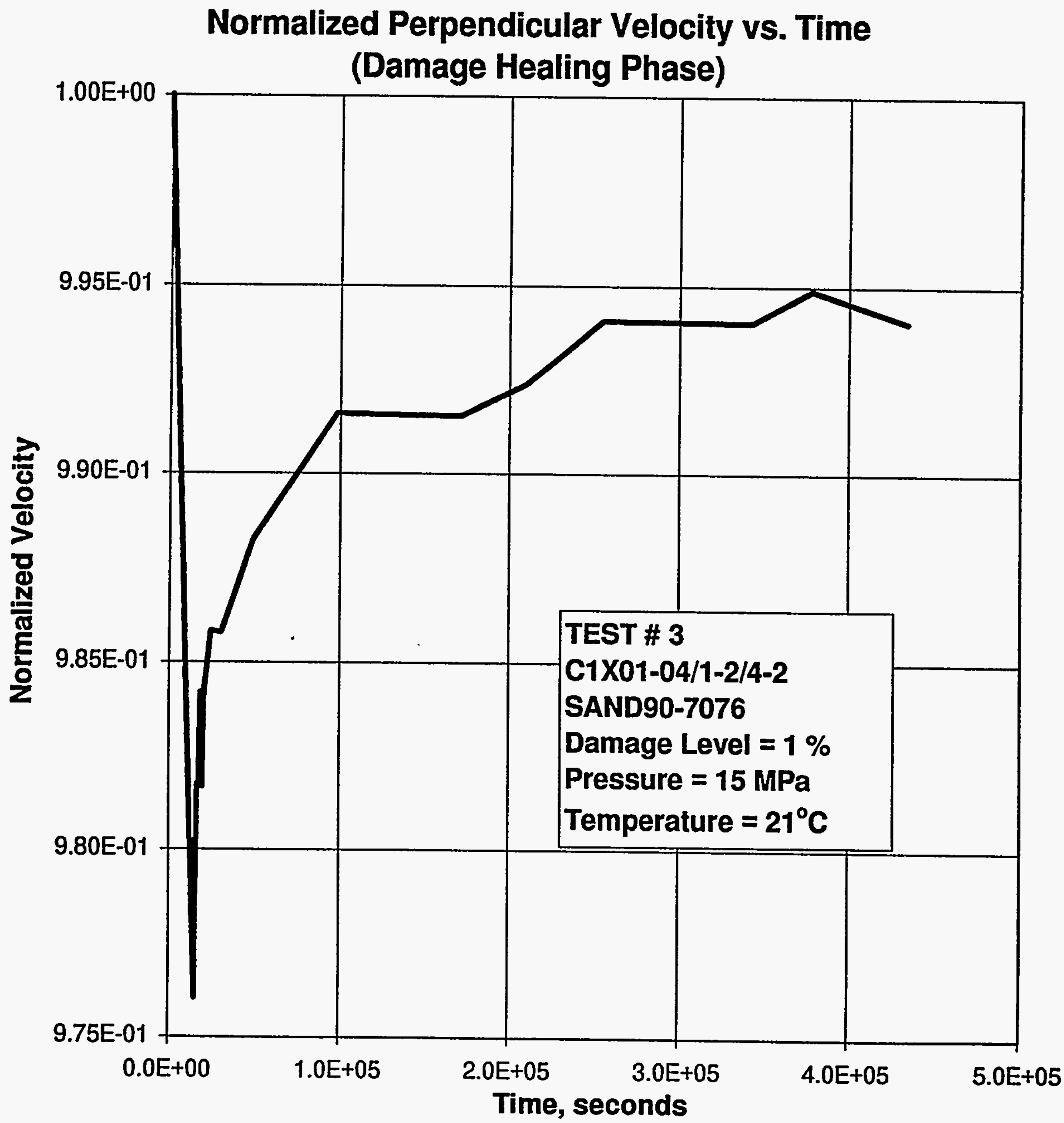

Figure E-69. Normalized Perpendicular Velocity as a Function of Time During the Hydrostatic Loading to Recover Damage in Specimen 2C1X01-04/1-2/4-2.

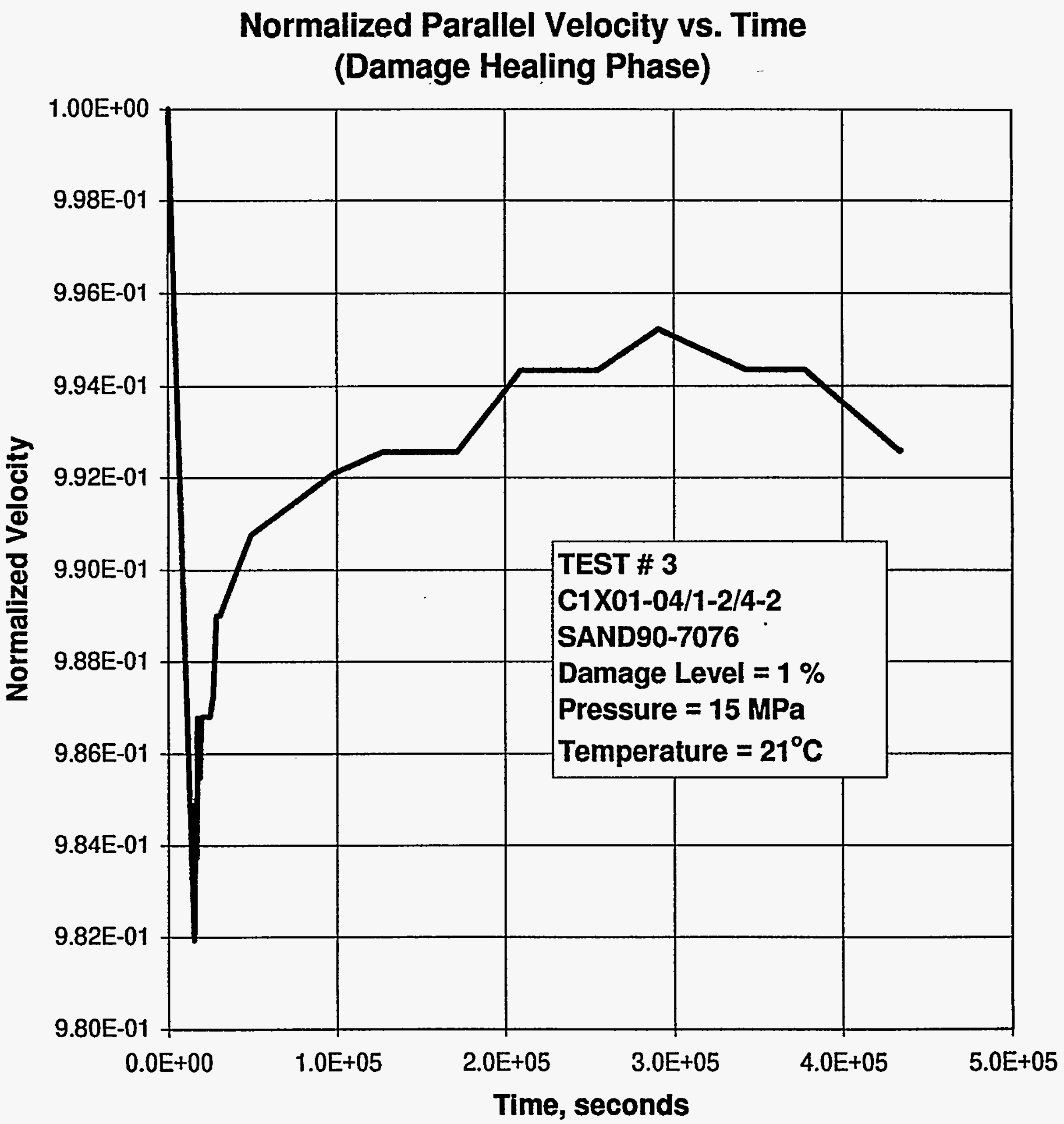

Figure E-70. Normalized Parallel Velocity as a Function of Time During the Hydrostatic Loading to Recover Damage in Specimen C1X01-04/1-2/4-2.

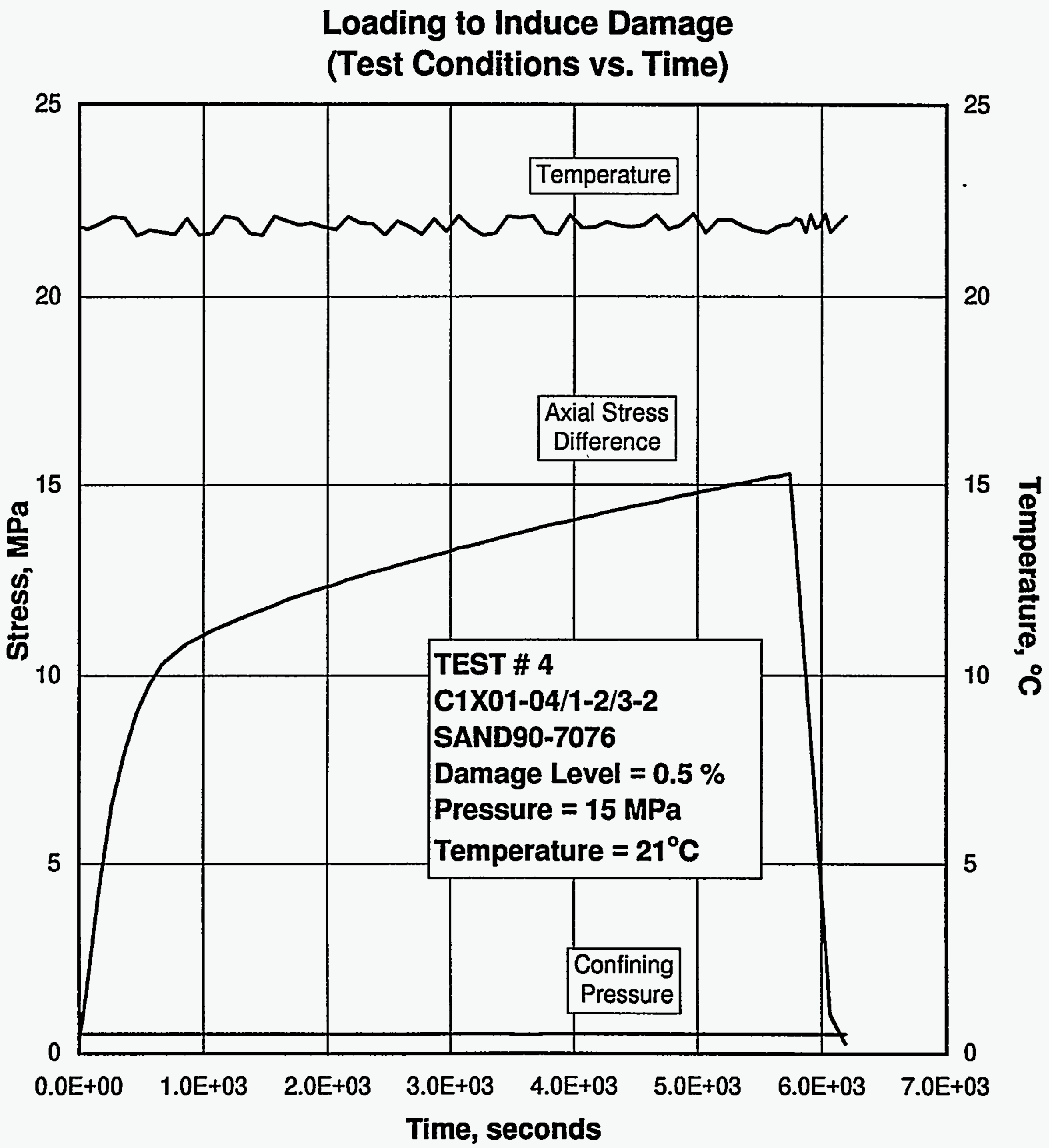

Figure E-71. Test Conditions as a Function of Time During the Quasi-Static Loading to Induce Damage in Specimen C1X01-04/1-2/3-2.

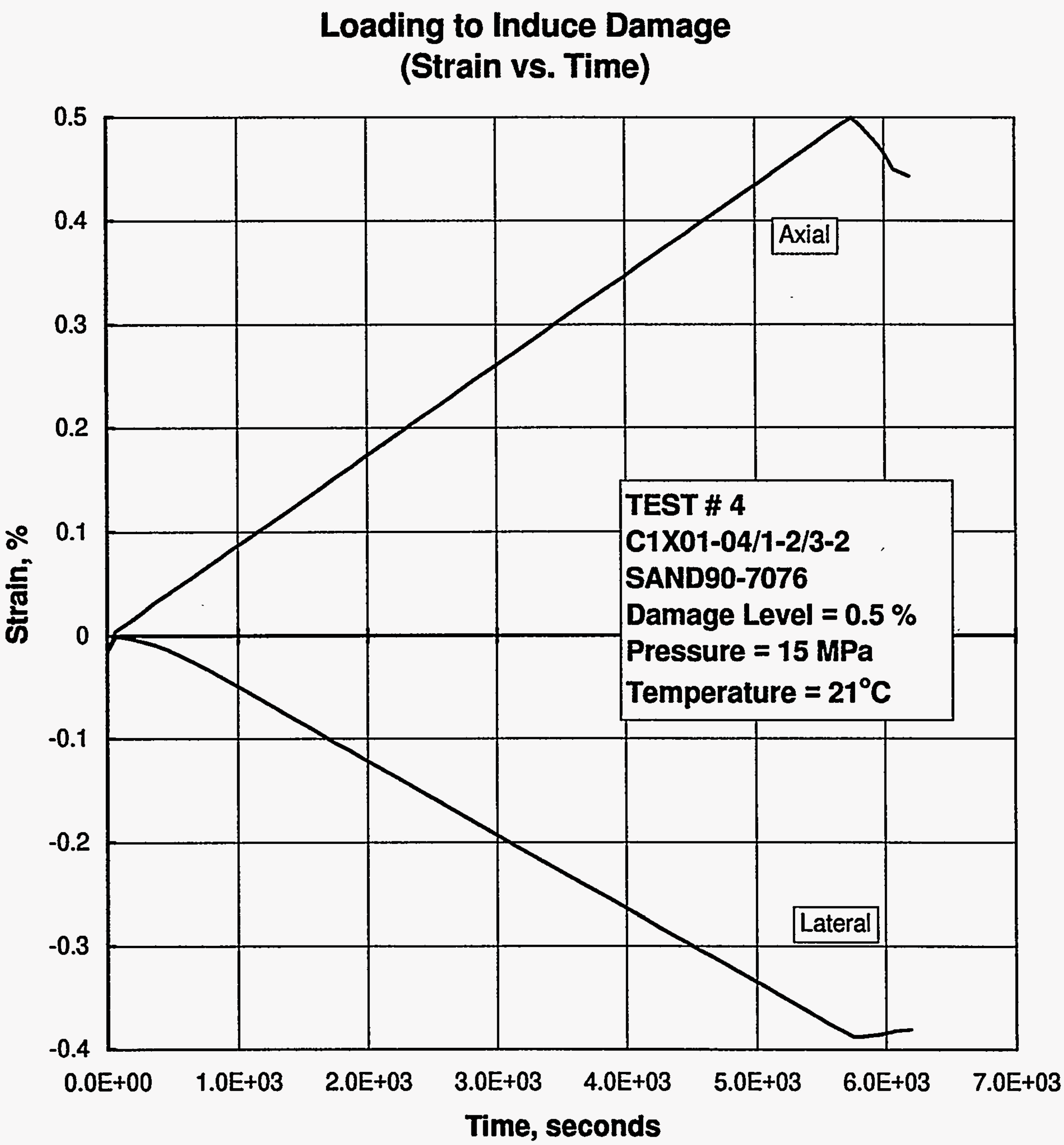

Figure E-72. Axial and Lateral Strain as a Function of Time During the Quasi-Static Loading to Induce Damage in Specimen C1X01-04/1-2/3-2.

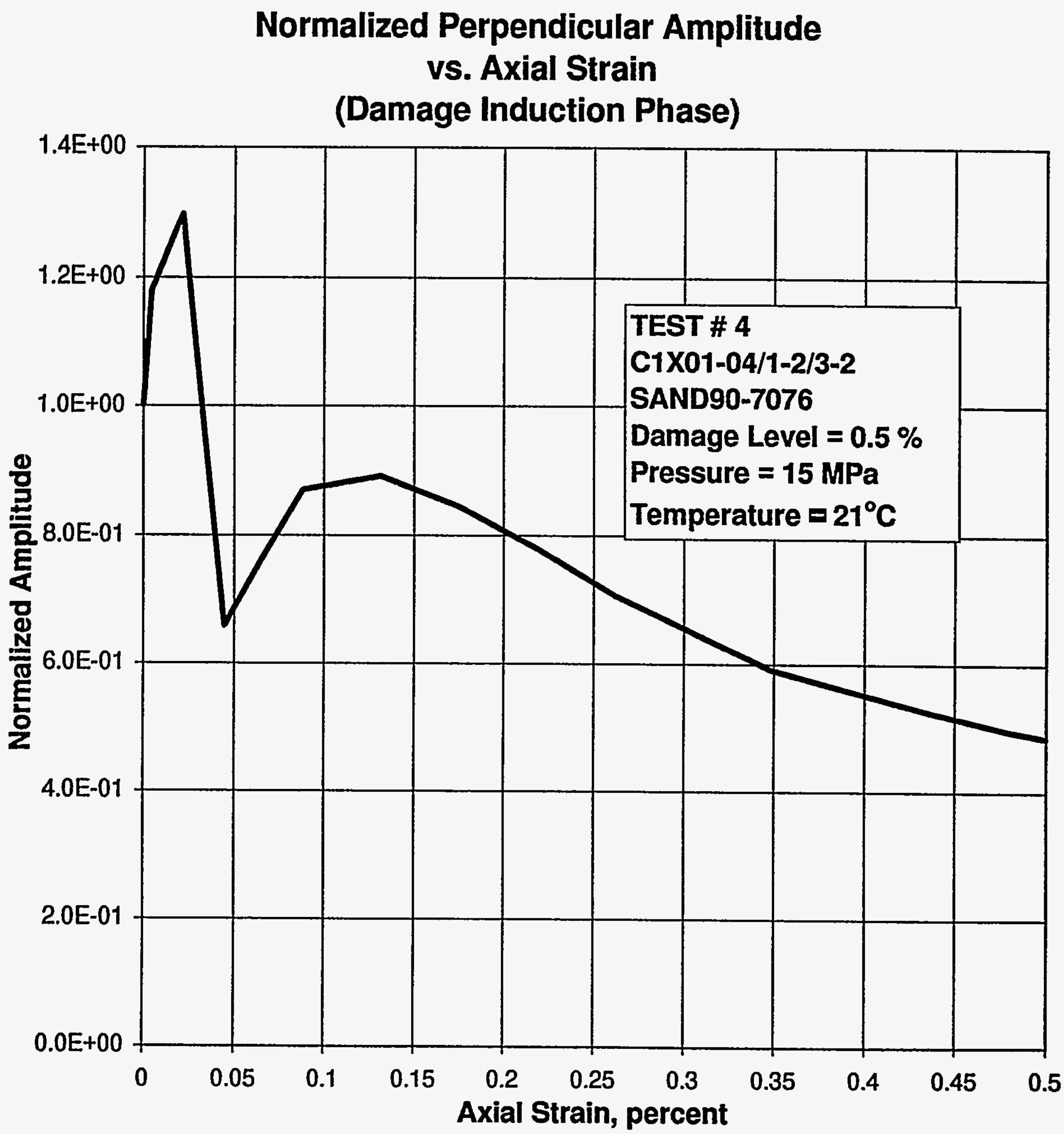

Figure E-73. Normalized Perpendicular Amplitude as a Function of Axial Strain During the Quasi-Static Loading to Induce Damage in Specimen C1X01-04/1-2/3-2.

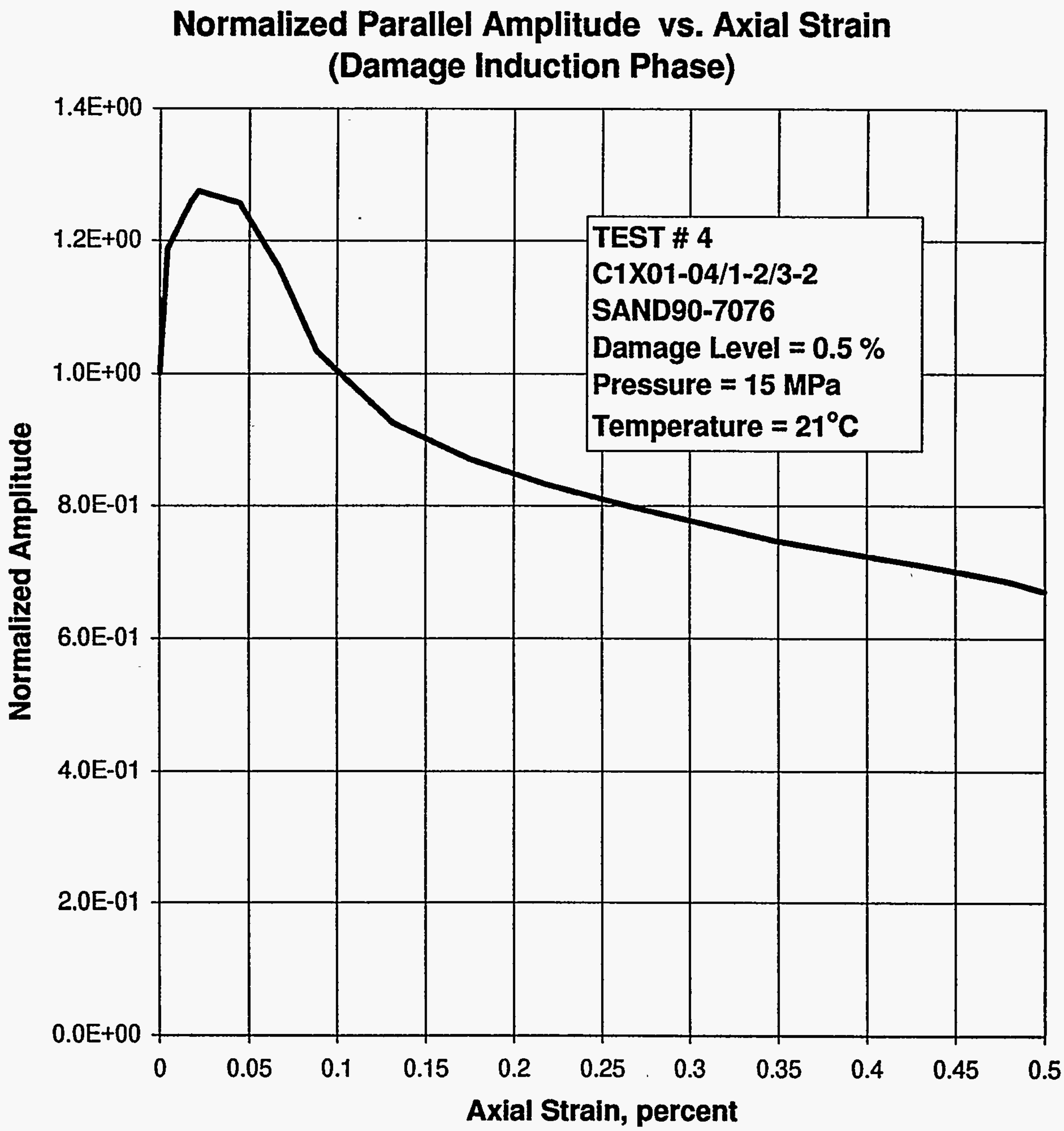

Figure E-74. Normalized Parallel Amplitude as a Function of Axial Strain During the Quasi-Static Loading to Induce Damage in Specimen C1X01-04/1-2/3-2.

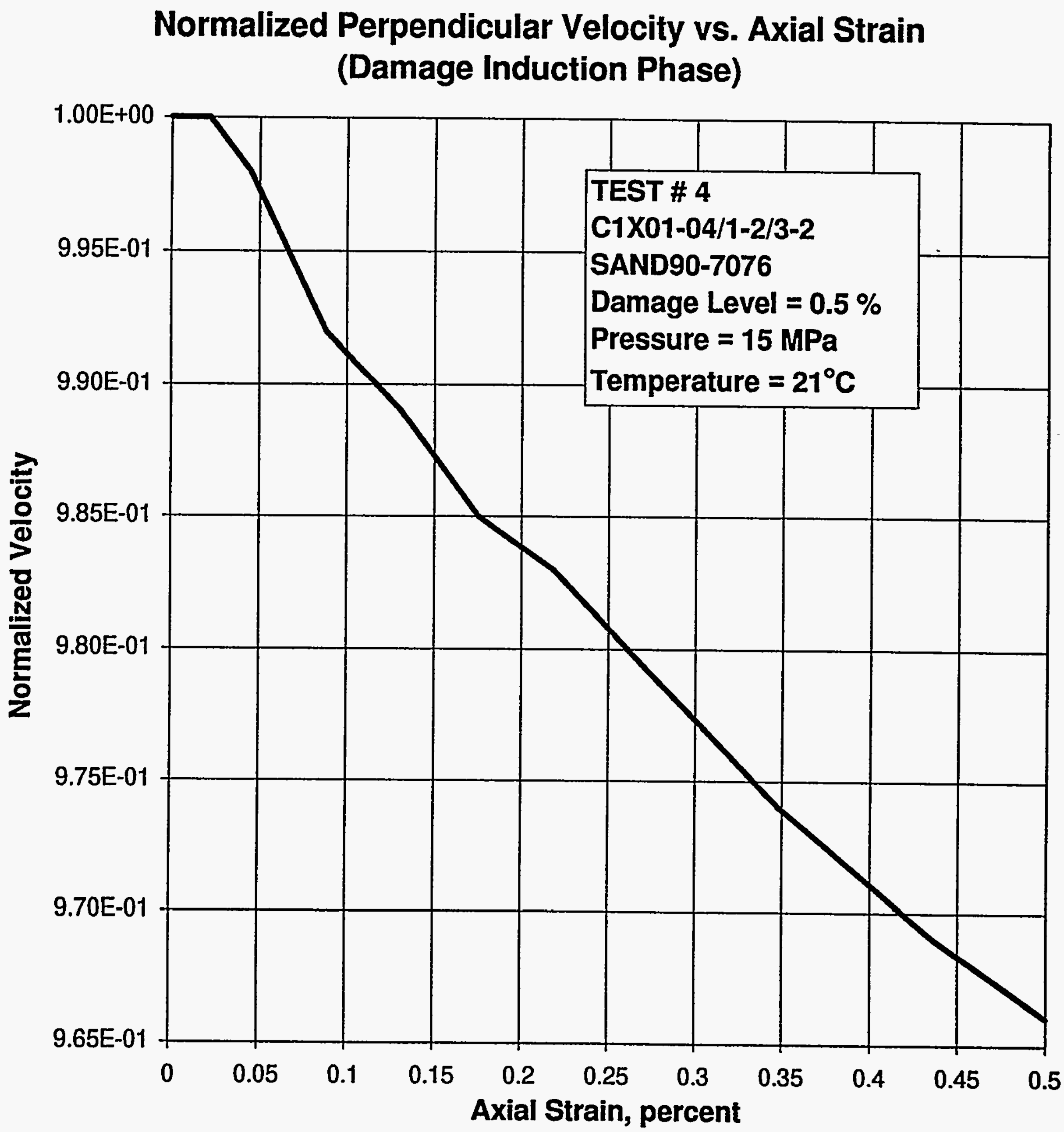

Figure E-75. Normalized Perpendicular Velocity as a Function of Axial Strain During the Quasi-Static Loading to Induce Damage in Specimen C1X01-04/1-2/3-2.

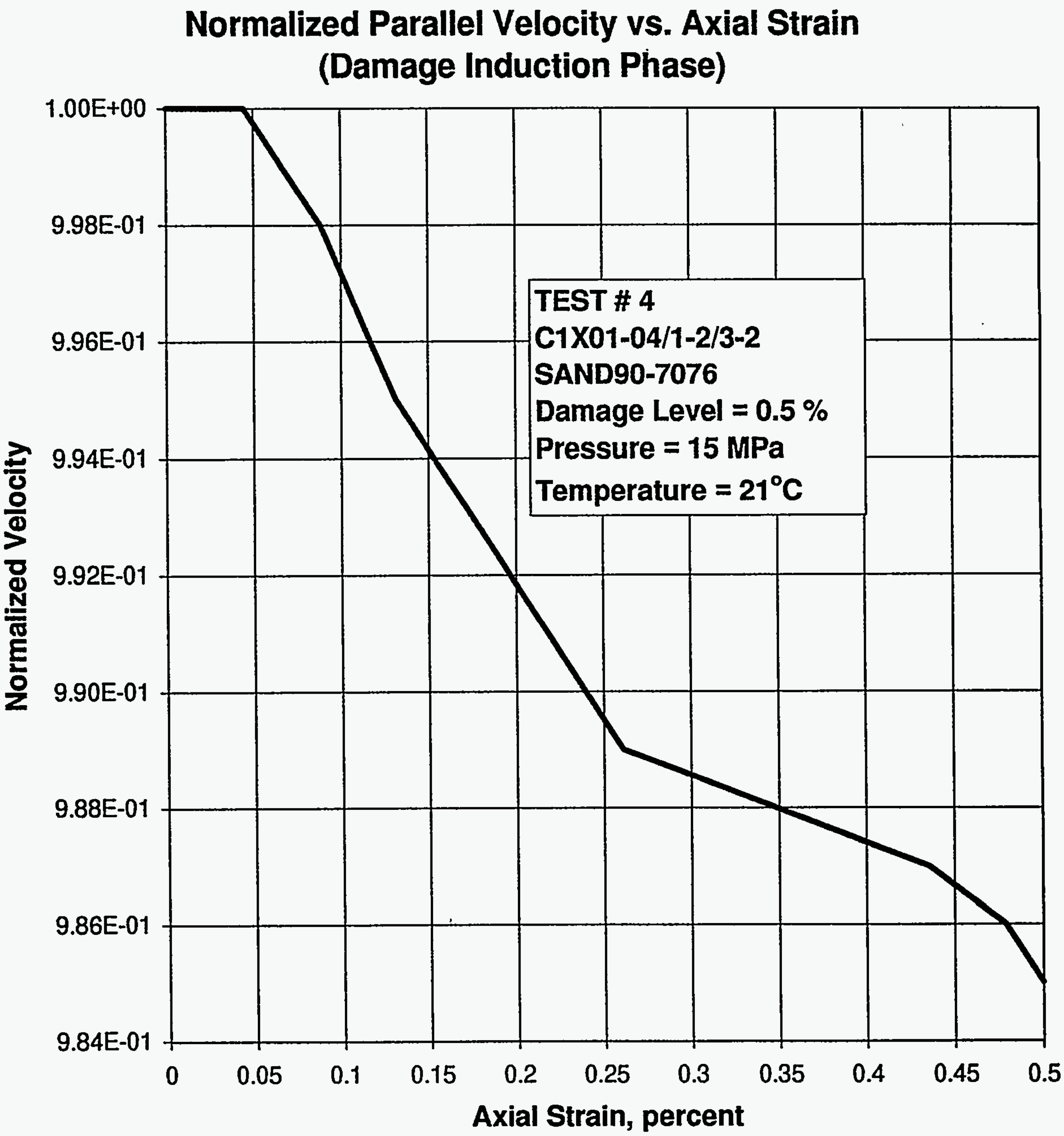

Figure E-76. Normalized Parallel Velocity as a Function of Axial Strain During the Quasi-Static Loading to Induce Damage in Specimen C1X01-04/1-2/3-2.

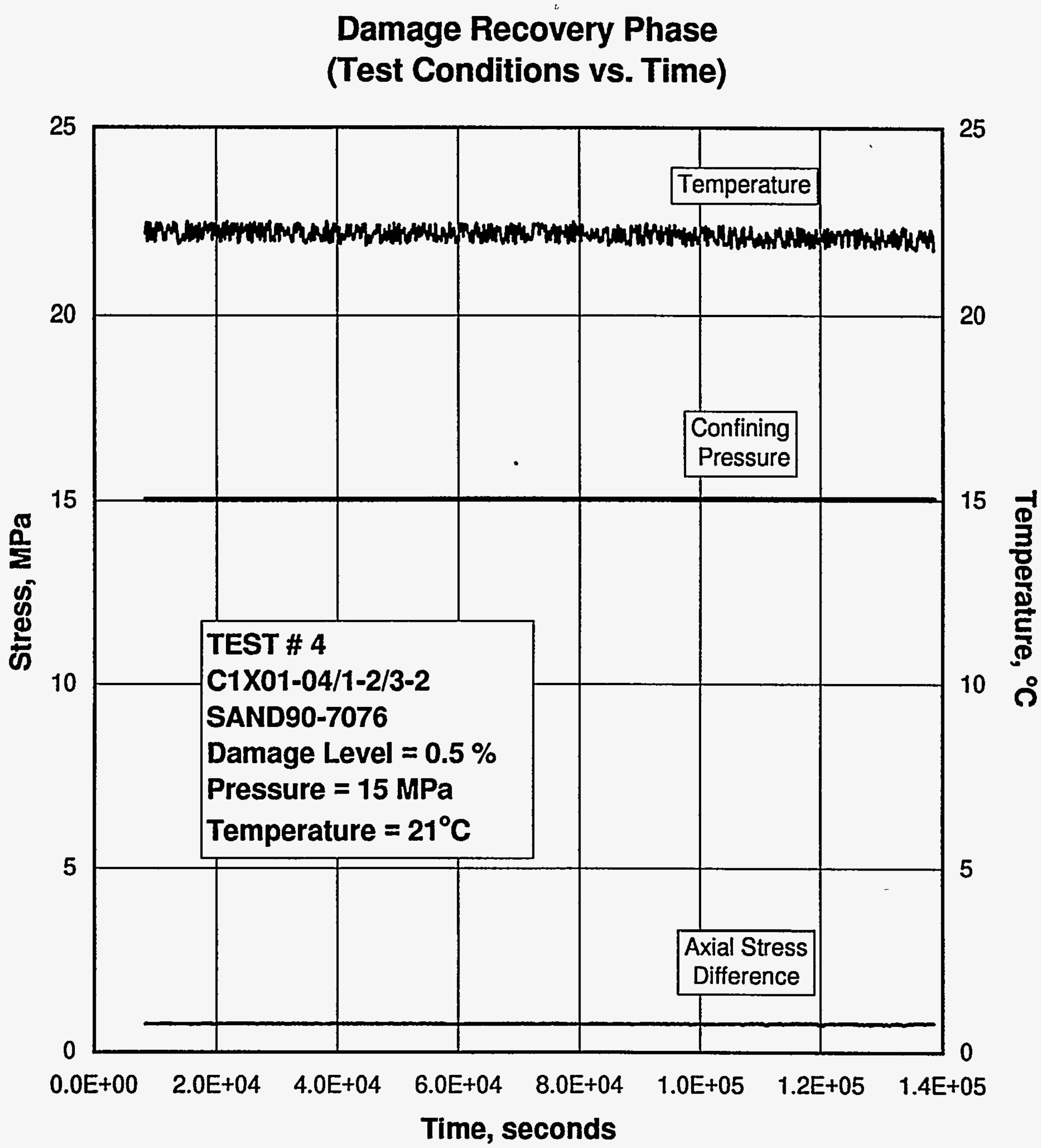

Figure E-77. Test Conditions as a Function of Time During the Hydrostatic Loading to Recover Damage in Specimen C1X01-04/1-2/3-2.

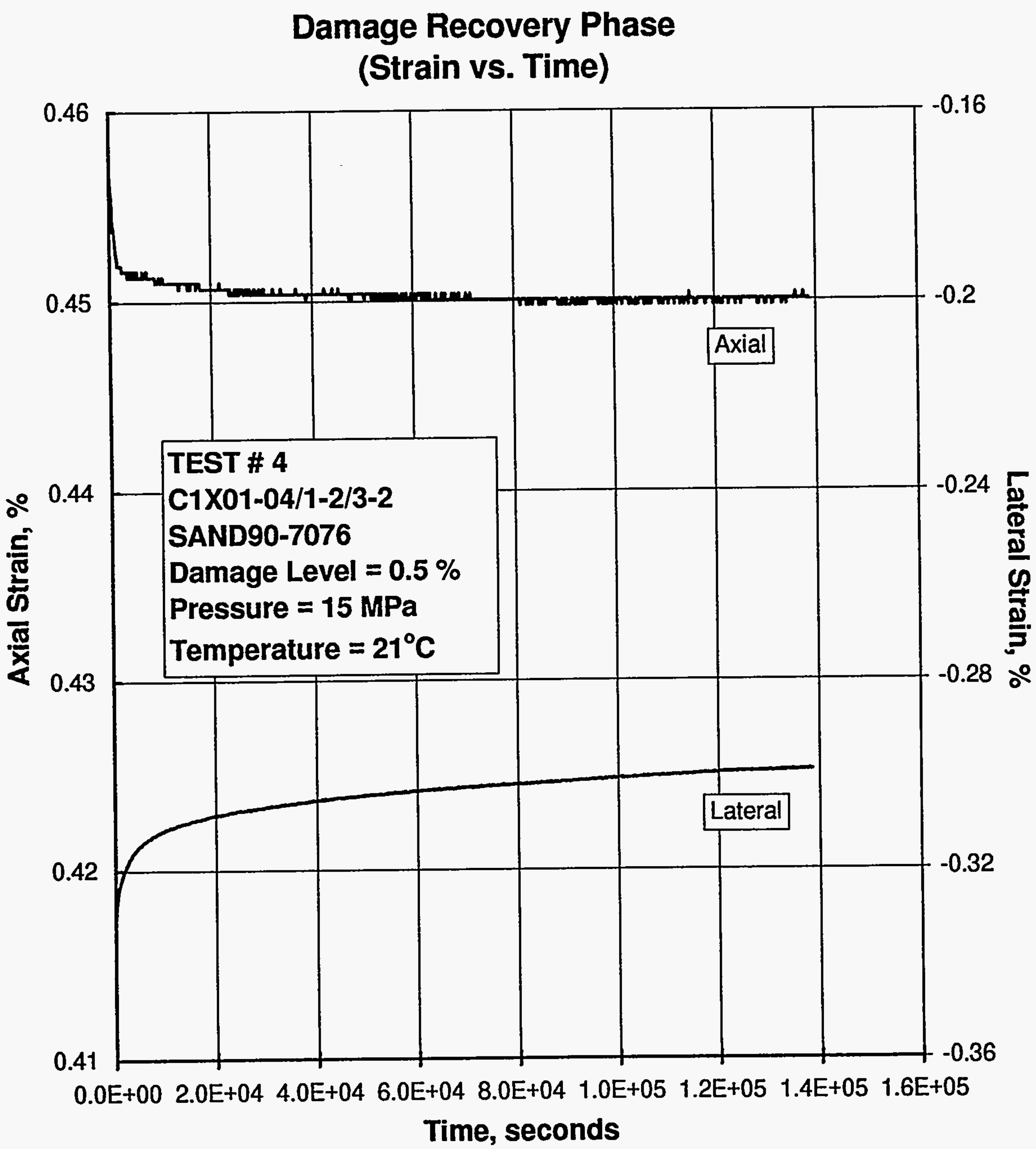

Figure E-78. Axial and Lateral Strain as a Function of Time During the Hydrostatic Loading to Recover Damage in Specimen C1X01-04/1-2/3-2.

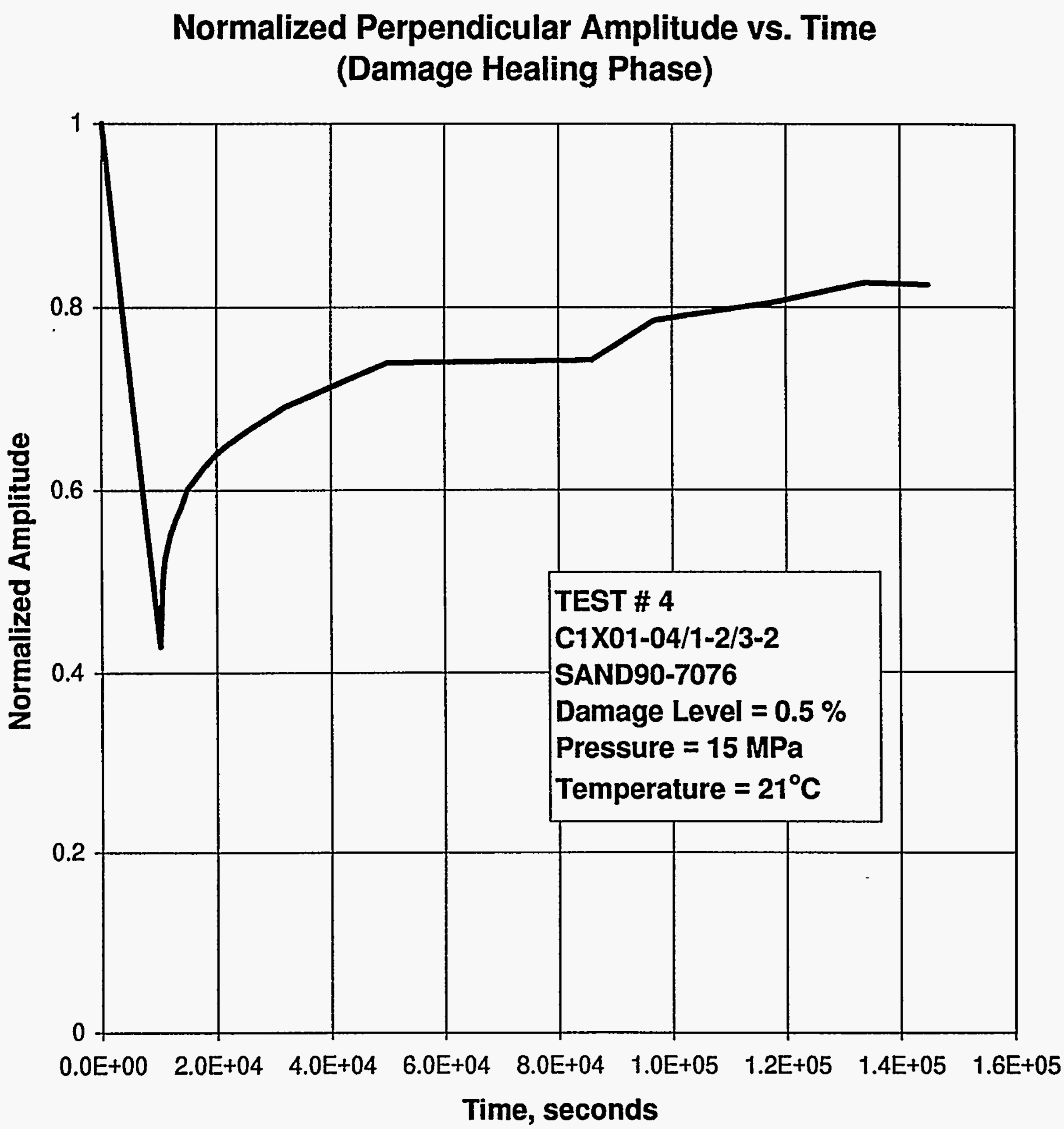

Figure E-79. Normalized Perpendicular Amplitude as a Function of Time During the Hydrostatic Loading to Recover Damage in Specimen C1X01-04/1-2/3-2.

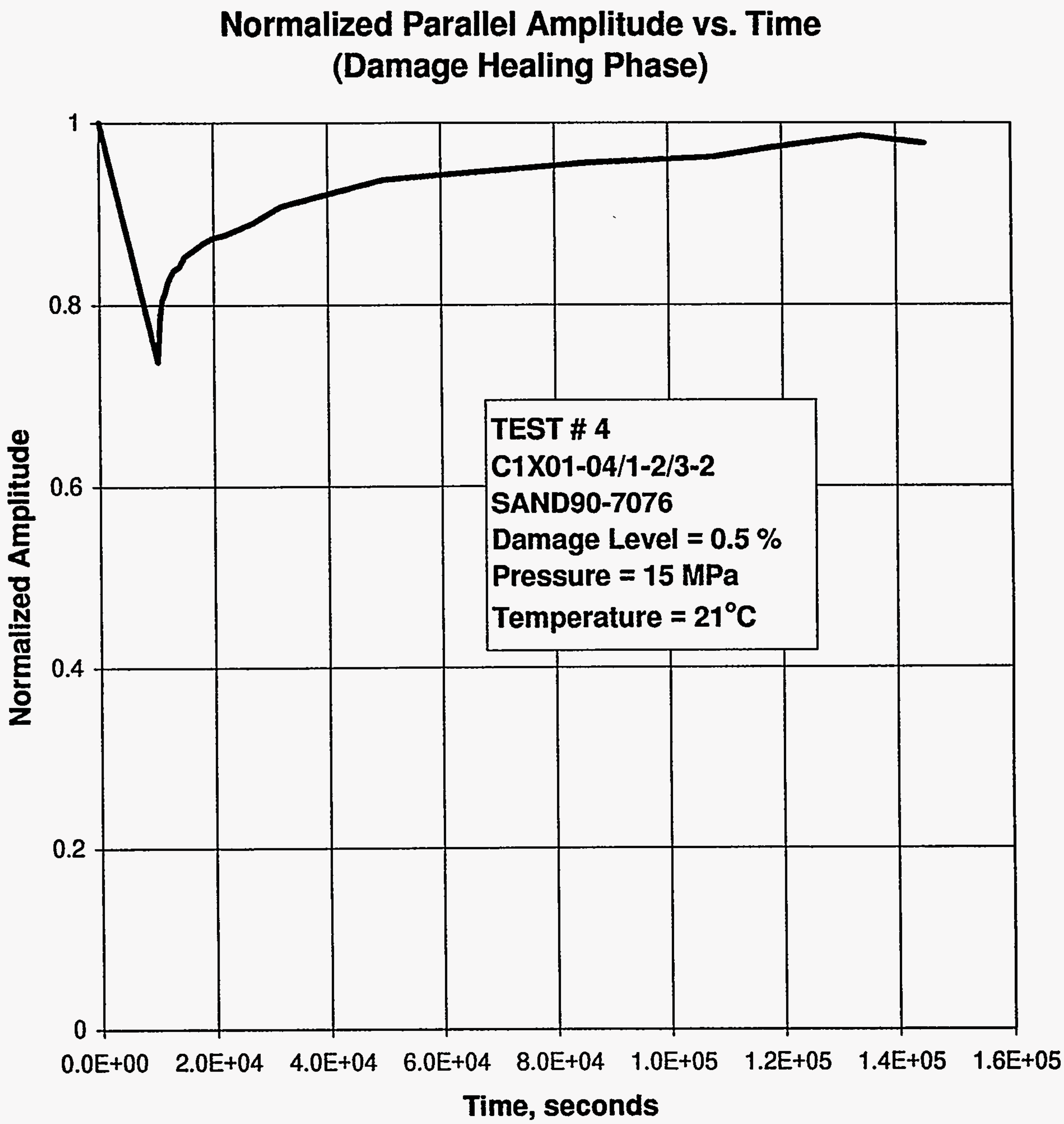

Figure E-80. Normalized Parallel Amplitude as a Function of Time During the Hydrostatic Loading to Recover Damage in Specimen C1X01-04/1-2/3-2.

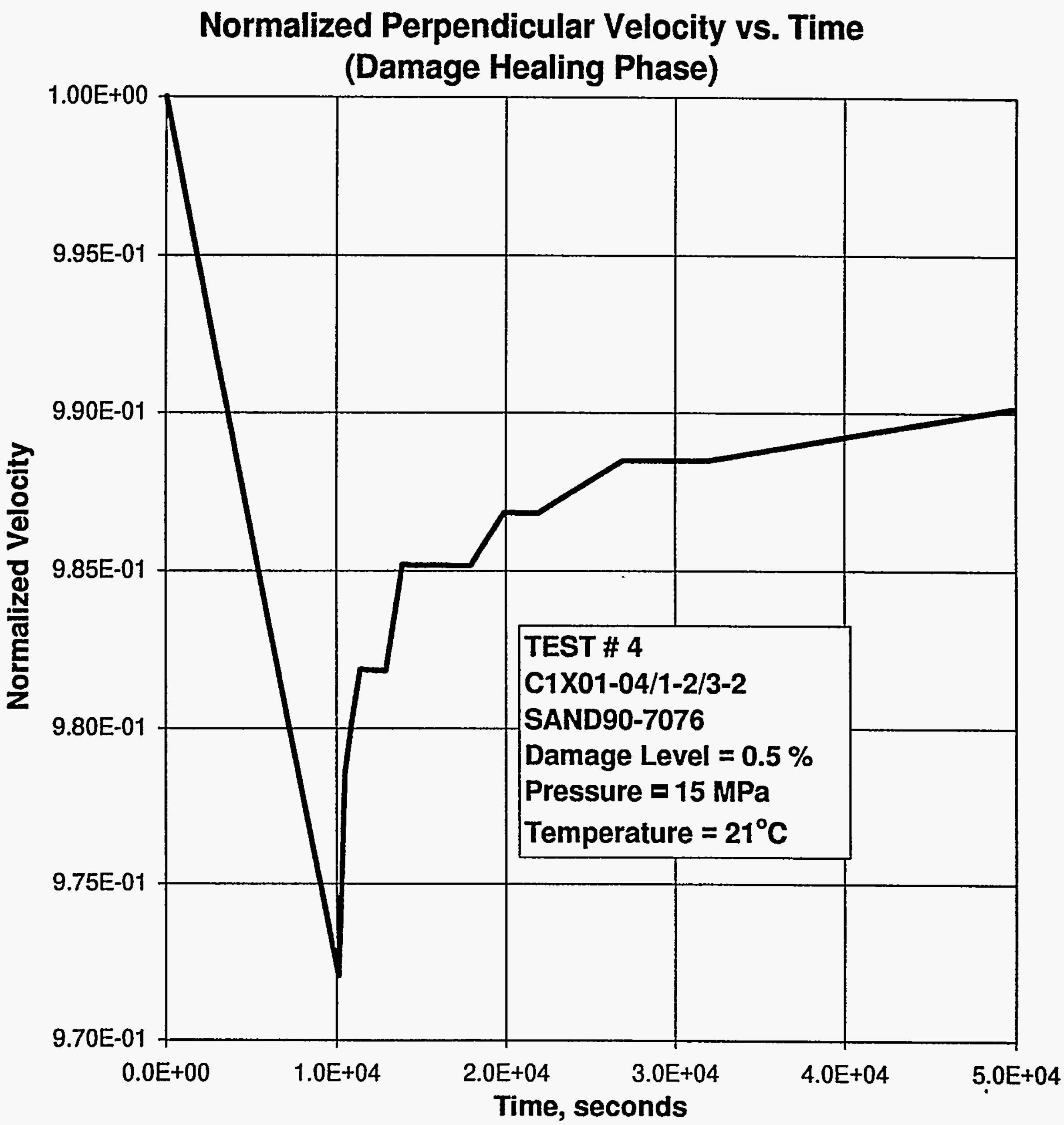

Figure E-81. Normalized Perpendicular Velocity as a Function of Time During the Hydrostatic Loading to Recover Damage in Specimen C1X01-04/1-2/3-2.

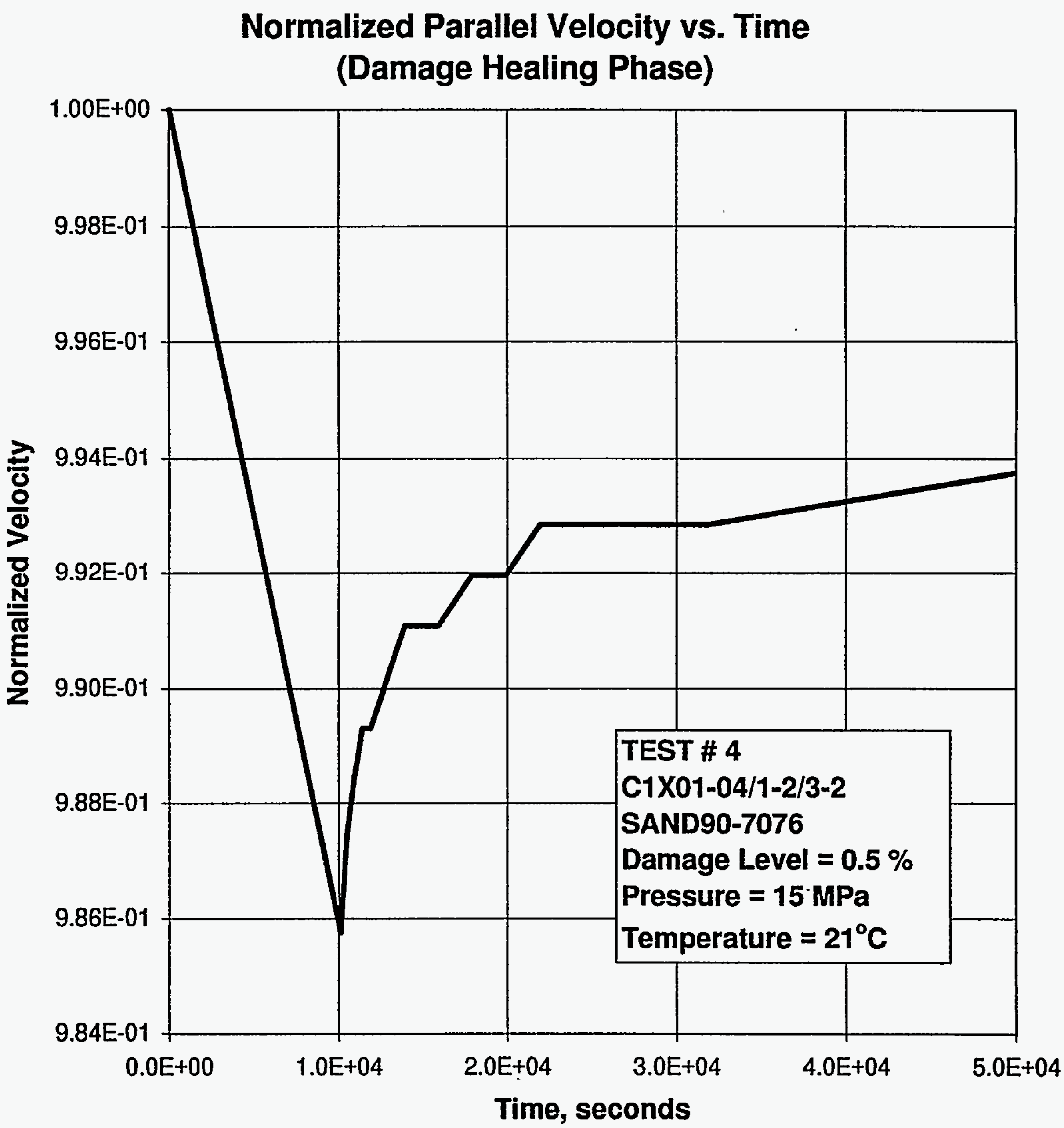

Figure E-82. Normalized Parallel Velocity as a Function of Time During the Hydrostatic Loading to Recover Damage in Specimen C1X01-04/1-2/3-2.

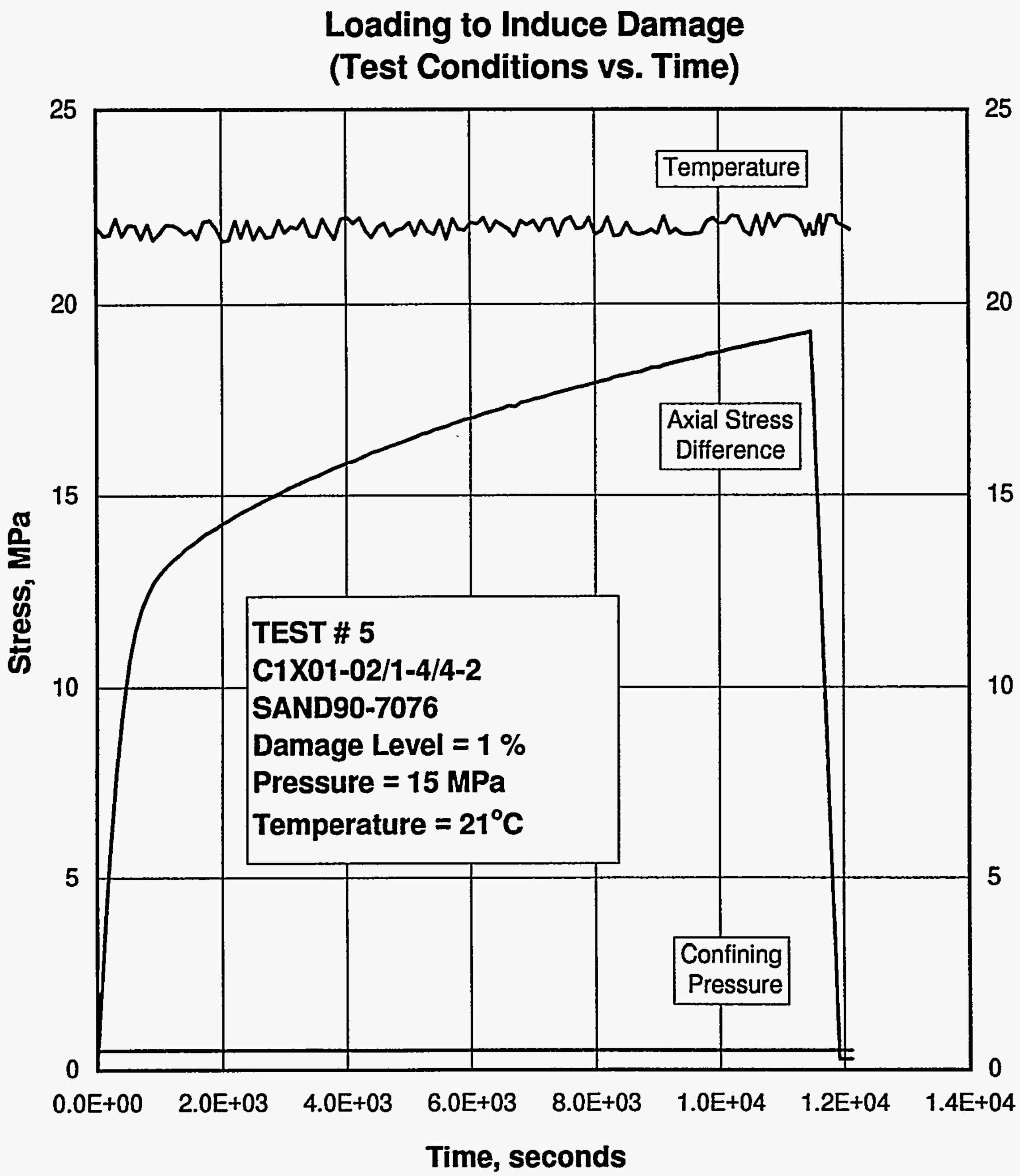

Figure E-83. Test Conditions as a Function of Time During the Quasi-Static Loading to Induce Damage in Specimen C1X01-02/1-4/4-2.

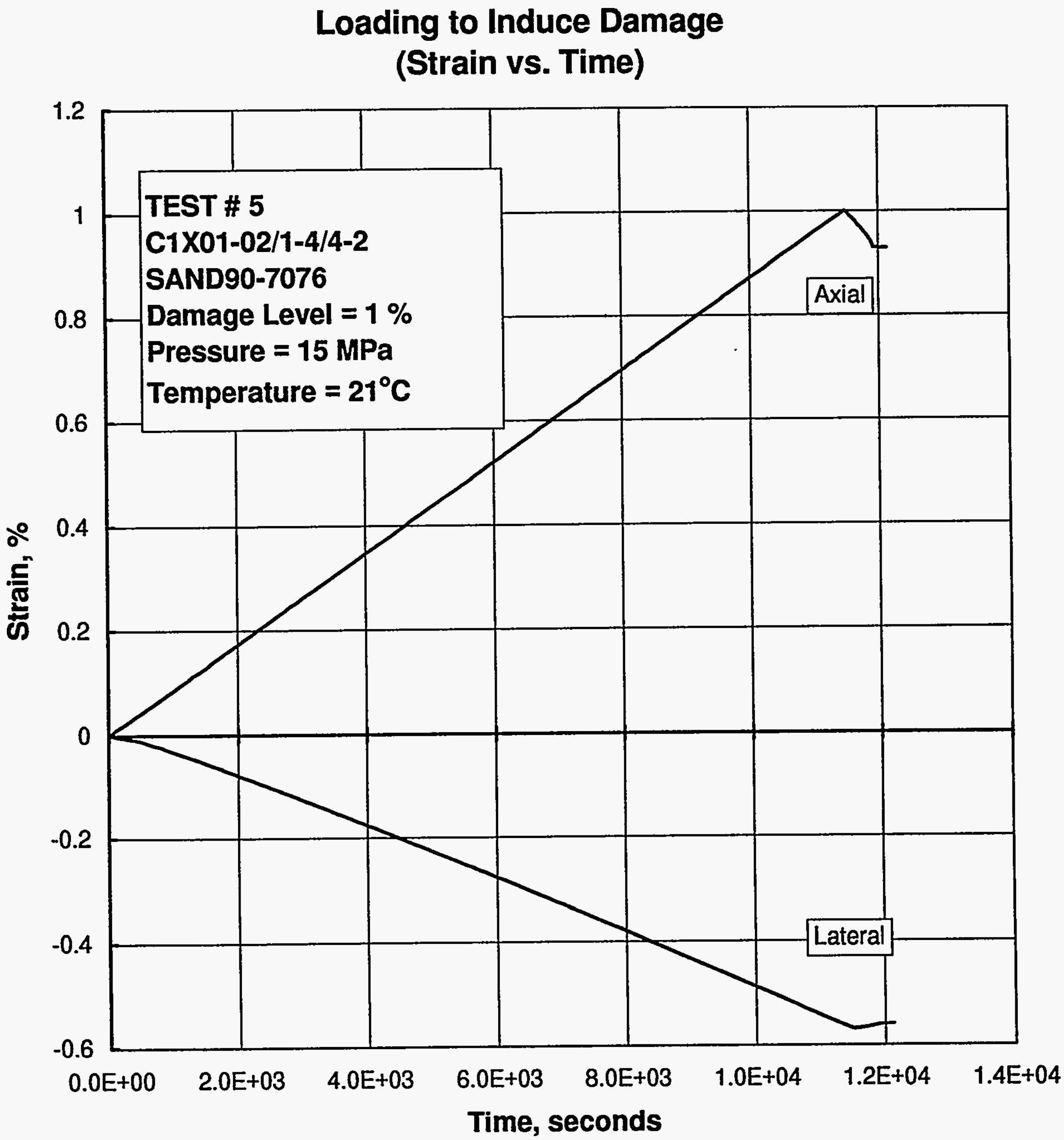

Figure E-84. Axial and Lateral Strain as a Function of Time During the Quasi-Static Loading to Induce Damage in Specimen C1X01-02/1-4/4-2.

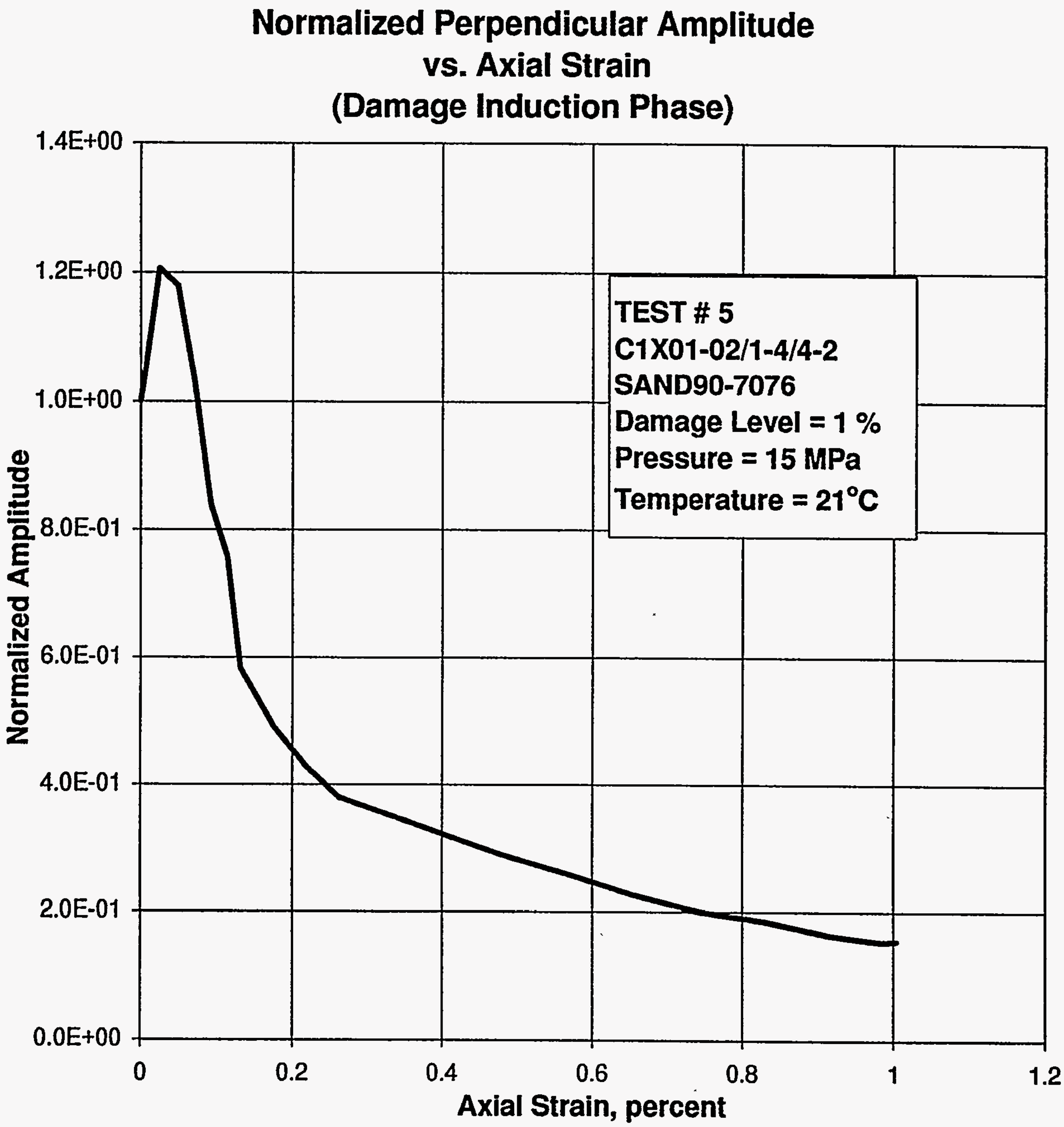

Figure E-85. Normalized Perpendicular Amplitude as a Function of Axial Strain During the Quasi-Static Loading to Induce Damage in Specimen C1X01-02/1-4/4-2.

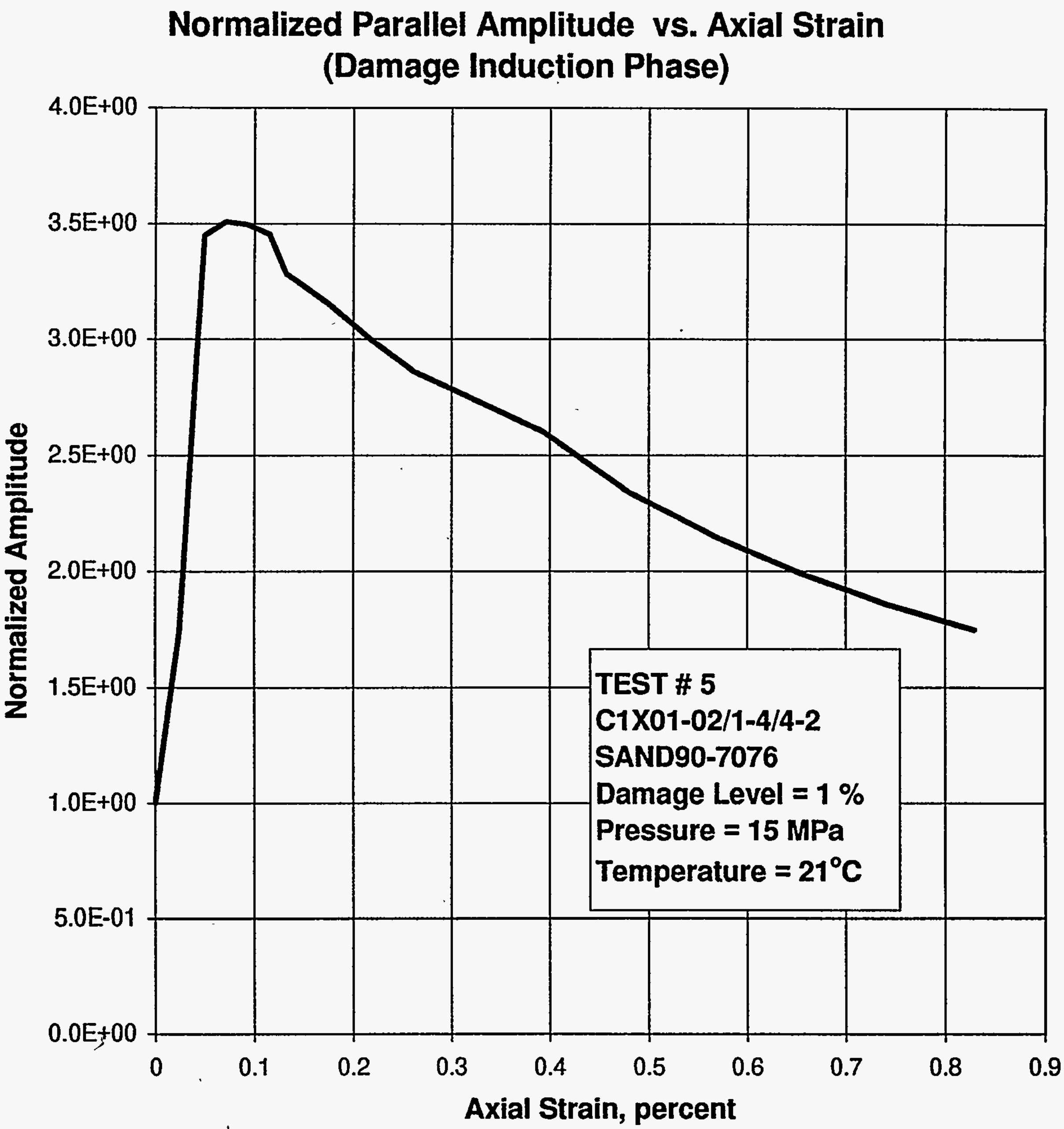

Figure E-86. Normalized Parallel Amplitude as a Function of Axial Strain During the Quasi-Static Loading to Induce Damage in Specimen C1X01-02/1-4/4-2.

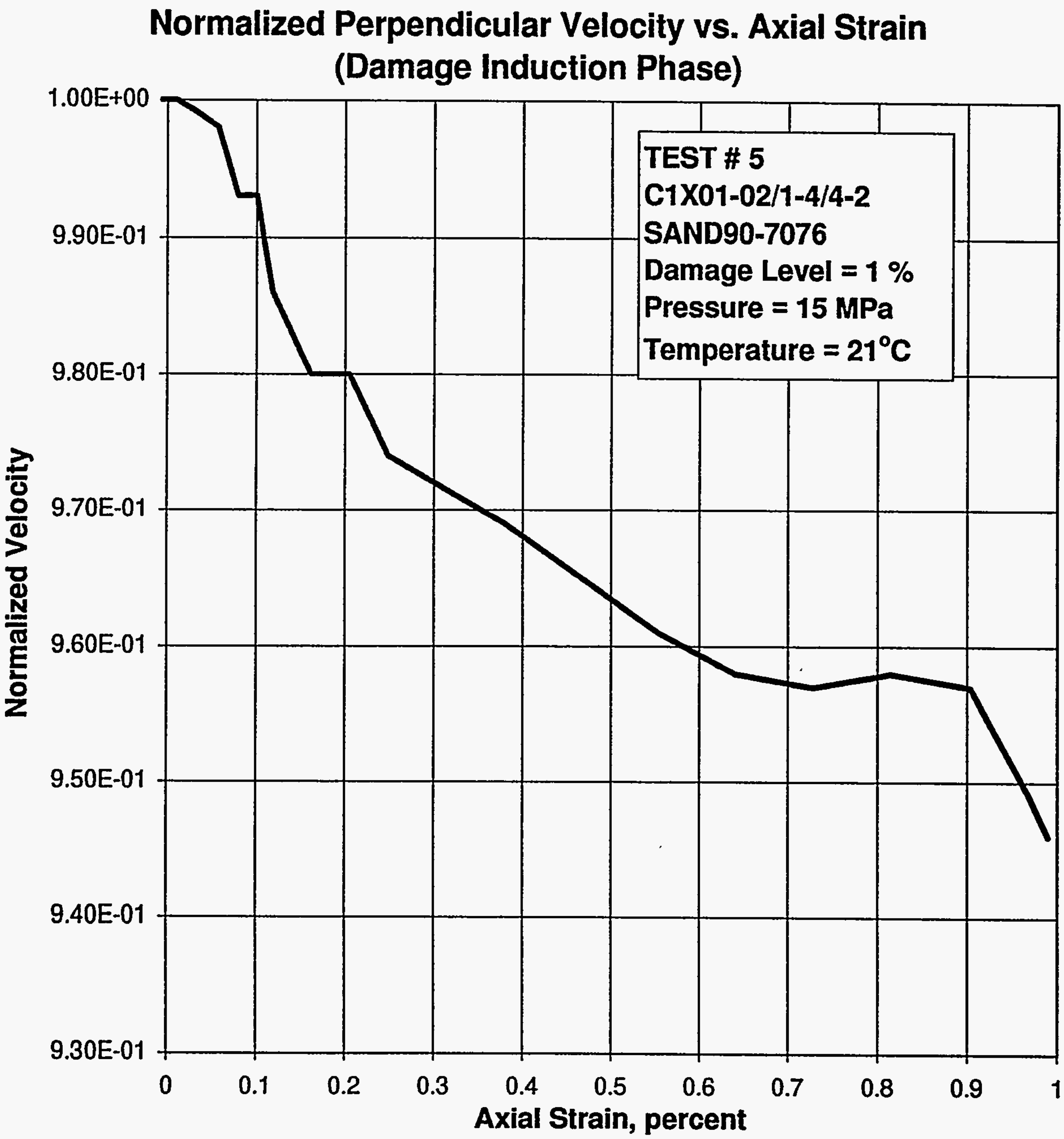

Figure E-87. Normalized Perpendicular Velocity as a Function of Axial Strain During the Quasi-Static Loading to Induce Damage in Specimen C1X01-02/1-4/4-2.

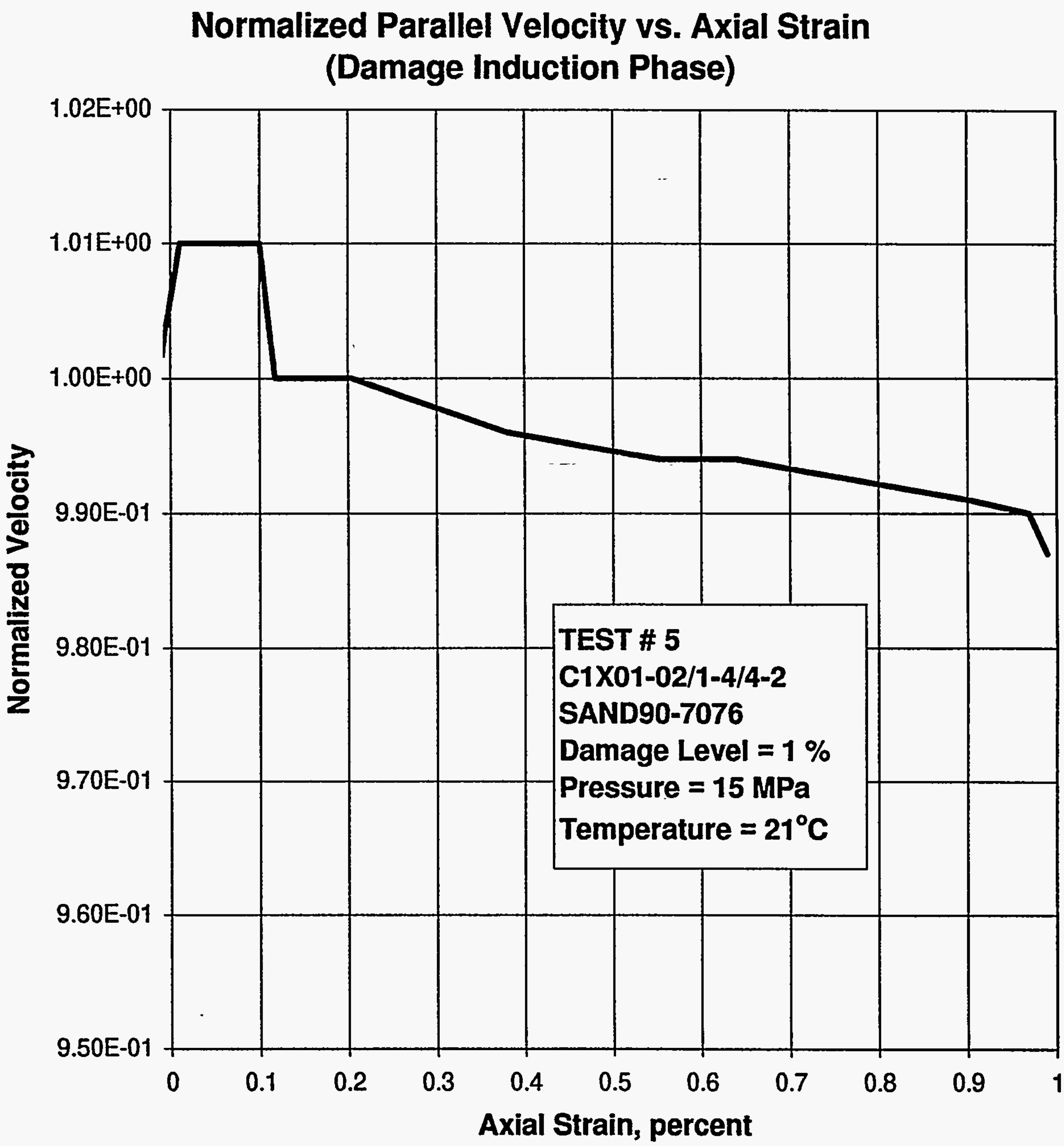

Figure E-88. Normalized Parallel Velocity as a Function of Axial Strain During the Quasi-Static Loading to Induce Damage in Specimen C1X01-02/1-4/4-2.

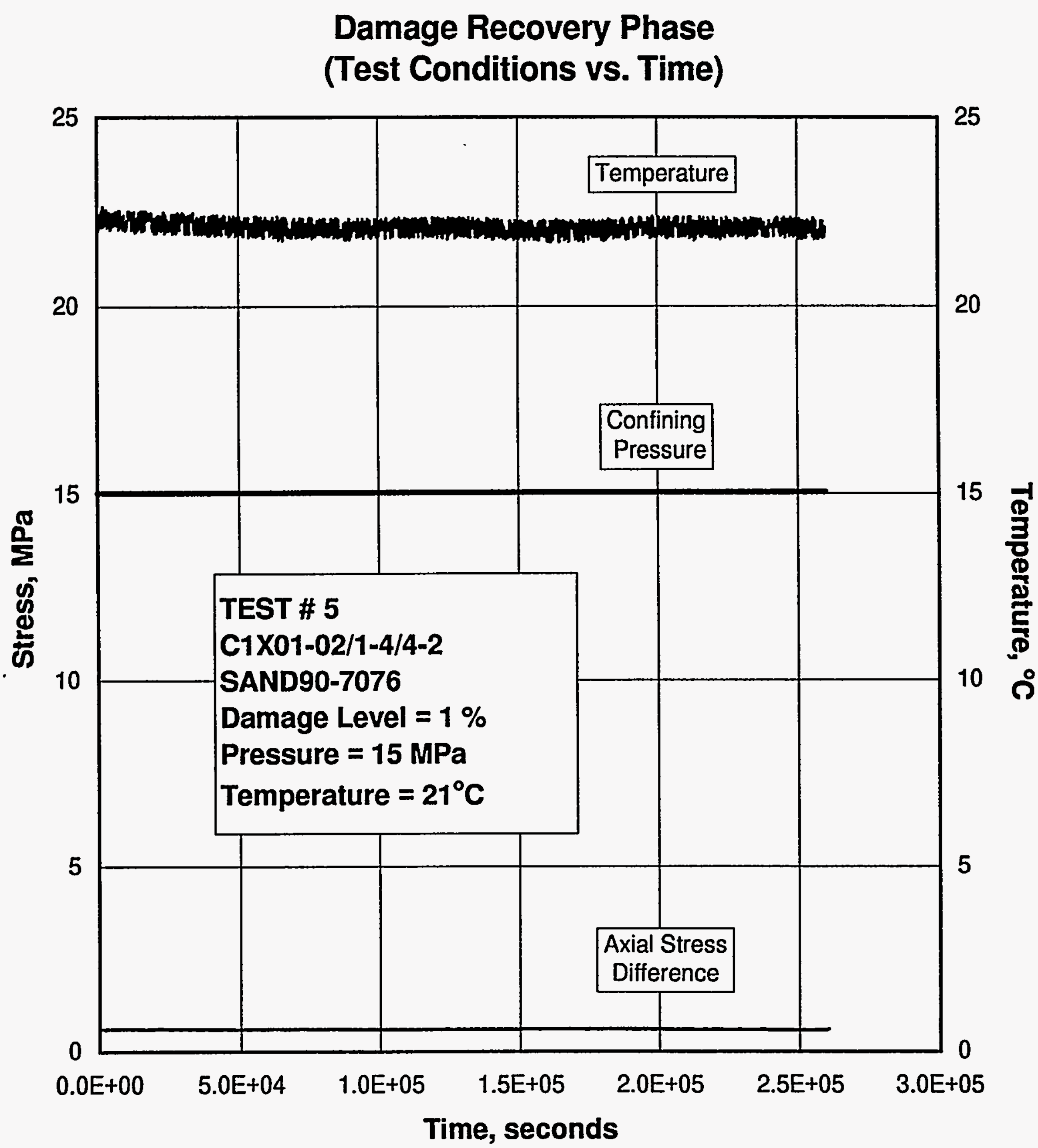

Figure E-89. Test Conditions as a Function of Time During the Hydrostatic Loading to Recover Damage in Specimen C1X01-02/1-4/4-2.

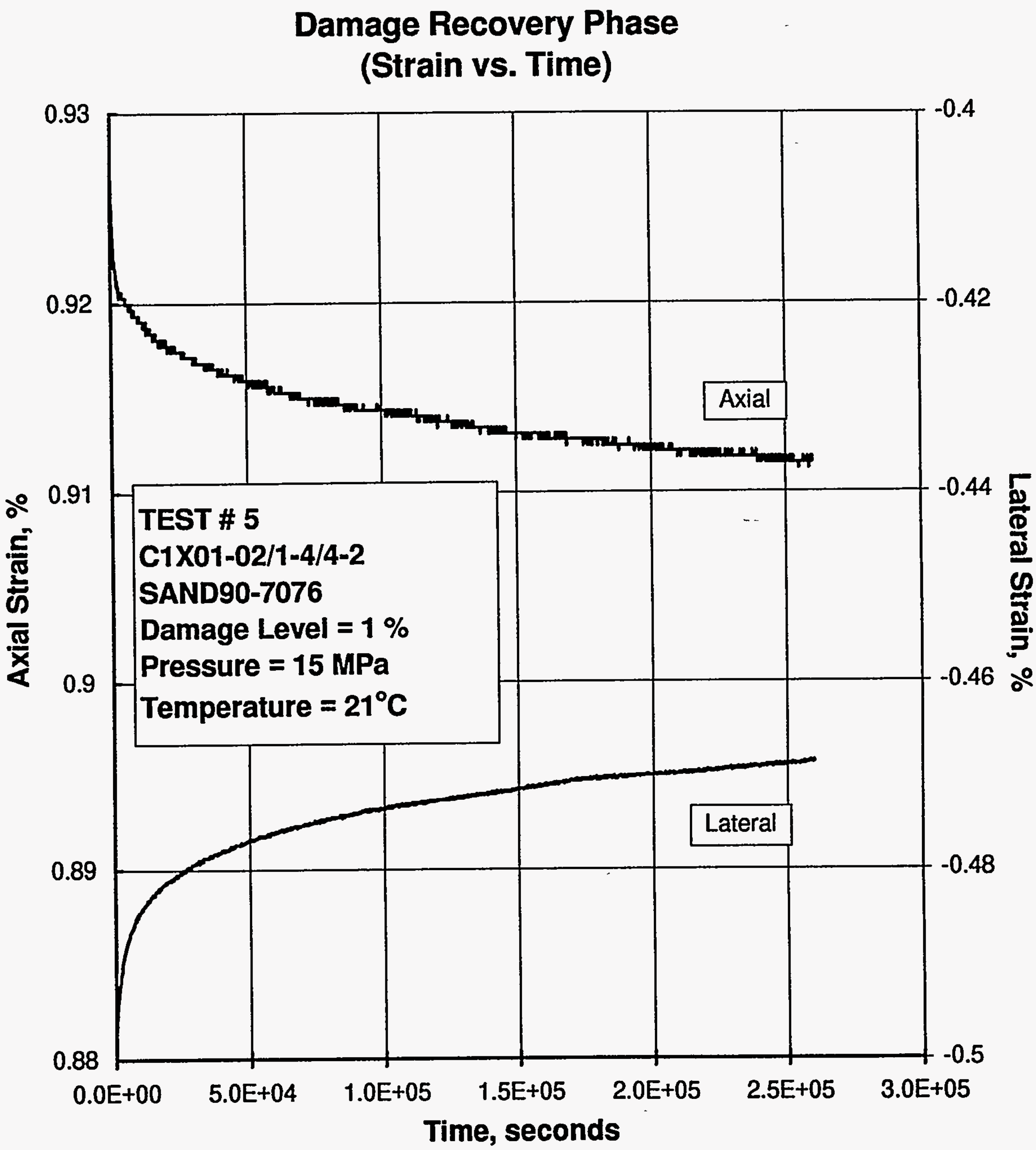

Figure E-90. Axial and Lateral Strain as a Function of Time During the Hydrostatic Loading to Recover Damage in Specimen C1X01-02/1-4/4-2.

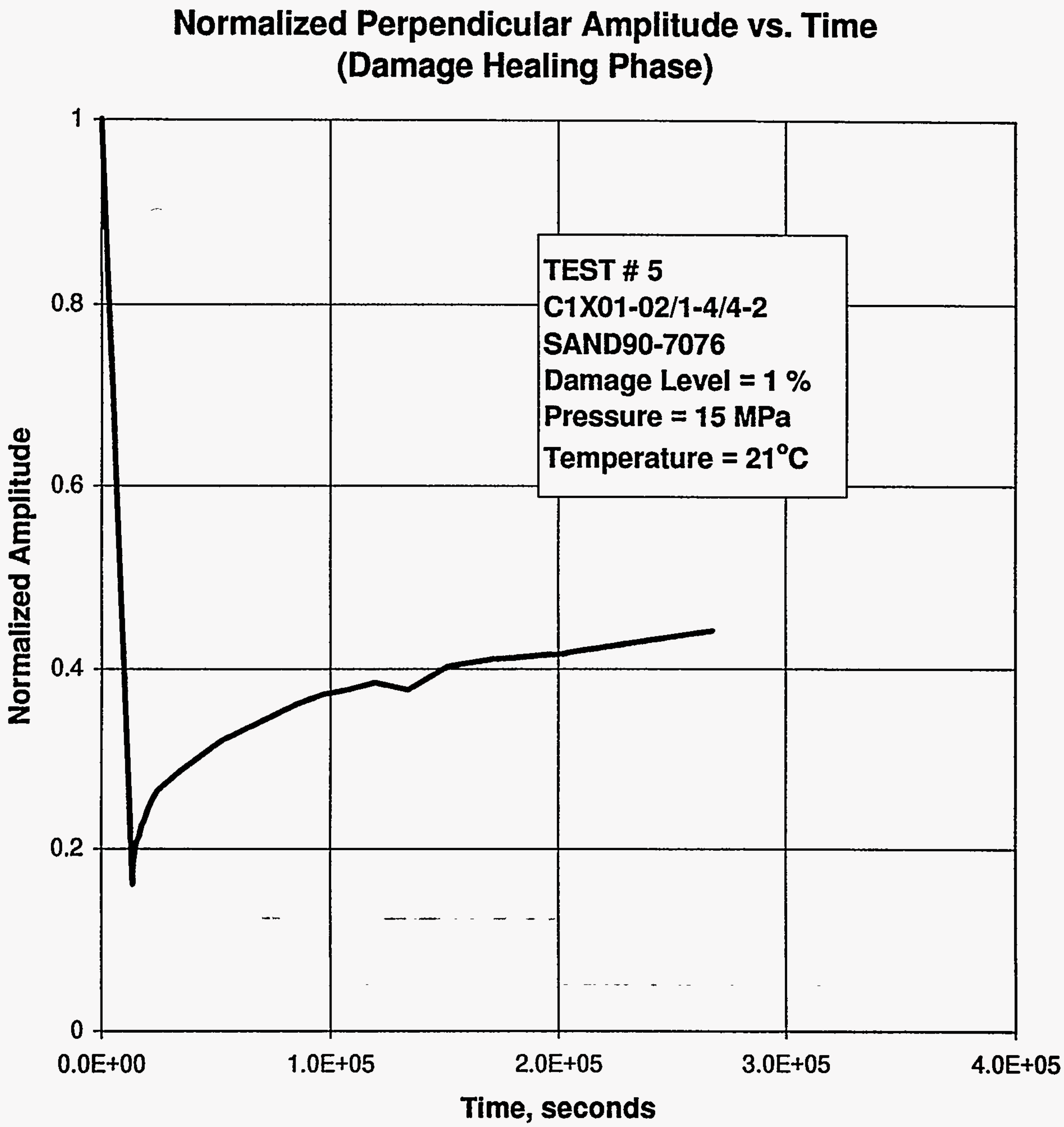

Figure E-91. Normalized Perpendicular Amplitude as a Function of Time During the Hydrostatic Loading to Recover Damage in Specimen C1X01-02/1-4/4-2.

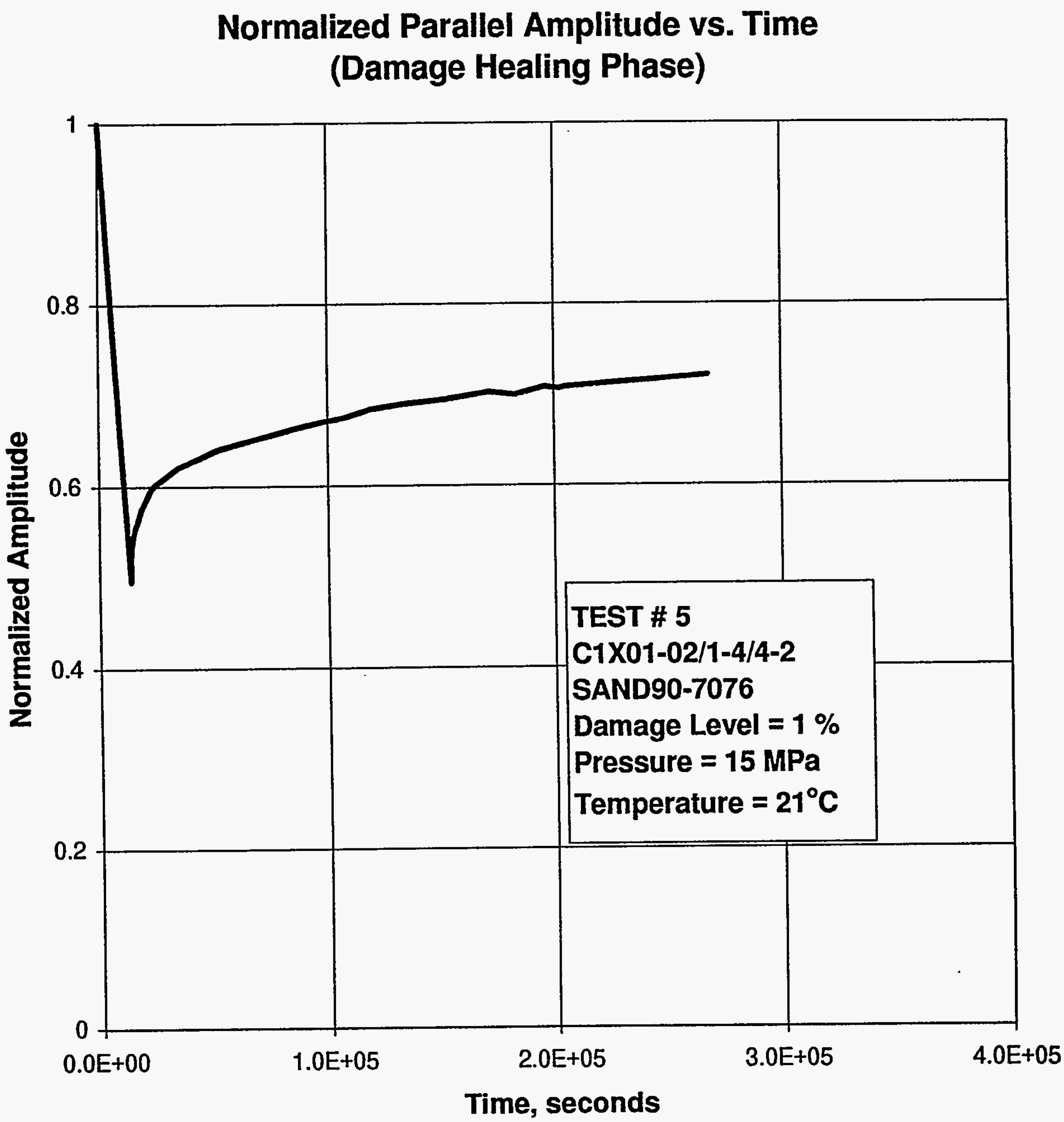

Figure E-92. Normalized Parallel Amplitude as a Function of Time During the Hydrostatic Loading to Recover Damage in Specimen C1X01-02/1-4/4-2.

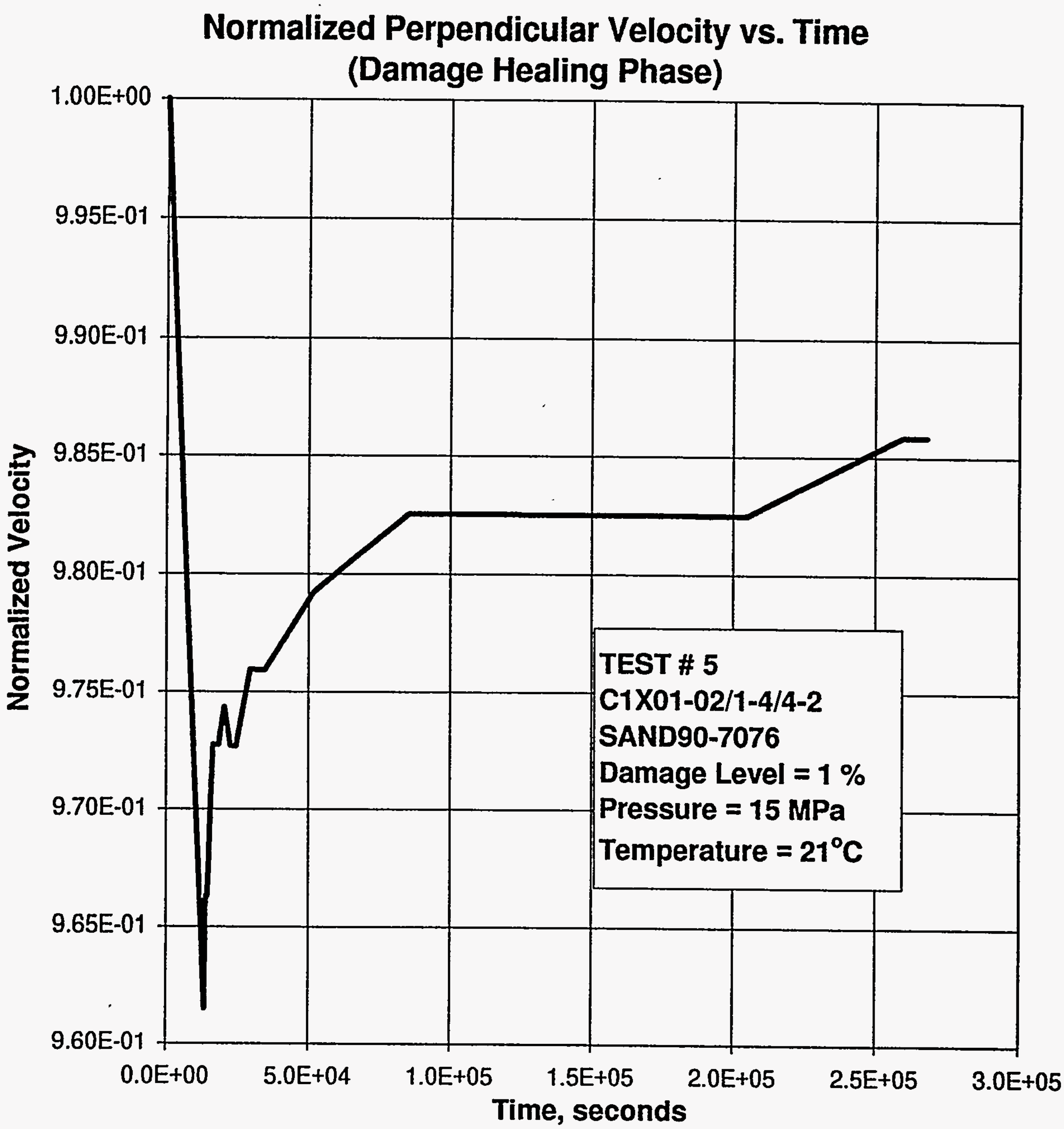

Figure E-93. Normalized Perpendicular Velocity as a Function of Time During the Hydrostatic Loading to Recover Damage in Specimen C1X01-02/1-4/4-2.

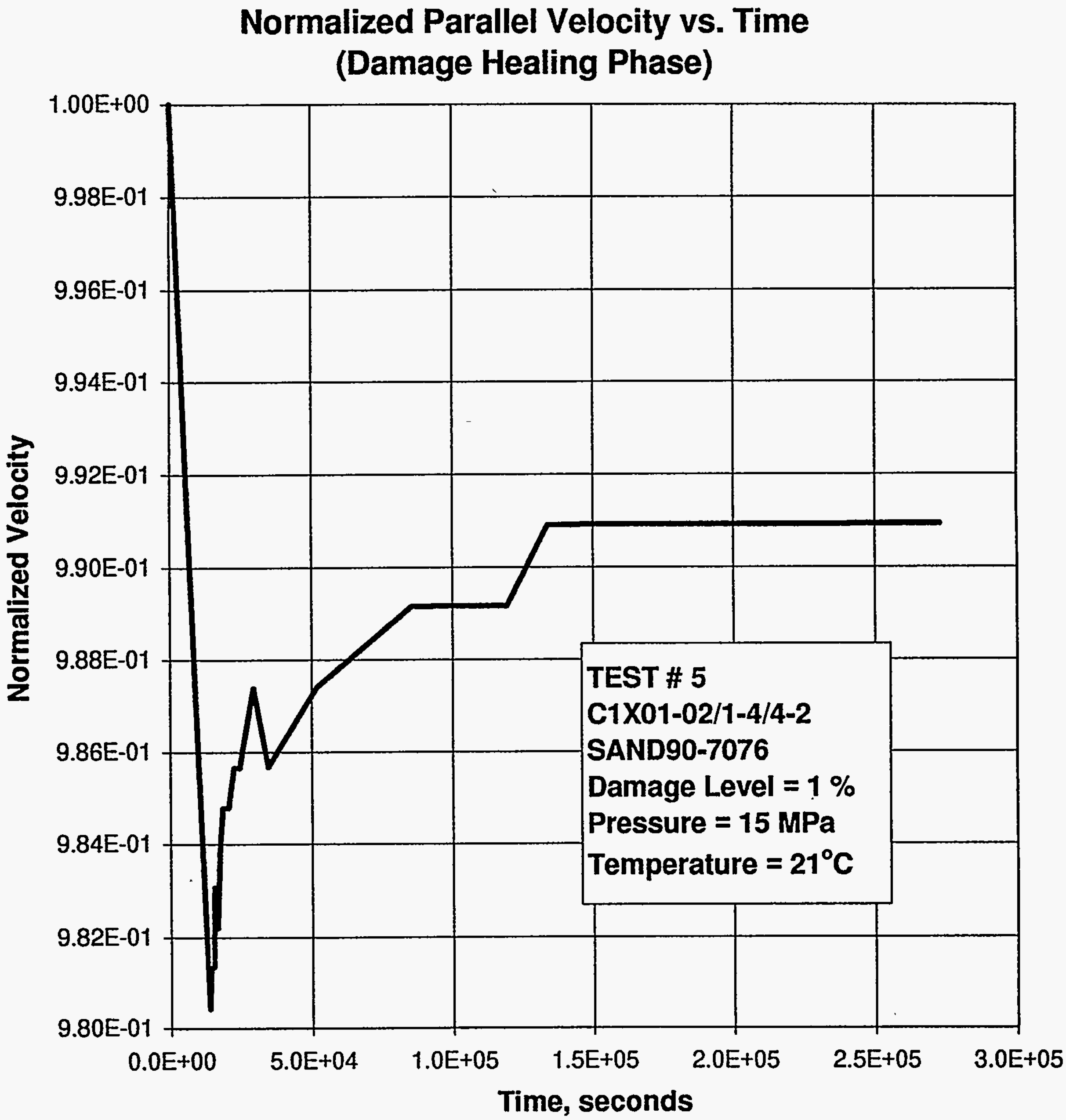

Figure E-94. Normalized Parallel Velocity as a Function of Time During the Hydrostatic Loading to Recover Damage in Specimen C1X01-02/1-4/4-2.

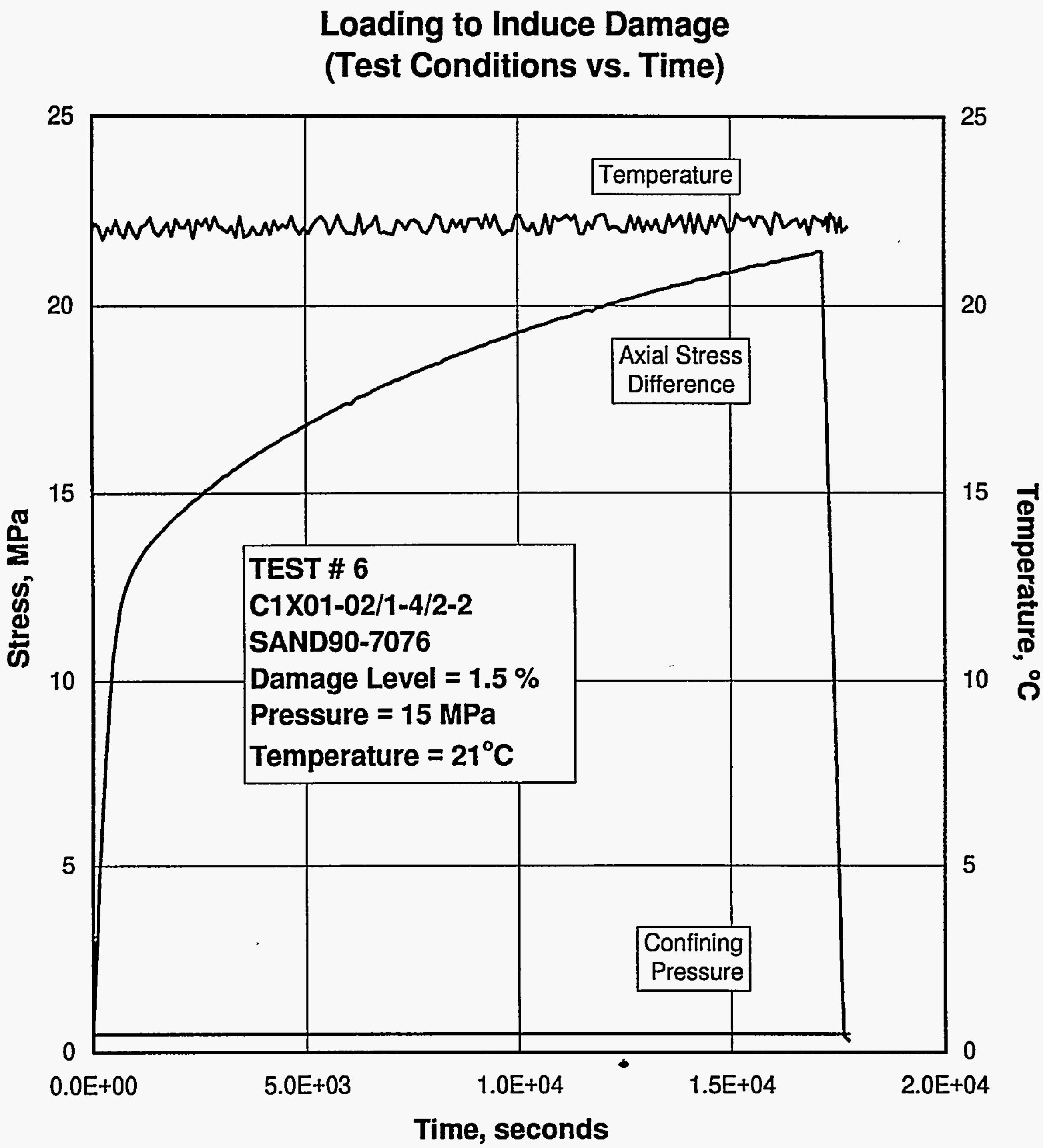

Figure E-95. Test Conditions as a Function of Time During the Quasi-Static Loading to Induce Damage in Specimen C1X01-02/1-4/2-2.

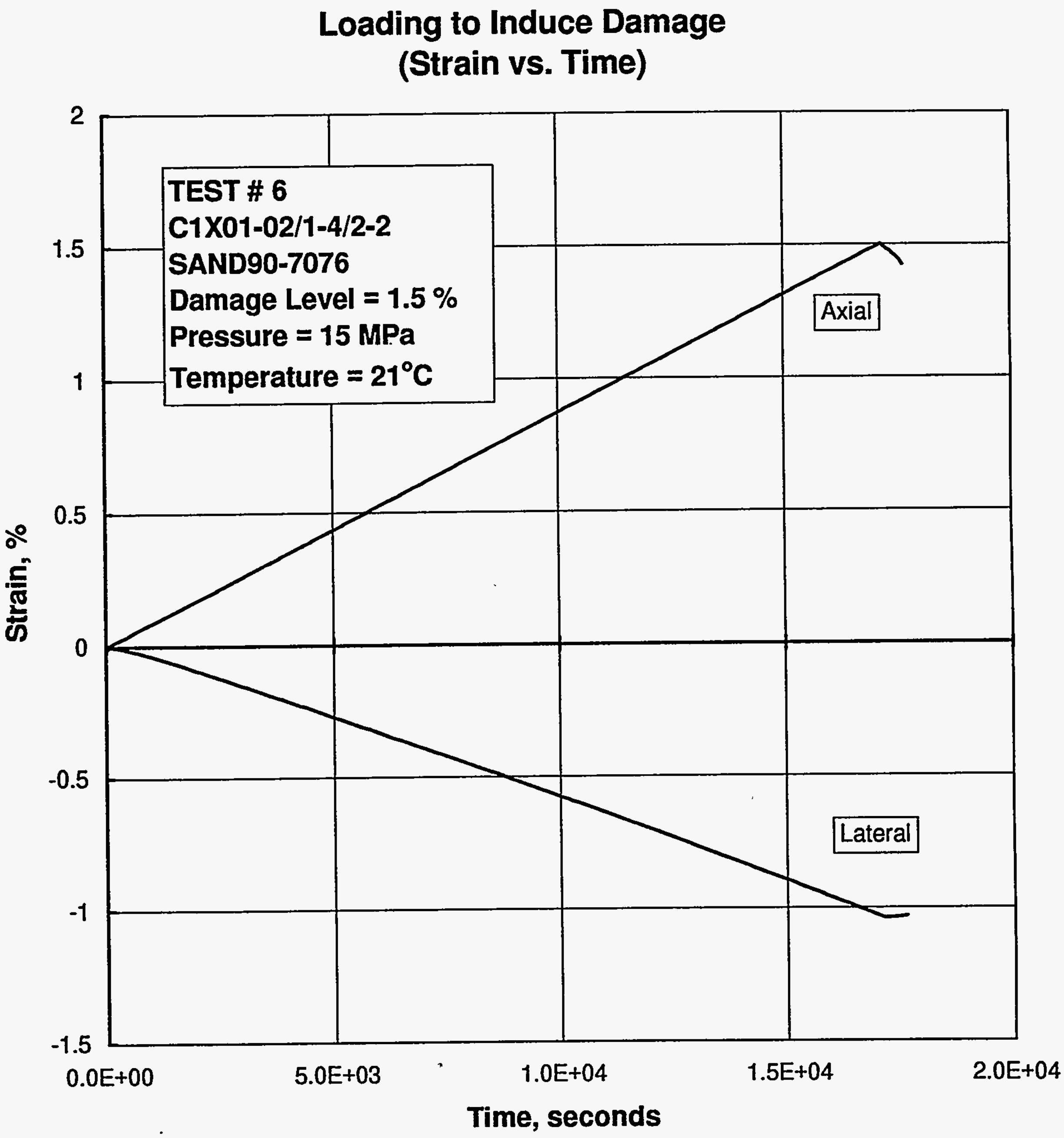

Figure E-96. Axial and Lateral Strain as a Function of Time During the Quasi-Static Loading to Induce Damage in Specimen C1X01-02/1-4/2-2.

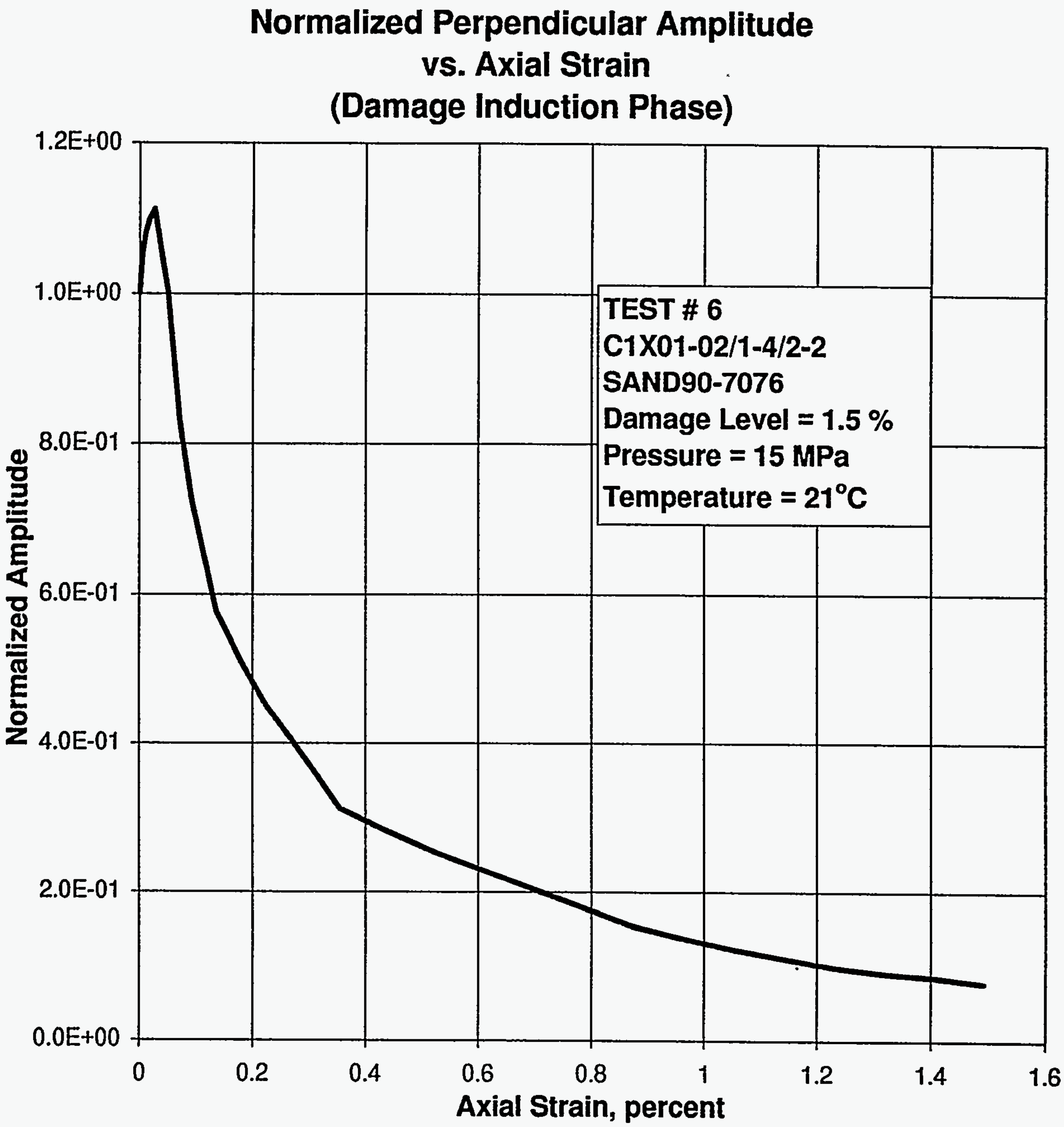

Figure E-97. Normalized Perpendicular Amplitude as a Function of Axial Strain During the Quasi-Static Loading to Induce Damage in Specimen C1X01-02/1-4/2-2.

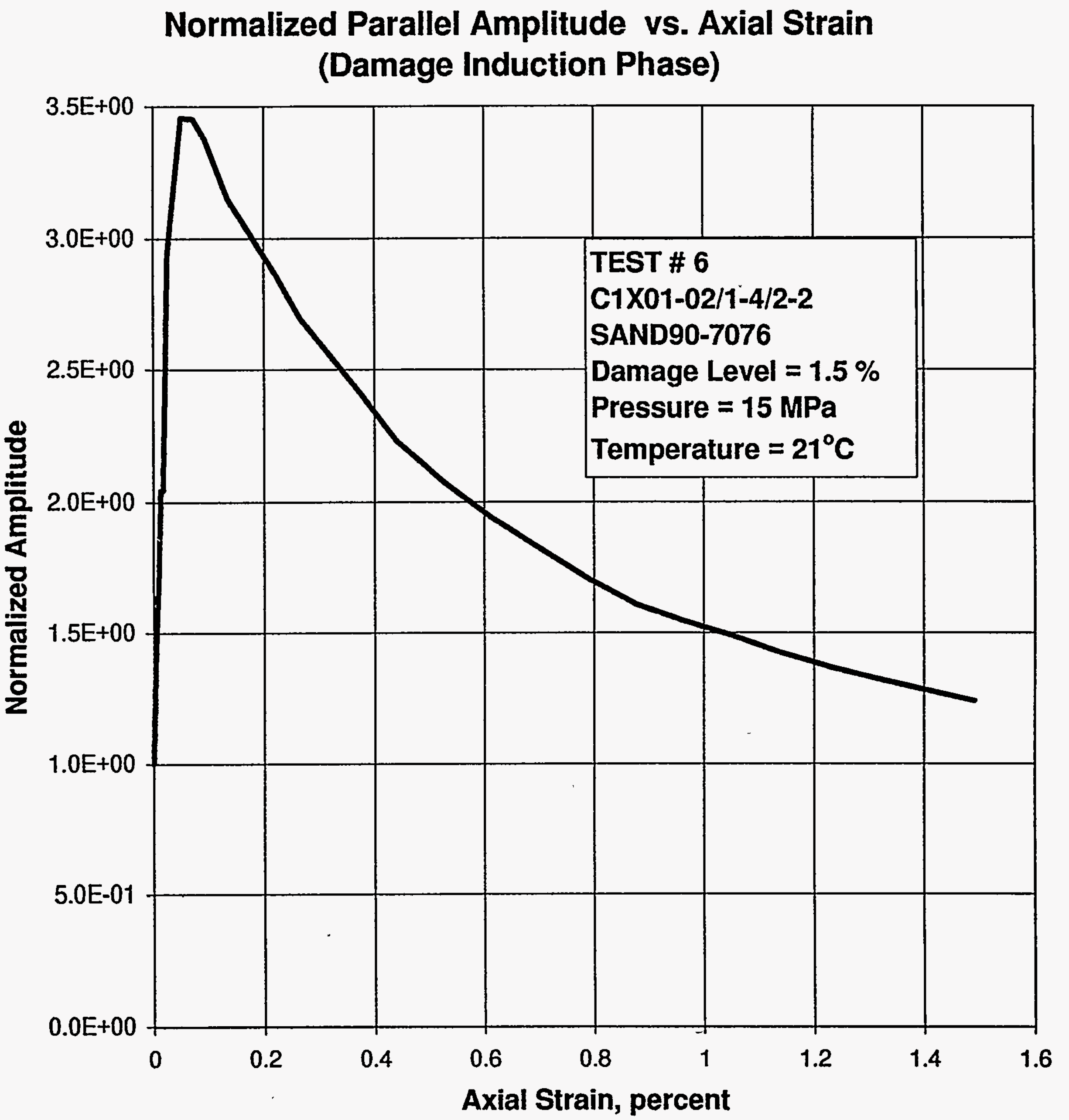

Figure E-98. Normalized Parallel Amplitude as a Function of Axial Strain During the Quasi-Static Loading to Induce Damage in Specimen C1X01-02/1-4/2-2.

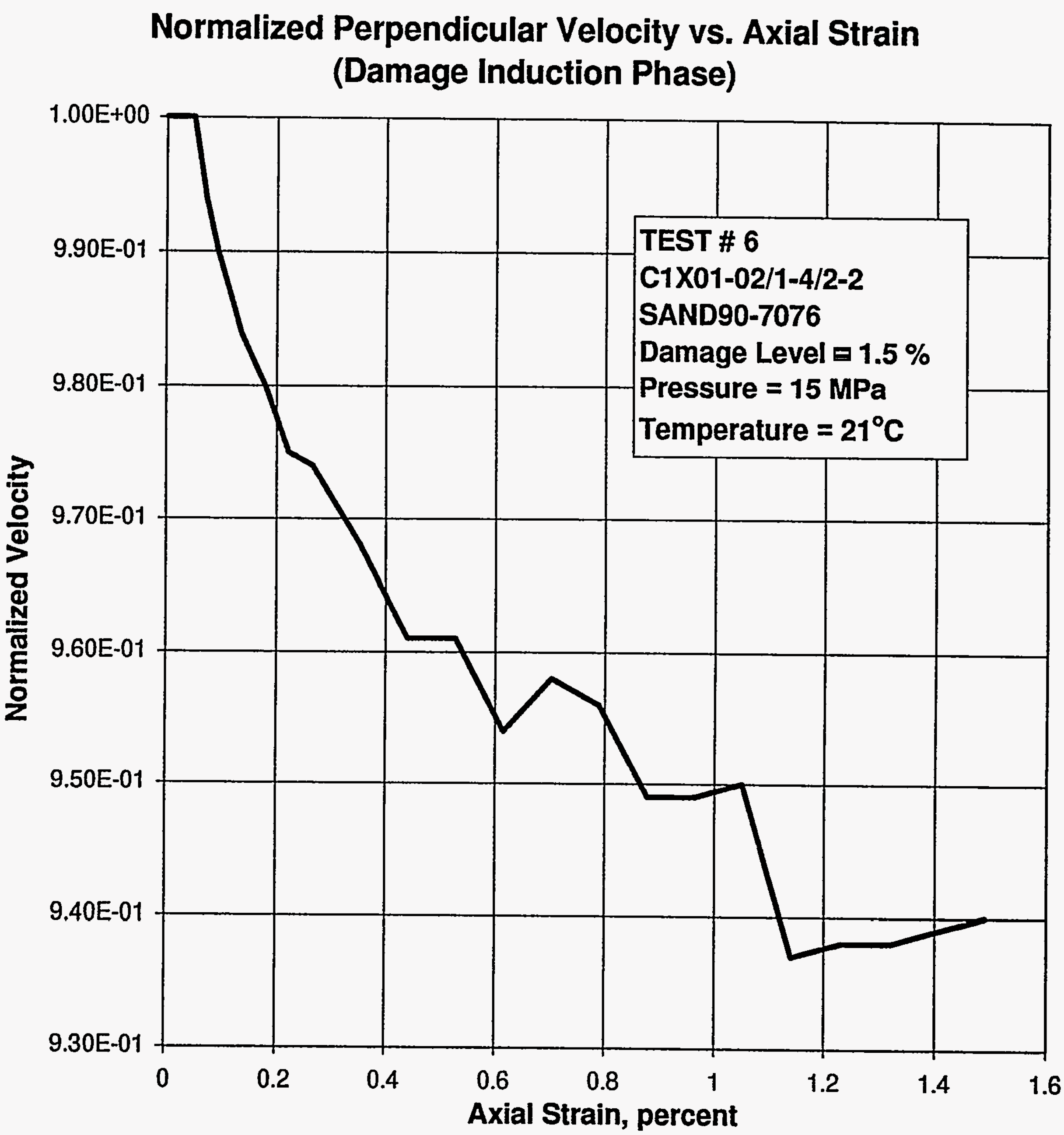

Figure E-99. Normalized Perpendicular Velocity as a Function of Axial Strain During the Quasi-Static Loading to Induce Damage in Specimen C1X01-02/1-4/2-2.

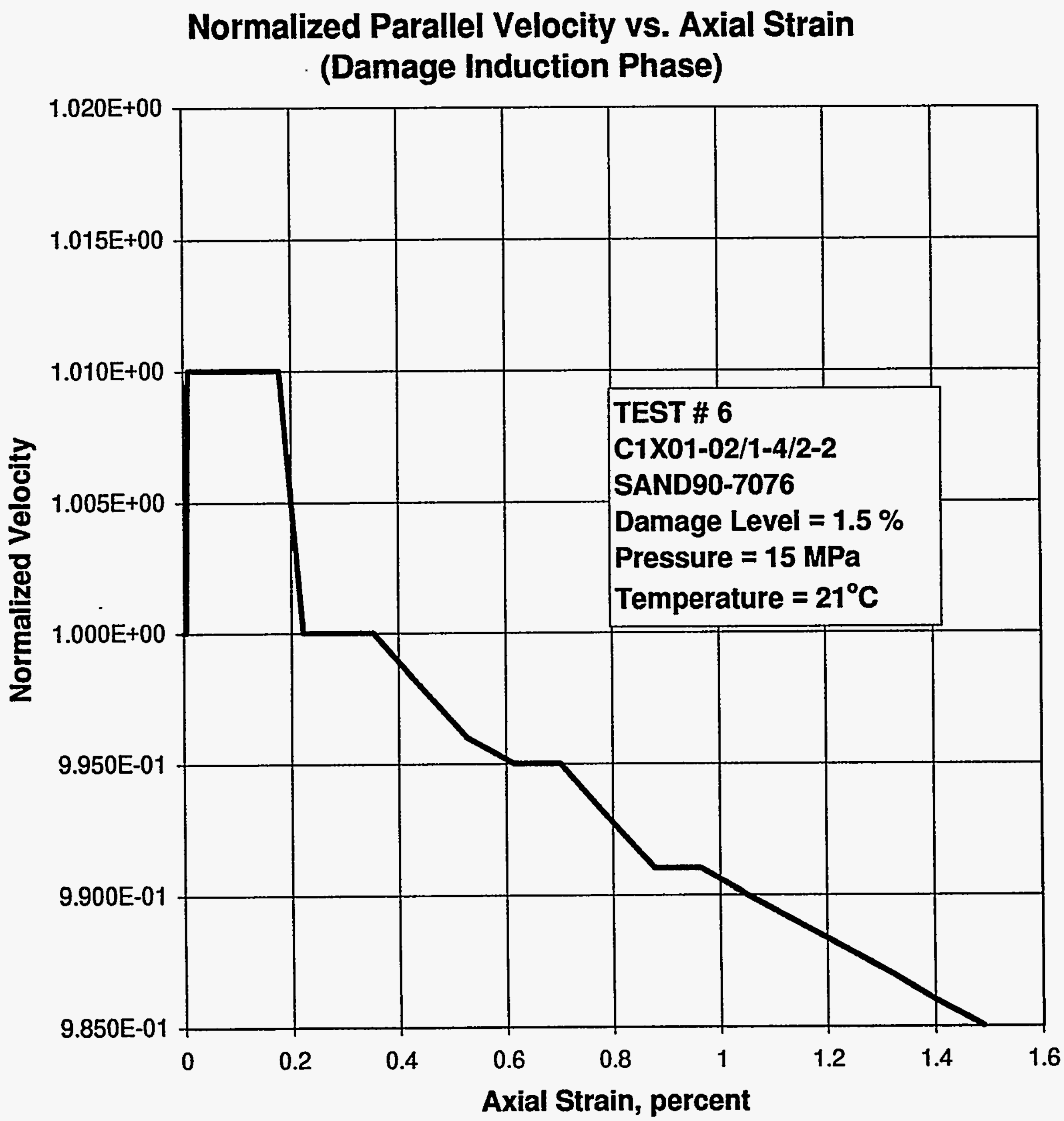

Figure E-100. Normalized Parallel Velocity as a Function of Axial Strain During the Quasi-Static Loading to Induce Damage in Specimen C1X01-02/1-4/2-2.

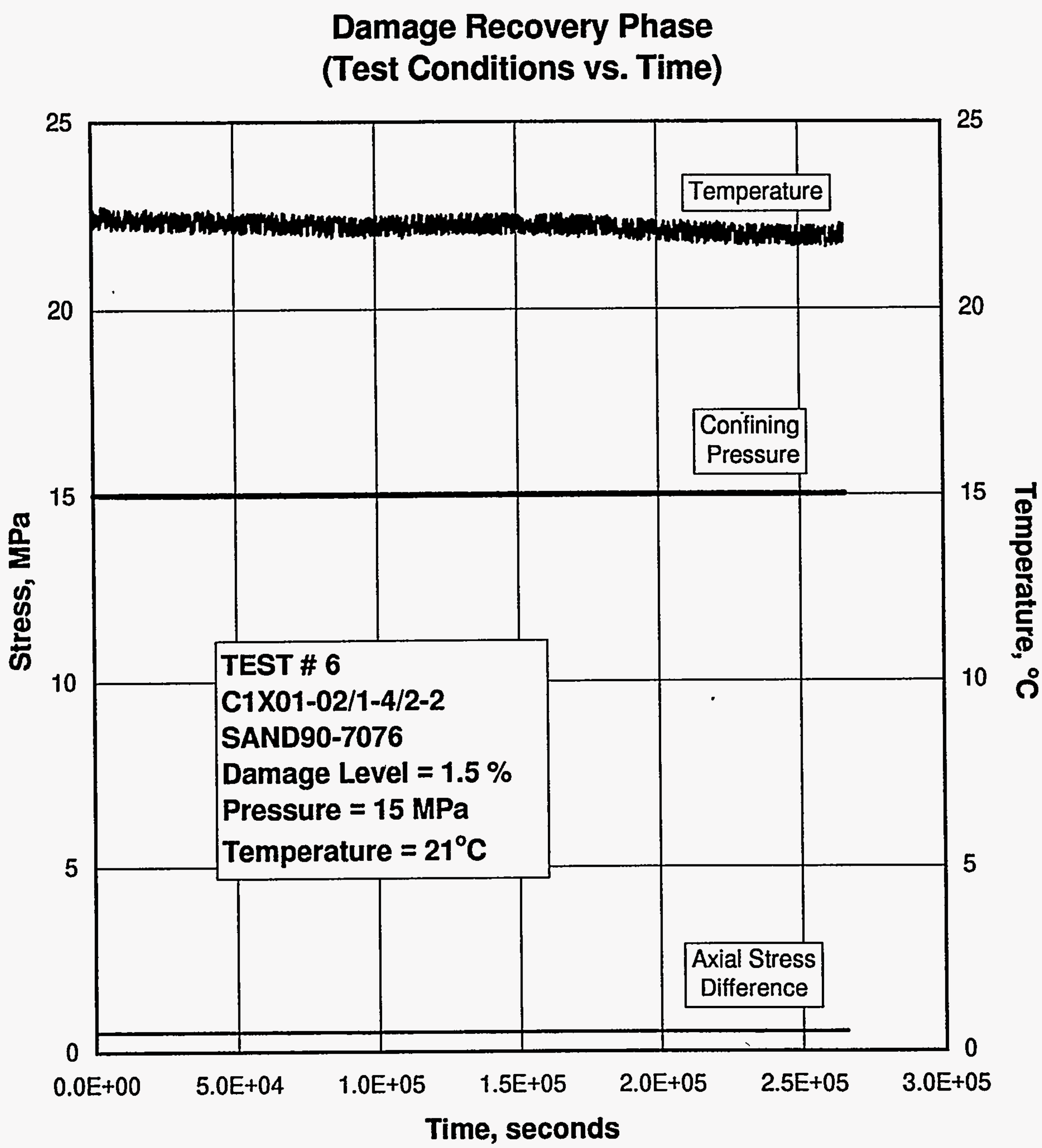

Figure E-101. Test Conditions as a Function of Time During the Hydrostatic Loading to Recover Damage in Specimen C1X01-02/1-4/2-2.

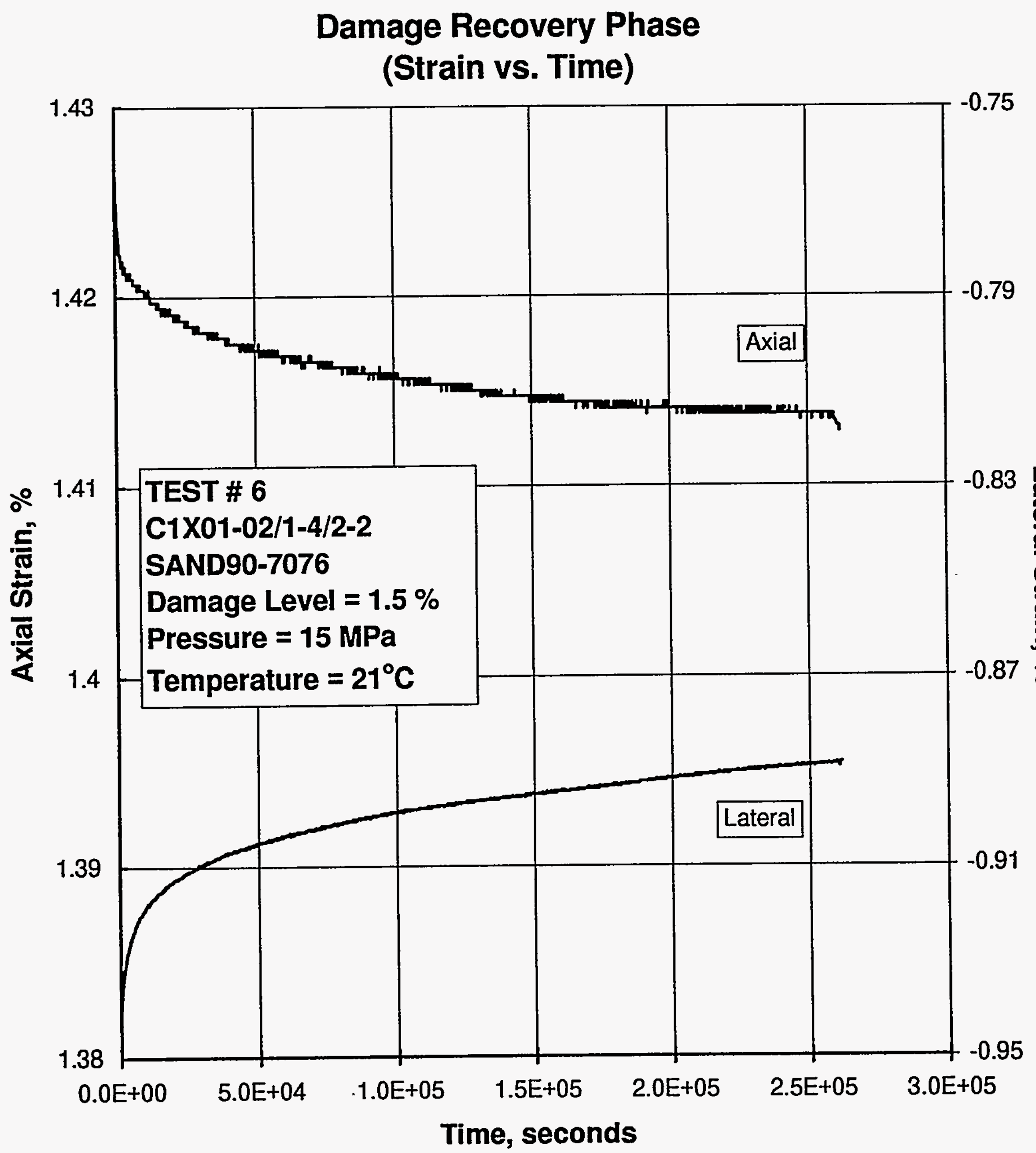

Figure E-102. Axial and Lateral Strain as a Function of Time During the Hydrostatic Loading to Recover Damage in Specimen C1X01-02/1-4/2-2.

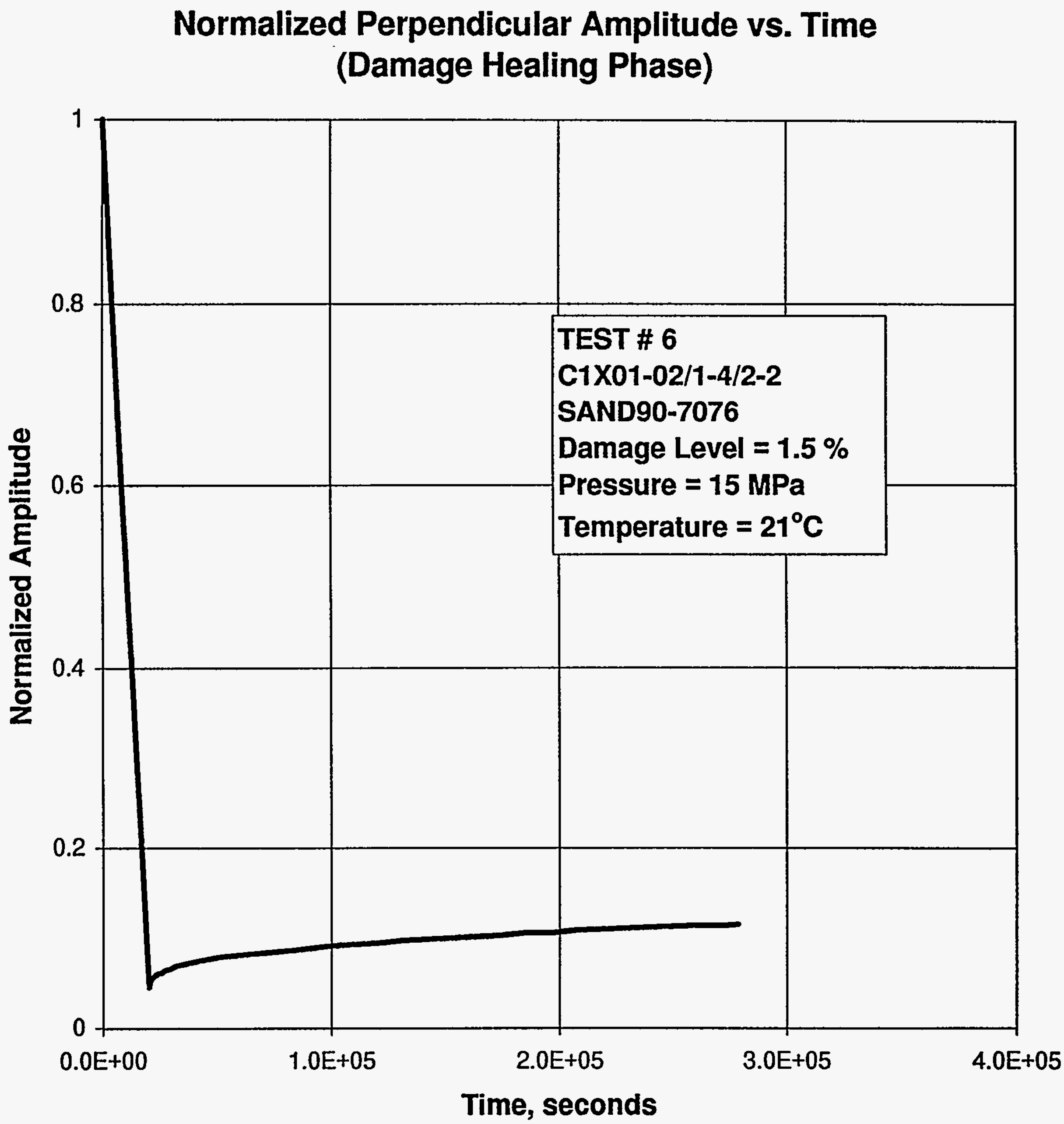

Figure E-103. Normalized Perpendicular Amplitude as a Function of Time During the Hydrostatic Loading to Recover Damage in Specimen C1X01-02/1-4/2-2.

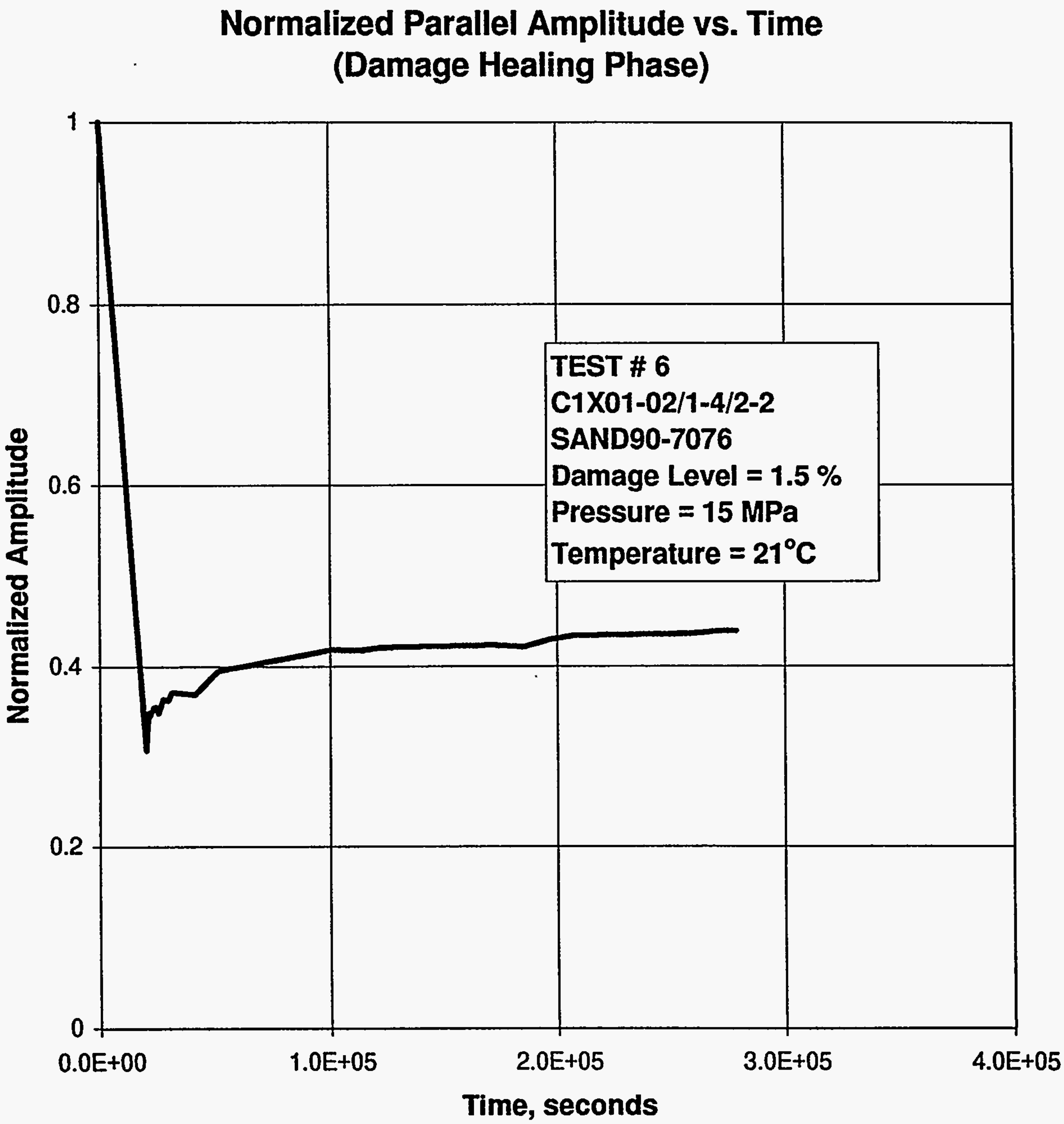

Figure E-104. Normalized Parallel Amplitude as a Function of Time During the Hydrostatic Loading to Recover Damage in Specimen C1X01-02/1-4/2-2.

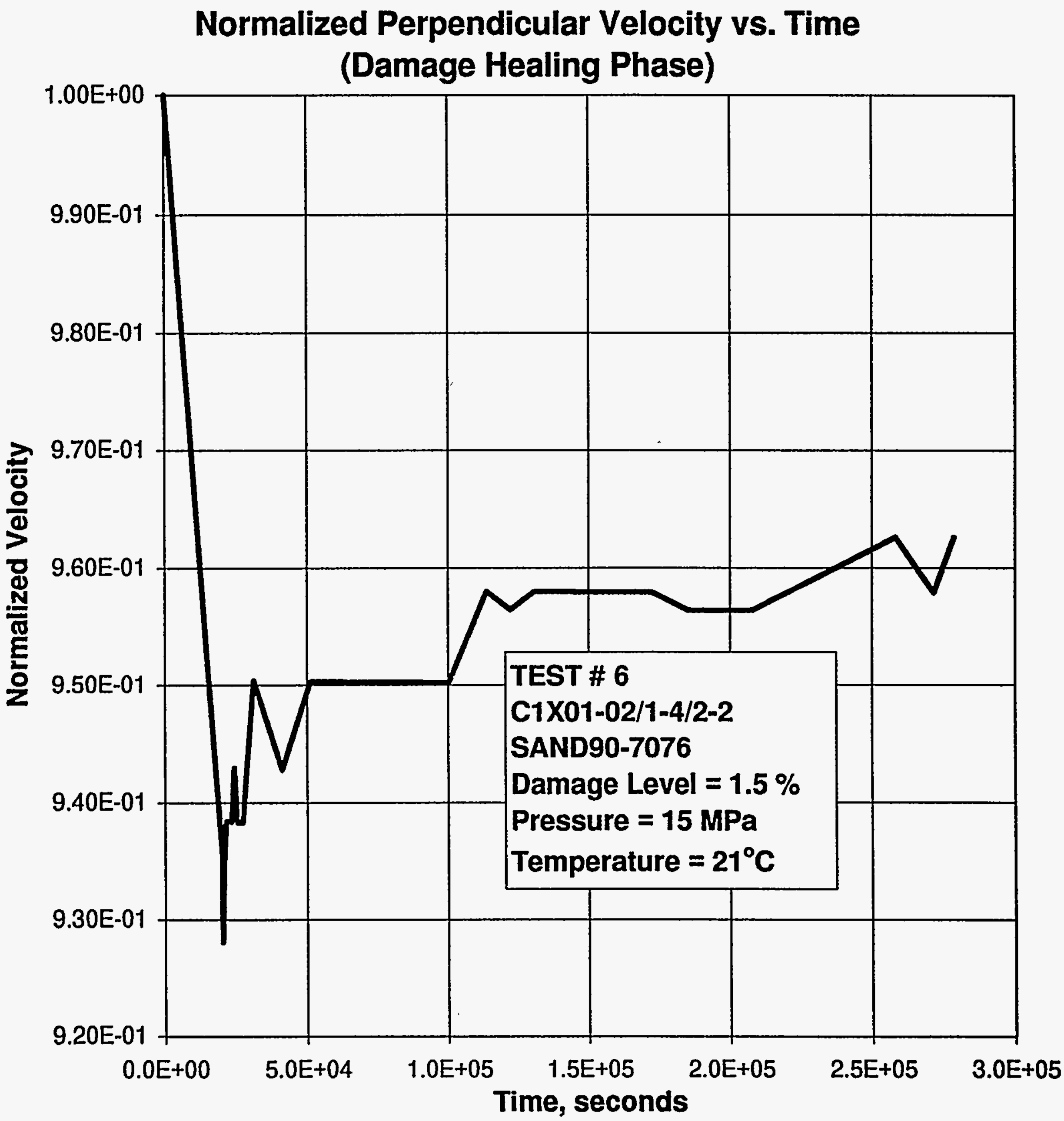

Figure E-105. Normalized Perpendicular Velocity as a Function of Time During the Hydrostatic Loading to Recover Damage in Specimen C1X01-02/1-4/2-2.

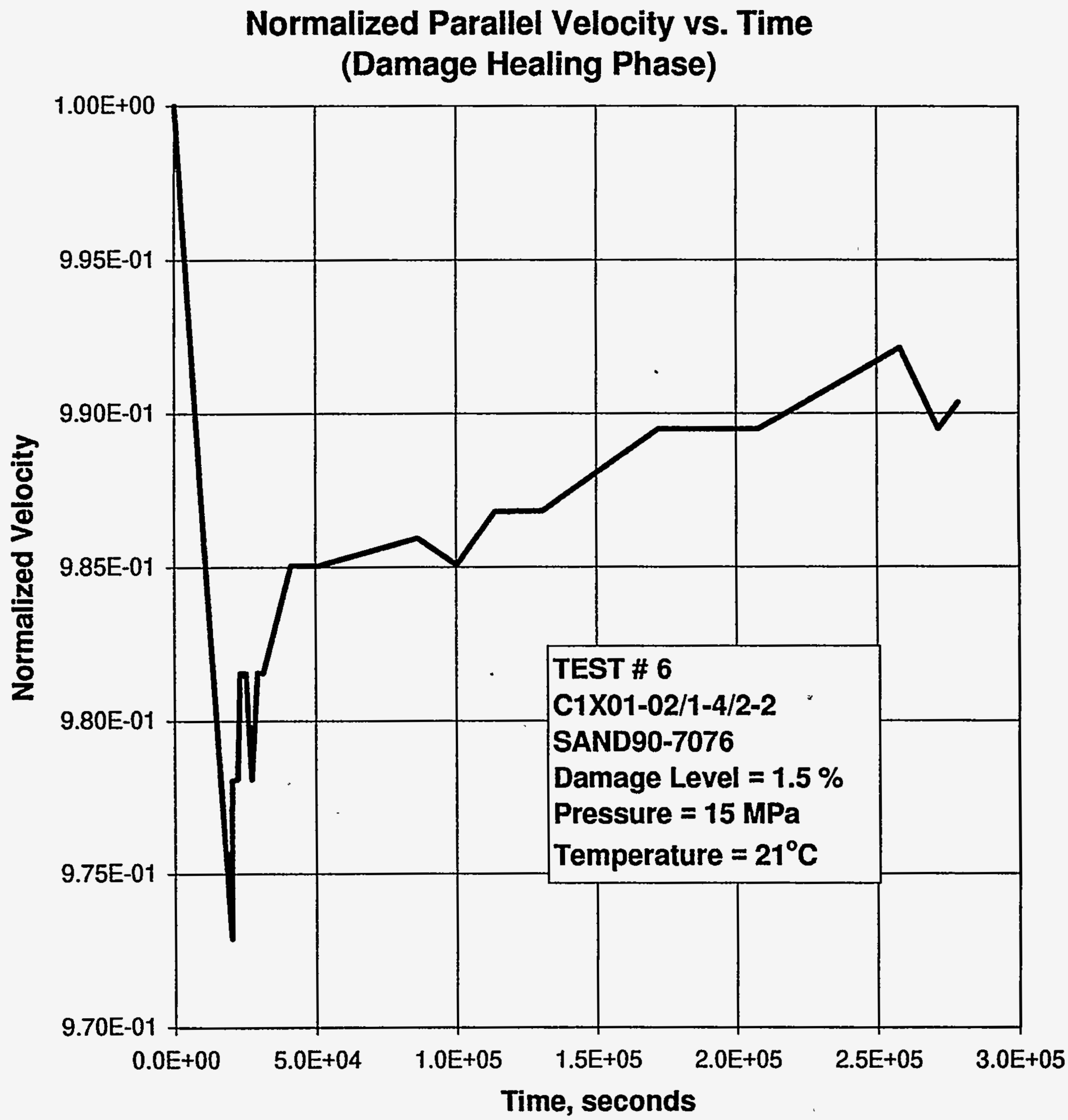

Figure E-106. Normalized Parallel Velocity as a Function of Time During the Hydrostatic Loading to Recover Damage in Specimen C1X01-02/1-4/2-2.

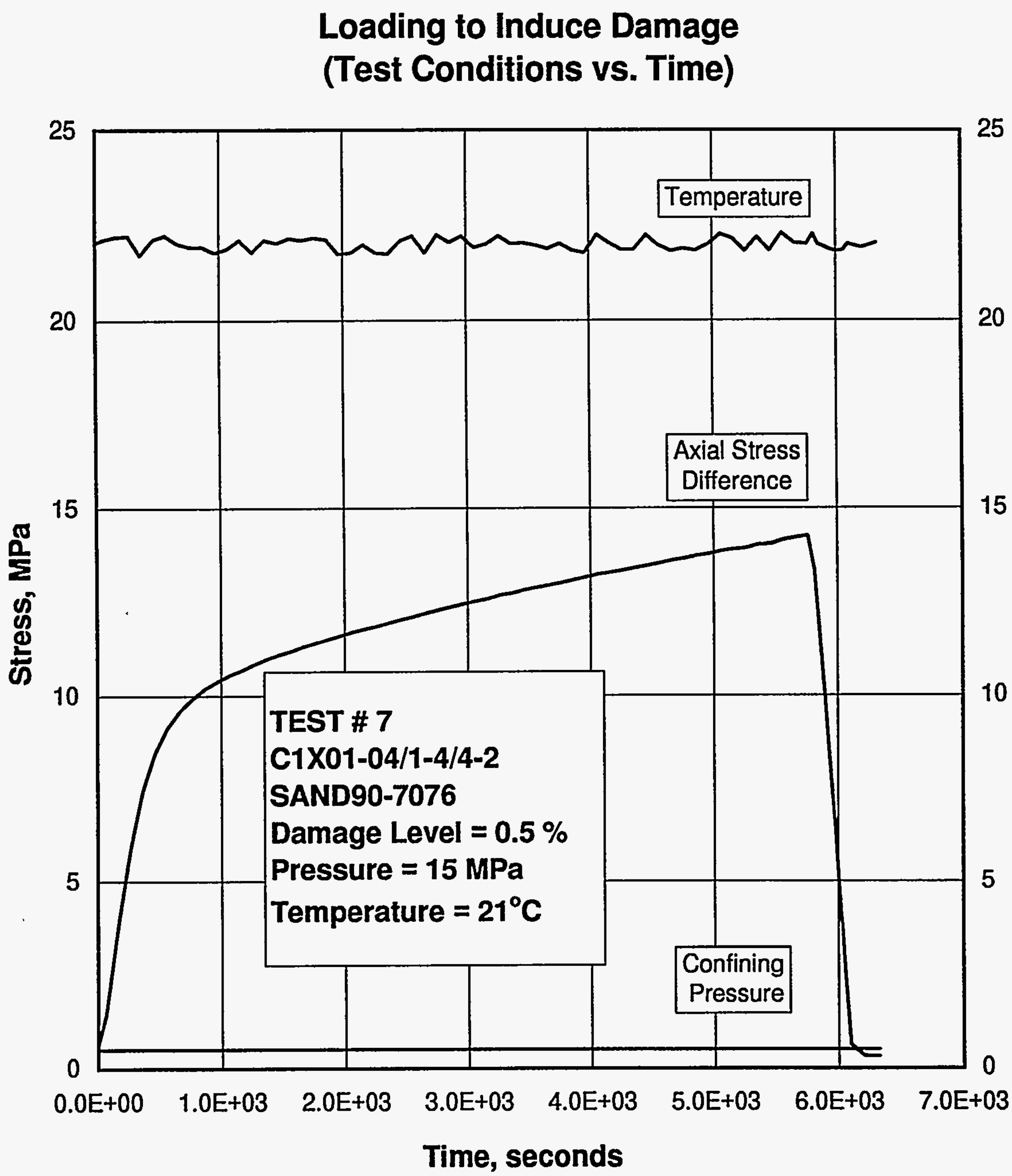

Figure E-107. Test Conditions as a Function of Time During the Quasi-Static Loading to Induce Damage in Specimen C1X01-04/1-4/4-2.

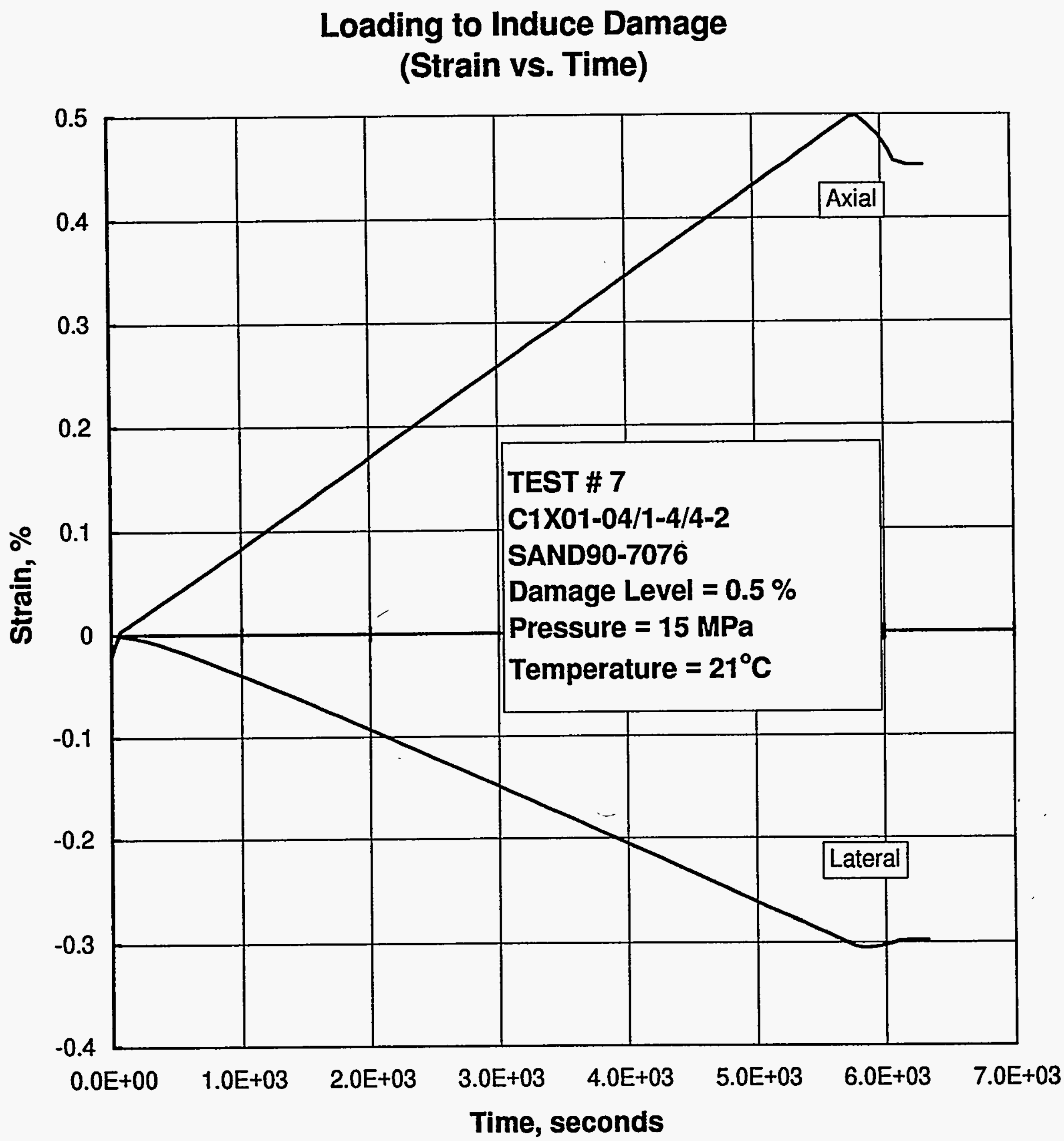

Figure E-108. Axial and Lateral Strain as a Function of Time During the Quasi-Static Loading to Induce Damage in Specimen C1X01-04/1-4/4-2.

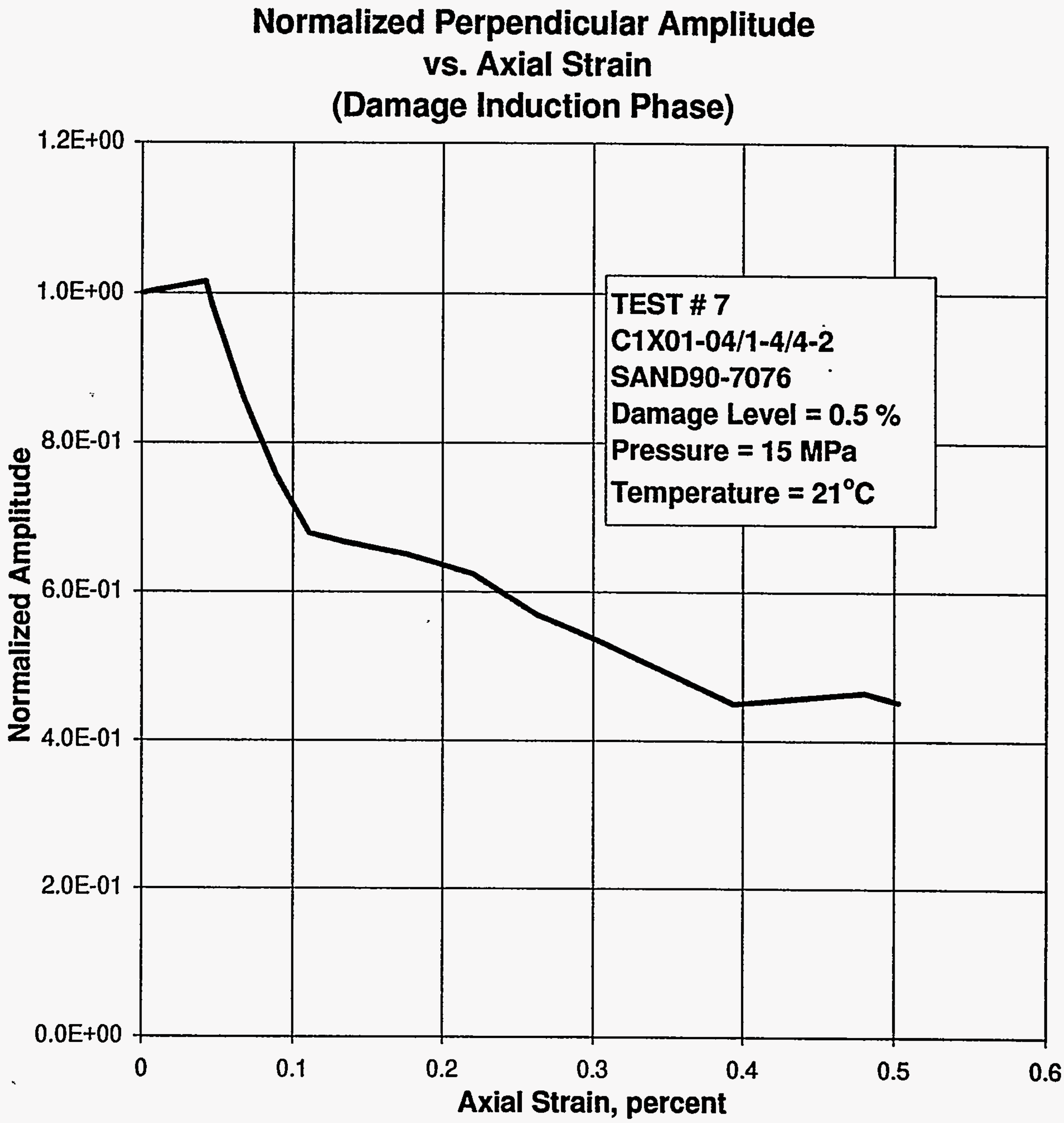

Figure E-109. Normalized Perpendicular Amplitude as a Function of Axial Strain During the Quasi-Static Loading to Induce Damage in Specimen C1X01-04/1-4/4-2.

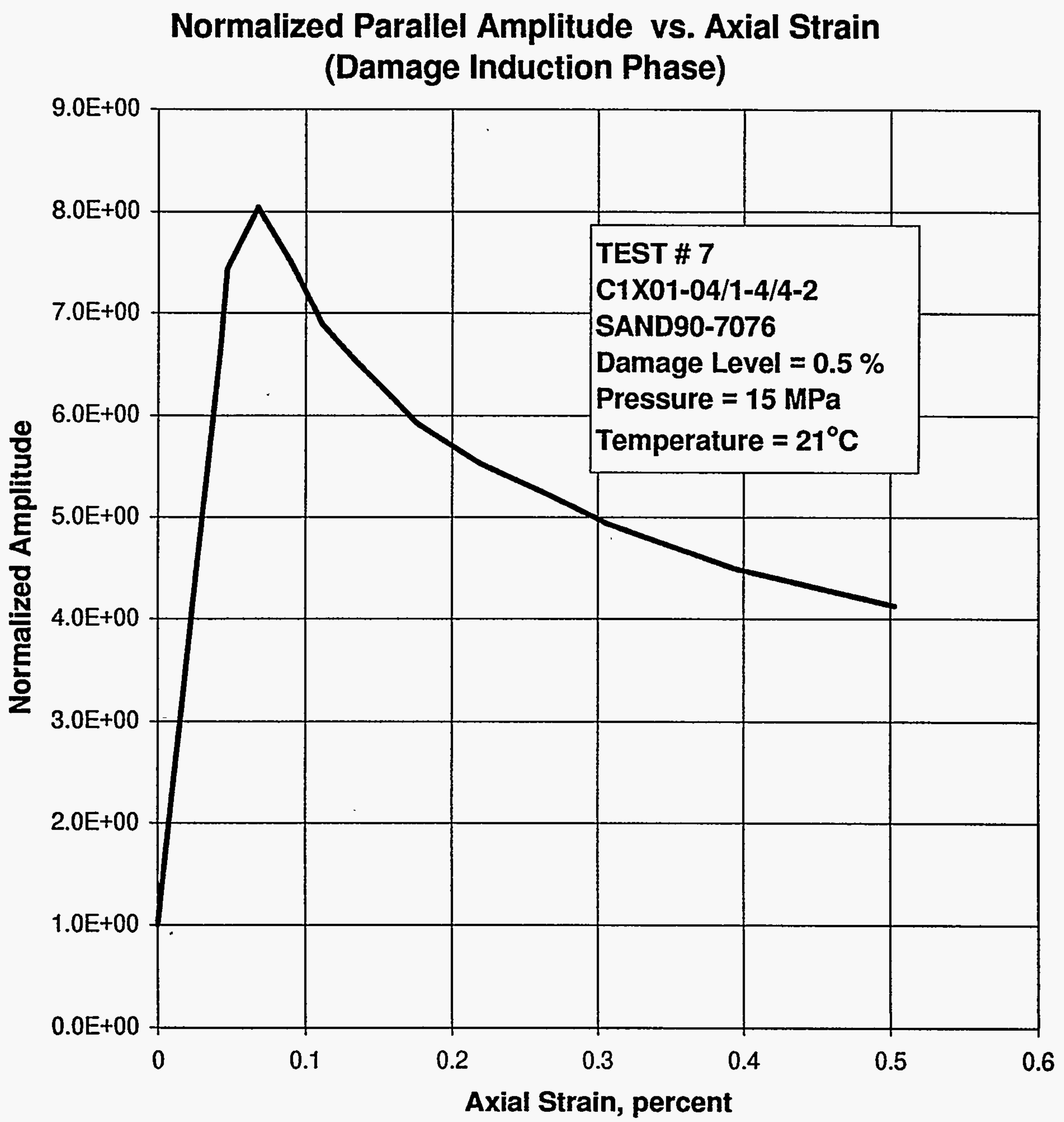

Figure E-110. Normalized Parallel Amplitude as a Function of Axial Strain During the Quasi-Static Loading to Induce Damage in Specimen C1X01-04/1-4/4-2.

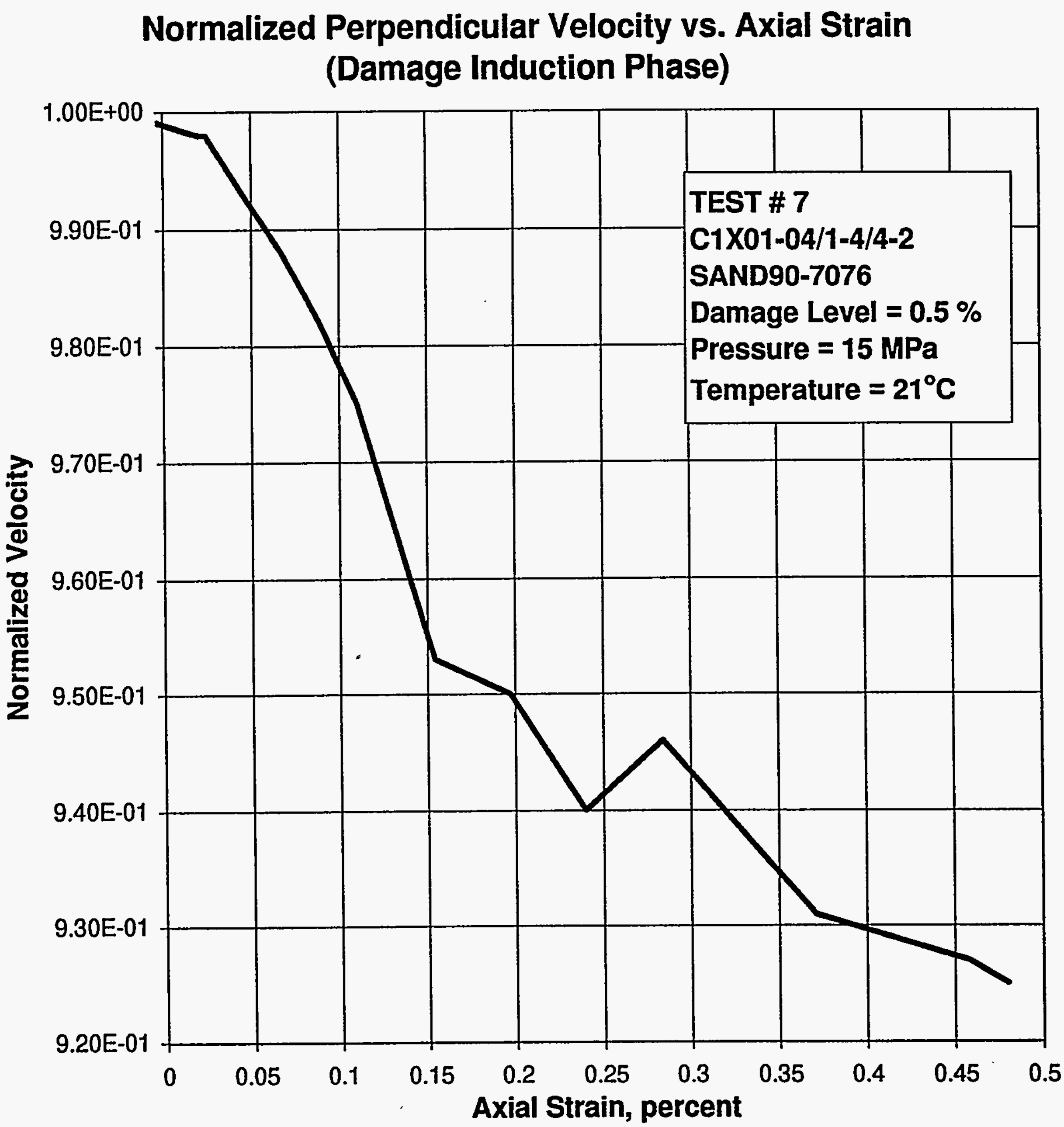

Figure E-111. Normalized Perpendicular Velocity as a Function of Axial Strain During the Quasi-Static Loading to Induce Damage in Specimen C1X01-04/1-4/4-2.

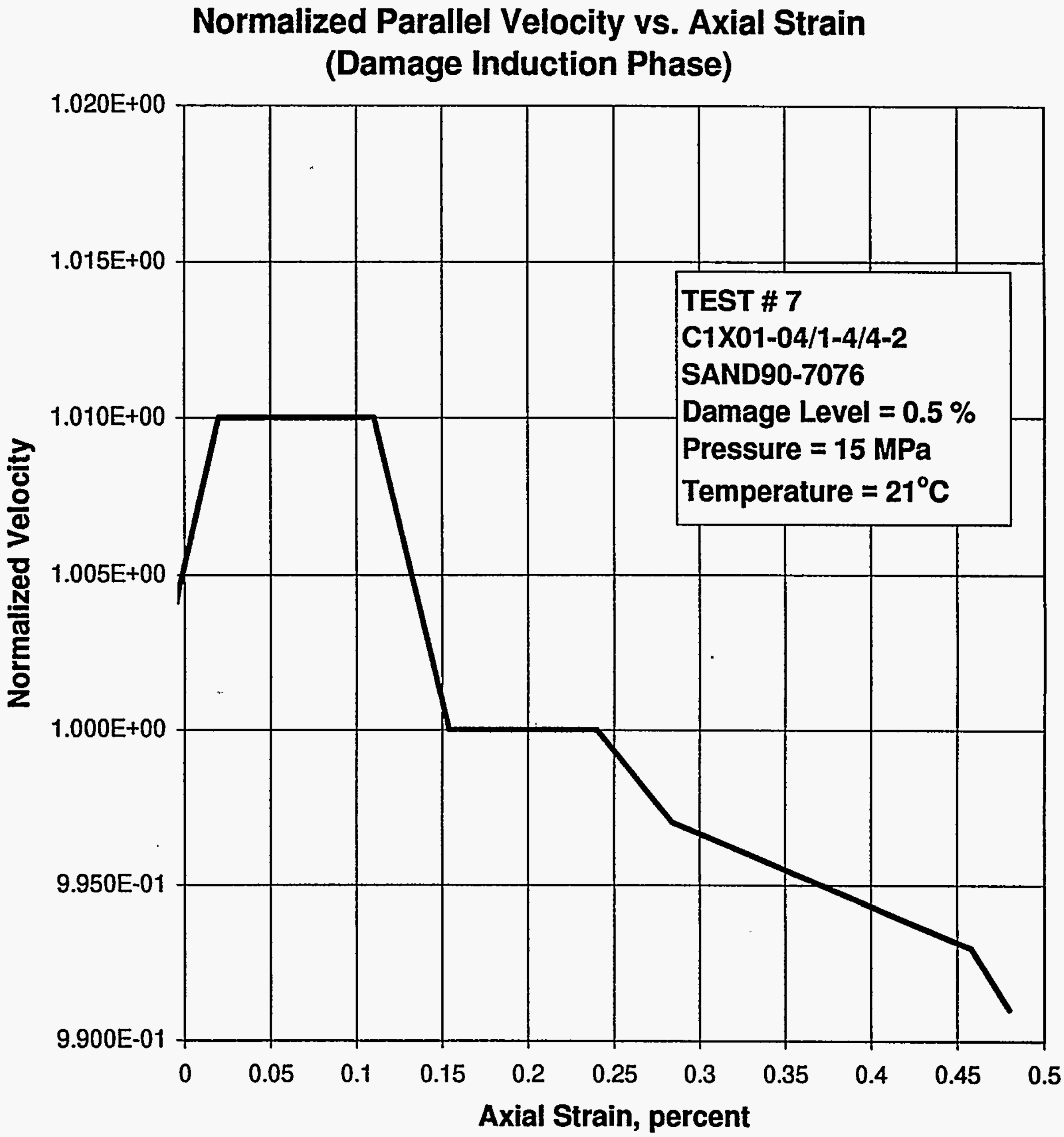

Figure E-112. Normalized Parallel Velocity as a Function of Axial Strain During the Quasi-Static Loading to Induce Damage in Specimen C1X01-04/1-4/4-2.

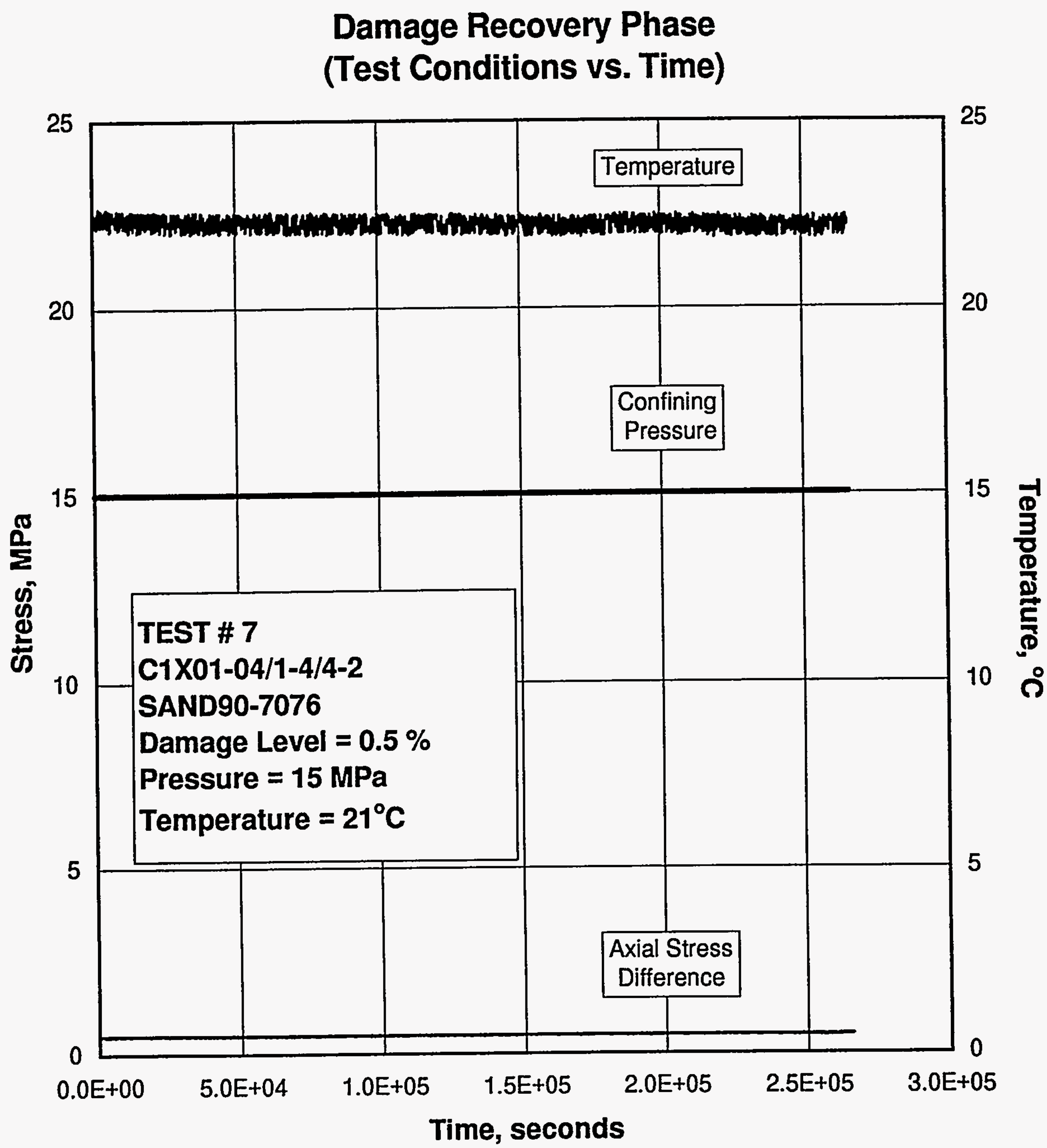

Figure E-113. Test Conditions as a Function of Time During the Hydrostatic Loading to Recover Damage in Specimen C1X01-04/1-4/4-2.

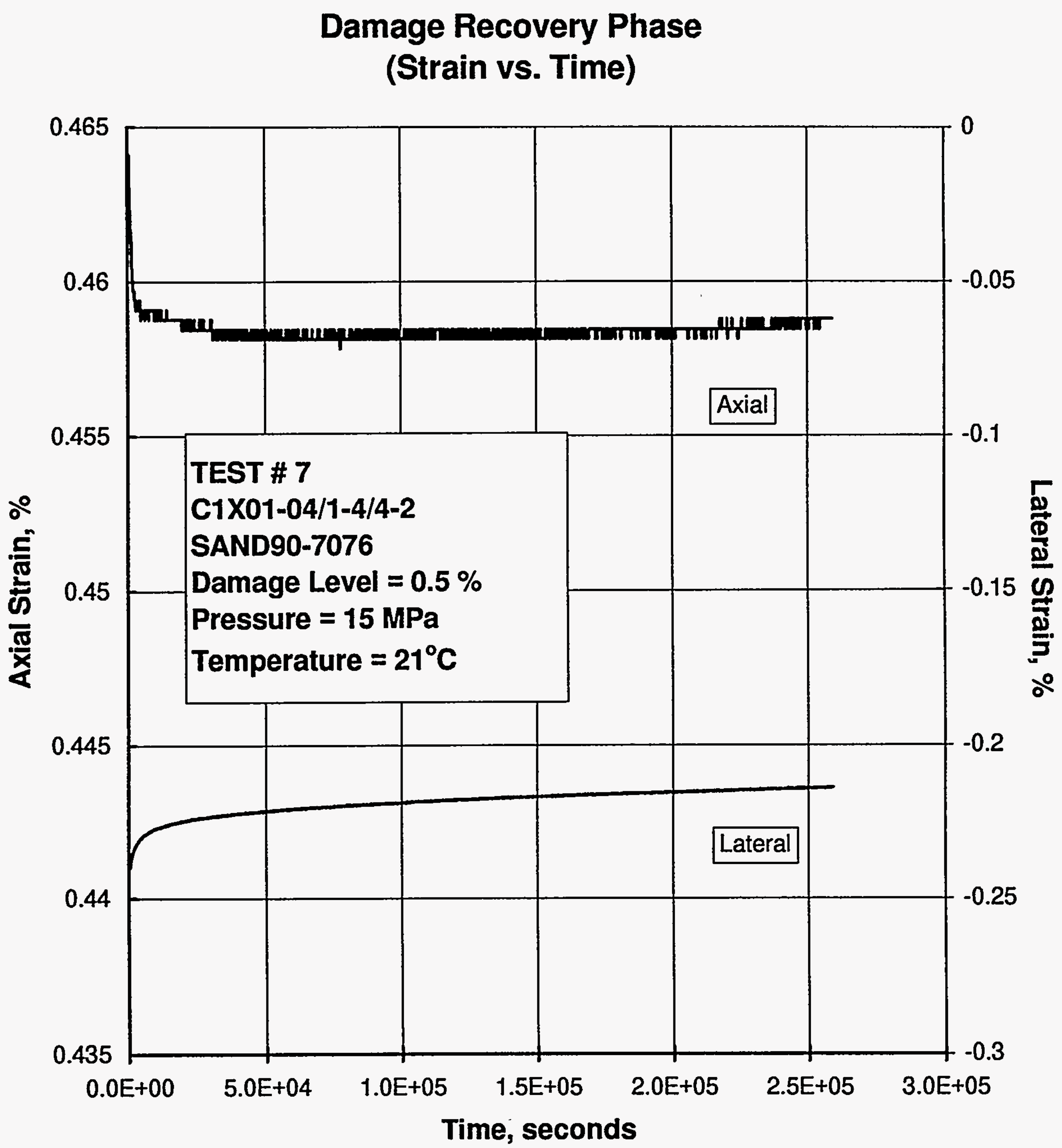

Figure E-114. Axial and Lateral Strain as a Function of Time During the Hydrostatic Loading to Recover Damage in Specimen C1X01-04/1-4/4-2.

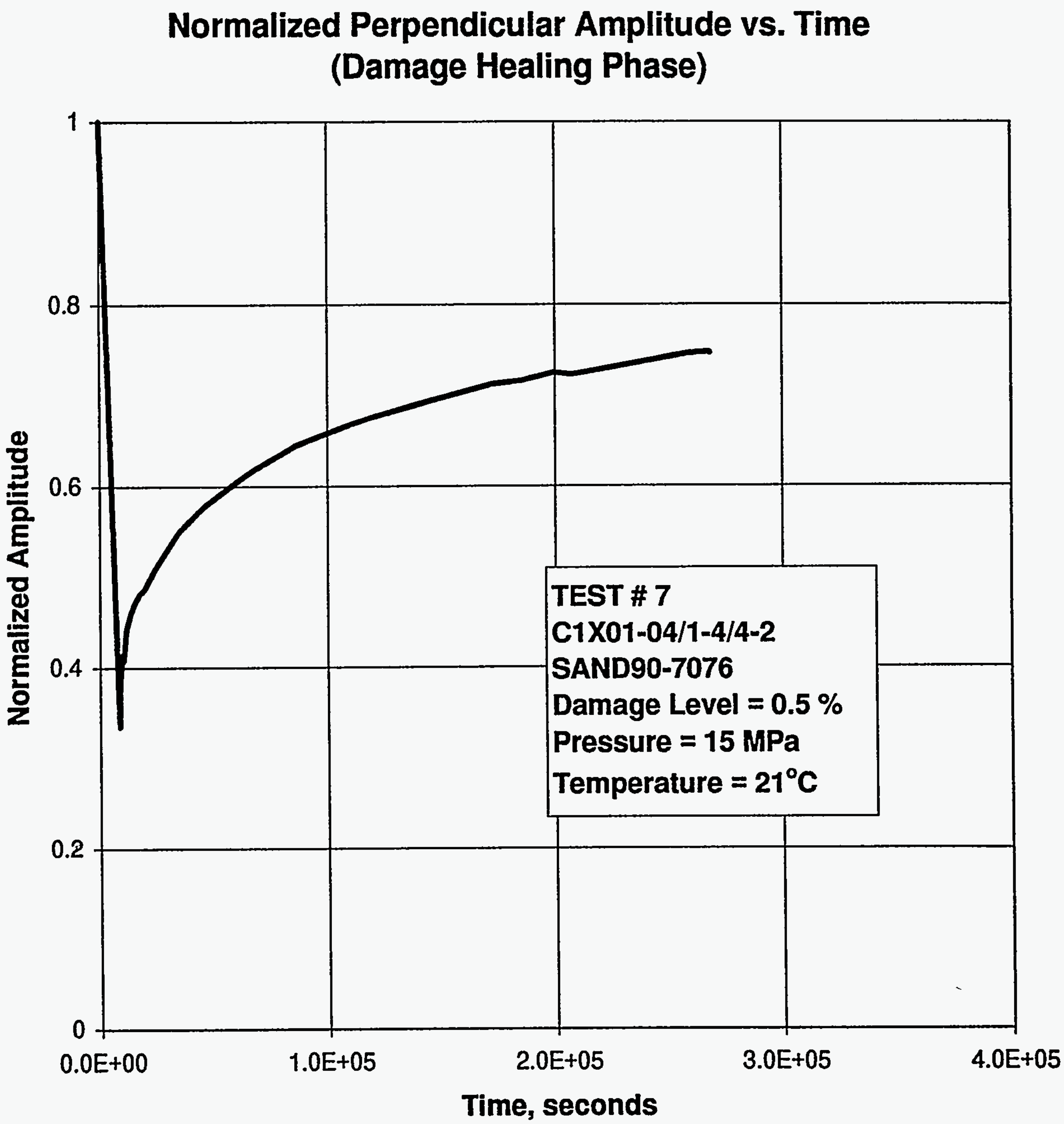

Figure E-115. Normalized Perpendicular Amplitude as a Function of Time During the Hydrostatic Loading to Recover Damage in Specimen C1X01-04/1-4/4-2.

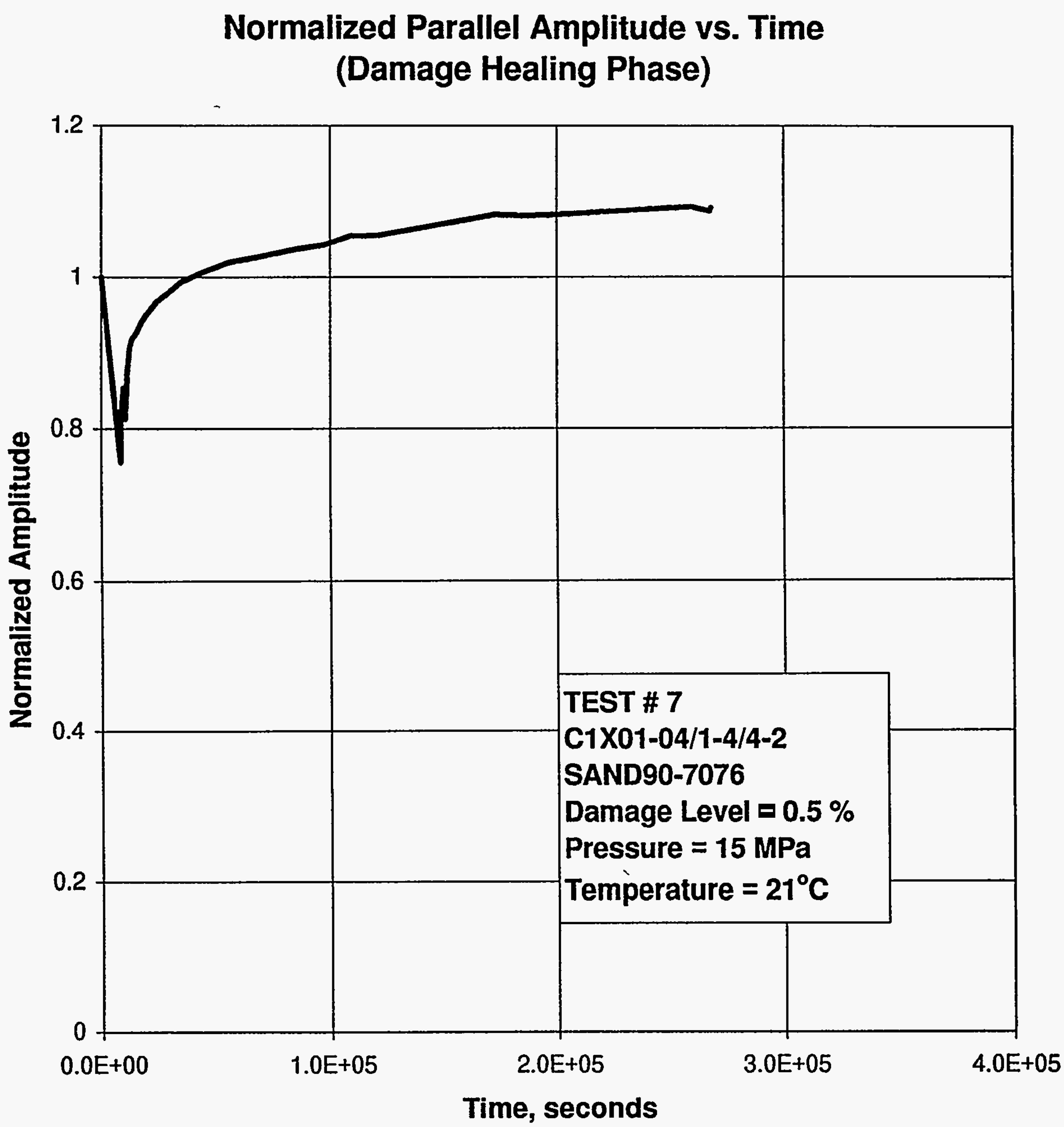

Figure E-116. Normalized Parallel Amplitude as a Function of Time During the Hydrostatic Loading to Recover Damage in Specimen C1X01-04/1-4/4-2.

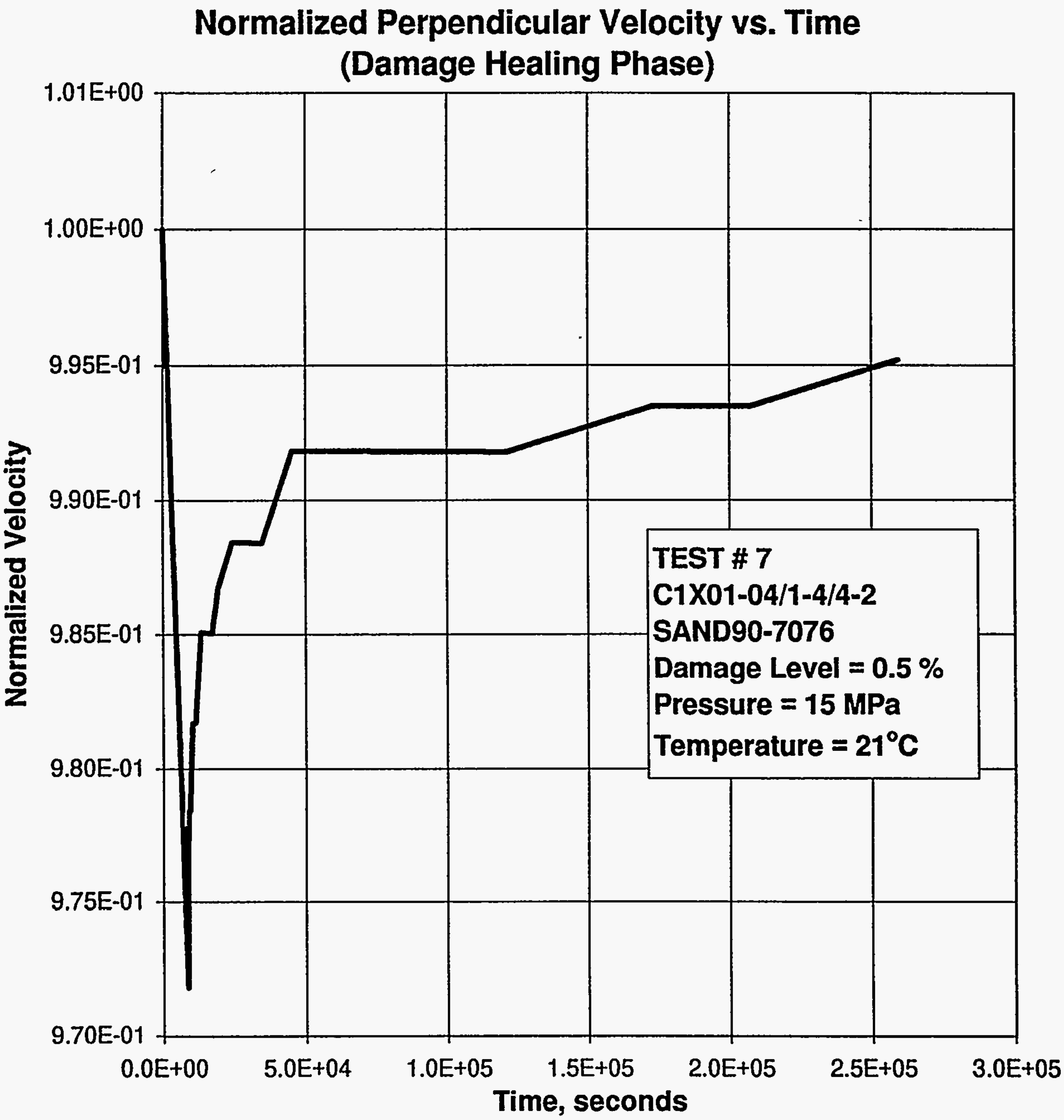

Figure E-117. Normalized Perpendicular Velocity as a Function of Time During the Hydrostatic Loading to Recover Damage in Specimen C1X01-04/1-4/4-2.

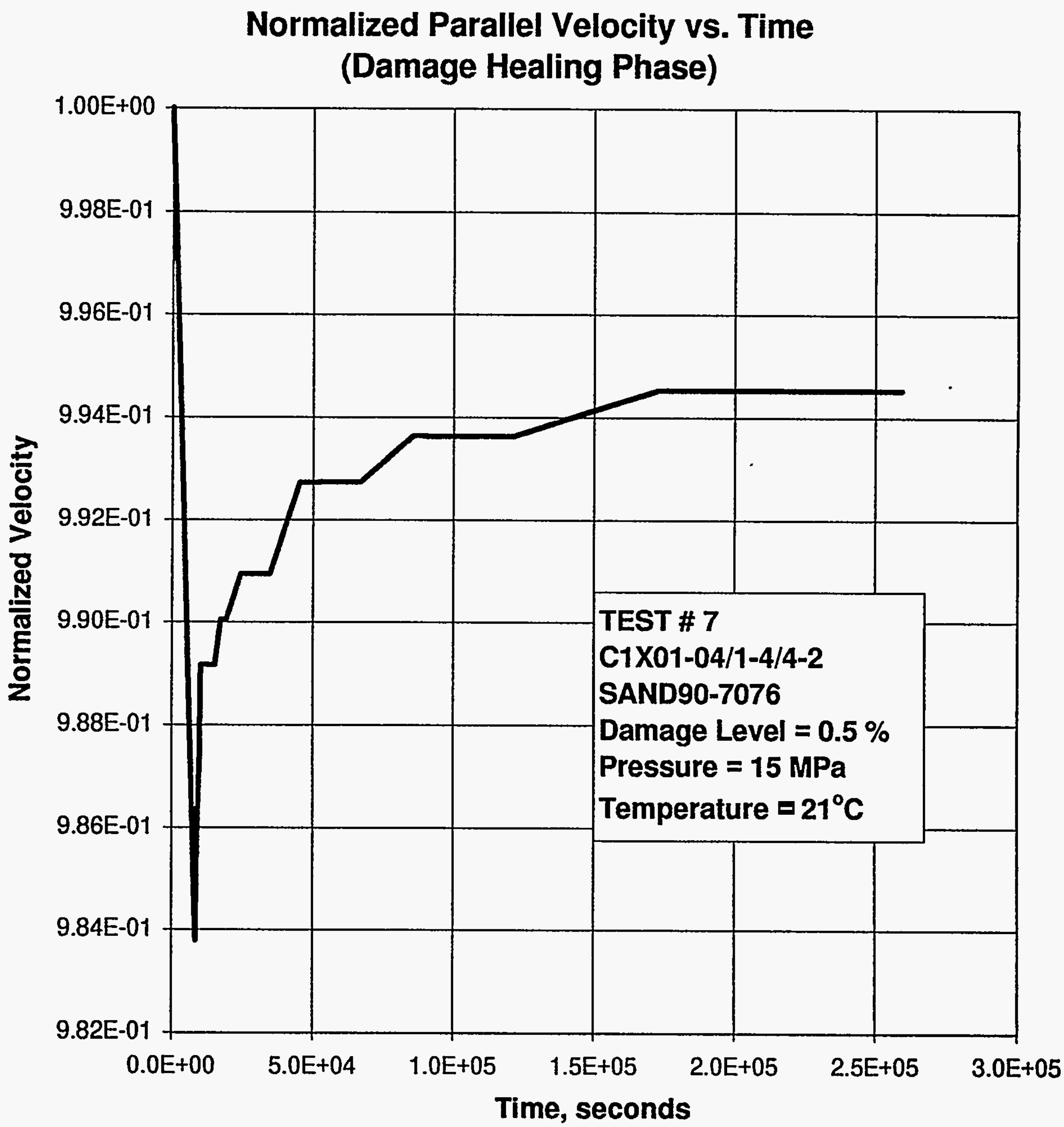

Figure E-118. Normalized Parallel Velocity as a Function of Time During the Hydrostatic Loading to Recover Damage in Specimen C1X01-04/1-4/4-2.

WIPP
UC721 - DISTRIBUTION LIST
SAND96-2765

Federal Agencies

US Department of Energy (6)
Office of Civilian Radioactive Waste Mgmt.
Attn: Deputy Director, RW-2
Acting Director, RW-10
Office of Human Resources & Admin.
Director, RW-30
Office of Program Mgmt. & Integ.
Director, RW-40
Office of Waste Accept., Stor., & Tran.
Director, RW-22
Analysis and Verification Division
Director, RW 4/5
Office of Strategic Planning and
International Programs
Forrestal Building
Washington, DC 20585

Attn: Project Director
Yucca Mountain Site Characterization Office
Director, RW-3
Office of Quality Assurance
101 Convention Center Drive, Suite #P-110
Las Vegas, NV 89109

US Department of Energy
Albuquerque Operations Office
Attn: National Atomic Museum Library
P.O. Box 5400
Albuquerque, NM 87185-5400

US Department of Energy
Research & Waste Management Division
Attn: Director
P.O. Box E
Oak Ridge, TN 37831

US Department of Energy (5)
Carlsbad Area Office
Attn: G. Dials
D. Galbraith
M. McFadden
R. Lark
J. A. Mewhinney
P.O. Box 3090
Carlsbad, NM 88221-3090

US Department of Energy
Office of Environmental Restoration and
Waste Management
Attn: J. Lytle, EM-30
Forrestal Building
Washington, DC 20585-0002

US Department of Energy
Attn: E. Young
Room E-178
GAO/RCED/GTN
Washington, DC 20545

US Department of Energy (3)
Office of Environmental Restoration and
Waste Management
Attn: M. Frei, EM-34, Trevion II
Washington, DC 20585-0002

US Department of Energy
Office of Environmental Restoration and
Waste Management
Attn: S. Schneider, EM-342, Trevion II
Washington, DC 20585-0002

US Department of Energy (2)
Office of Environment, Safety & Health
Attn: C. Borgstrom, EH-25
R. Pelletier, EH-231
Washington, DC 20585

US Department of Energy (2)
Idaho Operations Office
Fuel Processing & Waste Mgmt. Division
785 DOE Place
Idaho Falls, ID 83402

US Environmental Protection Agency (2)
Radiation Protection Programs
Attn: M. Oge
ANR-460
Washington, DC 20460

U.S. Nuclear Regulatory Commission
Division of Waste Management
Attn: H. Marson
MS 4-H-3
Washington, DC 20555

Boards

Defense Nuclear Facilities Safety Board
Attn: D. Winters
625 Indiana Ave. NW, Suite 700
Washington, DC 20004

Nuclear Waste Technical Review Board (2)
Attn: Chairman
S. J. S. Parry
1100 Wilson Blvd., Suite 910
Arlington, VA 22209-2297

Advisory Committee on Nuclear Waste
Nuclear Regulatory Commission
Attn: R. Major
7920 Norfolk Avenue
Bethesda, MD 20814

State Agencies

Attorney General of New Mexico
P.O. Drawer 1508
Santa Fe, NM 87504-1508

Environmental Evaluation Group (3)
Attn: Library
7007 Wyoming NE
Suite F-2
Albuquerque, NM 87109

NM Energy, Minerals, and Natural
Resources Department
Attn: Library
2040 S. Pacheco
Santa Fe, NM 87505

NM Environment Department (3)
Secretary of the Environment
Attn: Mark Weidler
1190 St. Francis Drive
Santa Fe, NM 87503-0968

NM Bureau of Mines & Mineral Resources
Socorro, NM 87801

NM Environment Department
WIPP Project Site
Attn: P. McCasland
P.O. Box 3090
Carlsbad, NM 88221

Laboratories/Corporations

Battelle Pacific Northwest Laboratories
Battelle Blvd.
Richland, WA 99352

INTERA, Inc.
Attn: G. A. Freeze
1650 University Blvd. NE, Suite 300
Albuquerque, NM 87102

INTERA, Inc.
Attn: J. F. Pickens
6850 Austin Center Blvd., Suite 300
Austin, TX 78731

INTERA, Inc.
Attn: W. Stensrud
P.O. Box 2123
Carlsbad, NM 88221

Los Alamos National Laboratory
Attn: B. Erdal, INC-12
P.O. Box 1663
Los Alamos, NM 87544

RE/SPEC, Inc
Attn: Angus Robb
4775 Indian School NE, Suite 300
Albuquerque, NM 87110-3927

RE/SPEC, Inc (10)
Attn: G.D. Callahan
P.O. Box 725
Rapid City, SD 57709

Southwest Research Institute (2)
Center for Nuclear Waste Regulatory Analysis
Attn: P.K. Nair
6220 Culebra Rd.
San Antonio, TX 78228-0510

Tech Reps, Inc. (4)
Attn: J. Chapman (2)
T. Peterson (2)
5000 Marble NE, Suite 222
Albuquerque, NM 87110

Westinghouse Electric Corporation (5)
Attn: Library
C. Cox
L. Fitch
B. A. Howard
R. Kehrman
P.O. Box 2078
Carlsbad, NM 88221

S. Cohen & Associates
Attn: Bill Thurber
1355 Beverly Road
McLean, VA 22101

National Academy of Sciences, WIPP Panel

Howard Adler
Oxyrase, Incorporated
7327 Oak Ridge Highway
Knoxville, TN 37931

Bob Andrews
Board of Radioactive Waste Management
GF456
2101 Constitution Ave.
Washington, DC 20418

Rodney C. Ewing
Department of Geology
University of New Mexico
Albuquerque, NM 87131

Charles Fairhurst
Department of Civil and Mineral Engineering
University of Minnesota
500 Pillsbury Dr. SE
Minneapolis, MN 55455-0220

B. John Garrick
PLG Incorporated
4590 MacArthur Blvd., Suite 400
Newport Beach, CA 92660-2027

Leonard F. Konikow
US Geological Survey
431 National Center
Reston, VA 22092

Carl A. Anderson, Director
Board of Radioactive Waste Management
National Research Council
HA 456
2101 Constitution Ave. NW
Washington, DC 20418

Christopher G. Whipple
ICF Kaiser Engineers
1800 Harrison St., 7th Floor
Oakland, CA 94612-3430

John O. Blomeke
720 Clubhouse Way
Knoxville, TN 37909

Sue B. Clark
University of Georgia
Savannah River Ecology Lab
P.O. Drawer E
Aiken, SC 29802

Konrad B. Krauskopf
Department of Geology
Stanford University
Stanford, CA 94305-2115

Della Roy
Pennsylvania State University
217 Materials Research Lab
Hastings Road
University Park, PA 16802

David A. Waite
CH_2 M Hill
P.O. Box 91500
Bellevue, WA 98009-2050

Thomas A. Zordon
Zordan Associates, Inc.
3807 Edinburg Drive
Murrysville, PA 15668

Universities

University of New Mexico
Geology Department
Attn: Library
141 Northrop Hall
Albuquerque, NM 87131

Pennsylvania State University
Dr. H. Reginald Hardy, Jr.
104 Mineral Science Building
University Park, PA 16802

University of Washington
College of Ocean & Fishery Sciences
Attn: G. R. Heath
583 Henderson Hall, HN-15
Seattle, WA 98195

Libraries

Thomas Brannigan Library
Attn: D. Dresp
106 W. Hadley St.
Las Cruces, NM 88001

Government Publications Department
Zimmerman Library
University of New Mexico
Albuquerque, NM 87131

New Mexico Junior College
Pannell Library
Attn: R. Hill
Lovington Highway
Hobbs, NM 88240

New Mexico State Library
Attn: N. McCallan
325 Don Gaspar
Santa Fe, NM 87503

New Mexico Tech
Martin Speere Memorial Library
Campus Street
Socorro, NM 87810

WIPP Public Reading Room
Carlsbad Public Library
101 S. Halagueno St.
Carlsbad, NM 88220

Foreign Addresses

Atomic Energy of Canada, Ltd.
Whiteshell Laboratories
Attn: B. Goodwin
Pinawa, Manitoba, CANADA R0E 1L0

Studecentrum Voor Kernenergie
Centre d'Energie Nuclaire
Attn: A. Bonne
SCK/CEN Boeretang 200
B-2400 Mol
BELGIUM

Professor Michel Aubertin
Ecole Polytechnique de Montreal
Mineral Engineering Dept.
P.O. Box 6079, Succursale Centre-Ville
Montreal Quebec H3C 3A7
CANADA

Pierre Berest
Laboratoire de Mecanique des Solides
Ecole Polytechnique
Palaiseau
FRANCE 91128

Jean-Pierre Oliver
OECD Nuclear Energy Agency
Division of Radiation Protection and
Waste Management
38 Boulevard Suchet
75016 Paris
FRANCE

Francois Chenevier (2)
ANDRA
Route de Panorama Robert Schumann
B. P. 38
92266 Fontenay-aux-Roses, Cedex
FRANCE

Claude Sombret
Centre d'Etudes Nucleaires de la Vallee Rhone
CEN/VALRHO
S.D.H.A. B.P. 171
30205 Bagnols-Sur-Ceze,
FRANCE

Commissariat a L'Energie Atomique
Attn: D. Alexandre
Centre d'Etudes de Cadarache
13108 Saint Paul Lez Durance Cedex
FRANCE

Bundesanstalt fur Geowissenschaften und
Rohstoffe
Attn: M. Langer
Postfach 510 153
D-30631 Hannover,
GERMANY

Bundesministerium fur Forschung und Technologie
Postfach 200 706
5300 Bonn 2,
GERMANY

Institut fur Tieflagerung
Attn: K. Kuhn
Theodor-Heuss-Strasse 4
D-3300 Braunschweig,
GERMANY

Gesellschaft fur Anlagen und Reaktorsicherheit (GRS)
Attn: B. Baltes
Schwertnergasse 1
D-50667 Cologne,
GERMANY

Physikalisch-Technische Bundesanstalt
Attn: P. Brenneke
Postfach 3345
D-3300 Braunschweig
GERMANY

Shingo Tashiro
Japan Atomic Energy Research Institute
Tokai-Mura, Ibaraki-Ken, 319-11
JAPAN

Netherlands Energy Research Foundation ECN
Attn: J. Prij
3 Westerduinweg
P.O. Box 1
1755 ZG Petten
THE NETHERLANDS

Svensk Karnbransleforsorjning AB
Attn: F. Karlsson
Project KBS (Karnbranslesakerhet)
Box 5864
S-102 48 Stockholm
SWEDEN

Nationale Genossenschaft fur die Lagerung Radioaktiver Abfalle (2)
Attn: S. Vomvoris
P. Zuidema
Hardstrasse 73
CH-5430 Wettingen
SWITZERLAND

AEA Technology
Attn: J. H. Rees
D5W/29 Culham Laboratory
Abington, Oxfordshire OX14 3DB
UNITED KINGDOM

AEA Technology
Attn: W. R. Rodwell
044/A31 Winfrith Technical Centre
Dorchester, Dorset DT2 8DH
UNITED KINGDOM

AEA Technology
Attn: J. E. Tinson
B4244 Harwell Laboratory
Didcot, Oxfordshire OX11 ORA
UNITED KINGDOM

D. R. Knowles
British Nuclear Fuels, plc
Risley, Warrington, Cheshire WA3 6AS
1002607 UNITED KINGDOM

Internal

MS	Org.	
0827	1502	P.J. Hommert
1324	6115	P. B. Davies
0706	6117	W. R. Wawersik
1320	6831	E. J. Nowak
1322	6121	J. R. Tillerson
1322	6121	D. E. Munson (10)
1328	6849	D. R. Anderson
1328	6848	H. N. Jow
1335	6801	M. Chu
1395	6121	F. D. Hansen
1341	6832	J. T. Holmes
1395	6800	L. Shephard
1395	6821	M. Marietta
1335	6000	W. Weart
1341	6347	D. R. Schafer
1341	6306	A. L. Stevens
1395	6841	V. H. Slaboszewicz
1330	6811	K. Hart (2)
1330	4415	NWM Library (20)
9018	8940-2	Central Technical Files
0899	4414	Technical Library (5)
0619	12630	Review and Approval Desk (2), For DOE/OSTI